MICROBIAL COMMUNITIES OF COASTAL EUTROPHIC SYSTEMS

EDITED BY: Savvas Genitsaris, Konstantinos (Kostas) Ar. Kormas and Maria Moustaka-Gouni

PUBLISHED IN: Frontiers in Marine Science and Frontiers in Microbiology

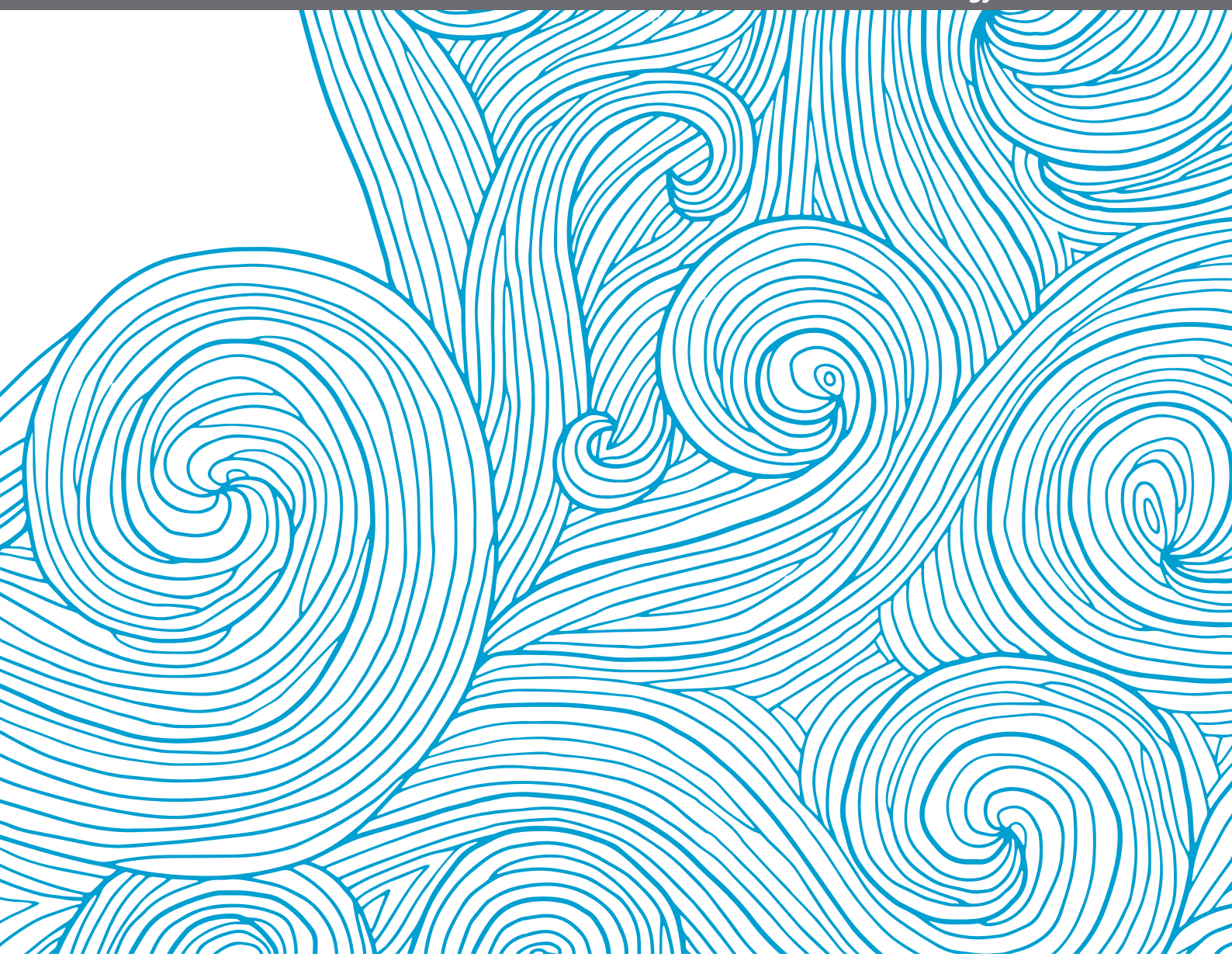

frontiers Research Topics

ISSN 1664-8714
ISBN 978-2-88971-907-5
DOI 10.3389/978-2-88971-907-5

About Frontiers

Frontiers is more than just an open-access publisher of scholarly articles: it is a pioneering approach to the world of academia, radically improving the way scholarly research is managed. The grand vision of Frontiers is a world where all people have an equal opportunity to seek, share and generate knowledge. Frontiers provides immediate and permanent online open access to all its publications, but this alone is not enough to realize our grand goals.

Frontiers Journal Series

The Frontiers Journal Series is a multi-tier and interdisciplinary set of open-access, online journals, promising a paradigm shift from the current review, selection and dissemination processes in academic publishing. All Frontiers journals are driven by researchers for researchers; therefore, they constitute a service to the scholarly community. At the same time, the Frontiers Journal Series operates on a revolutionary invention, the tiered publishing system, initially addressing specific communities of scholars, and gradually climbing up to broader public understanding, thus serving the interests of the lay society, too.

Dedication to Quality

Each Frontiers article is a landmark of the highest quality, thanks to genuinely collaborative interactions between authors and review editors, who include some of the world's best academicians. Research must be certified by peers before entering a stream of knowledge that may eventually reach the public - and shape society; therefore, Frontiers only applies the most rigorous and unbiased reviews.
Frontiers revolutionizes research publishing by freely delivering the most outstanding research, evaluated with no bias from both the academic and social point of view. By applying the most advanced information technologies, Frontiers is catapulting scholarly publishing into a new generation.

What are Frontiers Research Topics?

Frontiers Research Topics are very popular trademarks of the Frontiers Journals Series: they are collections of at least ten articles, all centered on a particular subject. With their unique mix of varied contributions from Original Research to Review Articles, Frontiers Research Topics unify the most influential researchers, the latest key findings and historical advances in a hot research area! Find out more on how to host your own Frontiers Research Topic or contribute to one as an author by contacting the Frontiers Editorial Office: frontiersin.org/about/contact

MICROBIAL COMMUNITIES OF COASTAL EUTROPHIC SYSTEMS

Topic Editors:
Savvas Genitsaris, National and Kapodistrian University of Athens, Greece
Konstantinos (Kostas) Ar. Kormas, University of Thessaly, Greece
Maria Moustaka-Gouni, Aristotle University of Thessaloniki, Greece

Citation: Genitsaris, S., Kormas., K. A., Moustaka-Gouni, M., eds. (2021). Microbial Communities of Coastal Eutrophic Systems. Lausanne: Frontiers Media SA. doi: 10.3389/978-2-88971-907-5

Table of Contents

frontiers in Marine Science

EDITORIAL
published: 28 October 2021
doi: 10.3389/fmars.2021.784112

Editorial: Microbial Communities of Coastal Eutrophic Systems

Savvas Genitsaris[1]*, *Konstantinos Ar. Kormas*[2] *and Maria Moustaka-Gouni*[3]

[1] Section of Ecology and Taxonomy, School of Biology, National and Kapodistrian University of Athens, Athens, Greece, [2] Department of Ichthyology and Aquatic Environment, University of Thessaly, Volos, Greece, [3] Department of Botany, School of Biology, Aristotle University of Thessaloniki, Thessaloniki, Greece

Keywords: plankton, eutrophication, urbanization, ecology, microbiome

Editorial on the Research Topic

Microbial Communities of Coastal Eutrophic Systems

Although climate change influences all life, microbes are generally not considered when discussing climate change impacts. We must explore not just how microorganisms affect climate change, including production and consumption of greenhouse gases, but also how they will be affected by climate change and other human activities (Cavicchioli et al., 2019). Indeed, coastal systems worldwide are in high risk of significant anthropogenic modifications as part of urbanization and global warming leading to increased eutrophication phenomena (Rabalais et al., 2009). Especially in these systems, where land-air-sea interactions are greater than at the open sea (Genitsaris et al., 2011), the first responders of high nutrient inputs and therefore biological indicators of the environmental status of these habitats are microbial communities. Coastal microbes, through their diverse morphology, functions, ecological strategies, and genetic content, play crucial roles in biogeochemical cycles, and food webs, which directly or indirectly affect human activities (Smith, 2003). This topic explores the responses of coastal microbial communities to environmental pressures of eutrophication and describes the complex processes that shape coastal system properties.

Coastal and estuarine sediments are drawing attention in recent years as systems highly threatened by multiple anthropogenic stressors that influence microbial populations of the benthos. Species that spend part of their life cycles in sediments, often reappear in the water column *via* resuspension of their resting stages, can rapidly increase in abundance under favorable growth conditions and influence planktonic food webs and biogeochemical cycles. Yi et al. reported that seasonality in bacterial assemblages of intertidal sediments in a subtropical river estuary affected by wastewaters, is related to rainfall and the monsoon climate; but spatial differences are attributed to pH variability and skewed nutrient inputs in the different sampling locations. Furthermore, RNA sequencing of sediment samples revealed higher expression patterns of multiple genes involved in bacterial stress responses far from localized anthropogenic stressors in well-flushed estuarine channels in Sydney Harbor, suggesting that bacterial communities might be more tolerant to urbanized eutrophication (Birrer et al.). Both studies suggest that several of the identified taxa with unique spatial distributions in the sediments of the sampled areas can be used as contaminant bioindicators in estuarine sediments. Complementing these contributions, Wallenius et al. reviewed the recent literature on anthropogenic and environmental constraints on the microbial methane cycle in coastal sediments. Although large amounts of methane are produced in hypoxic sediments of eutrophic coastal areas by methanogenic archaea, favored by global warming, the involvement of specific groups in methanogenesis is unclear. Furthermore, methane can be oxidized by aerobic methanotrophs in the upper sediment layers or in the water column, albeit the pathways involved, the key players and the factors controlling these processes

OPEN ACCESS

Edited and reviewed by:
Lasse Riemann,
University of Copenhagen, Denmark

***Correspondence:**
Savvas Genitsaris
genitsar@biol.uoa.gr

Specialty section:
This article was submitted to Aquatic Microbiology, a section of the journal Frontiers in Marine Science

Received: *27 September 2021*
Accepted: *07 October 2021*
Published: *28 October 2021*

Citation:
Genitsaris S, Kormas KA and Moustaka-Gouni M (2021) Editorial: Microbial Communities of Coastal Eutrophic Systems. Front. Mar. Sci. 8:784112. doi: 10.3389/fmars.2021.784112

is yet to be determined. Integration of the knowledge on microbial and geochemical processes is necessary to produce accurate predictions of methane emissions from coastal zones.

Contributions in this topic included studies on the roles of protease-producing bacteria in aquacultures, and the impacts of oyster aquaculture on nitrogen removal via bacterial processes in sediments. Protease-producing bacteria participate in the degradation processes of organic matter in aquaculture systems. Wei et al. found that protease-producing bacteria were more diverse and abundant in the sediment of tropical aquaculture systems than in the water column. Dissolved oxygen, chemical oxygen demand and salinity were the main factors with positive effects on the dominant assemblages. These findings lay the basis for the development of protease-producing bacterial agents for wastewater purification and the construction of an environment-friendly tropical aquaculture model. In parallel, Mara et al. compared three of the most common oyster aquaculture methods and their potential to enhance microbial nitrogen removal from coastal systems, through oyster biomass and particulate export to underlying sediments. All three methods enhanced nitrogen removal, albeit with different rates depending on the season, choice of gear and approach, indicating that monitoring for these shifts is essential for making decisions about siting and size of aquaculture sites from year to year.

Moving on from sediment microbes, Quéméneur et al. examined the prokaryotic diversity along environmental gradients in the water column of a Mediterranean site (Tunisian coast) for the first time. Their results support further investigation on the role of bacterioplankton in the biogeochemical cycles of the region. Knowledge on bacterial community composition and structure in the water column was considered the first step to further investigate the coupling of bacterio- and phyto-plankton in coastal areas. The resource competition between these two interdependent compartments of plankton, and how this is affecting the productivity of eutrophic sites was examined at the molecular expression level during a summer bloom in the Baltic Sea (Sörenson et al.). The expression of selected pathways of carbon, nitrogen and phosphorus metabolism varied over time, independently, for both phytoplankton and bacterioplankton, indicating partitioning of the available resources and functional flexibility, which are deemed necessary to maintain phytoplankton-bacterioplankton interactions at stable environmental conditions.

Unicellular eukaryotes were examined at the taxonomic and functional levels in the last two contributions in this topic. Wang et al. explored pico- and nanoeukaryotic diversity in coastal surface waters of northern China, and the influence of environmental factors. They concluded that taxonomic composition is related to dissolved oxygen, but functional composition is shaped by limiting nutrient gradients in a regional scale. In addition, Breton et al. applied a trait-based approach to explore the mechanisms of the seasonal species succession of diatoms and copepods in a nutrient-enriched coastal system marked by recurrent spring *Phaeocystis* blooms. Results suggest that the trade-off between the competition advantages and the costs of defense mechanisms played important roles in promoting species richness and in triggering *Phaeocystis* blooms in the meso-eutrophic Eastern English Channel. The seasonal maximum of the defense trait that is the start of *Phaeocystis* single cells transformation into mucilaginous colonies and the timing of the bloom initiation of *Phaeocystis* were synchronized. Copepod assemblage homogenization coincided with the harmful, foam producing *Phaeocystis* bloom, confirming that eutrophication favors biotic homogenization which leads to blooms of inedible species, such as *Phaeocystis*.

The advances in high-throughput sequencing accompanied by the technological innovations of classical microscopy have provided the researchers contributing to the topic the tools to address questions on the diverse and complex marine microbial communities of eutrophic coastal areas. These contributions highlight the magnitude of the unexplored microbial diversity, the complex responses of marine microbes to cultural eutrophication in terms of community structure and roles, and offer insights on the who, when, where, and how they are affecting ecosystem function and biogeochemical cycles.

AUTHOR CONTRIBUTIONS

All authors listed have made a substantial, direct and intellectual contribution to the work, and approved it for publication.

REFERENCES

Cavicchioli, R., Ripple, W. J., Timmis, K. N., Azam, F., Bakken, L. R., Baylis, M., et al. (2019). Scientists' warning to humanity: microorganisms and climate change. *Nat. Rev. Microbiol.* 17, 569–586. doi: 10.1038/s41579-019-0222-5

Genitsaris, S., Kormas, K. A., and Moustaka-Gouni, M. (2011). Airborne algae and cyanobacteria: Occurrence and related health effects. *Front. Biosci.* 3, 772–787. doi: 10.2741/e285

Rabalais, N. N., Turner, R. E., Díaz, R. J., and Justić, D. (2009). Global change and eutrophication of coastal waters. *ICES J. Mar. Sci.* 66, 1528–1537. doi: 10.1093/icesjms/fsp047

Smith, V. H. (2003). Eutrophication of freshwater and coastal marine ecosystems: A global problem. *Environ. Sci. Pollut. Res.* 10, 126–139. doi: 10.1065/espr2002.12.142

Conflict of Interest: The authors declare that the research was conducted in the absence of any commercial or financial relationships that could be construed as a potential conflict of interest.

frontiers in Marine Science

ORIGINAL RESEARCH
published: 22 October 2020
doi: 10.3389/fmars.2020.585970

Dynamics of Microbial Community Structure and Ecological Functions in Estuarine Intertidal Sediments

*Jun Yi[1], Linus Shing Him Lo[2] and Jinping Cheng[1,2]**

[1] State Key Laboratory of Estuarine and Coastal Research, East China Normal University, Shanghai, China, [2] Hong Kong Branch of Southern Marine Science and Engineering Guangdong Laboratory (Guangzhou) & Department of Ocean Science, School of Science, The Hong Kong University of Science and Technology, Kowloon, Hong Kong

Microbial communities are important indicators of aquatic ecosystem health, responsible for functional roles sustaining the ecosystem such as nutrient cycling, as well as environmental problems. Urbanized estuaries are vulnerable intersections between terrestrial and marine ecosystems and are susceptible to pressure and perturbation from both natural processes and human activities over time. The response by microbial communities toward changes in the environment should be closely monitored and studied. In this study, microbial communities in brackish intertidal sediments, sampled seasonally over a year along the coast of Yangtze River estuary, were analyzed using 16S rRNA gene sequencing. Potential compositional and functional changes in microbial communities resulting from temporal variation and associated physiochemical gradients in the environment were studied and notable patterns were observed over time. Summer season was recorded with the lowest microbial community α-diversity. For β-diversity, spatiotemporal differentiation in community structures was recorded with seasonal clustering. *Proteobacteria* was recorded as the most dominant phylum among all sampling sites throughout the year but its relative abundance showed no temporal changes. Instead, relative abundances of phyla *Actinobacteria*, *Chloroflexi,* and *Verrucomicrobia* were found to differ significantly over time, generally favoring the wet Spring and Summer. In contrast, temporal variation was observed for the class *Deltaproteobacteria* and some of the corresponding sulfate/sulfur-reducing bacterial genera, favoring the dry Autumn and Winter. However, there were no major temporal changes in ecological functions contributed by microbial communities throughout the study period. While results from redundancy analysis showed that the subtle changes in pH in the environment had the greatest impact on microbial community composition, the variation it explained remained relatively low. Alternatively, precipitation, distinguishing the dry and wet seasons of the subtropical monsoon climate zone, was suggested to be another potential key factor influencing microbial community composition and their relative abundances. The present study provides new data and insights on the impact of temporal variation on microbial community composition and ecological function in an urbanized estuarine ecosystem.

Keywords: Yangtze River estuary, intertidal sediments, microbial community, community composition, seasonal dynamics, ecological functions

OPEN ACCESS

Edited by:
Maria Moustaka-Gouni, Aristotle University of Thessaloniki, Greece

Reviewed by:
Alma Parada, Stanford University, United States
Alexandra Meziti, University of Thessaly, Greece

***Correspondence:**
Jinping Cheng
jincheng@ust.hk

Specialty section:
This article was submitted to Aquatic Microbiology, a section of the journal Frontiers in Marine Science

Received: *22 July 2020*
Accepted: *30 September 2020*
Published: *22 October 2020*

Citation:
Yi J, Lo LSH and Cheng J (2020) Dynamics of Microbial Community Structure and Ecological Functions in Estuarine Intertidal Sediments. Front. Mar. Sci. 7:585970. doi: 10.3389/fmars.2020.585970

INTRODUCTION

Microbes are important components of estuarine ecosystems responsible for driving many biogeochemical processes, ranging from regulatory functions for the cycling of nutrients, such as nitrogen, phosphorus, and sulfur (Falkowski et al., 2008), to biodegradation and decomposition of pollutants (Xie et al., 2016). However, the role and performance of microbial communities are susceptible to impact from changing environments (Suh et al., 2015).

Estuarine intertidal mudflats are known interactive zones between terrestrial and marine ecosystems. Intertidal sediment conditions can constantly change due to different natural processes such as freshwater input, terrestrial runoff, and incoming tides, as well as anthropogenic impact (Guo et al., 2018). This variability has resulted in microbial communities in intertidal sediments displaying richer composition and overall biodiversity, compared to marine ecosystems (Wang et al., 2012). In particular, the surface sediment layer has the highest microbial activity; the sensitive microbial communities from surface sediments can also be indicators of ecological health (Duarte et al., 2012; Kallmeyer et al., 2012). The status of the active and diverse microbial communities in estuarine ecosystems has great economic and ecological significance (Grizzetti et al., 2019).

In terms of environmental changes, temporal variation such as the succession of seasons can be an important factor, leading to differences in tides and precipitation. Subsequently, the amount of dissolved oxygen in surface sediments are often dynamic (Murphy et al., 2011; Peterson et al., 2013). Oxic-anoxic conditions have knock-on effects on the nutrient conditions of the environment and potential respiration rates of microbes (Karhu et al., 2014). Seasonal changes may have notable effects on microbial community composition patterns and corresponding ecological functions due to microbial adaptation (Gilbert et al., 2012; Aguirre et al., 2017). For marine ecosystems, previous long-term monitoring study showed that microbial communities can display seasonal patterns, and the data can be used to predict the effects microbial communities have on geochemical cycles (Giovannoni and Vergin, 2012). For urbanized estuarine ecosystems, spatiotemporal dynamics of microbial communities can be important indicators of water quality and ecological conditions, with human health consequences (Kaestli et al., 2017). Therefore, microbial ecology studies on community-level responses to temporal variations have important implications. They can provide beneficial data to help evaluate relevant long-term impact imposed on an ecosystem, and to identify patterns in microbial community diversity and ecological functions, especially for an ever-changing environment.

The urbanized Yangtze River estuary receives freshwater from Yangtze River and its tributaries and discharges to the East China Sea. With anthropogenic input including nutrients (Liu et al., 2003) and pollutants (Shi et al., 2014), Yangtze River estuary is a complex hydrological environment with rich fisheries resources and great economic significance (Kindong et al., 2020). Yangtze River is also a source of drinking water for nearby cities. The importance of Yangtze River estuary is well established, but to our knowledge, there are very limited field monitoring data available on the potential temporal or seasonal patterns of microbial communities in the estuarine intertidal mudflats, as previous studies have tended to focus on spatial differences or specific groups of bacteria (Guo et al., 2018; Niu et al., 2018; Xu et al., 2018). The advances in sequencing methods such as high throughput 16S rRNA gene sequencing have facilitated microbial studies on a community-level, allowing research on community composition, phylogeny, and ecology (Dyksma et al., 2016; Fan et al., 2016), as opposed to previous species-level approach. In the present study, microbial communities in the Yangtze River estuary, obtained along the brackish boundary region approaching the East China Sea, were characterized. Microbial communities were sampled seasonally over the course of one year with the aim to monitor and identify potential patterns and shifts in microbial community composition and corresponding ecological functions with changing seasons. Environmental factors which may be responsible for potential differences were evaluated to determine their correlation and contribution to compositional and functional changes. Results will help to inform and allow for timely decision making to better manage the valuable ecosystem. This study contributes to the understanding of microbial communities in coastal waters and will be a useful reference for future studies to evaluate impact on estuarine ecosystems.

MATERIALS AND METHODS

Site Description and Sample Collection

The Yangtze River estuary is the mouth of an urbanized waterway, carrying significant volumes of freshwater from Yangtze, subsidiary rivers, and lakes to the East China Sea. The Yangtze River is located in the subtropical monsoon climate zone, with warm, humid summer seasons during May to August, and cool, dry winter seasons during December to February, with an annual temperature range between 6 to 28°C, averaging at 16°C. The annual average precipitation is around 1057 mm, recorded mainly during the Summer season between May to October (Shen, 2020).

In this study, estuarine sediment samples were collected at seasonal intervals on April 12th (Spring), July 23rd (Summer), November 13th (Autumn) of 2016 and January 10th (Winter) of 2017. Five sampling sites were selected along the Yangtze River estuary (**Figure 1**), including Wusongkou (WSK, 31°24′ N, 121°30′ E), Shidongkou (SDK, 31°28′ N, 121°23′ E), Liuhekou (LHK, 31°31′ N, 121°17′ E), Qiyakou (QYK, 31°36′ N, 121°14′ E) and Xupu (XP, 31°45′ N, 120°57′ E) (**Supplementary Figures 1–5**). Sampling sites were coastal brackish intertidal mudflats. Notably, a wastewater treatment plant outlet is located near the SDK sampling site. For each season, intertidal sediments for all five sampling sites were collected on the same day. Dates and time were chosen according to the tidal table to allow efficient sample collection during low tide period for all sites.

A sterile polyethylene shovel was used for sample collection. Above surface sediments (0 - 5 cm) were removed using the shovel before collection of sediment samples (5 - 7 cm). At each

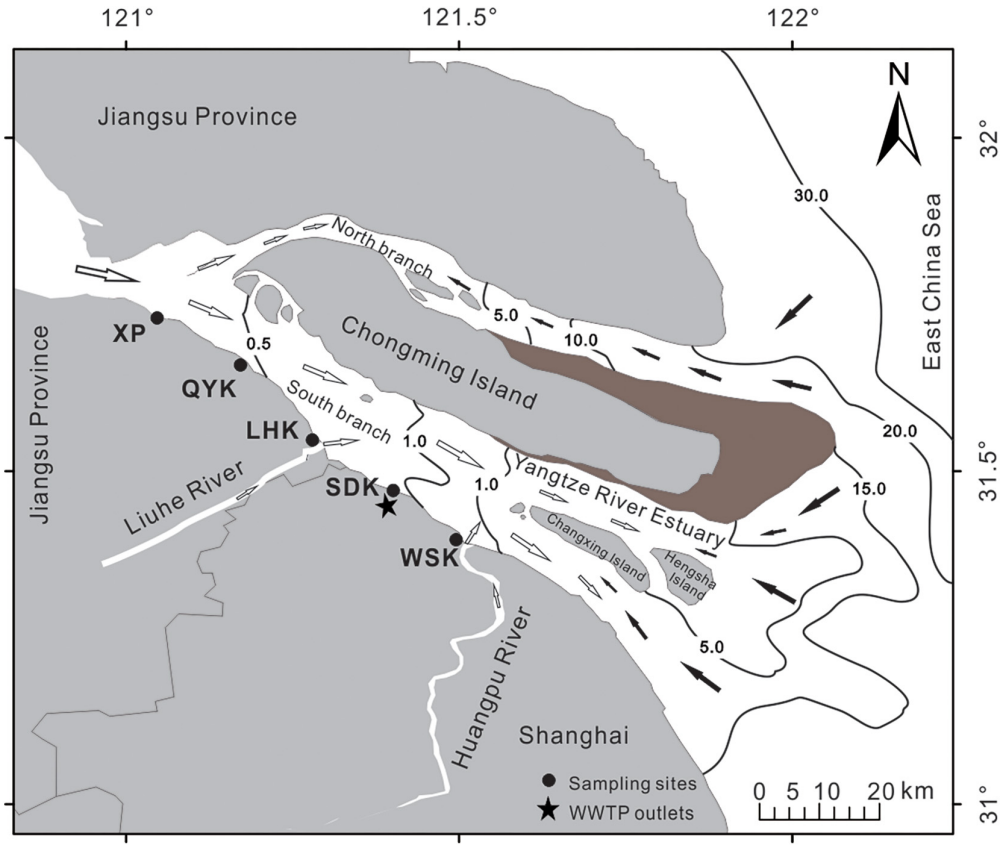

FIGURE 1 | Map of the locations of sampling sites along the Yangtze River estuary tidal mudflats. WSK = Wusongkou; SDK = Shidongkou; LHK = Liuhekou; QYK = Qiyakou; XP = Xupu. Black and white arrows indicate direction of saltwater and freshwater, respectively. Numbers on black lines represent salinity gradients. The black star indicates the outlet of Shidongkou wastewater treatment plant.

site, samples were collected in triplicates and pooled together as one representative sample for subsequent analytical purposes. Over the year, a total of 60 samples were collected and pooled into 20 samples. Samples collected were placed in individual sterile plastic bags in an ice box and transported back to laboratory on the same day. At the laboratory, samples collected were separated into two portions. A portion was stored at 4°C for the characterization of physicochemical properties of the sediments. The other portion was stored at −80°C for DNA extraction. All samples were prepared and handled within seven days after collection.

Characterization of Physicochemical Properties

Physicochemical properties of sediment samples were measured either *in situ* or in the laboratory. Salinity of pore water was measured *in situ* using a portable salinity meter (Model 30, YSI Incorporated, United States). Similarly, pH of pore water was measured *in situ* using a portable pH meter (SIN-PH170, Hangzhou Sinomeasure Automation, China). Sediment samples were then transported to the laboratory and dried at 50°C before measurement of grain size and nutrient concentrations. The grain size of sediments was analyzed using a laser granulometer (LS 13320, Beckman Coulter Corporation, United States). Total nitrogen (TN) concentration in sediments was measured using an elemental analyzer (Vario EL III, Elementar, Germany). Total organic carbon (TOC) concentration in sediments was determined using the $K_2Cr_2O_7$ redox titration method. Total phosphorus (TP) concentration in sediments was determined using the Murphy-Riley modified solution method (Murphy and Riley, 1962).

DNA Extraction and 16S rRNA Gene Sequencing

DNA extraction and isolation from sediment samples were carried out using the E.Z.N.A.^{TM} Soil DNA Kit (D5625-01, Omega Bio-tek, Inc., United States). Extracted DNA were measured through quantitation assays with a Qubit 2.0 Fluorometer (Invitrogen, United States) for subsequent PCR. Primers used for the amplification of bacterial 16S rRNA gene were 314F (5′-CCTACGGGNGGCWGCAG-3′) and 805R (5′-GACTACHVGGGTATCTAATCC-3′), targeting the V3–V4 hypervariable regions (Herlemann et al., 2011). A 30 μL PCR was carried out, containing: 15 μL of 2 × Taq Master Mix, 1 μL of Bar-PCR primer F (10 μM), 1 μL of Primer R (10 μM), 20 μg of DNA template, and deionized water. PCR was conducted

under the following cycling conditions: initial denaturation at 94°C for 3 min; followed by 5 cycles of amplification in which each cycle consisted of denaturation at 94°C for 30 s, primer annealing at 45°C for 20 s and extension at 65°C for 30 s; followed by 20 cycles of 94°C for 20 s, 55°C for 20 s and 72°C for 30 s; followed by final extension at 72°C for 5 min. Products of the first PCR were used as the template for subsequent PCR, with the addition of primers allowing for Illumina™ Bridge Amplification. Second round of PCR was conducted under the following cycling conditions: initial denaturation at 95°C for 3 min; followed by 5 cycles of amplification in which each cycle consisted of denaturation at 94°C for 30 s, primer annealing at 55°C for 20 s and extension at 72°C for 30 s; followed by final extension at 72°C for 5 min. Amplicon products were quantified using Qubit 2.0 Fluorometer. Finally, for each sample, 10 ng (20 pmol) of the product were paired-end sequenced using the Illumina™ MiSeq sequencing platform (Illumina, United States), conducted at Sangon Biotech (Shanghai, China). Sequences generated from the samples used in this study have been deposited in the Sequence Read Archive (SRA) database of the NCBI. Accession numbers for the 20 samples collected from the Yangtze River estuary are SRX 3851127 - 3851146.

Data Analysis

Bacterial OTU Clustering and Taxonomic Classification

Sequencing data were analyzed using the data processing tool Quantitative Insights Into Microbial Ecology 2 (QIIME2) (Bolyen et al., 2019). After importing raw sequencing data (FASTQ) into QIIME2, sequence reads from different samples were demultiplexed according to the barcode sequences. The bacterial paired-end reads were then merged using the VSEARCH pipeline (Rognes et al., 2016). After filtering chimeric and short sequences, reads were clustered into OTUs using closed-reference OTU picking based on a 98% similarity cutoff (Edgar et al., 2011; Rognes et al., 2016).

Classifying OTUs into taxonomy can allow further analysis of the microbial community composition at different taxonomic ranks (Lan et al., 2012). Representative sequences from each OTU were assigned to taxonomy according to the SILVA r138.1 reference database using QIIME2 at > 93% confidence (Quast et al., 2013). The relative abundances of bacterial communities were studied at different taxonomic levels, such as phylum, class and genus. At each level, taxa were considered dominant if the average relative abundance was above 1%.

α- and β-Diversity Analysis

An array of α- and β-diversity measures were calculated using QIIME2. The α-diversity of bacterial communities was analyzed using ACE, Chao1 and Shannon's indices, based on the assigned OTUs. Rarefaction curve for random sampling was established to assess species richness and diversity between samples (**Supplementary Figure 6**). The differences in α-diversity between microbial communities under the influence of different environmental factors were evaluated using Tukey's HSD test followed by Pearson's correlation.

The analysis of β-diversity was conducted through an unweighted UniFrac analysis, as it is sensitive toward rare species of low abundance and is more representative of microbial community diversity in the environment. Based on the UniFrac analysis, a principal coordinate analysis (PCoA) was used to compare microbial communities (Lozupone and Knight, 2005), using the QIIME2 pipeline. Differences between microbial communities were analyzed through Permutational Multivariate Analysis of Variance (PERMANOVA, Adonis test) using QIIME2 (Anderson, 2014).

Functional Annotation of Microbial Communities

Microbial ecological functions were annotated using Functional Annotation of Prokaryotic Taxa (FAPROTAX) based on OTU classification (Louca et al., 2016). FAPROTAX is one of the common predictive methods that utilizes 16S rRNA gene sequencing, extrapolating microbial taxa into putative functions based on literature and cultured microorganism database (Kumar et al., 2019).

Statistical Analysis

Differences in physicochemical properties between collected samples were analyzed using one-way ANOVA and Tukey's HSD test. Differences in relative abundances of microbial community compositions were analyzed using the Welch's *t*-test (White et al., 2009) and Statistical analysis of metagenomics profiles (STAMP) tool (Parks et al., 2014).

Principal component analysis (PCA) and redundancy analysis (RDA) were then carried out using Canoco5 to investigate the relationships between environmental factors, microbial community composition and abundance, and ecological functions (Ter Braak and Šmilauer, 2002). PCA can reflect spatial and temporal variation in microbial communities. Based on PCA, RDA can reveal the impact of different environmental factors on the composition and abundance of microbial communities, and determine whether they contribute significantly to changes (Sun et al., 2018). The used data were log (x + 1) transformed prior to the RDA.

The correlation between environmental factors, relative abundances of bacterial taxa, and their contribution toward ecological functions were analyzed using Spearman's correlation. Statistical analyses were carried out using the SPSS Statistics Version 22.0 (IBM Corp., United States) software. Differences were considered significant when $P < 0.05$.

RESULTS

Characteristics of the Estuarine Sediments

Physicochemical properties of estuarine sediments were summarized in **Table 1**. The salinity of pore water from sampled areas were generally low, ranging between 0.1–0.4. The pH values ranged between 7.20–7.82 and displayed no significant temporal or spatial differences. Salinity, pH, and grain size of sediments in intertidal mudflats of the Yangtze River estuary showed low variance throughout the year,

TABLE 1 | Physicochemical properties of intertidal sediments along the Yangtze River estuary at different seasons.

Sample	Salinity	pH	TOC (%)	TN (mg/kg)	TP (mg/kg)	Sand (%)	Silt (%)	Clay (%)
WSK-spring	0.3	7.76	0.701	570.41	784.64	13.3	73.6	13.1
SDK-spring	0.2	7.67	1.178	1062.94	877.96	20.3	62.9	16.9
LHK-spring	0.3	7.52	0.573	653.37	892.15	3.5	76.6	19.9
QYK-spring	0.3	7.44	0.567	684.11	764.47	4.7	77.7	17.5
XP-spring	0.2	7.82	0.685	562	757.24	5.3	73.0	21.8
WSK-summer	0.2	7.31	1.882	699.39	1238.77	6.6	72.2	21.2
SDK-summer	0.1	7.2	1.838	1328.17	1747.41	5.5	68.4	26.0
LHK-summer	0.2	7.43	0.946	596.87	942.06	7.8	70.7	21.4
QYK-summer	0.1	7.47	0.983	673.03	996.25	3.7	79.7	16.7
XP-summer	0.1	7.71	1.191	487.34	911.68	5.9	73.1	21.0
WSK-autumn	0.4	7.21	0.902	569.14	681.4	5.3	77.9	16.9
SDK-autumn	0.3	7.45	1.308	1767.83	1894.5	3.1	79.3	17.5
LHK-autumn	0.3	7.71	0.765	575.61	673.6	6.7	72.2	21.1
QYK-autumn	0.1	7.45	0.783	494.39	612.97	4.1	78.9	17.0
XP-autumn	0.2	7.62	1.224	350.57	796.2	4.8	70.7	24.5
WSK-winter	0.1	7.36	0.950	683.76	941.04	21.9	74.6	3.5
SDK-winter	0.1	7.4	0.920	907.44	1095.03	10.1	67.4	22.5
LHK-winter	0.2	7.67	1.102	1043.56	934.62	11.4	70.2	18.4
QYK-winter	0.1	7.52	0.888	666.94	785.36	5.6	75.3	19.1
XP-winter	0.2	7.44	1.069	769.02	782.42	3.5	69.3	27.2

whereas nutrient concentrations showed greater variability. The 20 samples were further separated into four seasonal groups to identify seasonal patterns. Results showed that only TOC concentrations displayed a significant temporal change from Spring to Summer ($P < 0.05$). It is suspected that anthropogenic sources of wastewater input and Liuhe River may have an impact on the environmental conditions of downstream sampling sites along Yangtze River estuary, such as WSK and SDK. By grouping the collected data based on location, results revealed that the TN concentrations of WSK and SDK region were significantly higher than its counterpart from LHK, QYK and XP region ($P = 0.03$). Similar patterns were found for TP, but the difference was statistically insignificant ($P = 0.07$).

Temporal Differences in Microbial Community Diversity

α-Diversity

The differences in α-diversity of microbial communities with changing seasons were calculated. A high Good's coverage value showed that the samples could be considered representative of the intertidal sediments. Overall, the structure of microbial communities was relatively stable. When samples were grouped according to sampling season, the Shannon index showed no significant change in overall diversity across all four seasons. However, during Summer, the OTUs in microbial communities were significantly lower compared to other seasons (Tukey's test, $P < 0.05$). Furthermore, the Chao1 index revealed that richness of microbial communities can show significant temporal differences, with Spring having the highest richness, followed by Winter, Autumn and Summer (Tukey's test, $P < 0.05$). Notably, only the difference between Winter and Autumn was insignificant (Tukey's test, $P = 0.801$). The α-diversity indices of the samples are summarized in **Table 2**.

Pearson's correlation was used to further investigate the relationship between microbial community richness, diversity, and physicochemical properties of sediments, as summarized in **Table 3**. Microbial community richness and diversity indices of the 20 samples showed significant positive correlation ($R = 0.503$, $P = 0.024$), confirming that as richness increases, diversity is also expected to increase. Among all the samples collected, there is a significant positive correlation between microbial community richness and pH values ($R = 0.531$, $P = 0.016$); and a significant negative correlation with TOC ($R = -0.633$, $P = 0.003$). Furthermore, microbial community diversity showed a significant negative correlation with TP of the sample ($R = -0.465$, $P = 0.039$).

β-Diversity

Significant spatial and/or temporal difference in microbial community structure can be observed between any two samples collected along the Yangtze River estuary, as shown in **Supplementary Table 1**; a score of 1 is assigned if communities were unrelated with 0% of shared sequences. When samples were grouped based on sampling season to identify seasonal patterns, PCoA results showed that microbial community structures within each seasonal group were relatively similar and clustered together, as shown in **Figure 2A**. Significant difference was found among the four seasonal groups (PERMANOVA, Adonis test, $P = 0.003$), reflected by the dispersed groups of colored points. The PCoA results were more visually distinguished when microbial community structures of collected samples were grouped based on wet and dry seasons (Spring and Summer, Autumn and Winter, respectively), as shown

TABLE 2 | Summary of the richness and diversity indices of microbial communities among different seasons.

Sample	Sequence number	OTUs	Shannon	Chao1	Coverage
WSK-spring	28216	4555	6.03	14957.26	0.89
SDK-spring	28809	6998	7.47	17844.58	0.85
LHK-spring	27131	5860	7.17	16069.85	0.86
QYK-spring	27792	7293	7.42	20425.93	0.83
XP-spring	29604	7049	7.31	19901.36	0.84
WSK-summer	27475	3097	6.39	4340.68	0.96
SDK-summer	28743	2476	5.93	3168.70	0.97
LHK-summer	30856	4268	6.96	5582.99	0.95
QYK-summer	28161	4024	6.93	5575.10	0.94
XP-summer	25333	3913	6.90	5157.06	0.94
WSK-autumn	61897	5680	6.63	7803.74	0.97
SDK-autumn	44830	5706	6.69	8937.88	0.94
LHK-autumn	54322	6378	6.89	9559.89	0.95
QYK-autumn	53658	6089	6.74	9395.95	0.95
XP-autumn	64510	7738	6.98	10809.38	0.95
WSK-winter	61042	6551	6.91	9959.52	0.95
SDK-winter	54951	5989	6.48	8507.48	0.96
LHK-winter	65719	7826	7.28	11497.49	0.95
QYK-winter	55954	7819	7.65	10888.70	0.95
XP-winter	70256	7834	7.66	9983.19	0.96

TABLE 3 | Summary of Pearson's correlation between the richness and diversity of microbial community, and physicochemical properties of sediments.

	OTU richness		Shannon	
	R	*P*	R	*P*
Chao1	1	-	0.503	**0.024**
Shannon	0.503	**0.024**	1	-
Salinity	0.376	0.102	−0.01	0.966
pH	0.531	**0.016**	0.332	0.153
TOC	−0.633	**0.003**	−0.41	0.073
TN	−0.117	0.624	−0.169	0.475
TP	−0.421	0.064	−0.465	**0.039**
Sand	0.204	0.388	−0.021	0.93
Silt	−0.018	0.94	−0.037	0.876
Clay	−0.197	0.405	0.058	0.808

The number is bold when P < 0.05.

in **Figure 2B**. Microbial community structures from samples collected in Spring and Summer were shown to cluster together; samples collected in Autumn and Winter also showed similar clustering. The two clusters were found to be significantly different (PERMANOVA, Adonis test, $P = 0.002$), suggesting precipitation as a potential key factor determining microbial community structures.

Temporal Differences in Relative Abundances of Dominant Bacterial Taxa

Dominant Phylum

The ten most dominant bacterial phyla, recorded from all sediment samples collected in this study, in descending order of mean relative abundance, were *Proteobacteria* (37.46%), *Acidobacteria* (9.38%), *Planctomycetes* (8.93%), *Chloroflexi* (8.89%), *Verrucomicrobia* (6.82%), *Bacteroidetes* (6.14%), *Firmicutes* (3.66%), *Actinobacteria* (3.24%), *Patescibacteria* (2.84%), and *Spirochaetes* (1.26%), as summarized in **Figure 3**. *Proteobacteria,* which is commonly found in estuarine sediments, had the highest relative abundance among all phyla reported from sampled microbial communities. The ten dominant bacterial phyla showed varying degree of differences in relative abundance with changing seasons, as summarized in **Table 4**. When the relative abundances of the ten phyla were compared between seasons and, on a broader scale, precipitation in dry and wet seasons, it is revealed that *Actinobacteria*, *Chloroflexi*, *Planctomycetes* and *Verrucomicrobia* showed occasional significant differences (Welch's *t*-test, $P < 0.05$). Among the four phyla, relative abundance of *Verrucomicrobia* displayed more obvious changes with changing seasons and precipitation; relative abundance was notably higher in Spring and, therefore, wet seasons. Alternatively, the Kruskal-Wallis H-test showed that the relative abundances of *Actinobacteria, Chloroflexi* and *Verrucomicrobia* were significantly different among the four seasons ($P < 0.05$). *Verrucomicrobia* is a methanotrophic phylum found in aquatic sediments and human fecal microbiota (Op, den Camp et al., 2009). *Actinobacteria* is a much more diverse phylum found in both aquatic and terrestrial ecosystems, known for its economic value in producing metabolites (Barka et al., 2016).

Dominant Class

Bacterial composition at the class level was further investigated to reveal potential temporal variations in microbial communities which may have been masked by the diversity within phyla. As shown in **Table 5**, the relative abundances of *Anaerolineae*, *Planctomycetacia,* and *Verrucomicrobiae* showed occasional significant differences between particular seasons or precipitation. For *Deltaproteobacteria*, significant difference was found between Spring and Winter ($P < 0.05$), favoring Winter. Kruskal-Wallis H-test results (**Figure 4**) showed that only classes *Anaerolineae* and *Verrucomicrobiae* were reported with relative abundances that differed significantly among the four seasons ($P < 0.05$). Both classes are major subdivisions of their respective phyla *Chloroflexi* and *Verrucomicrobia* and are directly responsible for the variation recorded at the phylum level.

SRB Genus

Deltaproteobacteria is a bacterial class known for its contributions in sulfate/sulfur-reduction. The subset of bacterial genera responsible for sulfate/sulfur-reduction was selected for study. Among the 15 bacterial genera, the relative abundances of *Desulfomonile* and *Desulfovibrio* had significant differences between Spring/Autumn and dry/wet seasons, respectively (**Table 6**). In addition, only the relative abundances of genera *Desulfuromonas* and *Desulfovirga* showed similar patterns and had significant differences among the four seasons (Kruskal-Wallis H-test, $P < 0.05$), favoring the dry seasons, as shown in **Figure 5**. While *Desulfovirga* is reportedly sulfate-reducing, *Desulfuromonas* is characterized as a genus of Gram-negative

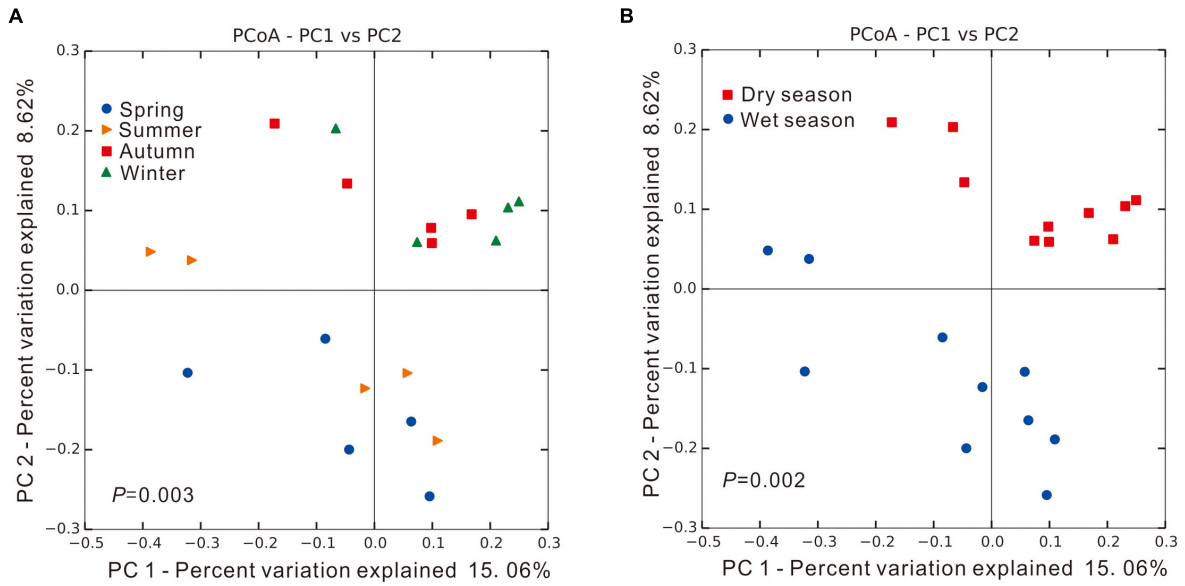

FIGURE 2 | The unweighted UniFrac principal coordinate analysis (PCoA) of microbial communities in intertidal sediments of Yangtze River estuary, among different **(A)** seasons and **(B)** precipitation (dry/wet season). Significant difference was identified using Adonis test in PERMANOVA, $P < 0.05$.

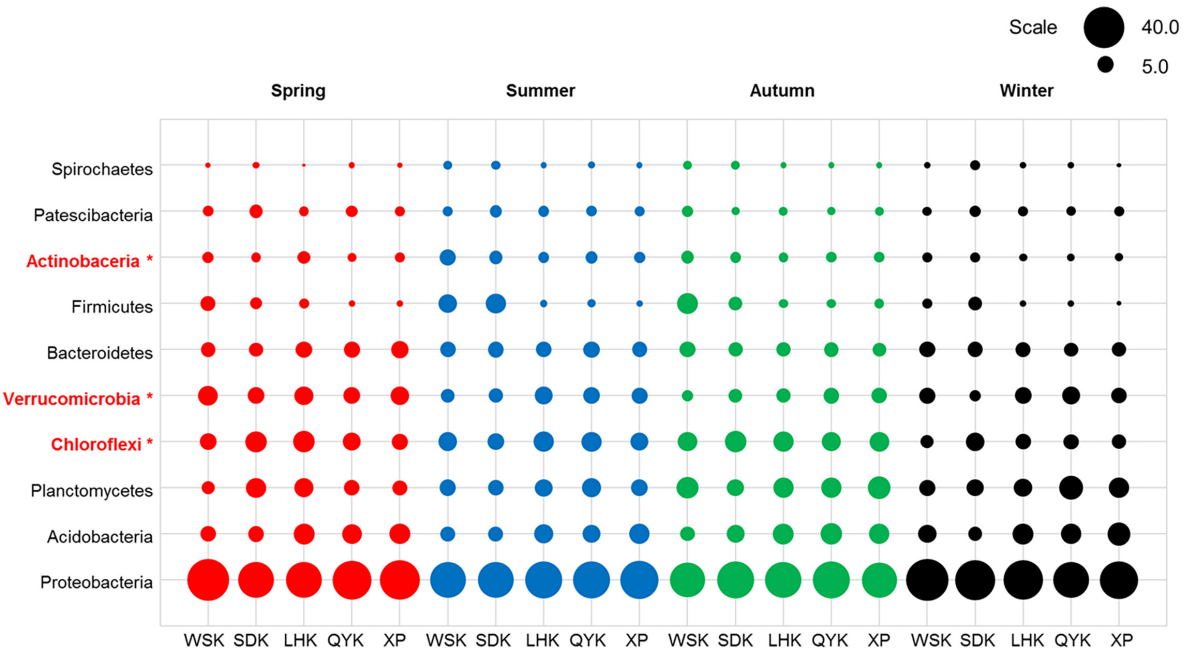

FIGURE 3 | Relative abundances of dominant bacterial phyla in sediments from different sampling sites among various seasons (Red = Spring, Blue = Summer, Green = Autumn, Black = Winter). Asterisks represent a significant difference among the seasons according to Kruskal-Wallis H-test from *STAMP* pipeline (Kruskal-Wallis H-test, $P < 0.05$).

bacteria capable of converting elemental sulfur into sulfide but does not reduce sulfate.

Dominant Phylum-Sediment Properties RDA

RDA was conducted to analyze the relationship between relative abundances of dominant bacterial compositions in microbial communities and physicochemical properties of sediments. As shown in **Figure 6A**, the two RDA axes explained 54.73% (49.13% and 5.60% for axes 1 and 2, respectively) of the variation. Physicochemical properties of sediments explained 62.6% of the variation in microbial compositions. The contribution of individual properties toward variation in microbial composition

TABLE 4 | Summary of temporal differences in relative abundances of dominant bacterial phyla in microbial communities (Welch's *t*-test, $P < 0.05$).

	Spr:Sum	Spr:Aut	Spr:Win	Sum:Aut	Sum:Win	Aut:Win	Dry:Wet
Acidobacteria	0.568	0.963	0.719	0.531	0.389	0.748	0.472
Actinobaceria	0.181	0.547	0.217	0.269	**0.034**	**0.009**	0.125
Bacteroidetes	0.868	0.311	0.550	0.085	0.415	0.322	0.162
Chloroflexi	0.831	0.458	0.078	0.287	**0.008**	**0.003**	0.288
Firmicutes	0.288	0.212	0.747	0.934	0.343	0.273	0.987
Patescibacteria	0.776	0.141	0.329	0.145	0.353	0.327	0.064
Planctomycetes	0.741	0.059	0.262	**0.033**	0.281	0.487	**0.022**
Proteobacteria	0.283	0.209	0.703	0.528	0.106	0.074	0.867
Spirochaetes	0.063	0.062	0.301	0.713	0.348	0.492	0.698
Verrucomicrobia	**0.037**	**0.002**	**0.028**	0.100	0.576	0.359	**0.008**

Spr = Spring; Sum = Summer; Aut = Autumn; Win = Winter. The number is bold when P < 0.05.

TABLE 5 | Summary of temporal differences in relative abundances of dominant bacterial classes in microbial communities (Welch's *t*-test, $P < 0.05$).

	Spr:Sum	Spr:Aut	Spr:Win	Sum:Aut	Sum:Win	Aut:Win	Dry:Wet
Alphaproteobacteria	0.583	0.367	0.975	0.648	0.621	0.397	0.736
Anaerolineae	0.778	0.504	0.073	0.465	**0.008**	**0.004**	0.238
Bacteroidia	0.552	0.181	0.365	0.087	0.507	0.276	0.103
Clostridia	0.273	0.435	0.472	0.683	0.217	0.333	0.591
Deltaproteobacteria	0.164	0.340	**0.029**	0.954	0.182	0.263	0.112
Gammaproteobacteria	0.110	0.091	0.576	0.689	0.307	0.258	0.546
Phycisphaerae	0.704	0.791	0.238	0.529	0.168	0.295	0.165
Planctomycetacia	0.767	0.059	0.539	**0.049**	0.646	0.097	0.061
Subgroup 6	0.285	0.416	0.546	0.927	0.698	0.820	0.643
Verrucomicrobiae	**0.037**	**0.002**	**0.028**	0.100	0.576	0.359	**0.008**

Spr = Spring; Sum = Summer; Aut = Autumn; Win = Winter. The number is bold when P < 0.05.

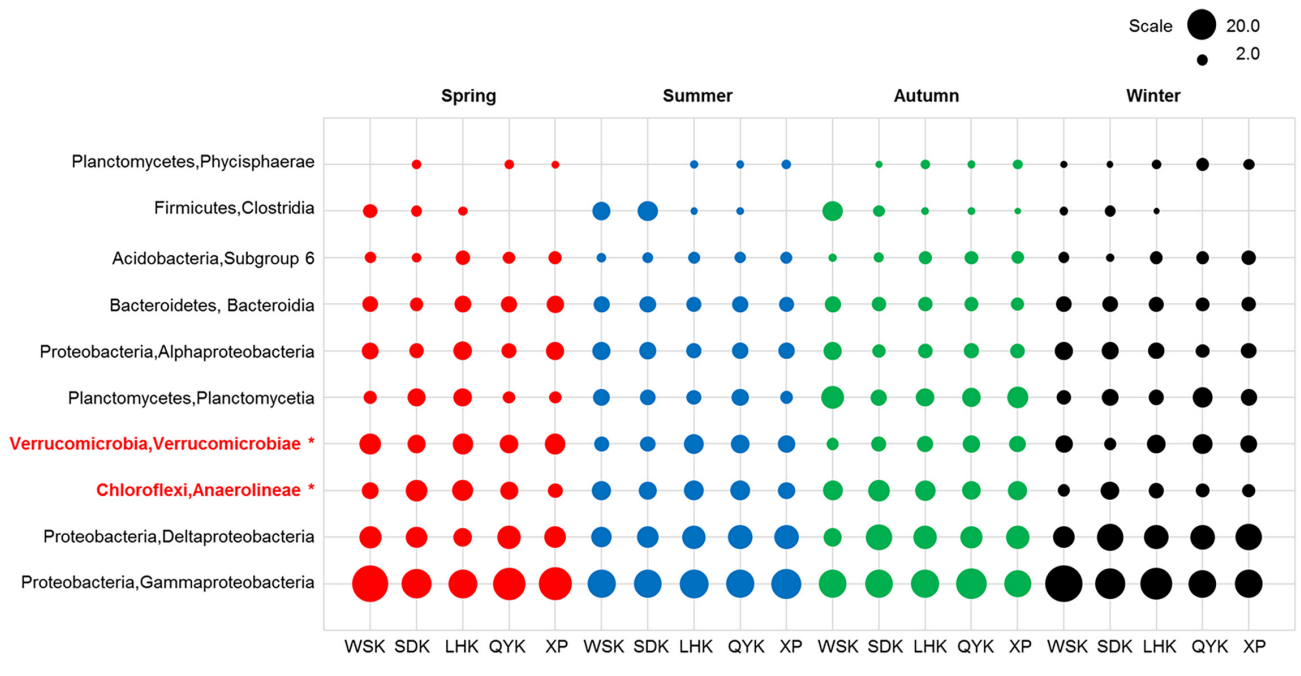

FIGURE 4 | Relative abundances of dominant bacterial classes in sediments from different sampling sites among various seasons (Red = Spring, Blue = Summer, Green = Autumn, Black = Winter). Asterisks represent a significant difference among the seasons according to Kruskal-Wallis H-test from *STAMP* pipeline (Kruskal-Wallis H-test, $P < 0.05$).

TABLE 6 | Summary of temporal differences in relative abundances of sulfate/sulfur-reducing bacterial genera in microbial communities (Welch's *t*-test, $P < 0.05$).

	Spr:Sum	Spr:Aut	Spr:Win	Sum:Aut	Sum:Win	Aut:Win	Dry:Wet
Desulfatiglans	0.252	0.199	0.375	0.925	0.581	0.404	0.521
Desulfatirhabdium	0.135	0.518	0.928	0.199	0.139	0.494	0.253
Desulfobacca	0.128	0.946	0.455	0.089	0.180	0.397	0.477
Desulfobacterium	1.000	1.000	0.374	1.000	0.374	0.374	0.343
Desulfobulbus	0.125	0.779	0.710	0.077	0.143	0.233	0.176
Desulfococcus	1.000	0.374	1.000	0.374	1.000	0.374	0.343
Desulfomicrobium	0.374	1.000	1.000	0.374	0.374	1.000	0.343
Desulfomonile	0.105	**0.007**	0.089	0.813	0.434	0.132	0.336
Desulfonema	0.207	0.160	0.543	0.874	0.384	0.352	0.805
Desulfoprunum	0.557	0.370	0.405	0.590	0.686	0.845	0.288
Desulforegula	1.000	0.374	1.000	0.374	1.000	0.374	0.343
Desulforhabdus	0.374	0.374	0.374	0.708	0.663	0.933	0.974
Desulfovibrio	0.374	0.154	0.245	0.098	0.095	0.442	**0.028**
Desulfovirga	1.000	0.075	**0.019**	0.075	**0.019**	0.467	**0.002**
Desulfuromonas	1.000	0.195	**0.034**	0.195	**0.034**	0.104	**0.013**

Spr = Spring; Sum = Summer; Aut = Autumn; Win = Winter. The number is bold when P < 0.05.

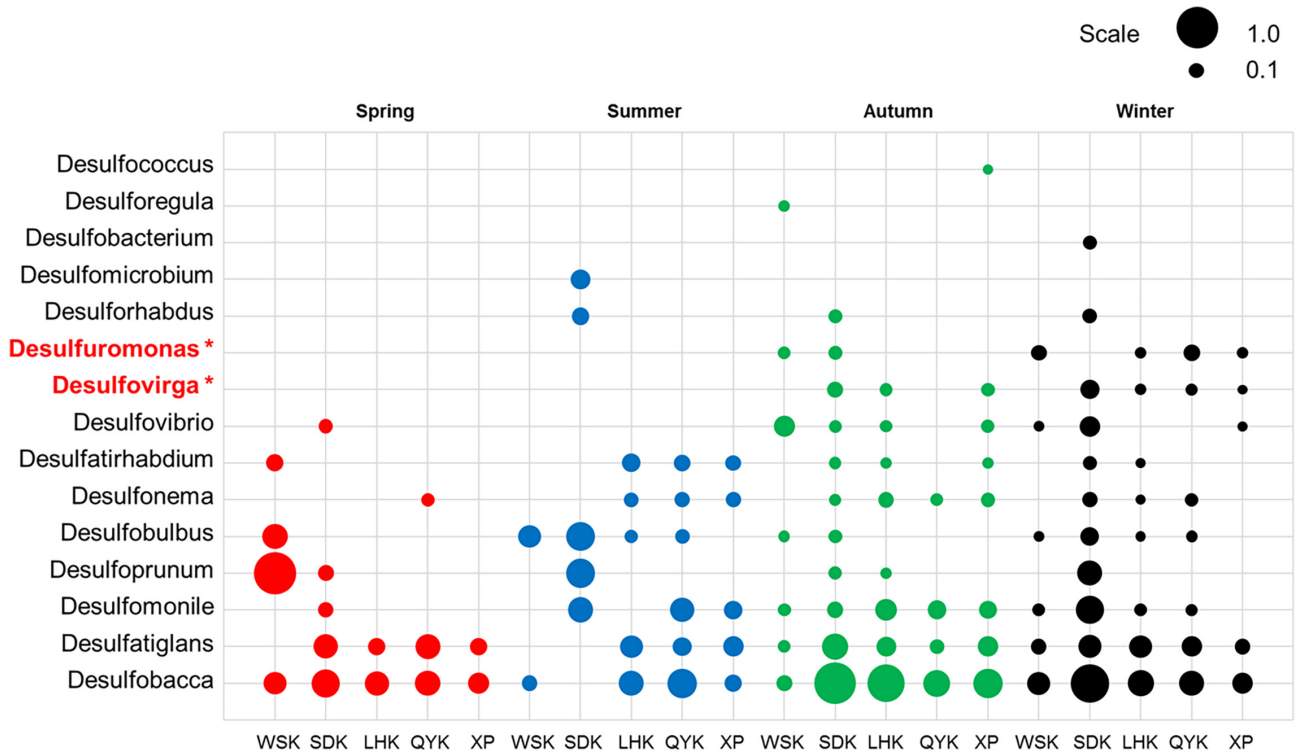

FIGURE 5 | Relative abundances of sulfate/sulfur-reducing bacterial genera in sediments from different sampling sites among various seasons (Red = Spring, Blue = Summer, Green = Autumn, Black = Winter). Asterisks represent a significant difference among the seasons according to Kruskal-Wallis H-test from *STAMP* pipeline (Kruskal-Wallis H-test, $P < 0.05$).

and abundance is summarized in **Supplementary Table 2**. Results showed that pH (Explains = 22.0%, F = 5.1, $P = 0.016$), TOC (Explains = 18.5%, F = 4.1, $P = 0.02$), and TP (Explains = 17.8%, F = 3.9, $P = 0.018$) were of significant impact. Among the three factors, pH was found to be the overall most impactful factor on microbial composition and abundance (Explains = 22.0%, F = 5.1, $P = 0.016$), as shown in **Supplementary Table 3**.

Dominant Class-Sediment Properties RDA

As shown in **Figure 6B**, the two RDA axes explained 56.06% (51.47% and 4.59% for axes 1 and 2, respectively) of the variation.

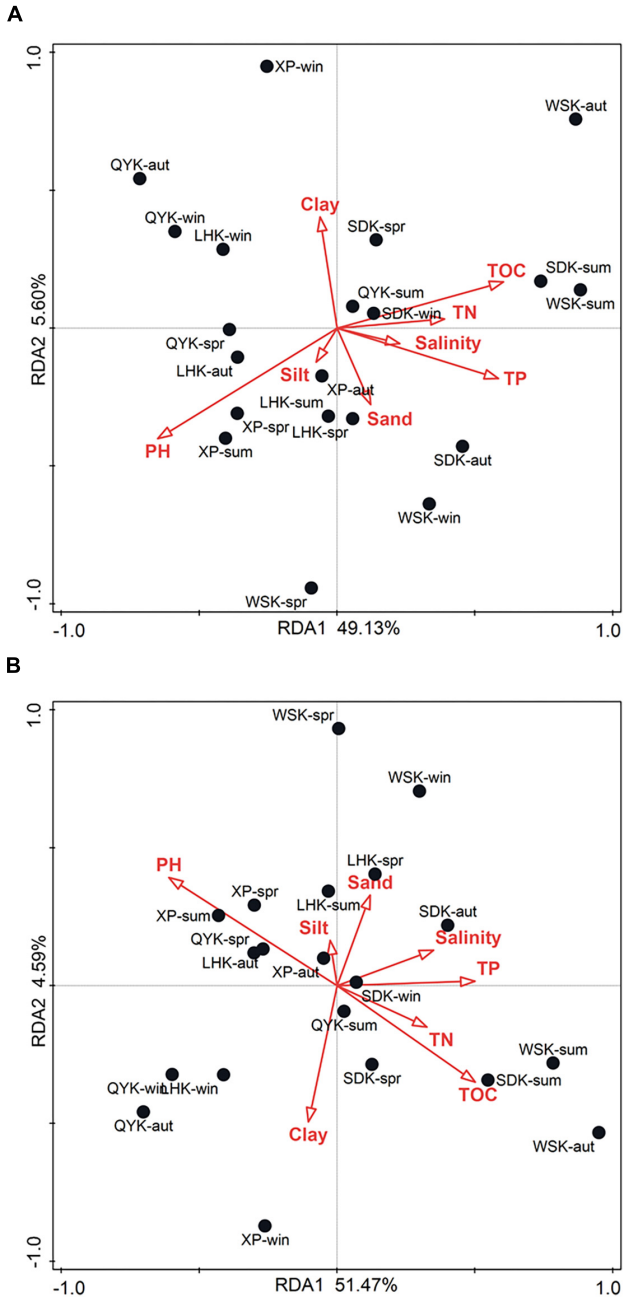

FIGURE 6 | Redundancy analysis (RDA) ordination plot of the composition and abundance of dominant bacterial **(A)** phyla and **(B)** classes in intertidal sediments of Yangtze River estuary, in relation to physicochemical properties of sediments.

Physicochemical properties of sediments explained 62.4% of the variation in microbial composition. The contribution of individual properties toward variation in microbial composition and abundance is summarized in **Supplementary Table 4**. Similarly, results showed that pH (Explains = 20.1%, F = 4.5, P = 0.024), TOC (Explains = 14.2%, F = 3.0, P = 0.0.04), and TP (Explains = 14.2%, F = 3.0, P = 0.042) were of significant impact. Among the three factors, pH was also determined the overall most impactful factor on microbial composition and abundance (Explains = 20.1%, F = 4.5, P = 0.028), as shown in **Supplementary Table 5**.

Relationship Between Microbial Community Ecological Functions and the Environment

The ecological functions of microbial communities were annotated using FAPROTAX. From the results, approximately 20% (15217) of the total sequence records (75719) were assigned with 82 ecological functions, contributing to a variety of biogeochemical processes. As shown in **Figure 7A**, the major ecological functions contributed by microbial communities, in descending order of relative contribution, were chemoheterotrophy, aerobic chemoheterotrophy, respiration of sulfur compounds, sulfate respiration, nitrification, aerobic nitrite oxidation, nitrate reduction, nitrate respiration, chlorate reducers, and fermentation.

The major ecological functions of microbial communities in studied sampling sites included both aerobic processes, such as aerobic chemoheterotrophy, and anaerobic processes, such as sulfate respiration. PCA was conducted to investigate the temporal variation in ecological functions contributed by microbial communities among all the sampling sites. Results revealed that the ten major ecological functions contributed by microbial communities show no temporal differences (**Figure 7B**; Kruskal-Wallis H-test). Only nine of the 82 ecological functions assigned showed differences with changing seasons, of which only two ecological functions had an average contribution above 1% (Animal parasites or symbionts, 1.85%; Human pathogens all, 1.57%).

DISCUSSION

The present study characterized intertidal sediments from the Yangtze River estuary and evaluated the effects of temporal variation on inhabiting microbial communities. Nutrient concentrations in sediments as well as α- and β-diversity of microbial communities showed some notable variation which may be attributed to seasonal differences, with summer conditions being reportedly least favorable for microbial diversity. The Summer season was reported with the lowest pH levels, and pH correlated positively with microbial community richness. At the phylum level, relative abundances of the dominant *Proteobacteria* did not show significant temporal variation. Instead, abundance of *Actinobacteria*, *Chloroflexi,* and *Verrucomicrobia* were reported to differ more significantly, favoring the wet seasons. Most of these phylum-level changes can be associated with similar patterns observed for a major subdivision at the class-level, such as *Anaerolineae* and *Verrucomicrobiae*. Notably, *Deltaproteobacteria*, a class known for containing most of the sulfate/sulfur-reducing bacteria, showed a significant difference in relative abundance between Spring and Winter, favoring Winter. Upon further investigation, sulfur-reducing bacteria at the genus level were also found to

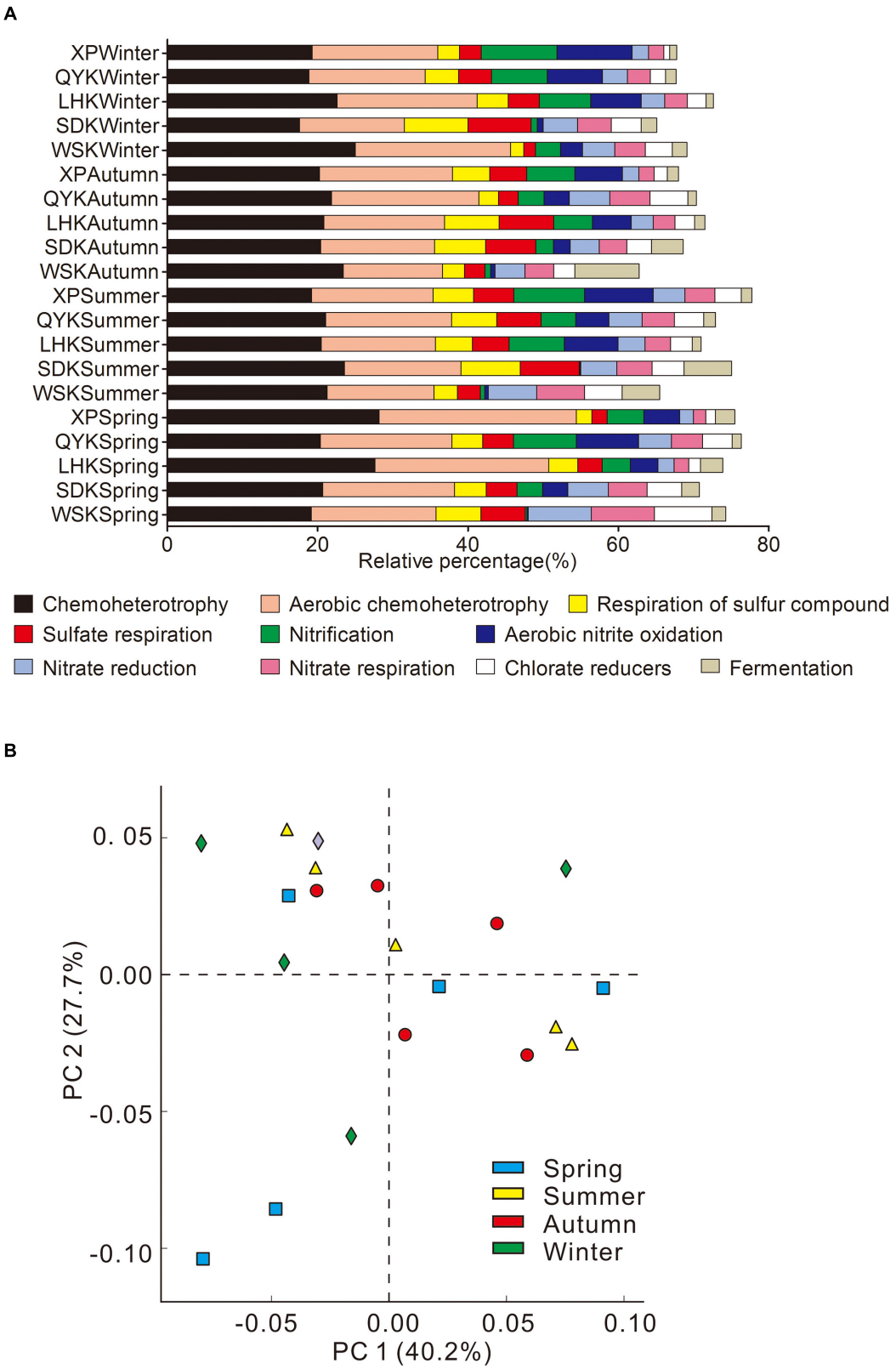

FIGURE 7 | Summary of major ecological functions **(A)** and principal component analysis (PCA) of ecological functions **(B)** contributed by microbial communities in the intertidal sediments of Yangtze River estuary, among different seasons (Kruskal-Wallis H-test).

favor Autumn and Winter, hence the dry seasons. However, such difference in sediment conditions, microbial diversity, and relative abundance did not translate to corresponding ecological functions showing significant temporal changes. Non-etheless, patterns recorded in the present study should not be overlooked. The composition of microbial communities was found to correlate with pH, TOC, and TP of the environment, but rainfall is proposed to be another important factor to consider, as discussed in the following sections.

Precipitation May Determine Patterns in Microbial Community Diversity

Summer seasons of the subtropical monsoon climate zone is characterized by high precipitation. Rainfall and subsequent run-off can be expected to erode and carry surface sediments, exposing sedimentary microbial community to further environmental perturbation. In this study, microbial communities sampled during the Summer season were reportedly of lower richness, despite having no significant difference in sediment physicochemical properties from succeeding seasons. Hence, it is suspected that the summer rainfall may be an unaccounted factor imposing an impact on microbial community diversity. However, throughout the year, species richness and diversity of sampled communities remained to be positively correlated. This meant that differences in microbial community structures were minor; for Yangtze River estuary, overall microbial diversity has displayed a degree of stability. The Summer season may have limited microbial species richness but did not fundamentally impact the community structures observed, reflecting the community's ability to adapt to changes in the environment (Shade et al., 2012).

In terms of β-diversity of microbial communities, clustering was observed for samples within the same season. The observation was much more distinct between dry and wet seasons, which may be further evidence supporting precipitation as an important factor (**Figure 2**). With global warming being an imminent issue, it is expected that rate of hydrological cycles will be enhanced, affecting precipitation on a global scale (Park et al., 2016). Previous study by Ren et al. (2018) showed that a reduction in precipitation had no effect on the formation of microbial community. However, this reduction lowered the total sedimentary biomass and bacterial abundance; total organic carbon and respiration rate were also affected by the reduced rainfall, and the two observations were positively correlated (Ren et al., 2018). A lack of rainfall can lead to lowered available water in soil, preventing carbon and nitrogen to be effectively utilized by microbial community and ultimately lowering the biomass (Schrama and Bardgett, 2016). However, some bacterial taxa within microbial communities can withstand the pressure imposed from a loss of water, such as Gram-positive bacteria and *Actinobacteria*, so the realistic impact on biomass and composition in the field environment may vary. In this study, microbial community diversity under conditions of high precipitation showed decreasing trends, and vice versa. An explanation for this is suggested to be the increase in precipitation causing lowered sediment pH, frequent runoffs, and constant changes in surface sedimentary conditions, which may be costly for the overall proliferation of microbial communities. Furthermore, as tides carry nutrients into intertidal sediments, there is no obvious lack in sediment carbon or nitrogen, even in dry seasons, which mitigates the possibility of a loss in biomass due to nutrient deprivation. Consequently, the present findings highlighted the importance of precipitation for microbial community diversity and provided new insights toward understanding the response of microbial communities to precipitation in a complex environment.

Key Microbial Phyla in Yangtze River Intertidal Sediments

In terms of bacterial abundance, *Proteobacteria* is the most dominant and diverse phylum, consisting of bacterial taxa which play important ecological roles in the cycling of carbon, nitrogen, and sulfur (Kersters et al., 2006). The metabolic functional diversity of *Proteobacteria* at lower taxonomic ranks meant that close to 40% of the microbial communities can adapt to different environmental conditions, especially in complex estuarine ecosystems. The adaptability toward oxic and anoxic environments may be an important trait for sedimentary bacteria, as oxygen levels in sediments can vary with vertical depth. In general, as vertical depth increases, sedimentary oxygen content decreases and form hypoxic layer or even anaerobic layer. In the present study, surface sediments were sampled, which should be considered the aerobic layer. Considering that all sediment samples were collected at the same vertical depth of the intertidal mudflats, oxygen content may not be a significant variable for this study. However, it is important to consider the implications that may be present. Since the relative abundance of phylum *Verrucomicrobia* showed significant differences with change in precipitation, it may be indicative of its adaptability toward the dynamic changes in oxygen. *Verrucomicrobia* (6.82%) is a dominant bacterial taxon in the Yangtze River estuary. However, very few studies on intertidal sedimentary microbial communities have reported it to be high in relative abundance (Zhang et al., 2014; Obi et al., 2016). In the study of Yu et al. (2012), *Verrucomicrobia* was reported as a major bacterial taxon (relative abundance of 0.21%). However, its relative contribution toward community abundance was only 1/192 than that of *Proteobacteria* (relative abundance of 40.5%). *Verrucomicrobia* is more commonly found in terrestrial environments and soil. Study by Bergmann et al. (2011) showed that among 181 soil samples, 180 were found to contain *Verrucomicrobia,* with its average abundance reaching 23%. Similarly, in marine environments, study showed that over 98% of the 506 collected terrestrial and marine environmental samples contained *Verrucomicrobia.* In fact, *Verrucomicrobia* was also common in marine environments with a reported average abundance of 2%, and a relative abundance of 1.4% in sediments (Freitas et al., 2012). In this study, Yangtze River estuary intertidal sediments were shown to support a rich community of *Verrucomicrobia,* with the relative abundances of *Verrucomicrobia* and its subtaxa

showing significant seasonal differences, especially between dry and wet seasons. A speculation would be precipitation causing water to carry terrestrial soil with relatively rich *Verrucomicrobia* content to move to estuarine sediments, leading to its widespread presence. The results can be important to address current gap in knowledge regarding patterns displayed by *Verrucomicrobia* in response to an ever-changing estuarine environment.

Limited Seasonal Change in Microbial Community Ecological Functions

Microbial communities in the Yangtze River estuary displayed diverse ecological functions, including aerobic chemosynthesis and nitrification, as well as anaerobic processes such as sulfate reduction and silver nitrate reduction. Previous study showed that sediments of intertidal mudflats at a depth range between 0–20 cm can be affected by periodic high tides, subsequently affecting microbial community composition and ecological functions (Zheng et al., 2016). Metabolic processes, both aerobic and anaerobic, of microbial communities in surface sediments tend to be more diverse and variable. However, in the present study, ecological function contributed by microbial communities in the field were shown to be stable and consistent, with insignificant temporal variations. For instance, the majority of sulfate/sulfur-reducing bacteria genus were recorded to favor Autumn and Winter in terms of relative abundances, yet the overall contributions by the functional group did not differ significantly, as seen for sulfate respiration (**Figure 7**). This suggests microbial communities in the Yangtze River estuary to be robust and resilient to changes in environment, instead of being vulnerable to constant perturbation. Investigating functional changes at the gene level e.g., sulfur metabolism gene *dsrA* can be beneficial for establishing a connection between bacterial community structure and corresponding ecological functions.

A notable factor that is not evaluated in the present study is the dissolved oxygen level in sediments. Periodic changes in tides is a key example of perturbation associated with temporal variation as it affects the utilization of sedimentary oxygen, which determines the composition and relative abundances of aerobes, facultative anaerobes, and anaerobes, in sedimentary microbial communities. Oxygen content and microbial community structure were implied to not follow any direct correlation according to previous study, which showed that aerobic methane-oxidizing bacteria have highest relative abundance and activity in surface sediments of depth range 2–3 cm, despite recording no oxygen content (Rahalkar et al., 2009). At slightly deeper (3–4 cm) sediments, relative abundance of methane-oxidizing bacteria remained at a noticeable level. However, methane-oxidizing activities were not recorded. This partly illustrates the historical problem of measuring oxygen content through instruments which were inaccurate and should be deemed inappropriate as a reference to distinguish aerobic and anaerobic bacterial communities. In addition, sedimentary oxygen may be under dynamic changes, meaning *in situ* measurements may not be sufficient to reflect the formation process of microbial communities under long-term selective pressure. In this study, intertidal sediment samples were collected at 5–7 cm range from surface. Although the oxygen content in sediments were not characterized, a recent study implied that intertidal sediments of 0 - 10 cm deep tend to contain a concentration of dissolved oxygen and do not form obvious oxic or anoxic layers (Wang et al., 2013). From the results of ecological functional predictions, the contributions of aerobic chemosynthesis regulated by microbial communities showed no spatial or seasonal changes. This may be evidence indicating the functional effectiveness of microbial communities under perceived perturbation.

Compared to temporal variations and potential adaptabilities displayed by the microbial communities, the significant differences in physicochemical properties resulting from different sampling sites may be more impactful for microbial communities. The heavy skew in nutrient concentrations in the SDK site made it a notable potential outlier among the five sites, suspected to be associated with input from Liuhe River. In addition, RDA had determined pH to be the most significant factor explaining the compositional differences. Although pH did not show significant spatiotemporal difference, it is possible that microbial communities were very sensitive to subtle changes. While it may be associated with anthropogenic sources, no convincing conclusion can be drawn at the current stage due to sample size at each sampling site. Spatial variation in microbial communities in estuarine ecosystems is an equally important research direction with ecological implications in human impacted areas, which can further the current understanding.

Overall, temporal variation has notable effects on intertidal sediment conditions and microbial community structure and diversity. This is thought to be related to rainfall conditions in the subtropical monsoon climate zones. At three months sampling intervals, patterns in microbial taxa were identified with respect to the environmental conditions of the intertidal sediments. Seasonality may be an explanation for the present observations but further investigations with rigorous sample collection will be required to provide confirmation. It is also shown that microbial communities and their contributions to ecological functions can be relatively robust and resilient to environmental changes. However, it should be noted that only approximately 20% of the microbial communities were functionally assigned in this study, which is an expected outcome due to limitations in analytical methods and the nature of predictive tools such as FAPROTAX. The drawback of mapping taxa inferred from short marker genes to manually constructed databases based on literature and cultured samples lies in the uncertainty with both data input and output. For 16S rRNA sequencing, results can be unclassified or identified at low specificity (e.g., to order level). Despite the relatively high taxonomic depth, the current database in use still reported 16% of the genus-level taxa to be unclassified. For output, the functional database of FAPROTAX is non-exhaustive, meaning that without frequent updates, new discoveries in the field are omitted, and assumptions have to be made. Nevertheless, the present study provided new temporal data and insights to help understand responses from microbial

communities under the changing environment of the urbanized Yangtze River estuary.

DATA AVAILABILITY STATEMENT

The datasets presented in this study can be found in online repositories. The names of the repository/repositories and accession number(s) can be found in the article/ **Supplementary Material**.

AUTHOR CONTRIBUTIONS

JY performed data curation, methodology, investigation, formal analysis, and writing – original draft. LL performed writing – original draft and writing – reviewing and editing. JC performed conceptualization, resources, supervision, funding acquisition, data curation, formal analysis, writing – original draft, and writing – reviewing and editing. All authors contributed to the article and approved the submitted version.

FUNDING

This work was supported by the Hong Kong Branch of Southern Marine Science and Engineering Guangdong Laboratory (Guangzhou) (SMSEGL20SC01).

SUPPLEMENTARY MATERIAL

The Supplementary Material for this article can be found online at: https://www.frontiersin.org/articles/10.3389/fmars.2020.585970/full#supplementary-material

REFERENCES

Aguirre, M., Abad, D., Albaina, A., Cralle, L., Goni-Urriza, M. S., Estonba, A., et al. (2017). Unraveling the environmental and anthropogenic drivers of bacterial community changes in the estuary of bilbao and its tributaries. *PLoS One* 12:e0178755. doi: 10.1371/journal.pone.0178755

Anderson, M. J. (2014). Permutational multivariate analysis of variance (PERMANOVA). *Wiley Statsref: Stat. Ref. Online* 1–15. doi: 10.1002/9781118445112.stat07841

Barka, E. A., Vatsa, P., Sanchez, L., Gaveau-Vaillant, N., Jacquard, C., Klenk, H. P., et al. (2016). Taxonomy, physiology, and natural products of Actinobacteria. *Microbiol. Mol. Biol. Rev.* 80, 1–43. doi: 10.1128/mmbr.00019-15

Bergmann, G. T., Bates, S. T., Eilers, K. G., Lauber, C. L., Caporaso, J. G., Walters, W. A., et al. (2011). The under-recognized dominance of Verrucomicrobia in soil bacterial communities. *Soil Biol. Biochem.* 43, 1450–1455. doi: 10.1016/j.soilbio.2011.03.012

Bolyen, E., Rideout, J. R., Dillon, M. R., Bokulich, N. A., Abnet, C. C., Al-Ghalith, G. A., et al. (2019). Reproducible, interactive, scalable and extensible microbiome data science using QIIME 2. *Nat. Biotechnol.* 37, 852–857.

Duarte, B., Freitas, J., and Caçador, I. (2012). Sediment microbial activities and physic-chemistry as progress indicators of salt marsh restoration processes. *Ecol. Indicators* 19, 231–239. doi: 10.1016/j.ecolind.2011.07.014

Dyksma, S., Bischof, K., Fuchs, B. M., Hoffmann, K., Meier, D., Meyerdierks, A., et al. (2016). Ubiquitous *Gammaproteobacteria* dominate dark carbon fixation in coastal sediments. *ISME J.* 10, 1939–1953. doi: 10.1038/ismej.2015.257

Edgar, R. C., Haas, B. J., Clemente, J. C., Quince, C., and Knight, R. (2011). UCHIME improves sensitivity and speed of chimera detection. *Bioinformatics* 27, 2194–2200. doi: 10.1093/bioinformatics/btr381

Falkowski, P. G., Fenchel, T., and Delong, E. F. (2008). The microbial engines that drive Earth's biogeochemical cycles. *Science* 320, 1034–1039. doi: 10.1126/science.1153213

Fan, M., Lin, Y., Huo, H., Liu, Y., Zhao, L., Wang, E., et al. (2016). Microbial communities in riparian soils of a settling pond for mine drainage treatment. *Water Res.* 96, 198–207. doi: 10.1016/j.watres.2016.03.061

Freitas, S., Hatosy, S., Fuhrman, J. A., Huse, S. M., Welch, D. B. M., Sogin, M. L., et al. (2012). Global distribution and diversity of marine Verrucomicrobia. *ISME J.* 6, 1499–1505. doi: 10.1038/ismej.2012.3

Gilbert, J. A., Steele, J. A., Caporaso, J. G., Steinbrück, L., Reeder, J., Temperton, B., et al. (2012). Defining seasonal marine microbial community dynamics. *ISME J.* 6, 298–308. doi: 10.1038/ismej.2011.107

Giovannoni, S. J., and Vergin, K. L. (2012). Seasonality in ocean microbial communities. *Science* 335, 671–676. doi: 10.1126/science.1198078

Grizzetti, B., Liquete, C., Pistocchi, A., Vigiak, O., Zulian, G., Bouraoui, F., et al. (2019). Relationship between ecological condition and ecosystem services in European rivers, lakes and coastal waters. *Sci. Total Environ.* 671, 452–465. doi: 10.1016/j.scitotenv.2019.03.155

Guo, X. P., Lu, D. P., Niu, Z. S., Feng, J. N., Chen, Y. R., Tou, F. Y., et al. (2018). Bacterial community structure in response to environmental impacts in the intertidal sediments along the Yangtze Estuary. *China. Mar. Pollut. Bull.* 126, 141–149. doi: 10.1016/j.marpolbul.2017.11.003

Herlemann, D. P., Labrenz, M., Jürgens, K., Bertilsson, S., Waniek, J. J., and Andersson, A. F. (2011). Transitions in bacterial communities along the 2000 km salinity gradient of the Baltic Sea. *ISME J.* 5, 1571–1579. doi: 10.1038/ismej.2011.41

Kaestli, M., Skillington, A., Kennedy, K., Majid, M., Williams, D., McGuinness, K., et al. (2017). Spatial and temporal microbial patterns in a tropical macrotidal estuary subject to urbanization. *Front. Microbiol.* 8:1313. doi: 10.3389/fmicb.2017.01313

Kallmeyer, J., Pockalny, R., Adhikari, R. R., Smith, D. C., and D'Hondt, S. (2012). Global distribution of microbial abundance and biomass in subseafloor sediment. *Proc. Natl. Acad. Sci.* 109, 16213–16216. doi: 10.1073/pnas.1203849109

Karhu, K., Auffret, M. D., Dungait, J. A., Hopkins, D. W., Prosser, J. I., Singh, B. K., et al. (2014). Temperature sensitivity of soil respiration rates enhanced by microbial community response. *Nature* 513, 81–84. doi: 10.1038/nature13604

Kersters, K., De Vos, P., Gillis, M., Swings, J., Vandamme, P., and Stackebrandt, E. (2006). "Introduction to the *Proteobacteria*," in *The Prokaryotes: a Handbook on the Biology of Bacteria*, eds M. Dworkin, S. Falkow, E. Rosenberg, K. H. Schleifer, and E. Stackebrandt (New York, NY: Springer), 3–37.

Kindong, R., Wu, J., Gao, C., Dai, L., Tian, S., Dai, X., et al. (2020). Seasonal changes in fish diversity, density, biomass, and assemblage alongside environmental variables in the Yangtze River Estuary. *Environ. Sci. Poll. Res.* 27, 25461–25474. doi: 10.1007/s11356-020-08674-8

Kumar, A., Ng, D. H., Wu, Y., and Cao, B. (2019). Microbial community composition and putative biogeochemical functions in the sediment and water of tropical granite quarry lakes. *Microbial. Ecol.* 77, 1–11. doi: 10.1007/s00248-018-1204-2

Lan, Y., Wang, Q., Cole, J. R., and Rosen, G. L. (2012). Using the RDP classifier to predict taxonomic novelty and reduce the search space for finding novel organisms. *PLoS One* 7:e32491. doi: 10.1371/journal.pone.0032491

Liu, S. M., Zhang, J., Chen, H. T., Wu, Y., Xiong, H., and Zhang, Z. F. (2003). Nutrients in the Changjiang and its tributaries. *Biogeochemistry* 62, 1–18.

Louca, S., Parfrey, L. W., and Doebeli, M. (2016). Decoupling function and taxonomy in the global ocean microbiome. *Science* 353, 1272–1277. doi: 10.1126/science.aaf4507

Lozupone, C., and Knight, R. (2005). UniFrac: a new phylogenetic method for comparing microbial communities. *Appl. Environ. Microbiol.* 71, 8228–8235. doi: 10.1128/aem.71.12.8228-8235.2005

Murphy, R. R., Kemp, W. M., and Ball, W. P. (2011). Long-term trends in Chesapeake Bay seasonal hypoxia, stratification, and nutrient loading. *Estuaries Coasts* 34, 1293–1309. doi: 10.1007/s12237-011-9413-7

Murphy, J., and Riley, J. P. (1962). A modified single solution method for the determination of phosphate in natural waters. *Anal. Chim. Acta*, 27, 31–36. doi: 10.1016/S0003-2670(00)88444-5

Niu, Z. S., Pan, H., Guo, X. P., Lu, D. P., Feng, J. N., Chen, Y. R., et al. (2018). Sulphate-reducing bacteria (SRB) in the Yangtze Estuary sediments: abundance, distribution and implications for the bioavailibility of metals. *Sci. Total Environ.* 634, 296–304. doi: 10.1016/j.scitotenv.2018.03.345

Obi, C. C., Adebusoye, S. A., Ugoji, E. O., Ilori, M. O., Amund, O. O., and Hickey, W. J. (2016). Microbial communities in sediments of Lagos Lagoon, Nigeria: elucidation of community structure and potential impacts of contamination by municipal and industrial wastes. *Front. Microbiol.* 7:1213. doi: 10.3389/fmicb.2016.01213

Op, den Camp, H. J., Islam, T., Stott, M. B., Harhangi, H. R., Hynes, A., et al. (2009). Environmental, genomic and taxonomic perspectives on methanotrophic Verrucomicrobia. *Environ. Microbiol. Rep.* 1, 293–306. doi: 10.1111/j.1758-2229.2009.00022.x

Park, J. Y., Bader, J., and Matei, D. (2016). Anthropogenic Mediterranean warming essential driver for present and future Sahel rainfall. *Nat. Climate Change* 6, 941–945. doi: 10.1038/nclimate3065

Parks, D. H., Tyson, G. W., Hugenholtz, P., and Beiko, R. G. (2014). STAMP: statistical analysis of taxonomic and functional profiles. *Bioinformatics* 30, 3123–3124. doi: 10.1093/bioinformatics/btu494

Peterson, J. O., Morgan, C. A., Peterson, W. T., and Lorenzo, E. D. (2013). Seasonal and interannual variation in the extent of hypoxia in the northern California Current from 1998–2012. *Limnol. Oceanography* 58, 2279–2292. doi: 10.4319/lo.2013.58.6.2279

Quast, C., Pruesse, E., Yilmaz, P., Gerken, J., Schweer, T., Yarza, P., et al. (2013). The SILVA ribosomal RNA gene database project: improved data processing and web-based tools. *Nucl. Acids Res.* 41, D590–D596.

Rahalkar, M., Deutzmann, J., Schink, B., and Bussmann, I. (2009). Abundance and activity of methanotrophic bacteria in littoral and profundal sediments of Lake Constance (Germany). *Appl. Environ. Microbiol.* 75, 119–126. doi: 10.1128/aem.01350-08

Ren, C., Chen, J., Lu, X., Doughty, R., Zhao, F., Zhong, Z., et al. (2018). Responses of soil total microbial biomass and community compositions to rainfall reductions. *Soil Biol. Biochem.* 116, 4–10. doi: 10.1016/j.soilbio.2017.09.028

Rognes, T., Flouri, T., Nichols, B., Quince, C., and Mahé, F. (2016). VSEARCH: a versatile open source tool for metagenomics. *PeerJ* 4:e2584. doi: 10.7717/peerj.2584

Schrama, M., and Bardgett, R. D. (2016). Grassland invasibility varies with drought effects on soil functioning. *J. Ecol.* 104, 1250–1258. doi: 10.1111/1365-2745.12606

Shade, A., Peter, H., Allison, S. D., Baho, D., Berga, M., Bürgmann, H., et al. (2012). Fundamentals of microbial community resistance and resilience. *Front. Microbiol.* 3:417. doi: 10.3389/fmicb.2012.00417

Shen, Z. (ed.) (2020). *Studies of the Biogeochemistry of Typical Estuaries, and Bays in China*. Berlin: Springer.

Shi, J., Liu, X., Chen, Q., and Zhang, H. (2014). Spatial and seasonal distributions of estrogens and bisphenol a in the Yangtze River Estuary and the adjacent East China Sea. *Chemosphere* 111, 336–343. doi: 10.1016/j.chemosphere.2014.04.046

Suh, S. S., Park, M., Hwang, J., Kil, E. J., Jung, S. W., Lee, S., et al. (2015). Seasonal dynamics of marine microbial community in the South Sea of Korea. *PLoS One* 10:e0131633. doi: 10.1371/journal.pone.0131633

Sun, Z., Brittain, J. E., Sokolova, E., Thygesen, H., Saltveit, S. J., Rauch, S., et al. (2018). Aquatic biodiversity in sedimentation ponds receiving road runoff–What are the key drivers? *Sci. Total Environ.* 610, 1527–1535. doi: 10.1016/j.scitotenv.2017.06.080

Ter Braak, C. J., and Šmilauer, P. (2002). *CANOCO Reference Manual and CanoDraw for Windows user's guide: Software for Canonical Community Ordination (version 4.5)*. www.canoco.com

Wang, L., Liu, L., Zheng, B., Zhu, Y., and Wang, X. (2013). Analysis of the bacterial community in the two typical intertidal sediments of Bohai Bay, China by pyrosequencing. *Mar. Poll. Bull.* 72, 181–187. doi: 10.1016/j.marpolbul.2013.04.005

Wang, Y., Sheng, H. F., He, Y., Wu, J. Y., Jiang, Y. X., Tam, N. F. Y., et al. (2012). Comparison of the levels of bacterial diversity in freshwater, intertidal wetland, and marine sediments by using millions of illumina tags. *Appl. Environ. Microbiol.* 78, 8264–8271. doi: 10.1128/aem.01821-12

White, J. R., Nagarajan, N., and Pop, M. (2009). Statistical methods for detecting differentially abundant features in clinical metagenomic samples. *PLoS Comput. Biol.* 5:e1000352. doi: 10.1371/journal.pcbi.1000352

Xie, Y., Wang, J., Wu, Y., Ren, C., Song, C., Yang, J., et al. (2016). Using in situ bacterial communities to monitor contaminants in river sediments. *Environ. Poll.* 212, 348–357. doi: 10.1016/j.envpol.2016.01.031

Xu, Z., Woodhouse, J. N., Te, S. H., Gin, K. Y. H., He, Y., Xu, C., et al. (2018). Seasonal variation in the bacterial community composition of a large estuarine reservoir and response to cyanobacterial proliferation. *Chemosphere* 202, 576–585. doi: 10.1016/j.chemosphere.2018.03.037

Yu, Y., Wang, H., Liu, J., Wang, Q., Shen, T., Guo, W., et al. (2012). Shifts in microbial community function and structure along the successional gradient of coastal wetlands in Yellow River Estuary. *Eur. J. Soil Biol.* 49, 12–21. doi: 10.1016/j.ejsobi.2011.08.006

Zhang, W., Bougouffa, S., Wang, Y., Lee, O. O., Yang, J., Chan, C., et al. (2014). Toward understanding the dynamics of microbial communities in an estuarine system. *PloS One* 9:e94449. doi: 10.1371/journal.pone.0094449

Zheng, Y., Hou, L., Liu, M., Liu, Z., Li, X., Lin, X., et al. (2016). Tidal pumping facilitates dissimilatory nitrate reduction in intertidal marshes. *Sci. Rep.* 6:21338.

Conflict of Interest: The authors declare that the research was conducted in the absence of any commercial or financial relationships that could be construed as a potential conflict of interest.

frontiers in Marine Science

ORIGINAL RESEARCH
published: 25 November 2020
doi: 10.3389/fmars.2020.608244

Resource Partitioning Between Phytoplankton and Bacteria in the Coastal Baltic Sea

*Eva Sörenson, Hanna Farnelid, Elin Lindehoff and Catherine Legrand**

Department of Biology and Environmental Science, Linnaeus University Centre of Ecology and Evolution and Microbial Model Systems, Linnaeus University, Kalmar, Sweden

Eutrophication coupled to climate change disturbs the balance between competition and coexistence in microbial communities including the partitioning of organic and inorganic nutrients between phytoplankton and bacteria. Competition for inorganic nutrients has been regarded as one of the drivers affecting the productivity of the eutrophied coastal Baltic Sea. Yet, it is unknown at the molecular expression level how resources are competed for, by phytoplankton and bacteria, and what impact this competition has on the community composition. Here we use metatranscriptomics and amplicon sequencing and compare known metabolic pathways of both phytoplankton and bacteria co-occurring during a summer bloom in the archipelago of Åland in the Baltic Sea to examine phytoplankton bacteria resource partitioning. The expression of selected pathways of carbon (C), nitrogen (N), and phosphorus (P) metabolism varied over time, independently, for both phytoplankton and bacteria, indicating partitioning of the available organic and inorganic resources. This occurs regardless of eukaryotic plankton growth phase (exponential or stationary), based on expression data, and microbial community composition. Further, the availability of different nutrient resources affected the functional response by the bacteria, observed as minor compositional changes, at class level, in an otherwise taxonomically stable bacterial community. Resource partitioning and functional flexibility seem necessary in order to maintain phytoplankton-bacteria interactions at stable environmental conditions. More detailed knowledge of which organisms utilize certain nutrient species are important for more accurate projections of the fate of coastal waters.

Keywords: phytoplankton, bacteria, coastal, community, interactions, resource partitioning, eutrophication

OPEN ACCESS

Edited by:
Konstantinos Ar. Kormas, University of Thessaly, Greece

Reviewed by:
Patricia M. Glibert, University of Maryland Center for Environmental Science (UMCES), United States
Andreas Oikonomou, Institute of Oceanography, Greece

****Correspondence:***
Catherine Legrand
catherine.legrand@lnu.se

Specialty section:
This article was submitted to Aquatic Microbiology, a section of the journal Frontiers in Marine Science

Received: *19 September 2020*
Accepted: *29 October 2020*
Published: *25 November 2020*

Citation:
Sörenson E, Farnelid H, Lindehoff E and Legrand C (2020) Resource Partitioning Between Phytoplankton and Bacteria in the Coastal Baltic Sea. Front. Mar. Sci. 7:608244. doi: 10.3389/fmars.2020.608244

INTRODUCTION

Coastal marine ecosystems have a key role of filtering nutrients and pollutants coming from land, before entering the pelagic environment (Bonsdorff et al., 1997; Rabalais et al., 2009; Carstensen et al., 2019). In coastal oceans, as along the coast of the Baltic Sea, allochthonous organic matter will get incorporated into the microbial food web, which may have large consequences for the nutrient balance between phytoplankton and bacteria (Andersson et al., 2015; Diner et al., 2016). During summer, low levels of inorganic nutrients (Nausch et al., 2018; Savchuk, 2018) limits phytoplankton growth (Granéli et al., 1990; Kivi and Setäl, 1995), while high levels of organic nutrients (Nausch et al., 2018; Savchuk, 2018) are present.

Effects of global warming including increased freshwater flow and allochtonous input of dissolved nutrients are likely to aggravate the long-term consequences of eutrophication in coastal ecosystems, such as archipelagic systems common to the brackish Baltic Sea, making it a suitable study system for the impacts of these effects. The consequences may include higher phytoplankton growth, oxygen deficiency, and a transition into a less productive ecosystem (Rönnberg and Bonsdorff, 2004; Rabalais et al., 2009). A complex interplay between autotrophic and heterotrophic marine microbes will determine how the accumulation and turnover of organic matter will be affected in a future climate scenario (Andersson et al., 2015; Zhou Y. et al., 2018). An understanding of how organic and inorganic nutrients are partitioned between phytoplankton and bacteria, and the dependence of phytoplankton on bacterial remineralization, is therefore important for predictions of status and knowledge of how to manage coastal ecosystems (Heiskanen et al., 2019).

One of the ways to investigate phytoplankton and bacteria interactions is by looking for co-occurrence patterns in the natural environment (Elifantz et al., 2005; Teeling et al., 2012; Landa et al., 2016). Several studies have investigated interactions during open water phytoplankton bloom conditions, and have shown that the different growth phases of blooms cause compositional changes in the co-occurring bacterial community, with successions of different bacterial groups assigned to Alpha-, Beta-, and Gamma-proteobacteria, Flavobacteria, Cytophagia, Actinobacteria, and Firmicutes (Teeling et al., 2012; Landa et al., 2016; Sison-Mangus et al., 2016; Camarena-Gómez et al., 2018). These changes have been attributed to the succession of exudates released by phytoplankton, differing both in quality (Cottrell and Kirchman, 2000; Elifantz et al., 2005; Camarena-Gómez et al., 2018; Mühlenbruch et al., 2018) and quantity (Sarmento et al., 2016) during their lifespan (Grossart et al., 2005; Grossart and Simon, 2007; Mühlenbruch et al., 2018). This suggests that a diverse bacterial community is important for the degradation of amino acids, proteins, extracellular polysaccharides and carbohydrates released by phytoplankton. This is also seen in the taxonomical difference among bacterial groups found either free-living or particle attached (Grossart et al., 2005; Rink et al., 2007; Sapp et al., 2007; Bagatini et al., 2014). Compositional shifts are often assumed to involve functional changes (Hunt et al., 2008; Williams et al., 2012), especially for bacteria, as different taxa are attributed with different functions, e.g., being copiotroph or oligotroph (Lauro et al., 2009), or generalists or specialists (Sarmento et al., 2016). However, composition studies alone limit the conclusions about which underlying processes and functions are selected for.

Using metatranscriptomics, capturing the actively expressed mRNA pool, with the inclusion of polyA and total mRNA, both the eukaryotic and prokaryotic transcriptional repertoire of a microbial community can be investigated (Dupont et al., 2015). Metatranscriptomics provide a glimps into the possible functions within a community at the time of sampling, while amplicon sequencing, using the ribosomal gene pool (16S and 18S rRNA gene), can be used for taxonomic identification. By combining the two methods both functional and compositional characterization of a microbial community can be made (McCarren et al., 2010; Teeling et al., 2012; Gifford et al., 2013; Alexander et al., 2015), thereby allowing for analysis of the connection between taxonomy and function. Functional analyses using transcriptomic data have suggested that bacterial species may avoid competition by ecological niche formation by having preferences for different types of algal substrates (Teeling et al., 2012) and of marine dissolved organic matter (McCarren et al., 2010). Taken together, this emphasizes the importance of resource partitioning and microbial community dynamics, encompassing both phytoplankton and bacteria, in the global carbon cycle.

In this study planktonic eukaryotes (PE $<$90 μm) and bacterioplankton (BAC) of an archipelagic bay in the Baltic Sea were sampled at two timepoints during late summer, with the aim of investigating carbon and nutrient (nitrogen and phosporus) utilization and partitioning between the two groups. The PE, consisting of phytoplankton (auto- and heterotrophic flagellated forms) and ciliates, and the BAC, dominated by heterotrophic bacteria with some cyanobacteria, were characterized separately, taxonomically, through both microscopic observation and amplicon sequencing, and functionally, focusing on the transcription of genes associated with uptake and assimilation of carbon, nitrogen, and phosphorus. The combination of morphological and molecular methods for characterization of the PE allows a more accurate identification of microbes, in light of known weaknesses such as high copy numbers for some protists (Gong and Marchetti, 2019) and brittleness when fixed for others (Mironova et al., 2009). Few, if any, studies have previously characterized the functional repertoire or resource partitioning of both phytoplankton and bacteria together, in such a coastal environment dominated by photosynthetic and often mixotrophic dinoflagellates.

MATERIALS AND METHODS

Field Sampling

Surface water (top 20 cm of water column, sieved through 90 μm) was collected 5–10 m off shore in a shallow bay off Lillängö, Åland archipelago, Northern Baltic Sea (60°5.86′N 20°30.3′E) at noon, on 27 July (T1) and 10 Aug (T2) 2016 (**Supplementary Figure 1**). Surface water temperature, salinity, and pH were recorded *in situ* at both occasions. Subsamples were taken for chlorophyll a measurement, filtered onto Whatman GF/C, stored at −20°C until extraction (ethanol) and fluorometric analysis (440 nm) according to Jespersen and Christoffersen (1987). Water samples for analyses of inorganic nutrients (200 mL, 2 replicates) such as nitrate, nitrite, phosphate and silica (**Table 1**) were kept frozen and dark until spectrophotometric analysis (UV-1600, VWR) following the method of Valderrama (1995).

For DNA and RNA collection at each sampling day, 3 replicates of 1 L of seawater were prefiltered through a 90 μm mesh, followed by filtration through a 3 μm membrane filter (Versapor, 47 mm), capturing both phytoplankton and the attached (AT) bacterial fraction. Subsequently, 300 mL of each filtrate were filtered through a 0.2 μm Supor filter (47 mm), capturing the free-living (FL) bacterial fraction. Filtrations were done using a hand operated vacuum pump. All filters were

TABLE 1 | Environmental parameters at sampling site.

	T1	T2
Temp (°C)	22.5	18.7
Sal (PSU)	5.9	5.8
pH	7.89	8.44
Chl a (μg Chla L^{-1})	3.5	3
$NO_3 + NO_2$ (μM)	0.11	0.11
PO_4 (μM)	0.41	0.18
Si (μM)	28.4	41.1
Bacterial abundance (10^6 × cells/ml)	5.73 std 0.16	5.25 std 0.06

immediately placed in pre-prepared cryotubes with RNAlater (Sigma) and stored in a cooler with ice packs. Samples were then stored at −20°C until arrival in the laboratory (<30 h), where they were stored at −80°C until DNA/RNA extraction, within 7 months of sampling.

Morphological Identification and Enumeration

For phytoplankton, subsamples (50 mL) were fixed using pH neutral Lugol's solution and stored in darkness. Phytoplankton cells sedimented in Utermöhl chambers were counted at 100x magnification using an inverted microscope (Olympus CKX 41). Phytoplankton, identified according to Hällfors (2004), were grouped as planktonic eukaryotes (PE) and cyanobacteria (filamentous). Phytoplankton biomass was calculated from cell biovolume and carbon content according to Olenina et al. (2006). Bacterial abundance (BAC) was measured by flow cytometry in 1.8 mL water subsamples fixed using 200 μL formaldehyde (1.5% final concentration) stored at−20°C for transport to the laboratory, were stored at −80°C until further processing. Samples were stained with SYBR green (Life Technologies) and bacterial cells were counted using a Cube8 flow cytometer (Partec). The cytograms were analyzed using FCS Express 4 flow cytometry data analysis software.

DNA Extraction and Preparation for Sequencing

Filters were cut into 4 quarters, of which one quarter was used for DNA extraction and the remaining 3 for RNA extraction. DNA was extracted using a phenol:chloroform protocol according to Boström et al. (2004). The V3-V4 region of the 16S rRNA gene was amplified, from both the AT and the FL size fractions, using primers 341F (CCTACGGGNGGCWGCAG) and 805R (GACTACHVGGGTATCTAATCC), and the V4-V5-region of the 18S rRNA gene was amplified, from the AT size fraction, using primers 574*F (CGGTAAYTCCAGCTCYV) and 1132R (CCGTCAATTHCTTYAART). Primers were connected to Illumina adapters, in accordance with Herlemann et al. (2011) and Hugerth et al. (2014). The PCR protocol used for 16S rRNA gene amplification was: (1x[98°C, 30 s], 28x[98°C, 10 s, 54°C, 30 s, 72°C, 15 s], 1x[72°C, 2 min]), modified from Bunse et al. (2016) and the protocol used for 18S rRNA gene amplification was: (1x[98°C, 30 s], 28x [98°C, 20 s, 50.4°C, 20 s, 72°C, 15 s], 1x [72°C, 2 min]). In a second PCR, Illumina handles and indexes (i7 and i5) were attached to both the 16S and 18S products using: (1x[98°C, 30 s], 12x[98°C, 20 s, 62°C, 30 s, 72°C, 30 s], 1x[72°C, 2 min]), modified from Hugerth et al. (2014). Fusion Mastermix (ThermoScientific) was used for all PCRs. The PCR products were purified both after the first and the second amplification steps, using the EZNA Cycle Pure kit (Omega Bio-tek) according to the manufacturer's instructions. Products were quantified with Qubit fluorometer (Invitrogen) and quality checked with Nanodrop 2000 spectrophotometer (Thermo Fisher Scientific). Fragment sizes were validated using gel electrophoresis. This resulted in 18 samples [16S: 6xT1(3xFL, 3xAT), 6xT2(3xFL, 3xAT); 18S: 3xT1, 3xT2] in total, that were pooled at equimolar concentrations and sequenced using Illumina MiSeq v3, PE (Illumina Inc), 2 × 300 base pairs (bp), at SciLifeLab/NGI (Stockholm, Sweden).

RNA Extraction and Sequencing for Metatranscriptomes

Filters were placed in petri dishes, on ice, and cut into smaller wedges with scissors, then placed in MatrixE tubes (MPbio), along with RLT-buffer (Qiagen), TE-buffer, β-mercaptoethanol (0.1 %) and Lysozyme (0.04 mg mL^{-1}). For the BAC samples, two vectors (pTZ19R, 546 bp and pFN18A, 970 bp) (**Supplementary Material 1**) at 0.1 ng μL^{-1} each, were added at this step to be used as internal standards, according to Satinsky et al. (2013). Cells were lysed using a FastPrep-24 instrument with a QuickPrep adaptor (MPbio), 3 rounds at 6 m s^{-1} for 40 s, with 1 min on ice in between, after which the Qiagen RNeasy mini kit was used for the extraction, according to protocol. The extracted RNA was treated with DNase to remove DNA (AMBIONTurbo DNA free, Invitrogen). The 6 samples intended for the BAC metatranscriptomes (0.2–3 μm size fraction) were rRNA depleted (RiboMinus Transcription isolation kit, Invitrogen) with a RiboMinus Concentration module, followed by cDNA to aRNA protocol (MessageAmp II-Bacteria RNA amplification kit, Invitrogen). To each of the 6 DNase treated samples intended for PE metatranscriptomes (3–90 μm size fraction) 0.02 pg spike-in ERCC Mix1 (Ambion) was added before they were sent for poly-A selection, which was followed by mRNA fragmentation and synthesis of cDNA, at SciLifeLab/NGI (Stockholm, Sweden). All 12 samples were then sequenced on one lane with Illumina HiSeq 2500 High Output mode v4, PE 2 × 125 bp, at SciLifeLab (Stockholm, Sweden).

Analysis of Sequencing Data

For the 16S and 18S gene amplicons, paired end sequences were analyzed in two separate rounds through the DADA2 pipeline, version 1.4.0 (Callahan et al., 2016) (available at https://github.com/benjjneb/dada2), implemented as a package in R, version 3.4.3. After the initial quality filtering 40% of the 16S reads and 25% of the 18S remained, resulting in 11 345 unique error corrected amplicon sequence variants (ASVs) for the 16S data and 29 642 unique error corrected ASVs for the 18S data (**Supplementary Table 1**). These were taxonomically assigned using Silva-128 db (Quast et al., 2013). To analyze the libraries,

packages in R (version 3.4.1) were used, vegan (nMDS, beta-diversity) (Oksanen et al., 2008, 2019) and tidyR to sort ASVs by annotation, and ggplot2 for all plotting (Wickham, 2016).

Metatranscriptome

The PE and the BAC metatranscriptome data were handled separately but using a similar pipeline for both datasets. After the initial quality check with FASTQC (0.11.5) (Andrews, 2009), adapters were cut with cutadapt (1.13) (Martin, 2011), and ERNE mapping program (Del Fabbro et al., 2013) was used for trimming and filtering with a custom rRNA database, removing <1% of the reads, in both datasets (**Supplementary Table 2**). Reads were digitally normalized using Khmer (2.1) (Crusoe et al., 2015). Internal standards were identified and removed using blast+. Both paired and single reads were included in the assembly, made with Megahit (1.1.2) (Li et al., 2016). The reads were assigned taxonomy with RefSeq using Diamond (0.8.22) (Buchfink et al., 2015). Megan (6.10.0) (Huson et al., 2016), with SEED db (version May 2015; Overbeek et al., 2014) was used for assigning functional annotations. The raw reads were mapped to the assembly using Bowtie2 (2.3.2) (Langmead and Salzberg, 2012). Samtools (1.5) (Li et al., 2009) were used to retrieve counts (**Supplementary Table 3**). The data was analyzed using R (3.4.4) (Core, 2018).

Statistics and Internal Standards

Differential expression analyses were made for both the PE and BAC metatranscriptome data using the DESeq2 (Love et al., 2014) package in R (version 3.4.4), with the internal standards (controlGenes) in the estimateSizeFactors function to normalize counts between samples (**Supplementary Table 3**) (Beier et al., 2018). Transcriptional changes of enzymes refer to relative log2 fold changes between contrasted timepoints (including triplicates), at an adjusted $p < 0.01$, unless otherwise stated (**Supplementary Tables 5, 7**). PE transcript raw counts were normalized using transcripts per kilobase million (TPM) for relative abundance analysis (Wagner et al., 2012). Bacterial absolute counts were calculated from raw counts using the formula from Satinsky et al. (2013) and used for abundance analyses. The vegan package (Oksanen et al., 2008) was used for permanova analysis.

Data Availability

Raw amplicon and metatranscriptome sequencing reads in our study were deposited at the European Nucleotide Archive under study accession numbers ERP107850 and EPR109469, with sample accession numbers ERS2571542-ERS2571562 and ERS2572272-ERS2572283, respectively.

RESULTS

Environmental Parameters

Samples were taken during a 2-week peak in sea surface temperature (SST), general for the whole Åland archipelago, Northern Baltic Sea (**Supplementary Figure 1**), with similar, warm temperatures at both sampling occasions (**Table 1**). Salinity, Chl-a and nitrate/nitrite levels were similar, while levels of inorganic phosphate decreased from T1 to T2 along with an increase of Si, and pH (**Table 1**). The bacterial abundance was slightly lower at T2 compared to T1. In all, the environmental parameters indicated stable environmental conditions during the studied period.

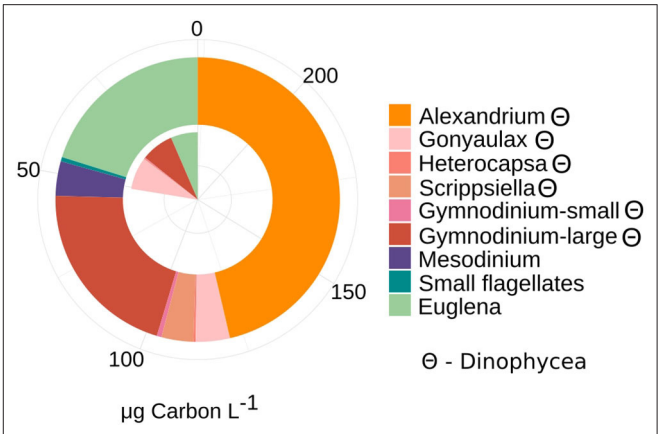

FIGURE 1 | Patterns of phytoplankton and autotrophic ciliate *Mesodinium*-like community composition (>3 µm) and contribution to total biomass (µg Carbon L^{-1}) at T1 and T2. Taxonomic composition was assessed by total microscopy counts and converted into biomass, using C conversion from cell to biomass as factors 0.17 for Cyanophycea (*filamentous*) and 0.15 for small phototrophic flagellates (Olenina et al., 2006). Carbon unit (pg C $cell^{-1}$) were calculated based on cell volume for the genera *Alexandrium* (7,723 pg C $cell^{-1}$), *Gonyaulax* (1,300 pg C $cell^{-1}$), *Heterocapsa* (160 pg C $cell^{-1}$), *Scrippsiella* (806 pg C $cell^{-1}$), *Gymnodinium* (large: 1,730, small: 51 pg C $cell^{-1}$), *Euglena* (120 pg C $cell^{-1}$), *Mesodinium* (2,630 pg C $cell^{-1}$) (Olenina et al., 2006). Θ denote taxa assigned to dinophycea (dinoflagellates). Twelve milliliter was counted in total at each date (T1 and T2).

Microbial Community Composition and Characterization of Subcommunities

Phytoplankton

The phytoplankton community consisted mostly of large dinoflagellates that contributed the most biomass (≈70%) to the phototrophic community at both sampling occasions. The planktonic eukaryotes (PE) community biomass increased 4-fold from T1 (50 µg C L^{-1}) to T2 (228 µg C L^{-1}) (**Figure 1**) while the proportion of dinoflagellates and green algae/Euglenoids (20–29%) remained stable. Among dinoflagellates, the potentially toxic *Alexandrium ostenfeldii* dominated the PE biomass (46 % of total biomass) at T2. The number of counted photosynthetic taxa increased between T1 and T2, among dinoflagellates (see list in legend of **Figure 1**) but also the filamentous nitrogen fixing cyanobacteria *(Anabaena/Dolichospermum,* 2 µg C L^{-1}), small flagellates (1 µg C L^{-1}) and the mixotrophic *Mesodinium rubrum*-like ciliate (9 µg C L^{-1}) were observed.

Analyses of the PE (18S) amplicon sequence data with nMDS, showed a distinction between the communities at T1 and T2, though not significant (permAnova $F = 5.76$, $R^2 = 0.59$, $P < 0.1$) (**Supplementary Figure 2**), while remaining at a similar diversity level [Shannon Index T1 (avg.) = 5.67, std = 0.26, T2 (avg.) = 5.87, std = 0.06] at

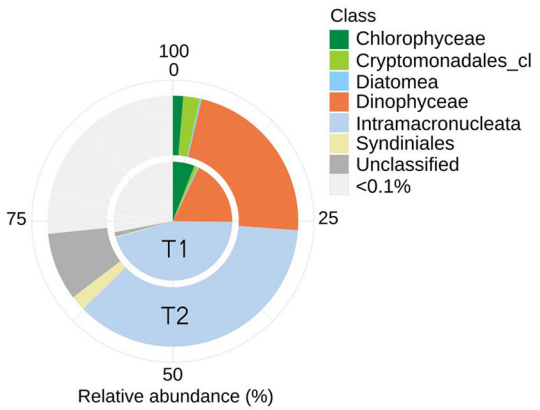

FIGURE 2 | Eukaryotic community composition (18S rRNA) including ASVs with an average (of triplicates) relative abundance >0.1% per timepoint (T1 or T2). Assigned taxonomy at class level. Intramacronucleata is a subphylum of ciliates and consists of heterotrophic species.

respective timepoint (**Supplementary Figure 2**). contrary to direct observations, the amplicon data indicate that ciliates (Intramacronucleata) was the dominating group within the PE fraction, followed by dinoflagellates (Dinophyceae) (**Figure 2**). There were also lower levels of green algae (Chlorophyceae), cryptophytes (Cryptomonadales), diatoms (Diatomea), and parasitic dinoflagellates (Syndiniales). From sampling T1 to T2, there was a change in the ASVs assigned to ciliates from 46 to 36% in relative abundance, involving heterotrophic species of the class Prostomatea (higher at T2) and the orders Oligotrichida (lower at T2) while Choreotrichida remained at similar levels (**Table 2**). ASVs assigned to the class Dinophyceae (order Gonyaulacales e.g., *Alexandrium ostenfeldii*, *Gonyaulax* sp., subclass Gymnodiniphycidae e.g., *Gymnodinium* spp., order Peridiniales e.g., *Heterocapsa triquetra*, family Thoracosphaeraceae e.g., genus *Scrippsiella*, order Suessiaceae e.g., *Symbiodinium*) increased from 18 to 22% in relative abundance at T1 and T2, respectively (**Table 2**). This was paralleled by the occurrence of green algae at T1 (*Tetracystis*-like, 4%), and a higher occurrence of mixotrophic Cryptomonadales (2%) at T2 (**Figure 2**, **Table 2**).

Bacteria

Bacterial abundance was similar (5–6 $\times$ 10^9 cells L^{-1}, **Table 1**) at both sampling occasions. Taxonomic profiles of the domain Bacteria (BAC) in both the attached fraction (AT, $>$ 3 µm) and the free-living fraction (FL, 0.2–3 µm) are visualized in **Figure 3**. Analysis with nMDS of BAC (16S) amplicon sequence data show a significant difference (permAnova F = 5.95, R^2 = 0.33, $P < 0.002^{**}$) between AT and FL (**Supplementary Figure 3**). However, within the same size fractions, no significant difference in BAC community composition was found between both sampling occasions: FL (T1 vs. T2): permAnova F = 4.72, R^2 = 0.54, $P < 0.1$; AT (T1 vs. T2): permAnova F = 4.12, R^2 = 0.51, $P < 0.1$. The FL fraction had a Shannon Index (avg.) = 6.41, std = 0.15, while AT (avg.) = 5.63, std = 0.57, indicating a higher diversity for the former (**Supplementary Figure 3**). The BAC community contained a large fraction of Actinobacteria (*Acidimicrobiiaceae, Microbacteriaceae, Sporichtyaceae*) mostly in the FL fraction, and Bacteroidetes (*Cytophagaceae*, *Flavobacteriaceae,* Sphingobacteriales), present in both the AT and the FL fractions (**Figure 3**, **Table 3**). The AT fraction was dominated by Gammaproteobacteria (*Pseudomonadacea*). Both Alpha- (*Pelagibacterales, Rhodobacteraceae*) and Betaproteobacteria (*Alcaligenaceae, Comamonadaceae)* were found in the AT and FL fractions, but they primarily occurred in the FL. There was a low occurrence of Verrucomicrobia (Opitutae) and Cyanobacteria in both size fractions (**Figure 3**, **Table 3**).

Microbial Community Functions

Metatranscriptome data from the PE and BAC parts of the community were analyzed to identify functional processes associated with uptake and assimilation of carbon, nitrogen and phosphorus, being the primary elements and nutrients utilized by both trophic levels. Differential expression (DE) analyses were made by contrasting the two timepoints (T1 and T2, in triplicates). For many of the ORFs assigned to the same functional annotation (SEED Rank1 and Rank3), the DE analysis resulted in a range of significant (padj $<$ 0.01) log2 fold change values, spanning from positive to negative [**Supplementary Tables 5** (PE), 7 (BAC)].

The taxonomic annotations of the PE metatranscriptome data did not correspond well with either the 18S rRNA gene amplicon annotations (**Supplementary Figure 4**) nor the microscopy counts at the family/genus level as only photosynthetic or potentially mixotrophic organisms were counted (**Figure 1**). Thus, no attempt was made to connect the identified PE functional processes with taxonomy. The taxonomy assigned to the BAC metatranscriptome data were more in accordance with the 16S rRNA gene amplicon results (**Supplementary Figure 5**), thus the assigned taxonomy from the BAC metatranscriptome was used together with that of the 16S rRNA gene amplicon-based annotation, to couple functional processes with taxonomy.

Carbon Utilization Pathways

Planktonic Eukaryotes (PE) expressed enzymes for uptake of both dissolved inorganic CO_2 through carbon fixation, by the expression of ribulose bisphosphate carboxylase (EC4.1.1.39) (Rubisco), and organic carbon through the uptake, degradation and biosynthesis of amino acids, by the expression of branched-chain amino acid aminotransferase (EC2.6.1.42) and branched-chain acyl-CoA dehydrogenase (EC1.3.99.12), mainly at T1 (**Figure 4A**). At T1 there was likely uptake and utilization of the sugars inositol, through the expression of inositol transport system sugar-binding protein and myo-inositol2-dehydrogenase1 (EC1.1.1.18), and maltose, by the predicted maltose transporter MalT. The rate of C-fixation is determined by the activity of Rubisco (Beer et al., 1991; MacIntyre et al., 1997), which at SEED Rank3 level per timepoint, contained ORFs with both positive and negative log2 fold change values (padj $<$ 0.01) (**Supplementary Table 5**), and the TPMs show very different levels of expression when

TABLE 2 | Taxons, at two levels, of representative PE ASVs (18S), with accession numbers for matches in GenBank with % identity.

		Repr. ASV	GenBank (%id)	Relative abundance of triplicates (%)	
				T1	T2
Intramacronucleata (subphylum)	Prostomatea (class)	seq_20	Paraspathidium_apofuscum FJ875140.1 (97)	0.31	3.88
	Oligotrichia (subclass)	seq_2	Strombidium_basimorphum FJ480419.1 (100)	39.25	17.74
	Choreotrichia (subclass)	seq_13	Cyttarocylis_acutiformis KY290316.1 (97.5)	4.17	3.83
	Haptoria (subclass)	seq_68	*Monodinium*_sp. DQ487196.1 (96.8)	0.57	1.44
	Nassophorea (class)	seq_54	Paraspathidium_apofuscum FJ875140.1 (97)	1.38	0.63
	Oligohymenophorea (class)	seq_79	Paraspathidium_apofuscum FJ875140.1 (97)	–	0.82
	Phyllopharyngea (class)	seq_339	Paraspathidium_apofuscum FJ875140.1 (97)	–	0.25
	Unclassified	seq_20	Paraspathidium_apofuscum FJ875140.1 (97)	0.40	7.12
	Total:			**46.08**	**35.71**
Dinophyceae (class)	Gonyaulacales (order)	seq_99	Amphidiniella_sedentaria LC057317.1 (93.5)	2.67	0.09
	Gymnodinium (genus)	seq_59	*Gymnodinium*_sp. KT860954.1 (100)	0.21	0.22
	Peridiniales (order)	seq_5	Heterocapsa_rotundata KY980397.1 (100)	3.71	7.60
	Suessiaceae (family)	seq_4	*Suessiaceae*_sp. LN898222.1 (100)	5.86	10.09
	Thoracospaeraceae (family)	seq_28	*Stoeckeria*_sp. HG005132.1 (99.7)	3.90	4.32
	Gymnodiniphycidae (family)	seq_59	*Gymnodinium*_sp. KT860954.1 (100)	1.48	0.05
	Unclassified	seq_179	Dissodinium_pseudolunula MK626523.1 (97.9)	0.15	0.08
	Total:			**17.98**	**22.45**
Chlorophyceae (class)	*Tetracystis* (genus)	seq_22	Tetracystis_vinatzeri MH102326.1 (97.2)	3.77	0.29
	Unclassified	seq_24	*Chlamydomonas*_sp. AB701511.2 (100)	2.14	1.04
Cryptomondales (order)	*Teleaulax* (genus)	seq_78	*Teleaulax*_sp. MF179478.1 (100)	0.18	0.98
	Unclassified	seq_52	Teleaulax_acuta LC334057.1 (100)	0.72	1.09
Diatomea (class)	*Nitzschia* (genus)	seq_119	*Nitzschia*_sp. KU179129.1 (100)	0.38	0.11
	Unclassified	seq_333	Thalassiosira_pseudonana MN080330.1 (100)	–	0.13
Syndiniales (order)	*Amoebophrya* (genus)	seq_111	*Amoebophrya*_sp. MK367927.1 (100)	0.29	1.56
	Unclassified	seq_158	*Amoebophrya*_sp. MK368189.1 (100)	–	0.37

Average relative abundance (in triplicates) of ASVs (>0.1% relative abundance) per timepoint. Totals provide sums of relative abundances for the two dominating taxonomic groups (Intramacronucleata and Dinophyceae).

comparing the replicates at each timepoints (**Figure 4A**). The expression analysis suggest that the rate of C-fixation was likely accelerated at T1 by the expression of carbonic anhydrase (EC4.2.1.1) (padj < 0.01) (**Figure 4A**). Expression levels of enzymes involved in glycolysis (NAD- and NADPH-dependent glyceraldehyde-3-phosphatedehydrogenase) (EC1.2.1.12,

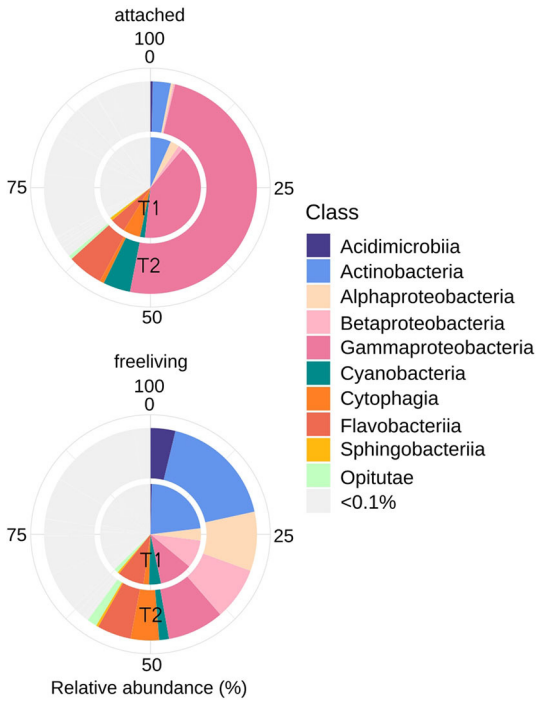

FIGURE 3 | Bacterial community composition (16S rRNA) including ASVs with an average (of triplicates) relative abundance >0.1% per timepoint (T1 or T2). Assigned taxonomy at class level.

EC1.2.1.13) (padj < 0.01) and the pentose phosphate pathway [Fructose-bisphosphate aldolase (EC4.1.2.13), Fructose-1,6-bisphosphatase (EC3.1.3.11)] (padj < 0.01) (assimilation of carbon), indicate lower activity at T2 (**Figure 4A**). Also, the expression of manganese superoxide dismutase (EC1.15.1.1) (padj < 0.01) was lower at T2. Both inorganic and different organic carbon sources were utilized at a higher rate at T1 compared to T2.

At T1, the BAC community seemed to primarily utilize simpler carbon molecules (padj < 0.01), through the expression of trehalase (EC3.2.1.28) (Bacteroidetes), for the conversion of disaccharide trehalose into glucose; expression of high affinity ABC-transporter of monosaccharide xylose, XylF (Actinobacteria and Alphaproteobacteria), and expression of sucrosephosphorylase (EC2.4.1.7) (Actinobacteria, Betaproteobacteria, and Bacteroidetes), for uptake of disaccharide maltose (**Figures 4B**, **7A**). At T2 the BAC mainly expressed (padj < 0.01) 6-phosphofructokinase (EC2.7.1.11) (Actinobacteria, Alpha- and Beta-proteobacteria, Bacteroidetes), for metabolism of linear monosaccharides tagatose and galactitol; predicted high-affinity ABC-transporter of the polyol erythritol (Alphaproteobacteria); myo-inositol-2-dehydrogenase (EC1.1.1.18) (Bacteroidetes and Gammaproteobacteria), for utilization of the polyol inositol; sucrose-6-phosphatehydrolase (EC3.2.1.B3) (Actinobacteria and Bacteroidetes), for metabolism of fructo-oligosaccharides and raffinose; and chitinase (EC3.2.1.14) (Bacteroidetes and other/unclassified), for utilization of high molecular weight chitin and its derivative acetyl glucosamine (**Figures 4B**, **7A**). There was also higher expression of phospholipid-lipopolysaccharide ABC transporter (padj < 0.06) (Bacteroidetes and Cyanobacteria) and branched-chain amino acid transport permease protein LivM (TC3.A.1.4.1) (padj < 0.01) (Alpha-, Beta-, and Gamma-proteobacteria, Actinobacteria) at T1, compared to T2 (**Figures 4B**, **7A**), for the possible uptake of alternative carbon sources.

The assimilation of carbon within the BAC community was significantly different at the two timepoints (padj < 0.01). At T1 both gluconeogenesis [fructose-1,6-bisphosphatase GlpX-type (EC3.1.3.11), fructose-bisphosphate aldolase class I & II (EC4.1.2.13) and phosphoglycerate kinase (EC2.7.2.3)] and the glyoxylate bypass (Malatesynthase G, EC2.3.3.9) were higher expressed than at T2, together accommodating for the use of other carbon sources than glucose, such as lipids and amino acids (**Figure 4C**). Also, the TCA-cycle [Malatedehydrogenase (EC1.1.1.37)], succinate dehydrogenase flavoprotein (EC1.3.99.1) and aconitatehydratase (EC4.2.1.3) was expressed at a higher level at T1 than at T2 (padj < 0.01) (**Figure 4C**). These processed were all seen in Actinobacteria, Alpha-, Beta-, and Gamma-proteobacteria, and Bacteroidetes to varying extents, while Cyanobacteria were only assigned to phosphoglycerate kinase and Acidimicrobiia to malatedehydrogenase (**Figure 7B**). The more complex molecules taken up at T2 seem to be channeled partly through the pentose phosphate pathway [6-phosphofructokinase (EC2.7.1.11), Ribose-phosphatepyrophosphokinase (EC2.7.6.1)] (Acidimicrobiia, Actinobacteria, Alpha-, Beta-, and Gamma-proteobacteria, and Bacteroidetes) followed by pyruvate metabolism: Aldehydedehydrogenase (EC1.2.1.3) and Pyruvatekinase (EC2.7.1.40), assigned to Actinobacteria, Alpha-, Beta-, and Gamma-proteobacteria, Cyanobacteria, and Bacteroidetes; L-lactatedehydrogenase (EC1.1.2.3) and lactoylglutathionelyase (EC4.4.1.5), assigned to primarily Alpha- and Beta-proteobacteria; Pyruvate dehydrogenase (EC1.2.4.1), subunits alpha and beta, assigned to primarily Bacteroidetes, Alphaproteobacteria, Cyanobacteria, and Actinobacteria. Both the pentose phosphate pathway and pyruvate metabolism associated enzymes were expressed at similar or slightly higher levels at T2 compared to T1 (padj < 0.01) (**Figures 4C**, **7B**).

Nitrogen Acquisition

The PE expressed high levels of inorganic nitrogen transporters (padj < 0.01), for high-affinity uptake of ammonium (Ammonium transporter, Amt), methylammonium permease and nitrate/nitrite (Nrt) (**Figure 5A**). The expression of Amt and Nrt was higher at T1 than at T2, while methylammonium permease was higher at T2. Nitrogen assimilation was lower at T2 (padj < 0.01), and occurred via the activity of nitrite reductase (EC1.7.1.4), allantoicase (EC3.5.3.4), the urea cycle [acetylornithine aminotransferase (EC2.6.1.11) and argininosuccinate synthase (EC6.3.4.5)], biosynthesis of arginine and glutamine synthetase type II (EC6.3.1.2) (located in chloroplast) and type III (EC6.3.1.2) [located in mitochondrion (Siaut et al., 2007)] with the ability to assimilate NO_3^- (Takabayashi et al., 2005) or NH_4^+ (Glibert

TABLE 3 | Taxons, at class and family level, of representative BAC ASVs (16S), with accession numbers for matches in GenBank with % identity.

Class	Family	Repr. ASV	GenBank (%id)	Relative abundance of triplicates (%)			
				AT		FL	
				T1	T2	T1	T2
Actinobacteria	*Acidimicrobiaceae*	seq_81	Actinobacterium HQ663610.1 (99.8)	–	0.34	0.43	3.77
	Microbacteriaceae	seq_12	*Candidatus_Aquiluna_rubra* AM999977.1 (99.5)	6.61	2.07	20.84	8.27
	Sporichthyaceae	seq_35	Actinobacterium HQ663229.1 (94.7)	–	0.63	1.76	9.22
Flavobacteriia	*Flavobacteriaceae*	seq_23	Flavobacterium HQ836451.1 (99.6)	3.04	4.63	7.07	3.96
	Cryomorphaceae	seq_58	*Cryomorphaceae* KM279028.1 (94.2)	1.81	0.76	1.43	1.20
Cytophagia	*Cytophagaceae*	seq_101	*Arcicella* AM988939.1 (99.3)	5.44	–	0.77	–
	Cyclobacteriaceae	*seq_28*	*Algoriphagus_BAL317 KM586916.1 (99.6)*	0.08	0.66	1.02	4.32
Sphingobacteriia	*NS11-12_marine_group*	seq_80	Uncultured_Sphingobacteriales MF042627.1 (99.8)	0.90	–	0.57	0.31
Gammaproteobacteria	*Pseudomonadaceae*	seq_1seq_3	Pseudomonas MH018904.1 (99.6)	40.45	47.68	9.86	7.06
	Other/Unclassified			0.27	1.68	0.75	1.54
Alphaproteobacteria	*Chesapeake-Delaware_Bay*	seq_18	Pelagibacterales MK603696.1 (99.3)	0.03	0.39	1.40	6.97
	Rhodobacteraceae	seq_79	Rhodobacter KT720393.1 (99.1)	2.81	–	2.50	0.75
	Other/Unclassified			0.01	–	–	1.28
Betaproteobacteria	*Comamonadaceae*	Seq_43seq_27	*Betaproteobacterium_BAL58* AY317112.1 (99.6) Hydrogenophaga AM110076.2 (99.3)	1.57	0.17	8.51	6.21
	Alcaligenaceae	seq_104	Burkholderiales KU382376.1 (99.6)	–	0.09	0.51	1.61
Opitutae	*Unclassified*	seq_39	Verrucomicrobia HQ663618.1 (98.3)	0.21	0.58	1.38	1.50
Cyanobacteria	*Family I*	seq_77	*Aphanizomenon_flos-aquae* AJ630442.1 (99.5)	1.58	4.13	3.81	1.48

Average relative abundance (in triplicates) of ASVs (>0.1% relative abundance) per timepoint and size fractions: FL (freeliving, 0.2–3 μm), AT (attached, 3–90 μm).

et al., 2016), respectively (**Figure 5A**). Expressed were also enzymes involved in the decomposition of cyanate [Cyanate hydratase (EC4.2.1.104)], as a possible source of nitrogen, at both timepoints, albeit lower at T2 (padj < 0.01) (**Figure 5A**).

The BAC expression pattern of enzymes associated with nitrogen uptake and assimilation suggest that different strategies dominated the two timepoints (**Figure 5B**). Initially, at T1, nitrogen was derived from degradation of nucleotides (purines), via the highly expressed allantoicase (EC3.5.3.4) (Pomati et al., 2001) (padj < 0.01) (Gammaproteobacteria) (**Figure 7B**). There was also expression of nitric oxide reductase (NorQ) (Other/Unclassified), and manganese superoxide dismutase (EC1.15.1.1) (Bacteroidetes, Cyanobacteria) (padj < 0.01) (**Figures 5B**, **7A**), which both are involved in detoxification of NO, an intermediate from denitrification, resulting in nitrous oxide (N_2O) or hydrogen peroxide (H_2O_2), respectively. In comparison, at T2 there was higher expression of high-affinity ammonium transporters (Amt) (padj < 0.01) (Actinobacteria, Alpha- and Beta-proteobacteria) together with lower expression of high-affinity ABC-transporters of urea (padj < 0.053) (Actinobacteria and Alphaproteobacteria) and the N-rich amino acid histidine (HisPQ) (TC3.A.1.3.1) (padj < 0.013) (Betaproteobacteria) (**Figures 5B**, **7A**). Expression of both urea cycle and arginine biosynthesis related compounds [Ornithinecarbamoyltransferase (EC2.1.3.3), Argininosuccinatelyase (EC4.3.2.1), Argininosuccinatesynthase (EC6.3.4.5), Arginase (EC3.5.3.1)] were higher at T2 than at T1 (padj < 0.01) (Actinobacteria, Alpha- and Beta-proteobacteria, Bacteroidetes, and Cyanobacteria) (**Figures 5B**, **7A**). The

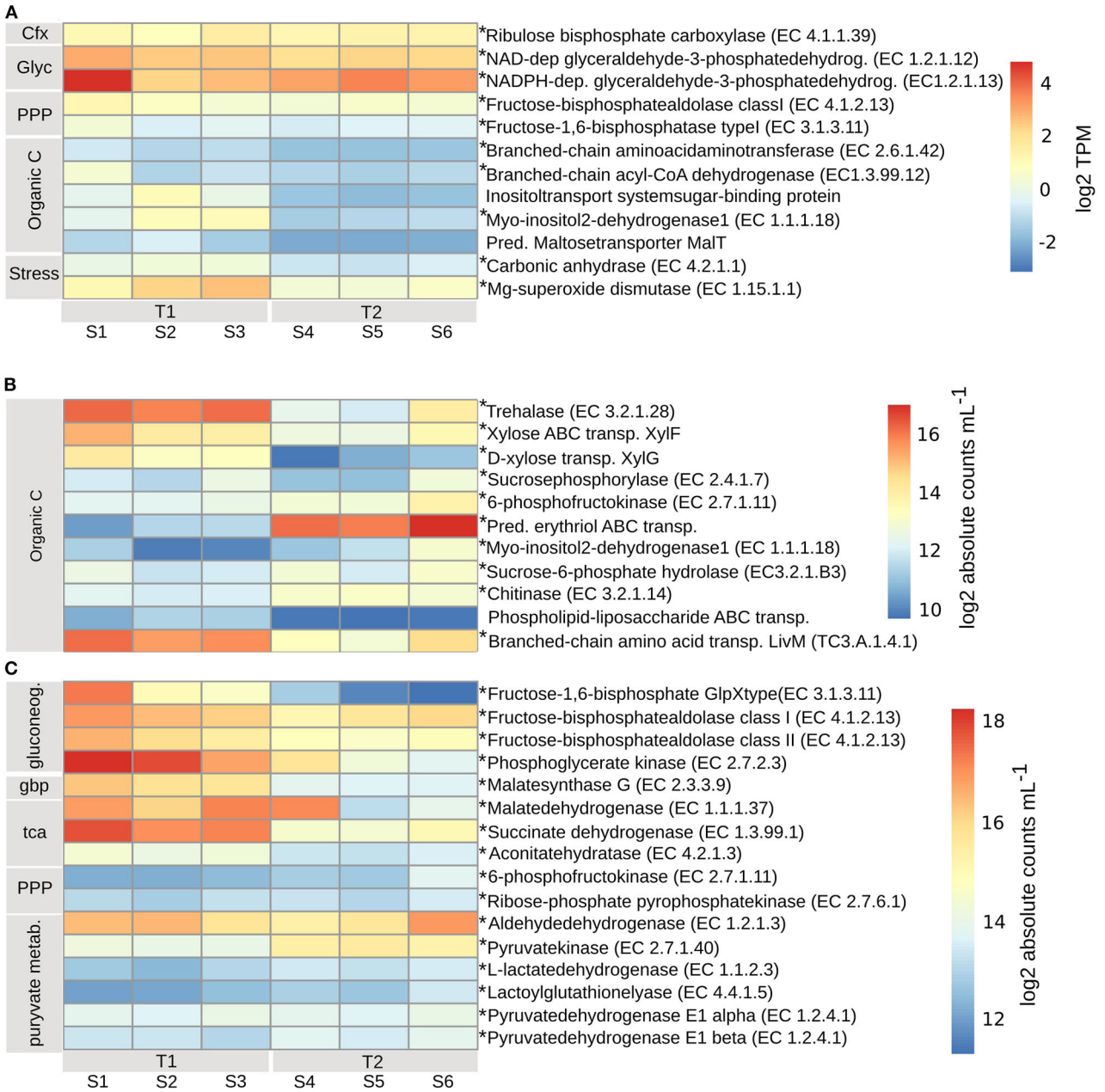

FIGURE 4 | Transcripts involved in inorganic and organic carbon uptake and assimilation for **(A)** planktonic eukaryotes (PE), transcripts per kilobase million (TPM) (grouped by SEED Rank3) log2 transformed. TPM values with standard errors (SE) can be found in **Supplementary Table 4**. **(B)** bacterial (BAC) carbon uptake and utilization, **(C)** carbon cycling. Bacterial absolute transcript counts per mL (grouped by SEED Rank3), calculated according to formula in Satinsky et al. (2013) can be found in **Supplementary Table 6**. To account for transcript length, counts were normalized to one mRNA standard at a time: pTZ19R (546nt), pFN19R (970nt) from which the mean was calculated (Beier et al., 2018), and then log2 transformed. Bacterial absolute transcript counts per mL (grouped by SEED Rank3), with standard errors (SE), calculated according to formula in Satinsky et al. (2013) can be found in **Supplementary Table 6**. Asterisks indicate enzymes that significantly changed from T1 to T2 (adjusted $p < 0.01$). T1, first timepoint (samples S1–S3); T2, second timepoint (samples S4–S6); *Cfx*, carbon fixation; *Glyc*, glycolysis; *PPP*, pentose phosphate pathway; *Organic C*, organic carbon; *Stress*, response to nutrient stress; *gluconeog*, gluconeogenesis; *gbp*, glyoxylate bypass; *tca*, tca cycle; *pyruvate metab*, pyruvate metabolism.

expression of glutamine synthetase (EC6.3.1.2) and NAD-specific glutamatedehydrogenase (EC1.4.1.2) was higher at T2 (padj < 0.01) (Actinobacteria, Alpha-, Beta-, and Gamma-proteobacteria, Cyanobacteria, and Bacteroidetes), along with its activator uridylyltransferase (EC2.7.7.59) (padj < 0.01) (Alpha-, Beta-, and Gamma-proteobacteria) (**Figures 5B**, **7A**), together increasing the potential for ammonium assimilation.

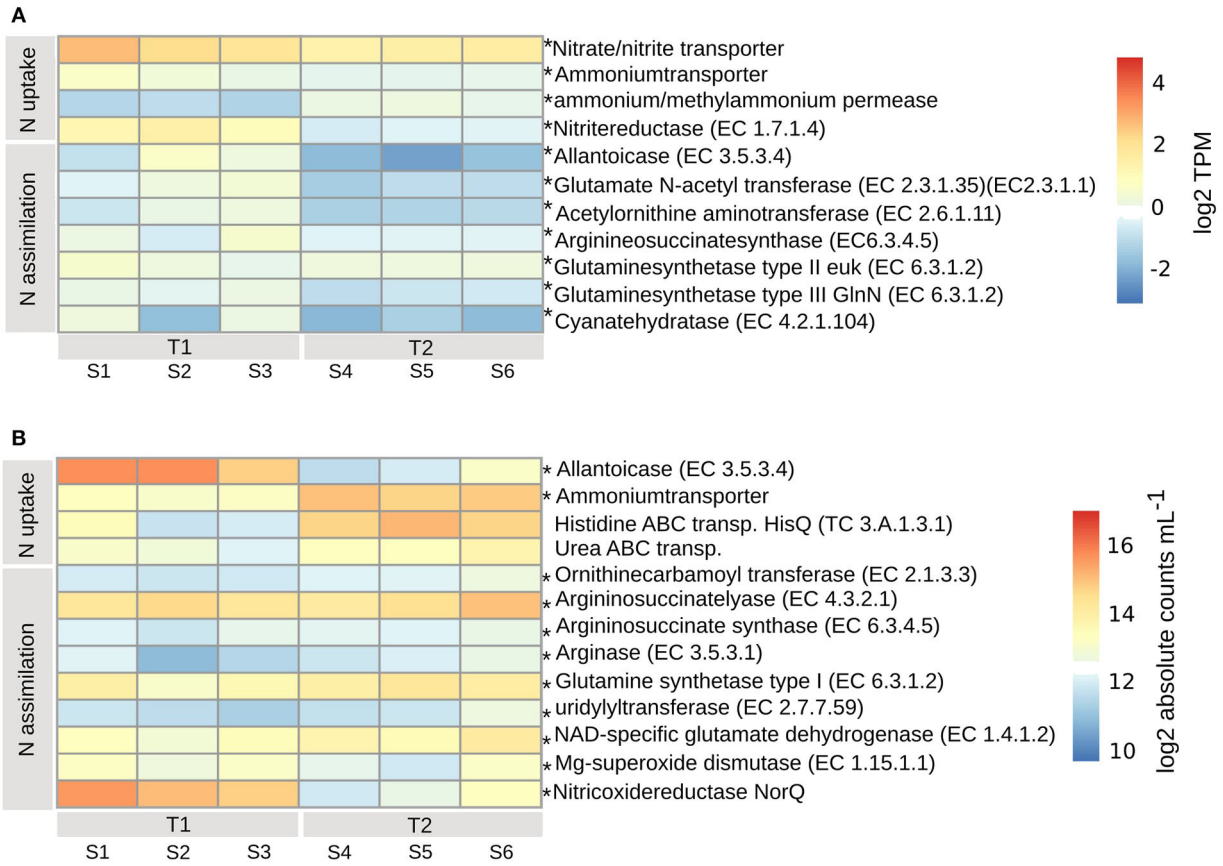

FIGURE 5 | Transcripts involved in nitrogen uptake and assimilation for PE **(A)** and BAC **(B)**, calculated according to legend in **Figure 4**. Asterisks indicate enzymes that were significantly changed from T1 to T2 (adjusted $p < 0.01$). T1, first timepoint (samples S1–S3); T2, second timepoint (samples S4–S6); *N uptake*, uptake of nitrogen; *N assimilation*, nitrogen assimilation.

Phosphorus Acquisition

The PE expressed both high and low affinity transporters for uptake of either inorganic or organic phosphorus. Expressed at both timepoints (padj < 0.01) was a probable low-affinity inorganic phosphate transporter (**Figure 6A**). The ABC transporters of less biologically available organic phosphate (TC3.A.1.7.1, PstS), phosphonate (TC3.A.1.9.1) (padj < 0.04) and oligopeptides (TC3.A.1.5.1, OppA) (padj < 0.01) were expressed at higher levels at T1 compared to T2, along with a sodium-dependent phosphate transporter (**Figure 6A**). A complementary strategy for the PE to obtain biologically available inorganic phosphorus, mainly at T1 but also at T2 (padj < 0.01), was through the expression of alkaline phosphatase (EC3.1.3.1), that transform extracellular dissolved organic phosphorus to inorganic phosphorus (Pi) for subsequent transporter mediated uptake. The likely sinks for intracellular inorganic phosphate, ubiquinone (EC7.1.1.2, EC1.6.99.3) and ATP-synthase (EC3.6.3.14), which are both part of the oxidative phosphorylation/electron transport chain, were higher in one replicate at T1, otherwise at similar or higher levels at T2, indicating a similar need for phosphorus at both timepoints (**Figure 6A**).

Among the BAC, alkaline phosphatase (EC3.1.3.1) (Actinobacteria, Alpha-, Beta-, and Gamma-proteobacteria, Cyanobacteria, and primarily Bacteroidetes) was expressed higher at T1 compared to T2 (padj < 0.01) while inorganic phosphate ABC transporter protein, PstS (TC3.A.1.7.1) (Acidimicrobiia, primarily Actinobacteria, Alpha-, Beta-, and Gamma-proteobacteria, Cyanobacteria, and Bacteroidetes), had a less distinct difference between the timepoints (padj < 0.01) (**Figures 6B**, **7A**). At T2 oligopeptide ABC-transporter proteins, OppD and F (TC3.A.1.5.1) (Beta- and Gamma-proteobacteria, other/unclassified), were both expressed higher than at T1 (padj < 0.01), indicating uptake of organic phosphate. Also, phosphonate ABC-transporters (TC3.A.1.9.1) (Alphaproteobacteria, Cyanobacteria) were higher at T2 than T1 (padj < 0.01), along with phosphate transport system regulatory protein, PhoU (Actinobacteria, Alpha-, Beta-, and Gamma-proteobacteria) (**Figures 6B**, **7A**), which is activated at low intracellular inorganic phosphate levels (Gardner et al., 2014). Both ATP-synthase (EC3.6.3.14) (Acidimicrobia, Actinobacteria, Alpha-, Beta-, and Gamma-proteobacteria, Cyanobacteria, and mainly Bacteroidetes) and ubiquinole (EC1.10.2.2) (Acidimicrobiia, Actinobacteria, Alpha-, Beta-, and

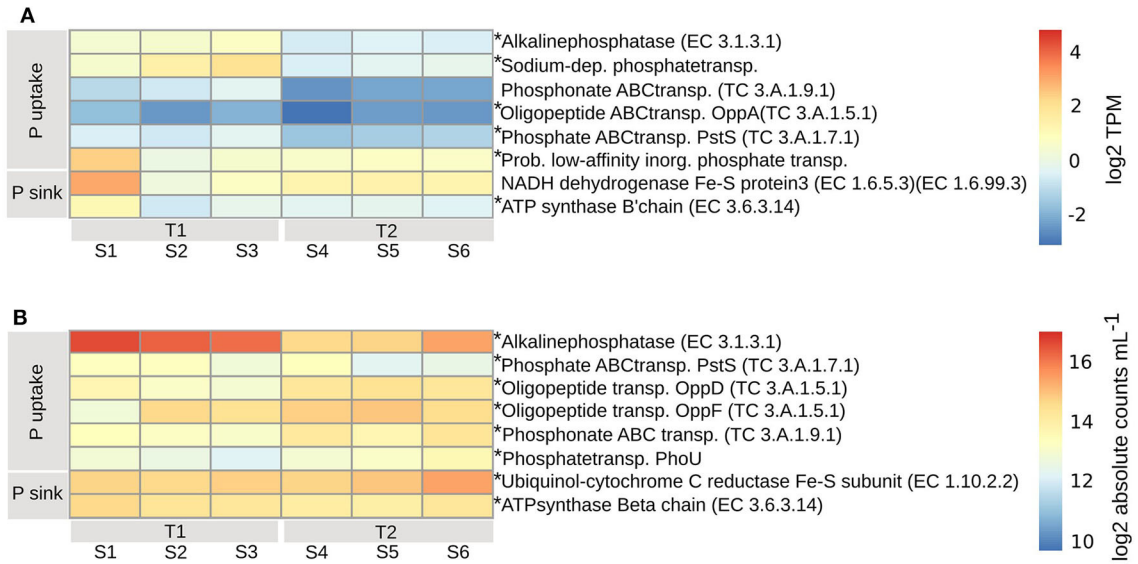

FIGURE 6 | Transcripts involved in phosphorous uptake and assimilation for PE **(A)** and BAC **(B)**, calculated according to legend in **Figure 4**. Asterisks indicate enzymes that were significantly changed from T1 to T2 (adjusted $p < 0.01$). T1, first timepoint (samples S1–S3); T2, second timepoint (samples S4–S6); *P uptake*, uptake of phosphorous; *P sink*, phosphorous utilization.

Gamma-proteobacteria) were expressed at similar levels (padj < 0.01), indicating a similar need for energy production at both timepoints (**Figures 6B**, **7A**).

DISCUSSION

In this study we show that resources (organic and inorganic forms of C, N, and P) were partitioned between planktonic eukaryotes (PE) and heterotrophic bacteria (BAC). This indicates a broad functional ability for resource acquisition and utilization within a coastal microbial community at stable environmental conditions. Our findings also reveal that changes in resource partitioning between PE and BAC does not necessarily result in large-scale taxonomic shifts in the bacterial fraction. Previously, a decoupling between function and taxonomy among bacteria has been proposed (Louca et al., 2017, 2018), suggesting that the environmental conditions select for necessary metabolic functions leading to a specific, but unpredictable, taxonomic composition of the bacterial population. Partly contradicting this, our results indicate that both environmental (nutrient conditions) and biotic (plankton species present) conditions select which bacterial taxa, with suitable metabolic functions are found at the study site. This is exemplified by that members (*Flavobacteriaceae* and *Comamonadaceae*) of the previously suggested *A. ostenfeldii* core microbiome, isolated from the brackish Baltic Sea (Sörenson et al., 2019), being the dominating dinoflagellate species among the PE, were found to be frequent among the BAC, both in the free-living and the attached fractions. Further, our findings indicate that while only minor BAC taxonomic shifts occurred, in both size fractions, during the dinoflagellate bloom (T1: exponential growth, T2: stationary phase), the expression of functions both related to resource acquisition and to metabolic pathways varied in relation to the availability of carbon, nitrogen and phosphorus. This can be seen in the conceptual model in **Figure 8**, illustrating the relevant transcripts that has been more highly expressed at either T1 or T2, or remained at similar expression levels. When compared to systems with supposed weaker biotic interactions, such as bacteria found in bromeliad cups (Louca et al., 2017), our study suggests that the interactions between PE and BAC are of importance for which plankton and bacteria are found within the community and that resource partitioning and a functional flexibility are necessary in order to maintain these interactions at stable environmental conditions, such as those seen in this coastal bay. Resource partitioning, allowing different species to coexist both temporally and spatially by the division of available resources, has previously been shown to exist among organisms within planktonic microbial communities. Hunt et al. (2008) show that within a single bacterial family there are signs of broad resource partitioning, likely dependent on nutrient utilization and season. Also, among coexisting diatom species, different inorganic and organic nitrogen and phosphorus resources have been suggested to be partitioned (Alexander et al., 2015). Previous studies have focused either on the partitioning of carbon, between primary and secondary producers on a broad scale (encompassing viruses to fish) in the Baltic Sea (Sandberg et al., 2004), and among bacteria associated with different phases of a phytoplankton bloom (Landa et al., 2016; Berg et al., 2018), or of nitrogen and phosphorus (Alexander et al., 2015).

In this field study of a natural archipelagic environment, the microbial plankton community was dominated by mainly phototrophic dinoflagellates (Gonyaulacales, Peridiniales, Suessiaceae) including mixotrophic species, and heterotrophic

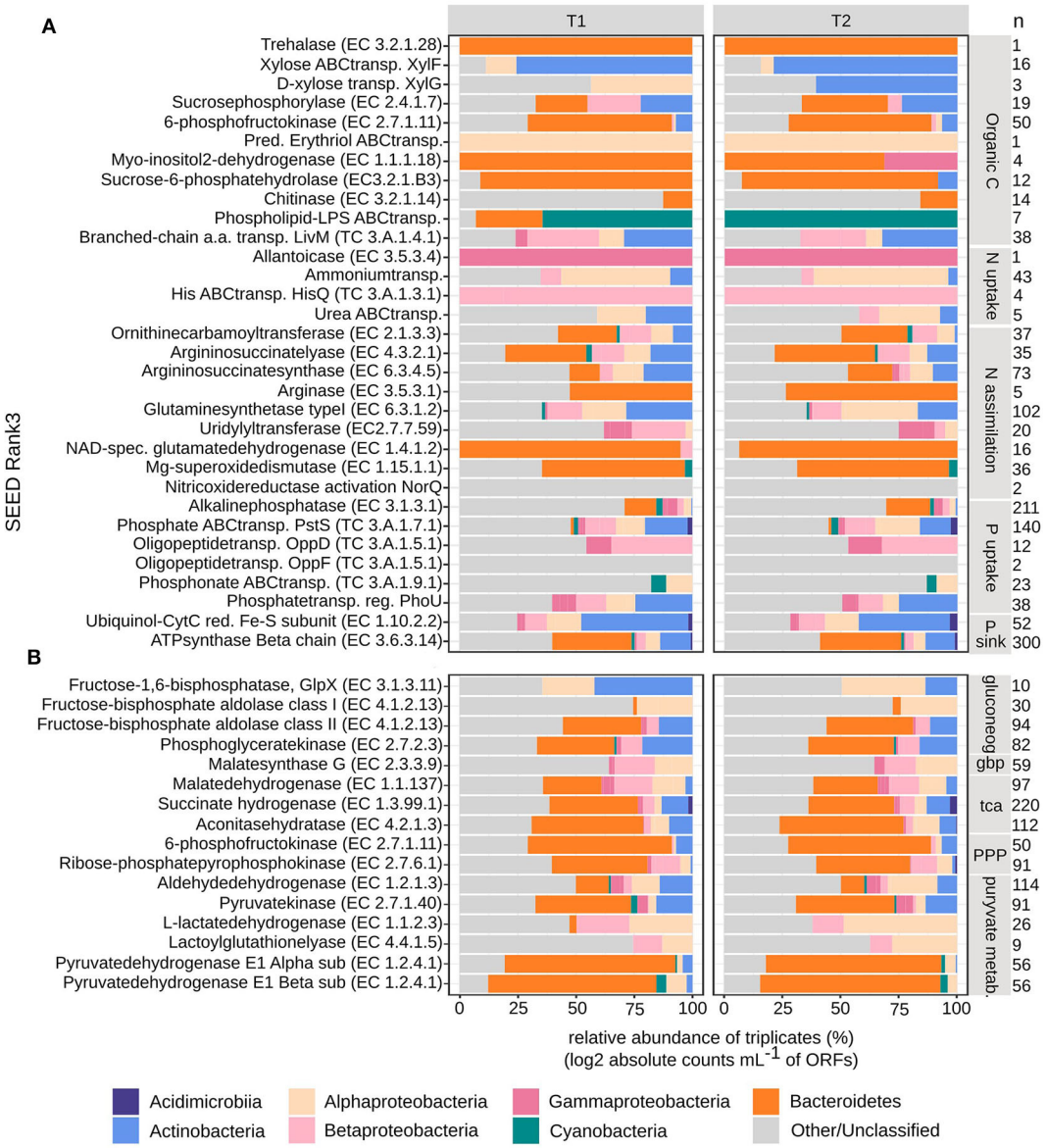

FIGURE 7 | Taxonomical distribution of bacterial metatranscriptome ORFs grouped into SEED Rank3. Absolute counts mL^{-1} were log2 transformed and then relative abundances were calculated per timepoint (T1 and T2, in triplicates). Taxonomical groups are given at phylum or class level. **(A)** Carbon, nitrogen and phosphorous uptake and assimilation, **(B)** carbon cycling, n, signify the number of ORFs per Rank3 category.

ciliates (Oligotrichia, Choreotrichia) along with primarily heterotrophic bacteria [Actinobacteria (*Microbacteriaceae, Sporichthyaceae*), Bacteroidetes (*Flavobacteriaceae, Cytophagaceae*), Proteobacteria (*Pseudomonadaceae,* Pelagibacter, and *Comamonadaceae*)], in line with taxa frequently occurring in the Baltic Sea (Johansson et al., 2004; Riemann et al., 2008; Kremp et al., 2009; Herlemann et al., 2011; Wohlrab et al., 2018). Discrepancies in phytoplankton genus/taxa composition between light microscopy observations and 18S rRNA amplicon sequencing have been reported previously (Xiao et al., 2014) and illustrate the benefit of a combined approach. In our study, the discrepancies in PE community structure between observations using microscopy (dominance of Dinophycea) and those resulting from 18S rRNA (dominated by Intramacronucleata) could depend on that sequences in public database are still insufficient for identifying diverse eukaryotic microbes (Kataoka and Kondo, 2019) and that there are large differences in copy number of the 18S rRNA gene between ciliates (high copy number) and other protists such as dinoflagellates (Gong and Marchetti, 2019). Taking this into consideration, we did not pursue a function to taxonomy analysis of the PE community based on molecular results.

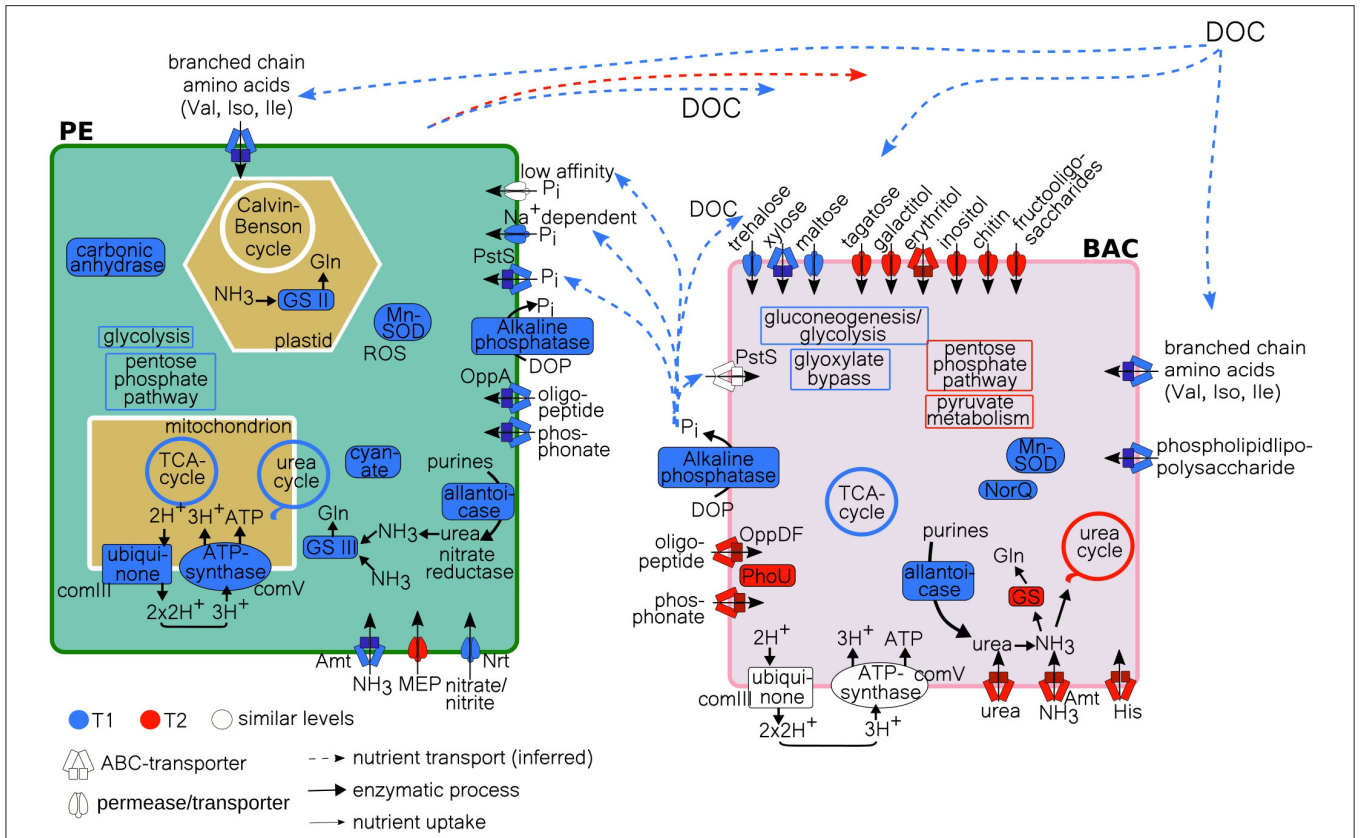

FIGURE 8 | Model of PE and BAC C, N, and P processes at T1 and T2, with inferred nutrient transport of DOC and Pi, based on metatranscriptome data analysis. Uptake/transport by either high-affinity ABC-transporters, low-affinity transporters or permeases. Processes more highly expressed at T1 (blue), at T2 (red), or at similar levels (white), according to TPM (PE) and absolute counts (BAC) (**Supplementary Tables 4, 6**). *GS,* glutamine synthetase; *MEP*, methylammonium permease; *DOC,* dissolved organic carbon (allochtonous and autochtonous); *Gln,* glutamine; *complex III and V,* of oxidative phosphorylation/electron transport chain; *Gln,* glycine; *Val,* valine; *Leu,* leucine; *Ile,* isoleucine; *His,* histidine; *ROS,* reactive oxygen species; *Mn-SOD,* manganese sodium dismutase; *NorQ,* nitric oxide reductase Q; *PE*, planktonic eukaryotes; *BAC*, bacteria.

Carbon Partition

The functional analysis of the metatranscriptome indicated a partitioning in the acquisition and uptake of organic and inorganic carbon between the PE and BAC, which contribute to explaining the coexistence of both eukaryotes and prokaryotes (**Figure 8**). The microplankton PE part of the community was constituted of both phototrophic and heterotrophic taxa. Dinoflagellates were mainly phototrophic, including mixotrophic and primarily heterotrophic genera with kleptochloroplasts or algal endosymbionts (Stoecker, 1999; Gómez, 2012), while the ciliates mostly belonged to heterotrophic taxa (Johansson et al., 2004) and the mixotrophic *Mesodinium rubrum* (Lips and Lips, 2017). This explains the occurrence of both carbon fixation and assimilation of amino acids and uptake of sugars observed within this part of the community. During bloom development (T1), carbon uptake associated processes were highly expressed, indicating a larger need for both inorganic and organic carbon, suggesting a more rapidly growing community. This trend is supported by the higher expression of carbonic anhydrase at T1, known to accelerate the HCO_3^- conversion to CO_2 upon inorganic carbon limitation, caused by high levels of aerobic metabolism (Rost et al., 2006). The expression of carbonic anhydrase indicates an increased efficiency of carbon fixation leading to a reduction in oxygen production (Foyer and Harbinson, 1994). This would result in the formation of reactive oxygen species and their scavenger, manganese-superoxide dismutase. Both carbonic anhydrase and manganese-superoxide dismutase were expressed at higher levels at T1 compared to T2, an expression pattern previously seen during a dinoflagellate bloom peak (Zhuang et al., 2015). In addition, the number of 18S reads after quality filtration were lower at T1 (avg.) = 213,024, std = 15,201, compared to T2 (avg.) = 222,557, std = 3,330, pointing to a higher richness among the PE during T2, which indicate that the community had progressed through the more homogenous bloom phase (Sison-Mangus et al., 2016; Zhou J. et al., 2018). Taken together, this suggested that the PE community at T1 was sampled during an exponential growth phase while the community at T2 represents a more stationary growth phase.

In comparison, BAC had similar expression levels of uptake and assimilation of organic carbon at T1 and T2 (**Figure 4C**), indicating an actively growing community at both

timepoints. Possibly, the difference between growth phases of the phytoplankton is reflected in the variety of organic carbon sources available to the heterotrophic bacteria. During active PE growth (T1), the BAC enzymes were associated with the utilization of the monosaccharides maltose and xylose and the disaccharide trehalose, while during PE slower growth (T2) the expression levels of organic carbon utilization mechanisms encompassed mono-, di- and tri-saccharides, two polyols, of which erythritol was especially highly expressed, and chitinase. The initial bacterial uptake of simple sugars appeared to go with the uptake of lipids and amino-acids, through the expression of phospholipid-lipopolysaccharide ABC transporter and branched-chain amino acid transport permease protein LivM. These carbon sources were likely channeled through gluconeogenesis and the glyoxylate bypass, more costly pathways that allow the conversion of proteins and lipids into glucose, which had higher expression levels at T1. Concomitantly, there was also a high occurrence of transcripts of components in the tricarboxylic acid cycle (TCA), likely providing glucose for growth, via pyruvate metabolism. This implies that during PE rapid growth, the need for carbon was higher also for the BAC, leading to a functional diversification to utilize several different variants of carbon.

While the PE, containing phototrophs, mixotrophs, and heterotrophs, utilizes both inorganic and simple organic carbon sources (amino-acids and sugars), the BAC has a wider functional repertoire to acquire varied forms of organic carbon, including amino-acids and a wide range of sugars, at both timepoints. During bloom development and active PE growth, when there are indications of a higher total energy demand (T1), there are however indications that the PE and BAC possibly compete for the same types of organic carbon (sugars and amino-acids), likely derived from both allochthonous sources and phytoplankton, though the BAC primarily utilizes other sugars than the PE. Taken together, this suggest that the PE and BAC partition the available organic carbon resources, primarily during PE active growth, in order to sustain growth and avoid competition for this valuable resource.

Nitrogen and Phosphorus Partition

Nutrient conditions in the Föglö archipelago indicated inorganic nitrogen (N) limitation and low phosphate concentrations, reflecting summer conditions in the shallow coastal Baltic Sea. In these conditions, phytoplankton and bacteria have to compete for limiting nutrients (Mayali and Doucette, 2002), and coexist despite competition for essential nutrient sources. Limiting levels of inorganic nutrients promote competition between trophic levels (Tilman, 1982), and the conditions in the bay, including the presence of mixotrophic eukaryotes, suggest that nutrient-based competition between eukaryotes and prokaryotes could be expected.

During bloom development (T1), along with a high carbon demand, the actively growing PE showed a high demand for the, likely limited resource, nitrogen. The PE expressed high-affinity N transporters for the inorganic N sources ammonium and nitrate/nitrite (Morey et al., 2011). This type of expression is indicative of low nutrient availability and these transporters have previously been seen to be upregulated in N starved diatoms (Alipanah et al., 2015). Another indication of the high N demand is the expression of cyanate hydratase (**Figure 5A**), shown to be related to limited nitrogen access (Alipanah et al., 2015). This expression coincides with expression of components for reduction of nitrite and N assimilation via the urea cycle. The expression of cyanate hydratase, primarily at T1, indicates that cyanate was also utilized as an organic N source. Cyanate has previously been observed to be taken up by dinoflagellates (Hu et al., 2012; Zhuang et al., 2015). This broad repertoire for accessing both inorganic and organic N has previously been reported for a coastal dinoflagellate bloom (Zhuang et al., 2015). In our study, the N uptake coincided with the expression of glutamine synthetase, both located in plastids and mitochondria, which is important for both nitrate and ammonium assimilation (Glibert et al., 2016). Expression of glutamine synthetase indicate limiting levels of internal nitrogen, and has previously been shown to be highly expressed in dinoflagellates during N stress (Parker and Armbrust, 2005; Morey et al., 2011; Zhuang et al., 2015). During PE slow growth (bloom stationary phase, T2), lower expression levels of these N assimilation enzymes with the addition of ammonium/methylammonium permease point to a lower N demand. As the PE community diversity increases at T2, a broadening of PE functions is likely, which could lead to a wider N uptake repertoire (Cardinale et al., 2006; Ptacnik et al., 2008). Nitrogen limited conditions seem to enforce the use of many strategies by the PE to access both organic and inorganic N, at both timepoints (**Figure 8**).

Nitrogen utilization mechanisms by aquatic bacteria in N-limited conditions have been much studied (Voss et al., 2013). Recent findings highlight the diverse N utilization strategies used by microbial communities to adapt to different N conditions and the ecological importance of the urea metabolism in N-limited regimes (Li et al., 2018). Our results confirm these findings as both the PE and BAC utilize a variation of strategies to acquire N. While the bacterial N demand was similar at both timepoints, the BAC expressed different N uptake mechanisms than the PE. Early in the bloom, the enzyme allantoicase was actively expressed, meeting the N demand by the intracellular formation of urea from purines (Solomon et al., 2010), as an organic N source. This process is known to occur in cyanobacteria and belongs to purine catabolism (Pomati et al., 2001; Solomon et al., 2010). Nitric oxide reductase activation protein NorQ, along with manganese superoxide dismutase, were also expressed in parallel, which suggests that both ammonium and nitrate transporters were inhibited by nitric oxide (Glibert et al., 2016). During late bloom (T2), direct acquisition of inorganic ammonium, organic urea, and amino acid histidine prevailed in the BAC N uptake strategy, of which all represent nitrogen species frequently associated with heterotrophic bacterial nutrient uptake (Kirchman, 1994; Fouilland et al., 2007).

Altogether, these results support a clear partition of the available N resources between PE and BAC at the different PE growth phases (**Figure 8**). Where the actively growing PE preferably utilize the scarce inorganic N sources and/or organic N-cyanate to sustain their growth, while the BAC

is restricted to degrade organic purines in order to obtain nitrogen. In comparison, the PE, in a more stationary growth phase, utilize less inorganic N while the BAC switch to acquiring N from both inorganic and diverse organic extracellular resources. This illustrates how PE and BAC partition available N resources, in different ways depending on both the PE growth phase and likely the availability of different nitrogen species.

Phosphate is the preferred P substrate for photosynthetic and heterotrophic microbial growth in aquatic systems, and ambient phosphate concentrations were relatively high in the Föglö archipelago compared to the offshore Baltic Sea during summer (Savchuk, 2018). The rapid uptake of phosphate by phytoplankton, and to a minor extent by large macrophytes (e.g., *Phragmites* in this study) in the coastal zone, the subsequent production of dissolved organic phosphorus (DOP), and the P uptake (adsorption) by organic matter regulate the P availability for the microbial community (White and Dyhrman, 2013). At low phosphate levels, eukaryotic phytoplankton and heterotrophic bacteria can efficiently scavenge P from DOP through hydrolysis using alkaline phosphatase (AP) enzymes, which has been observed both in the coastal Baltic Sea and elsewhere (Chróst, 1991; Tanaka et al., 2006; Traving et al., 2017). Though, during bloom development (T1) in Föglö, high levels of AP were expressed among both BAC and in PE, suggesting limiting levels of internal Pi despite relatively high external Pi (PO_4) levels ($>0.2\,\mu M$). This could be reflecting high carbon and nitrogen turn-over (Baltar et al., 2016) in the coastal bay, rich in dissolved organic matter (DOM). Alternatively, as dissolved organic carbon (DOC) has a contributory effect on microbial AP response (Stewart et al., 1982), the release of simple sugars during PE active growth may trigger higher expression of AP among BAC (Anderson, 2018). Whether it is to alleviate bacterial P limitation or to satisfy BAC organic C demand is unclear. Dinoflagellates, that dominate the PE fraction, have a high diversity of AP genes that can confer diverse strategies to access and utilize DOP (Lin et al., 2012). Whether actively growing mixotrophic dinoflagellates would increase their AP response in relation to organic C sources and not P limitation is unknown. In addition, the PE expressed mechanisms for uptake of several inorganic and organic P sources during active growth, which was not seen in the BAC (**Figure 8**). This supports that some of the PO_4 transformed by BAC-AP at T1 may be directly used by the PE, and that the BAC mainly used the resulting carbon products (Benitez-Nelson and Buesseler, 1999; Santos-Beneit, 2015). During late bloom (T2), the assumed lower eukaryotic C and N demand may link to the lower AP expression by PE and their expression of a low-affinity sodium dependent Pi transporter. The fact that BAC expressed uptake of two types of high-affinity organic P transporters, along with the expression of the Pi uptake repressor PhoU, suggests that there is a higher demand for organic P, but a lower demand for Pi at this timepoint (Santos-Beneit, 2015). Our findings demonstrate partitioning of the macronutrient P between PE and BAC, over bloom phase, by type (organic or inorganic) and nutrient species, beyond the direct coupling of composition and functional shifts.

Function and Community Composition

In the archipelago of Föglö, northern Baltic Proper, the taxonomic composition, based on amplicon sequencing analyses of both the PE and the BAC, did not vary significantly during the summer bloom while significant differences in resource acquisition were observed. The decoupling between bacterial community taxonomy and function previously suggested by Louca et al. (2016) has recently been evaluated experimentally (Louca et al., 2020) and showed that taxonomy shifts do not systematically affect metabolic rates. Our findings also point toward a decoupling between taxonomic composition and function in the field. For uptake of organic C, the same BAC taxa (Bacteroidetes, Actinobacteria, Alpha- and Beta-proteobacteria) initially utilize trehalose, xylose and maltose while during stationary bloom phase they instead utilize the more complex organic C compounds tagatose/galactitol, erythritol, inositol, raffinose, and chitin. The exception is gammaproteobacterial expression associated with uptake of inositol seen only during the later bloom stage. Traditionally, Bacteroidetes and Actinobacteria are correlated to algal blooms conditions (Riemann et al., 2008) and are often associated to late bloom phase due to their metabolic capacity to degrade HMW carbon compounds (Pinhassi et al., 1997) or polyaromatic compounds such as chitin (Beier and Bertilsson, 2013). This traditional view may perhaps not be so clear cut at this coastal location. Regarding BAC uptake of N, the results suggest that distinct organic and inorganic N resources were acquired and utilized during the two bloom phases. While these transcripts were assigned to several different BAC taxa, the same groups were represented throughout the bloom (Bacteroidetes, Actinobacteria, Cyanobacteria, Alpha-, Beta-, and Gamma-proteobacteria). Similarly, the transcripts associated with BAC acquisition and metabolism of P partly varied between the bloom phases, primarily with higher expression of alkaline phosphatase during the initial stage. These processes were annotated to a variety of BAC taxa, which were all represented during the whole bloom (Acidimicrobiia, Actinobacteria, Bacteroidetes, Cyanobacteria, Alpha-, Beta-, and Gamma-proteobacteria). Taken together, these results suggest that the community composition of BAC in association with a PE bloom is stable despite distinct metabolic and functional variations in C, N, and P resource usage. Thus, a decoupling between taxonomy and function is clear, it does however seem to be dependent on both the abiotic (availability of nutrients) and biotic (PE and BAC interactions) conditions in the bay.

CONCLUSIONS

In this eutrophied archipelagic environment, with high organic:inorganic nutrient ratio, interactions in the form of competition for highly desirable inorganic (nitrate, nitrite, ammonium, Pi) and organic (sugars, amino acids, oligo-peptides, phosphonates, urea, cyanate) nutrients, was characterized by an observed resource partitioning between PE (primarily phototrophs and mixotrophs) and BAC (primarily heterotrophs). This pattern was evident both when the PE were in exponential and stationary phase, implying that uptake

and assimilation of resources may be partitioned regardless of growth stage. This resulted in a range of metabolic functions, dependent on the resources available, which did not result in taxonomic shifts, suggesting a decoupling of function from taxonomy among BAC. This study shows the importance of BAC remineralization of allochthonous organic nutrients and of how PE and BAC divide available C, N, and P species, both in type and over time. At unbalanced nutrient conditions, these mechanisms likely enable phytoplankton growth, and even the development of blooms. This study reveals the potential importance of mixotrophic nutrition of PE in brackish coastal systems, which is still not taken into account in biogeochemical models. The results provide insight into how phytoplankton and bacteria in natural communities interact, and opens up for new questions such as how are resources partitioned at low organic:inorganic nutrient ratio, and what effect would a reduction of land run-off have on the microbial community and the nutrient distribution?

DATA AVAILABILITY STATEMENT

The datasets presented in this study can be found in online repositories. The names of the repository/repositories and accession number(s) can be found at: https://www.ebi.ac.uk/ena, ERS2571542-ERS2571562; https://www.ebi.ac.uk/ena, ERS2572272-ERS2572283; https://www.ebi.ac.uk/ena, PRJEB25883; https://www.ebi.ac.uk/ena, PRJEB27395.

AUTHOR CONTRIBUTIONS

ES designed the study, performed the sampling together with EL, handled all bioinformatic work, and led the writing of the manuscript, to which all authors contributed. ES, EL, and HF performed the laboratory work. All authors contributed to the interpretation of the results and the methods used for analysis.

FUNDING

The study was supported by funding from the Strategic Research Environment-ECOCHANGE funded by the Swedish Research Council Formas (CL), the Marie Skłodowska-Curie grant, Grant/Award Number: 659453 (EL), the Linnaeus University Centre of Ecology and Evolution in Microbial Model Systems (EEMiS) (CL and HF).

ACKNOWLEDGMENTS

The authors are grateful to Moritz Buck, at the National Bioinformatics Infrastructure Sweden at SciLifeLab, for bioinformatic advice, and Adina Howe, at Iowa State University, and Sara Beier, at Leibniz Institute for Baltic Sea Research, for computational support (AH) and advice (SB) on the calculations for use of internal standards with the metatranscriptome data. The authors acknowledge support from the National Genomics Infrastructure in Stockholm funded by Science for Life Laboratory, the Knut and Alice Wallenberg Foundation and the Swedish Research Council, and SNIC/Uppsala Multidisciplinary Center for Advanced Computational Science for assistance with massively parallel sequencing and access to the UPPMAX computational infrastructure.

SUPPLEMENTARY MATERIAL

The Supplementary Material for this article can be found online at: https://www.frontiersin.org/articles/10.3389/fmars.2020.608244/full#supplementary-material

REFERENCES

Alexander, H., Jenkins, B. D., Rynearson, T. A., and Dyhrman, S. T. (2015). Metatranscriptome analyses indicate resource partitioning between diatoms in the field. *Proc. Natl. Acad. Sci. U.S.A.* 112, E2182–E2190. doi: 10.1073/pnas.1421993112

Alipanah, L., Rohloff, J., Winge, P., Bones, A. M., and Brembu, T. (2015). Whole-cell response to nitrogen deprivation in the diatom *Phaeodactylum tricornutum*. *J. Exp. Bot*. 66, 6281–6296. doi: 10.1093/jxb/erv340

Anderson, O. R. (2018). Evidence for coupling of the carbon and phosphorus biogeochemical cycles in freshwater microbial communities. *Front. Mar. Sci.* 5, 1–6. doi: 10.3389/fmars.2018.00020

Andersson, A., Meier, H. E. M., Ripszam, M., Rowe, O., Wikner, J., Haglund, P., et al. (2015). Projected future climate change and Baltic sea ecosystem management. *Ambio* 44(Suppl. 3), 345–356. doi: 10.1007/s13280-015-0654-8

Andrews, S. (2009). *FastQC. A Quality Control Tool for High Throughput Sequence Data*. Available online at: http://www.bioinformatics.babraham.ac.uk/projects/fastqc/

Bagatini, I. L., Eiler, A., Bertilsson, S., Klaveness, D., Tessarolli, L. P., and Vieira, A. A. H. (2014). Host-specificity and dynamics in bacterial communities associated with bloom-forming freshwater phytoplankton. *PLoS ONE* 9:e85950. doi: 10.1371/journal.pone.0085950

Baltar, F., Lundin, D., Palovaara, J., Lekunberri, I., Reinthaler, T., Herndl, G. J., et al. (2016). Prokaryotic responses to ammonium and organic carbon reveal alternative CO_2 fixation pathways and importance of alkaline phosphatase in the mesopelagic North Atlantic. *Front. Microbiol.* 7:1670. doi: 10.3389/fmicb.2016.01670

Beer, S., Sand-Jensen, K., Madsen, T. V., and Nielsen, S. L. (1991). The carboxylase activity of Rubisco and the photosynthetic performance in aquatic plants. *Oecologia* 87, 429–434. doi: 10.1007/BF00634602

Beier, S., and Bertilsson, S. (2013). Bacterial chitin degradation-mechanisms and ecophysiological strategies. *Front. Microbiol.* 4:149. doi: 10.3389/fmicb.2013.00149

Beier, S., Holtermann, P., Numberger, D., Schott, T., Umlauf, L., and Jürgens, K. (2018). A metatranscriptomics based assessment of small scale mixing of sulfidic and oxic waters on redoxcline prokaryotic communities. *Environ. Microbiol.* 21, 1462–2920. doi: 10.1111/1462-2920.14499

Benitez-Nelson, C. R., and Buesseler, K. O. (1999). Variability of inorganic and organic phosphorus turnover rates in the coastal ocean. *Nature* 398, 502–505. doi: 10.1038/19061

Berg, C., Dupont, C. L., Asplund-Samuelsson, J., Celepli, N. A., Eiler, A., Allen, A. E., et al. (2018). Dissection of microbial community functions during a cyanobacterial bloom in the Baltic sea via metatranscriptomics. *Front. Mar. Sci.* 5:55. doi: 10.3389/fmars.2018.00055

Bonsdorff, E., Blomqvist, E. M., Mattila, J., and Norkko, A. (1997). Coastal eutrophication: causes, consequences and perspectives in the Archipelago areas of the northern Baltic sea. *Estuar. Coast. Shelf Sci.* 44, 63–72. doi: 10.1016/S0272-7714(97)80008-X

Boström, K. H., Simu, K., Hagström, Å., and Riemann, L. (2004). Optimization of DNA extraction for quantitative marine bacterioplankton community analysis. *Limnol. Oceanogr. Methods* 2, 365–373. doi: 10.4319/lom.2004.2.365

Buchfink, B., Xie, C., and Huson, D. H. (2015). Fast and sensitive protein alignment using DIAMOND. *Nat. Methods* 12, 59–60. doi: 10.1038/nmeth.3176

Bunse, C., Bertos-Fortis, M., Sassenhagen, I., Sildever, S., Sjöqvist, C., Godhe, A., et al. (2016). Spatio-temporal interdependence of bacteria and phytoplankton during a Baltic sea spring bloom. *Front. Microbiol.* 7:517. doi: 10.3389/fmicb.2016.00517

Callahan, B. J., McMurdie, P. J., Rosen, M. J., Han, A. W., Johnson, A. J. A., and Holmes, S. P. (2016). DADA2: high-resolution sample inference from Illumina amplicon data. *Nat. Methods* 13, 581–583. doi: 10.1038/nmeth.3869

Camarena-Gómez, M. T., Lipsewers, T., Piiparinen, J., Eronen-Rasimus, E., Perez-Quemaliños, D., Hoikkala, L., et al. (2018). Shifts in phytoplankton community structure modify bacterial production, abundance and community composition. *Aquat. Microb. Ecol.* 81, 149–170. doi: 10.3354/ame01868

Cardinale, B. J., Srivastava, D. S., Emmett Duffy, J., Wright, J. P., Downing, A. L., Sankaran, M., et al. (2006). Effects of biodiversity on the functioning of trophic groups and ecosystems. *Nature* 443, 989–992. doi: 10.1038/nature05202

Carstensen, J., Conley, D. J., Almroth-Rosell, E., Asmala, E., Bonsdorff, E., Fleming-Lehtinen, V., et al. (2019). Factors regulating the coastal nutrient filter in the Baltic sea. *Ambio* 49, 1194–1210. doi: 10.1007/s13280-019-01282-y

Chróst, R. J. (Ed.). (1991). "Environmental control of the synthesis and activity of aquatic microbial ectoenzymes," in *Microbial Enzymes in Aquatic Environments* (New York, NY: Springer Verlag), 29–59.

Core, T. R. (2018). *R: A Language and Environment for Statistical Computing*. Available online at: https://www.r-project.org/

Cottrell, M. T., and Kirchman, D. L. (2000). Natural assemblages of marine proteobacteria and members of the cytophaga-flavobacter cluster consuming low- and high-molecular-weight dissolved organic matter. *Appl. Environ. Microbiol.* 66, 1692–1697. doi: 10.1128/AEM.66.4.1692-1697.2000

Crusoe, M. R., Alameldin, H. F., Awad, S., Boucher, E., Caldwell, A., Cartwright, R., et al. (2015). The khmer software package: enabling efficient nucleotide sequence analysis. *F1000Research* 4:900. doi: 10.12688/f1000research.6924.1

Del Fabbro, C., Scalabrin, S., Morgante, M., and Giorgi, F. M. (2013). An extensive evaluation of read trimming effects on illumina NGS data analysis. *PLoS ONE* 8:e85024. doi: 10.1371/journal.pone.0085024

Diner, R. E., Schwenck, S. M., McCrow, J. P., Zheng, H., and Allen, A. E. (2016). Genetic manipulation of competition for nitrate between heterotrophic bacteria and diatoms. *Front. Microbiol.* 7:880. doi: 10.3389/fmicb.2016.00880

Dupont, C. L., McCrow, J. P., Valas, R., Moustafa, A., Walworth, N., Goodenough, U., et al. (2015). Genomes and gene expression across light and productivity gradients in eastern subtropical Pacific microbial communities. *ISME J.* 9, 1076–1092. doi: 10.1038/ismej.2014.198

Elifantz, H., Malmstrom, R. R., Cottrell, M. T., and Kirchman, D. L. (2005). Assimilation of polysaccharides and glucose by major bacterial groups in the Delaware Estuary. *Appl. Environ. Microbiol.* 71, 7799–7805. doi: 10.1128/AEM.71.12.7799-7805.2005

Fouilland, E., Gosselin, M., Rivkin, R. B., Vasseur, C., and Mostajir, B. (2007). Nitrogen uptake by heterotrophic bacteria and phytoplankton in Arctic surface waters. *J. Plankton Res.* 29, 369–376. doi: 10.1093/plankt/fbm022

Foyer, C., and Harbinson, J. (1994). "Oxygen metabolism and the regulation of photosynthetic electron transport," in C*auses of Photooxidative Stress and Amelioration of Defense Systems in Plant*, eds C. Foyer and P. Mullineaux (Boca Raton, FL: CRC Press), 1–42.

Gardner, S. G., Johns, K. D., Tanner, R., and McCleary, W. R. (2014). The PhoU protein from *Escherichia coli* interacts with PhoR, PstB, and metals to form a phosphate-signaling complex at the membrane. *J. Bacteriol.* 196, 1741–1752. doi: 10.1128/JB.00029-14

Gifford, S. M., Sharma, S., Booth, M., and Moran, M. A. (2013). Expression patterns reveal niche diversification in a marine microbial assemblage. *ISME J.* 7, 281–298. doi: 10.1038/ismej.2012.96

Glibert, P. M., Wilkerson, F. P., Dugdale, R. C., Raven, J. A., Dupont, C. L., Leavitt, P. R., et al. (2016). Pluses and minuses of ammonium and nitrate uptake and assimilation by phytoplankton and implications for productivity and community composition, with emphasis on nitrogen-enriched conditions. *Limnol. Oceanogr.* 61, 165–197. doi: 10.1002/lno.10203

Gómez, F. (2012). A quantitative review of the lifestyle, habitat and trophic diversity of dinoflagellates (Dinoflagellata, Alveolata). *Syst. Biodivers.* 10, 267–275. doi: 10.1080/14772000.2012.721021

Gong, W., and Marchetti, A. (2019). Estimation of 18S gene copy number in marine eukaryotic plankton using a next-generation sequencing approach. *Front. Mar. Sci.* 6:219. doi: 10.3389/fmars.2019.00219

Granéli, E., Wallström, K., Larsson, U., Granéli, W., and Elmgren, R. (1990). Nutrient limitation of primary production in the Baltic sea. *Ambio* 13, 142–151.

Grossart, H.-P., Levold, F., Allgaier, M., Simon, M., and Brinkhoff, T. (2005). Marine diatom species harbour distinct bacterial communities. *Environ. Microbiol.* 7, 860–873. doi: 10.1111/j.1462-2920.2005.00759.x

Grossart, H. P., and Simon, M. (2007). Interactions of planktonic algae and bacteria: effects on algal growth and organic matter dynamics. *Aquat. Microb. Ecol.* 47, 163–176. doi: 10.3354/ame047163

Hällfors, G. (2004). *Checklist of Baltic Sea Phytoplankton Species*. Helsinki Commission; Baltic Marine Environment protection Commission. Available online at: http://helcom.fi/Lists/Publications/BSEP95.pdf

Heiskanen, A. S., Bonsdorff, E., and Joas, M. (2019). "Baltic Sea: a recovering future from decades of eutrophication," in *Coasts and Estuaries*, eds E. Wolanski, J. Day, M. Elliott, and R. Ramesh (Amsterdam: Elsevier), 343–362. doi: 10.1016/b978-0-12-814003-1.00020-4

Herlemann, D. P., Labrenz, M., Jürgens, K., Bertilsson, S., Waniek, J. J., and Andersson, A. F. (2011). Transitions in bacterial communities along the 2000 km salinity gradient of the Baltic sea. *ISME J.* 5, 1571–1579. doi: 10.1038/ismej.2011.41

Hu, Z., Mulholland, M. R., Duan, S., and Xu, N. (2012). Effects of nitrogen supply and its composition on the growth of *Prorocentrum donghaiense*. *Harmful Algae* 13, 72–82. doi: 10.1016/j.hal.2011.10.004

Hugerth, L. W., Muller, E. E. L., Hu, Y. O. O., Lebrun, L. A. M., Roume, H., Lundin, D., et al. (2014). Systematic Design of 18S rRNA gene primers for determining eukaryotic diversity in microbial consortia. *PLoS ONE* 9:e95567. doi: 10.1371/journal.pone.0095567

Hunt, D. E., David, L. A., Gevers, D., Preheim, S. P., Alm, E. J., and Polz, M. F. (2008). Resource partitioning and sympatric differentiation among closely related bacterioplankton. *Science* 320, 1081–1085. doi: 10.1126/science.1157890

Huson, D. H., Beier, S., Flade, I., Górska, A., El-Hadidi, M., Mitra, S., et al. (2016). MEGAN community edition - interactive exploration and analysis of large-scale microbiome sequencing data. *PLOS Comput. Biol.* 12:e1004957. doi: 10.1371/journal.pcbi.1004957

Jespersen, A., and Christoffersen, K. (1987). Measurements of chlorophyll-a from phytoplankton using ethanol as extraction solvent. *Arch. Hydrobiol.* 109, 445–454.

Johansson, M., Gorokhova, E., and Larsson, U. (2004). Annual variability in ciliate community structure, potential prey and predators in the open northern Baltic sea proper. *J. Plankton Res.* 26, 67–80. doi: 10.1093/plankt/fbg115

Kataoka, T., and Kondo, R. (2019). Data on taxonomic annotation and diversity of 18S rRNA gene amplicon libraries derived from high throughput sequencing. *Data Br.* 25:104213. doi: 10.1016/j.dib.2019.104213

Kirchman, D. L. (1994). The uptake of inorganic nutrients by heterotrophic bacteria. *Microb. Ecol.* 28, 255–271. doi: 10.1007/BF00166816

Kivi, K., and Setäl, O. (1995). Simultaneous measurement of food particle selection and clearance rates of planktonic oligotrich ciliates (Ciliophora:Oligotrichina). *Mar. Ecol. Prog. Ser.* 119, 125–137. doi: 10.3354/meps119125

Kremp, A., Lindholm, T., Dreßler, N., Erler, K., Gerdts, G., Eirtovaara, S., et al. (2009). Bloom forming *Alexandrium ostenfeldii* (Dinophyceae) in shallow waters of the Åland Archipelago, Northern Baltic sea. *Harmful Algae* 8, 318–328. doi: 10.1016/j.hal.2008.07.004

Landa, M., Blain, S., Christaki, U., Monchy, S., and Obernosterer, I. (2016). Shifts in bacterial community composition associated with increased carbon cycling in a mosaic of phytoplankton blooms. *ISME J.* 10, 39–50. doi: 10.1038/ismej.2015.105

Langmead, B., and Salzberg, S. L. (2012). Fast gapped-read alignment with Bowtie 2. *Nat. Methods* 9, 357–359. doi: 10.1038/nmeth.1923

Lauro, F. M., McDougald, D., Thomas, T., Williams, T. J., Egan, S., Rice, S., et al. (2009). The genomic basis of trophic strategy in marine bacteria. *Proc. Natl. Acad. Sci. U.S.A.* 106, 15527–15533. doi: 10.1073/pnas.0903507106

Li, D., Luo, R., Liu, C.-M., Leung, C.-M., Ting, H.-F., Sadakane, K., et al. (2016). MEGAHIT v1.0: a fast and scalable metagenome assembler driven by advanced methodologies and community practices. *Methods* 102, 3–11. doi: 10.1016/j.ymeth.2016.02.020

Li, H., Handsaker, B., Wysoker, A., Fennell, T., Ruan, J., Homer, N., et al. (2009). The sequence alignment/map format and SAMtools. *Bioinformatics* 25, 2078–2079. doi: 10.1093/bioinformatics/btp352

Li, Y.-Y., Chen, X.-H., Xie, Z.-X., Li, D.-X., Wu, P.-F., Kong, L.-F., et al. (2018). Bacterial diversity and nitrogen utilization strategies in the upper layer of the Northwestern Pacific Ocean. *Front. Microbiol.* 9:797. doi: 10.3389/fmicb.2018.00797

Lin, X., Zhang, H., Cui, Y., and Lin, S. (2012). High sequence variability, diverse subcellular localizations, and ecological implications of alkaline phosphatase in dinoflagellates and other eukaryotic phytoplankton. *Front. Microbiol.* 3:235. doi: 10.3389/fmicb.2012.00235

Lips, I., and Lips, U. (2017). The importance of *Mesodinium rubrum* at post-spring bloom nutrient and phytoplankton dynamics in the vertically stratified Baltic sea. *Front. Mar. Sci.* 4:407. doi: 10.3389/fmars.2017.00407

Louca, S., Jacques, S. M. S., Pires, A. P. F., Leal, J. S., Srivastava, D. S., Parfrey, L. W., et al. (2017). High taxonomic variability despite stable functional structure across microbial communities. *Nat. Ecol. Evol.* 1:15. doi: 10.1038/s41559-016-0015

Louca, S., Parfrey, L. W., and Doebeli, M. (2016). Decoupling function and taxonomy in the global ocean microbiome. *Science* 353, 1272–1277. doi: 10.1126/science.aaf4507

Louca, S., Polz, M. F., Mazel, F., Albright, M. B. N., Huber, J. A., O'Connor, M. I., et al. (2018). Function and functional redundancy in microbial systems. *Nat. Ecol. Evol.* 2, 936–943. doi: 10.1038/s41559-018-0519-1

Louca, S., Rubin, I. N., Madilao, L. L., Bohlmann, J., Doebeli, M., and Wegener Parfrey, L. (2020). Effects of forced taxonomic transitions on metabolic composition and function in microbial microcosms. *Environ. Microbiol. Rep.* 12, 514–524. doi: 10.1111/1758-2229.12866

Love, M. I., Huber, W., and Anders, S. (2014). Moderated estimation of fold change and dispersion for RNA-seq data with DESeq2. *Genome Biol.* 15:550. doi: 10.1186/s13059-014-0550-8

MacIntyre, H. L., Sharkey, T. D., and Geider, R. J. (1997). Activation and deactivation of ribulose- 1,5-bisphosphate carboxylase/oxygenase (Rubisco) in three marine microalgae. *Photosynth. Res.* 51, 93–106. doi: 10.1023/A:1005755621305

Martin, M. (2011). Cutadapt removes adapter sequences from high-throughput sequencing reads. *EMBnet J.* 17, 10–12. doi: 10.14806/ej.17.1.200

Mayali, X., and Doucette, G. J. (2002). Microbial community interactions and population dynamics of an algicidal bacterium active against *Karenia brevis* (Dinophyceae). *Harmful Algae* 1, 277–293. doi: 10.1016/S1568-9883(02)00032-X

McCarren, J., Becker, J. W., Repeta, D. J., Shi, Y., Young, C. R., Malmstrom, R. R., et al. (2010). Microbial community transcriptomes reveal microbes and metabolic pathways associated with dissolved organic matter turnover in the sea. *Proc. Natl. Acad. Sci. U.S.A.* 107, 16420–16427. doi: 10.1073/pnas.1010732107

Mironova, E. I., Telesh, I. V., and Skarlato, S. O. (2009). Planktonic ciliates of the Baltic sea (a review). *Inl. Water Biol.* 2, 13–24. doi: 10.1134/S1995082909010039

Morey, J. S., Monroe, E. A., Kinney, A. L., Beal, M., Johnson, J. G., Hitchcock, G. L., et al. (2011). Transcriptomic response of the red tide dinoflagellate, *Karenia brevis*, to nitrogen and phosphorus depletion and addition. *BMC Genomics* 12:346. doi: 10.1186/1471-2164-12-346

Mühlenbruch, M., Grossart, H.-P., Eigemann, F., and Voss, M. (2018). Mini-review: Phytoplankton-derived polysaccharides in the marine environment and their interactions with heterotrophic bacteria. *Environ. Microbiol.* 20, 2671–2685. doi: 10.1111/1462-2920.14302

Nausch, M., Achterberg, E. P., Bach, L. T., Brussaard, C. P. D., Crawfurd, K. J., Fabian, J., et al. (2018). Concentrations and uptake of dissolved organic phosphorus compounds in the Baltic sea. *Front. Mar. Sci.* 5:386. doi: 10.3389/fmars.2018.00386

Oksanen, J., Blanchet, F. G., Friendly, M., Kindt, R., Legendre, P., McGlinn, D., et al. (2019). *vegan: Community Ecology Package*. Available online at: https://cran.r-project.org/package=vegan

Oksanen, J., Kindt, R., Legendre, P., O'Hara, B., Simpson, G. L., Solymos, P. M., et al. (2008). *The vegan Package. Community Ecology Package*, 190. Available online at: https://bcrc.bio.umass.edu/biometry/images/8/85/Vegan.pdf

Olenina, I., Edler, L., Andersson, A., Wasmund, N., Busch, S., Göbel, J., et al. (2006). *Biovolumes and Size-Classes of Phytoplankton in the Baltic Sea*. Helsinki Commission; Baltic Marine Environment Protection Commission. Available online at: http://helcom.fi/Lists/Publications/BSEP106.pdf

Overbeek, R., Olson, R., Pusch, G. D., Olsen, G. J., Davis, J. J., Disz, T., et al. (2014). The SEED and the Rapid Annotation of microbial genomes using Subsystems Technology (RAST). *Nucl. Acids Res.* 42, D206–D214. doi: 10.1093/nar/gkt1226

Parker, M. S., and Armbrust, E. V. (2005). Synergistic effects of light, temperature, and nitrogen source on transcription of genes for carbon and nitrogen metabolism in the centric diatom *Thalassiosire pseudonana* (Bacillariophyceae). *J. Phycol.* 41, 1142–1153. doi: 10.1111/j.1529-8817.2005.00139.x

Pinhassi, J., Zweifel, U. L., and Hagström, A. (1997). Dominant marine bacterioplankton species found among colony-forming bacteria. *Appl. Environ. Microbiol.* 63, 3359–3366. doi: 10.1128/AEM.63.9.3359-3366.1997

Pomati, F., Manarolla, G., Rossi, O., Vigetti, D., and Rossetti, C. (2001). The purine degradation pathway. *Environ. Int.* 27, 463–470. doi: 10.1016/S0160-4120(01)00101-5

Ptacnik, R., Solimini, A. G., Andersen, T., Tamminen, T., Brettum, P., Lepistö, L., et al. (2008). Diversity predicts stability and resource use efficiency in natural phytoplankton communities. *Proc. Natl. Acad. Sci. U.S.A.* 105, 5134–5138. doi: 10.1073/pnas.0708328105

Quast, C., Pruesse, E., Yilmaz, P., Gerken, J., Schweer, T., Yarza, P., et al. (2013). The SILVA ribosomal RNA gene database project: improved data processing and web-based tools. *Nucl. Acids Res.* 41, 590–596. doi: 10.1093/nar/gks1219

Rabalais, N. N., Turner, R. E., Díaz, R. J., and Justić, D. (2009). Global change and eutrophication of coastal waters. *ICES J. Mar. Sci.* 66, 1528–1537. doi: 10.1093/icesjms/fsp047

Riemann, L., Leitet, C., Pommier, T., Simu, K., Holmfeldt, K., Larsson, U., et al. (2008). The native bacterioplankton community in the central Baltic sea is influenced by freshwater bacterial species. *Appl. Environ. Microbiol.* 74, 503–515. doi: 10.1128/AEM.01983-07

Rink, B., Seeberger, S., Martens, T., Duerselen, C., Simon, M., and Brinkhoff, T. (2007). Effects of phytoplankton bloom in a coastal ecosystem on the composition of bacterial communities. *Aquat. Microb. Ecol.* 48, 47–60. doi: 10.3354/ame048047

Rönnberg, C., and Bonsdorff, E. (2004). "Baltic sea eutrophication: area-specific ecological consequences," in *Biology of the Baltic Sea*, eds H. Kautsky and P. Snoeijs (Dordrecht: Springer Netherlands), 227–241.

Rost, B., Richter, K.-U., Riebesell, U., and Hansen, P. J. (2006). Inorganic carbon acquisition in red tide dinoflagellates. *Plant Cell Environ.* 29, 810–822. doi: 10.1111/j.1365-3040.2005.01450.x

Sandberg, J., Andersson, A., Johansson, S., and Wikner, J. (2004). Pelagic food web structure and carbon budget in the northern Baltic sea: potential importance of terrigenous carbon. *Mar. Ecol. Prog. Ser.* 268, 13–29. doi: 10.3354/meps268013

Santos-Beneit, F. (2015). The Pho regulon: a huge regulatory network in bacteria. *Front. Microbiol.* 6, 1–13. doi: 10.3389/fmicb.2015.00402

Sapp, M., Schwaderer, A. S., Wiltshire, K. H., Hoppe, H. G., Gerdts, G., and Wichels, A. (2007). Species-specific bacterial communities in the phycosphere of microalgae? *Microb. Ecol.* 53, 683–699. doi: 10.1007/s00248-006-9162-5

Sarmento, H., Morana, C., and Gasol, J. M. (2016). Bacterioplankton niche partitioning in the use of phytoplankton-derived dissolved organic carbon: quantity is more important than quality. *ISME J.* 10, 2582–2592. doi: 10.1038/ismej.2016.66

Satinsky, B. M., Gifford, S. M., Crump, B. C., and Moran, M. A. (2013). "Use of internal standards for quantitative metatranscriptome and metagenome analysis," in *Methods in Enzymology* 531, 237–250. doi: 10.1016/B978-0-12-407863-5.00012-5

Savchuk, O. P. (2018). Large-scale nutrient dynamics in the Baltic sea, 1970–2016. *Front. Mar. Sci.* 5:95. doi: 10.3389/fmars.2018.00095

Siaut, M., Heijde, M., Mangogna, M., Montsant, A., Coesel, S., Allen, A., et al. (2007). Molecular toolbox for studying diatom biology in *Phaeodactylum tricornutum*. *Gene* 406, 23–35. doi: 10.1016/j.gene.2007.05.022

Sison-Mangus, M. P., Jiang, S., Kudela, R. M., and Mehic, S. (2016). Phytoplankton-associated bacterial community composition and succession

during toxic diatom bloom and non-bloom events. *Front. Microbiol.* 7:1433. doi: 10.3389/fmicb.2016.01433

Solomon, C., Collier, J., Berg, G., and Glibert, P. (2010). Role of urea in microbial metabolism in aquatic systems: a biochemical and molecular review. *Aquat. Microb. Ecol.* 59, 67–88. doi: 10.3354/ame01390

Sörenson, E., Bertos-Fortis, M., Farnelid, H., Kremp, A., Krüger, K., Lindehoff, E., et al. (2019). Consistency in microbiomes in cultures of *Alexandrium* species isolated from brackish and marine waters. *Environ. Microbiol. Rep*. 11, 425–433. doi: 10.1111/1758-2229.12736

Stewart, A. J., Robert, G., and Wetzel, W. K. (1982). Influence of dissolved humic materials on carbon assimilation and alkaline phosphatase activity in natural algal-bacterial assemblages. *Freshw. Biol.* 12, 369–380. doi: 10.1111/j.1365-2427.1982.tb00630.x

Stoecker, D. K. (1999). Mixotrophy among Dinoflagellates. *J. Eukaryot. Microbiol.* 46, 397–401. doi: 10.1111/j.1550-7408.1999.tb04619.x

Takabayashi, M., Wilkerson, F. P., and Robertson, D. (2005). Response of glutamine synthetase gene transcription and enzyme activity to external nitrogen sources in the diatom *Skeletonema costatum* (Bacillariophyceae). *J. Phycol.* 41, 84–94. doi: 10.1111/j.1529-8817.2005.04115.x

Tanaka, T., Henriksen, P., Lignell, R., Olli, K., Seppälä, J., Tamminen, T., et al. (2006). Specific affinity for phosphate uptake and specific alkaline phosphatase activity as diagnostic tools for detecting phosphorus-limited phytoplankton and bacteria. *Estuaries Coasts* 29, 1226–1241. doi: 10.1007/BF02781823

Teeling, H., Fuchs, B. M., Becher, D., Klockow, C., Gardebrecht, A., Bennke, C. M., et al. (2012). Substrate-controlled succession of marine bacterioplankton populations induced by a phytoplankton bloom. *Science* 336, 608–611. doi: 10.1126/science.1218344

Tilman, D. (1982). *Resource Competition and Community Structure*. Princeton, NJ: Princeton University Press.

Traving, S. J., Rowe, O., Jakobsen, N. M., Sørensen, H., Dinasquet, J., Stedmon, C. A., et al. (2017). The effect of increased loads of dissolved organic matter on estuarine microbial community composition and function. *Front. Microbiol.* 8:351. doi: 10.3389/fmicb.2017.00351

Valderrama, J. C. (1995). "Methods of nutrient analysis," in *Manual on Harmful Marine Microalgae, IOC Manuals and Guides*, eds G. M. Hallagraeff, D. M. Anderson, and A. D. Cembella (Paris: UNESCO), 251–268.

Voss, M., Bange, H. W., Dippner, J. W., Middelburg, J. J., Montoya, J. P., and Ward, B. (2013). The marine nitrogen cycle: recent discoveries, uncertainties and the potential relevance of climate change. *Philos. Trans. R. Soc. B Biol. Sci*. 368:0121. doi: 10.1098/rstb.2013.0121

Wagner, G. P., Kin, K., and Lynch, V. J. (2012). Measurement of mRNA abundance using RNA- seq data: RPKM measure is inconsistent among samples. *Theory Biosci.* 131, 281–285. doi: 10.1007/s12064-012-0162-3

White, A., and Dyhrman, S. (2013). The marine phosphorus cycle. *Front. Microbiol.* 4:105. doi: 10.3389/fmicb.2013.00105

Wickham, H. (2016). *ggplot2: Elegant Graphics for Data Analysis*. New York, NY: Springer International Publishing.

Williams, T. J., Long, E., Evans, F., DeMaere, M. Z., Lauro, F. M., Raftery, M. J., et al. (2012). A metaproteomic assessment of winter and summer bacterioplankton from Antarctic Peninsula coastal surface waters. *ISME J.* 6, 1883–1900. doi: 10.1038/ismej.2012.28

Wohlrab, S., Falcke, J. M., Lin, S., Zhang, H., Neuhaus, S., Elferink, S., et al. (2018). Metatranscriptome profiling indicates size-dependent differentiation in plastic and conserved community traits and functional diversification in dinoflagellate communities. *Front. Mar. Sci.* 5:358. doi: 10.3389/fmars.2018.00358

Xiao, X., Sogge, H., Lagesen, K., Tooming-Klunderud, A., Jakobsen, K. S., and Rohrlack, T. (2014). Use of high throughput sequencing and light microscopy show contrasting results in a study of phytoplankton occurrence in a freshwater environment. *PLoS ONE* 9:e106510. doi: 10.1371/journal.pone.0106510

Zhou, J., Richlen, M. L., Sehein, T. R., Kulis, D. M., Anderson, D. M., and Cai, Z. (2018). Microbial community structure and associations during a marine dinoflagellate bloom. *Front. Microbiol.* 9:1201. doi: 10.3389/fmicb.2018.01201

Zhou, Y., Davidson, T. A., Yao, X., Zhang, Y., Jeppesen, E., de Souza, J. G., et al. (2018). How autochthonous dissolved organic matter responds to eutrophication and climate warming: evidence from a cross-continental data analysis and experiments. *Earth Sci. Rev.* 185, 928–937. doi: 10.1016/j.earscirev.2018.08.013

Zhuang, Y., Zhang, H., Hannick, L., and Lin, S. (2015). Metatranscriptome profiling reveals versatile n-nutrient utilization, CO_2 limitation, oxidative stress, and active toxin production in an *Alexandrium fundyense* bloom. *Harmful Algae* 42, 60–70. doi: 10.1016/j.hal.2014.12.006

Conflict of Interest: The authors declare that the research was conducted in the absence of any commercial or financial relationships that could be construed as a potential conflict of interest.

frontiers in Microbiology

ORIGINAL RESEARCH
published: 01 December 2020
doi: 10.3389/fmicb.2020.593540

Prokaryotic Diversity and Distribution Along Physical and Nutrient Gradients in the Tunisian Coastal Waters (South Mediterranean Sea)

Marianne Quéméneur[1], Malika Bel Hassen[2], Fabrice Armougom[1], Yosra Khammeri[2], Rim Lajnef[2] and Amel Bellaaj-Zouari[2]*

[1] Aix-Marseille Univ, University of Toulon, CNRS, IRD, MIO UM 110, Mediterranean Institute of Oceanography, Marseille, France, [2] Institut National des Sciences et Technologies de la Mer, Salammbô, Tunis, Tunisia

OPEN ACCESS

Edited by:
Savvas Genitsaris, International Hellenic University, Greece

Reviewed by:
Sandi Orlic, Rudjer Boskovic Institute, Croatia
John Paul Balmonte, Evolutionary Biology Centre, Uppsala University, Sweden
Rachel Jane Parsons, Bermuda Institute of Ocean Sciences, Bermuda

***Correspondence:**
Marianne Quéméneur
marianne.quemeneur@ird.fr; marianne.quemeneur@mio.osupytheas.fr

Specialty section:
This article was submitted to Aquatic Microbiology, a section of the journal Frontiers in Microbiology

Received: *10 August 2020*
Accepted: *26 October 2020*
Published: *01 December 2020*

Citation:
Quéméneur M, Bel Hassen M, Armougom F, Khammeri Y, Lajnef R and Bellaaj-Zouari A (2020) Prokaryotic Diversity and Distribution Along Physical and Nutrient Gradients in the Tunisian Coastal Waters (South Mediterranean Sea). Front. Microbiol. 11:593540. doi: 10.3389/fmicb.2020.593540

Prokaryotes play an important role in biogeochemical cycling in marine ecosystems, but little is known about their diversity and composition, and how they may contribute to the ecological functioning of coastal areas in the South Mediterranean Sea. This study investigated bacterial and archaeal community diversity in seawater samples along the Tunisian coast subject to important physicochemical disturbances. The 16S amplicon sequencing survey revealed higher prokaryotic diversity in the northern Tunisian bays than in southeastern waters (Gulf of Gabès). The major taxonomic groups identified in all samples were *Alphaproteobacteria* (40.9%), *Gammaproteobacteria* (18.7%), Marine Group II *Euryarchaeota* (11.3%), and *Cyanobacteria* (10.9%). Among them, the relative abundance of *Alteromonadales*, *Prochlorococcus*, and some clades of *Pelagibacterales* (SAR11) significantly differed between the northern and the southern bays, whereas no difference was observed across coastal waters in the archaeal *Candidatus* Poseidoniales (MGII), *Synechococcus*, and *Pelagibacteraceae* (SAR11 clade Ia), for which no relationship was observed with the environmental variables. Both *Pseudoalteromonas* and *Alteromonas* levels increased with the increasing salinity, density and nutrients (NH_4^+ and/or PO_4^{3-}) gradients detected toward the southern waters, while the SAR11 clades Ib and IV and *Prochlorococcus*, decreased in the shallow, salty and nutrient-rich coastal waters of the Gulf of Gabès. *Rhodobacteraceae* was positively correlated with *Synechococcus* and chlorophyll levels, suggesting a relationship with phytoplankton biomass. The present study provides the first insights into planktonic prokaryotic community composition in the South Mediterranean Sea through the analysis of Tunisian seawaters, which may support further investigations on the role of bacterioplankton in the biogeochemistry of these ecosystems.

Keywords: bacteria, archaea, bacterioplankton, diversity, Tunisia, Gulf of Gabès, seawater

INTRODUCTION

Prokaryotes are abundant in marine ecosystems, with number estimates of 1×10^{29} in oceans and concentration estimates of 10^3 bacteria per microliter in surface seawater (Azam and Malfatti, 2007; Flemming and Wuertz, 2019). They are the most diverse metabolically and phylogenetically organisms on Earth (Oren, 2004). They also play a central role in biogeochemical cycles, marine food chains and global climate change (Shively et al., 2001; Cotner and Biddanda, 2002; Azam and Malfatti, 2007; Falkowski et al., 2008; Strom, 2008; Liu et al., 2010; Zehr and Kudela, 2011; Bao et al., 2018). Photosynthetic prokaryotes are responsible for a large proportion of the total primary production (Azam and Malfatti, 2007; Flombaum et al., 2013), while heterotrophs play an important role in the microbial loop by the remineralization of organic compounds (Carlson et al., 2010). Photosynthetic *Cyanobacteria* and photoheterotrophic *Alphaproteobacteria* of the order *Pelagibacterales* (also known as SAR11) are among the most abundant prokaryotes in marine waters (Chisholm et al., 1988; Morris et al., 2002; Carlson et al., 2009; Flombaum et al., 2013; Evans et al., 2015; Giovannoni, 2017). In the Mediterranean Sea, most studies have identified SAR11 as the dominant bacteria (ranging between 25 and 45% of the reported sequences and contributing to $36 \pm 6\%$ of total prokaryotic abundance; Laghdass et al., 2012), followed by other *Alphaproteobacteria* (belonging to the family *Rhodobacteriaceae*; Zaballos et al., 2006; Alonso-Sáez et al., 2007; Feingersch et al., 2010; Salter et al., 2015). *Cyanobacteria* (*Prochlorococcus* and *Synechococcus*), *Gammaproteobacteria* (e.g., *Alteromonadales*) and *Bacteroidetes* constitute the remaining of the dominant bacterial diversity with some divergences depending on depth, seasons, and distance from land (Estrada and Vaqué, 2014). Diverse archaeal communities have also been observed in the Mediterranean Sea water column and their structure also varied depending on depth, geographic areas, and seasons (Massana et al., 2000; Galand et al., 2010; Hugoni et al., 2013; Martin-Cuadrado et al., 2015). Marine planktonic *Archaea* are currently classified into four main groups belonging the phyla *Thaumarchaeota* (formerly Marine Group I archaea) and *Euryarchaeota* (Marine Groups II, III, and IV; Santoro et al., 2019). Although many studies have evaluated the spatiotemporal diversity of prokaryotes in several marine regions throughout the world, including the Mediterranean Sea (Ghiglione et al., 2005; Feingersch et al., 2010; Galand et al., 2010; Techtmann et al., 2015), their responses to environmental changes remain largely unknown in many specific coastal areas, especially along the southern coasts of the Mediterranean Sea, impacted by anthropogenic activities, climatic changes, and a complex water circulation pattern (Bel Hassen et al., 2009a; Coll et al., 2010; Zouch et al., 2018; Béjaoui et al., 2019).

The Mediterranean Sea is a semi-enclosed oligotrophic sea characterized by high variations in environmental conditions (e.g., temperature, salinity, current, and nutrient availability) leading to high change in biodiversity depending on depth, seasons, and location (Coll et al., 2010). The salinity, temperature and nutrient gradients are especially pronounced off the coasts of Tunisia, comprising the Strait of Sicily, which represent the natural conjunction between the western and the eastern Mediterranean basins (Khammeri et al., 2020). This eastern basin is the most oligotrophic area of the Mediterranean Sea, and their phytoplanktonic communities were mainly composed of ultraphytoplankton (<10 μm), which play an important role in the primary production (Bel Hassen et al., 2009b; Estrada and Vaqué, 2014; Khammeri et al., 2020). In the eastern Mediterranean basin, the Gulf of Gabès is one of the most productive Mediterranean area (Ayata et al., 2018), due to the favorable climatic conditions and the high nutrient availability, contrasting with the oligotrophic waters of the eastern basin (Béjaoui et al., 2019). Changes in picoeukaryotic assemblages, phytoplankton abundance and ultraphytoplankton composition have been largely studied in the shallow waters of the Gulf of Gabès (Bel Hassen et al., 2009a,b; Rekik et al., 2014; Hamdi et al., 2015; Bellaaj-Zouari et al., 2018). Recently, the ultraphytoplankton distribution have been evaluated by flow cytometry analysis along the Tunisian coast, showing a gradual increase from the North to the South in *Synechococcus*, picoeucaryotes, nanoeukaryotes and cryptophytes, mainly concentrated in the Gulf of Gabès, except for *Prochloroccocus* more abundant in northern coast (Khammeri et al., 2020). Although prokaryotic structure and dynamics have been well studied in the North Western and Eastern Mediterranean Sea (Zaballos et al., 2006; Laghdass et al., 2012; Hazan et al., 2018; Haber et al., 2020), the diversity of planktonic prokaryotes, especially heterotrophic prokaryotes, has not yet been studied in the South Mediterranean Sea (including the Gabès Gulf), despite their potential important role in biogeochemical cycles.

In this study, we evaluated for the first time the diversity and composition of prokaryotic communities in seawater samples collected along the Tunisian coast subjected to physicochemical gradients (from the North to the South), in order to understand how environmental variables, affect both archaeal and bacterial community structure. The first step to describe the microbial communities was to determine the diversity and relative abundances of different phylogenetic groups using Illumina sequencing of 16S rRNA genes. Then, we examined the relationships between the prokaryotic community composition/distribution and the water physicochemical characteristics (i.e., salinity, nutrients, physical properties, chlorophyll content). Finally, we investigate the relationships between the dominant microbial groups to highlight their potential ecological role in this specific area of the Mediterranean Sea.

MATERIALS AND METHODS

Sample Collection

Seawater samples (n = 20) were collected at two depths (1 m below the surface and 2 to 3 m above the bottom) from 10 stations along the eastern coast of Tunisia (South Mediterranean Sea, Eastern Mediterranean basin; **Figures 1A,B**) in November 2013 during the INCOMMET cruise aboard the

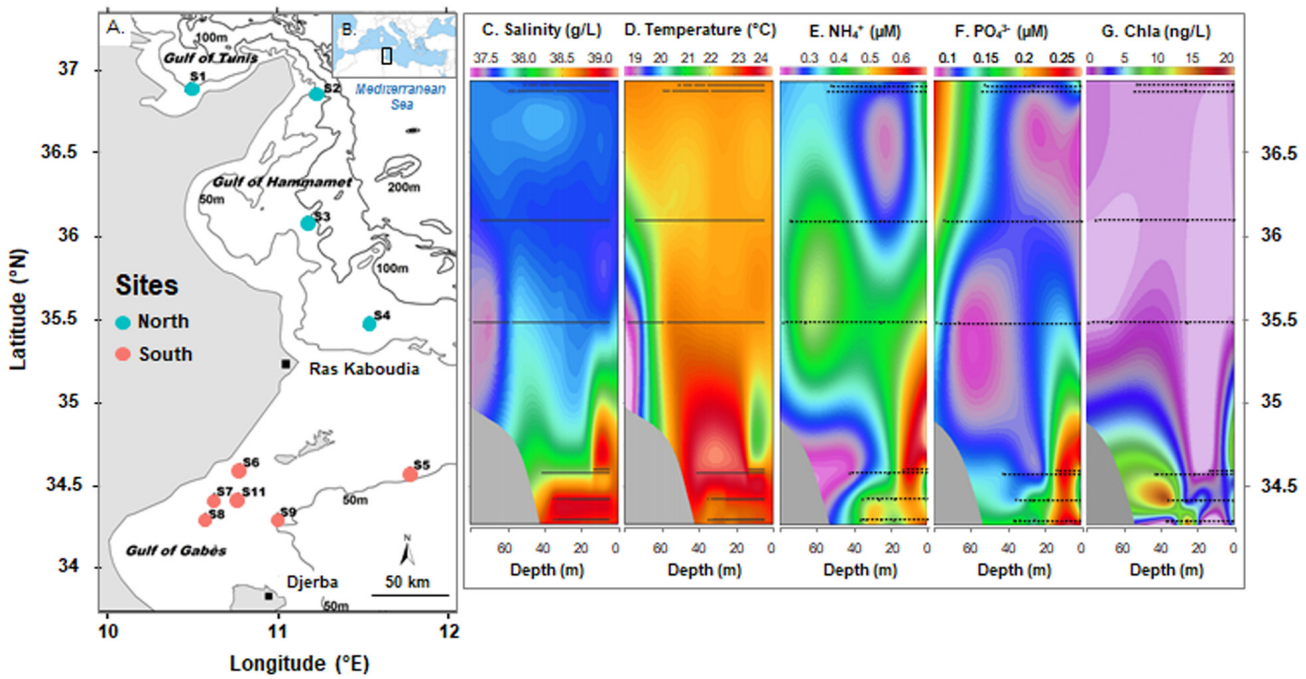

FIGURE 1 | Sampling sites along the Tunisian coast during INCOMMET cruise **(A)** in the South Mediterranean Sea **(B)** with vertical profiles of salinity **(C)**, temperature **(D)**, ammonium **(E)**, orthophosphate **(F)**, and chlorophyll *a* (Chla) **(G)** concentrations along the section defined by the station latitude from the Gulf of Tunis to the Gulf of Gabès (modified from Khammeri et al., 2020). Stations are indicated by blue or red circles (for North or South bays) on map. Stations and sample depth are indicated by line in vertical profiles.

N/O Hannibal. Samples analyzed in this study were selected out of the 30 collected from 11 sites previously described in an ultraphytoplankton community study (Khammeri et al., 2020). Surface (S) and bottom (B) waters were collected using 12-L Niskin bottles fitted on a Rosette sampler equipped with conductivity, temperature, and depth (CTD) sensors (SBE 9, Sea-Bird Electronics) that led to the salinity and temperature data reported in the **Figures 1C,D**.

Sampling sites were in different bays along the Tunisian coast from North (S1, S2, S3, and S4, located in the Gulf of Tunis and the Gulf of Hammamet) to South (S5, S6, S7, S8, S9, and S11, located in the Gulf of Gabès). These areas are subjected to different physical water properties: the Modified Atlantic Water mass was reported along the northeastern coasts whereas the saltier and warmer Modified Mediterranean Water (MMW) was detected in the Gulf of Gabès (Khammeri et al., 2020). Study area and methodologies used to collect and analyze environmental samples have been described in detail by Khammeri et al. (2020). Water biophysicochemical parameters, such as salinity, temperature, inorganic nutrients (i.e., nitrite: NO_2^-, nitrate: NO_3^-, ammonium: NH_4^+ (**Figure 1E**), orthophosphate: PO_4^{3-} (**Figure 1F**), silicate: $Si(OH)_4$, chlorophyll *a* (Chla) (**Figure 1G**) and planktonic population densities derived by flow-cytometry (i.e., *Synechococcus*, *Prochlorococcus*, pico-, and nano-eukaryotes) have been reported in **Table 1**.

For molecular diversity studies of prokaryotic communities, 3L seawater samples were first prefiltered through a 20-µm pore size mesh, then filtered on 2.7-µm pore size, 47-mm-diameter, GF/D filters, to remove large organisms. Picoplanktonic cells were subsequently collected on 0.2-µm pore size, 47-mm-diameter polyethersulfone (PES) filters before being transferred into cryovial tubes containing 3 mL of filtered (0.2-µm) lysis buffer (0.75 M sucrose, 50 mM Tris-HCl and 40 mM EDTA, pH = 8; Massana et al., 2004). Cryovials were immediately frozen in liquid nitrogen.

DNA Extraction, PCR, and Sequencing Analyses of 16S rRNA Gene Fragments

DNA extraction from 0.2-µm filters was carried out using a phenol/chloroform protocol detailed by Bellaaj-Zouari et al. (2018). The quality and concentration of DNA extracts was measured using a Nanodrop spectrophotometer (Nano Drop 2000 Thermo). DNA samples were stored at −80°C.

Bacterial and archaeal 16S rRNA gene V4 variable regions were amplified by PCR using the Pro341F/Pro805R prokaryotic universal primer set (Takahashi et al., 2014), with barcode on the forward primer, as previously described by Dowd et al. (2008), and were sequenced by the MiSeq Illumina (paired-end 2 × 300 bp) platform of the Molecular Research Laboratory (TX, United States).

Raw amplicon sequencing data were processed using DADA2 version 1.12.1, a model-based approach for correcting amplicon sequencing errors (Callahan et al., 2016). After the inspection of quality read profiles, the data processing steps includes quality filtering, dereplication, denoising, merging, inference of ASVs

TABLE 1 | Physicochemical parameters for seawater samples collected along the Tunisian coast in November 2013.

Samples	Location	Coordinates	Chla (ng/L)	Depth (m)	Density (mg/m^3)	Temperature (°C)	Salinity (g/L)	NO_2^- (μM)	NO_3^- (μM)	NH_4^+ (μM)	PO_4^{3-} (μM)	NT (μM)	PT (μM)	$Si(OH)_4$ (μM)
S1B	Tunis Gulf[1]	36.90 N 10.49 E	0	52	26.00	22.73	37.62	0.26	0.89	0.32	0.13	9.95	3.57	1.81
S2B	Hammamet Gulf[1]	36.80 N 11.23 E	0	59	26.05	22.68	37.66	0.11	1.13	0.33	0.07	9.38	3.39	2.59
S2S	Hammamet Gulf[1]	36.87 N 11.23 E	0	1	26.01	22.69	37.62	0.23	0.71	0.45	0.11	8.82	3.35	3.38
S3B	Hammamet Gulf[1]	36.09 N 11.18 E	0	74	26.30	21.53	37.55	0.06	1.16	0.37	0.17	8.99	2.57	1.44
S3S	Hammamet Gulf[1]	36.09 N 11.18 E	0	1	26.03	22.56	37.60	0.10	0.79	0.37	0.10	7.85	2.52	1.66
S4B	Hammamet Gulf[1]	35.48 N 11.54 E	0	78	26.94	18.85	37.45	0.10	1.09	0.35	0.14	8.69	3.13	2.46
S4S	Hammamet Gulf[1]	35.48 N 11.54 E	0	78	26.94	18.85	37.45	0.10	1.09	0.35	0.14	8.69	3.13	2.46
S5B	Gabès Gulf[2]	34.58 N 11.79 E	10.2	42	26.10	24.19	38.32	0.10	1.14	0.22	0.13	8.62	3.14	2.03
S5S	Gabès Gulf[2]	34.58 N 11.79 E	0	1	26.11	24.18	38.32	0.14	0.79	0.27	0.11	9.15	3.06	2.67
S6B	Gabès Gulf[2]	34.60 N 10.78 E	0	13	27.32	22.02	39.09	0.25	0.77	0.63	0.24	9.01	3.46	2.21
S6S	Gabès Gulf[2]	34.60 N 10.78 E	13.4	1	27.32	22.05	39.09	0.25	0.93	0.65	0.27	8.78	3.23	3.00
S7B	Gabès Gulf[2]	34.42 N 10.63 E	0	26	26.75	23.67	38.97	0.16	0.90	0.49	0.18	8.97	4.12	3.02
S7S	Gabès Gulf[2]	34.42 N 10.63 E	0	1	26.75	23.68	38.97	0.17	1.10	0.43	0.18	8.26	3.18	1.20
S8B	Gabès Gulf[2]	34.30 N 10.58 E	0	33	26.94	23.12	39.01	0.25	0.57	0.53	0.17	8.40	3.13	3.87
S8S	Gabès Gulf[2]	34.30 N 10.58 E	13.2	1	26.87	23.31	38.99	0.26	0.66	0.67	0.25	8.99	3.84	3.64
S9B	Gabès Gulf[2]	34.31 N 11.07 E	17.2	25	27.01	22.63	38.91	0.11	0.67	0.49	0.13	8.95	4.04	3.91
S9S	Gabès Gulf[2]	34.31 N 11.07 E	6.2	1	26.82	22.95	38.78	0.14	0.64	0.37	0.17	9.82	3.69	3.61
S11B	Gabès Gulf[2]	34.43 N 10.77 E	18.2	35	26.96	23.03	39.00	0.08	0.76	0.47	0.12	9.54	4.14	3.32
S11S	Gabès Gulf[2]	34.43 N 10.77 E	14.0	1	26.87	23.29	38.98	0.11	0.96	0.52	0.14	8.69	4.33	4.61

[1] *Tunisian northern bays.*
[2] *Tunisian southern bay.*

(Amplicon Sequence Variants, i.e., the true error-free sequences), and chimera removal. This process generates an error-corrected table of the abundances of ASVs in each sample. Because of low sequence number, one sample (S1S) was removed from the dataset for further analysis. The taxonomic assignment of ASVs were performed using the SILVA 16S rRNA gene reference (release 132) database (Quast et al., 2012). Finally, sub-sampling normalization, alpha and beta diversity were investigated by the Phyloseq and vegan R packages (McMurdie and Holmes, 2013; Oksanen et al., 2016).

Sequences from archaeal MGII ASVs were aligned using Muscle (Edgar, 2004) with related sequences from NCBI databases and sequences of *Thaumarchaeota* (MGI) which were used as outgroup. A phylogenetic tree was built with MEGA7 (Kumar et al., 2016) using the Maximum Likelihood method (Tamura and Nei, 1993). Tree topology confidence was determined by bootstrap analysis on 1000 replicates (Felsenstein, 1985).

Raw sequence data are available in the Sequence Read Archive (SRA) of NCBI under BioProject PRJNA632896, BioSamples SAMN14927758–SAMN14927776.

Statistical Analyses

Statistical analyses were performed with R version 3.6.0 (R Core Team, 2013) using R Studio environment version 1.2.1335. The alpha diversity was assessed by calculating global richness (number of observed ASVs), Shannon (Shannon and Weaver, 1949) and Simpson (Simpson, 1949) indices. The level of sequencing effort was evaluated by rarefaction curves of the observed richness using the *rarecurve* function implemented in the vegan R package. Principal coordinate analysis (PCoA) of beta diversity based on Bray-Curtis distance matrix (from ASVs) was performed for visualizing the distribution of samples along the Tunisian coast with the contribution of the 25 most abundant ASVs. Samples were categorized based on sampling location (North or South, i.e., Gulf of Gabès) or depth (surface, S, or bottom, B). Difference in the alpha diversity indices, the relative abundance of microbial taxa (phylum/class/order/family/genus) or water physicochemical parameters depending on sampling location or depth were assessed using the non-parametric Kruskal-Wallis test followed by Dunn's test with Bonferroni correction (according to the results of a Shapiro-Wilk normality test). *P* values of <0.05 were considered as statistically significant differences. A Spearman rank correlation test was chosen to investigate the correlations among abundant bacterial taxa (at genus level $>1\%$ of sequences per sample in average) and environmental parameters, and we accepted correlation coefficients (r_S) with associated *p*-values <0.05. Dominant genera were also analyzed by a heatmap based on *Z*-scores and a double hierarchical clustering (Ward method). The relationship between the dominant ASVs (selection of the top 40 ASVs, mean relative abundance $>0.5\%$) and environmental factors was carried out by Canonical correspondence analysis (CCA) with Vegan package. The *bioenv* function in the vegan R package selected the best combination of all environmental factors to explain the spatial patterns in the biological matrix. The CCA function used the ASV abundance matrix (transformed by log1p function) with the best combination of environmental factors. The *envfit* (permutation = 999) function fitted environmental factors onto the ordination for those with a *p*-value <0.05.

RESULTS

16S rRNA Gene Analysis and Alpha Diversity

A total of 20 seawater samples were collected and analyzed for prokaryotic community variation along the Tunisian coast, including 12 samples from the Gulf of Gabès (**Table 1**). The 16S rRNA gene sequencing of samples resulted in 868,099 raw sequences, which were further reduced to 438,375 after filtering, denoising, merging, and chimera checking. The rarefaction curves reached to asymptote (**Supplementary Figure S1**), indicating a sufficient sequencing effort to collect the overall prokaryotic diversity from the sampling.

The number of reads for each sample is reported in **Supplementary Table S1**. Across all samples, a total of 1,028 unique ASVs were identified. The number of observed ASVs varied from one sampling site to another, with a maximum (290 ASVs) for the station in the Gulf of Hammamet (North bay) at more than 60 m (S3F) and a minimum (143 ASVs) for the station near Sfax (South bay, Gabès Gulf, S6S). Based on the Simpson (D) and Shannon (H) indices, the microbial diversity in the northern samples ($D_{North} = 0.98 \pm 0.01$; $H_{North} = 4.43 \pm 0.22$) was statistically higher than that in the southern samples ($D_{South} = 0.96 \pm 0.01$; $H_{South} = 4.06 \pm 0.20$; $p_D = 0.012$; $p_H = 0.016$; **Figure 2**). Regarding all surface (S) and bottom (B) waters group samples, no difference in diversity indices was observed ($p > 0.05$). However, within the northern

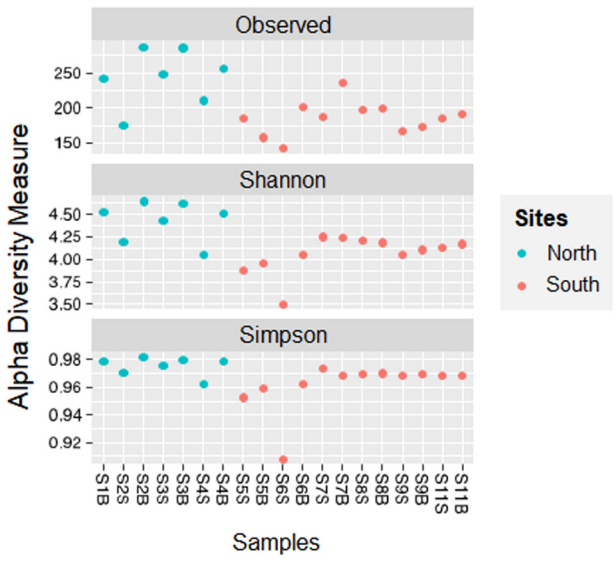

FIGURE 2 | Comparison of alpha diversity indices (Observed, Shannon, Simpson) between sampling sites and location groups (from North or South bays) along Tunisian coast.

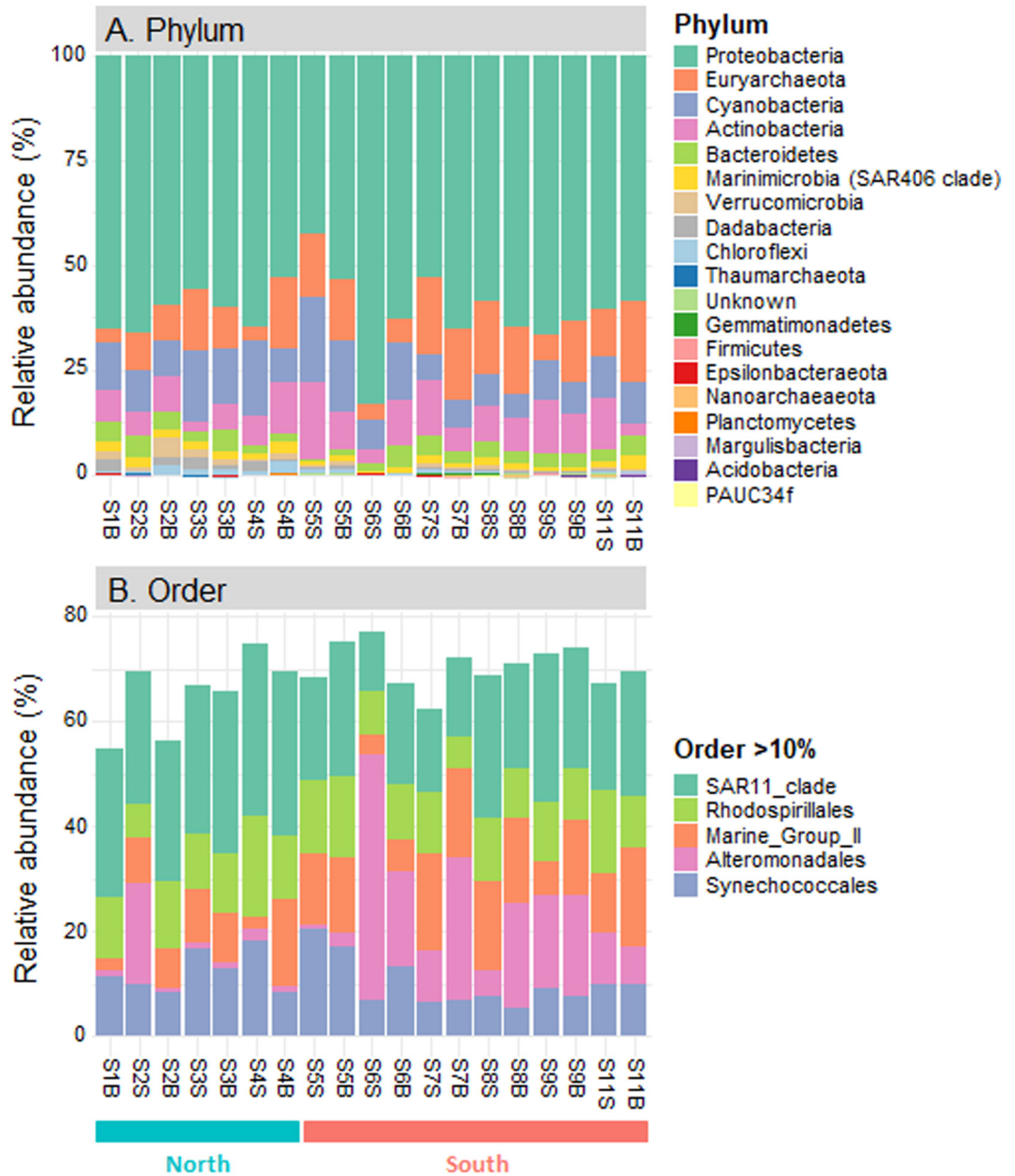

FIGURE 3 | Composition of prokaryotic communities in the seawater samples along the Tunisian coast (South Mediterranean Sea). Relative abundance of all prokaryotic phyla **(A)** and dominant orders (>10% in average, **B**).

waters, the diversity indices were higher at the bottom (B) than at the surface (S; $p_D = 0.049$; $p_H = 0.026$).

Prokaryotic Community Composition

Eighteen different phyla were identified across the seawater samples collected along the Tunisian coast, including *Acidobacteria*, *Actinobacteria*, *Bacteroidetes*, *Chloroflexi*, *Cyanobacteria*, *Dadabacteria*, *Epsilonbacteraeota*, *Euryarchaeota*, *Firmicutes*, *Gemmatimonadetes*, *Margulisbacteria*, *Marinimicrobia* (SAR406 clade), *Nanoarchaeaeota*, PAUC34f, *Planctomycetes*, *Proteobacteria*, *Thaumarchaeota*, and *Verrucomicrobia* (**Figure 3A**). Half of them (nine phyla) were present in all sampling sites and represented more than 99.9% of prokaryotic sequences. Among these nine ubiquitous phyla, *Proteobacteria* was predominant in all samples (60.8 ± 8.0%, 42.8–82.5%), followed by *Cyanobacteria* (10.9 ± 4.4%, 5.8–20.2%) and *Euryarchaeota* (12.0 ± 5.5, 2.8–19.5%; **Figure 3A**). These three major phyla (each >10% in average) accounted for 84.0% of all prokaryotic sequences. In addition, six other ubiquitous phyla were present at lower proportions, including *Actinobacteria* (8.6 ± 4.0%), *Bacteroidetes* (3.0 ± 1.4), and *Marinimicrobia* (SAR406 clade; 1.6 ± 0.7%), followed by

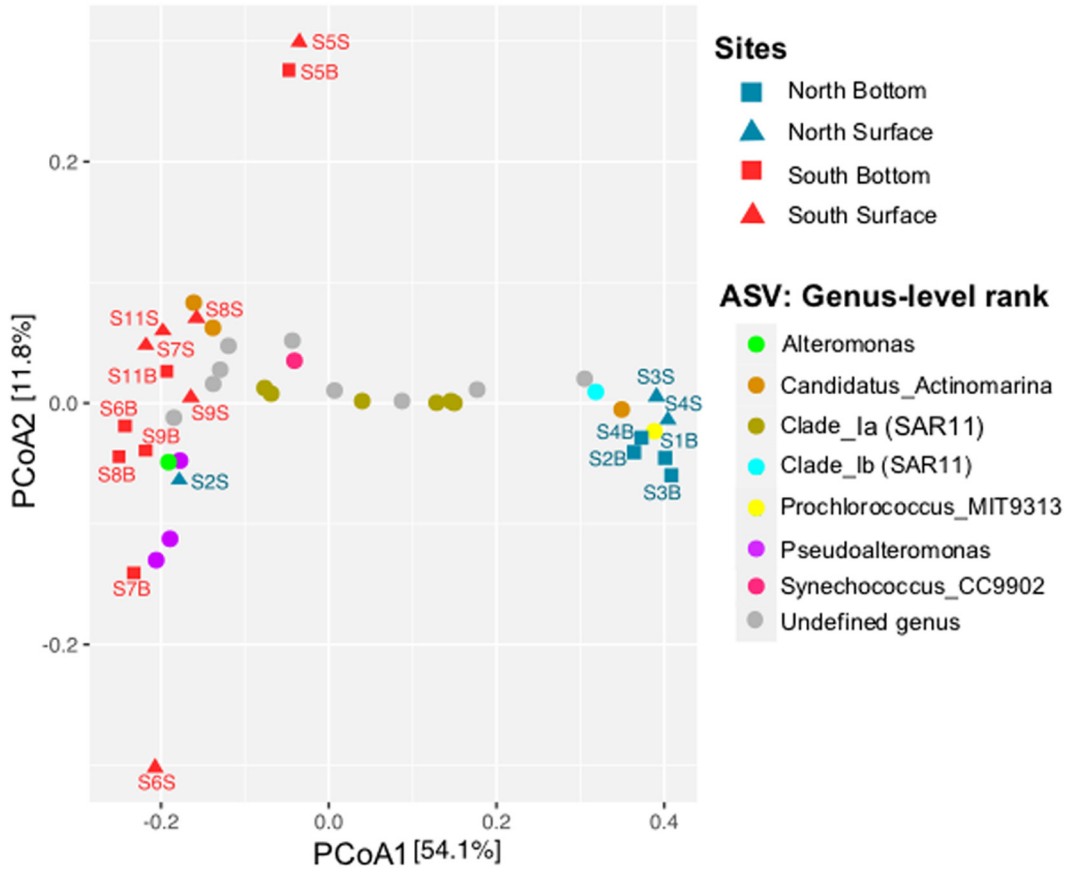

FIGURE 4 | Principal Coordinate Analysis (PCoA) ordination based on Bray-Curtis distance matrix from the prokaryotic community (ASV level) across all seawater samples collected along Tunisian coast. Sample locations are indicated by blue (North) or red (South) symbols (squares or triangles for bottom or surface waters, respectively). The distribution of the 25 most abundant ASVs is indicated by circles of different colors and their taxonomic affiliations are given in the legend at genus-level rank.

Verrucomicrobia, *Chloroflexi* (SAR202 cluster) and *Dadabacteria* (<1% in average). At lower taxonomic ranks, the prokaryotic communities were dominated by five dominant orders (each >10% in average): alphaproteobacterial *Pelagibacterales* (SAR11, 23.9% in average) and *Rhodospirillales* (11.4%), followed by archaeal Marine Group II (MGII, 11.3%), gammaproteobacterial *Alteromonadales* (11.0%) and cyanobacterial *Synechococcales* (10.9%) (**Figure 3B**).

Spatial Distribution of Abundant Prokaryotic Taxa

The PCoA plot based on the Bray-Curtis distance matrix of the prokaryotic community (ASV level) showed a spatial dichotomy between the North and the South sites (**Figure 4**). Indeed, the northern samples were ordinated close together (on the right, except for S2S), and separated from the southern samples by the first dimension (PCo1, 54.1% of the total variation). The southern samples (Gulf of Gabès) were relatively grouped together (on the left), but higher variability in the prokaryotic composition of the samples were observed compared to the North. Moreover, the southern samples S5S and S5B (located North of the Gabès Gulf) were mainly separated from the other samples by the second dimension (PCo2, 11.8% of the total variation). Regarding the spatial distribution of samples according to depth, surface (S) vs. bottom (B), no depth-related pattern in the prokaryotic community profiles were identified, regardless of the taxonomic rank ($p > 0.05$).

To examine at a finer resolution the differences in the prokaryotic communities within the samples, the contribution of the 25 most abundant ASVs was also visualized on the Bray-Curtis based PCoA plot (**Figure 4**). A heatmap with dendrogram was constructed using the 16 dominant genera (each >1% in average and accounting for 81.8% of sequences; **Figure 5**). The distribution of representative ASVs of each dominant genera was visualized by histograms (**Figure 6**). Both PCoA and heatmap clustering analysis revealed some differences in the prokaryotic relative abundance at ASV and genus levels between the northern or the southern bays, as observed at higher taxonomic ranks, e.g., class, order (**Figure 3B**).

At the genus level, *Prochlorococcus* and proteobacterial SAR11 Ib and II, SAR86, and SAR116 were more abundant in the North than in the South waters ($p < 0.005$, **Figure 5**). On the contrary, dominant gammaproteobacterial genera

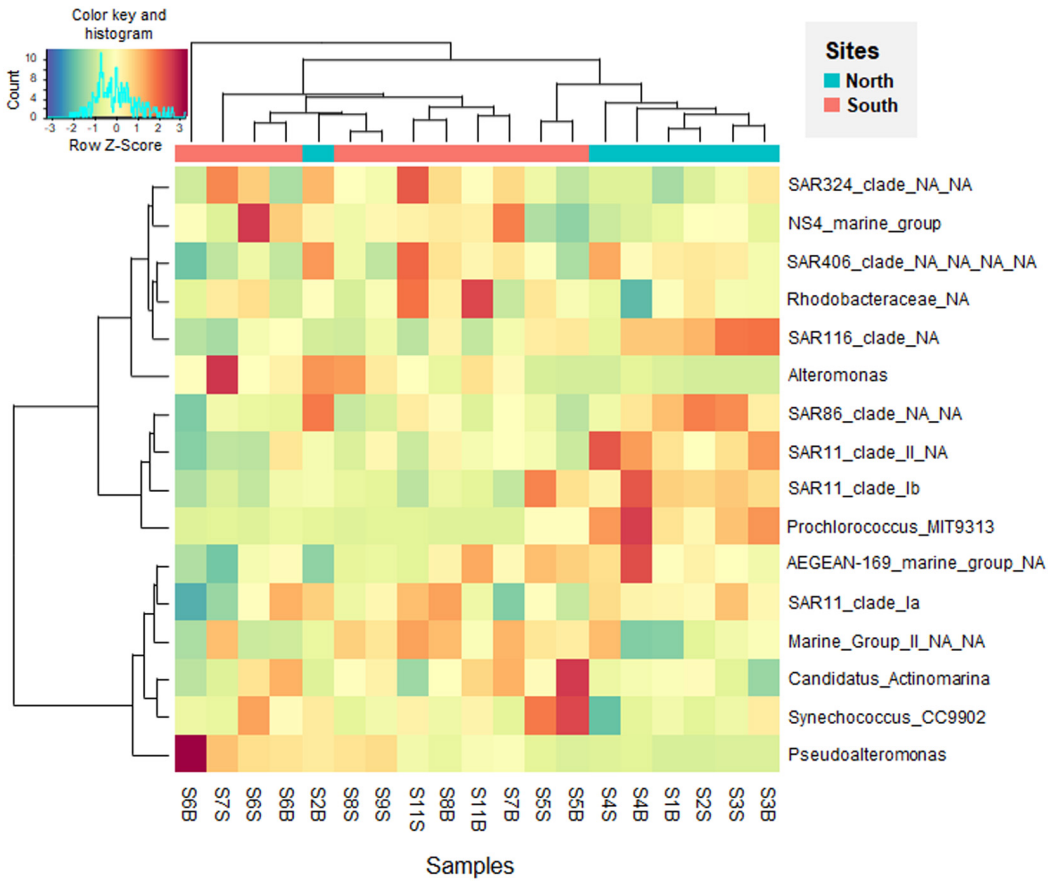

FIGURE 5 | Heatmap visualizing the *Z*-score distribution from the relative abundance of the dominant genera (> 1% in average) in the seawater samples along the Tunisian coast (South Mediterranean Sea). The dendogram clusters according to the Bray-Curtis similarity index.

Pseudoalteromonas (9.28% in average, dominated by ASVs 4 and 7) and *Alteromonas* (1.69%, dominated by ASV 15), significantly increased in the South (**Figures 5** and **6,** $p = 0.002$ and $p = 0.035$, respectively). Both *Alteromonas* and the deltaproteobacterial SAR324 (abundantly found in the South) were also detected in high proportion in the northern sample S2B grouped with southern samples (**Figure 5**), indicating that *Proteobacteria* seems to drive the northern site clustering with southern sites.

At ASV level, *Prochlorococcus* was related to the northern site clustering (in term of abundance, **Figure 4**), with SAR11 Ib and *Candidatus* Actinomarina, while both *Alteromonas* and *Pseudoalteromonas* ASVs were related to the southern site clustering (**Figure 4**). Pronounced differences between North and South waters were also observed at ASV level in the relative abundance of dominant archaeal MGIIb (ASV 29), and bacterial ASVs, such as AEGEAN_169 marine ASVs (e.g., ASVs 5 and 9; **Figure 6**). However, some difference disappeared at higher taxonomic rank (due to the ASV grouping into genus, family, and order). Indeed, no difference between the North and the South ($p \geq 0.05$) was observed in the distribution of the following major bacterial groups (at the genus level): SAR11 clade Ia (mainly represented by ASV 2), *Synechococcus* (dominated by ASV 1), AEGEAN_169 marine group (*Rhodospirillales*) and *Rhodobacteraceae* (**Figures 5**, **6**). No difference was also globally observed for the major archaeal order (MGII), dominated by ASV3 affiliated to the MGIIb representative, *Candidatus* Thalassoarchaea mediterranii (**Supplementary Figure S2**).

Relationships Between Prokaryotic Diversity and Environmental Variables

Canonical correspondence analysis was used to identify the biological and physicochemical environmental parameters that could influence prokaryotic composition in the coastal Tunisian waters (**Figure 7**). The first two constrained axes explained 49% (CCA1) and 9% (CCA2) of the total inertia (**Figure 7**). The first axis mostly separated the northern sites from the southern sites, while the second axis separated only the S5 site (South) from the others. The CCA analysis indicated that the prokaryotic composition was significantly related to three environmental factors including NH_4^+ ($p = 0.049$), temperature ($p = 0.012$) and silicates ($p = 0.003$). The highest levels of these three parameters were found at the southern sites (excepted S5 and S2B samples) (**Table 1**). The salinity parameter, which was not plotted, reaches the limit of significance ($p = 0.052$), and PO_4^{3-} was also not significant ($p < 0.05$).

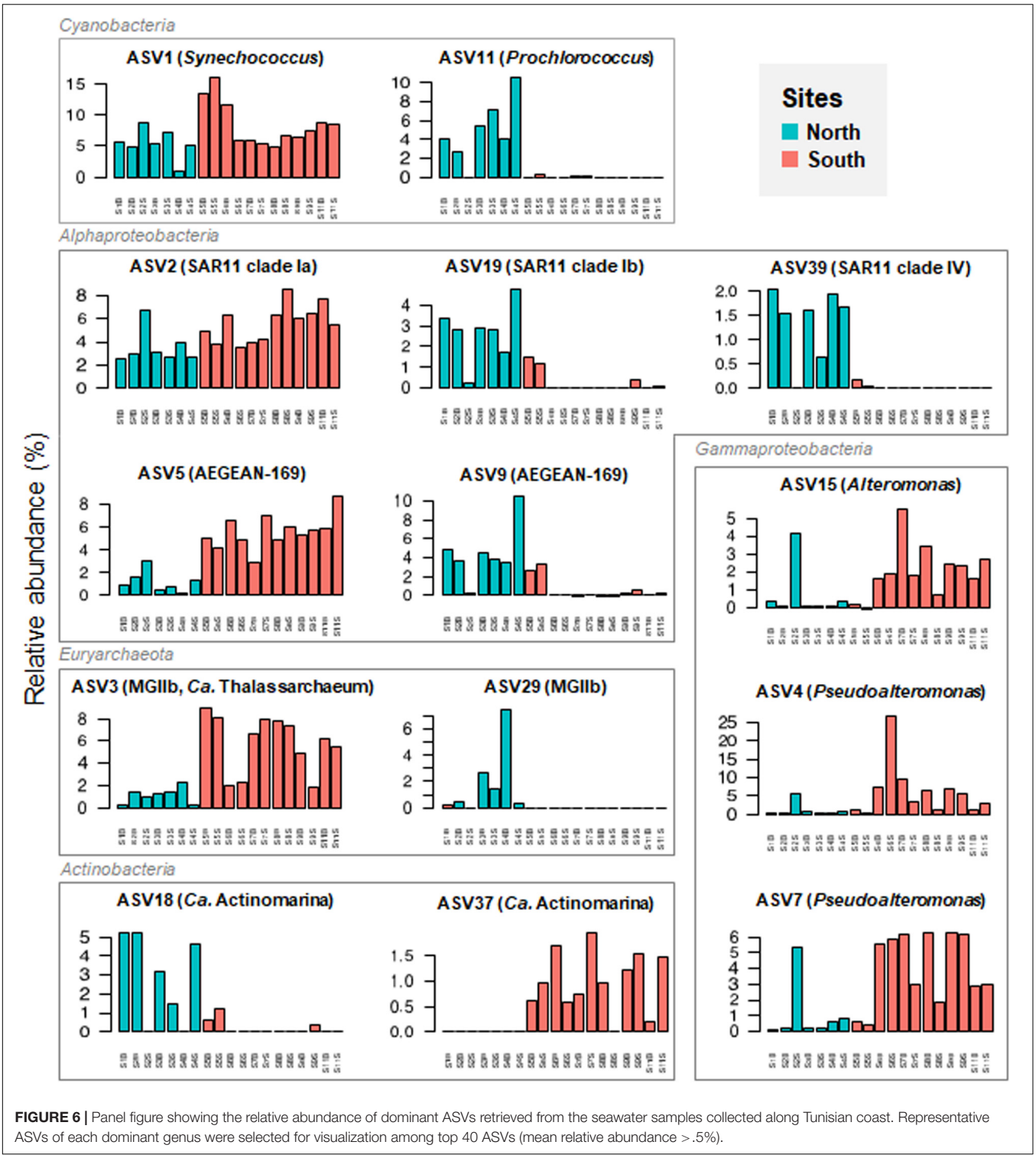

FIGURE 6 | Panel figure showing the relative abundance of dominant ASVs retrieved from the seawater samples collected along Tunisian coast. Representative ASVs of each dominant genus were selected for visualization among top 40 ASVs (mean relative abundance >.5%).

A Spearman's rank correlation analysis was also used to examine the relationships between the microbial diversity mainly represented by the abundant genera (>1%) and the environmental variables (**Supplementary Table S2**). Five environmental variables (Chla, density, NH_4^+, salinity, temperature) increased significantly in the southern samples ($p < 0.05$), with a more marked rise in salinity ($p < 0.0001$) and no significant correlation regarding the abundant *Synechococcus* and SAR11 clade Ia ($p > 0.05$; **Supplementary Table S2**). On the contrary, the gammaproteobacterial *Alteromonas* and *Pseudoalteromonas* proportions ($r = 0.83$, $p < 0.05$) were positively correlated with salinity ($r = 0.55$ and 0.70, respectively,

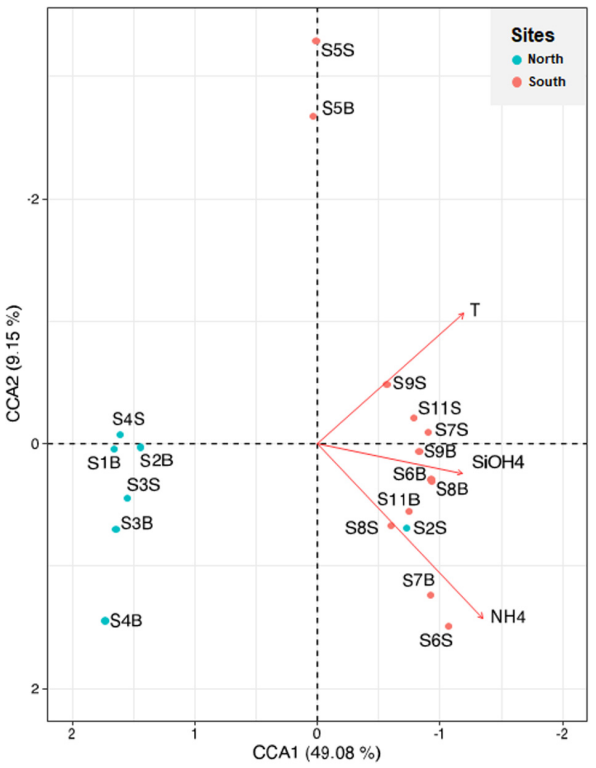

FIGURE 7 | Canonical correspondence analysis visualizing the relationships between physicochemical environmental variables (arrows) and sampling sites (black circles) derived from ASV abundance data. Significant environmental variables are displayed ($p < 0.05$). S1 to S4 sample originated from North Tunisian coast; S5 to S11 samples originate from South Tunisian coast. B and S mean Bottom and Surface waters, respectively.

$p < 0.05$), NH_4^+ ($r = 0.66$ and 0.75, respectively, $p < 0.05$), PO_4^{3-} and water densities (for *Pseudoalteromonas*, $r = 0.57$ and 0.63, respectively, $p < 0.05$), found in high levels in the Gabès Gulf waters. Rather, these *Alteromonadales* were negatively correlated with the levels of SAR11 subclades Ib and II and *Prochlorococcus* ($r = -0.74$–0.77, $p < 0.05$; **Supplementary Table S3**), which were negatively correlated with salinity ($r = -0.81$–0.92, $p < 0.05$), NH_4^+ ($r = -0.79$–0.86, $p < 0.05$), PT, PO_4^{3-} and water densities ($r = -0.50$–0.55 and $r = -0.52$–0.60, respectively, $p < 0.05$; **Supplementary Table S2**). Both SAR11 Ib and II were positively associated with *Prochloroccocus* ($r = -0.82$–0.83, $p < 0.05$; **Supplementary Table S3**), which were positively correlated with depth ($r = -0.50$–0.55, $p < 0.05$; **Supplementary Table S2**). *Rhodobacteraceae* was the only one to be positively correlated with the Chla levels ($r = 0.63$, $p < 0.05$), *Synechococcus* abundance, obtained by flow cytometry; $r = 0.82$, $p < 0.05$ (**Supplementary Table S4**) and *Synechococcus* relative abundance obtained by 16S rRNA gene sequencing analysis; $r = 0.59$, $p < 0.05$, while the archaeal MGII group was the only one to be positively correlated with temperature ($r = 0.59$, $p < 0.05$). Shannon and Simpson indices were inversely related to *Synechococcus* and *Prochlorococcus* proportions ($r = -0.52$–0.57, $p < 0.05$; **Supplementary Table S4**).

DISCUSSION

To date, diversity studies on prokaryotic communities using molecular approaches have received limited attention in coastal waters of the South Mediterranean Sea, despite the presence of marked physicochemical gradients and ecological threat caused by climatic changes and anthropogenic impacts, such as intensive agricultural and industrial activities, as well as international shipping and tourism development. To fill this gap, the planktonic prokaryotic diversity was investigated along the Tunisian coast. This study highlighted changes in the distribution of some microbial taxa from the northern to the southern waters depending on the following environmental variables: Chla, density, nutrients, salinity, and temperature. However, the absence of a depth-related variation in the overall prokaryotic community structure could be explained by the shallowness of the water column sampled and the absence of water stratification in all stations except the deepest station S4 (**Figure 1**). Indeed, the hydrodynamic conditions measured during the cruise are typically associated with the end of summer-fall stratification in the Mediterranean Sea and the beginning of winter mixing (Bel Hassen et al., 2009b; Bellaaj-Zouari et al., 2018).

The order *Pelagibacteriales* (SAR11) is the most relatively abundant prokaryotic component thriving in coastal Tunisian seawaters, in agreement with previous studies on other Mediterranean Sea areas (Zaballos et al., 2006; Alonso-Sáez et al., 2007; Feingersch et al., 2010; Grote et al., 2012; Laghdass et al., 2012; Viklund et al., 2013; Estrada and Vaqué, 2014; Haber et al., 2020). It was dominated by the genus *Pelagibacter* (SAR11 subclade Ia; 15.3% of the prokaryotes), represented by very small cultivated species adapted to nutrient-limited conditions, and involved in the remineralization of low molecular weight organic matter (Morris et al., 2002; Rappé et al., 2002; Giovannoni et al., 2005; Brown et al., 2012). Along the Tunisian coast, no significant spatial difference in the *Pelagibacter* proportion was observed, while the occurrences of some SAR11 subclades (Ib, II, and IV) decreased significantly from North to South (Gulf of Gabès). Since SAR11 contributed up to 25% of total prokaryotes in Tunisian waters, the distribution changes within the subclades may have important implications on the biogeochemical cycles. Despite its ubiquity and abundance, the distribution and activity of the different SAR11 subclades depending on environmental variables were still unclear, as previously reported in the northwestern Mediterranean surface waters (Laghdass et al., 2012; Salter et al., 2015). In our study, the levels of SAR11 Ib and II were negatively correlated to salinity ($r = -0.85$ and -0.76, respectively) and SAR11 Ib was also negatively correlated to NH_4^+ ($r = -0.79$) and PO_4^{3-} ($r = -0.64$), suggesting that the low proportions of these SAR11 subclades in the Gabes Gulf may be due to its salty, and nutrient-rich waters. Unlike a previous study conducted along a halocline in the Balic Sea (Herlemann et al., 2014), these subclades have not been substituted in the Gabes Gulf by others oligotrophic SAR11 subclades, which prefer low-nutrient environments (Giovannoni, 2017).

Pronounced differences in the cyanobacterial relative abundances were also observed between the northern and the southern Tunisian seawaters. Changes in the *Prochlorococcus*

distribution along the Tunisian coast were consistent with previous flow cytometry data obtained according to the described water masses (Khammeri et al., 2020). The *Prochlorococcus* abundance was high in the North corresponding to the MAW and considerably decreased in the shallow, salty, and nutrient-rich waters of the South (where they were absent in the samples S6F, S6S, S8S, S8F, and S11S) corresponding to the MMW. Here, *Prochlorococcus* proportion was negatively correlated to NH_4^+ ($r = -0.86$), PO_4^{3-} ($r = -0.55$) and salinity ($r = -0.92$), found in high levels in the Gabès Gulf waters. Indeed, *Prochlorococcus* preferentially thrives in oligotrophic (nutrient-poor), warm, and stratified waters, usually in summer/fall and is generally absent from eutrophic areas (Chisholm et al., 1988; Partensky et al., 1999b; Durand et al., 2001; Mella-Flores et al., 2012). The highest proportions of the ubiquitous *Synechococcus* observed in southern samples (S5S, S5B, and S6S), suggesting that *Synechococcus* is more adapted than *Prochlorococcus* to the hydrodynamic and nutrient-rich conditions of the Gabès Gulf. Indeed, *Synechococcus* genus is known to be widely distributed, but it is most abundant in well-lit and nutrient-rich waters, usually in a well-mixed coastal water column (Waterbury et al., 1979; Partensky et al., 1999a; Zwirglmaier et al., 2008). Similar trend was also observed along the eastern coast of the Adriatic Sea located North of the Eastern Mediterranean basin (Šantić et al., 2011) and in other marine areas (Flombaum et al., 2013; van den Engh et al., 2017).

The gammaproteobacterial order *Alteromonadales* was more prevalent in the southern waters (Gabès Gulf), than in northern waters (except in S2S). Both *Alteromonas* and *Pseudoalteromonas* proportions were positively correlated with salinity, NH_4^+, PO_4^{3-} and water densities, found in high levels in the Gabès Gulf waters. *Pseudoalteromonas* was more abundant than *Alteromonas* in the Gabès Gulf waters, especially in the surface waters S6S (near the Sfax City), where it accounted for 43.81% of the prokaryotes. These typical marine heterotrophs play important roles in the biodegradation of marine organic matter, such as organic nitrogen and phosphorous mineralization, owing to their high production of proteases and extracellular alkaline phosphatases (Thomas et al., 2008; Zhou et al., 2009; Li et al., 2015; Liu and Liu, 2020). Indeed, higher organic phosphorous in the South than in the North (Khammeri et al., 2020) may induce active biodegradation processes by these heterotrophic organisms. Other heterotrophs detected in nutrient-rich Gabès Gulf waters were related to *Deltaproteobacteria* (SAR324 clade, also involved in sulfur oxidation and carbon fixation, Sheik et al., 2014), as well as to *Actinobacteria* (Ca. *Actinomarina*) and *Bacteroidetes* (NS4 marine group) also known as key players of the organic matter processing (i.e., transport and degradation) in oceans (Kirchman, 2002; Ghai et al., 2013; Anandan et al., 2016). Several studies have reported changes in microbial community composition with a dominance of heterotrophs in marine mesocosms and Mediterranean ecosystems enriched with minerals and nutrients, such as coastal urbanized areas (Allers et al., 2007; Rekik et al., 2014; Richa et al., 2017). The Gulf of Gabès is impacted by industrial and municipal discharges that increase toxic metals (such as cadmium) and nutrients (such as PO_4^{3-}) in marine environment, that cause seawater pollution (e.g., eutrophication) and microbial diversity changes (Zouch et al., 2017, 2018; Chifflet et al., 2019).

Beyond abiotic factors, heterotrophic microorganisms can impact and interact with a wide range of prokaryotic organisms in marine ecosystems. Heterotrophic *Pseudoalteromonas* species exhibit high extracellular activities and antimicrobial properties allowing them to hydrolyze complex molecules and to be extremely competitive for nutrients (Holmström and Kjelleberg, 1999). In our study, the relative abundance of both heterotrophic *Pseudoalteromonas* and *Alteromonas* were negatively correlated with photosynthetic *Prochlorococcus* ($r = -0.71$–0.75), accordingly to previous co-culture findings (Becker et al., 2019). On the contrary, the relative abundance of *Prochlorococcus* was positively correlated with some SAR11 clades (Ib and IV) ($r = 0.82$–0.83), in agreement with the study of Becker et al. (2019) showing that SAR11 grew faster in co-culture with *Prochlorococcus*, likely due to the production and release of glycine betaine by this latter. This result suggests that some SAR11 clades, detected in low abundance in the South, might be also influenced by the *Prochlorococcus* decrease in the Gabès Gulf. The relative abundance of *Rhodobacteraceae* was also positively correlated to *Synechococcus* and chlorophyll *a* ($r = 0.63$–0.71), suggesting a link with phytoplankton biomass, as revealed by a previous study in marine water mesocosms (Allers et al., 2007).

Archaea were well represented in all Tunisian coastal seawater samples (>10% of the prokaryotes) and were mainly composed of the candidate order "Poseidoniales" (MGII), as observed in coastal northwest Mediterranean Sea and in surface waters of different marine areas around the world (Galand et al., 2010; Hugoni et al., 2013; Pereira et al., 2019; Rinke et al., 2019; Santoro et al., 2019). In our winter study, the MGIIb group (Candidatus *Thalassarchaeaceae*, represented by the ASVs 3, 21, 29, 40) was more abundant that the MGIIa (represented by the ASVs 28 and 41) in seawaters. These results agree with previous data on the northwest Mediterranean Sea showing MGIIb as a major archaeal group in winter, while MGIIa predominated in summer (Galand et al., 2010; Hugoni et al., 2013; Martin-Cuadrado et al., 2015). Recent MGII genomic analyses provide evidence for a photoheterotrophic lifestyle combining phototrophy via proteorhodopsins with organic matter remineralization (Martin-Cuadrado et al., 2015; Tully, 2019). In shallow Tunisian coastal waters, both MGIII and *Thaumarchaeota* (mainly ammonia-oxidizing *Nitrososphaera*) were detected in low abundance (<1% and <0.1% of the prokaryotes, respectively), in accordance with their known prevalence in deep waters (Techtmann et al., 2015; Santoro et al., 2019). The predominance of MGIII in the surface waters of the Gulf of Hammamet (S3S, 4.56% of the prokaryotes), displaying the lowest level of PO_4^{3-}, may be explained by the presence in its genomes of photolyase genes and phosphonate uptake, which may serve as a phosphorus source in inorganic phosphorus-deficient waters (Santoro et al., 2019). Finally, *Nanoarchaeota* were exclusively found in extremely low proportion (around 0.02%) in the bottom waters of the Gabès Gulf and they are known as small parasitic or symbiotic Archaea (Amils, 2014).

In conclusion, our findings on prokaryotic diversity in seawater samples along the Tunisian coast increase our knowledge on microbial biodiversity and potential ecosystem functioning in the understudied regions of the South Mediterranean Sea. Amplicon sequencing-based prokaryotic community analysis allowed us to identify typical dominant and ubiquitous marine taxa affiliated to phyla *Proteobacteria* (alphaproteobacterial SAR11 clade and gammaproteobacterial *Alteromonadales*), *Cyanobacteria* (*Synechococcales*), and *Euryarchaeota* ("Poseidoniales"). Our comparative analysis between the North and South Tunisian bays showed several changes in the prokaryotic community composition, especially within the SAR11 clade, the order *Alteromonadales* and the order *Synechococcales*. A significant increase in the levels of the genera *Pseudoalteromonas* and *Alteromonas* were observed in the southern waters (Gulf of Gabès), compared to northern bays, and was inversely related to *Prochlorococcus* proportion. These changes may be explained by the difference in physical water properties, mainly temperature and nutrient content and Chla concentrations, in accordance with previous studies in the Mediterranean Sea. It is worthy to continue analyzing the diversity of the microbial community in future investigations toward larger spatial and temporal scales in the South Mediterranean Sea, in order to confirm these microbial biodiversity patterns and better understand the important biogeochemical processes mediated by specific microbial groups in a context of global climatic change and/or human-induced environmental changes.

DATA AVAILABILITY STATEMENT

The datasets presented in this study can be found in online repositories. The names of the repository/repositories and accession number(s) can be found in the article/ **Supplementary Material**.

AUTHOR CONTRIBUTIONS

AB-Z, MB, and YK performed the water sampling during the INCOMMET cruise aboard the *N/O Hannibal*. YK performed core parameter analyses. AB-Z performed DNA extraction. MQ processed the Illumina MiSeq data with the help of FA. MQ wrote the first draft of the manuscript. All authors were involved in the critical revision and approval of the final version.

FUNDING

This study was partially financed by the European funded project "Improving National Capacities in Observation and Management of Marine Environment in Tunisia" (INCOMMET, 295009), the Institute of Research for Development (IRD), and the Tunisian Ministry of Higher Education and Scientific Research through the Laboratoire Mixte International (LMI) COSYS-Med (Contaminants et Ecosystèmes Marins Sud Méditerranéens).

ACKNOWLEDGMENTS

We would like to thank the captain and the crew of the RV "Hannibal" for their help during the INCOMMET cruise. The project leading to this publication has received funding from European FEDER Fund under project 1166-39417.

SUPPLEMENTARY MATERIAL

The Supplementary Material for this article can be found online at: https://www.frontiersin.org/articles/10.3389/fmicb.2020.593540/full#supplementary-material

REFERENCES

Allers, E., Gomez-Consarnau, L., Pinhassi, J., Simek, K., Gasol, J. M., and Pernthaler, J. (2007). Population dynamics of Alteromonas and Roseobacter in marine mesocosms after substrate and nutrient manipulations. *Environ. Microbiol.* 9, 2417–2429.

Alonso-Sáez, L., Balagué, V., Sà, E. L., Sánchez, O., González, J. M., Pinhassi, J., et al. (2007). Seasonality in bacterial diversity in north-west Mediterranean coastal waters: assessment through clone libraries, fingerprinting and FISH. *FEMS Microbiol. Ecol.* 60, 98–112. doi: 10.1111/j.1574-6941.2006.00276.x

Amils, R. (2014). "Nanoarchaeota," in *Encyclopedia of Astrobiology*, eds R. Amils et al. (Heidelberg: Springer).

Anandan, R., Dharumadurai, D., and Manogaran, G. P. (2016). "An introduction to actinobacteria," in *Actinobacteria-Basics and Biotechnological Applications*, eds D. Dhanasekaran and Y. Jiang (Rijeka: Intechopen), 3–37.

Ayata, S. D., Irisson, J. O., Aubert, A., Berline, L., Dutay, J. C., Mayot, N., et al. (2018). Regionalisation of the Mediterranean basin, a MERMEX synthesis. *Progr. Oceanogr.* 163, 7–20. doi: 10.1016/j.pocean.2017.09.016

Azam, F., and Malfatti, F. (2007). Microbial structuring of marine ecosystems. *Nat. Rev. Microbiol.* 5, 782–791. doi: 10.1038/nrmicro1747

Bao, P., Li, G.-X., Sun, G.-X., Xu, Y.-Y., Meharg, A. A., and Zhu, Y.-G. (2018). The role of sulfate-reducing prokaryotes in the coupling of element biogeochemical cycling. *Sci. Total Environ.* 61, 398–408. doi: 10.1016/j.scitotenv.2017.09.062

Becker, J. W., Hogle, S. L., Rosendo, K., and Chisholm, S. W. (2019). Co-culture and biogeography of *Prochlorococcus* and SAR11. *ISME J.* 13, 1506–1519. doi: 10.1038/s41396-019-0365-4

Béjaoui, B., Ben Ismail, S., Othmani, A., Ben Hadj Hamida, O., Chevalier, C., Feki, W., et al. (2019). Synthesis review of the Gulf of Gabes (eastern Mediterranean Sea, Tunisia): morphological, climatic, physical oceanographic, biogeochemical and fisheries features. *Estuar. Coast. Shelf Sci.* 219, 395–408. doi: 10.1016/j.ecss.2019.01.006

Bel Hassen, M., Drira, Z., Hamza, A., Ayadi, H., Akrout, F., Messaoudi, S., et al. (2009a). Phytoplankton dynamics related to water mass properties in the Gulf of Gabès, ecological implications. *J. Mar. Syst.* 75, 216–226. doi: 10.1016/j.jmarsys.2008.09.004

Bel Hassen, M., Hamza, A., Drira, Z., Zouari, A., Akrout, F., Messaoudi, S., et al. (2009b). Phytoplankton-pigment signatures and their relationship to spring–summer stratification in the Gulf of Gabes. *Estuar. Coast. Shelf Sci.* 83, 296–306. doi: 10.1016/j.ecss.2009.04.002

Bellaaj-Zouari, A., Belhassen, M., Balagué, V., Sahli, E., Kacem, M. Y. B., Akrout, F., et al. (2018). Picoeukaryotic diversity in the Gulf of Gabès: variability patterns and relationships to nutrients and water masses. *Aquat. Microb. Ecol.* 81, 37–53. doi: 10.3354/ame01857

Brown, M. V., Lauro, F. M., DeMaere, M. Z., Muir, L., Wilkins, D., Thomas, T., et al. (2012). Global biogeography of SAR11 marine bacteria. *Mol. Syst. Biol* 8:595. doi: 10.1038/msb.2012.28

Callahan, B. J., McMurdie, P. J., Rosen, M. J., Han, A. W., Johnson, A. J. A., and Holmes, S. P. (2016). DADA2: high-resolution sample inference from Illumina amplicon data. *Nat. Methods* 13, 581–583. doi: 10.1038/nmeth.3869

Carlson, C. A., Hansell, D. A., Nelson, N. B., Siegel, D. A., Smethie, W. M., and Khatiwala, S. (2010). Dissolved organic carbon export and subsequent remineralization in the mesopelagic and bathypelagic realms of the North Atlantic basin. *Deep Sea Res. II Top. Stud. Oceanogr.* 57, 1433–1445. doi: 10.1016/j.dsr2.2010.02.013

Carlson, C. A., Morris, R., Parsons, R., Giovannoni, S. J., and Vergin, K. (2009). Seasonal dynamics of SAR11 populations in the euphotic and mesopelagic zones of the northwestern Sargasso Sea. *ISME J.* 3, 283–295. doi: 10.1038/ismej.2008.117

Chifflet, S., Tedetti, M., Zouch, H., Fourati, R., Zaghden, H., Elleuch, B., et al. (2019). Dynamics of trace metals in a shallow coastal ecosystem: insights from the Gulf of Gabès (southern Mediterranean Sea). *AIMS Environ. Sci.* 6, 277–297. doi: 10.3934/environsci.2019.4.277

Chisholm, S. W., Olson, R. J., Zettler, E. R., Goericke, R., Waterbury, J. B., and Welschmeyer, N. A. (1988). A novel free-living prochlorophyte abundant in the oceanic euphotic zone. *Nature* 334, 340–343. doi: 10.1038/334340a0

Coll, M., Piroddi, C., Steenbeek, J., Kaschner, K., Lasram, F. B. R., Aguzzi, J., et al. (2010). The biodiversity of the Mediterranean Sea: estimates, patterns, and threats. *PLoS One* 5:e11842. doi: 10.1371/journal.pone.0011842

Cotner, J. B., and Biddanda, B. A. (2002). Small players, large role: microbial influence on biogeochemical processes in pelagic aquatic ecosystems. *Ecosystems* 5, 105–121. doi: 10.1007/s10021-001-0059-3

Dowd, S. E., Callaway, T. R., Wolcott, R. D., Sun, Y., McKeehan, T., Hagevoort, R. G., et al. (2008). Evaluation of the bacterial diversity in the feces of cattle using 16S rDNA bacterial tag-encoded FLX amplicon pyrosequencing (bTEFAP). *BMC Microbiol.* 8:125. doi: 10.1186/1471-2180-8-125 doi: 10.1186/1471-2180-8-125

Durand, M. D., Olson, R. J., and Chisholm, S. W. (2001). Phytoplankton population dynamics at the Bermuda Atlantic Time-series station in the Sargasso Sea. *Deep Sea Res. II Top. Stud. Oceanogr.* 48, 1983–2004. doi: 10.1016/s0967-0645(00)00166-1

Edgar, R. C. (2004). MUSCLE: multiple sequence alignment with high accuracy and high throughput. *Nucleic Acids Res.* 32, 1792–1797. doi: 10.1093/nar/gkh340

Estrada, M., and Vaqué, D. (2014). "Microbial components," in *The Mediterranean Sea*, eds S. Goffredo and Z. Dubinsky (Dordrecht: Springer), 87–111. doi: 10.1007/978-94-007-6704-1_6

Evans, C., Gómez-Pereira, P. R., Martin, A. P., Scanlan, D. J., and Zubkov, M. V. (2015). Photoheterotrophy of bacterioplankton is ubiquitous in the surface oligotrophic ocean. *Prog. Oceanogr.* 135, 139–145. doi: 10.1016/j.pocean.2015.04.014

Falkowski, P. G., Fenchel, T., and Delong, E. F. (2008). The microbial engines that drive Earth's biogeochemical cycles. *Science* 320, 1034–1039. doi: 10.1126/science.1153213

Feingersch, R., Suzuki, M. T., Shmoish, M., Sharon, I., Sabehi, G., Partensky, F., et al. (2010). Microbial community genomics in eastern Mediterranean Sea surface waters. *ISME J.* 4, 78–87. doi: 10.1038/ismej.2009.92

Felsenstein, J. (1985). Confidence limits on phylogenies: an approach using the bootstrap. *Evolution* 39, 783–791. doi: 10.2307/2408678

Flemming, H. C., and Wuertz, S. (2019). Bacteria and archaea on Earth and their abundance in biofilms. *Nat. Rev. Microbiol.* 17, 247–260. doi: 10.1038/s41579-019-0158-9

Flombaum, P., Gallegos, J. L., Gordillo, R. A., Rincón, J., Zabala, L. L., Jiao, N., et al. (2013). Present and future global distributions of the marine Cyanobacteria *Prochlorococcus* and *Synechococcus*. *Proc. Natl Acad. Sci. U.S.A.* 110, 9824–9829.

Galand, P. E., Gutiérrez-Provecho, C., Massana, R., Gasol, J. M., and Casamayor, E. O. (2010). Inter-annual recurrence of archaeal assemblages in the coastal NW Mediterranean Sea (Blanes Bay Microbial Observatory). *Limnol. Oceanogr.* 55, 2117–2125. doi: 10.4319/lo.2010.55.5.2117

Ghai, R., Mizuno, C. M., Picazo, A., Camacho, A., and Rodriguez-Valera, F. (2013). Metagenomics uncovers a new group of low GC and ultra-small marine Actinobacteria. *Sci. Rep.* 3:2471.

Ghiglione, J. F., Larcher, M., and Lebaron, P. (2005). Spatial and temporal scales of variation in bacterioplankton community structure in the NW Mediterranean Sea. *Aquat. Microb. Ecol.* 40, 229–240. doi: 10.3354/ame040229

Giovannoni, S. J. (2017). SAR11 bacteria: the most abundant plankton in the oceans. *Annu. Rev. Mar. Sci.* 9, 231–255. doi: 10.1146/annurev-marine-010814-015934

Giovannoni, S. J., Tripp, H. J., Givan, S., Podar, M., Vergin, K. L., Baptista, D., et al. (2005). Genome streamlining in a cosmopolitan oceanic bacterium. *Science* 309, 1242–1245. doi: 10.1126/science.1114057

Grote, J., Thrash, J. C., Huggett, M. J., Landry, Z. C., Carini, P., Giovannoni, S. J., et al. (2012). Streamlining and core genome conservation among highly divergent members of the SAR11 clade. *mBio* 3:e00252-12.

Haber, M., Rosenberg, D. R., Lalzar, M., Burgsdorf, I., Saurav, K., Lionheart, R., et al. (2020). Microbial communities in an ultraoligotrophic sea are more affected by season than by distance from shore. *bioRxiv* [Preprint]. doi: 10.1101/2020.04.17.044305

Hamdi, I., Denis, M., Bellaaj-Zouari, A., Khemakhem, H., Hassen, M. B., Hamza, A., et al. (2015). The characterisation and summer distribution of ultraphytoplankton in the Gulf of Gabès (Eastern Mediterranean Sea, Tunisia) by using flow cytometry. *Cont. Shelf Res.* 93, 27–38. doi: 10.1016/j.csr.2014.10.002

Hazan, O., Silverman, J., Sisma-Ventura, G., Ozer, T., Gertman, I., Shoham-Frider, E., et al. (2018). Mesopelagic prokaryotes alter surface phytoplankton production during simulated deep mixing experiments in eastern mediterranean sea waters. *Front. Mar. Sci.* 5:1. doi: 10.3389/fmars.2018.00001

Herlemann, D. P. R., Woelk, J., Labrenz, M., and Jürgens, K. (2014). Diversity and abundance of "Pelagibacterales" (SAR11) in the Baltic Sea salinity gradient. *Syst. Appl. Microbiol.* 37, 601–604. doi: 10.1016/j.syapm.2014.09.002

Holmström, C., and Kjelleberg, S. (1999). Marine Pseudoalteromonas species are associated with higher organisms and produce biologically active extracellular agents. *FEMS Microbiol. Ecol.* 30, 285–293. doi: 10.1016/s0168-6496(99)00063-x

Hugoni, M., Taib, N., Debroas, D., Domaizon, I., Dufournel, I. J., Bronner, G., et al. (2013). Structure of the rare archaeal biosphere and seasonal dynamics of active ecotypes in surface coastal waters. *Proc. Natl Acad. Sci. U.S.A.* 110, 6004–6009. doi: 10.1073/pnas.1216863110

Khammeri, Y., Bellaaj-Zouari, A., Hamza, A., Medhioub, W., Sahli, E., Akrout, F., et al. (2020). Ultraphytoplankton community composition in Southwestern and Eastern Mediterranean Basin: relationships to water mass properties and nutrients. *J. Sea Res.* 158:101875. doi: 10.1016/j.seares.2020.101875

Kirchman, D. L. (2002). The ecology of *Cytophaga*-Flavobacteria in aquatic environments. *FEMS Microbiol. Ecol.* 39, 91–100. doi: 10.1016/s0168-6496(01)00206-9

Kumar, S., Stecher, G., and Tamura, K. (2016). MEGA7: molecular evolutionary genetics analysis version 7.0 for bigger datasets. *Mol. Biol. Evol.* 33, 1870–1874. doi: 10.1093/molbev/msw054

Laghdass, M., Catala, P., Caparros, J., Oriol, L., Lebaron, P., and Obernosterer, I. (2012). High contribution of SAR11 to microbial activity in the north west Mediterranean Sea. *Microb. Ecol.* 63, 324–333. doi: 10.1007/s00248-011-9915-7

Li, M., Baker, B. J., Anantharaman, K., Jain, S., Breier, J. A., and Dick, G. J. (2015). Genomic and transcriptomic evidence for scavenging of diverse organic compounds by widespread deep-sea archaea. *Nat. Commun.* 6:8933.

Liu, J., Weinbauer, M. G., Maier, C., Dai, M., and Gattuso, J. P. (2010). Effect of ocean acidification on microbial diversity and on microbe-driven biogeochemistry and ecosystem functioning. *Aquat. Microb. Ecol.* 61, 291–305. doi: 10.3354/ame01446

Liu, S., and Liu, Z. (2020). Distinct capabilities of different Gammaproteobacterial strains on utilizing small peptides in seawater. *Sci. Rep.* 10:464.

Martin-Cuadrado, A. B., Garcia-Heredia, I., Molto, A. G., Lopez-Ubeda, R., Kimes, N., López-García, P., et al. (2015). A new class of marine Euryarchaeota group II from the mediterranean deep chlorophyll maximum. *ISME J.* 9, 1619–1634. doi: 10.1038/ismej.2014.249

Massana, R., Balagué, V., Guillou, L., and Pedros-Alio, C. (2004). Picoeukaryotic diversity in an oligotrophic coastal site studied by molecular and culturing approaches. *FEMS Microbiol. Ecol.* 50, 231–243. doi: 10.1016/j.femsec.2004.07.001

Massana, R., DeLong, E. F., and Pedrós-Alió, C. (2000). A few cosmopolitan phylotypes dominate planktonic archaeal assemblages in widely different oceanic provinces. *Appl. Environ. Microbiol.* 66, 1777–1787. doi: 10.1128/aem.66.5.1777-1787.2000

McMurdie, P. J., and Holmes, S. (2013). phyloseq: an R package for reproducible interactive analysis and graphics of microbiome census data. *PLoS One* 8:e61217. doi: 10.1371/journal.pone.0061217

Mella-Flores, D., Six, C., Ratin, M., Partensky, F., Boutte, C., Le Corguillé, G., et al. (2012). *Prochlorococcus* and *Synechococcus* have evolved different adaptive mechanisms to cope with light and UV stress. *Front. Microbiol.* 3:285. doi: 10.3389/fmicb.2012.00285

Morris, R. M., Rappé, M. S., Connon, S. A., Vergin, K. L., Siebold, W. A., Carlson, C. A., et al. (2002). SAR11 clade dominates ocean surface bacterioplankton communities. *Nature* 420, 806–810. doi: 10.1038/nature01240

Oksanen, J., Blanchet, F., Kindt, R., Legendre, P., and O'Hara, R. (2016). *Vegan: Community Ecology Package. R Package* 2.3-3.

Oren, A. (2004). Prokaryote diversity and taxonomy: current status and future challenges. *Philos. Trans. R. Soc. Lond. B Biol. Sci.* 359, 623–638. doi: 10.1098/rstb.2003.1458

Partensky, F., Blanchot, J., and Vaulot, D. (1999a). "Differential distribution and ecology of *Prochlorococcus* and *Synechococcus* in oceanic waters: a review," in *Marine Cyanobacteria*, eds L. Charpy and A. Larkum (Monaco: Musée Océanographique), 457–475.

Partensky, F., Hess, W. R., and Vaulot, D. (1999b). *Prochlorococcus*, a marine photosynthetic prokaryote of global significance. *Microbiol. Mol. Biol. Rev.* 63, 106–127. doi: 10.1128/mmbr.63.1.106-127.1999

Pereira, O., Hochart, C., Auguet, J. C., Debroas, D., and Galand, P. E. (2019). Genomic ecology of Marine Group II, the most common marine planktonic Archaea across the surface ocean. *Microbiologyopen* 8:e00852.

Quast, C., Pruesse, E., Yilmaz, P., Gerken, J., Schweer, T., Yarza, P., et al. (2012). The SILVA ribosomal RNA gene database project: improved data processing and web-based tools. *Nucleic Acids Res.* 41, D590–D596.

R Core Team (2013). *R: A Language and Environment for Statistical Computing*. Vienna: R Foundation for Statistical Computing.

Rappé, M. S., Connon, S. A., Vergin, K. L., and Giovannoni, S. J. (2002). Cultivation of the ubiquitous SAR11 marine bacterioplankton clade. *Nature* 418, 630–633. doi: 10.1038/nature00917

Rekik, A., Denis, M., Dugenne, M., Barani, A., Maalej, S., and Ayadi, H. (2014). Seasonal distribution of ultraphytoplankton and heterotrophic prokaryotes in relation to abiotic variables on the north coast of Sfax after restoration. *Mar. Pollut. Bull.* 84, 280–305. doi: 10.1016/j.marpolbul.2014.05.003

Richa, K., Balestra, C., Piredda, R., Benes, V., Borra, M., Passarelli, A., et al. (2017). Distribution, community composition, and potential metabolic activity of bacterioplankton in an urbanized Mediterranean Sea coastal zone. *Appl. Environ. Microbiol.* 83:e00494-17.

Rinke, C., Rubino, F., Messer, L. F., Youssef, N., Parks, D. H., Chuvochina, M., et al. (2019). A phylogenomic and ecological analysis of the globally abundant Marine Group II archaea (Ca. Poseidoniales ord. nov.). *ISME J.* 13, 663–675. doi: 10.1038/s41396-018-0282-y

Salter, I., Galand, P. E., Fagervold, S. K., Lebaron, P., Obernosterer, I., Oliver, M. J., et al. (2015). Seasonal dynamics of active SAR11 ecotypes in the oligotrophic Northwest Mediterranean Sea. *ISME J.* 9, 347–360. doi: 10.1038/ismej.2014.129

Šantić, D., Krstulović, N., Šolić, M., and Kušpilić, G. (2011). Distribution of Synechococcus and Prochlorococcus in the central Adriatic Sea. *Acta Adriat.* 52, 101–114.

Santoro, A. E., Richter, R. A., and Dupont, C. L. (2019). Planktonic marine archaea. *Annu. Rev. Mar. Sci.* 11, 131–158. doi: 10.1146/annurev-marine-121916-063141

Shannon, C. E., and Weaver, W. (1949). *The Mathematical Theory of Information*. (Champaign, IL: University of Illinois Press), 97.

Sheik, C. S., Jain, S., and Dick, G. J. (2014). Metabolic flexibility of enigmatic SAR 324 revealed through metagenomics and metatranscriptomics. *Environ. Microbiol.* 16, 304–317. doi: 10.1111/1462-2920.12165

Shively, J., English, R. S., Baker, S., and Cannon, G. (2001). Carbon cycling: the prokaryotic contribution. *Curr. Opin. Microbiol.* 4, 301–306. doi: 10.1016/s1369-5274(00)00207-1

Simpson, E. H. (1949). Measurement of diversity. *Nature* 163:688.

Strom, S. L. (2008). Microbial ecology of ocean biogeochemistry: a community perspective. *Science* 320, 1043–1045. doi: 10.1126/science.1153527

Takahashi, S., Tomita, J., Nishioka, K., Hisada, T., and Nishijima, M. (2014). Development of a prokaryotic universal primer for simultaneous analysis of bacteria and archaea using next-generation sequencing. *PLoS One* 9:e105592. doi: 10.1371/journal.pone.0105592

Tamura, K., and Nei, M. (1993). Estimation of the number of nucleotide substitutions in the control region of mitochondrial DNA in humans and chimpanzees. *Mol. Biol. Evol.* 10, 512–526.

Techtmann, S. M., Fortney, J. L., Ayers, K. A., Joyner, D. C., Linley, T. D., Pfiffner, S. M., et al. (2015). The unique chemistry of Eastern Mediterranean water masses selects for distinct microbial communities by depth. *PLoS One* 10:e0120605. doi: 10.1371/journal.pone.0120605

Thomas, T., Evans, F. F., Schleheck, D., Mai-Prochnow, A., Burke, C., Penesyan, A., et al. (2008). Analysis of the *Pseudoalteromonas tunicata* genome reveals properties of a surface-associated life style in the marine environment. *PLoS One* 3:e3252. doi: 10.1371/journal.pone.0003252

Tully, B. J. (2019). Metabolic diversity within the globally abundant Marine Group II Euryarchaea offers insight into ecological patterns. *Nat. Commun.* 10:271.

van den Engh, G. J., Doggett, J. K., Thompson, A. W., Doblin, M. A., Gimpel, C. N. G., and Karl, D. M. (2017). Dynamics of *Prochlorococcus* and *Synechococcus* at Station ALOHA Revealed through Flow Cytometry and High-Resolution Vertical Sampling. *Front. Mar. Sci.* 4:359. doi: 10.3389/fmars.2017.00359

Viklund, J., Martijn, J., Ettema, T. J., and Andersson, S. G. (2013). Comparative and phylogenomic evidence that the alphaproteobacterium HIMB59 is not a member of the oceanic SAR11 clade. *PLoS One* 8:e78858. doi: 10.1371/journal.pone.0078858

Waterbury, J. B., Watson, S. W., and Valoius, F. (1979). The contribution of *Synechococcus* to oceanic primary productivity. *Paper Presented at the 4th International Symposium on Photosynthetic Procaryotes*, Bombannes.

Zaballos, M., Lopez-Lopez, A., Ovreas, L., Bartual, S. G., D'Auria, G., Alba, J. C., et al. (2006). Comparison of prokaryotic diversity at offshore oceanic locations reveals a different microbiota in the Mediterranean Sea. *FEMS Microbiol. Ecol.* 56, 389–405. doi: 10.1111/j.1574-6941.2006.00060.x

Zehr, J. P., and Kudela, R. M. (2011). Nitrogen cycle of the open ocean: from genes to ecosystems. *Annu. Rev. Mar. Sci.* 3, 197–225. doi: 10.1146/annurev-marine-120709-142819

Zhou, M. Y., Chen, X. L., Zhao, H. L., Dang, H. Y., Luan, X. W., Zhang, X. Y., et al. (2009). Diversity of both the cultivable protease-producing bacteria and their extracellular proteases in the sediments of the South China Sea. *Microb. Ecol.* 58, 582–590. doi: 10.1007/s00248-009-9506-z

Zouch, H., Cabrol, L., Chifflet, S., Tedetti, M., Karray, F., Zaghden, H., et al. (2018). Effect of acidic industrial effluent release on microbial diversity and trace metal dynamics during resuspension of coastal sediment. *Front. Microbiol.* 9:3103. doi: 10.3389/fmicb.2018.03103

Zouch, H., Karray, F., Armougom, F., Chifflet, S., Hirschler-Réa, A., Kharrat, H., et al. (2017). Microbial diversity in sulfate-reducing marine sediment enrichment cultures associated with anaerobic biotransformation of coastal stockpiled phosphogypsum (Sfax, Tunisia). *Front. Microbiol.* 8:1583. doi: 10.3389/fmicb.2017.01583

Zwirglmaier, K., Jardillier, L., Ostrowski, M., Mazard, S., Garczarek, L., Vaulot, D., et al. (2008). Global phylogeography of marine *Synechococcus* and *Prochlorococcus* reveals a distinct partitioning of lineages among oceanic biomes. *Environ. Microbiol.* 10, 147–161.

Conflict of Interest: The authors declare that the research was conducted in the absence of any commercial or financial relationships that could be construed as a potential conflict of interest.

frontiers in Microbiology

ORIGINAL RESEARCH
published: 03 December 2020
doi: 10.3389/fmicb.2020.601037

Taxonomic Diversity of Pico-/Nanoeukaryotes Is Related to Dissolved Oxygen and Productivity, but Functional Composition Is Shaped by Limiting Nutrients in Eutrophic Coastal Oceans

Yaping Wang[1,2†], Guihao Li[1,2†], Fei Shi[3], Jun Dong[3], Eleni Gentekaki[4], Songbao Zou[3], Ping Zhu[5], Xiaoli Zhang[3] and Jun Gong[1,2,6]*

[1] School of Marine Sciences, Sun Yat-sen University, Zhuhai, China, [2] Southern Marine Science and Engineering Guangdong Laboratory (Zhuhai), Zhuhai, China, [3] Yantai Institute of Coastal Zone Research, Chinese Academy of Sciences, Yantai, China, [4] School of Science, Mae Fah Luang University, Chiang Rai, Thailand, [5] School of Life Sciences, Ludong University, Yantai, China, [6] Guangdong Provincial Key Laboratory of Marine Resources and Coastal Engineering, Guangzhou, China

OPEN ACCESS

Edited by:
Savvas Genitsaris, International Hellenic University, Greece

Reviewed by:
André M. Comeau, Dalhousie University, Canada
Ingrid Sassenhagen, Université du Littoral Côte d'Opale, France

***Correspondence:**
Jun Gong
gongj27@mail.sysu.edu.cn

[†] These authors have contributed equally to this work

Specialty section:
This article was submitted to Aquatic Microbiology, a section of the journal Frontiers in Microbiology

Received: 31 August 2020
Accepted: 13 November 2020
Published: 03 December 2020

Citation:
Wang Y, Li G, Shi F, Dong J, Gentekaki E, Zou S, Zhu P, Zhang X and Gong J (2020) Taxonomic Diversity of Pico-/Nanoeukaryotes Is Related to Dissolved Oxygen and Productivity, but Functional Composition Is Shaped by Limiting Nutrients in Eutrophic Coastal Oceans. Front. Microbiol. 11:601037. doi: 10.3389/fmicb.2020.601037

Pico-/nanoeukaryotes (P/NEs) comprise both primary producers and bacterial predators, playing important biogeochemical and ecological roles in the marine microbial loop. Besides the difference in size, these small-sized fractions can be distinguished from microplankton by certain functional and ecological traits. Nevertheless, little information is available regarding patterns of their taxonomic and functional diversity and community composition along environmental gradients in coastal marine ecosystems. In this study, we applied high-throughput sequencing of 18S rRNA gene to assess the taxonomic species richness and community composition of P/NEs in surface waters of Bohai Sea and North Yellow Sea, northern China spanning a 600-km distance during summer and winter of 2011. The richness of operational taxonomic units (OTUs) formed a U-shaped relationship with concentration of chlorophyll *a* (Chl-*a*, a proxy of primary productivity), but a stronger, negative relationship with concentration of dissolved oxygen (DO). These two factors also significantly co-varied with the OTU-based community composition of P/NEs. The effect of geographic distance on community composition of P/NEs was negligible. Among the three functional groups defined by trophic traits, heterotrophs had the highest OTU richness, which exhibited a U-shaped relationship with both DO and Chl-*a*. The community of P/NEs was dominated by heterotrophs and mixotrophs in terms of read numbers, which showed a trade-off along the gradient of phosphate, but no significant changes along DO and Chl-*a* gradients, indicating functional redundancy. Similarly, the proportion of phototrophs was significantly and positively correlated with the concentration of silicate. Our results indicate that taxonomic and functional composition of P/NEs are decoupled on a regional scale, and limiting nutrients are important factors in modulating functional

composition of these microorganisms in the studied area. These findings contribute toward gaining a better understanding of how diversity of small eukaryotes and their functions are structured in coastal oceans and the effect of environmental changes on the structuring process.

Keywords: functional redundancy, metabarcoding, mixotrophy, nutrient limitation, productivity

INTRODUCTION

Pico- (0.2–2 μm) and nano-sized (2–20 μm) eukaryotic plankton constitute important components in marine microbial food webs. They frequently comprise major primary producers (Worden and Not, 2008), parasites, symbionts, decomposers (Sherr et al., 2007), and bacterial grazers (Linley et al., 1983; Sherr and Sherr, 1994; Christaki et al., 1999; Massana et al., 2009; Hartmann et al., 2012; Unrein et al., 2014). Due to their small cell size and lack of conspicuous morphological features, pico-/nanoeukaryotes (P/NEs; 0.2–20 μm) are generally difficult to enumerate and identify with high taxonomic resolution using traditional microscopy, especially at the lower hierarchical levels (Moreira and Lopez-Garcia, 2002; Massana, 2011). In the last two decades, application of 18S rRNA gene-based molecular tools has revealed high taxonomic diversity of these small eukaryotes, and picoeukaryotes in particular, in various marine environments, e.g., deep seas (Lopez-Garcia et al., 2001), a bottom euphotic layer of the Pacific Ocean (Moon-van der Staay et al., 2001), a coastal site of English Channel (Romari and Vaulot, 2004), pan-European coastal waters (Massana et al., 2015), and open oceans (de Vargas et al., 2015). Nevertheless, research studies focused on exploring the molecular diversity and biogeography of small marine eukaryotes (Hernandez-Ruiz et al., 2018; Piwosz et al., 2018; Gong et al., 2020), particularly in eutrophic marginal oceans on a large spatial scale are limited.

Concentration of chlorophyll *a* (Chl-*a*) has been widely used as a proxy of phytoplankton biomass and primary productivity, both of which are highly variable across seasons and regions in temperate coastal ecosystems. Picoeukaryotes and nanoeukaryotes are important components in plankton biomass, and often exhibit similar ecological patterns along a productivity gradient. Increase of total Chl-*a* is accompanied by a corresponding increase of the biomass of both pico- and nanophytoplankton. Nevertheless, the relative contributions of these microbial eukaryotes to overall phytoplankton biomass and primary production decline systematically in marine ecosystems (Marañón et al., 2012). This contrasts with microphytoplankton, which contributes an increasing portion of biomass and productivity in more eutrophic waters (Bell and Kalff, 2001; Marañón et al., 2012). Phytoplankton release approximately 20% of their photosynthetic products as dissolved organic carbon (DOC) in surrounding waters in both oligotrophic and eutrophic aquatic habitats (Baines and Pace, 1991; Marañón et al., 2005). The high availability of DOC in eutrophic waters, results in bacterioplankton becoming more productive (Cole et al., 1988; Baines and Pace, 1991), which in turn enhances the abundance and activity of bacterivorus picoeukaryotes and heterotrophic/mixotrophic nanoeukaryotes (Burney et al., 1981; Lonsdale et al., 2006; Šolić et al., 2010). Apart from this bottom-up effect, the abundance of both bacteria and pico-/nanoeukaryotic plankton is controlled in a top-down fashion by microzooplankton (e.g., ciliates), especially under eutrophic conditions (e.g., Šolić et al., 2010; Šimek et al., 2019). Studies that have taken plankton size-fraction into account have shown that a large proportion of oxygen (O_2) production came from microplankton, whereas pico- and nanoplankton consumed most of the dissolved oxygen (DO) in surface waters of the Canadian Arctic (Harrison, 1986) and a coastal upwelling system (Hernandez-Ruiz et al., 2018). The functional diversity of pico- and nano-sized protists is higher than that of microplankton in coastal oceans (Ramond et al., 2019). Therefore, pico- and nanoplankton are, to some extent, more similar to each other in ecological, physiological and functional aspects than to microplankton, which has prompted us to consider pico- and nanoeukaryotes as a whole in ecological and biogeographic studies. The relationship of overall marine phytoplankton richness with productivity is unimodal (Vallina et al., 2014) and driven by temperature and environmental variability (Righetti et al., 2019). Nevertheless, similar studies on size fractions of plankton have yet to be performed. Furthermore, variability of community composition and structure of P/NEs (including the heterotrophs) in relation to phytoplankton biomass (or productivity) and the main environmental factors driving these changes remain little explored topics.

The Bohai Sea (BHS) and the northern Yellow Sea (NYS) are two shallow and eutrophic coastal basins northwest of the Pacific. These basins are semi-closed, with an average depth of 18 and 40 m, respectively. The recent economic development in the Bohai Economic Circle has resulted in gradually increasing levels of dissolved inorganic nitrogen (DIN), as well as, DIN to phosphate ratio (N:P), thus turning the BHS and NYS into nitrogen-rich and phosphorus-limited basins (Zhao et al., 2016; Yang et al., 2018; Wang et al., 2019). The BHS and NYS ecosystems are variable and mainly controlled by physical processes, including monsoons, tides, and seasonal stratification (Guan, 1994; Wei et al., 2004). The Yellow River directly discharges into the BHS leading to lower salinity and higher nutrient levels in this basin compared to NYS (Chen, 2009). The freshwater discharge causes nutrient replenishment resulting in phytoplankton blooms in spring and August–September. The blooms are accompanied by changes in the concentration of Chl-*a*, which shows distinct seasonality and regional variations (Wei et al., 2004; Liu et al., 2014; Zhou et al., 2017). In general, both Chl-*a* and N:P ratio are higher in the BHS than NYS (Xie et al., 2012). These distinct seasonal and regional attributes of BHS and NYS provide an ideal testing ground for understanding the environmental drivers of the diversity and distribution of

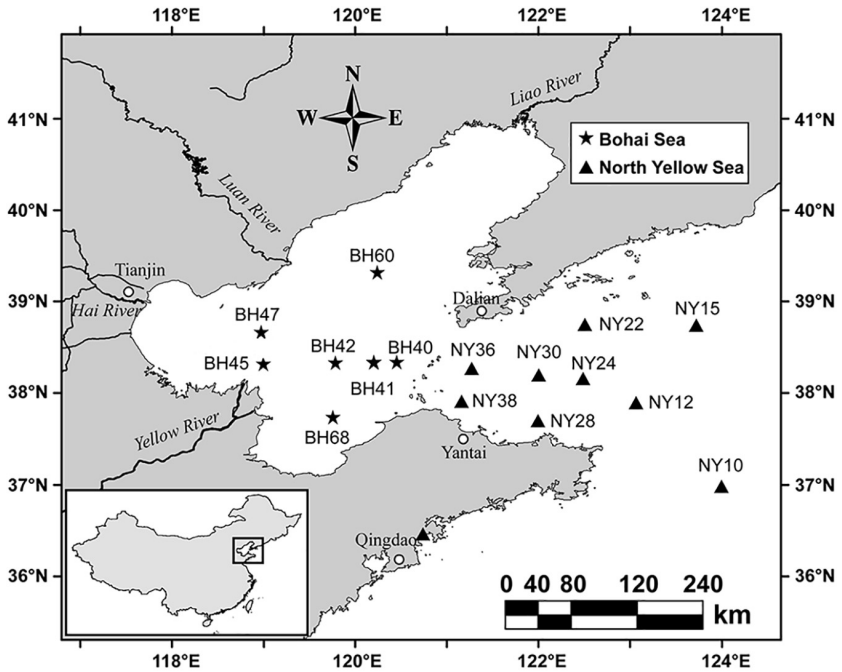

FIGURE 1 | Map of sampling stations at Bohai Sea and North Yellow Sea.

P/NEs in coastal oceans that are highly affected by anthropogenic activities. This knowledge is essential for optimizing ecosystem and biogeochemical models (by incorporating or parameterizing pico-/nanoplanktonic components) toward stronger predictive power and subsequent management of such ecosystems.

In this study, we investigated the temporal (summer-winter) and regional variability of diversity and community structure of pico-/nanoeukaryotic plankton in the surface waters of BHS and NYS using high-throughput sequencing of 18S rRNA genes. We hypothesized that: (i) the diversity and community structure of P/NEs would change significantly along the productivity (i.e., Chl-*a*) gradient; (ii) there would be substantial differences in community structure between summer and winter and between the two basins; and (iii) due to higher bioavailability of DOC and primary productivity (Chl-*a*) under highly eutrophic conditions, the pico-/nanoeukaryote community would become functionally more heterotrophic, which would be reflected in increased relative abundance of rRNA gene copies of heterotrophs.

MATERIALS AND METHODS

Sampling and Characterization of Environmental Variables

Samples were collected from BHS and NYS during the summer (June 21–28) and winter (November 13–19) cruises of R/V *Dong Fang Hong 2* in 2011 (**Figure 1**). A total of 28 (16 summertime and 12 wintertime) surface water samples were collected at a depth of 3 m with a rosette of Niskin bottles attached to a conductivity, temperature, depth (CTD) probe frame. At each station, a water sample of 1.5 L was prefiltered through a 20-μm-pore-sized mesh to remove larger plankton and debris, then gently filtered using 0.22-μm-pore-sized polycarbonate membrane filters (47 mm in diameter; Millipore, United States). All membranes bearing the pico- and nano-sized plankton biomass were placed in cryovial tubes and stored in liquid nitrogen for subsequent molecular analyses.

In situ measurements of water temperature (Temp), salinity (Sal), depth, and DO concentration were recorded using CTD. Concentration of total chlorophyll *a* (Chl-*a*) was measured on site using an electronic probe (Hydrolab MS5; Hach, United States). At each site, a subsample volume of 100 ml was filtered on board the research vessel through 0.45-μm-pore-sized polyethersulfone membrane filters (25 mm in diameter; Jinteng, Beijing, China) and stored at −20°C for determination of nutrients. The concentrations of nitrate (NO_3^-), nitrite (NO_2^-), ammonium (NH_4^+), dissolved inorganic phosphate (PO_4^{3-}), and silicate (SiO_3^{2-}) in all subsamples were determined with a nutrient AutoAnalyzer (Seal, Germany). Dissolved organic nitrogen (DON) was measured with a TOC-VCPH TOC analyzer (Shimadzu, Japan). The sample ID, sampling sites and dates, as well as, environment variables are supplied in **Supplementary Table 1**.

DNA Preparation, Polymerase Chain Reaction (PCR) Amplification, and High-Throughput Sequencing

The FastDNA Spin Kit (MP Biomedical, United States) was used to extract and purify DNA according to the manufacturer's

instructions. The quality of extracted DNA was assessed using gel electrophoresis (1% agarose gels) and quantified using a NanoDrop 2000c spectrophotometer (Thermo Fisher Scientific, United States).

A fragment spanning the V2 and V3 regions of the 18S rRNA gene was amplified using the universal eukaryotic primers 82F (López-García et al., 2003) and 516R (Casamayor et al., 2002). A 10-bp barcode specific to each sample was added to the forward primers. The reaction solutions for PCR were made according to standard conditions for Platinum *Pfx* DNA polymerase (Invitrogen) with 20 ng of environmental DNA as template. Reactions were performed under the following conditions: initial denaturation at 95°C for 2 min; 20 cycles of 95°C for 30 s, 60°C for 30 s, and 72°C for 1 min; and a final extension at 72°C for 7 min. Pyrosequencing was performed with GS-FLX Titanium LV emPCR Kit (Lib-L) on a Roche 454 GS-FLX Titanium sequencer by the BGI Company (Shenzhen, China).

The raw sequencing data (246,066 reads) were processed and analyzed using QIIME (Caporaso et al., 2010) and Mothur v.1.35.1 (Schloss et al., 2009). Quality filtering was performed according to the following criteria: (i) no N's; (ii) quality score > 25; (iii) no sequencing mismatches within the PCR primer regions; (iv) minimum sequence length of 200 bp and maximum length of 500 bp (excluding PCR primers); and (v) homopolymers ≤ 6. After quality filtering, the wintertime sample NY10W was excluded as only very few reads remained. Putative chimeras were identified with the UCHIME module of USEARCH v.6.0.203 based on the Silva database (release 119) and discarded. The remaining reads were grouped into operational taxonomic units (OTUs) based on a 97% similarity threshold using the UCLUST algorithm. Singletons were excluded from further analysis. Taxonomy annotation was performed against the PR^2 database (a version based on GenBank v. 230) (Guillou et al., 2012) using UCLUST with default settings. Unassigned reads were discarded. The reads assigned to macroorganisms (e.g., Metazoa, Streptophyta, Rhodophyta, and Ulvophyceae) were treated as contaminants, and hence excluded from subsequent analysis for P/NEs.

To calculate OTU richness, 1590 reads from each sample were randomly re-sampled 10 times. The OTU richness was also partitioned into major groups (e.g., Alveolata, Stramenopiles, Hacrobia, and Opisthokonta), which were subsequently analyzed for spatial and seasonal variability and correlations with environmental variables. For beta diversity analysis, the OTU table was normalized using *edgeR* v. 3.12.1 package (Robinson et al., 2010) in R (R Development Core Team, 2013). This method allows for detection of differentially abundant species as appose to common normalization approaches, such as using simple proportions or rarefying of counts (McMurdie and Holmes, 2014).

The functional structure of P/NEs was assessed using a trait-based approach as previously described (Genitsaris et al., 2015; Ramond et al., 2019). We used the simplified trophic traits (autotrophy, heterotrophy, and mixotrophy) largely because the level of DO, which was mainly driven by photosynthesis and respiration by these trophic groups, was the most important environmental factor co-varying with alpha and beta diversities of P/NEs in this study. The OTU richness and read proportions of these three functional groups were calculated by accumulating those of the affiliated taxonomic groups in a given community (**Supplementary Table 2**).

Statistical Analyses

The normality of all variables was tested using Shapiro–Wilk analysis. Student's *t* tests (for normally distributed variables) and non-parametric Mann–Whitney *U* test (for the variables that showed non-normal distribution) were performed to identify differences in environmental factors, alpha diversity estimators, and the relative proportion of a given taxonomic group between seasons and regions, and among trophic and DO levels. Pearson or Spearman's correlations between alpha diversity and environmental factors were performed using SPSS v.11.5 (SPSS, Chicago, IL, United States). The statistical differences of the relative proportions of pico-/nanoeukaryotic taxa between the levels of DO and Chl-*a* were assessed by one-way ANOVA and least significant difference (LSD) *post hoc* test. Visualization of community relatedness was conducted using non-metric multiple dimensional scaling (NMDS), which was based on Bray-Curtis similarity matrices. Redundancy analysis (RDA) was used to explore the co-variations between environmental parameters and community structure of P/NEs. Only the variables (i.e., Chl-*a* and DO) that were statistically significant based on forward selection were plotted. Analysis of Similarity (ANOSIM) was executed to test hypotheses regarding variation of community structure of P/NEs between seasons, regions, or among different levels of environmental variables. All analyses of community structure were carried out using *vegan* in R (v. 2.4-3) (Oksanen et al., 2013).

RESULTS

Spatial and Seasonal Variations of Environmental Factors

Most of the environmental variables determined for the 28 surface water samples (i.e., temperature, DO, pH, Chl-*a*, NO_3^-, NO_2^-, SiO_3^{2-}, TN, DON, and P:Si) demonstrated distinct seasonality (**Supplementary Table 1**). The water temperature ranged from 13.15 to 21.47°C in summer and from 12.09 to 13.67°C in winter across BHS and NYS ($P < 0.001$). The level of Chl-*a* was significantly higher in summer (mean ± SE, 3.34 ± 0.32 μg L^{-1}) than in winter (0.27 ± 0.03 μg L^{-1}; $P < 0.001$), and so was the concentration of DO (7.41 ± 0.17 vs. 3.95 ± 0.04 mg L^{-1}, $P < 0.001$). The concentrations of NO_3^- (1.20 ± 0.16 vs. 2.49 ± 0.23 μM, $P < 0.001$), NO_2^- (0.25 ± 0.02 vs. 0.52 ± 0.06 μM, $P < 0.001$), DON (9.52 ± 1.03 vs. 13.56 ± 1.71 μM, $P = 0.050$), and SiO_3^{2-} (1.10 ± 0.16 vs. 4.30 ± 0.63 μM, $P < 0.001$) were relative lower in the summertime samples, due to highly abundant phytoplankton standing stock in summer and increased nutrient uptake. NH_4^+ was the dominant DIN species (78%). The N:P ratios varied greatly across all samples, ranging from 19.7 to 2170, with relatively higher values in winter (440 ± 175) than in summer

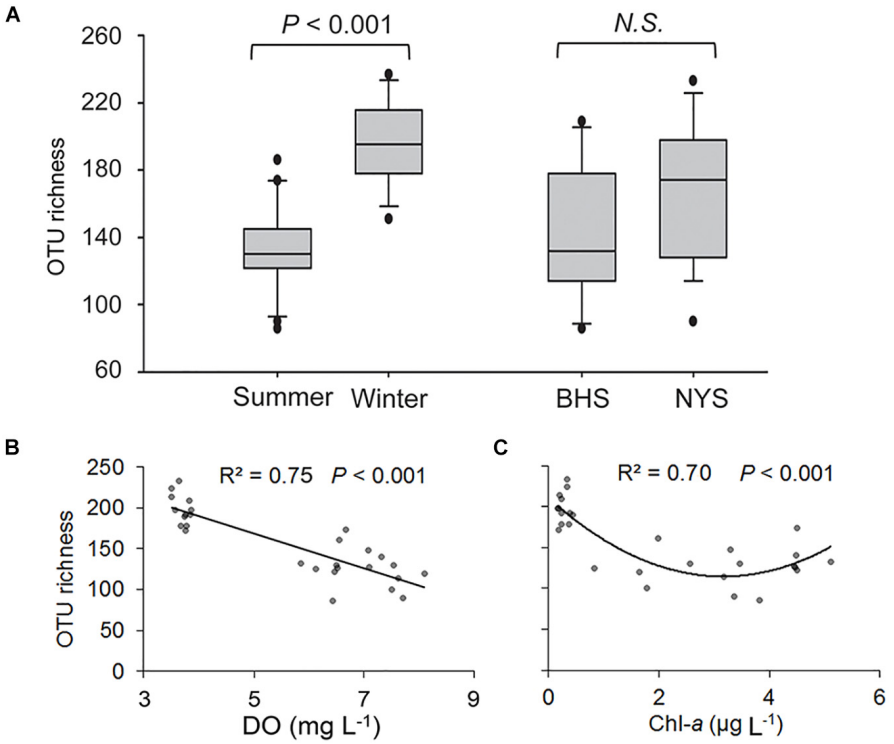

FIGURE 2 | Variations in OTU richness of pico-/nanoeukaryotes in surface waters of Bohai Sea (BHS) and North Yellow Sea (NYS). **(A)** Box plots showing the OTU richness was significantly higher in winter than in summer across two basins, but not between BHS and NYS. **(B,C)** Regression analyses showing the relationships between OTU richness and two of the most important factors, dissolved oxygen (DO, **B**) and chlorophyll *a* (Chl-*a*, **C**). *N.S.*, no significant differences ($P > 0.05$).

(138 ± 20). The N:Si ratio ranged from 0.7 to 50, but was not significantly different between these two seasons (14.7 ± 3.6 vs. 8.8 ± 3.7, $P = 0.070$). The concentrations of Chl-*a*, DO, pH, NO_3^-, NO_2^-, DON, and SiO_3^{2-} were higher in the BHS, while salinity, NH_4^+, PO_4^{3-}, N:P, and N:Si tended to be higher in the NYS, but these differences were not significant.

Variations in Richness of Pico-/Nanoeukaryotes

After quality filtering, a total of 94,642 reads and 893 OTUs were retained for the 28 surface samples, among which 417 OTUs were detected in both summer and winter samples, and 611 OTUs in both basins (**Supplementary Table 3**). The OTU richness of P/NEs was significantly higher in the winter (198 ± 5) than in summer (131 ± 7) across the whole area studied ($P < 0.001$; **Figure 2A**). The P/NEs in NYS (167 ± 10) appeared to be more diverse than in BHS (143 ± 12), however, this basin-wise difference was not statistically supported ($P = 0.147$, **Figure 2A**).

Both linear and non-linear regression analyses were performed to explore the relationships between OTU richness of P/NEs and the abiotic or biotic factors, among which DO and Chl-*a* had the highest coefficients of determination. The OTU richness linearly decreased with DO, which explained 75% of observed variance ($P < 0.001$; **Figure 2B**), whereas a lower variance (70%) was explained by Chl-*a* in a quadratic fitting ($P < 0.001$; **Figure 2C**). In particular, the relationship between OTU richness of P/NEs and Chl-*a* was U-shaped, i.e., richness decreased and then increased along the Chl-*a* gradient, reaching the minimum at an intermediate level (∼ 3 μg Chl-*a* L^{-1}) of phytoplankton biomass (**Figure 2C**).

A quarter of pico-/nanoeukaryote OTUs were affiliated with Dinophyceae, of which the percentage of OTU number varied greatly (15 ∼ 44%) among samples. The OTU numbers of Hacrobia (on average 10%), Ciliophora (7%), Archaeplastida (8%), marine stramenopiles (MASTs, 6%), and Syndiniales (5%) were also abundant. Significant summer-winter differences in percentage of OTU number were observed for Dinophyceae (28 vs. 19%), Hacrobia (11 vs. 9%), Archaeplastida (10 vs. 6%), Syndiniales (5 vs. 4%), and Rhizaria (5 vs. 4%), whereas the opposite was true for Ciliophora (5 vs. 11%) and MASTs (5 vs. 7%; **Figure 3A**). The OTU richness of Syndiniales, Ciliophora, MASTs, Bacillariophyta, Cryptophyta, Choanoflagellida, and Apicomplexa formed U-shaped relationships with both DO and Chl-*a*, with the exception of Cryptophyta and Apicomplexa, which formed a negative relationship with DO ($0.29 \leq R^2 \leq 0.80$, $P \leq 0.004$; **Supplementary Figures 1**, **2**).

Community Structure, Seasonal, and Regional Variations

Overall, the reads of pico-/nanoeukaryotes were dominated by Alveolata (61.1%), which was comprised of Dinophyceae (33.4%), Syndiniales (24.0%), Ciliophora (3.6%), Apicomplexa

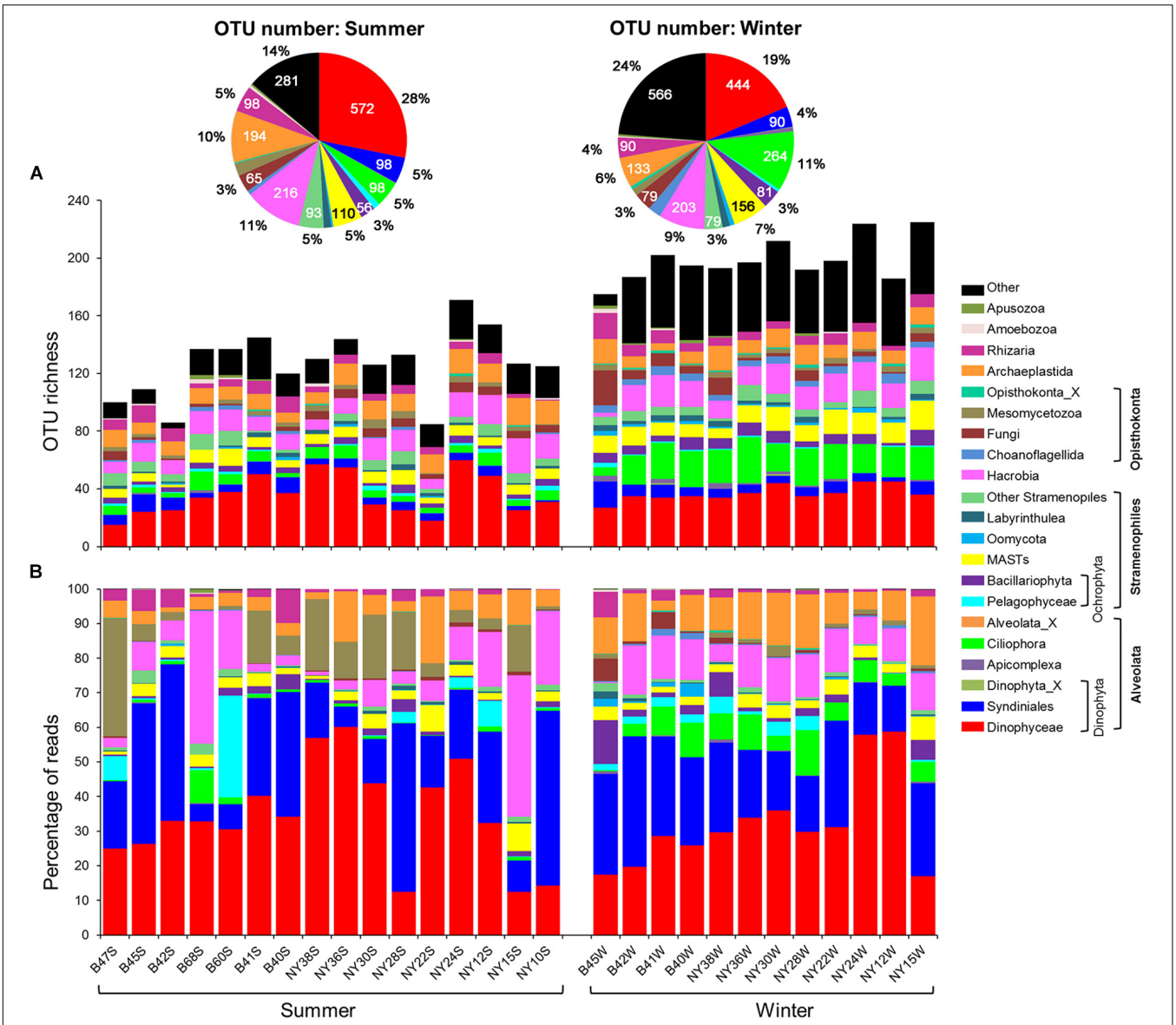

FIGURE 3 | Variations in OTU richness and community composition of pico-/nanoeukaryotes. **(A)** The column chart shows the variation in OTU numbers of major taxa among samples; the pie charts summarize the OTU numbers and proportions of major taxa in summer and winter, respectively. **(B)** Relative proportions of pyrotags of major taxa across samples. MASTs, marine stramenopiles.

(0.1%), and Perkinsida (0.01%; **Figure 3B**). Hacrobia (11.0%; mostly Haptophyta and Cryptophyta), Stramenopiles (10.1%), Chlorophyta (8.3%), Opisthokonta (7.2%), and Rhizaria (2.2%) were also present. Most of Stramenopiles was affiliated with MASTs (3.3%), Pelagophyceae (2.7%), Bacillariophyta (2.2%), Labyrinthulea (0.4%), Oomycota (0.4%), Chrysophyceae-Synurophyceae (0.2%), and Bicoecea (0.2%). The reads of marine Ochrophyta (MOCH), *Pirsonia*, Dictyochophyceae, Bolidophyceae-and-relatives, Eustigmatophyceae, and Raphidophyceae were each less than 0.1%. Over 50% of reads of Chlorophyta belonged to Mamiellophyceae. The read percentages of other higher-ranking taxa, such as Apusozoa and Amoebozoa, were on average less than 1% (**Figure 3B**).

The NMDS plot showed that the community structure of P/NEs in the summertime samples of both basins was more divergent and well separated from the wintertime samples (**Figure 4A**). The community structure of P/NEs was significantly different between summer and winter (ANOSIM, $R = 0.698$, $P = 0.001$, **Table 1**), whereas this was not the case between BHS and NYS ($R = 0.023$, $P = 0.278$, **Table 1**). The RDA plot revealed that the community structure of P/NEs co-varied significantly with DO and Chl-*a* ($P < 0.05$; **Figure 4B**). Correlations between paired community Bray-Curtis similarity and pairwise differences in DO and Chl-*a* also showed a stronger effect of the former ($R = -0.65$, $P < 0.001$) than the latter ($R = -0.44$, $P < 0.001$; **Figures 4C,D**). The effect of geographic distance

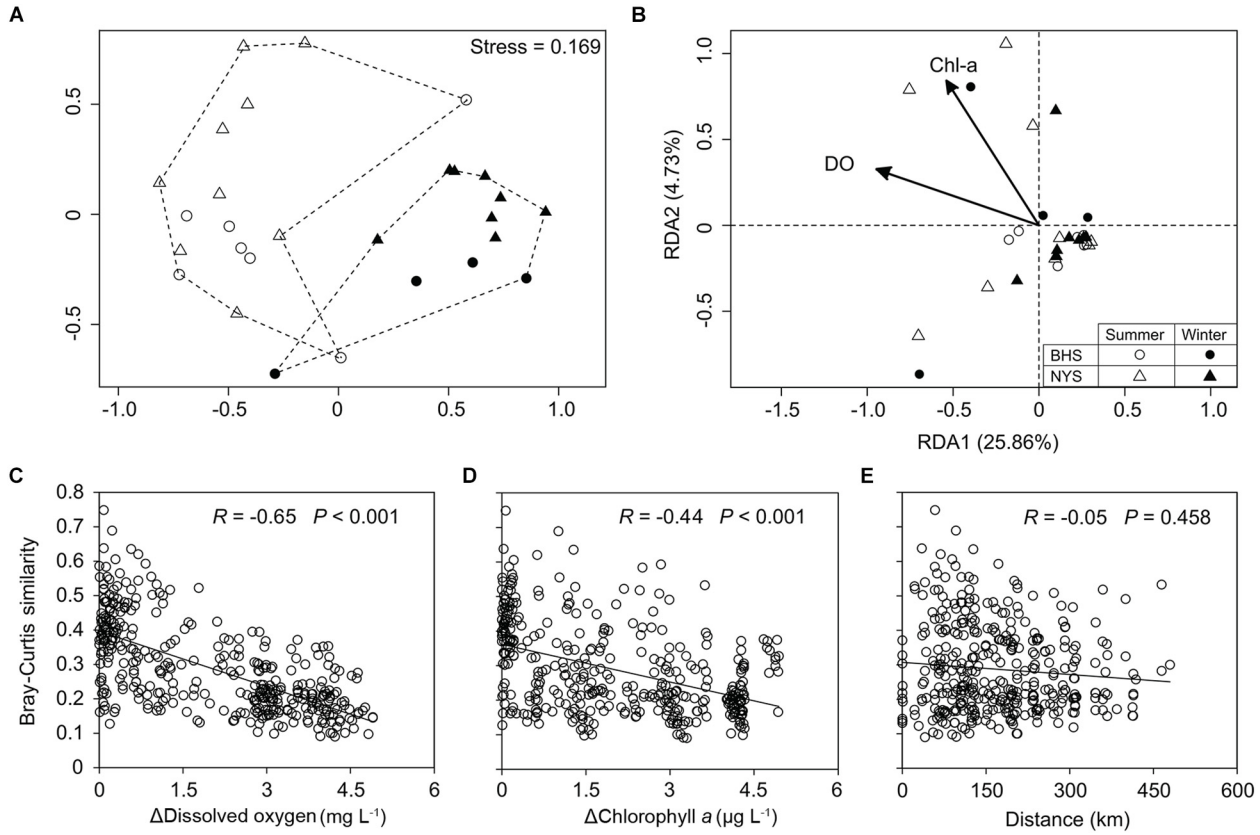

FIGURE 4 | Variations in taxonomic community composition of pico-/nanoeukaryotes. **(A)** A non-metric multidimensional scaling plot depicting the distinct seasonality of taxonomic community structure in NYS and BHS. **(B)** Plot of redundancy analysis (RDA) showing dissolved oxygen and chlorophyll *a* significantly (Monte Carlo test, $P < 0.05$) co-varied with the taxonomic community composition. **(C–E)** Scatter plots showing that the similarity in taxonomic community composition was significantly decreased with the differences in dissolved oxygen **(C)** and chlorophyll *a* **(D)**, but not with that of geographic distance between samples **(D)**.

TABLE 1 | ANOSIM testing the differences in taxonomic community structure of P/NEs between seasons (summer and winter), basins (BHS and NYS), and among levels of dissolved oxygen (DO) and Chl-*a*.

	R	*P*
Season	0.698	**0.001**
Basin	0.023	0.278
DO (Global test)	0.806	**0.001**
3–5 vs. 5–7 mg L^{-1}	0.860	**0.001**
3–5 vs. 7–9 mg L^{-1}	0.931	**0.001**
5–7 vs. 7–9 mg L^{-1}	0.324	**0.001**
Chl-*a* (Global test)	0.662	**0.001**
0–1 vs. 1–4 μg L^{-1}	0.828	**0.001**
0–1 vs. 4–6 μg L^{-1}	0.676	**0.001**
1–4 vs. 4–6 μg L^{-1}	0.069	0.265

Significant P-values (≤0.05) are highlighted in bold.

on the taxonomic community composition of P/NEs was not significant ($R = -0.05$, $P = 0.46$; **Figure 4E**).

Comparisons between summer and winter revealed that the read percentages of many groups showed a distinct seasonality (**Figure 5** and **Supplementary Table 4**). The proportions of Suessiales (7.2 ± 0.92 vs. 1.9 ± 0.50%) and Mesomycetozoa (9.6 ± 2.36 vs. 0.9 ± 0.25%) were much higher in the summer than in the winter ($P < 0.001$). In contrast, Dino-Group-II (3.4 ± 0.44 vs. 12.1 ± 1.82%), Dino-Group-III (0.2 ± 0.05 vs. 0.8 ± 0.23%), Dino-Group-IV (0 vs. 0.1 ± 0.02%), Ciliophora (1.4 ± 0.55 vs. 6.5 ± 1.02%), Mamiellophyceae (1.7 ± 0.21 vs. 8.0 ± 1.13%), Chytridiomycota (0.1 ± 0.03 vs. 0.3 ± 0.07%), Oomycota (0.1 ± 0.04 vs. 0.8 ± 0.32%), MAST-4 (0.0 ± 0.03 vs. 0.5 ± 0.10%), and MAST-7 (0.0 ± 0.01 vs. 0.3 ± 0.09%) were significantly more abundant in the winter ($P < 0.05$). Dino-Group-I was the most abundant among the four Dino-groups, accounting for approximately 20.5 and 10.8% of pico-/nanoeukaryotic reads in summer and winter, respectively, but this seasonal difference was not significant ($P = 0.19$; **Supplementary Table 4**).

Despite the community structures of P/NEs not being significantly different between BHS and NYS, basin-wise differences in relative proportion were detected for several lineages (**Figure 5** and **Supplementary Table 4**). These included Mamiellophyceae (2.9 ± 0.76 vs. 5.3 ± 1.12%), MAST-8 (0.0 ± 0.02 vs. 0.1 ± 0.03%), Prasino-Clade-V (0.1 ± 0.03 vs.

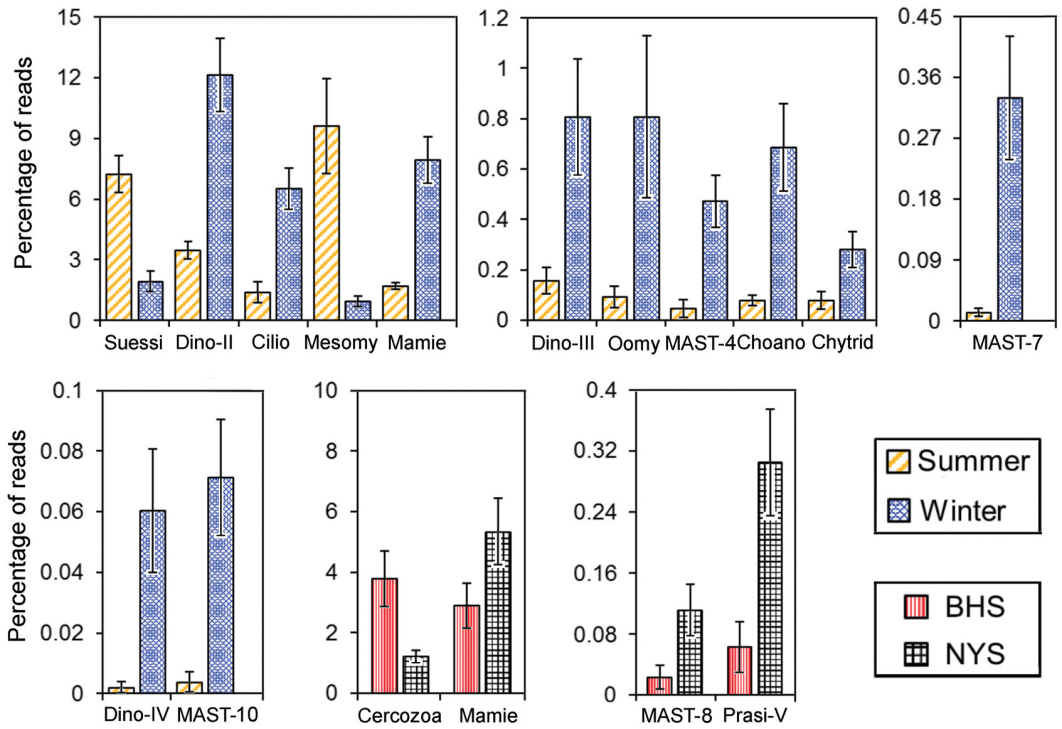

FIGURE 5 | The pico-/nanoeukaryotic taxa of which the relative proportions were significantly different ($P \leq 0.05$ by Student's *t*-test or Mann–Whitney *U* test) between summer and winter, or between BHS and NYS. The error bars indicate standard errors. Asco, Ascomycota; Basidio, Basidiomycota; Choano, Choanoflagellida; Chytrid, Chytridiomycota; Cilio, Ciliophora; Crypto, Cryptophyta; Dino-II, Dino-Group-II; Dino-III, Dino-Group-III; Dino-IV, Dino-Group-IV; Labyri, Labyrinthulea; Mamie, Mamiellaceae; MASTs, marine stramenopiles; Mesomy, Mesomycetozoa; Oomy, Oomycota; Prasi-V, Prasino-Clade-V; Prym, Prymnesiales; Suessi, Suessiales.

$0.3 \pm 0.07\%$), and Cercozoa (3.8 ± 0.92 vs. $1.2 \pm 0.21\%$) (**Figure 5** and **Supplementary Table 4**).

Changes in Taxonomic Composition Along Dissolved Oxygen Gradient and Productivity

In order to explore how these two factors affected community structure, the relative proportions of major lineages were statistically compared among three levels of DO (low: 3–5 mg L^{-1}; intermediate: 5–7 mg L^{-1}; and high: 7–9 mg L^{-1}) and Chl-*a* (low: 0–1 μg L^{-1}; intermediate: 1–4 μg L^{-1}; and high: 4–6 μg L^{-1}; **Figure 6** and **Supplementary Table 5**). Along the DO gradient, 11 taxonomic groups had the highest pyrotag proportions under low DO conditions. These included Dino-Group-II (mean 12.1, 3.4, and 3.5%); Bathycoccaceae + Mamiellaceae (7.9, 1.8, and 1.2%), Choreotrichia + Oligotrichia (5, 2.1, and 0.5%), Dino-Group-III (0.8, 0.3, and 0.1%); Choanoflagellida (0.7, 0.1, and 0.1%), MAST-4 (0.5%, 0.1%, and 0); Chytridiomycota (0.3, 0.1, and 0.1%); MAST-7 (0.3%, 0, and 0); MAST-10 (0.1%, 0, and 0); Dino-Group-IV (0.1%, 0, and 0); and Bolidophyceae (0.2%, 0, and 0; **Figure 6**). The pyrotag proportions of these taxa were the highest at the lowest level of Chl-*a* as well (**Figure 6**).

In contrast, among the three levels of DO, Prymnesiophyceae (2.9, 9.7, and 2.1%), Katablepharidophyta (0.5, 1.9, and 0.6%), Chrysophyceae-Synurophyceae (0.2, 0.6, and 0.1%), and Dictyochophyceae (0.1%, 0.3%, and 0) exhibited significantly higher proportions at intermediate DO ($P < 0.05$). However, the pyrotag proportions of these taxa were not significantly different among any of the three Chl-*a* levels ($P > 0.05$; **Figure 6**). Finally, only pyrotags of Mesomycetozoa (0.9, 5.6, and 12.8%) and Suessiales (1.9, 5.9, and 8.2%; **Figure 6**) peaked under high DO conditions and at intermediate levels of Chl-*a*.

Variations in Richness of Functional Groups and in Community Functional Structure

The OTU richness of heterotrophs ranged from 37 to 143, ranging from 41.5 to 69.3% across all samples. In contrast, the OTU richness of mixotrophs (20 ∼ 70) and phototrophs (10 ∼ 30) was much lower and with narrower ranges in the pico-/nanoeukaryote communities (**Figure 7A**). Regarding seasonal and basin-wise comparisons, a significant difference in OTU richness was only found for the heterotrophs between winter (126 ± 3.0) and summer (60 ± 2.4; $P < 0.001$). Among all determined environmental variables, DO ($R^2 = 0.92$, $P < 0.001$) and Chl-*a* ($R^2 = 0.85$, $P < 0.001$) were the most significant, consistently showing a U-shaped relationship with heterotrophic OTU richness (**Figures 7B,C**). The richness of phototrophs, mixotrophs and mixotrophs + phototrophs

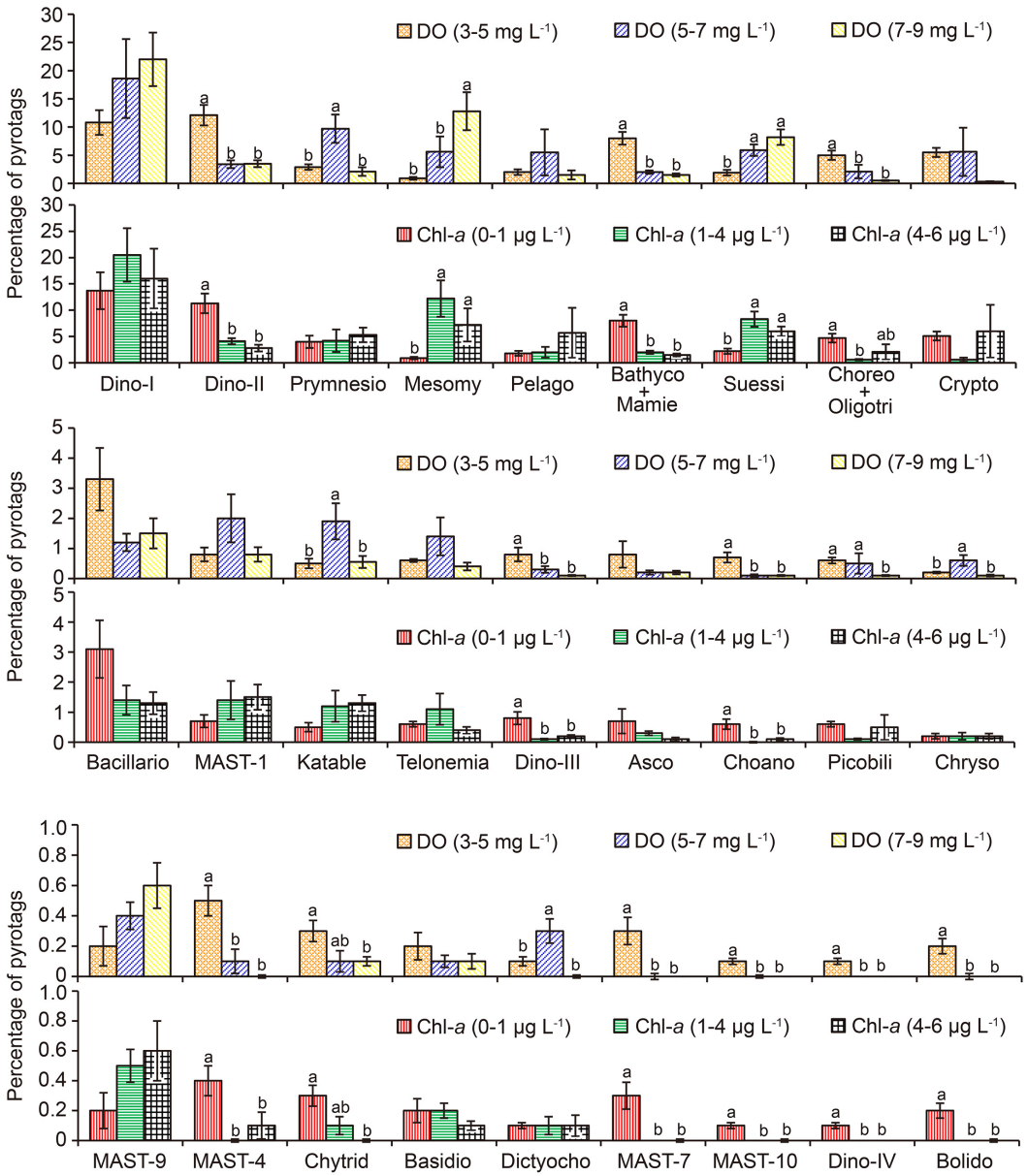

FIGURE 6 | Comparisons of the relative proportions of pico-/nanoeukaryotic taxa between the levels of dissolved oxygen (DO) and chlorophyll *a* (Chl-*a*). The error bars indicate standard errors. Different lowercase letters indicate significant differences ($P \leq 0.05$ using Least-Significant Difference test) in percentage of pyrotags of a taxon between two levels of DO or Chl-*a*. Absence of letters indicates insignificant effect ($P > 0.05$ by one-way ANOVA) of DO or Chl-*a* on the relative proportion of a taxon. Asco, Ascomycota; Bacillario, Bacillariophyta; Basidio, Basidiomycota; Bathyco + Mamie, Bathycoccaceae + Mamiellaceae; Bolido, Bolidophyceae; Choano, Choanoflagellida; Choreo + Oligotri, Choreotrichia + Oligotrichia; Chryso, Chrysophyceae-Synurophyceae; Chytrid, Chytridiomycota; Crypto, Cryptophyta; Dictyocho, Dictyochophyceae; Dino-I, Dino-Group-I; Dino-II, Dino-Group-II; Dino-III, Dino-Group-III; Dino-IV, Dino-Group-IV; Katable, Katablepharidophyta; MASTs, marine stramenopiles; Mesomy, Mesomycetozoa; Pelago, Pelagophyceae; Picobili, Picobiliphyta; Prymnesio, Prymnesiophyceae; Suessi, Suessiales.

(i.e., pico-/nanophytoplankton) tended to be maximized at the intermediate levels of DO, while richness was minimized at the intermediate Chl-*a* concentrations; nevertheless, these quadratic relations were weak and not statistically supported ($R^2 < 0.2$, $P > 0.05$; **Figures 7D–I**).

The read proportions of the three ecological groups in the pico-/nanoeukaryotic community varied greatly across the two seasons and regions (**Figure 8A**). The percentages of heterotrophs (Hetero%) and mixotrophs (Mixo%) in the community varied greatly, accounting for 18∼74% and 15∼67% among all samples, respectively. The contribution of phototrophs (Photo%) was consistently low (2∼36%). The pyrotag proportions of heterotrophs and mixotrophs appeared to be higher in the summer, whereas phototrophs became more abundant in the winter; however, these differences were not statistically supported ($P > 0.05$; **Figure 8B**). Similarly,

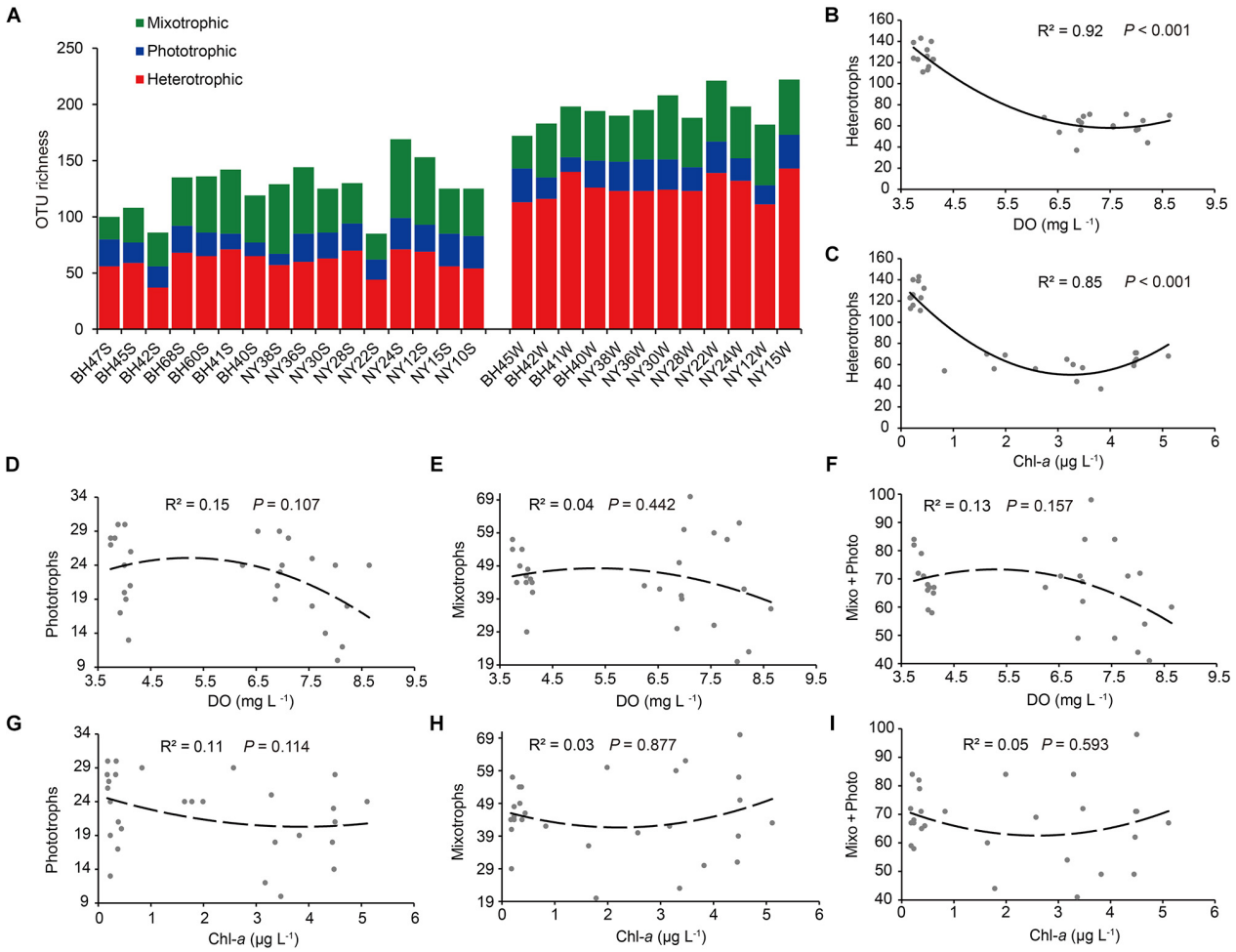

FIGURE 7 | (A) The OTU richness of heterotrophs, phototrophs, and mixotrophs. **(B–I)** Variations in OTU numbers of these functional groups in relation to dissolved oxygen (DO) and chlorophyll *a* (Chl-*a*) concentrations. Note that the relationships between OTU richness of heterotrophs and DO and Chl-*a* are highly significant and U-shaped. The abbreviation "Mixo + Photo" refers to pigmented pico-/nanoeukaryotes.

the proportions of these three functional groups were not significantly different between BHS and NYS either ($P > 0.05$). Correlations between the proportions of functional groups and all determined environmental variables showed contrasting patterns: the Hetero% was significantly and negatively correlated with PO_4^{3-} ($R = -0.42$, $P = 0.026$), whereas both the Mixo% ($R = 0.38$) and the ratio of mixotrophs to heterotrophs (Mixo/Hetero; $R = 0.45$) were significantly and positively correlated with PO_4^{3-} ($P < 0.05$) (**Figure 8C**). The Photo% increased linearly with the concentration of SiO_3^{2-} ($R = 0.42$, $P = 0.027$). Nevertheless, the correlation between the ratio of phototrophs to heterotrophs (Photo/Hetero) and SiO_3^{2-} was weak and insignificant ($R = 0.24$, $P > 0.05$; **Figure 8C**).

The changes in functional groups across the three DO levels showed some general trends. Hetero% appeared to be the highest (47.6%) in the highly oxygenated waters; Photo% was highest (17.0%) at low DO level, but progressively decreased at intermediate (10.4%) and high DO levels; and Mixo% peaked (50%) at the intermediate DO level (**Figure 8D**). Nevertheless, the statistical comparisons among the three levels were not significant ($P > 0.05$). Across the gradient of phytoplankton biomass, the functional structure of P/NEs was not discernible either (data not shown), despite there being a high and positive correlation between DO and Chl-*a* ($R = 0.78$, $P < 0.001$). This was probably due to the fact that in the present study the increase of DO with Chl-*a* was not monotonic and could fit better with a parabolic curve instead ($R^2 = 0.90$, $P < 0.01$; **Figure 8E**): when Chl-*a* was relatively lower (<3 μg L^{-1}), the DO in surface waters increased along with Chl-*a*; whereas the slope became negative when Chl-*a* was beyond the turning point (>3 μg L^{-1}; **Figure 8E**).

DISCUSSION

The nutrient levels in the surface waters of BHS and NYS determined in this study showed that the DIN was dominated by high concentration of NH_4^+ in summer and by NO_3^-

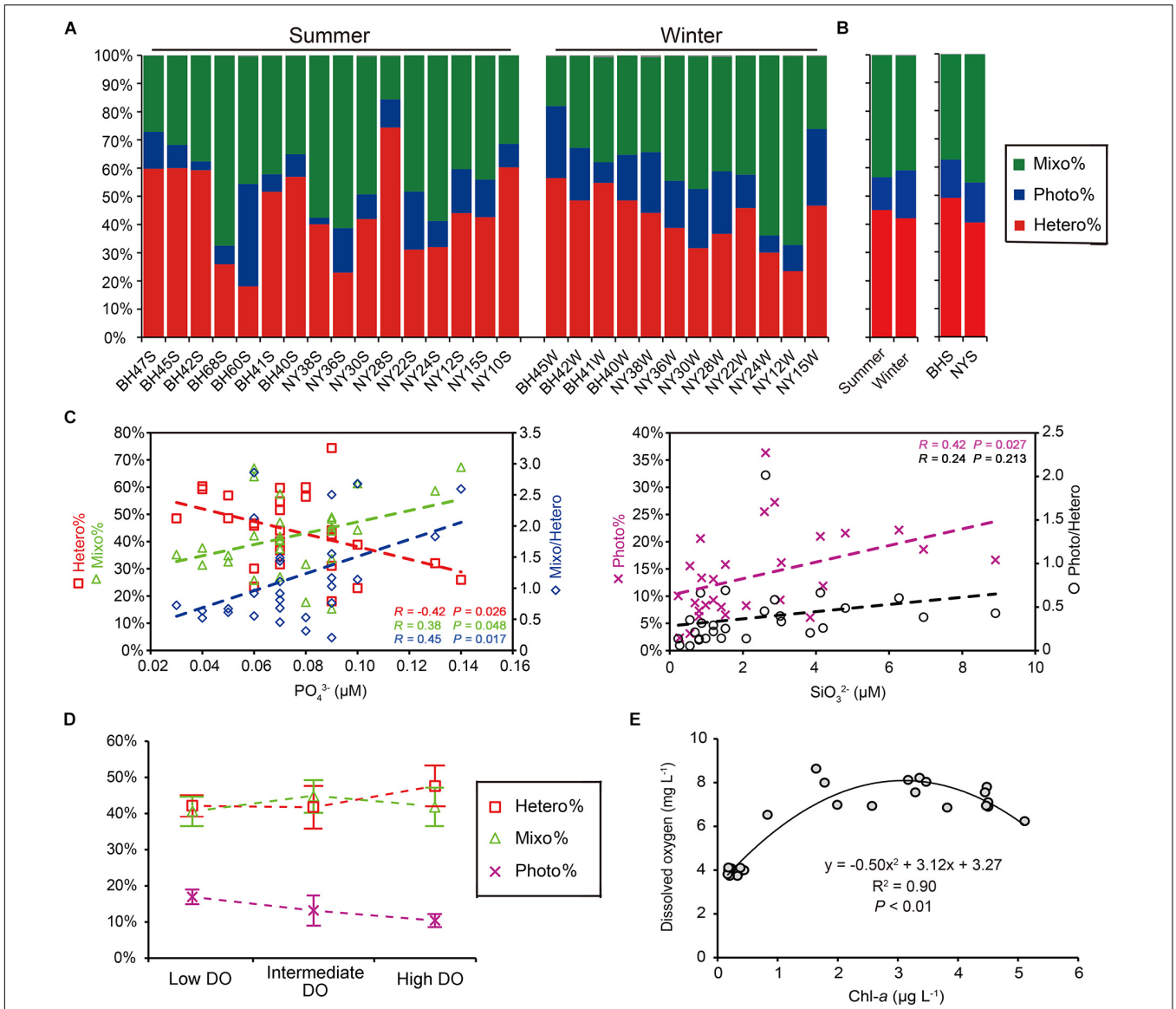

FIGURE 8 | Functional composition of pico-/nanoeukaryotic community as shown by the pyrotag proportions of heterotrophs (Hetero%), phototrophs (Photo%), and Mixotrophs (Mixo%) in the communities. **(A)** Variation among individual samples. **(B)** Comparisons between two seasons and between basins, none of which was significant ($P > 0.05$). **(C)** The Hetero% was negatively correlated with concentration of phosphate, and Mixo% was positively correlated with concentration of phosphate, resulting in a higher Mixo/Hetero ratio at a higher level of phosphate ($P < 0.05$). Both Photo% was positively related to concentration of silicate ($P < 0.05$), whereas the ratio of phototrophs to heterotrophs (Photo/Hetero) was not. **(D)** There were no significantly differences in percentages of pyrotags (mean and standard error) of three trophic groups across the low, intermediate and high levels of dissolved oxygen (DO). **(E)** The humped relationship between concentrations of DO and chlorophyll-*a* observed in the present study.

in winter; the on average concentration of PO_4^{3-} was very low (0.068 μM); and N:P ratio (on average 355) was much higher than the Redfield ratio (16:1). These results collectively indicate a N-rich and P-limited regime of BHS and NYS, which is largely consistent with previous reports for these regions (Yang et al., 2018; Wang et al., 2019; Xin et al., 2019). Our measurements of surface Chl-*a* were generally low (<1 μg L^{-1}) in winter and higher (>1 μg L^{-1}) in summer, indicating a higher contribution of pico-/nanophytoplankton in the total phytoplankton biomass in the winter in the studied areas (Marañón et al., 2012). The characteristics of phytoplankton size classes in BHS and NYS have been demonstrated by *in situ* measurements of size-fractionated Chl-*a* and satellite-based observations (Sun D. et al., 2019; Sun X. et al., 2019). Nevertheless, our study contributes knowledge on the genetic diversity and taxonomic community composition, as well as, seasonal and spatial variability of P/NEs. Moreover, the trophic types (autotrophs, mixotrophs, and heterotrophs) of pico-/nanoeukaryotic components in the microbial loop of the studied areas are revealed.

Operational Taxonomic Unit Richness of P/NEs Across Productivity and Dissolved Oxygen Gradients

The local and regional species richness and productivity relationship (SPR) is one of the central topics in community ecology. The curves describing SPR can be linear positive, hump-shaped (unimodal), linear negative, U-shaped, or of non-significant pattern. The unimodal relationship has been the most frequently recognized one in macroorganisms (Mittelbach et al., 2001; Scheiner and Willig, 2005; Whittaker, 2010) and marine phytoplankton (Vallina et al., 2014), while the U-shaped relationship has been found only rarely in microorganisms (Smith, 2007). Therefore, our observation of a U-shaped relationship between pico-/nanoeukaryotic richness and Chl-*a* is somewhat extraordinary. In this type of relationship, richness achieves a clear minimum at intermediate productivity levels. Nonetheless, the mechanisms underlying this pattern have yet to be understood. The U-shaped curve (**Figure 2C**) was mainly attributed to Syndiniales, ciliates and MASTs (**Supplementary Figure 2**), all of which comprise mostly heterotrophs. On the negative side of the curve, the OTU numbers of these three groups sharply decreased with Chl-*a*. This observation might be attributed to certain species getting increasingly dominant during the bloom, leading to a decrease in OTU richness temporarily. However, at the intermediate Chl-*a* levels, additional DOC released by phytoplankton could promote overgrowth of certain bacterial groups (for example, Gammaproteobacteria; Alonso-Sáez et al., 2009). This could lower diversity of bacterial communities, alter the overall digestibility of bacterioplankton (Gong et al., 2016), and in turn select for specific bacterivorous populations of ciliates and MAST grazers (Jürgens and Güde, 1994). On the positive side of the curve, whereby Chl-*a* is sustained at even higher levels, Dinophyceae are consistently present in high proportions in the communities (**Supplementary Table 5**), which might stimulate parasitic Syndiniales in pico-fractions (Chambouvet et al., 2008). Alternatively, the increased OTU richness of Syndiniales might be due to release of additional phylotypes into the pico-/nano-sized pool, when highly abundant infected micro-sized host cells burst. Thus, the top-down and bottom-up effects and species turnover of heterotrophs and mixotrophs seemed to determine the variation of richness of P/NEs along the Chl-*a* gradient in this study. This idea agrees well with Scheiner and Willig (2005), who proposed a theoretical framework to explain U-shaped patterns, i.e., the inflection point of the curve was a consequence of trade-off or shift in two dominating mechanisms that control the number of individuals.

Notably, DO had a stronger and negative relationship with the OTU richness of P/NEs than Chl-*a* in surface waters of the studied regions (**Figures 2B,C**), suggesting that oxygenation status reflects species richness of P/NEs more comprehensively than productivity. From a biological point of view, DO is usually correlated with Chl-*a* (i.e., a higher phytoplankton biomass and primary production tends to yield more photosynthetically produced O_2 leading to higher level of DO in the water), and it is often difficult to disentangle the effects of these two factors. Nevertheless, the unimodal relationship between Chl-*a* and DO observed in our study (**Figure 8E**) indicates existence of an ecological feedback mechanism, whereby DO peaks at intermediate levels of Chl-*a*. Previous studies have shown that under highly eutrophic conditions (Chl-*a* $> 3\ \mu g\ L^{-1}$), both carbon fixation and O_2 production were mainly contributed by microphytoplankton (Marañón et al., 2012), accompanied by release of a higher amount of DOC (Baines and Pace, 1991; Marañón et al., 2005). Under these conditions, productivity and oxygen consumption by heterotrophic prokaryotes was enhanced (Cole et al., 1988; Baines and Pace, 1991), thus lowering the DO levels in surrounding waters. Due to relatively larger sizes, protists have much higher apparent half-saturation constants for O_2 uptake (Fenchel and Finlay, 2008). Thus, a high DO concentration might relieve the competitive pressure of heterotrophic eukaryotes against bacteria, leading to an increase of their proportions in biomass (**Figure 8D**) and contributing to low species richness. In addition to bacterioplankton, P/NEs could also contribute significantly to community respiration (Harrison, 1986; Hernandez-Ruiz et al., 2018). Therefore, the DO level reflects the balance between biological production and consumption of O_2. These processes are involved in not only maintaining the standing stock of autotrophs and heterotrophs, but also their physiological activities, both of which are controlled by a range of environmental variables (e.g., light availability and temperature). Apart from these biological effects, physical processes (e.g., wind induced air-water interface exchange) and diel cycle (some of the samples herein were collected at night, when Chl-*a* level was relatively steady, but the DO was lower compared with that during daytime) are also among the controlling factors of DO dynamics (Hull et al., 2008). The observed stronger relationship of richness with DO rather than Chl-*a* in this study, along with the highly dynamic nature of DO in surface waters, suggests that DO is likely a more important environmental factor than productivity in reflecting the richness of P/NEs in coastal oceans. Nevertheless, more accurate measurements of Chl-*a* concentration (e.g., using high performance liquid chromatography), and direct determination of primary productivity using ^{14}C method would be worth applying in the future to more accurately explore the richness-productivity relationship.

Limiting Nutrients Drive the Functional Composition of Pico-/Nanoeukaryote Community

A number of studies have investigated the functional traits of protistan communities based on metabarcoding data of 18S rRNA genes (e.g., Charvet et al., 2014; de Vargas et al., 2015; Genitsaris et al., 2015; Ramond et al., 2019). Using a similar approach, our study indicated functional redundancy of P/NEs in the BHS and NYS. While the taxonomic community composition of P/NEs was significantly correlated with DO (**Figures 4B,C**) and differed between seasons (**Table 1**), the functional traits (trophic strategies) of the community (Photo%, Hetero%, and Mixo% in read proportion) did not follow any of these correlations and trends (**Figures 8B,D**). This observed

decoupling contrasts with the study by Ramond et al. (2019), who found that the taxonomic and functional diversity of marine planktonic protists of pico-, nano- and micro-size classes in the Atlantic were tightly coupled. Compared with ours, their samples were collected from stations spanning a much larger geographic distance (over 3600 vs. 600 km) and latitude gradient; it is likely that the large scale of sampling resulted in higher variability of functional diversity, as has already been observed for taxonomic diversity (Martiny et al., 2006). Our sampling of surface waters [vs. surface, deep chlorophyll maximum (DCM) and mesopelagic zone] in the open ocean (vs. open water, estuaries, and upwelling) exhibited relatively low environmental heterogeneity (e.g., in terms of irradiance, organic carbon sources, and abundance and composition of bacterial food), which might account for the observed reduced functional variability of the pico-/nanoeukaryotic communities in this study.

Unexpectedly, the functional composition of pico-/nanoeukaryotic communities was significantly related to PO_4^{3-}, a limiting nutrient in the BHS and NYS basins (**Figure 8C**). Under conditions of P-deficit, mixotrophic eukaryotes can obtain nutrients by predating on bacteria (e.g., Nygaard and Tobiesen, 1993). Nevertheless, this switch to heterotrophy might come with a cost, in that mixotrophs might not be as competitive as strict heterotrophs in ingesting and digesting bacterial prey. When the level of PO_4^{3-} increased beyond a threshold (e.g., 0.08 μM), the use of both inorganic and bacterial resources might have led to a distinct advantage of the mixotrophs over the heterotrophs. Our observation of the trade-off between mixotrophs and heterotrophs along the nutrient gradient is in line with the model predicted by Edwards (2019). Nevertheless, the percentage of phototrophs in the pico-/nanoeukaryotic community was not significantly correlated with PO_4^{3-}, which was likely due to their capability of using non-phosphorus membrane lipids for growth in the face of P-limitation (Van Mooy et al., 2009). While the concentration of PO_4^{3-} was positively correlated with Chl-*a* in our samples, that of SiO_3^{2-} had a negative correlation with Chl-*a*. This suggests that uptake of SiO_3^{2-} by phytoplankton (especially large-celled diatoms) led to the low level of SiO_3^{2-} observed in this study. Therefore, the lower percentage of autotrophs at lower SiO_3^{2-} supply might be a consequence of immobilization and competition for Si between nano- and micro-sized diatoms.

DATA AVAILABILITY STATEMENT

The datasets presented in this study can be found in online repositories. The names of the repository/repositories and accession number(s) can be found in the article/**Supplementary Material**.

AUTHOR CONTRIBUTIONS

YW and GL analyzed the data. FS and JD performed the sample preparation, DNA extraction, and submission to sequencing. SZ, PZ, and XZ took part in cruises for sampling and obtaining metadata. EG and JG revised the manuscript. YW, GL, and JG wrote the manuscript. JG conceived the research and designed the experiment. All authors approved the final version of the manuscript and agreed to its submission for publication.

FUNDING

This work was supported by the National Natural Science Foundation of China (No. 41976128), the Marine S and T Fund of Shandong Province for Pilot National Laboratory for Marine Science and Technology (Qingdao) (No. 2018SDKJ0406-4), the Research Fund Program of Guangdong Provincial Key Laboratory of Marine Resources and Coastal Engineering, the Key Research Project of Frontier Science, CAS (No. QYZDB-SSW-DQC013-1), and the Fundamental Research Funds for the Central Universities, China (No. 42000-31611178).

SUPPLEMENTARY MATERIAL

The Supplementary Material for this article can be found online at: https://www.frontiersin.org/articles/10.3389/fmicb.2020.601037/full#supplementary-material

REFERENCES

Alonso-Sáez, L., Unanue, M., Latatu, A., Azua, I., Ayo, B., Artolozaga, I., et al. (2009). Changes in marine prokaryotic community induced by varying types of dissolved organic matter and subsequent grazing pressure. *J. Plankton Res.* 31, 1373–1383. doi: 10.1093/plankt/fbp081

Baines, S. B., and Pace, M. L. (1991). The production of dissolved organic matter by phytoplankton and its importance to bacteria: patterns across marine and freshwater systems. *Limnol. Oceanogr.* 36, 1078–1090. doi: 10.4319/lo.1991.36.6.1078

Bell, T., and Kalff, J. (2001). The contribution of picophytoplankton in marine and freshwater systems of different trophic status and depth. *Limnol. Oceanogr.* 46, 1243–1248. doi: 10.4319/lo.2001.46.5.1243

Burney, C. M., Davis, P. G., Johnson, K. M., and Sieburth, J. M. (1981). Dependence of dissolved carbohydrate concentrations upon small scale nanoplankton and bacterioplankton distributions in the western Sargasso Sea. *Mar. Biol.* 65, 289–296. doi: 10.1007/BF00397124

Caporaso, J. G., Kuczynski, J., Stombaugh, J., Bittinger, K., Bushman, F. D., Costello, E. K., et al. (2010). QIIME allows analysis of high-throughput community sequencing data. *Nat. Methods* 7, 335–336. doi: 10.1038/nmeth.f.303

Casamayor, E. O., Massana, R., Benlloch, S., Øvreås, L., Díez, B., Goddard, V. J., et al. (2002). Changes in archaeal, bacterial and eukaryal assemblages along a salinity gradient by comparison of genetic fingerprinting methods in a multipond solar saltern. *Environ. Microbiol.* 4, 338–348. doi: 10.1046/j.1462-2920.2002.00297.x

Chambouvet, A., Morin, P., Marie, D., and Guillou, L. (2008). Control of toxic marine dinoflagellate blooms by serial parasitic killers. *Science* 322, 1254–1257. doi: 10.1126/science.1164387

Charvet, S., Vincent, W. F., and Lovejoy, C. (2014). Effects of light and prey availability on Arctic freshwater protist communities examined by high-throughput DNA and RNA sequencing. *FEMS Microbiol. Ecol.* 88, 550–564. doi: 10.1111/1574-6941.12324

Chen, C.-T. A. (2009). Chemical and physical fronts in the Bohai, Yellow and East China seas. *J. Mar. Syst.* 78, 394–410. doi: 10.1016/j.jmarsys.2008.11.016

Christaki, U., Wambeke, F. V., and Dolan, J. R. (1999). Nanoflagellates (mixotrophs, heterotrophs and autotrophs) in the oligotrophic eastern Mediterranean: standing stocks, bacterivory and relationships with bacterial production. *Mar. Ecol. Prog. Ser.* 181, 297–307. doi: 10.3354/meps181297

Cole, J. J., Findlay, S., and Pace, M. L. (1988). Bacterial production in fresh and saltwater ecosystems: a cross-system overview. *Mar. Ecol. Prog. Ser.* 43, 1–10. doi: 10.3354/meps043001

de Vargas, C., Audic, S., Henry, N., Decelle, J., Mahe, F., Logares, R., et al. (2015). Eukaryotic plankton diversity in the sunlit ocean. *Science* 348:1261605. doi: 10.1126/science.1261605

Edwards, K. F. (2019). Mixotrophy in nanoflagellates across environmental gradients in the ocean. *Proc. Natl. Acad. Sci. U.S.A.* 116, 6211–6220. doi: 10.1073/pnas.1814860116

Fenchel, T., and Finlay, B. (2008). Oxygen and the spatial structure of microbial communities. *Biol. Rev.* 83, 553–569. doi: 10.1111/j.1469-185X.2008.00054.x

Genitsaris, S., Monchy, S., Viscogliosi, E., Sime-Ngando, T., Ferreira, S., and Christaki, U. (2015). Seasonal variations of marine protist community structure based on taxon-specific traits using the eastern English Channel as a model coastal system. *FEMS Microbiol. Ecol.* 91:fiv034. doi: 10.1093/femsec/fiv034

Gong, F., Li, G., Wang, Y., Liu, Q., Huang, F., Yin, K., et al. (2020). Spatial shifts in size structure, phylogenetic diversity, community composition and abundance of small eukaryotic plankton in a coastal upwelling area of the northern South China Sea. *J. Plankton Res.* 42, 650–667. doi: 10.1093/plankt/fbaa046

Gong, J., Qing, Y., Zou, S., Fu, R., Su, L., Zhang, X., et al. (2016). Protist-bacteria associations: Gammaproteobacteria and Alphaproteobacteria are prevalent as digestion-resistant bacteria in ciliated protozoa. *Front. Microbiol.* 7:498. doi: 10.3389/fmicb.2016.00498

Guan, B. X. (1994). "Patterns and structures of the currents in Bohai, Huanghai and East China Seas," in *Oceanology of China Seas*, eds D. Zhou, Y.-B. Liang, and C.-K. Zeng (Dordrecht: Springer), 17–26. doi: 10.1007/978-94-011-0862-1_3

Guillou, L., Bachar, D., Audic, S., Bass, D., Berney, C., Bittner, L., et al. (2012). The protist ribosomal reference database (PR2): a catalog of unicellular eukaryote small sub-unit rRNA sequences with curated taxonomy. *Nucleic Acids Res.* 41, D597–D604. doi: 10.1093/nar/gks1160

Harrison, W. (1986). Respiration and its size-dependence in microplankton populations from surface waters of the Canadian Arctic. *Polar Biol.* 6, 145–152. doi: 10.1007/BF00274877

Hartmann, M., Grob, C., Tarran, G. A., Martin, A. P., Burkill, P. H., Scanlan, D. J., et al. (2012). Mixotrophic basis of Atlantic oligotrophic ecosystems. *Proc. Natl. Acad. Sci. U.S.A.* 109, 5756–5760. doi: 10.1073/pnas.1118179109

Hernandez-Ruiz, M., Barber-Lluch, E., Prieto, A., Alvarez-Salgado, X. A., Logares, R., and Teira, E. (2018). Seasonal succession of small planktonic eukaryotes inhabiting surface waters of a coastal upwelling system. *Environ. Microbiol.* 20, 2955–2973. doi: 10.1111/1462-2920.14313

Hull, V., Parrella, L., and Falcucci, M. (2008). Modelling dissolved oxygen dynamics in coastal lagoons. *Ecol. Model.* 211, 468–480. doi: 10.1016/j.ecolmodel.2007.09.023

Jürgens, K., and Güde, H. (1994). The potential importance of grazing-resistant bacteria in planktonic systems. *Mar. Ecol. Prog. Ser.* 112, 169–188.

Linley, E., Newell, R., and Lucas, M. (1983). Quantitative relationships between phytoplankton, bacteria and heterotrophic microflagellates in shelf waters. *Mar. Ecol. Prog. Ser.* 12, 77–89. doi: 10.3354/meps012077

Liu, F., Su, J., Moll, A., Krasemann, H., Chen, X., Pohlmann, T., et al. (2014). Assessment of the summer–autumn bloom in the Bohai Sea using satellite images to identify the roles of wind mixing and light conditions. *J. Mar. Syst.* 129, 303–317. doi: 10.1016/j.jmarsys.2013.07.007

Lonsdale, D. J., Greenfield, D. I., Hillebrand, E. M., Nuzzi, R., and Taylor, G. T. (2006). Contrasting microplanktonic composition and food web structure in two coastal embayments (Long Island, NY, USA). *J. Plankton Res.* 28, 891–905. doi: 10.1093/plankt/fbl027

López-García, P., Philippe, H., Gail, F., and Moreira, D. (2003). Autochthonous eukaryotic diversity in hydrothermal sediment and experimental microcolonizers at the Mid-Atlantic Ridge. *Proc. Natl. Acad. Sci. U.S.A.* 100, 697–702. doi: 10.1073/pnas.0235779100

Lopez-Garcia, P., Rodriguez-Valera, F., Pedros-Alio, C., and Moreira, D. (2001). Unexpected diversity of small eukaryotes in deep-sea Antarctic plankton. *Nature* 409, 603–607. doi: 10.1038/35054537

Marañón, E., Cermeño, P., and Pérez, V. (2005). Continuity in the photosynthetic production of dissolved organic carbon from eutrophic to oligotrophic waters. *Mar. Ecol. Prog. Ser.* 299, 7–17. doi: 10.3354/meps299007

Marañón, E., Cermeno, P., Latasa, M., and Tadonléké, R. D. (2012). Temperature, resources, and phytoplankton size structure in the ocean. *Limnol. Oceanogr.* 57, 1266–1278. doi: 10.4319/lo.2012.57.5.1266

Martiny, J. B. H., Bohannan, B. J. M., Brown, J. H., Colwell, R. K., Fuhrman, J. A., Green, J. L., et al. (2006). Microbial biogeography: putting microorganisms on the map. *Nat. Rev. Microbiol.* 4, 102–112. doi: 10.1038/nrmicro1341

Massana, R. (2011). Eukaryotic picoplankton in surface oceans. *Annu. Rev. Microbiol.* 65, 91–110. doi: 10.1146/annurev-micro-090110-102903

Massana, R., Gobet, A., Audic, S., Bass, D., Bittner, L., Boutte, C., et al. (2015). Marine protist diversity in European coastal waters and sediments as revealed by high-throughput sequencing. *Environ. Microbiol.* 17, 4035–4049. doi: 10.1111/1462-2920.12955

Massana, R., Unrein, F., Rodriguez-Martinez, R., Forn, I., Lefort, T., Pinhassi, J., et al. (2009). Grazing rates and functional diversity of uncultured heterotrophic flagellates. *ISME J.* 3, 588–596. doi: 10.1038/ismej.2008.130

McMurdie, P. J., and Holmes, S. (2014). Waste not, want not: why rarefying microbiome data is inadmissible. *PLoS Comput. Biol.* 10:e1003531. doi: 10.1371/journal.pcbi.1003531

Mittelbach, G. G., Steiner, C. F., Scheiner, S. M., Gross, K. L., Reynolds, H. L., Waide, R. B., et al. (2001). What is the observed relationship between species richness and productivity? *Ecology* 82, 2381–2396.

Moon-van der Staay, S. Y., De Wachter, R., and Vaulot, D. (2001). Oceanic 18S rDNA sequences from picoplankton reveal unsuspected eukaryotic diversity. *Nature* 409, 607–610. doi: 10.1038/35054541

Moreira, D., and Lopez-Garcia, P. (2002). The molecular ecology of microbial eukaryotes unveils a hidden world. *Trends Microbiol.* 10, 31–38. doi: 10.1016/S0966-842X(01)02257-0

Nygaard, K., and Tobiesen, A. (1993). Bacterivory in algae: a survival strategy during nutrient limitation. *Limnol. Oceanogr.* 38, 273–279. doi: 10.4319/lo.1993.38.2.0273

Oksanen, J., Blanchet, F. G., Kindt, R., Legendre, P., Minchin, P. R., O'hara, R., et al. (2013). *Package 'vegan'. Community Ecology Package, version, 2, 1-295*. Available online at: https://cran.r-project.org (accessed May 5, 2016).

Piwosz, K., Całkiewicz, J., Gołębiewski, M., and Creer, S. (2018). Diversity and community composition of pico-and nanoplanktonic protists in the Vistula River estuary (Gulf of Gdańsk, Baltic Sea). *Estuar. Coast. Shelf Sci.* 207, 242–249. doi: 10.1016/j.ecss.2018.04.013

R Development Core Team (2013). *R: A Language and Environment for Statistical Computing*. Vienna: R Foundation for Statistical Computing.

Ramond, P., Sourisseau, M., Simon, N., Romac, S., Schmitt, S., Rigaut-Jalabert, F., et al. (2019). Coupling between taxonomic and functional diversity in protistan coastal communities. *Environ. Microbiol.* 21, 730–749. doi: 10.1111/1462-2920.14537

Righetti, D., Vogt, M., Gruber, N., Psomas, A., and Zimmermann, N. E. (2019). Global pattern of phytoplankton diversity driven by temperature and environmental variability. *Sci. Adv.* 5:eaau6253. doi: 10.1126/sciadv.aau6253

Robinson, M. D., McCarthy, D. J., and Smyth, G. K. (2010). edgeR: a bioconductor package for differential expression analysis of digital gene expression data. *Bioinformatics* 26, 139–140. doi: 10.1093/bioinformatics/btp616

Romari, K., and Vaulot, D. (2004). Composition and temporal variability of picoeukaryote communities at a coastal site of the English Channel from 18S rDNA sequences. *Limnol. Oceanogr.* 49, 784–798. doi: 10.4319/lo.2004.49.3.0784

Scheiner, S. M., and Willig, M. R. (2005). Developing unified theories in ecology as exemplified with diversity gradients. *Am. Nat.* 166, 458–469. doi: 10.1086/444402

Schloss, P. D., Westcott, S. L., Ryabin, T., Hall, J. R., Hartmann, M., Hollister, E. B., et al. (2009). Introducing mothur: open-source, platform-independent, community-supported software for describing and comparing microbial communities. *Appl. Environ. Microbiol.* 75, 7537–7541. doi: 10.1128/AEM.01541-09

Sherr, B. F., Sherr, E. B., Caron, D. A., Vaulot, D., and Worden, A. Z. (2007). Oceanic protists. *Oceanography* 20, 130–134.

Sherr, E. B., and Sherr, B. F. (1994). Bacterivory and herbivory: key roles of phagotrophic protists in pelagic food webs. *Microb. Ecol.* 28, 223–235. doi: 10.1007/BF00166812

Šimek, K., Grujčić, V., Nedoma, J., Jezberová, J., Šorf, M., Matoušů, A., et al. (2019). Microbial food webs in hypertrophic fishponds: omnivorous ciliate taxa are major protistan bacterivores. *Limnol. Oceanogr.* 64, 2295–2309. doi: 10.1002/lno.11260

Smith, V. H. (2007). Microbial diversity–productivity relationships in aquatic ecosystems. *FEMS Microbiol. Ecol.* 62, 181–186. doi: 10.1111/j.1574-6941.2007.00381.x

Šolić, M., Krstulović, N., Kušpilić, G., Gladan, ŽN., Bojanić, N., Šestanović, S., et al. (2010). Changes in microbial food web structure in response to changed environmental trophic status: a case study of the Vranjic Basin (Adriatic Sea). *Mar. Environ. Res.* 70, 239–249. doi: 10.1016/j.marenvres.2010.05.007

Sun, D., Huan, Y., Wang, S., Qiu, Z., Ling, Z., Mao, Z., et al. (2019). Remote sensing of spatial and temporal patterns of phytoplankton assemblages in the Bohai Sea, Yellow Sea, and East China Sea. *Water Res.* 157, 119–133. doi: 10.1016/j.watres.2019.03.081

Sun, X., Shen, F., Brewin, R. J., Liu, D., and Tang, R. (2019). Twenty-year variations in satellite-derived Chlorophyll-*a* and phytoplankton size in the Bohai Sea and Yellow Sea. *J. Geophys. Res. Oceans* 124, 8887–8912. doi: 10.1029/2019JC015552

Unrein, F., Gasol, J. M., Not, F., Forn, I., and Massana, R. (2014). Mixotrophic haptophytes are key bacterial grazers in oligotrophic coastal waters. *ISME J.* 8, 164–176. doi: 10.1038/ismej.2013.132

Vallina, S. M., Follows, M., Dutkiewicz, S., Montoya, J. M., Cermeno, P., and Loreau, M. (2014). Global relationship between phytoplankton diversity and productivity in the ocean. *Nat. Commun.* 5:4299. doi: 10.1038/ncomms5299

Van Mooy, B. A., Fredricks, H. F., Pedler, B. E., Dyhrman, S. T., Karl, D. M., Koblížek, M., et al. (2009). Phytoplankton in the ocean use non-phosphorus lipids in response to phosphorus scarcity. *Nature* 458, 69–72. doi: 10.1038/nature07659

Wang, J., Yu, Z., Wei, Q., and Yao, Q. (2019). Long-term nutrient variations in the Bohai Sea over the past 40 years. *J. Geophys. Res. Oceans* 124, 703–722. doi: 10.1029/2018JC014765

Wei, H., Sun, J., Moll, A., and Zhao, L. (2004). Phytoplankton dynamics in the Bohai Sea—observations and modelling. *J. Mar. Syst.* 44, 233–251. doi: 10.1016/j.jmarsys.2003.09.012

Whittaker, R. J. (2010). Meta-analyses and mega-mistakes: calling time on meta-analysis of the species richness-productivity relationship. *Ecology* 91, 2522–2533. doi: 10.1890/08-0968.1

Worden, A. Z., and Not, F. (2008). "Ecology and diversity of picoeukaryotes," in *Microbial Ecology of the Ocean*, 2nd Edn, ed. D. L. Kirchman (Hoboken, NJ: John Wiley and Sons), 159–205. doi: 10.1002/9780470281840.ch6

Xie, L., Sun, X., Wang, B., and Xin, M. (2012). Temporal and spatial distributions of trophic structure and potential nutrient limitation in the Bohai Sea and the Yellow Sea. *Mar. Sci.* 36, 45–53.

Xin, M., Wang, B., Xie, L., Sun, X., Wei, Q., Liang, S., et al. (2019). Long-term changes in nutrient regimes and their ecological effects in the Bohai Sea, China. *Mar. Pollut. Bull.* 146, 562–573. doi: 10.1016/j.marpolbul.2019.07.011

Yang, F., Wei, Q., Chen, H., and Yao, Q. (2018). Long-term variations and influence factors of nutrients in the western North Yellow Sea, China. *Mar. Pollut. Bull.* 135, 1026–1034. doi: 10.1016/j.marpolbul.2018.08.034

Zhao, C., Zang, J., Liu, J., Sun, T., and Ran, X. (2016). Distribution and budget of nitrogen and phosphorus and their influence on the ecosystem in the Bohai Sea and Yellow Sea. *China Environ. Sci.* 36, 2115–2127.

Zhou, Y., Zhang, C., Shi, X., and Su, R. (2017). Distribution characteristics of chlorophyll *a* and its influencing environmental factors in Bohai Sea and Yellow Sea. *China Environ. Sci.* 37, 4259–4265. doi: 10.3969/j.issn.1000-6923.2017.11.031

Conflict of Interest: The authors declare that the research was conducted in the absence of any commercial or financial relationships that could be construed as a potential conflict of interest.

frontiers in Microbiology

ORIGINAL RESEARCH
published: 04 February 2021
doi: 10.3389/fmicb.2021.638129

Community Structure of Protease-Producing Bacteria Cultivated From Aquaculture Systems: Potential Impact of a Tropical Environment

Yali Wei[1,2†], Jun Bu[1,3,4†], Hao Long[1,3,4], Xiang Zhang[1,3,4], Xiaoni Cai[1,3,4], Aiyou Huang[1,3,4], Wei Ren[1,3,4] and Zhenyu Xie[1,3,4*]*

[1]State Key Laboratory of Marine Resource Utilization in the South China Sea, Hainan University, Haikou, China, [2]Ministry of Education Key Laboratory of Cell Activities and Stress Adaptations, School of Life Sciences, Lanzhou University, Lanzhou, China, [3]Hainan Provincial Key Laboratory for Tropical Hydrobiology and Biotechnology, Hainan University, Haikou, China, [4]College of Marine Sciences, Hainan University, Haikou, China

OPEN ACCESS

Edited by:
Konstantinos Ar. Kormas, University of Thessaly, Greece

Reviewed by:
Jiazhang Chen, Chinese Academy of Fishery Sciences, China
Hailun He, Central South University, China

***Correspondence:**
Wei Ren
renweifly@126.com
Zhenyu Xie
xiezyscuta@163.com;
994394@hainanu.edu.com

†These authors have contributed equally to this work

Specialty section:
This article was submitted to Aquatic Microbiology, a section of the journal Frontiers in Microbiology

Received: *05 December 2020*
Accepted: *05 January 2021*
Published: *04 February 2021*

Citation:
Wei Y, Bu J, Long H, Zhang X, Cai X, Huang A, Ren W and Xie Z (2021) Community Structure of Protease-Producing Bacteria Cultivated From Aquaculture Systems: Potential Impact of a Tropical Environment. Front. Microbiol. 12:638129. doi: 10.3389/fmicb.2021.638129

Protease-producing bacteria play vital roles in degrading organic matter of aquaculture system, while the knowledge of diversity and bacterial community structure of protease-producing bacteria is limited in this system, especially in the tropical region. Herein, 1,179 cultivable protease-producing bacterial strains that belonged to Actinobacteria, Firmicutes, and Proteobacteria were isolated from tropical aquaculture systems, of which the most abundant genus was *Bacillus*, followed by *Vibrio*. The diversity and relative abundance of protease-producing bacteria in sediment were generally higher than those in water. Twenty-one genera from sediment and 16 genera from water were identified, of which *Bacillus* dominated by *Bacillus hwajinpoensis* in both and *Vibrio* dominated by *Vibrio owensii* in water were the dominant genera. The unique genera in sediment or water accounted for tiny percentage may play important roles in the stability of community structure. Eighty *V. owensii* isolates were clustered into four clusters (ET-1–ET-4) at 58% of similarity by ERIC-PCR (enterobacterial repetitive intergenic consensus-polymerase chain reaction), which was identified as a novel branch of *V. owensii*. Additionally, *V. owensii* strains belonged to ET-3 and ET-4 were detected in most aquaculture ponds without outbreak of epidemics, indicating that these protease-producing bacteria may be used as potential beneficial bacteria for wastewater purification. Environmental variables played important roles in shaping protease-producing bacterial diversity and community structure in aquaculture systems. In sediment, dissolved oxygen (DO), chemical oxygen demand (COD), and salinity as the main factors positively affected the distributions of dominant genus (*Vibrio*) and unique genera (*Planococcus* and *Psychrobacter*), whereas temperature negatively affected that of *Bacillus* (except *B. hwajinpoensis*). In water, *Alteromonas* as unique genus and *Photobacterium* were negatively affected by NO_3^--N and NO_2^--N, respectively, whereas pH as the main factor positively affected the distribution of *Photobacterium*. These findings will lay a foundation for the development of protease-producing bacterial agents for wastewater purification and the construction of an environment-friendly tropical aquaculture model.

Keywords: protease-producing bacteria, *Vibrio owensii*, tropical aquaculture, enterobacterial repetitive intergenic consensus-polymerase chain reaction, environmental variables, *Bacillus hwajinpoensis*, bacterial community structure

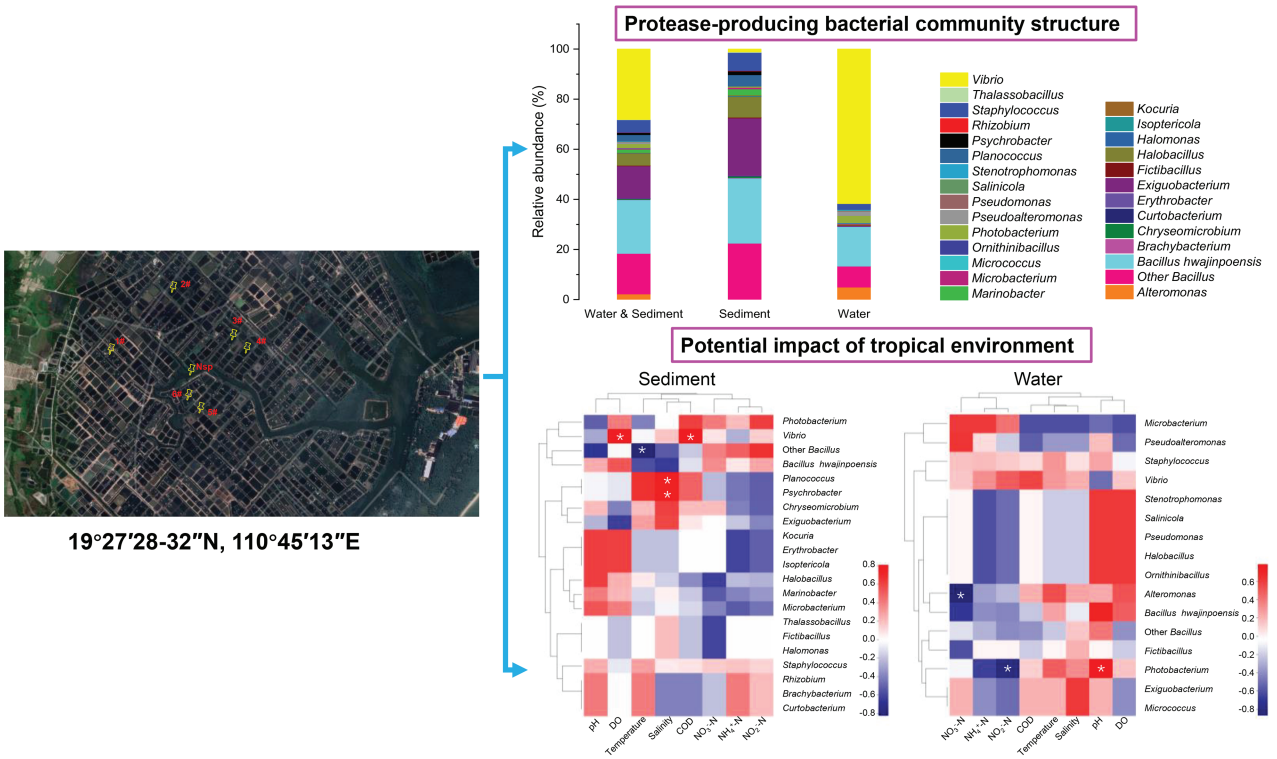

GRAPHICAL ABSTRACT | Community structure of protease-producing bacteria cultivated from aquaculture systems: potential impact of a tropical environment, in the case of Wenchang, Hainan, China.

INTRODUCTION

Aquaculture as an important food production has become an important economic activity in many countries (Hamza et al., 2017; Santos and Ramos, 2018). However, with the rapid development of aquaculture industry, a large number of animal residues, residual feed, and excrement have been produced, thereby aggravating the accumulation of organic matter in aquaculture (Lin and Chen, 2001, 2003; Kuhn et al., 2010; Guo et al., 2016; Li et al., 2020; Mariane de Morais et al., 2020). The main sources of nitrogen and carbon of aquaculture are from the particulate organic matters containing large amounts of proteins and amino acids. Generally, particulate organic matter is difficult to be dissolved, which should be first decomposed into dissolved form. In turn, the dissolved organic matter can be transformed into nitrogen gas by ammonification, nitrification, and denitrification. Bacteria play key roles in these processes by secreting degradation enzymes (Olson and Lesser, 2013; Su et al., 2020).

Protease-producing bacteria as the main degraders of organic matter can effectively hydrolyze the organic matter into peptides and amino acids by secreting extracellular proteases (Su et al., 2020). As we all know, peptides and amino acids are essential for subsequent catabolism of organisms. Reportedly, protease-producing bacteria could not only improve protein digestibility and growth of the host, but also reduce organic pollutants in aquaculture (Shi et al., 2016; Amin, 2018; Su et al., 2020). Protease-producing bacteria that belong to four major phyla, Proteobacteria, Firmicutes, Actinobacteria, and Bacteroidetes, have been identified, which are dominated by *Bacillus*, *Pseudomonas*, and *Pseudoalteromonas* genera (Su et al., 2020).

Many methods have been developed to enhance protein digestibility of aquafeed in aquaculture. However, the application of exogenous enzymes has been limited because of expensive and poor stability in various processing conditions. During the feed processing, dietary enzymes may lose their activities under high temperature and pressure conditions. Fortunately, an increasingly accepted method by supplementing protease-producing bacteria considered as an environment-friendly method was good for growth enhancement (Shi et al., 2016; Amin, 2018), which has been confirmed to not only enhance protein digestibility, but also reduce organic pollutants produced by undigested feed (Suzer et al., 2008; Ambas et al., 2015; Reda and Selim, 2015). Reportedly, feed by supplementing 1.0×10^{10} CFU/g protease-producing bacteria could improve growth and nonspecific immune system of Nile tilapia (Selim and Reda, 2015).

Protease-producing bacteria play a vital role in degrading organic matter. However, the diversity and community of protease-producing bacteria have seldom been addressed in aquaculture. As a consequence, in this article, 1,179 cultivable

protease-producing bacterial strains were isolated and screened from sediment and water samples in Wenchang (Hainan, China), and then their diversity and community structure were investigated. Additionally, the physicochemical factors related to diversity and distribution of protease-producing bacterial communities in sediment and water were comprehensively analyzed, respectively. The dominant protease-producing *Vibrio owensii* strains in aquaculture water were classified using enterobacterial repetitive intergenic consensus-polymerase chain reaction (ERIC-PCR).

MATERIALS AND METHODS

Study Site Description and Sample Collection

Surface sediment (2- to 3-cm thickness) and aquaculture water (1-m water depth) samples were collected from six prawn ponds (19°27'28-32"N, 110°45'13"E) and one nature sea pool (closed to the prawn ponds) located at Huiwen Town, Wenchang City, China. The special geographical position is shown in **Supplementary Figure S1**. The experimental ponds are summarized in **Supplementary Table S1**.

Isolation and Screening of Protease-Producing Bacteria

Sediment (0.5 g) and water (100 μl) samples were serially diluted with sterile normal saline solution (0.85% NaCl) within 24 h of collection to obtain 1:10, 1:100, and 1:1,000 dilutions. One hundred microliters of each diluted sample was spread-plated on marine 2216E agar and incubated at 30°C for 18 h, which was finally ascertained by preliminary selection for the condition of cultural bacteria. For screening of protease-producing bacteria, 2 μl of overnight growth culture in the marine 2216E of each bacterial isolate was spot plated on casein-gelatin agar [containing 0.2% yeast extract, 0.3% xasein, sodium salt, 5% gelatin, 0.13% $(NH_4)_2SO_4$, 0.05% $MgSO_4{\cdot}7H_2O$, and 1.5% agar and seawater; pH 7.5–8.0]. The protease-producing bacterial isolates were further used for DNA extraction.

Quantification of Protease Activity

Protease activity was elevated in terms of hydrolytic capacity (HC); the pure bacterial isolates were cultured in 2166E broth. A solution with OD at 600 nm of 0.2 ml was set, of which 1 μl was pipetted out and dropped on casein-gelatin agar plate in duplicates. Diameters of bacterial colonies and related-clearance zones were measured after 24-h incubation at 28°C ± 2°C. The HC value determined the protease activity was calculated from the ratio between the diameter of the caseinolytic zone and the diameter of the bacterial colony. In this study, we selected only colonies with a ratio greater than three.

DNA Extraction and PCR Amplification

Bacterial strain with the highest protease activity was identified using genotypic assay. Genomic DNAs of culturable protease-producing bacteria were extracted using a commercial DNA extraction kit (Tiangen Biotech, Beijing, China; Sun et al., 2008; Marquez-Santacruz et al., 2010), after bacterial growth on 2216E medium and incubation at 30°C for 18 h. The 16S rDNA genes were amplified from genomic DNA by PCR using the universal primers 27F (5'-AGAGTTTGATCCTGGCTCAG-3') and 1492R (5'-GGCTACCTTGTTACGACTT-3'). PCR amplifications were performed using the following conditions: initial denaturation of template DNA (95°C for 2 min), then 1 cycle consisting of denaturation (30 s at 95°C), annealing (30 s at 60°C), extension (1 min at 72°C), 25 cycles, and a final extension at 72°C for 5 min. Bacteria sequences obtained by culture-dependent approach were compared with 16S rDNA reference gene sequences by BLAST.[1]

Genetic Diversity of Dominant *V. owensii* Using ERIC-PCR

All the dominant isolates identified and confirmed as *V. owensii* were chosen for further molecular typing by ERIC-PCR. One microliter of the extracted DNA was added to 12.5 μl of PCR amplification mixture, containing 9.5 μl ddH_2O, and 2 μl primers (forward and reverse). Amplification reactions were carried out in a thermal cycler (Bio-Rad, United States) using the primer set ERIC-1R 5'-AAGTAAGTGACTGGGGTGAGCG-3', and ERIC-2F 5'-ATGTAAGCTCCTGGGGATTCAC-3'. The amplification program was as follows: an initial denaturation step at 95°C for 7 min, denaturation 90°C for 30 min; annealing at 52°C for 1 min; extension at 65°C for 8 min; and after 35 cycles, a final extension at 65°C for 16 min. Six microliters of each amplified product was electrophoresed on 1% agarose gel with DNA safe stain (Greenview Plus, Andy Gold™, United States) 1 × TAE buffer along with 1 Kb DNA Ladder (Thermo Fischer Scientific, United States) and M2-DL2000 marker (Takara, Japan), at 180 V for 50 min. The amplification was repeated three times.

Gels were viewed by Gel Imaging System (Tanon3500R, Shanghai, China). The images were captured for further analysis. In turn, "1" and "0" were assigned for the presence or lack of the banding pattern and recorded in sequence according to the reading direction. The genetic patterns were calculated according to the molecular weights and quantification of the bands in each sample. Simpson's Index of Diversity was used to calculated the discriminatory index of ERIC-PCR (Pishbin and Mehrabian, 2020), and the "unweighted pair group method with dice similarity coefficient" option in NTSYS v. 12 program (Bakhshi et al., 2018) was used to cluster the *V. owensii* isolates.

RESULTS

Analysis of Diversity and Distribution of Cultivable Protease-Producing Bacterial Strains

There were 1,179 cultivable protease-producing bacterial strains isolated and screened from sediment (654 strains) and water (525 strains) samples of aquaculture systems, and the bacterial counts

[1]http://eztaxon-e.ezbiocloud.net

of sediment and water varied from 2×10^4 to 2.6×10^5 CFU/g and 658 to 2.1×10^3 CFU/ml, respectively (**Table 1**). All of the isolates belonged to three phyla, Actinobacteria, Firmicutes, and Proteobacteria, and classified into 27 genera dominated by *Bacillus* (37.7%) and *Vibrio* (28.1%) genera (**Figure 1**, "Water & Sediment" bars), of which Firmicutes accounted for the highest proportion. Additionally, *Bacillus hwajinpoensis* in *Bacillus* was dominant species in whole tropical aquaculture system (**Figure 1B**). Twenty-one genera from sediment belonged to Actinobacteria, Firmicutes, and Proteobacteria, and bacterial diversity was found to be maximum (up to about 91.6%) in the phylum of Firmicutes. The largest genus was *Bacillus* (*B. hwajinpoensis* as the dominant species, 26%), followed by *Exiguobacterium* in sediment (**Figure 1**, "Sediment" bars). Additionally, 12 unique genera were isolated only from sediment samples, namely *Brachybacterium*, *Chryseomicrobium*, *Curtobacterium*, *Erythrobacter*, *Halomonas*, *Isoptericola*, *Kocuria*, *Marinobacter*, *Planococcus*, *Psychrobacter*, *Rhizobium*, and *Thalassobacillus*. Sixteen genera from aquaculture water samples also belonged to Actinobacteria, Firmicutes, and Proteobacteria, whereas their relative abundance displayed significant differences with those in sediment samples. The relative abundance of Proteobacteria was up to about 71.6%, followed by Firmicutes (28.0%), and the largest genus was *Vibrio* (61.7%) as the dominant group in aquaculture water samples (**Figure 1**, "Water" bars). Meanwhile, there were seven unique genera from water samples, namely, *Alteromonas*, *Micrococcus*, *Ornithinibacillus*, *Pseudoalteromonas*, *Pseudomonas*, *Salinicola*, and *Stenotrophomonas*. Previous studies have reported that protease-producing bacteria were extremely diverse, including main genera such as *Acinetobacter*, *Aeromonas*, *Enterobacter*, *Enterococcus*, *Microbacterium*, *Micrococcus*, *Pseudomonas*, *Staphylococcus*, *Stenotrophomonas*, and *Streptomyces*, as well as other unclassified bacteria especially *Bacillus* and *Vibrio*, which were similar to our results (Dat et al., 2019). In this work, 80 *V. owensii* strains among the dominant *Vibrio* genus were isolated. It is worth noting that cultivable protease-producing bacterial diversity of sediment was generally higher than that of water (**Figure 1B** and **Table 1**).

The diversity and distribution of cultivable protease-producing bacterial strains in different sampling stations were investigated (**Figure 2**). The results showed obviously different protease-producing bacterial community structures displayed between each aquaculture pond at the genus level. Interestingly, *Vibrio* from water samples was found in all sampling stations (**Supplementary Table S2**) and accounted for the relatively higher proportion (**Figure 2**). *Bacillus* also displayed high abundance in most sampling stations.

TABLE 1 | Distribution of cultivable protease-producing bacteria in tropical aquaculture systems.

Ponds	Sediment		Water	
	$\times 10^3$ CFU/g	Isolates	$\times 10^3$ CFU/ml	Isolates
1#	234.0	148	1.090	79
2#	44.7	62	0.728	93
3#	104.7	54	1.050	105
4#	20.5	148	1.450	45
5#	285.0	132	0.658	76
6#	88.3	75	2.10	113
Nsp	260.0	35	1.820	14
Total		654		525

The aquaculture ponds are coded 1#–6#, and Nsp represents nature seawater pool.

Comparison of Cultivable Protease-Producing Bacterial Distribution of Sediments and Water in Aquaculture Systems

As shown in **Figure 3**, of the 1,179 total cultivable protease-producing bacterial strains from different genera, most strains were found in both sediment and water samples, whereas the sediment and water samples harbored only 70 and 41 unique strains, respectively. *Planococcus* (42.9%) and *Marinobacter* (22.9%) were notably abundant in the unique genus of sediment samples, whereas *Alteromonas* (63.4%) displayed the highest relative abundance in the unique genus of water samples. Among the genera in both locations, *Vibrio* (31.0%) as the dominant group accounted for the highest proportion.

Genetic Diversity of Dominant *V. owensii* Using ERIC-PCR

In this study, 80 *V. owensii* strains as the dominant cultivable protease-producing bacteria were isolated from aquaculture systems. In view of the high-importance *Vibrio* and their increased prevalence in aquaculture, the genetic linkage of these isolates was investigated by ERIC-PCR. In the extragenic regions of *V. owensii* genome, the sequences of enterobacterial repetitive intergenic consensus consist of highly conserved central inverted repeats. In this study, 80 *V. owensii* isolates were fingerprinted by ERIC-PCR. This technique generated two to six amplification bands ranging in size from 800 to 7,500 bp (**Supplementary Figure S2**). Adopting 58% of similarity, 80 *V. owensii* isolates were clustered into four clusters (**Figure 4** and **Supplementary Table S3**), ET-1, ET-2, ET-3, and ET-4. The predominant clusters were ET-3 and ET-4, as most isolates had a common banding pattern (7,000 bp; **Supplementary Figure S2**). Only three strains were clustered into ET-1, and nine strains were clustered into ET-2. The Simpson's Index of Diversity was used to elevate the discriminatory power of this typing method.

Overview of Physicochemical Parameters in the Survey Area

Temperature varied among different sampling aquaculture ponds, ranging from 28.1 to 29.7°C. pH was relatively stable and varied slightly among the different sampling ponds. Salinity ranged from 20.29‰ to 29.98‰. The differences in dissolved inorganic N, such as NH_4^+-N, NO_2^-N, and NO_3^--N, were obvious. Physical-chemical parameters of the survey areas were summarized in **Table 2**.

DISCUSSION

With the rapid development of aquaculture industry, aquaculture system is loaded with abundant organic matter,

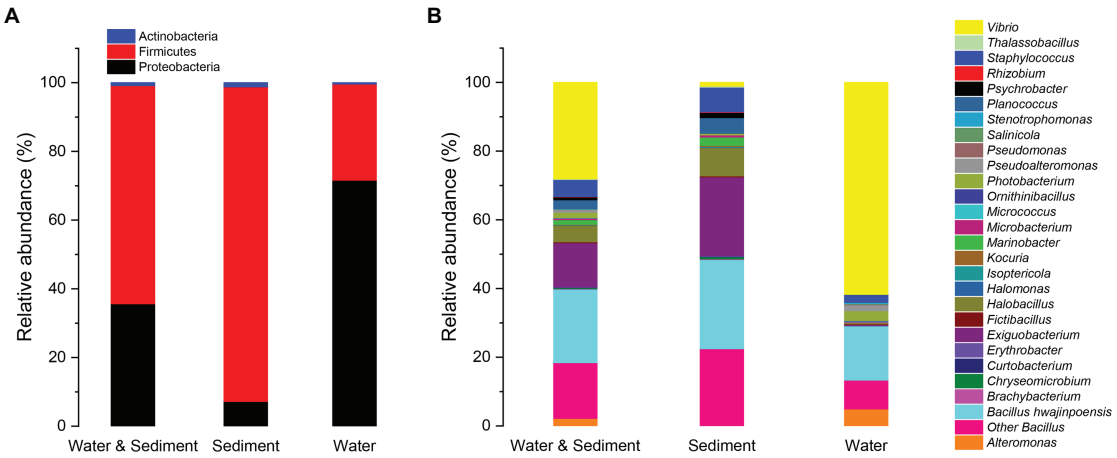

FIGURE 1 | Relative abundances of cultivable protease-producing bacterial strains in water and sediment, sediment, and water of aquaculture systems at the level of phylum **(A)** and genus **(B)**, respectively.

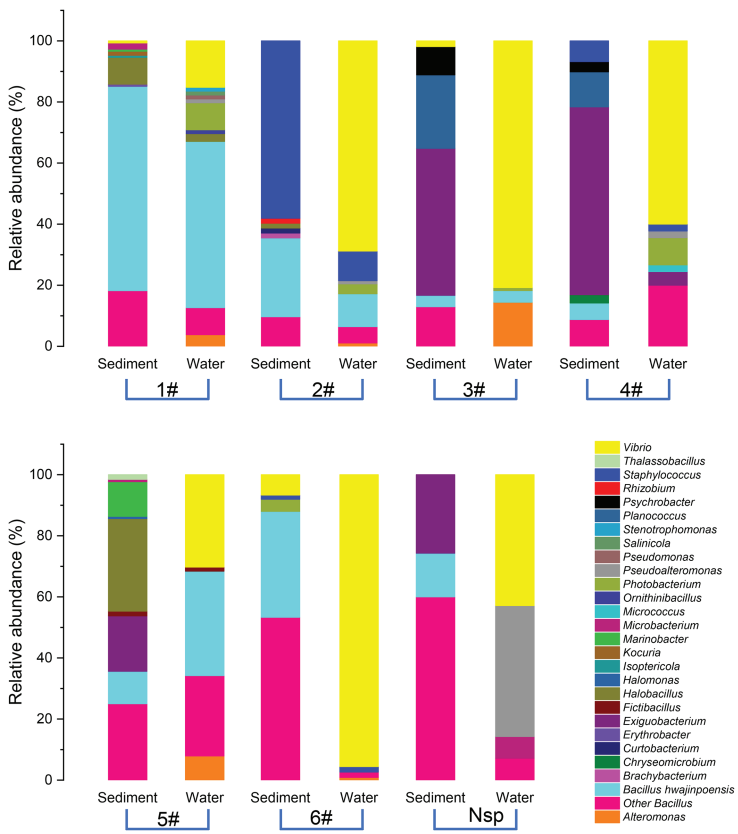

FIGURE 2 | Relative abundances of cultivable protease-producing bacterial strains in sediment and water of aquaculture ponds on the level of genus. The aquaculture ponds are coded 1#–6#, and Nsp represents nature seawater pool.

ammonia-nitrogen, and phosphorus due to high concentration of organic and inorganic pollutants from uneaten feed and aquaculture animal excreta (Dat et al., 2019), and long-term use of antibiotics and chemicals to prevent diseases in aquaculture has led to a series of environmental problems, such as water eutrophication and atmospheric pollution (caused

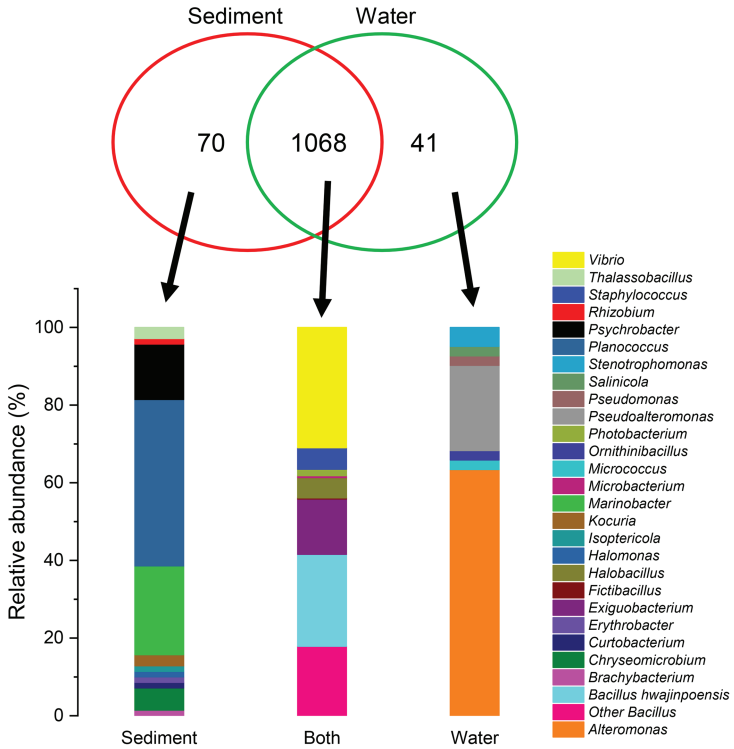

FIGURE 3 | Comparison of the cultivable protease-producing bacteria distribution of sediment and water samples at the genus level. Proportional Venn diagram showing the number of strains found only in sediment samples, only in water samples, and in both. These strains were used to create the relative abundance bar graphs at the genus level under the panel Venn.

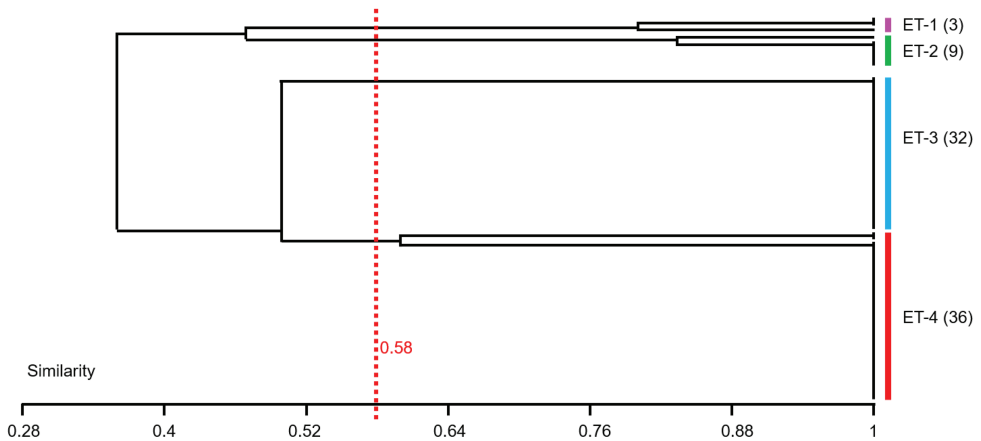

FIGURE 4 | Dendrogram obtained from ERIC-PCR fingerprinting of 80 *Vibrio owensii* strains. Adopting 58% of similarity, isolates were clustered into four clusters, ET-1, ET-2, ET-3, and ET-4.

by volatilization of ammonia and hydrogen sulfide; Hai, 2015), which greatly hinders the sustainable development of aquaculture industry. Therefore, exploring a harmless and recyclable technology for reducing excessive organic matter in aquaculture system is necessary to ensure the sustainable development of aquaculture and for environmental protection. Microorganisms such as potential probiotic biocontrol candidates play important roles in diseases resistance and improvement of water quality (Blancheton et al., 2013; Hucheng et al., 2020). Abundant enzymes produced by microorganisms, such as protease, lipase, and amylase, can effectively decompose the excessive bait and other organic matter, which play a

TABLE 2 | Physical-chemical parameters of sampling stations.

Ponds	Temperature (°C)	Salinity (%)	pH	DO (mg/L)	NH_4^+-N (mg/L)	NO_2^--N (mg/L)	NO_3^--N (mg/L)	COD (mg/L)
1#	28.9	25.68	7.77	3.12	0.27	0.91	0.025	129.6
2#	29.5	21.87	7.66	2.82	3.01	0.74	0.074	74.8
3#	29.7	26.58	7.41	2.95	1.27	0.25	0.027	141.0
4#	29.4	29.98	7.56	2.42	0.92	0.91	0.025	140.0
5#	29.2	26.30	7.49	2.61	2.20	0.20	0.073	82.0
6#	28.8	26.00	7.28	3.01	2.36	0.99	0.450	147.0
Nsp	28.1	20.29	7.28	1.42	4.03	6.18	0.130	38.8

The aquaculture ponds are coded 1#–6#, and Nsp represents nature seawater pool.

key role in material transformation and energy metabolism in aquaculture system. Intensive aquaculture system is a closed or semiclosed material circulation system. Protein and other high-molecular substances from bait are the main sources of pollution in aquaculture system. Therefore, aquaculture system is highly dependent on functional bacteria that can promote the decomposition of high-molecular substances, such as protease-producing bacteria. Meanwhile, tropical marine region with unique climate and environmental condition harbors diverse bacterial communities with unique metabolic and physiological capabilities (Hamza et al., 2017; Ren et al., 2018, 2019). Wenchang in Hainan Island belonging to a tropical marine region is one of the largest aquaculture production areas in China, but the knowledge of protease-producing bacterial community structure in this area, especially in aquaculture system, is extremely limited.

For this purpose, we herein communicate that protease-producing bacteria displayed high diversity and complex community structure. The diversity and relative abundance of protease-producing bacteria in aquaculture sediments were generally higher than those in aquaculture water. Similar results were also found in Guangdong (China) aquaculture system (Wenguang et al., 2015). All of the protease-producing bacteria isolates from the survey aquaculture systems belonged to three phyla, Actinobacteria, Firmicutes, and Proteobacteria, of which Firmicutes accounted for the highest proportion, and the dominant genera were *Bacillus* (37.7%) and *Vibrio* (28.1%) in aquaculture system, which were similar with that in aquacultured yellowtail (Ramírez and Romero, 2017). However, the relative abundances of these phyla in sediment and water of aquaculture had significant differences. Firmicutes (91.6%) in sediment and Proteobacteria (71.6%) in water accounted for the highest proportion, respectively. Reportedly, some cultivable members of these phyla from aquaculture systems belonged to antibiotic resistance bacteria with (fluoro) quinolone-resistant, sulfamethoxazole-resistant, and oxytetracycline-resistant and were most abundant in fish ponds (Akinbowale et al., 2010; Hoa et al., 2011; Takasu et al., 2011; Wenguang et al., 2015). Firmicutes was described as the most predominant in the intestinal content of aquacultured animals (Ramírez and Romero, 2017). Some researchers reported that the dominant phyla of aquaculture system in Guangdong, China, were Proteobacteria, Bacteroidetes, and Firmicutes in sediment and Proteobacteria, Actinobacteria, and Bacteroidetes in water (Wenguang et al., 2015). Although only less than 1% bacteria of the microbial community could be detected by culture-dependent approach, the living bacteria can be obtained (Ramírez and Romero, 2017), which is an essential method for various researches. We only focused on culturable protease-producing bacterial community structure of tropical aquaculture system in this study; it still indirectly implied significant differences in bacterial community structure between tropical aquaculture system and other regional aquaculture systems. Reportedly, the microbiome of aquaculture systems could be more similar to structure of aquatic animal microbiomes (Ramírez and Romero, 2017).

Additionally, the composition and relative abundance of protease-producing bacteria at the genus level in sediment and water also displayed significantly different in aquaculture systems. Reportedly, *Bacillus*, *Lactobacillus*, and *Enterococcus* as protease-producing bacteria positively affected the bait digestibility and growth of aquaculture animals (Yanbo and Zirong, 2006; Ghosh et al., 2008; Suzer et al., 2008; Iehata et al., 2009; Askarian et al., 2011). In this study, *Bacillus* dominated by *B. hwajinpoensis* displayed high relative abundance in both sediment and aquaculture water. *Bacillus* as probiotic has been commonly selected to improve water quality by reducing organic matter, ammonia-nitrogen, and phosphorus accumulation and inhibit certain pathogenic bacteria of fishery by producing antimicrobial peptides, thereby making them more suitable candidates compared to other probiotics (Rengpipat et al., 1998; Verschuere et al., 2000; Hai, 2015; Kumari et al., 2016; Saravanan et al., 2018; Sonune and Garode, 2018; Yi et al., 2018; Kuebutornye et al., 2019; Wang et al., 2019). SW-72^T from a tidal flat of the Yellow Sea in Korea was the first reported *B. hwajinpoensis* (Yoon et al., 2003). The function of heterotrophic nitrification-aerobic denitrification of *B. hwajinpoensis* has been reported (Cheng et al., 2016), which can effectively improve water quality by removing inorganic nitrogen and total nitrogen.

The unique genera of sediment or water were also isolated in this work. Twelve unique genera were only isolated from sediment samples, *Brachybacterium*, *Chryseomicrobium*, *Curtobacterium*, *Erythrobacter*, *Halomonas*, *Isoptericola*, *Kocuria*, *Marinobacter*, *Planococcus*, *Psychrobacter*, *Rhizobium*,

and *Thalassobacillus*. Meanwhile, there were seven unique genera from water samples, *Alteromonas*, *Micrococcus*, *Ornithinibacillus*, *Pseudoalteromonas*, *Pseudomonas*, *Salinicola*, and *Stenotrophomonas*. Although these unique genera accounted for tiny percentage in sediment or water, we reason that they played important roles in the stability of community structure. For example, *Brachybacterium* from *Lates calcarifer* showed inhibitory activities against *Lysinibacillus*, *Paenibacillus*, *Pseudomonas*, *Escherichia coli*, and *Mesorhizobium* (Orsod et al., 2012); *Halomonas* could improve the survival, growth, water quality, and robustness and modifies the gut microbial composition of shrimp (Gao et al., 2019); *Kocuria* as probiotic from the intestinal microbiota of rainbow trout showed resistance to sulphatriad and had health benefits in aquaculture (Sharifuzzaman et al., 2018); *Marinobacter* from a recycling aquaculture system could perform only aerobic denitrification but not nitrification (Liu et al., 2016); *Pseudomonas* showed antibiofilm properties and reduced the risk of pathogenic infection to aquaculture animals by their exopolysaccharides (Ang et al., 2020).

It is worth to note that *Vibrio* as the dominant genus was isolated from most aquaculture ponds (**Figure 2** and **Supplementary Table S2**), which were dominated by *V. owensii* species (80 strains). The DY05^T and 47,666-1 belonging to the *Harveyi* clade of the genus were the first reported *V. owensii* strains from diseased cultured crustaceans (Cano-Gomez et al., 2010). So far, most of *Vibrio* from aquaculture systems in southern China belonged to *V. harveyi*, *V. alginolyticus*, *V. parahaemolyticus*, *V. splendidus*, and *V. fischeri*, whereas no *V. owensii* was detected. In this study, *V. owensii* as dominate species in tropical aquaculture systems could be isolated from most sampling stations, indicating that *V. owensii* in tropical region may be a normal species and played important roles in material circulation. Reportedly, *V. owensii* were potential bacterial pathogens in mariculture systems (Yu et al., 2013; Liu et al., 2018), necessitating the designation of an appropriate typing approach to completely fathom their transmission tactics and control infection strategies. So far, there were many reports on the molecular types of *V. alginolyticus* (Kahla-Nakbi et al., 2006), *V. tapetis* (Rodríguez et al., 2006), and *V. parahaemolyticus* (Chen et al., 2012), but no reports on that of *V. owensii*. ERIC-PCR as an easy and cost-effective genotyping approach for discriminating different strains types (Bakhshi et al., 2018) has urged us to use this technique to inspect phylogenetic closeness of *V. owensii* isolates. All 80 *V. owensii* isolates produced banding patterns after amplification by ERIC-PCR (**Supplementary Figure S2**), indicating the complete type ability of *V. owensii* using this technology, which were clustered into four clusters (ET-1–ET-4) at 58% of similarity (**Figure 4**). We found that all *V. owensii* had a common band around 7,000 bp (**Supplementary Figure S2**), indicating that they had a similar genetic background. We reason that the common band may be an effective molecular marker for *V. owensii*. The predominant clusters, ET-3 and ET-4, contained most isolates, indicating that these two genotypes were representative strains in tropical aquaculture. Additionally, the *V. owensii* strains belonging to ET-3 and ET-4 were detected in most ponds without outbreak of epidemics in this region (**Supplementary Table S1**) and significantly different from *V. owensii* DY05^T from other regions on the basis of 16S rDNA (**Supplementary Figure S3**), implying that *V. owensii* strains in this area may be potential beneficial bacteria for the wastewater purification and the construction of an environment-friendly aquaculture model in tropical region, especially in Hainan Island.

Our experimental design aimed to determine the relative influence of environmental variables of aquaculture on protease-producing microbial communities in aquaculture system. Environmental variables must play important roles in shaping protease-producing bacterial diversity and community structure in aquaculture systems (Holmström and Kjelleberg, 1999; Li et al., 2018). Therefore, Spearman rank correlation coefficient between relative abundance of protease-producing bacterial communities and environmental variables at the genus level was investigated (**Figure 5**). As shown in **Figure 5A**, DO and COD were the main factors positively affecting the distributions of dominant *Vibrio* in sediment, and salinity as a main factor also positively affected the distributions of unique genera of sediment, *Planococcus* and *Psychrobacter*. *Planococcus* spp. were associated with biological sulfamethoxazole degradation pathway, which can respond more quickly and adapt to environmental changes in aquaculture system (Kong et al., 2020). It is worth mentioning that the antagonistic effect against pathogenic species of *Psychrobacter* has been demonstrated and reported (Sun et al., 2009), and *Psychrobacter* could be commonly found in intestinal microbiota of several fish (Ringo et al., 2006; Sun et al., 2009; Yang et al., 2011; Ramirez and Romero, 2017). Reportedly, *Psychrobacter* could also improve immunological parameters and growth performance in tilapia (Makled et al., 2017), whereas temperature was the main factor negatively affecting the distribution of dominant *Bacillus* (except *B. hwajinpoensis*) in sediment, which was agreed with some previous studies in different regional oceans (Pomeroy and Wiebe, 2001; Fuhrman et al., 2008; Li et al., 2018). In this study, DO, COD, salinity, and temperature played important roles in shaping bacterial diversity of aquaculture sediment by affecting the key species. The conditions with low concentration of NO_3^--N and NO_2^--N were more suitable for the growth of *Alteromonas* and *Photobacterium*, and pH as a main factor positively affecting the distribution of *Photobacterium* in water (**Figure 5B**). *Photobacterium* genus was detected worldwide in aquaculture systems and identified as pathogens causing wound infections and hemorrhagic septicemia (Terceti et al., 2018; Labella et al., 2020). It is worth noticing that *Alteromonas* was only isolated from aquaculture water, which was identified as probiotic bacteria in aquaculture system (Kesarcodi-Watson et al., 2010; Torres et al., 2016). In conclusion, DO, temperature, salinity, and COD as the main factor could affect the protease-producing bacterial community structure of sediment, whereas pH, NO_2^-N, and NO_3^--N were the main factors affecting that of aquaculture water.

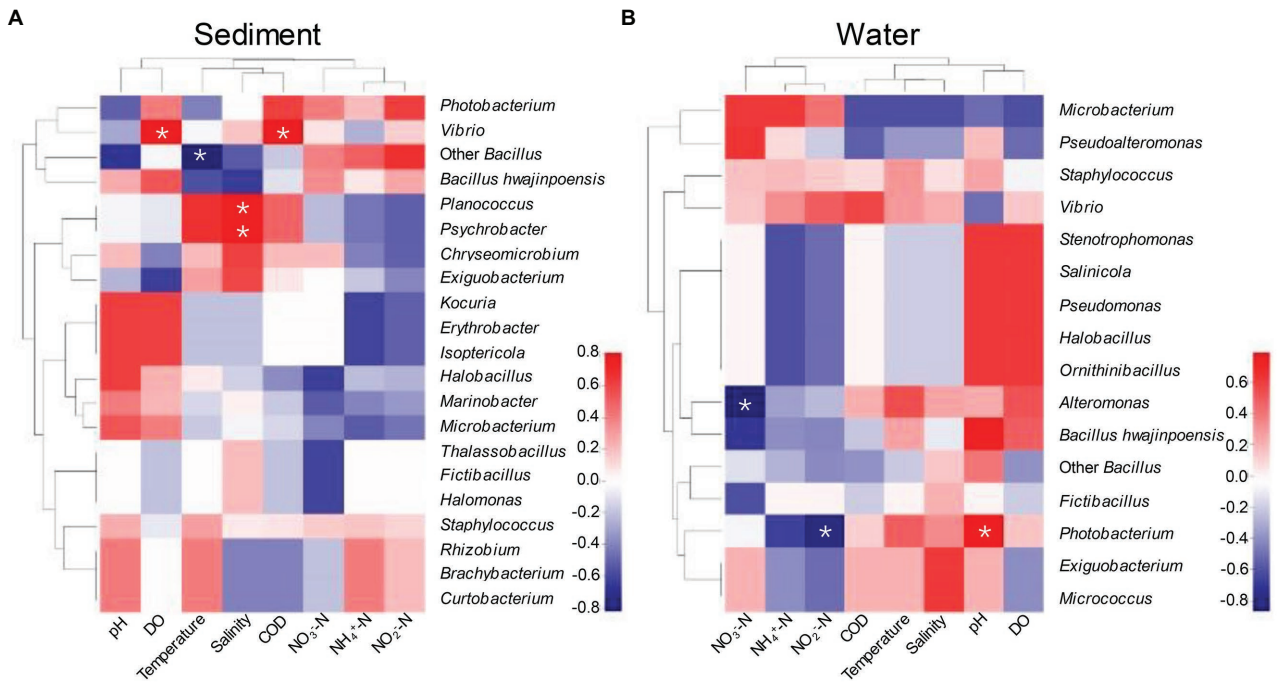

FIGURE 5 | Spearman rank correlation coefficient between relative abundance of bacterial communities in sediment **(A)** and aquaculture water **(B)** and environmental variables at the genus. *$p < 0.05$ indicates significant correlation level.

CONCLUSION

In this study, cultivable protease-producing bacterial community structures in sediment and water of tropical aquaculture systems were completely surveyed. The protease-producing bacteria displayed high diversity and complex community structure. *Bacillus* genera in sediment and *Vibrio* in aquaculture water were the dominant genera. *V. owensii* strains as the dominant *Vibrio* species were clustered into four clusters, which was identified as a novel branch of *V. owensii*. Additionally, temperature, DO, COD, salinity, NO_3^--N, NO_2^-N, and pH of aquaculture system played important roles in shaping protease-producing bacterial diversity and community structure in aquaculture system. These results will help the development useful and practical strategies for the improvement of water quality in the marine recirculating aquaculture system.

DATA AVAILABILITY STATEMENT

The original contributions presented in the study are included in the article/**Supplementary Material**, further inquiries can be directed to the corresponding authors.

AUTHOR CONTRIBUTIONS

YW, JB, WR, and ZX designed the study and wrote the manuscript. YW, JB, HL, XZ, XC, and AH performed the experiments. YW, WR, and ZX analyzed the data. YW and JB contributed equally to this work. All authors contributed to the article and approved the submitted version.

FUNDING

This research was financially supported by the Key Research and Development Project of Hainan Province (ZDYF2020088), the National Key Research and Development Project of China (2020YFD0901100), Marine Economic and Innovative Demonstration City Project of State Oceanic Administration (HHCL201802 and HHCL201813), the Foundation of Hainan Agricultural and Rural Department (NY-2019-819), the National Natural Science Foundation of China (31660744), and the Scientific Research Foundation of Hainan University (KYQD(ZR)1967, KYQD(ZR)1819 and KYQD(ZR)20060).

ACKNOWLEDGMENTS

We are thankful to the reviewers who helped improve this paper. We are also thankful to Mengjie Cheng from Hainan University for her support in data analysis.

SUPPLEMENTARY MATERIAL

The Supplementary Material for this article can be found online at: https://www.frontiersin.org/articles/10.3389/fmicb.2021.638129/full#supplementary-material

REFERENCES

Akinbowale, O. L., Peng, H., and Barton, M. D. (2010). Diversity of tetracycline resistance genes in bacteria from aquaculture sources in Australia. *J. Appl. Microbiol.* 103, 2016–2025. doi: 10.1111/j.1365-2672.2007.03445.x

Ambas, I., Buller, N., and Fotedar, R. (2015). Isolation and screening of probiotic candidates from marron, *C herax cainii* (Austin, 2002) gastrointestinal tract (GIT) and commercial probiotic products for the use in marron culture. *J. Fish Dis.* 38, 467–476. doi: 10.1111/jfd.12257

Amin, M. (2018). Marine protease-producing bacterium and its potential use as an abalone probiont. *Aquacult. Rep.* 12, 30–35. doi: 10.1016/j.aqrep.2018.09.004

Ang, C. Y., Sano, M., Dan, S., Leelakriangsak, M., and Lal, T. M. (2020). Postbiotics applications as infectious disease control agent in aquaculture. *Biocontrol Sci.* 25, 1–7. doi: 10.4265/bio.25.1

Askarian, F., Kousha, A., Salma, W., and Ringø, E. (2011). The effect of lactic acid bacteria administration on growth, digestive enzyme activity and gut microbiota in Persian sturgeon (*Acipenser persicus*) and beluga (*Huso huso*) fry. *Aquac. Nutr.* 17, 488–497. doi: 10.1111/j.1365-2095.2010.00826.x

Bakhshi, B., Afshari, N., and Fallah, F. (2018). Enterobacterial repetitive intergenic consensus (ERIC)-PCR analysis as a reliable evidence for suspected *Shigella* spp. outbreaks. *Braz. J. Microbiol.* 49, 529–533. doi: 10.1016/j.bjm.2017.01.014

Blancheton, J., Attramadal, K., Michaud, L., D'orbcastel, E. R., and Vadstein, O. (2013). Insight into bacterial population in aquaculture systems and its implication. *Aquac. Eng.* 53, 30–39. doi: 10.1016/j.aquaeng.2012.11.009

Cano-Gomez, A., Goulden, E. F., Owens, L., and Høj, L. (2010). *Vibrio owensii* sp. nov., isolated from cultured crustaceans in Australia. *FEMS Microbiol. Lett.* 302, 175–181. doi: 10.1111/j.1574-6968.2009.01850.x

Chen, W., Xie, Y., Xu, J., Wang, Q., Gu, M., Yang, J., et al. (2012). Molecular typing of *Vibrio parahaemolyticus* isolates from the middle-east coastline of China. *Int. J. Food Microbiol.* 153, 402–412. doi: 10.1016/j.ijfoodmicro.2011.12.001

Cheng, Y., Li, Q. -F., Fei, Y. -T., and Zhang, Y. (2016). Screening and nitrogen removing characteristics of heterotrophic nitrification-aerobic denitrification bacteria SLWX2 from sea water. *Huanjing Kexue.* 37, 2681–2688. doi: 10.13227/j.hjkx.2016.07.035

Dat, T., Tam, V., Dung, T., Bui, L., Anh, H., and Oanh, P. (2019). Isolation and screening of cellulose and organic matter degrading bacteria from aquaculture ponds for improving water quality in aquaculture. *IOP Conf. Se.: Earth and Environ. Sci.* 266:012002. doi: 10.1088/1755-1315/266/1/012002

Fuhrman, J. A., Steele, J. A., Hewson, I., Schwalbach, M. S., Brown, M. V., Green, J. L., et al. (2008). A latitudinal diversity gradient in planktonic marine bacteria. *Proc. Natl. Acad. Sci. U. S. A.* 105, 7774–7778. doi: 10.1073/pnas.0803070105

Gao, M., Du, D., Bo, Z., and Sui, L. (2019). Poly-beta-hydroxybutyrate (PHB)-accumulating *Halomonas* improves the survival, growth, robustness and modifies the gut microbial composition of *Litopenaeus vannamei* postlarvae. *Aquaculture* 500, 607–612. doi: 10.1016/j.aquaculture.2018.10.032

Ghosh, S., Sinha, A., and Sahu, C. (2008). Dietary probiotic supplementation in growth and health of live-bearing ornamental fishes. *Aquac. Nutr.* 14, 289–299. doi: 10.1111/j.1365-2095.2007.00529.x

Guo, H., Xian, J. -A., and Wang, A. L. (2016). Analysis of digital gene expression profiling in hemocytes of white shrimp *Litopenaeus vannamei* under nitrite stress. *Fish Shellfish Immunol.* 56, 1–11. doi: 10.1016/j.fsi.2016.06.059

Hai, N. (2015). The use of probiotics in aquaculture. *J. Appl. Microbiol.* 119, 917–935. doi: 10.1111/jam.12886

Hamza, F., Satpute, S., Banpurkar, A., Kumar, A. R., and Zinjarde, S. (2017). Biosurfactant from a marine bacterium disrupts biofilms of pathogenic bacteria in a tropical aquaculture system. *FEMS Microbiol. Ecol.* 93:fix140. doi: 10.1093/femsec/fix140

Hoa, P. T. P., Managaki, S., Nakada, N., Takada, H., Shimizu, A., Anh, D. H., et al. (2011). Antibiotic contamination and occurrence of antibiotic-resistant bacteria in aquatic environments of northern Vietnam. *Sci. Total Environ.* 409, 2894–2901. doi: 10.1016/j.scitotenv.2011.04.030

Holmström, C., and Kjelleberg, S. (1999). Marine *Pseudoalteromonas* species are associated with higher organisms and produce biologically active extracellular agents. *FEMS Microbiol. Ecol.* 30, 285–293. doi: 10.1111/j.1574-6941.1999.tb00656.x

Hucheng, J., Xiaohui, C., Wenji, B., Longlong, F., Qin, Q., Liqiang, Z., et al. (2020). Comparison of bacterial communities in channel catfish *Ictalurus punctatus* culture ponds of an industrial ecological purification recirculating aquaculture system. *Aquac. Res.* 51, 2432–2442. doi: 10.1111/are.14587

Iehata, S., Inagaki, T., Okunishi, S., Nakano, M., Tanaka, R., and Maeda, H. (2009). Colonization and probiotic effects of lactic acid bacteria in the gut of the abalone *Haliotis gigantea*. *Fish. Sci.* 75, 1285–1293. doi: 10.1007/s12562-009-0138-5

Kahla-Nakbi, A. B., Chaieb, K., Besbes, A., Zmantar, T., and Bakhrouf, A. (2006). Virulence and enterobacterial repetitive intergenic consensus PCR of *Vibrio alginolyticus* strains isolated from Tunisian cultured gilthead sea bream and sea bass outbreaks. *Vet. Microbiol.* 117, 321–327. doi: 10.1016/j.vetmic.2006.06.012

Kesarcodi-Watson, A., Kaspar, H., Lategan, M. J., and Gibson, L. (2010). *Alteromonas macleodii* 0444 and *Neptunomonas* sp. 0536, two novel probiotics for hatchery-reared Greenshell ™ mussel larvae, *Perna canaliculus*. *Aquaculture* 309, 49–55. doi: 10.1016/j.aquaculture.2010.09.019

Kong, S., Zhao, Y. -G., Guo, L., Gao, M., Jin, C., and She, Z. (2020). Transcriptomics of *Planococcus kocurii* O516 reveals the degrading metabolism of sulfamethoxazole in marine aquaculture wastewater. *Environ. Pollut.* 265:114939. doi: 10.1016/j.envpol.2020.114939

Kuebutornye, F. K., Abarike, E. D., and Lu, Y. (2019). A review on the application of Bacillus as probiotics in aquaculture. *Fish Shellfish Immunol.* 87, 820–828. doi: 10.1016/j.fsi.2019.02.010

Kuhn, D. D., Smith, S. A., Boardman, G. D., Angier, M. W., Marsh, L., and Flick, G. J. Jr. (2010). Chronic toxicity of nitrate to pacific white shrimp, *Litopenaeus vannamei*: impacts on survival, growth, antennae length, and pathology. *Aquaculture* 309, 109–114. doi: 10.1016/j.aquaculture.2010.09.014

Kumari, V., Yadav, A., Haq, I., Kumar, S., Bharagava, R. N., Singh, S. K., et al. (2016). Genotoxicity evaluation of tannery effluent treated with newly isolated hexavalent chromium reducing *Bacillus cereus*. *J. Environ. Manag.* 183, 204–211. doi: 10.1016/j.jenvman.2016.08.017

Labella, A. M., Rosado, J. J., Balado, M., Lemos, M. L., and Borrego, J. J. (2020). Virulence properties of three new *Photobacterium* species affecting cultured fish. *J. Appl. Microbiol.* 129, 37–50. doi: 10.1111/jam.14437

Li, Y. -Y., Chen, X. -H., Xie, Z. -X., Li, D. -X., Wu, P. -F., Kong, L. -F., et al. (2018). Bacterial diversity and nitrogen utilization strategies in the upper layer of the northwestern Pacific Ocean. *Front. Microbiol.* 9:797. doi: 10.3389/fmicb.2018.00797

Li, Y., Wang, L., Yan, Z., Chao, C., Yu, H., Yu, D., et al. (2020). Effectiveness of dredging on internal phosphorus loading in a typical aquacultural lake. *Sci. Total Environ.* 744:140883. doi: 10.1016/j.scitotenv.2020.140883

Lin, Y. C., and Chen, J. C. (2001). Acute toxicity of ammonia on *Litopenaeus vannamei* Boone juveniles at different salinity levels. *J. Exp. Mar. Biol. Ecol.* 259, 109–119. doi: 10.1016/S0022-0981(01)00227-1

Lin, Y. -C., and Chen, J. -C. (2003). Acute toxicity of nitrite on *Litopenaeus vannamei* (Boone) juveniles at different salinity levels. *Aquaculture* 224, 193–201. doi: 10.1016/S0044-8486(03)00220-5

Liu, Y., Ai, G. -M., Miao, L. -L., and Liu, Z. -P. (2016). *Marinobacter* strain NNA5, a newly isolated and highly efficient aerobic denitrifier with zero N_2O emission. *Bioresour. Technol.* 206, 9–15. doi: 10.1016/j.biortech.2016.01.066

Liu, L., Xiao, J., Zhang, M., Zhu, W., Xia, X., Dai, X., et al. (2018). A *Vibrio owensii* strain as the causative agent of AHPND in cultured shrimp, *Litopenaeus vannamei*. *J. Invertebr. Pathol.* 153, 156–164. doi: 10.1016/j.jip.2018.02.005

Makled, S. O., Hamdan, A. M., El-Sayed, A. -F. M., and Hafez, E. E. (2017). Evaluation of marine psychrophile, *Psychrobacter namhaensis* SO89, as a probiotic in Nile tilapia (*Oreochromis niloticus*) diets. *Fish Shellfish Immunol.* 61, 194–200. doi: 10.1016/j.fsi.2017.01.001

Mariane De Morais, A. P., Abreu, P. C., Wasielesky, W., and Krummenauer, D. (2020). Effect of aeration intensity on the biofilm nitrification process during the production of the white shrimp *Litopenaeus vannamei* (Boone, 1931) in Biofloc and clear water systems. *Aquaculture* 514:734516. doi: 10.1016/j.aquaculture.2019.734516

Marquez-Santacruz, H. A., Hernandez-Leon, R., Orozco-Mosqueda, M. C., Velazquez-Sepulveda, I., and Santoyo, G. (2010). Diversity of bacterial endophytes in roots of Mexican husk tomato plants (*Physalis ixocarpa*) and their detection in the rhizosphere. *Genet. Mol. Res.* 9, 2372–2380. doi: 10.4238/vol9-4gmr921

Olson, N. D., and Lesser, M. P. (2013). Diazotrophic diversity in the Caribbean coral, *Montastraea cavernosa*. *Arch. Microbiol.* 195, 853–859. doi: 10.1007/s00203-013-0937-z

Orsod, M., Joseph, M., and Huyop, F. (2012). Characterization of exopolysaccharides produced by *Bacillus cereus* and *Brachybacterium* sp. isolated from Asian sea bass (*Lates calcarifer*). *Mal. J. Microbiol.* 8, 170–174. doi: 10.1006/geno.2001.6469

Pishbin, Z., and Mehrabian, S. (2020). Molecular analysis of *Proteus mirabilis* isolated from urine samples using ERIC-PCR. *Gene Reports.* 19:100637. doi: 10.1016/j.genrep.2020.100637

Pomeroy, L. R., and Wiebe, W. J. (2001). Temperature and substrates as interactive limiting factors for marine heterotrophic bacteria. *Aquat. Microb. Ecol.* 23, 187–204. doi: 10.3354/ame01431

Ramirez, C., and Romero, J. (2017). Fine flounder (*Paralichthys adspersus*) microbiome showed important differences between wild and reared specimens. *Front. Microbiol.* 8:271. doi: 10.3389/fmicb.2017.00271

Ramírez, C., and Romero, J. (2017). The microbiome of *Seriola lalandi* of wild and aquaculture origin reveals differences in composition and potential function. *Front. Microbiol.* 8:1844. doi: 10.3389/fmicb.2017.01844

Reda, R. M., and Selim, K. M. (2015). Evaluation of *Bacillus amyloliquefaciens* on the growth performance, intestinal morphology, hematology and body composition of Nile tilapia, *Oreochromis niloticus*. *Aquac. Int.* 23, 203–217. doi: 10.1007/s10499-014-9809-z

Ren, W., Cai, R., Yan, W., Lyu, M., Fang, Y., and Wang, S. (2018). Purification and characterization of a biofilm-degradable dextranase from a marine bacterium. *Mar. Drugs* 16:51. doi: 10.3390/md16020051

Ren, W., Liu, L., Gu, L., Yan, W., Feng, Y. L., Dong, D., et al. (2019). Crystal structure of GH49 dextranase from *Arthrobacter oxidans* KQ11: identification of catalytic base and improvement of thermostability using semirational design based on B-factors. *J. Agric. Food Chem.* 67, 4355–4366. doi: 10.1021/acs.jafc.9b01290

Rengpipat, S., Phianphak, W., Piyatiratitivorakul, S., and Menasveta, P. (1998). Effects of a probiotic bacterium on black tiger shrimp *Penaeus monodon* survival and growth. *Aquaculture* 167, 301–313. doi: 10.1016/S0044-8486(98)00305-6

Ringo, E., Sperstad, S., Myklebust, R., Refstie, S., and Krogdahl, A. (2006). Characterisation of the microbiota associated with intestine of Atlantic cod (*Gadus morhua L.*) - the effect of fish meal, standard soybean meal and a bioprocessed soybean meal. *Aquaculture* 261, 829–841. doi: 10.1016/j.aquaculture.2006.06.030

Rodríguez, J. M., López-Romalde, S., Beaz, R., Alonso, M. C., Castro, D., and Romalde, J. L. (2006). Molecular fingerprinting of *Vibrio tapetis* strains using three PCR-based methods: ERIC-PCR, REP-PCR and RAPD. *Dis. Aquat. Org.* 69, 175–183. doi: 10.3354/dao069175

Santos, L., and Ramos, F. (2018). Antimicrobial resistance in aquaculture: current knowledge and alternatives to tackle the problem. *Int. J. Antimicrob. Agents* 52, 135–143. doi: 10.1016/j.ijantimicag.2018.03.010

Saravanan, M., Barik, S. K., Mubarakali, D., Prakash, P., and Pugazhendhi, A. (2018). Synthesis of silver nanoparticles from *Bacillus brevis* (NCIM 2533) and their antibacterial activity against pathogenic bacteria. *Microb. Pathog.* 116, 221–226. doi: 10.1016/j.micpath.2018.01.038

Selim, K. M., and Reda, R. M. (2015). Improvement of immunity and disease resistance in the Nile tilapia, *Oreochromis niloticus*, by dietary supplementation with *Bacillus amyloliquefaciens*. *Fish Shellfish Immunol.* 44, 496–503. doi: 10.1016/j.fsi.2015.03.004

Sharifuzzaman, S. M., Rahman, H., Austin, D. A., and Austin, B. (2018). Properties of probiotics *Kocuria* SM1 and *Rhodococcus* SM2 isolated from fish guts. *Probiotics Antimicrob. Proteins.* 10, 534–542. doi: 10.1007/s12602-017-9290-x

Shi, Z., Li, X. -Q., Chowdhury, M. K., Chen, J. -N., and Leng, X. -J. (2016). Effects of protease supplementation in low fish meal pelleted and extruded diets on growth, nutrient retention and digestibility of gibel carp, *Carassius auratus gibelio*. *Aquaculture* 460, 37–44. doi: 10.1016/j.aquaculture.2016.03.049

Sonune, N., and Garode, A. (2018). Isolation, characterization and identification of extracellular enzyme producer *Bacillus licheniformis* from municipal wastewater and evaluation of their biodegradability. *Biotechnol. Res. Inno.* 2, 37–44. doi: 10.1016/j.biori.2018.03.001

Su, H., Xiao, Z., Yu, K., Huang, Q., Wang, G., Wang, Y., et al. (2020). Diversity of cultivable protease-producing bacteria and their extracellular proteases associated to scleractinian corals. *PeerJ.* 8:e9055. doi: 10.7717/peerj.9055

Sun, L., Qiu, F., Zhang, X., Dai, X., Dong, X., and Song, W. (2008). Endophytic bacterial diversity in rice (*Oryza sativa* L.) roots estimated by 16S rDNA sequence analysis. *Microb. Ecol.* 55, 415–424. doi: 10.1007/s00248-007-9287-1

Sun, Y., Yang, H., Ling, Z., Chang, J., and Ye, J. (2009). Gut microbiota of fast and slow growing grouper *Epinephelus coioides*. *Afr. J. Microbiol. Res.* 3, 637–640. doi: 10.5897/AJMR.9000353

Suzer, C., Çoban, D., Kamaci, H. O., Saka, Ş., Firat, K., Otgucuoğlu, Ö., et al. (2008). *Lactobacillus* spp. bacteria as probiotics in gilthead sea bream (*Sparus aurata*, L.) larvae: effects on growth performance and digestive enzyme activities. *Aquaculture* 280, 140–145. doi: 10.1016/j.aquaculture.2008.04.020

Takasu, H., Suzuki, S., Reungsang, A., and Viet, P. H. (2011). Fluoroquinolone (FQ) contamination does not correlate with occurrence of FQ-resistant bacteria in aquatic environments of Vietnam and Thailand. *Microbes Environ.* 26, 135–143. doi: 10.1264/jsme2.ME10204

Terceti, M. S., Vences, A., Matanza, X. M., Dalsgaard, I., Pedersen, K., and Osorio, C. R. (2018). Molecular epidemiology of *Photobacterium damselae* subsp *damselae* outbreaks in marine rainbow trout farms reveals extensive horizontal gene transfer and high genetic diversity. *Front. Microbiol.* 9:2155. doi: 10.3389/fmicb.2018.02155

Torres, M., Rubio-Portillo, E., Anton, J., Ramos-Espla, A. A., Quesada, E., and Llamas, I. (2016). Selection of the *N*-Acylhomoserine lactone-degrading bacterium *Alteromonas stellipolaris* PQQ-42 and of its potential for biocontrol in aquaculture. *Front. Microbiol.* 7:646. doi: 10.3389/fmicb.2016.00646

Verschuere, L., Rombaut, G., Sorgeloos, P., and Verstraete, W. (2000). Probiotic bacteria as biological control agents in aquaculture. *Microbiol. Mol. Biol. Rev.* 64, 655–671. doi: 10.1023/A:1024127100993

Wang, Y., Bi, L., Liao, Y., Lu, D., Zhang, H., Liao, X., et al. (2019). Influence and characteristics of *Bacillus stearothermophilus* in ammonia reduction during layer manure composting. *Ecotoxicol. Environ. Saf.* 180, 80–87. doi: 10.1016/j.ecoenv.2019.04.066

Wenguang, X., Yongxue, S., Tong, Z., Ding, X., Li, Y., Wang, M., et al. (2015). Antibiotics, antibiotic resistance genes, and bacterial community composition in fresh water aquaculture environment in China. *Microb. Ecol.* 70, 425–532. doi: 10.1007/s00248-015-0583-x

Yanbo, W., and Zirong, X. (2006). Effect of probiotics for common carp (*Cyprinus carpio*) based on growth performance and digestive enzyme activities. *Anim. Feed Sci. Technol.* 127, 283–292. doi: 10.1016/j.anifeedsci.2005.09.003

Yang, H. L., Sun, Y. Z., Ma, R. L., Li, J. S., and Huang, K. P. (2011). Probiotic *Psychrobacter* sp. improved the autochthonous microbial diversity along the gastrointestinal tract of grouper *Epinephelus coioides*. *J. Aquac. Res. Dev.* s1:001. doi: 10.4172/2155-9546.S1-001

Yi, Y., Zhang, Z., Zhao, F., Liu, H., Yu, L., Zha, J., et al. (2018). Probiotic potential of *Bacillus velezensis* JW: antimicrobial activity against fish pathogenic bacteria and immune enhancement effects on *Carassius auratus*. *Fish Shellfish Immunol.* 78, 322–330. doi: 10.1016/j.fsi.2018.04.055

Yoon, J. -H., Kim, I. -G., Kang, K. H., Oh, T. -K., and Park, Y. -H. (2003). *Bacillus marisflavi* sp. nov. and *Bacillus aquimaris* sp. nov., isolated from sea water of a tidal flat of the Yellow Sea in Korea. *J. Med. Microbiol.* 53, 1297–1303. doi: 10.1016/S0370-2693(97)01497-4

Yu, Y. -P., Gong, T., Jost, G., Liu, W. -H., Ye, D. -Z., and Luo, Z. -H. (2013). Isolation and characterization of five lytic bacteriophages infecting a *Vibrio* strain closely related to *Vibrio owensii*. *FEMS Microbiol. Lett.* 348, 112–119. doi: 10.1111/1574-6968.12277

Conflict of Interest: The authors declare that the research was conducted in the absence of any commercial or financial relationships that could be construed as a potential conflict of interest.

frontiers in Microbiology

REVIEW
published: 18 February 2021
doi: 10.3389/fmicb.2021.631621

Anthropogenic and Environmental Constraints on the Microbial Methane Cycle in Coastal Sediments

Anna J. Wallenius[1], Paula Dalcin Martins[1], Caroline P. Slomp[2] and Mike S. M. Jetten[1]*

[1] Department of Microbiology, Institute for Water and Wetland Research, Radboud University Nijmegen, Nijmegen, Netherlands, [2] Department of Earth Sciences, Faculty of Geosciences, Utrecht University, Utrecht, Netherlands

Large amounts of methane, a potent greenhouse gas, are produced in anoxic sediments by methanogenic archaea. Nonetheless, over 90% of the produced methane is oxidized via sulfate-dependent anaerobic oxidation of methane (S-AOM) in the sulfate-methane transition zone (SMTZ) by consortia of anaerobic methane-oxidizing archaea (ANME) and sulfate-reducing bacteria (SRB). Coastal systems account for the majority of total marine methane emissions and typically have lower sulfate concentrations, hence S-AOM is less significant. However, alternative electron acceptors such as metal oxides or nitrate could be used for AOM instead of sulfate. The availability of electron acceptors is determined by the redox zonation in the sediment, which may vary due to changes in oxygen availability and the type and rate of organic matter inputs. Additionally, eutrophication and climate change can affect the microbiome, biogeochemical zonation, and methane cycling in coastal sediments. This review summarizes the current knowledge on the processes and microorganisms involved in methane cycling in coastal sediments and the factors influencing methane emissions from these systems. In eutrophic coastal areas, organic matter inputs are a key driver of bottom water hypoxia. Global warming can reduce the solubility of oxygen in surface waters, enhancing water column stratification, increasing primary production, and favoring methanogenesis. ANME are notoriously slow growers and may not be able to effectively oxidize methane upon rapid sedimentation and shoaling of the SMTZ. In such settings, ANME-2d (*Methanoperedenaceae*) and ANME-2a may couple iron- and/or manganese reduction to AOM, while ANME-2d and NC10 bacteria (*Methylomirabilota*) could couple AOM to nitrate or nitrite reduction. Ultimately, methane may be oxidized by aerobic methanotrophs in the upper millimeters of the sediment or in the water column. The role of these processes in mitigating methane emissions from eutrophic coastal sediments, including the exact pathways and microorganisms involved, are still underexplored, and factors controlling these processes are unclear. Further studies are needed in order to understand the factors driving methane-cycling pathways and to identify the responsible microorganisms. Integration of the knowledge on microbial pathways and geochemical processes is expected to lead to more accurate predictions of methane emissions from coastal zones in the future.

Keywords: marine microbiology, methane oxidation, eutrophication, methanogenesis, sediment, climate change, greenhouse gases

OPEN ACCESS

Edited by:
Konstantinos Ar. Kormas, University of Thessaly, Greece

Reviewed by:
Jakob Zopfi, University of Basel, Switzerland
Maxim Rubin-Blum, Israel Oceanographic and Limnological Research (IOLR), Israel

****Correspondence:***
Anna J. Wallenius
a.wallenius@science.ru.nl

Specialty section:
This article was submitted to Aquatic Microbiology, a section of the journal Frontiers in Microbiology

Received: *20 November 2020*
Accepted: *29 January 2021*
Published: *18 February 2021*

Citation:
Wallenius AJ, Dalcin Martins P, Slomp CP and Jetten MSM (2021) Anthropogenic and Environmental Constraints on the Microbial Methane Cycle in Coastal Sediments. Front. Microbiol. 12:631621. doi: 10.3389/fmicb.2021.631621

INTRODUCTION

Methane is an important greenhouse gas, contributing to 16% of global warming (Ciais et al., 2013). Total methane emissions to the atmosphere are estimated at 500–600 Tg CH_4 yr^{-1} with yearly fluctuations in sinks and sources. The recently measured atmospheric concentration (1,870 ppb in June 2020; Dlugokencky, 2020) is 2.5-fold higher than that for pre-industrial times (720 ppb). Anthropogenic activity is believed to be the main cause for this rapid increase of atmospheric methane (Ciais et al., 2013), as human activity is responsible for an estimated 50–75% of total methane emissions (Conrad, 2009). Oxidation by hydroxyl radicals is the main sink for methane in the atmosphere, accounting for 90% of all removal (Kirschke et al., 2013). Microbial methane production and oxidation, which occurs both aerobically and anaerobically by bacterial and archaeal species, regulates the amount of methane released into the atmosphere (Hanson and Hanson, 1996; Knittel and Boetius, 2009).

Methane is released from various sources including the Earth's crust (thermogenic origin), incomplete combustion of fossil fuels and biomass (pyrogenic origin), and microbial metabolism (biogenic origin; Kirschke et al., 2013). Most biogenic methane is produced by microorganisms, mainly methanogenic archaea, as the last step in the breakdown of organic matter in anoxic environments, via the process of methanogenesis. Smaller amounts of methane are produced from methylphosphonates in oxic waters by cyanobacteria and other phytoplankton, and in the ocean by Thaumarchaea (Metcalf et al., 2012; Klintzsch et al., 2019; Bižiæ et al., 2020).

Methanogens are found both in natural and human-influenced systems, frequently where all electron acceptors other than CO_2 are exhausted. Anthropogenic sources include rice fields, ruminant guts, landfills and sewage systems, which are ideal habitats for methanogens and emit significant amounts of methane into the atmosphere (Conrad, 2009). Natural methane sources include wetlands, other freshwater and marine systems, termites and thawing permafrost soils. Wetlands contribute almost to a third of overall global emissions, with estimates ranging from 80 Tg CH_4 yr^{-1} to 280 Tg CH_4 yr^{-1} (Bridgham et al., 2013). However, while oceans cover 70% of the Earth's surface, they contribute only 1–2% of the global emissions (6–12 Tg CH_4 yr^{-1}; Weber et al., 2019). A significant portion of this, up to 75%, originates from coastal environments, which cover only a fraction of the total ocean area (Hamdan and Wickland, 2016). Degradation of organic matter in marine sediments produces large amounts of methane, but due to efficient removal by methane oxidation over 90% of this methane is microbially filtered and removed prior to emission (Knittel and Boetius, 2009).

In marine sediments, methanogens inhabit the deep anoxic layers where methanogenesis is the terminal step in organic matter degradation (Ferry, 1992). Archaeal methanogens use the enzyme complex methyl-coenzyme M reductase (MCR) to produce methane. Methanogens use a limited number of substrates, i.e., formate, acetate, hydrogen or methylated compounds (Reeburgh, 2007). The type of substrates used depends on the microorganisms present and the quality of the organic matter being degraded, which varies in different environments (e.g., LaRowe et al., 2020).

Above the methanogenic zone in marine sediments is a layer called the sulfate-methane transition zone (SMTZ) where upward diffusing methane and downward diffusing sulfate meet and are both removed (Barnes and Goldberg, 1976). At the start of the 21st century, the pathways and responsible organisms for this removal were identified (Boetius et al., 2000; Orphan et al., 2001, 2002; Knittel and Boetius, 2009). In the SMTZ, methane is oxidized by anaerobic methane-oxidizing archaea (ANME) with sulfate-reducing bacteria (SRB) serving as the electron sink for the reaction (Knittel et al., 2018). ANME are phylogenetically related to methanogens and are divided into three clades (ANME-1, ANME-2 and ANME-3). Based on the Genome Taxonomy Database (GTDB), ANME-2 and ANME-3 belong to different *Methanosarcinales* clades, while ANME-1 is currently assigned to the Candidatus *Syntropharchaeia* class (Parks et al., 2020). All clades use a reverse methanogenesis pathway to oxidize methane, but some clades have been hypothesized to use the enzyme machinery for methane production as well (Lloyd et al., 2011). Members of the ANME-1 clade were recently identified as the main contributors to methane removal and potentially also methanogenesis in estuarine sediments, and the preferred metabolic process may be partly regulated by hydrogen concentrations (Kevorkian et al., 2020).

Sulfate-dependent anaerobic methane oxidation (S-AOM) by ANME consortia efficiently filters most of the upward diffusing methane in the SMTZ of deep marine sediments. The SRB can also couple dissimilatory sulfate reduction to organic matter degradation, and, given the sulfate concentration of 28 mM in seawater, they are the main microorganisms responsible for organic matter mineralization in these sediments (Jørgensen et al., 2019). As SRB have a high affinity for methanogenic substrates such as acetate and hydrogen, SRB can outcompete methanogens (Kristjansson et al., 1982; Schönheit et al., 1982). Therefore, methanogenesis usually does not occur above the zone of S-AOM but does dominate in deeper sediments where most, if not all sulfate, has been exhausted and still enough organic matter is present. However, cryptic methane cycling fueled by methylotrophic methanogenesis has been reported in sulfate-rich surface sediments of Aarhus Bay in Denmark (Xiao et al., 2018) and in the SMTZ at multiple sites in the Baltic Sea, where ANME-1 were hypothesized to mediate such activity (Beulig et al., 2019).

Although in most marine sediments with a well-defined SMTZ and steady ANME community methane removal is typically efficient (Knittel and Boetius, 2009), this is less so in many coastal sediments. One reason is that the SMTZ is generally located closer to the sediment-water interface, because of a lower salinity and associated lower sulfate concentrations. The smaller distance to the overlying water allows more methane to escape from the sediment through either diffusion or advection (Egger et al., 2018). Furthermore, the highly dynamic conditions in many coastal systems, i.e., linked to seasonal changes in temperature and primary production and/or variations in sedimentation rates, can impact the balance between methanogenesis and methane oxidation in the sediment. The key factors regulating methane cycling in coastal sediments are, however, not well understood (Hamdan and Wickland, 2016).

Besides S-AOM, various other pathways of methane oxidation may be quantitatively important in coastal sediments. In oxic surface sediment layers, aerobic methane-oxidizing bacteria (MOB) are expected to dominate (Rasigraf et al., 2017). MOB belonging to the phyla Proteobacteria and Verrucomicrobia use a particulate or soluble methane monooxygenase (pMMO; sMMO) to oxidize methane seeping through the SMTZ (Hanson and Hanson, 1996; Op den Camp et al., 2009). There is also accumulating evidence for anaerobic methane oxidation with nitrate, metal oxides and humic substances in freshwater and brackish coastal habitats (e.g., Raghoebarsing et al., 2006; Sivan et al., 2011; Haroon et al., 2013; Segarra et al., 2013; Egger et al., 2015b; Scheller et al., 2016; Martinez-Cruz et al., 2017; Valenzuela et al., 2017; Bai et al., 2019; van Grinsven et al., 2020). While bacteria of the NC10 candidate phylum named '*Candidatus* Methylomirabilis oxyfera' can couple methane oxidation to nitrite reduction and nitric oxide dismutation (Ettwig et al., 2010), archaea belonging to the ANME-2 subclade ANME-2d (also known as family *Methanoperedenaceae*) can couple methane oxidation to reduction of nitrate (Haroon et al., 2013). Members of *Methanoperedenaceae* have also being identified as responsible organisms for methane oxidation coupled to iron and manganese reduction (Ettwig et al., 2016; Cai et al., 2018; Leu et al., 2020).

Coastal environments are vulnerable ecosystems that differ from open marine habitats by being more dynamic. Environmental conditions can change rapidly due to seasonal changes in temperature and salinity, in the composition of organic matter in terrestrial run-off, fluctuating rates of primary production and changes in hydrological conditions (Bauer et al., 2013). As the barrier between marine and terrestrial habitats, coastal sediments play an important role in the biogeochemical cycling of carbon, nitrogen, phosphorus, and metals (Sundby, 2006). Mineralization of organic compounds in coastal sediments is generally very rapid due to a high biodegradability of organic matter and a sufficient supply of electron acceptors, in addition to oxygen. Due to a complex network of metabolic processes, small changes in environmental factors may affect the redox zonation and biogeochemical functioning, including the methane cycle. Therefore, anthropogenic activity typically has a large impact on biogeochemical processes in coastal ecosystems. For example, eutrophication affects the redox state and microbial communities of coastal sediments (Doney, 2010).

Anthropogenically-induced nutrient inputs to coastal waters feed primary production in the form of intense algal spring blooms, which can result in bottom water oxygen depletion and high burial rates of organic matter (Diaz and Rosenberg, 2008). Additionally, climate change impacts hydrological conditions, which can lead to changes in bottom water salinity and/or water level. Global warming affects gas solubility, rates of chemical reactions and microbial activity (Doney, 2010). However, little is known about how these changes will influence element cycling in eutrophic coastal areas.

This review aims to summarize the current state of research on methane cycling in coastal sediments and the different factors driving methanogenic and methanotrophic processes. As anthropogenic eutrophication and global warming are increasing, coastal systems are severely impacted. Rapid burial of organic matter, changes in temperature and oxygen availability together with a high availability of alternative electron acceptors such as metal oxides and nitrate all alter the methane-filtering potential in coastal habitats. The impact of these changing factors is not well understood, and it is therefore difficult to estimate, let alone predict, future coastal methane emissions. However, we urgently need more accurate models to predict the role that different types of sediments have in increasing or decreasing methane emissions from coastal zones in the future.

THE EFFECT OF EUTROPHICATION AND CLIMATE CHANGE ON SEDIMENT BIOGEOCHEMISTRY AND METHANE FLUXES

Eutrophication of coastal areas is of growing concern, as human activities cause major disturbances of coastal ecosystems. Land management practices such as agriculture, dam building, peatland draining and wetland removal alter the amount and content of organic carbon delivered to coastal areas (Bauer et al., 2013). Further, constant development of coastal areas may directly affect the methane cycling in estuaries, with sediments from estuaries subject to a higher intensity of human modification potentially emitting more methane into the water column (Wells et al., 2020). Anthropogenically-driven climate change results in higher average annual temperatures and induces hydrological and oceanographic variations, such as changes in water level and river flows, and might increase greenhouse gas emissions (IPCC, 2014). Flooding events in rivers have been shown to increase estuarine stratification and hypoxia (Kerimoglu et al., 2020) as well as methane emissions (Sieczko et al., 2016), with the composition of the terrestrial organic matter possibly determining which greenhouse gases are released (Schade et al., 2016). Increased hypoxia alters biogeochemical processes, with anaerobic pathways of organic matter degradation, including methanogenesis, gaining importance. Upon mild hypoxia, however, responses may be variable and difficult to predict (Foster and Fulweiler, 2019; LaRowe et al., 2020). Eutrophication can lead to an upward shift of the SMTZ (Crill and Martens, 1983), with past eutrophication potentially affecting rates of methanogenesis observed today (Myllykangas et al., 2020a).

Influence of Sedimentation Rates on Coastal Methane Emissions

At the global scale, sedimentation rates, organic matter input, the depth of the SMTZ and the upward flux of methane to the sediment-water interface are related (Egger et al., 2018): the higher the sedimentation rate, the more organic carbon burial and the shallower the SMTZ because of increased methane production at depth. Hence, variations in sedimentation rate contribute to the difference in the average depth of the SMTZ in coastal and inner shelf sediments ($\leq$2 m below the sea floor) when compared to sediments from more offshore areas ($>$4 m below the seafloor) (Egger et al., 2018). The shallower the SMTZ, the more chance of escape of methane from the sediment

to the overlying water and, ultimately, to the atmosphere (Borges and Abril, 2012).

For example, elevated methane fluxes across the sediment-water interface due to high rates of sedimentation were reported for the Himmerfjärden estuary (Sweden) in the Baltic Sea (Thang et al., 2013). Porewater analysis at three sites in the estuary revealed a shallow SMTZ at 20 cm below the sediment surface, as defined by the depth of sulfate penetration (Thang et al., 2013). Overlapping sulfate and methane depth profiles indicate that the sediments at Himmerfjärden had a poor methane removal capacity in the SMTZ. Methane concentrations below the SMTZ were highest at the site closest to the shore, located directly downstream from a sewage treatment plant. At this site, the sedimentation rate and organic matter burial rates, were also highest (**Table 1**). This suggests that nutrients and organic matter leaking from the sewage treatment plant contributed to eutrophication in the nearby coastal areas. Organic carbon burial rates were, overall, relatively high at all stations. The high organic matter burial rates and shallow SMTZ allowed labile organic matter as well as reactive iron to be buried below the SMTZ. Active methanogenesis was observed in and below the SMTZ. Together, the weakened methane-filtering ability in the SMTZ, caused by the high sedimentation and organic matter burial rates, were suggested to increase methane emissions (Thang et al., 2013). A similar relationship between sedimentation rate and less efficient methane removal was described in a field study in Lake Grevelingen, a saline coastal reservoir suffering from eutrophication (Egger et al., 2016b). Porewater profiles combined with records of sedimentation and organic matter burial showed a link between eutrophication and rise in methane fluxes. The high rates of sedimentation and organic matter burial, when compared to many other coastal sediments (**Table 1**), are not unusual for coastal reservoirs and likely explain the shallow position of the SMTZ. The isotopic composition of upward diffusing methane in Lake Grevelingen sediment indicated that methanogenesis occurred within the SMTZ. Most of the methane bypassed the SMTZ and was likely either oxidized at the oxic surface of the sediment by aerobic methanotrophs or escaped to the overlying water (Egger et al., 2016b).

Rapid sediment accumulation in coastal areas such as the Himmelfjärden estuary and Lake Grevelingen is associated with high organic matter input resulting from anthropogenic-driven eutrophication. The longer eutrophication persists, the more the redox zonation and biogeochemical functioning of the sediment may alter. Rapid sedimentation changes the depth of the SMTZ by bringing it closer to the sediment surface. This results in a shorter residence time of organic matter in the sulfate reduction zone, thereby leaving more substrate for methanogenesis below the SMTZ (Sundby, 2006; Dale et al., 2019).

The most common substrates for methanogens in coastal sediments are acetate (acetoclastic methanogenesis) and hydrogen (hydrogenotrophic methanogenesis; Crill and Martens, 1986). Little is known about the importance of methylotrophic methanogenesis in coastal ecosystems so far (Zhuang et al., 2017).

Methanogenesis is usually observed only in deeper sediments where all other electron acceptors have been exhausted, because SRB can outcompete methanogens on substrates such as acetate and hydrogen. Therefore, the SMTZ is usually a barrier for methane production. In many offshore marine sediments, sulfate-AOM in the SMTZ is so efficient that all methane is removed at the top of this zone (Reeburgh, 2007). Furthermore, methane could be produced in the SMTZ in addition to the layer below, due to a high abundance of methanogenic substrates. Combined with sulfate limitation, SRB can no longer outcompete methanogens for all the substrates in such a situation. In addition, methylated compounds such as dimethyl sulfide are non-competitive substrates and, therefore, methylotrophic methanogens may also be commonly present in the SMTZ (Mitterer, 2010).

In addition to the high abundance of substrates to support simultaneous sulfate reduction, AOM and methanogenesis, the SMTZ might also have a reduced ability to filter methane, regardless of the increased production. High sediment accumulation rates such as the one recorded at the Himmerfjärden estuary mean that the residence time of the microbial community in the SMTZ is only 20–30 years (Thang et al., 2013) and even shorter in Lake Grevelingen where the sedimentation rate is 10-fold higher (Egger et al., 2016b). The main organisms responsible for methane removal, ANME archaea, are known to be very slow growers (Knittel et al., 2018), and can possibly not establish enough biomass, as approximately 60 years are needed for ANME to create a steady-state AOM biomass (Dale et al., 2008a). Therefore, it is possible that the

TABLE 1 | Sedimentation rates and reported diffusive CH_4 fluxes from sediments to the overlying water for selected coastal sediments.

Location (water depth (m))	Sedimentation rate (cm yr^{-1})	Organic matter accumulation rate (mol C m^{-2} yr^{-1})	Diffusive CH_4 efflux (mol m^{-2} yr^{-1})*	References
Lake Grevelingen (45)	13	91	0.2–0.8	Egger et al., 2016b
Himmerfjärden estuary station H5; downstream from sewage plant (25)	0.98	9.5	0.37	Thang et al., 2013
Himmerfjärden estuary station H3 (50)	0.82	9.3	0.25	Thang et al., 2013
Himmerfjärden estuary station H2 (30)	0.77	8.9	0.11	Thang et al., 2013
Average Inner shelf** (0–50)	0.56	7.8	0.21	Egger et al., 2018
Average Outer shelf** (50–200)	0.14	3.4	0.05	Egger et al., 2018

**Diffusive fluxes are calculated from porewater profiles and bottom water concentrations and do not include ebullition. **Based on literature review. For a recent overview of benthic release of CH_4 in coastal systems, see Egger et al. (2016b).*

methane removal in these sediments is impaired, as the methane-oxidizing consortia cannot keep up with the rapid accumulation. The decreased ability to remove methane in the SMTZ, added to the increased methanogenic potential below this layer, strongly indicates that rapid sedimentation rates cause increased methane emissions from coastal sediments.

Impact of Spreading Coastal Hypoxia on Sediment Processes

Hypoxia occurs in water bodies that are poorly ventilated and/or receive large inputs of organic matter (Middelburg and Levin, 2009). In these systems, hypoxia can be seasonal or more long lasting depending on the balance between the oxygen supply and demand. Human impact has extended the duration and spatial extent of hypoxia in many coastal systems. Following the widespread use of fertilizers since the 1950's, many coastal areas have seen an introduction or expansion of hypoxia ($\leq$2 mg O_2 L^{-1}; Breitburg et al., 2018). Examples of such areas are the Baltic Sea (Carstensen et al., 2014) and East China Sea (Wang et al., 2012). Hypoxia develops as eutrophication increases organic matter input, which promotes oxygen-consuming mineralization of organic matter. The degrading organic matter releases reduced compounds such as ammonium, and leads to release of Mn (II), Fe (II), and H_2S, and their oxidation can deplete the remaining oxygen (Sundby, 2006). Higher average temperatures caused by global warming decrease the solubility of dissolved oxygen in coastal waters and may increase primary production and respiration. Consequently, oxygen is depleted faster in coastal waters (Diaz and Rosenberg, 2008). The longer the hypoxia remains, the larger the consequences are for the microbial and benthic community as well as the biogeochemical cycling of elements in the sediment (Middelburg and Levin, 2009).

A decrease in bottom water oxygen alters the pathways of organic matter mineralization and methane cycling in sediments. In sediments covered by oxic bottom waters, various electron acceptors are typically available which can be used for organic matter mineralization in the following sequence (based on the Gibbs free energy yield): oxygen, nitrate (NO_3^-), manganese [Mn(IV)], iron [Fe(III)], sulfate (SO_4^{2-}), and finally CO_2, for methanogenesis (**Figure 1**; Froelich et al., 1979; LaRowe et al., 2020). Many of these electron acceptors are also involved in additional redox reactions, including methane oxidation (**Figure 1**) and cryptic cycling of Fe and S. In sediments overlain by hypoxic and anoxic bottom waters, however, the redox zonation will become more compressed and, especially upon persistent anoxia, may include only the zones of sulfate reduction and methanogenesis. Upon prolonged periods of bottom water anoxia, the mineralization of organic matter in the sediment may not be as effective (Hartnett et al., 1998; Middelburg and Levin, 2009). Seasonal bottom water hypoxia, however, could accelerate organic matter conversion, as studies have shown that alternating oxic-anoxic cycles were most efficient for mineralization (Sundby, 2006).

Bioturbation may also alter the sediment redox zonation. Macrofauna can transfer fresh organic matter and electron acceptors from surface sediments and the overlying seawater to deeper sediment layers, thereby changing the microbial community structure and composition and potentially accounting for the dominance of bacteria over archaea in marine sediments (Chen et al., 2017; Deng et al., 2020). In the Baltic Sea, macrofauna may increase methane release (up to

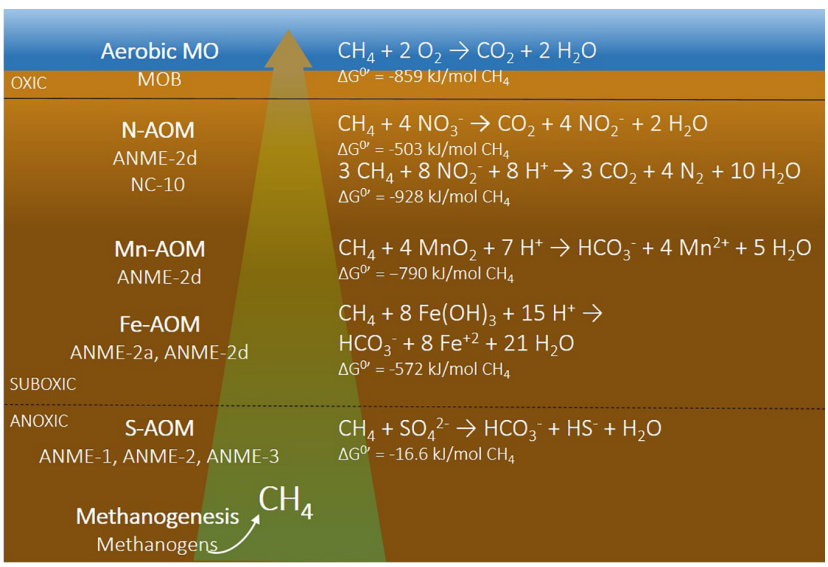

FIGURE 1 | Schematic presentation of microbial processes and microorganisms **(left)** and reaction equations with different electron acceptors **(right)** involved in methane cycling. N-AOM can couple either nitrate (ANME-2d) or nitrite (NC-10) to methane oxidation. MO, methane oxidation; N-AOM, nitrate/nitrite-dependent anaerobic oxidation of methane; Mn-AOM, manganese-dependent anaerobic oxidation of methane; Fe-AOM, iron-dependent anaerobic oxidation of methane; S-AOM, sulfate-dependent anaerobic oxidation of methane. References for the Gibbs free energies are the following: aerobic MO (Regnier et al., 2011), N-AOM (In' t Zandt et al., 2018), Mn-AOM and Fe-AOM (Sturm et al., 2019), and S-AOM (Meulepas et al., 2010).

eightfold) from sediments in relation to macrofauna-devoid sediments, potentially accounting for an estimated 9.5% of total emissions from this marine ecosystem (Bonaglia et al., 2017). The hypothesized mechanism for macrofauna-induced benthic methane efflux was a combination of a flush-out effect and methanogen symbionts of macrofauna. However, this does not exclude the hypothesis that macrofaunal activity could also enhance methane oxidation due to the introduction of electron acceptors into deeper sediment layers (Kogure and Wada, 2005). On the other hand, hypoxia and anoxia often disperse or completely eliminate macrofauna from coastal marine sediments, promoting the further accumulation of reduced compounds, including sulfide (Middelburg and Levin, 2009). Sulfide might not affect methanogenic activity, but could be toxic to ANME archaea (Timmers et al., 2015), potentially decreasing anaerobic oxidation of methane. The complex mechanisms and impacts of the presence or absence of macrofaunal activity remain to be fully elucidated.

A direct link between seasonal hypoxia and higher methane fluxes was recently observed in the eutrophic Chesapeake Bay, United States (Gelesh et al., 2016). Upon oxygen depletion in the bottom water following the algal spring bloom, benthic methane release increased. By the end of summer, methane was detected across the stratified water column up to the surface waters and was thus likely released to the atmosphere. However, once oxygen was reintroduced in the bottom waters, methane concentrations decreased significantly, and disappeared to background levels during winter. One possibility for the observed methane trend is that methanogenesis rates increased in the anoxic sediments, and the anaerobic oxidation was too slow to respond. Another explanation for the sudden decrease in methane levels during summer is the transport of dissolved methane from elsewhere, due to seasonal storms or algal blooms, to the measurement site (Gelesh et al., 2016). However, as biogeochemical processes regulating the sediment methane cycle are very complex and affected by changes in many factors such as sedimentation rate, temperature and availability of electron acceptors in addition to spatial and temporal depletion of oxygen, more field studies are needed to establish a connection between hypoxia and methane emissions.

Climate Change-Induced Rising Temperatures and Sediment Biogeochemistry

Human-driven climate change is increasing average seasonal temperatures globally. Since pre-industrial times, global temperature has risen 1°C, with much greater increases locally, especially in polar and sub-tropical coastal zones (IPCC, 2014). In coastal areas, increasing temperatures have been linked to increases in greenhouse gas emissions, such as elevated sediment-water fluxes of methane in coastal waters of Belgium (Borges et al., 2019) and Baltic Sea (Humborg et al., 2019) during a heatwave in 2018.

Local methane emissions may also increase due to long-term warming, as was demonstrated in artificial freshwater ponds with 4°C warming over a decade (Zhu et al., 2020). The over twofold increase in emissions was linked to disproportionate increase in methanogenesis activity, in comparison to other processes. Methanogenesis is known to strongly depend on temperature (Westermann et al., 1989; Schulz et al., 2006) and many methanogens may have a significantly higher optimum temperatures than their *in situ* habitat (Blake et al., 2020). Thus, a warming climate may favor methanogens and increase their activity, but the potential increase of methane production is difficult to link directly to higher emissions. Notably, Yvon-Durocher et al. (2014) used meta-analyses to show that the temperature dependence of methane production in natural ecosystems is higher than that of other carbon-cycling processes with a 4:1 ratio for CH_4:CO_2, resulting in potentially relatively higher global methane emissions in a warmer climate.

Methanogenesis using different substrates may also respond differently to rising temperature. Long-term warming shifted a freshwater community toward hydrogenotrophic methanogenesis, and hydrogen was favored over acetate also in incubation studies (Zhu et al., 2020). Similarly, laboratory incubations of coastal sediments from Gulf of Mexico showed the strongest effect of temperature on hydrogenotrophic methanogenesis, and methylotrophic methanogenesis were much less affected (Zhuang et al., 2018). These studies suggest that the different methanogenic clades inhabiting the sediments might determine the level of impact that temperature plays on increasing methane production rates.

Temperature dependence of methane oxidation is less understood. ANME archaea have mainly been characterized in cold, high-pressure environments such as deep sea vents (Boetius et al., 2000) where methane dissolves easier. Studies show that the optimal AOM rates vary between ANME clades, but are within a narrow range of 5–25°C (Bhattarai et al., 2018; Nauhaus et al., 2005), therefore suggesting that their activity would not increase significantly in warmer temperatures. However, more studies on the effect of temperature on AOM are needed to know whether anaerobic oxidation of methane is equally affected by global warming as methanogenesis, since this will determine the strength of the positive feedback loop of climate warming and increases in atmospheric methane concentrations.

EUTROPHICATION ALTERS THE REDOX ZONATION IN COASTAL SEDIMENTS AND COULD SUPPORT ALTERNATIVE ELECTRON ACCEPTORS FOR AOM

In freshwater environments with non-detectable amounts of sulfate, AOM has been linked to metal oxide, nitrate and nitrite reduction (Raghoebarsing et al., 2006; Segarra et al., 2013; He et al., 2016). In coastal areas with rapid rates of sedimentation and a decreased salinity, sulfate only penetrates the surface layers a few centimeters, and a large amount of reactive organic matter and metal oxides can be buried below the SMTZ (Egger et al., 2015a, 2016b; Rooze et al., 2016; Rasigraf et al., 2020). Run-off of nitrogen products from agricultural fertilizers also deliver more reactive nitrogen products to the coastal waters (Jickells, 1998). Therefore, anthropogenically-induced eutrophication might create conditions to supply AOM

with alternative electron acceptors and these processes might become more important to understand the future in coastal areas affected by human activity. As the methane-removing efficiency is often compromised in coastal areas due to rapid sedimentation rates and high organic matter load (Thang et al., 2013; Egger et al., 2015b), it is important to understand how these alternative AOM processes contribute to methane removal.

Metal Oxides Buried Below the SMTZ Could Serve as Electron Acceptors for AOM

In marine sediments, ANME-1, ANME-2 and ANME-3 have been linked to S-AOM in the SMTZ and are considered key microorganisms involved in methane removal (Knittel et al., 2018). In freshwater sediments where sulfate concentrations are low to non-existent, AOM may be coupled to more energetically favorable electron acceptors such as oxides of iron (Fe-AOM) and manganese (Mn-AOM; Cai et al., 2018). Alternatively, in such environments, manganese and iron oxides could lead to the oxidation of reduced sulfur species to sulfate, sustaining S-AOM by a syntrophic consortium of *Methanoperedenaceae* (ANME-2d) and sulfate-reducing *Desulfobulbaceae* (Su et al., 2020). Due to a high salinity and, hence, high availability of sulfate in marine sediments, iron oxides are usually not available as electron acceptors in the SMTZ, as they react with dissolved sulfide formed from sulfate reduction (Reeburgh, 2007). However, the possibility for Fe-AOM and Mn-AOM in marine settings was shown already a decade ago (Beal et al., 2009), but direct evidence for this process and details on the responsible microorganisms are still scarce.

Genomic and transcriptomic analysis of a freshwater sediment enrichment culture identified ANME-2d clade members as being responsible for coupling methane oxidation to the reduction of iron and manganese oxides (Cai et al., 2018; Leu et al., 2020), but these organisms are yet to be connected to potential Fe-AOM and Mn-AOM in marine sediments. Interestingly, also aerobic Proteobacterial methanotrophs were recently reported to be capable of coupling methane oxidation to metal reduction under hypoxia (Zheng et al., 2020). Furthermore, contradictory to previous knowledge, methanogens may benefit from iron oxides (Kato and Igarashi, 2019) and have been suggested to play a role in Fe-AOM (Elul et al., 2020) and be able to switch between methanogenesis and iron reduction in varying conditions (Sivan et al., 2016). These findings reveal the complexity of iron and methane cycling in sediments, highlighting the importance of unraveling the responsible microorganisms and biogeochemical pathways used.

Egger et al. (2015b) provided geochemical evidence for Fe-AOM in brackish coastal sediments of the Bothnian Sea from porewater profiles and laboratory incubations. Sediments in this deep part of the Bothnian Sea (214 m) are characterized by a shallow SMTZ, which is attributed to high inputs of organic matter and rates of sedimentation (**Table 1**). Below the SMTZ, high concentrations of iron oxides and dissolved Fe^{2+} were observed, as well as indications for active methanogenesis, based on isotopically depleted CH_4. Slurry incubations of methanogenic layers with ^{13}C-CH_4 and iron oxides in the absence of sulfate showed increased $^{13}CO_2$ production compared to those supplied only with methane, suggesting sulfate-independent AOM. This suggests Fe-AOM can occur in sediments where iron oxides and reactive organic matter are buried below the SMTZ. The potential controls on Fe-AOM at this site were explored further by Rooze et al. (2016) using a transient reactive transport model. The results confirm that increased organic matter input over several decades can lead to increased rates of methanogenesis and iron reduction, and a shoaling of the SMTZ. Inputs of Fe oxide and bottom water sulfate concentrations are also major controls on Fe-AOM rates, with sulfate inhibiting both methanogenesis and Fe-AOM.

Even though the ANME-2d clade has been linked to Fe-AOM and Mn-AOM in enrichment cultures isolated from freshwater sediments (Ettwig et al., 2016; Cai et al., 2018; Leu et al., 2020), very little is known about the microorganisms involved and their abundance and significance in other environments. Aromokeye et al. (2020) enriched a different subclade of ANME-2; ANME-2a, from methanic marine sediments of the Helgoland Mud area in the North Sea in incubations with iron oxides, whereas ANME-2d reads were not detected in the sediments. The incubations showed active Fe-AOM in the absence of sulfate, albeit at a rate of only 2% of the S-AOM rate recorded in the SMTZ (**Table 2**). In addition, 16S rRNA gene reads of dissimilatory iron-reducing bacteria increased in relative abundance in the same incubations. While active manganese reduction was seen in the porewater profiles, incubations amended with manganese oxides showed no active methane oxidation (Aromokeye et al., 2020).

In another study, the microbial community composition in the Bothnian Sea, ANME-2a abundance was also linked to the presence of methane and iron oxides (Rasigraf et al., 2020). However, regardless of the parallel enrichment of iron-reducing bacterial taxa with ANME-2a (Aromokeye et al., 2020), it is not clear whether ANME-2a can oxidize methane independently, possibly via an extracellular electron acceptor, or whether they need a bacterial partner similar to the SRB in S-AOM. Incubation or enrichments fed with artificial electron acceptors, or transcriptomic profile of both bacterial and archaeal species could help to gain more insight into the physiology of Fe-AOM.

The evidence for Mn-AOM in coastal sediments is less clear. Although no indication of Mn-AOM was observed in Helgoland Mud sediment incubations (Aromokeye et al., 2020), Mn-AOM was recorded in incubations of sediments from deep methane seeps (Beal et al., 2009), coastal freshwaters, and brackish wetlands (Segarra et al., 2013). These differences could be due to disparities in the microbial community composition. Sulfate reduction was deliberately inhibited only in the Helgoland Mud incubations, indicating that observed Mn-AOM rates in other studies could have resulted from S-AOM if sulfate was available. Recently, Leu et al. (2020) showed active Mn reduction coupled to methane oxidation in a bioreactor enriched with members of the ANME-2d clade. Hence, further insight is needed in the potential role of manganese oxides as electron acceptors in AOM, the ANME clades capable of Mn-AOM, and the environmental factors favoring Fe-AOM and Mn-AOM in coastal and freshwater sediments.

The rates recorded for Fe-AOM are significantly lower than S-AOM, accounting for less than 5% of methane oxidation in

TABLE 2 | Comparison of estimated Fe-AOM and S-AOM rates from selected coastal sediments.

Location	Fe-AOM rate (μmol CH_4 cm^{-3} yr^{-1})	S-AOM rate in SMTZ (μmol CH_4 cm^{-3} yr^{-1})	Method	References
North Sea	0.035	2.0	Laboratory incubations	Aromokeye et al., 2020
Bothnian Sea (US5B)	1.3	–	Laboratory incubations	Egger et al., 2015a
Bothnian Sea (US5B)	0.08	0.79	Reactive transport model	Rooze et al., 2016
Bothnian Sea Öre estuary (NB8)	0.15	9.5	Reactive transport model	Lenstra et al., 2018; Rasigraf et al., 2020
Dover Bluff salt marsh	1.4	2.4	Laboratory incubations	Segarra et al., 2013
Black Sea	$1.46*10^{-5}$	0.073	Reactive transport model	Egger et al., 2016a
Baltic Sea, Bornholm Basin	$9.1*10^{-4}$	0.029	Reactive transport model	Dijkstra et al., 2018; Ash et al., 2019
Baltic Sea Landsort Deep	$1.1*10^{-3}$	0.27	Reactive transport model	Egger et al., 2017

coastal marine sediments (**Table 2**). However, eutrophication causes several changes that might favor Fe-AOM in deep methanic sediments. If the SMTZ is moved upward and the organic matter load is high, iron oxides spend less time in this layer and can be buried below the SMTZ before reacting with dissolved sulfide (**Figure 2**; Rooze et al., 2016). Over time, iron oxides will become abundant and may serve as electron acceptors for AOM (Egger et al., 2015b). Iron oxides may also be more available for Fe-AOM in sediments of shallower coastal waters, as is suggested with a minimum 10-fold difference in iron reduction rates determined via reactive transport models from offshore sites (**Table 2**). Potentially, in deeper sediments the more reactive iron oxides are already exhausted, or estimated Fe-AOM rates correspond instead to dissimilatory iron reduction.

An increased Fe input upon the expansion of eutrophication-driven hypoxia is, for example, recorded in sediments of the open

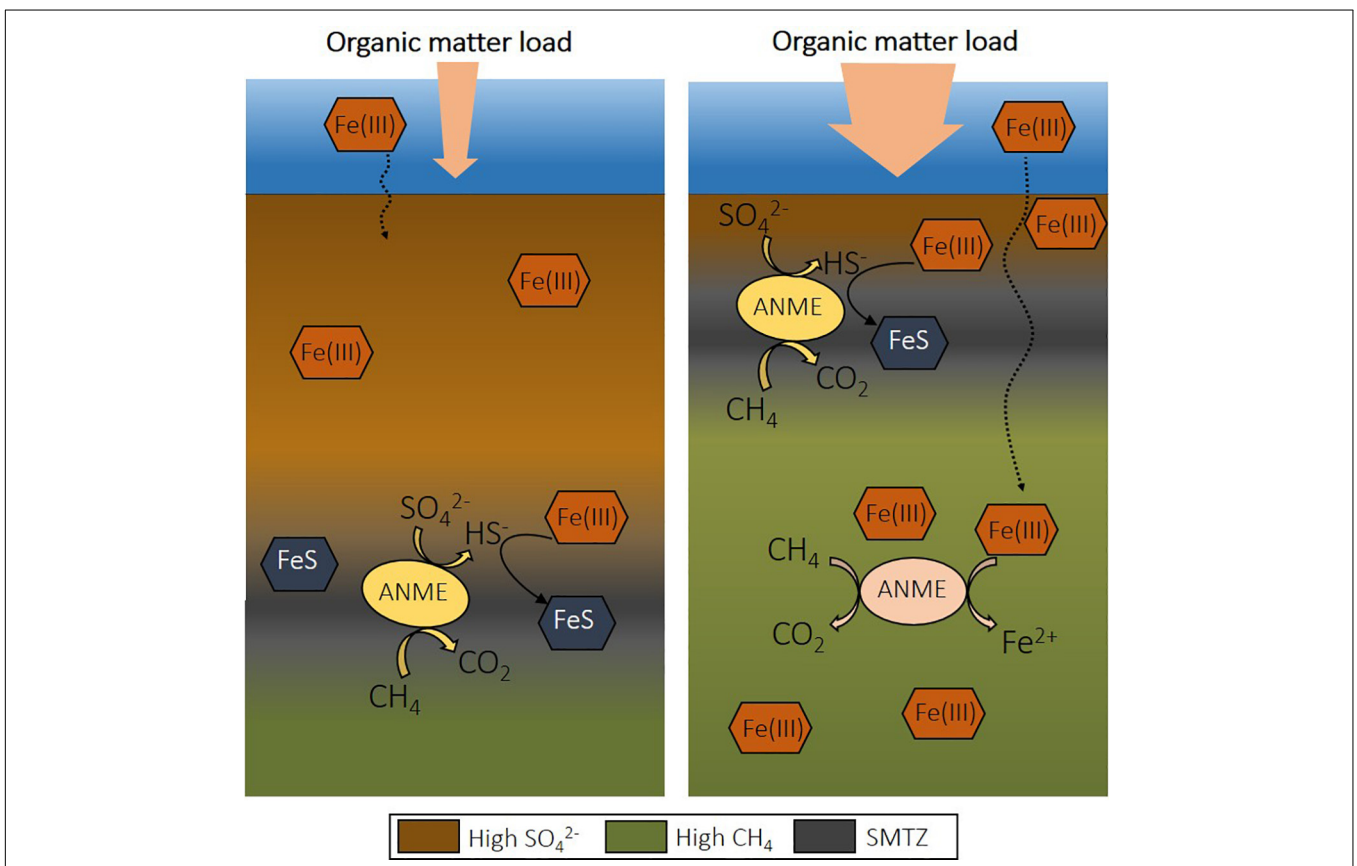

FIGURE 2 | The effect of eutrophication on the depth of the sulfate-methane transition zone (SMTZ) in coastal sediment and the potential for Fe-AOM. Upon increase of organic matter load, the depth of sulfate penetration decreases due to organic matter degradation coupled to sulfate reduction. This shifts the SMTZ upward and allows the presence of iron oxides at deeper depths, creating a niche for Fe-AOM. Fe-AOM, iron-dependent anaerobic oxidation of methane; S-AOM, sulfate-dependent anaerobic oxidation of methane.

Baltic Sea (Reed et al., 2016). Changes in land-use and/or climate may also lead to episodic increased terrestrial inputs of organic matter and Fe oxides to coastal sediments (Lenstra et al., 2018). As a consequence, iron oxides could be available over a wide depth interval. As the SMTZ in coastal areas is usually located at a shallow depth, a relatively wide Fe-AOM zone could increase the role of this alternative methane oxidation pathway.

Nitrate and Nitrite as Electron Acceptors for AOM

Methane oxidation coupled to nitrate/nitrite reduction (N-AOM) by both bacterial and archaeal species has been observed in freshwater sediments (Raghoebarsing et al., 2006; Luesken et al., 2011; Shen et al., 2015), and could also play a role in removing methane in coastal marine sediments (Shen et al., 2016; Wang J. et al., 2019) and marine oxygen minimum zones (Padilla et al., 2016; Thamdrup et al., 2019). The N-AOM *Candidatus* Methylomirabilis oxyfera bacteria can couple methane oxidation to nitrite reduction and nitric oxide dismutation (nitrite-AOM) using intracellularly produced oxygen and the aerobic methane oxidation pathway (Ettwig et al., 2010). The archaeal species belonging to the ANME-2 subclade ANME-2d (also known as family *Methanoperedenaceae*) can couple methane oxidation to reduction of nitrate (Haroon et al., 2013). In contrast to S-AOM, nitrate-dependent AOM (nitrate-AOM) does not require syntrophy. However, *Candidatus* Methanoperedens nitroreducens is often found in a community together with nitrite scavengers such as anammox and N-AOM bacteria (Haroon et al., 2013; Vaksmaa et al., 2017; Gambelli et al., 2018) to prevent inhibition by nitrite. Moreover, dissimilatory nitrate reduction to ammonium by *Methanoperedenaceae* has been recently reported to suffice as ammonium supply for anammox activity in a bioreactor enrichment culture (Nie et al., 2020). Several genomes of Methylomirabilis bacteria and ANME-2d archaea have been sequenced (Ettwig et al., 2010; Haroon et al., 2013; Arshad et al., 2015; Berger et al., 2017; Vaksmaa et al., 2017; Versantvoort et al., 2018) and recently the major protein complexes involved in the central metabolism of both microorganisms have been elucidated (Versantvoort et al., 2019; Berger et al., 2021).

Despite rapidly emerging new studies on N-AOM, the factors affecting the rates of nitrate- and nitrate-AOM and abundance of the responsible organisms are not well understood (Welte et al., 2016), and even less is known about the actual contribution of N-AOM to methane removal in coastal sediments. As anthropogenic eutrophication brings more organic matter to coastal sediments and increases nutrient concentrations in bottom waters, substantial amounts of nitrate and nitrite may become available as electron acceptors (Kraft et al., 2014). Increases in global eutrophication might therefore make these processes more important in methane removal, especially in sediments where sulfate concentrations are generally low and S-AOM is further compromised by shoaling of the SMTZ.

Significant rates of N-AOM were observed in coastal wetland and estuary sediments in China, with high concentrations of nitrate and nitrite in the sub-surface sediment (He et al., 2019; Wang J. et al., 2019). Molecular analysis revealed an abundant NC10 bacterial community in the layers below the oxygen penetration zone and the recorded rate for nitrite-AOM was faster than the S-AOM rate in deeper layers. Most of the methane was removed at the same depth where NC10 sequences were present, indicating their important role as a methane sink in these sediments. However, ANME-2d were also abundant and present in all samples showing N-AOM activity by isotopic tracing of $^{13}CO_2$, indicating a potential niche separation of microorganisms performing nitrite- and nitrate-AOM.

The depth distribution of *Ca.* M. oxyfera and ANME was hypothesized to result from better oxygen tolerance of *Ca.* M. oxyfera bacteria. However, oxygen exposure studies showed that oxygen as low as 2% (vol/vol) for *Ca.* M. oxyfera (Luesken et al., 2012) and 5% for archaea *Ca.* Methanoperedens nitroreducens (Guerrero-Cruz et al., 2018) can cause oxidative stress and a rapid decrease in methane oxidation potential. Nevertheless, genomes of both organisms indicate the potential to counteract exposure to oxygen. Therefore, other biogeochemical factors probably play a role in the observed depth profile of nitrate- and nitrite-AOM, but further studies are needed to understand the spatial and temporal dynamics of N-AOM in coastal sediments with fluctuating oxygen concentration.

In general, N-AOM has been shown to be downregulated by the presence of sulfate (Wang J. et al., 2019) and salinity (Shen et al., 2016). In contrast, temperature, ammonia and nitrate were positively correlated to N-AOM. This could imply that regardless of the inhibiting effect of sulfate, N-AOM activity will increase in coastal areas upon an increase in nutrient load as well as higher temperatures. Curiously, S-AOM has been shown to be inhibited by exogenous nitrogen addition (Zhang et al., 2020), emphasizing the potential role of N-AOM in eutrophic sediments. Furthermore, N-AOM is energetically more favorable than S-AOM, and therefore might have a higher methane removal potential if the organisms are able to grow faster than S-AOM ANME archaea (Wang J. et al., 2019). However, more information on the community structure and methane oxidation rates under different conditions is necessary to assess how eutrophication affects N-AOM in coastal sediments and its contribution to methane removal.

RECENT ADVANCES AND CHALLENGES IN THE IDENTIFICATION AND CHARACTERIZATION OF METHANE-CYCLING MICROORGANISMS IN COASTAL MARINE SEDIMENTS

The discovery of anaerobic methanotrophs capable of converting methane with electron acceptors other than sulfate has brought us a step closer to understanding and predicting methane cycling in different coastal environments. However, the methane cycle is only a small though important fraction of an entire network of microbial metabolism involved in the decomposition of organic matter, which drives element cycling in sediments

(Jørgensen et al., 2019; LaRowe et al., 2020). Geochemical porewater profiles do not reveal the complex active microbial network in sediments, as locations with a similar redox zonation might harbor an entirely different microbiome and active metabolic pathways (Grossart et al., 2020). Therefore, understanding the microbial community composition of sediments, including their metabolic potential and interactions with the abiotic environment is a major challenge.

The advances in high throughput gene sequencing and metagenomic analysis in the last decade have enabled numerous studies on the microbial community composition of diverse aquatic environments using pyro-, 16S rRNA gene, and metagenome sequencing (reviewed in Grossart et al., 2020). Yet, linking specific activity to the genes and microorganisms present is difficult. Fortunately, the database of metagenomic sequences extracted from different sediments is growing, and linking this genome information to geochemical data is increasing our understanding of factors influencing the sediment microbiome involved in biogeochemical processes such as nitrogen cycling (Rasigraf et al., 2017; Reyes et al., 2017) and iron reduction (Reyes et al., 2016; Vuillemin et al., 2018).

Anaerobic Methanotrophs

Metagenomic approaches have revealed the diversity and distribution of methane-cycling microbes such as the ANME archaea (**Table 3**). The ANME clades identified so far appear to prefer different conditions and substrates and are often linked to specific environments. For example, ANME-2d, which are capable of Fe-AOM/Mn-AOM, are usually found in freshwater sediments (Cai et al., 2018; Leu et al., 2020), whereas ANME-2a are observed in marine environments (Aromokeye et al., 2020). ANME-1 are traditionally classified as a marine clade performing S-AOM together with SRB (Knittel et al., 2018), but related sequences have been found in ferruginous freshwater sediments poor in sulfate, hinting at potential for Fe-AOM (Vuillemin et al., 2018). Another explanation could be that the detected ANME-1 cells are involved in methanogenesis as suggested in other studies (Lee et al., 2016; Kevorkian et al., 2020). Targeting iron-reducing microorganisms and/or genes, has increased the understanding of potential habitats for Fe-AOM activity. Furthermore, new bioinformatic tools are arising for screening of ubiquitous genes such as those involved in iron cycling (FeGenie; Garber et al., 2020), possibly enabling identification of novel taxa involved in iron reduction in coastal sediments. Similarly, genomic approaches have identified separate niches for N-AOM organisms showing that nitrate-reducing ANME archaea often prefer deeper sediments, whereas nitrite-reducing *Ca.* M. oxyfera-like bacteria are found closer to the oxic zone, regardless of the distribution of their substrate (He et al., 2019; Xie et al., 2020).

Metagenomic approaches can be used to gain knowledge of the metabolic potential of unclassified or poorly known microbes. Rasigraf et al. (2020) combined porewater profiles, 16S rRNA amplicon sequencing and functional gene analysis of metagenome-assembled genomes (MAGs) to study the metabolic potential and microbial community composition linked to the geochemical characteristics of Bothnian Sea sediments. The dominant bacterial and archaeal taxa followed the redox zones at the sampled sites, and ANME-2a was found to directly correlate with the presence of methane and iron oxides at two sites. However, despite this similarity in redox zonation, the microbial community composition at the sites differed noticeably. For example, an abundant community of aerobic methanotrophs was observed in the surface at the most offshore site. Dominant taxa involved in organic matter mineralization at each site also indicated that the active biogeochemical processes were different. To analyze the metabolic potential, MAG construction and functional gene analysis targeting main metabolic pathways for S, N, and C cycling was performed on one methanogenic sediment layer. The characterization of the most dominant microbes complemented the geochemical and phylogenetic data and revealed a vast metabolic potential adapted to low availability of substrates and anoxia. Main pathways for all element cycling could be identified, such as denitrification for N-reduction and three different pathways for methanogenesis (Rasigraf et al., 2020). However, a metagenomic profile of the microbiome is only a snapshot in time and fails to reveal the active metabolisms. To link a metabolic process with a gene or a group of microbes, metatranscriptomic and -proteomic methods preferably at the single cell level would give a more accurate indication. Metatranscriptomic methods reveal the transcribed genes in the community and help identifying microorganisms involved in methane cycling, as was done for ANME-2a capable of Mn-AOM and Fe-AOM (Cai et al., 2018; Leu et al., 2020), and N-AOM activity in ANME-2d (Haroon et al., 2013). They are also critical when studying the factors affecting gene expression and methane-oxidizing activity in different environments (e.g., Narrowe et al., 2019; Vigneron et al., 2019). Finally, metaproteomics, the analysis of all expressed proteins in a community, is rising as an important method to unravel the physiology of microbes involved in biogeochemical cycling in coastal sediments and the influence of environmental factors on these processes (Saito et al., 2019; Grossart et al., 2020).

Methanogens

Methanogenic archaea are better characterized than ANME, as there are several isolated representatives of different taxonomic groups. Metagenomic studies are rapidly adding new groups to the canonical methanogenic orders (i.e., *Methanococcales*, *Methanopyrales*, *Methanobacteriales*, *Methanosarcinales*, *Methanomicrobiales,* and *Methanocellales*), such as *Methanomassiliicoccales*, *Methanofastidiosa,* and *Methanonatronarchaeia*. In addition, the (reverse) methanogenesis marker gene *mcrA* has been repeatedly found outside *Euryarchaeota* in diverse environments, expanding the methanogenic metabolic potential in other archaeal phyla (Evans et al., 2019). *Bathyarchaeota* are some of the most dominant archaeal phyla in anoxic marine sediments and they are speculated to be important in degradation of diverse organic compounds as well as carbon cycling, potentially via methane metabolism (Zhou et al., 2018).

The methanogenic groups found in sediments depend greatly on physiochemical conditions such as salinity, pH, temperature, and available substrates (Webster et al., 2015). A global meta-analysis on biogeographical distribution of *mcrA* sequences showed that estuaries harbor the highest diversity

TABLE 3 | Distribution of ANME archaea clades and their suggested metabolism in marine and freshwater sediments as found in metagenomic studies.

Location (mbsf)	Sediment characteristics	Method	Detected ANME clades	Suggested AOM-pathway	References
Gulf of California Guaymas basin hydrothermal sediment (2011)	Hydrothermal, hydrocarbon rich sediment; SMTZ/SR; 4–6, 8–11 cm deep	Metagenomics and metatranscriptomics	ANME-1, ANME-2c	S-AOM; multi-carbon alkane oxidizing archaea	Dombrowski et al., 2017; Wang Y. et al., 2019
Gulf of Mexico, cold seep (>1,000)	Biogenic methane seep;	Metagenomics, metatranscriptomics, 16S rRNA gene sequencing	ANME-1(b)	SRB-independent S-AOM	Vigneron et al., 2017, 2019
	Thermogenic methane seep, top layer (0–15 cm)		ANME-2c	S-AOM in syntrophy with SRB	Vigneron et al., 2019
South China Sea, Dongsha area (1,024)	High methane flux (methane clathrates below); above SMTZ; 10–330 cm deep	Metagenomics, 16S rRNA gene sequencing	ANME-1b	S-AOM and Fe-AOM based on presence of Fe(III)/Fe(II) and Fe-reduction genes (supported by geochemical data)	Li et al., 2019
East Sea of Korea, Ulleung Basin (>1,000)	SMTZ, methane hydrate-bearing sediment	Metagenomics	ANME-1b	S-AOM	Lee et al., 2016
Nyegga cold seep, Norwegian Sea (746)	Methane seep; top 15 cm	Metagenomics and metaproteomics	ANME-1	SRB-independent S-AOM	Stokke et al., 2012
Bothnian Sea (Öre estuary 21–33; offshore 214)	Methanic; rich in Fe-oxides; below SMTZ (16S first 50 cm)	Metagenomics (Öre estuary) 16S rRNA gene sequencing (all)	ANME-2a	Fe-AOM; ANME-2a correlates to methane and Fe-oxides below SMTZ	Rasigraf et al., 2020
Baltic Sea, Aarhus Bay (27)	SMTZ	Metagenomics	ANME-1	S-AOM and methanogenesis (cryptic CH_4 cycling)	Beulig et al., 2019
Marine Lake Grevelingen, the Netherlands (45)	SMTZ	16S rRNA gene sequencing, batch incubations	ANME-3	SRB-independent S-AOM	Bhattarai et al., 2017
Pojo Bay estuary, Finland (7–34)	SMTZ and below	Metagenomics, 16S rRNA gene sequencing, batch incubations	ANME-2a/b	Fe-AOM	Myllykangas et al., 2020b
Lake Towuti, Indonesia, ferruginous lake (60; 200)	Top 50 cm	Metagenomics, 16S rRNA gene sequencing	ANME-1	Unclear – Fe-AOM?	Vuillemin et al., 2018
Gold Creek Reservoir, Australia (10)	Enrichment culture of top sediment layer	Metagenomics, metatranscriptomics, 16S rRNA gene sequencing (enrichment culture)	ANME-2d	Fe-AOM	Cai et al., 2018
Ferruginous terrestrial mud volcano, Taiwan (0)	0–160 cm depth profile	Metagenomics, 16S rRNA gene sequencing	ANME-2a	Fe-AOM (possibly with a synthrophic bacterial partner)	Tu et al., 2017

of methanogenic lineages (Wen et al., 2017), potentially due to availability of various substrates of terrestrial and marine origin as well as a salinity gradient, which could create micro niches with ideal conditions for several lineages. Conventionally, methanogens are thought to inhabit and produce methane only in the deep methanic zones below the SMTZ via acetoclastic and hydrogenotrophic methanogenesis (Reeburgh, 2007), and this view is often supported by porewater methane profiles. However, vertical depth profiles of 16S rRNA gene sequences and MAGs combined with gas flux measurements and activity assays have questioned this view. Especially in eutrophic coastal sediments, methanogens are not necessarily outcompeted by SRB and may produce methane even close to the sediment-water interface due to a high abundance of both competitive (i.e., acetate) and non-competitive (i.e., methanol) substrates (Maltby et al., 2016; Zhuang et al., 2016; Sela-Adler et al., 2017; Kallistova et al., 2020). Therefore, methylotrophic methanogenesis may be an important but previously overlooked methane source in coastal shallow sediments (Conrad, 2020), and trimethylamine, dimethylsulfide, and dimethylsulfoniopropionate may be more common methanogenic substrates in marine sediments than currently thought (Zhuang et al., 2017), especially under higher salinity. Methylotrophic methanogens can co-exist with acetogens, SRB and ANME in OMZ sediments (Bhattacharya et al., 2020) and deep sea methane seeps (Li et al., 2020; Xu et al., 2020), and methanogenesis in the sulfate-reducing zone has been identified in coastal sediments (Maltby et al., 2016). However, whether these microorganisms compete for the same substrates or exist in separate niches remains unclear.

Aerobic Methanotrophs

Aerobic MOB are widespread and active in marine ecosystems, with lineages that appear to thrive exclusively in marine environments, such as *Methylomicrobium japanense*-like organisms, and lineages deep sea-1 to -5 (Lüke and Frenzel, 2011). MOB have been detected in deep methane seepage sediments (Case et al., 2017), shallow hydrothermal systems (Hirayama et al., 2014), and in marine animals as symbionts (Petersen and Dubilier, 2009). MOB communities seem to differ between high methane seepage sediments and the overlying water column, the latter potentially hosting novel, poorly understood MOB lineages (Tavormina et al., 2008). In coastal areas of the Baltic Sea, aerobic methane oxidation rates in the water column achieve a maximum of 11.6 nmol L^{-1} d^{-1} over summer, when oxygen concentrations are lowest, highlighting that methanotrophs adapted to hypoxia may contribute significantly to mitigating methane emissions in such ecosystems (Steinle et al., 2017).

However, in coastal sediments, MOB seem to be present at low abundances. For instance, while in coastal sites of the Bothnian Sea only few Type I methanotrophic *Methylococcaceae* sequences were detected, the relative abundance of this group reached 6% of total bacterial reads at an offshore site (Rasigraf et al., 2020). Similarly, in coastal sediments of the Baltic Sea, the relative abundance and RNA transcripts attributed to the aerobic methanotrophy marker protein pMMO of the dominant methanotroph *Methylococcales* were significantly higher in deeper coastal offshore areas compared to adjacent shallow zones, which had higher surface water methane concentrations (Broman et al., 2020). The authors hypothesized that, in coastal sites, ebullition prevented the access of MOB to methane, limiting their growth, and that light might inhibit methanotrophic activity. Nonetheless, experimental oxygenation of Baltic Sea sediments resulted in increased MOB activity, as suggested by *pmoAB* RNA transcripts and 16S rRNA genes matching *Methylococcales* (Broman et al., 2017), indicating that MOB in coastal sediments may become active under favorable conditions. Similarly, MOB were found at maximum relative abundances of 0.012% in top sediments of the East China Sea coast, but were enriched after incubation with methane (He et al., 2019). Given that the most abundant MOB affiliated to the Type II methanotroph *Methylosinus*, which have a high affinity for methane, the authors hypothesized that these MOB could be surviving on "methane leftovers" after the activity of ANME and NC10 microorganisms. Moreover, MOB, at low abundances, may be found together with ANME in coastal sediments, suggesting potential effects of bioturbation (Myllykangas et al., 2020b).

Marine MOB may utilize alternative terminal electron acceptors. *Methylococcales* were identified as partially denitrifying methanotrophs in the OMZ of Gulfo Dulce via 16S rRNA gene analyses, metagenomics and metatranscriptomics (Padilla et al., 2017). It has been experimentally shown that aerobic MOB can couple methane oxidation to nitrate reduction under oxygen limitation (Kits et al., 2015). More recently, pure cultures of *Methylomonas* and *Methylosinus* were shown to couple methane oxidation to ferrihydrite reduction under oxygen limitation (Zheng et al., 2020). Such metabolisms are poorly investigated in marine ecosystems. Moreover, MOB in coastal sediments may have distinct biochemistry and be phylogenetically diverse. Some novel MOB isolated from North Sea sediments, including the first cultivated marine Alphaproteobacterial methanotroph, rely solely on a soluble methane monooxygenase for methane oxidation (Vekeman et al., 2016a), while others utilize a lanthanide-dependent XoxF5-type methanol dehydrogenase for methanol oxidation (Vekeman et al., 2016b). MOB affiliated to the phylum Verrucomicrobia (*Ca.* Methylacidiphilum) have been identified at low abundances in the coastal sediments of the Baltic Sea (Myllykangas et al., 2020b). Additionally, poorly classified Verrucomicrobia sequences have been identified in coastal sediments of the Bothnian Sea (Rasigraf et al., 2020), which were used for inoculation of a methane and iron-fed bioreactor that enriched Verrucomicrobia under oxygen limitation (Dalcin Martins et al., 2020). Further studies are needed to elucidate the roles as well as metabolic and phylogenetic diversity of MOB in coastal sediments.

Identifying and Understanding Responses of Methane-Cycling Microbial Communities to Anthropogenic Disturbances

As the metabolic potential of most microorganisms is still not known, it is difficult to understand how complex biogeochemical cycles and microorganisms of coastal sediments are linked.

Studies using 16S rRNA genes for phylogenetic analysis have shown a quite similar vertical diversity of bacterial and archaeal sequences both in freshwater (Borrel et al., 2012; Rissanen et al., 2019) and marine sediments (Petro et al., 2017; Rasigraf et al., 2020). The microbial diversity is highest in surface sediments, while it decreases in deeper layers, with only a few key taxa abundant in all layers. Methanogenic Euryarchaeota often dominate the deepest sediments, which harbor a large fraction of unclassified or less known taxa, such as Bathyarchaeota (Evans et al., 2015; Rissanen et al., 2019). The physiology of these recently identified archaea is poorly understood, and without cultivated representatives, phylogenetic studies do not tell us about the active metabolic pathways in the deep methanogenic zones.

Sediment redox zones can change rapidly upon variations in bottom water salinity, temperature, oxygen and nutrient concentrations and/or the input and composition of organic matter. While microbial activity in sediments is sensitive to these changes, the response could be delayed because of a lack of sufficient biomass for a given reaction (Dale et al., 2008a). In addition, bacterial and archaeal species may react to changes differently, e.g., archaea may be less sensitive to salinity changes but may respond to increases in organic carbon (Swan et al., 2010). Therefore, to estimate the effect of anthropogenic eutrophication and climate change on coastal methane emissions, the factors driving changes in the microbial community need to be understood. Increased hypoxia in eutrophic areas may have long-term effects on the microbiome, promoting methane emissions (Egger et al., 2016b). However, Broman et al. (2017) showed that restoration efforts for re-oxygenation may reverse increased methane fluxes. Metatranscriptomic analysis found elevated levels of transcripts for methanotrophic genes already one month after the return of oxic conditions in Baltic Sea sediment incubations.

Natural coastal areas are also affected by human-induced modifications, and, in recent years, many areas such as salt marshes and wetlands are being restored to their previous state. A microbiome investigation of salt marshes, habitats rich in organic matter and potential greenhouse gas sources, saw vast differences between the sediment microbiomes in nearby locations before and after restoration (Morris et al., 2019). In Jamaica Bay (United States), native salt marshes harbored higher taxonomic diversity than restored marshes. The younger the restored marsh was, the more distinct the bacterial communities were when compared to the microbiome of the natural, degraded marsh. In addition to loss of diversity in restored coastal sediments, Thomas et al. (2019) observed a loss of the SRB community in newly amended marshes in the US East coast. As sulfate reduction is the main pathway for organic matter degradation in salt marshes and an inhibitor/competitor of methanogenesis (Giani et al., 1996), the change in the microbiome might alter the metabolic pathways possibly resulting in increased methanogenesis in anoxic sediments below the oxic sediment layer. As the microbial community is very sensitive to changes in sediment redox zones, oxygenation, and organic matter composition, it is important to understand the consequences of restoration effects of different coastal areas. Even though reoxygenation may mitigate methane emissions via aerobic methane oxidation, restoring other areas to their natural state may disturb a stable microbial community and the functioning metabolic pathways, which may have unforeseen effects on the biogeochemical cycling and greenhouse gas emissions.

ESTIMATING METHANE EMISSIONS FROM COASTAL SEDIMENTS

Eutrophication and climate change resulting from anthropogenic activity are strongly affecting coastal ecosystems, their biogeochemical functioning and microbiome. High rates of sedimentation combined with a high organic matter input, bottom water oxygen depletion and rising temperatures alter rates of organic matter burial and the electron acceptors available for its mineralization in coastal sediments. All of these processes affect methane production and oxidation. In order to mitigate emissions from coastal sediments, it is important to have a quantitative understanding of how methane-cycling processes respond to environmental change.

Whereas in offshore marine sediments methane emissions are regulated by a stable SMTZ (Weber et al., 2019), estimating methane sinks and sources across more complex coastal systems is challenging. Frequently, fluctuating hydrological conditions and seasonality affect sulfate concentrations, salinity, nutrient input and the type and abundance of organic matter, which all have an influence on methanogenic and –trophic processes.

Rapid sediment accumulation can be a cause for both increased methanogenesis and decreased AOM, as more labile organic carbon substances are buried below a shallow SMTZ with poorly constructed ANME consortia (Egger et al., 2016b). For instance, S-AOM can be replaced by Fe-AOM and/or N-AOM, which often occur in coastal sediments with low sulfate concentration (Egger et al., 2015b; Shen et al., 2016). ANME-2 archaea and NC10 bacteria responsible for N-AOM and Fe-AOM can also exist in the methanogenic zone and outcompete methanogens for their substrates, thereby mitigating the effects of increased methanogenesis. However, these methane oxidation pathways are regulated by the abundance of sulfate, methane, iron oxides and salinity, among many factors, and therefore the local conditions will determine their effectiveness.

Methanogens can use various substrates for methane production, thus the rate of methanogenesis can be difficult to estimate without knowing the sediment composition in the methanogenic layers (Reeburgh, 2007). Furthermore, in coastal sediments, methanogenic archaea and anaerobic methanotrophs can co-exist across the sediment profile. This leads to an overlap in redox zones, shoaling of the SMTZ and burial of more labile organic matter in the methanic zone (Rooze et al., 2016). In addition, the microbial community composition can play an important role, as ANME-1 may be capable of both methanogenesis and AOM, depending on the amount of hydrogen/methane being available (Kevorkian et al., 2020). All these interactions contribute to the methane cycle in sediments and make the potential processes difficult to predict.

Reactive transport models are useful in integrating geochemical data from field studies to quantify methane dynamics in sediments (e.g., Dale et al., 2008b; Regnier et al., 2011; Mogollón et al., 2012; Rooze et al., 2016). Reactive transport models can be used to reconstruct changes in sediment biogeochemistry and methane dynamics on time scales of decades (Rooze et al., 2016) to millennia (Mogollón et al., 2012; Egger et al., 2017). This can help to estimate how the effects of eutrophication will be propagated. Additionally, eutrophication can cause many local changes depending on hydrological conditions, oxygen concentration, water level and for example the location of sewage treatment plants close by Thang et al. (2013). These local differences can make the model predictions less reliable. Another factor making the model outcome less precise is seasonality. As shown in the Gulf of Mexico (Gelesh et al., 2016), methane emissions are affected by seasonal hypoxia, but many other factors such as sudden weather changes also affect the amount of methane released. Therefore, both spatial and temporal trends of methane emissions are difficult to capture by upscaling local data with reactive transport models. To allow the development of larger scale models, better recording of sediment profiles together with better understanding on the factors regulating the microbial methane production and oxidation in eutrophic conditions are needed.

Microorganisms play a critical role in controlling biogeochemical processes in sediments. At present, we cannot predict how these processes will respond to environmental change, because this may depend on the composition of the active microbial community. Gene-centric models, which are biogeochemical models that include an explicit representation of microbial processes, have the potential to greatly enhance our insights in coupled elemental cycling in sediments (Reed et al., 2014; Louca et al., 2016; Kreft et al., 2017). As the functional genes involved in methane production and oxidation are well known, meta-omics could be applied to target key genes and active metabolic processes. Combined with 16S rRNA gene analyses and geochemical profiles, these improved models could make better predictions of methane emissions from coastal sediments. To achieve this, a major focus of future research should be on understanding of the complex network of the microbial methane cycle and identifying the responsible microorganisms.

CONCLUSION

Methane cycling in coastal environments is a complex process with many factors regulating both methane production and oxidation. Anthropogenic eutrophication and climate change are greatly impacting coastal ecosystems and are likely enhancing methane emissions from these environments in the future. Rapid sedimentation rates, bottom water oxygen depletion and rising temperatures can all contribute to increased methane production in coastal sediments. Further increased organic matter inputs and lower salinity reduce the rates of S-AOM which decreases the methane-filtering potential of coastal sediments. Influx of nutrients, especially nitrate and metal oxides on the other hand can serve as electron acceptors for alternative AOM pathways Taken together the consequences of eutrophication and climate change most likely will increase overall methane emissions. Establishing better gene-centric models including the activity of the responsible microorganisms will be an important study area to better understand and predict the microbial methane cycle in coastal systems.

AUTHOR CONTRIBUTIONS

AW collected the data and literature, wrote the draft version, and composed the tables and figures. PDM, CS, and MJ critically reviewed and discussed the subsequent versions, and rewrote several sections. All authors contributed to the article and approved the submitted version.

FUNDING

This research was supported by OCW/NOW NESSC 024002001, OCW/NOW SIAM 024002002, and ERC SYNERGY MARIX 854088.

REFERENCES

Aromokeye, D. A., Kulkarni, A. C., Elvert, M., Wegener, G., Henkel, S., Coffinet, S., et al. (2020). Rates and microbial players of iron-driven anaerobic oxidation of methane in methanic marine sediments. *Front. Microbiol.* 10:3041. doi: 10.3389/fmicb.2019.03041

Arshad, A., Speth, D. R., De Graaf, R. M., Op den Camp, H. J. M., Jetten, M. S. M., and Welte, C. U. (2015). A metagenomics-based metabolic model of nitrate-dependent anaerobic oxidation of methane by Methanoperedens-like archaea. *Front. Microbiol.* 6:1423. doi: 10.3389/fmicb.2015.01423

Ash, J. L., Egger, M., Treude, T., Kohl, I., Cragg, B., Parkes, R. J., et al. (2019). Exchange catalysis during anaerobic methanotrophy revealed by 12CH2D2 and 13CH3D in methane. *Geochem. Perspect. Lett.* 10, 26–30. doi: 10.7185/geochemlet.1910

Bai, Y. N., Wang, X. N., Wu, J., Lu, Y. Z., Fu, L., Zhang, F., et al. (2019). Humic substances as electron acceptors for anaerobic oxidation of methane driven by ANME-2d. *Water Res.* 164:114935. doi: 10.1016/j.watres.2019.114935

Barnes, R. O., and Goldberg, E. D. (1976). Methane production and consumption in anoxic marine sediments. *Geology* 4, 297–300.

Bauer, J. E., Cai, W. J., Raymond, P. A., Bianchi, T. S., Hopkinson, C. S., and Regnier, P. A. G. (2013). The changing carbon cycle of the coastal ocean. *Nature* 504, 61–70. doi: 10.1038/nature12857

Beal, E. J., House, C. H., and Orphan, V. J. (2009). Manganese- and iron-dependent marine methane oxidation. *Science* 325, 184–187. doi: 10.1126/science.1169984

Berger, S., Cabrera-Orefice, A., Jetten, M. S. M., Brandt, U., and Welte, C. U. (2021). Investigation of central energy metabolism-related protein complexes of ANME-2d methanotrophic archaea by complexome profiling. *Biochim. Biophys. Acta Bioenerget.* 1862:148308. doi: 10.1016/j.bbabio.2020.148308

Berger, S., Frank, J., Martins, P. D., Jetten, M. S. M., and Welte, C. U. (2017). High-quality draft genome sequence of "*Candidatus methanoperedens* sp." strain BLZ2, a nitratereducing anaerobic methane-oxidizing archaeon enriched in an anoxic bioreactor. *Genome Announc.* 5:e01159-17. doi: 10.1128/genomeA.01159-17

Beulig, F., Røy, H., McGlynn, S. E., and Jørgensen, B. B. (2019). Cryptic CH4 cycling in the sulfate–methane transition of marine sediments apparently

mediated by ANME-1 archaea. *ISME J.* 13, 250–262. doi: 10.1038/s41396-018-0273-z

Bhattacharya, S., Mapder, T., Fernandes, S., Roy, C., Sarkar, J., Jameela Rameez, M., et al. (2020). Sedimentation rate and organic matter dynamics shape microbiomes across a continental margin. *bioRxiv* [Preprint]. doi: 10.1101/2020.10.03.324590

Bhattarai, S., Cassarini, C., Gonzalez-Gil, G., Egger, M., Slomp, C. P., Zhang, Y., et al. (2017). Anaerobic methane-oxidizing microbial community in a coastal marine sediment: anaerobic methanotrophy dominated by ANME-3. *Microb. Ecol.* 74, 608–622. doi: 10.1007/s00248-017-0978-y

Bhattarai, S., Zhang, Y., and Lens, P. N. L. (2018). Effect of pressure and temperature on anaerobic methanotrophic activities of a highly enriched ANME-2a community. *Environ. Sci. Pollut. Res.* 25, 30031–30043. doi: 10.1007/s11356-018-2573-2

Bižiæ, M., Klintzsch, T., Ionescu, D., Hindiyeh, M. Y., Günthel, M., Muro-Pastor, A. M., et al. (2020). Aquatic and terrestrial cyanobacteria produce methane. *Sci. Adv.* 6:eaax5343. doi: 10.1126/sciadv.aax5343

Blake, L. I., Sherry, A., Mejeha, O. K., Leary, P., Coombs, H., Stone, W., et al. (2020). An unexpectedly broad thermal and salinity-tolerant estuarine methanogen community. *Microorganisms* 8:1467. doi: 10.3390/microorganisms8101467

Boetius, A., Ravenschlag, K., Schubert, C. J., Rickert, D., Widdel, F., Gleseke, A., et al. (2000). A marine microbial consortium apparently mediating anaerobic oxidation methane. *Nature* 407, 623–626. doi: 10.1038/35036572

Bonaglia, S., Brüchert, V., Callac, N., Vicenzi, A., Chi Fru, E., and Nascimento, F. J. A. (2017). Methane fluxes from coastal sediments are enhanced by macrofauna. *Sci. Rep.* 7. doi: 10.1038/s41598-017-13263-w

Borges, A. V., and Abril, G. (2012). Carbon dioxide and methane dynamics in estuaries. *Treat. Estuarine Coast. Sci.* 4, 119–161. doi: 10.1016/B978-0-12-374711-2.00504-0

Borges, A. V., Royer, C., Martin, J. L., Champenois, W., and Gypens, N. (2019). Response of marine methane dissolved concentrations and emissions in the Southern North Sea to the European 2018 heatwave. *Continent.l Shelf Res.* 190:104004. doi: 10.1016/j.csr.2019.104004

Borrel, G., Lehours, A. C., Crouzet, O., Jézéquel, D., Rockne, K., Kulczak, A., et al. (2012). Stratification of Archaea in the deep sediments of a freshwater meromictic lake: vertical shift from methanogenic to uncultured Archaeal lineages. *PLoS One* 7:e0043346. doi: 10.1371/journal.pone.0043346

Breitburg, D., Levin, L. A., Oschlies, A., Grégoire, M., Chavez, F. P., Conley, D. J., et al. (2018). Declining oxygen in the global ocean and coastal waters. *Science* 359:eaam7240. doi: 10.1126/science.aam7240

Bridgham, S. D., Cadillo-Quiroz, H., Keller, J. K., and Zhuang, Q. (2013). Methane emissions from wetlands: biogeochemical, microbial, and modeling perspectives from local to global scales. *Glob. Change Biol.* 19, 1325–1346. doi: 10.1111/gcb.12131

Broman, E., Sjöstedt, J., Pinhassi, J., and Dopson, M. (2017). Shifts in coastal sediment oxygenation cause pronounced changes in microbial community composition and associated metabolism. *Microbiome* 5:96. doi: 10.1186/s40168-017-0311-5

Broman, E., Sun, X., Stranne, C., Salgado, M. G., Bonaglia, S., Geibel, M., et al. (2020). Low abundance of methanotrophs in sediments of shallow boreal coastal zones with high water methane concentrations. *Front. Microbiol.* 11:1536. doi: 10.3389/fmicb.2020.01536

Cai, C., Leu, A. O., Xie, G. J., Guo, J., Feng, Y., Zhao, J. X., et al. (2018). A methanotrophic archaeon couples anaerobic oxidation of methane to Fe(III) reduction. *ISME J.* 12, 1929–1939. doi: 10.1038/s41396-018-0109-x

Carstensen, J., Andersen, J. H., Gustafsson, B. G., and Conley, D. J. (2014). Deoxygenation of the baltic sea during the last century. *Proc. Natl. Acad. Sci. U. S. A.* 111, 5628–5633. doi: 10.1073/pnas.1323156111

Case, D. H., Ijiri, A., Morono, Y., Tavormina, P., Orphan, V. J., and Inagaki, F. (2017). Aerobic and anaerobic methanotrophic communities associated with methane hydrates exposed on the seafloor: a high-pressure sampling and stable isotope-incubation experiment. *Front. Microbiol.* 8:2569. doi: 10.3389/fmicb.2017.02569

Chen, X., Andersen, T. J., Morono, Y., Inagaki, F., Jørgensen, B. B., and Lever, M. A. (2017). Bioturbation as a key driver behind the dominance of Bacteria over Archaea in near-surface sediment. *Sci. Rep.* 7:2400. doi: 10.1038/s41598-017-02295-x

Ciais, P., Sabine, C., Bala, G., Bopp, L., Brovkin, V., Canadell, J., et al. (2013). "Carbon and other biogeochemical cycles," in *Proceedings pf the Contribution of Working Group I to the Fifth Assessment Report of the Inter- governmental Panel on Climate Change*, (Cambridge, MA: Cambridge Univ. Press), 465–570.

Conrad, R. (2009). The global methane cycle: recent advances in understanding the microbial processes involved. *Environ. Microbiol. Rep.* 1, 285–292. doi: 10.1111/j.1758-2229.2009.00038.x

Conrad, R. (2020). Importance of hydrogenotrophic, aceticlastic and methylotrophic methanogenesis for methane production in terrestrial, aquatic and other anoxic environments: a mini review. *Pedosphere* 30, 25–39. doi: 10.1016/S1002-0160(18)60052-9

Crill, P. M., and Martens, C. S. (1983). Spatial and temporal fluctuations of methane production in anoxic coastal marine sediments. *Limnol. Oceanogr.* 28, 1117–1130. doi: 10.4319/lo.1983.28.6.1117

Crill, P. M., and Martens, C. S. (1986). Methane production from bicarbonate and acetate in an anoxic marine sediment. *Geochim. Cosmochim. Acta* 50, 2089–2097. doi: 10.1016/0016-7037(86)90262-0

Dalcin Martins, P., De Jong, A., Lenstra, W. K., Van Helmond, N. A. G. M., Slomp, C. P., Jetten, M. S. M., et al. (2020). Enrichment of novel Verrucomicrobia, Bacteroidetes and Krumholzibacteria in an oxygen-limited, methane-and iron-fed bioreactor inoculated with Bothnian Sea sediments. *bioRxiv* [Preprint]. doi: 10.1101/2020.09.22.307553

Dale, A. W., Flury, S., Fossing, H., Regnier, P., Røy, H., Scholze, C., et al. (2019). Kinetics of organic carbon mineralization and methane formation in marine sediments (Aarhus Bay, Denmark). *Geochim. Cosmochim. Acta* 252, 159–178. doi: 10.1016/j.gca.2019.02.033

Dale, A. W., Regnier, P., Knab, N. J., Jørgensen, B. B., and Van Cappellen, P. (2008b). Anaerobic oxidation of methane (AOM) in marine sediments from the Skagerrak (Denmark): II. Reaction-transport modeling. *Geochim. Cosmochim. Acta* 72, 2880–2894. doi: 10.1016/j.gca.2007.11.039

Dale, A. W., Van Cappellen, P., Aguilera, D. R., and Regnier, P. (2008a). Methane efflux from marine sediments in passive and active margins: estimations from bioenergetic reaction–transport simulations. *Earth Planet. Sci. Lett.* 265, 329–344. doi: 10.1016/j.epsl.2007.09.026

Deng, L., Bölsterli, D., Kristensen, E., Meile, C., Su, C.-C., Bernasconi, S. M., et al. (2020). Macrofaunal control of microbial community structure in continental margin sediments. *Proc. Natl. Acad. Sci.* 117:201917494. doi: 10.1073/pnas.1917494117

Diaz, R. J., and Rosenberg, R. (2008). Spreading dead zones and consequences for marine ecosystems. *Science* 321, 926–929. doi: 10.1126/science.1156401

Dijkstra, N., Hagens, M., Egger, M., and Slomp, C. P. (2018). Post-depositional formation of vivianite-type minerals alters sediment phosphorus records. *Biogeosciences* 15, 861–883. doi: 10.5194/bg-15-861-2018

Dlugokencky, E. J. (2020). *ESRL Global Monitoring Division - Global Greenhouse Gas Reference Network*. Available online at: https://www.esrl.noaa.gov/gmd/ccgg/trends_ch4/ (accessed 20 January, 2020).

Dombrowski, N., Seitz, K. W., Teske, A. P., and Baker, B. J. (2017). Genomic insights into potential interdependencies in microbial hydrocarbon and nutrient cycling in hydrothermal sediments. *Microbiome* 5:106. doi: 10.1186/s40168-017-0322-2

Doney, S. C. (2010). The growing human footprint on coastal and open-ocean biogeochemistry. *Science* 328, 1512–1516. doi: 10.1126/science.1185198

Egger, M., Hagens, M., Sapart, C. J., Dijkstra, N., van Helmond, N. A. G. M., Mogollón, J. M., et al. (2017). Iron oxide reduction in methane-rich deep Baltic Sea sediments. *Geochim. Cosmochim. Acta* 207, 256–276. doi: 10.1016/j.gca.2017.03.019

Egger, M., Jilbert, T., Behrends, T., Rivard, C., and Slomp, C. P. (2015a). Vivianite is a major sink for phosphorus in methanogenic coastal surface sediments. *Geochim. Cosmochim. Acta* 169, 217–235. doi: 10.1016/j.gca.2015.09.012

Egger, M., Kraal, P., Jilbert, T., Sulu-Gambari, F., Sapart, C. J., Röckmann, T., et al. (2016a). Anaerobic oxidation of methane alters sediment records of sulfur, iron and phosphorus in the Black Sea. *Biogeosciences* 13, 5333–5355. doi: 10.5194/bg-13-5333-2016

Egger, M., Lenstra, W., Jong, D., Meysman, F. J. R. R., Sapart, C. J., Van Der Veen, C., et al. (2016b). Rapid sediment accumulation results in high methane effluxes from coastal sediments. *PLoS One* 11:e0161609. doi: 10.1371/journal.pone.0161609

Egger, M., Rasigraf, O., Sapart, C. J., Jilbert, T., Jetten, M. S. M., Röckmann, T., et al. (2015b). Iron-mediated anaerobic oxidation of methane in brackish coastal sediments. *Environ. Sci. Technol.* 49, 277–283. doi: 10.1021/es503663z

Egger, M., Riedinger, N., Mogollón, J. M., and Jørgensen, B. B. (2018). Global diffusive fluxes of methane in marine sediments. *Nat. Geoscience* 11, 421–425. doi: 10.1038/s41561-018-0122-8

Elul, M., Rubin-Blum, M., Ronen, Z., Bar-Or, I., Eckert, W., and Sivan, O. (2020). Metagenomic insights into the metabolism of microbial communities that mediate iron and methane cycling in Lake Kinneret sediments. *Biogeosci. Discuss.* [Epub ahead of print]. doi: 10.5194/bg-2020-329

Ettwig, K. F., Butler, M. K., Le Paslier, D., Pelletier, E., Mangenot, S., Kuypers, M. M. M., et al. (2010). Nitrite-driven anaerobic methane oxidation by oxygenic bacteria. *Nature* 464, 543–548. doi: 10.1038/nature08883

Ettwig, K. F., Zhu, B., Speth, D., Keltjens, J. T., Jetten, M. S. M., and Kartal, B. (2016). Archaea catalyze iron-dependent anaerobic oxidation of methane. *Proc. Natl. Acad. Sci. U.S.A.* 113, 12792–12796. doi: 10.1073/pnas.1609534113

Evans, P. N., Boyd, J. A., Leu, A. O., Woodcroft, B. J., Parks, D. H., Hugenholtz, P., et al. (2019). An evolving view of methane metabolism in the Archaea. *Nat. Rev. Microbiol.* 17, 219–232. doi: 10.1038/s41579-018-0136-7

Evans, P. N., Parks, D. H., Chadwick, G. L., Robbins, S. J., Orphan, V. J., Golding, S. D., et al. (2015). Methane metabolism in the archaeal phylum Bathyarchaeota revealed by genome-centric metagenomics. *Science* 350, 434–438. doi: 10.1126/science.aac7745

Ferry, J. G. (1992). Biochemistry of methanogenesis. *Crit. Rev. Biochem. Mol. Biol.* 27:992. doi: 10.3109/10409239209082570

Foster, S. Q., and Fulweiler, R. W. (2019). Estuarine sediments exhibit dynamic and variable biogeochemical responses to hypoxia. *J. Geophys. Res. Biogeosci.* 124, 737–758. doi: 10.1029/2018JG004663

Froelich, P. N., Klinkhammer, G. P., Bender, M. L., Luedtke, N. A., Heath, G. R., Cullen, D., et al. (1979). Early oxidation of organic matter in pelagic sediments of the eastern equatorial Atlantic: suboxic diagenesis. *Geochim. Cosmochim. Acta* 43, 1075–1090. doi: 10.1016/0016-7037(79)90095-4

Gambelli, L., Guerrero-Cruz, S., Mesman, R. J., Cremers, G., Jetten, M. S. M., Op den Camp, H. J. M., et al. (2018). Community composition and ultrastructure of a nitrate-dependent anaerobic methaneoxidizing enrichment culture. *Appl. Environ. Microbiol.* 84:e02186-17. doi: 10.1128/AEM.02186-17

Garber, A. I., Nealson, K. H., Okamoto, A., McAllister, S. M., Chan, C. S., Barco, R. A., et al. (2020). FeGenie: a comprehensive tool for the identification of iron genes and iron gene neighborhoods in genome and metagenome assemblies. *Front. Microbiol.* 11:37. doi: 10.3389/fmicb.2020.00037

Gelesh, L., Marshall, K., Boicourt, W., and Lapham, L. (2016). Methane concentrations increase in bottom waters during summertime anoxia in the highly eutrophic estuary, Chesapeake Bay, U.S.A. *Limnol. Oceanogr.* 61, S253–S266. doi: 10.1002/lno.10272

Giani, L., Dittrich, K., Martsfeld-Hartmann, A., and Peters, G. (1996). Methanogenesis in saltmarsh soils of the North Sea coast of Germany. *Eur. J. Soil Sci.* 47, 175–182. doi: 10.1111/j.1365-2389.1996.tb01388.x

Grossart, H. P., Massana, R., McMahon, K. D., and Walsh, D. A. (2020). Linking metagenomics to aquatic microbial ecology and biogeochemical cycles. *Limnol. Oceanogr.* 2, S2–S20. doi: 10.1002/lno.11382

Guerrero-Cruz, S., Cremers, G., van Alen, T. A., Op den Camp, H. J. M., Jetten, M. S. M., Rasigraf, O., et al. (2018). Response of the anaerobic methanotroph "*Candidatus Methanoperedens nitroreducens*" to oxygen stress. *Appl. Environ. Microbiol.* 84:e01832-18. doi: 10.1128/AEM.01832-18

Hamdan, L. J., and Wickland, K. P. (2016). Methane emissions from oceans, coasts, and freshwater habitats: new perspectives and feedbacks on climate. *Limnol. Oceanogr.* 61, S3–S12. doi: 10.1002/lno.10449

Hanson, R. S., and Hanson, T. E. (1996). Methanotrophic bacteria. *Microbiol. Rev.* 60, 439–471. doi: 10.1128/mmbr.60.2.439-471.1996

Haroon, M. F., Hu, S., Shi, Y., Imelfort, M., Keller, J., Hugenholtz, P., et al. (2013). Anaerobic oxidation of methane coupled to nitrate reduction in a novel archaeal lineage. *Nature* 500, 567–570. doi: 10.1038/nature12375

Hartnett, H. E., Keil, R. G., Hedges, J. I., and Devol, A. H. (1998). Influence of oxygen exposure time on organic carbon preservation in continental margin sediments. *Nature* 391, 572–574. doi: 10.1038/35351

He, Z., Cai, C., Wang, J., Xu, X., Zheng, P., Jetten, M. S. M., et al. (2016). A novel denitrifying methanotroph of the NC10 phylum and its microcolony. *Sci. Rep.* 6:32241. doi: 10.1038/srep32241

He, Z., Wang, J., Hu, J., Yu, H., Jetten, M. S. M., Liu, H., et al. (2019). Regulation of coastal methane sinks by a structured gradient of microbial methane oxidizers. *Environ. Pollut.* 244, 228–237. doi: 10.1016/j.envpol.2018.10.057

Hirayama, H., Abe, M., Miyazaki, M., Nunoura, T., Furushima, Y., Yamamoto, H., et al. (2014). *Methylomarinovum caldicuralii* gen. nov., sp. nov., a moderately thermophilic methanotroph isolated from a shallow submarine hydrothermal system, and proposal of the family Methylothermaceae fam. nov. *Int. J. Syst. Evol. Microbiol.* 64(Pt_3), 989–999. doi: 10.1099/ijs.0.058172-0

Humborg, C., Geibel, M. C., Sun, X., McCrackin, M., Mörth, C.-M., Stranne, C., et al. (2019). High emissions of carbon dioxide and methane from the coastal baltic sea at the end of a summer heat wave. *Front. Mar. Sci.* 6:493. doi: 10.3389/fmars.2019.00493

In' t Zandt, M. H., de Jong, A. E., Slomp, C. P., and Jetten, M. S. (2018). The hunt for the most-wanted chemolithoautotrophic spookmicrobes. *FEMS Microbiol. Ecol.* 94:fiy064. doi: 10.1093/femsec/fiy064

IPCC (2014). *Climate Change 2014: Synthesis Report. Contribution of Working Groups I, II and III to the Fifth Assessment Report of the Intergovernmental Panel on Climate Change, Kristin Seyboth (USA)*. Geneva: IPCC.

Jickells, T. D. (1998). Nutrient biogeochemistry of the coastal zone. *Science* 217–222. doi: 10.1126/science.281.5374.217

Jørgensen, B. B., Findlay, A. J., and Pellerin, A. (2019). The biogeochemical sulfur cycle of marine sediments. *Front. Microbiol.* 10:849. doi: 10.3389/fmicb.2019.00849

Kallistova, A., Merkel, A., Kanapatskiy, T., Boltyanskaya, Y., Tarnovetskii, I., Perevalova, A., et al. (2020). Methanogenesis in the Lake Elton saline aquatic system. *Extremophiles* 24, 657–672. doi: 10.1007/s00792-020-01185-x

Kato, S., and Igarashi, K. (2019). Enhancement of methanogenesis by electric syntrophy with biogenic iron-sulfide minerals. *MicrobiologyOpen* 8:e00647. doi: 10.1002/mbo3.647

Kerimoglu, O., Voynova, Y. G., Chegini, F., Brix, H., Callies, U., Hofmeister, R., et al. (2020). Interactive impacts of meteorological and hydrological conditions on the physical and biogeochemical structure of a coastal system. *Biogeosciences* 17, 5097–5127. doi: 10.5194/bg-17-5097-2020

Kevorkian, R., Callahan, S., Winstead, R., and Lloyd, K. G. (2020). ANME-1 archaea drive methane accumulation and removal in estuarine sediments. *bioRxiv* [Preprint]. doi: 10.1101/2020.02.24.963215

Kirschke, S., Bousquet, P., Ciais, P., Saunois, M., Canadell, J. G., Dlugokencky, E. J., et al. (2013). Three decades of global methane sources and sinks. *Nat. Geosci.* 6, 813–823. doi: 10.1038/ngeo1955

Kits, K. D., Klotz, M. G., and Stein, L. Y. (2015). Methane oxidation coupled to nitrate reduction under hypoxia by the Gammaproteobacterium *Methylomonas denitrificans*, sp. nov. type strain FJG1. *Environ. Microbiol.* 17, 3219–3232. doi: 10.1111/1462-2920.12772

Klintzsch, T., Langer, G., Nehrke, G., Wieland, A., Lenhart, K., and Keppler, F. (2019). Methane production by three widespread marine phytoplankton species: release rates, precursor compounds, and potential relevance for the environment. *Biogeosciences* 16, 4129–4144. doi: 10.5194/bg-16-4129-2019

Knittel, K., and Boetius, A. (2009). Anaerobic oxidation of methane: progress with an unknown process. *Annu. Rev. Microbiol.* 63, 311–334. doi: 10.1146/annurev.micro.61.080706.093130

Knittel, K., Wegener, G., and Boetius, A. (2018). "Anaerobic methane oxidizers," in *Microbial Communities Utilizing Hydrocarbons and Lipids: Members, Metagenomics and Ecophysiology*, ed. T. J. McGenity (Cham: Springer), 1–21.

Kogure, K., and Wada, M. (2005). Impacts of macrobenthic bioturbation in marine sediment on bacterial metabolic activity. *Microbes Environ.* 20, 191–199. doi: 10.1264/jsme2.20.191

Kraft, B., Tegetmeyer, H. E., Sharma, R., Klotz, M. G., Ferdelman, T. G., Hettich, R. L., et al. (2014). The environmental controls that govern the end product of bacterial nitrate respiration. *Science* 345, 676–679. doi: 10.1126/science.1254070

Kreft, J. U., Plugge, C. M., Prats, C., Leveau, J. H. J., Zhang, W., and Hellweger, F. L. (2017). From genes to ecosystems in microbiology: modeling approaches and the importance of individuality. *Front. Microbiol.* 8:2299. doi: 10.3389/fmicb.2017.02299

Kristjansson, J. K., Schönheit, P., and Thauer, R. K. (1982). Different Ks values for hydrogen of methanogenic bacteria and sulfate reducing bacteria: an explanation for the apparent inhibition of methanogenesis by sulfate. *Arch. Microbiol.* 131, 278–282. doi: 10.1007/BF00405893

LaRowe, D. E. E., Arndt, S., Bradley, J. A. A., Estes, E. R. R., Hoarfrost, A., Lang, S. Q. Q., et al. (2020). The fate of organic carbon in marine sediments - New insights from recent data and analysis. *Earth Sci. Rev.* 204:103146. doi: 10.1016/j.earscirev.2020.103146

Lee, J. W., Kwon, K. K., Bahk, J. J., Lee, D. H., Lee, H. S., Kang, S. G., et al. (2016). Metagenomic analysis reveals the contribution of anaerobic methanotroph-1b in the oxidation of methane at the Ulleung Basin, East Sea of Korea. *J. Microbiol.* 54, 814–822. doi: 10.1007/s12275-016-6379-y

Lenstra, W. K., Egger, M., van Helmond, N. A. G. M., Kritzberg, E., Conley, D. J., and Slomp, C. P. (2018). Large variations in iron input to an oligotrophic Baltic Sea estuary: impact on sedimentary phosphorus burial. *Biogeosciences* 15, 6979–6996. doi: 10.5194/bg-15-6979-2018

Leu, A. O., Cai, C., McIlroy, S. J., Southam, G., Orphan, V. J., Yuan, Z., et al. (2020). Anaerobic methane oxidation coupled to manganese reduction by members of the Methanoperedenaceae. *ISME J.* 14, 1030–1041. doi: 10.1038/s41396-020-0590-x

Li, H., Yang, Q., and Zhou, H. (2020). Niche differentiation of sulfate- and iron-dependent anaerobic methane oxidation and methylotrophic methanogenesis in deep sea methane seeps. *Front. Microbiol.* 11:1409. doi: 10.3389/fmicb.2020.01409

Li, J., Li, L., Bai, S., Ta, K., Xu, H., Chen, S., et al. (2019). New insight into the biogeochemical cycling of methane, S and Fe above the Sulfate-Methane Transition Zone in methane hydrate-bearing sediments: a case study in the Dongsha area, South China Sea. *Deep Sea Res. Part I Oceanogr. Res. Pap.* 145, 97–108. doi: 10.1016/j.dsr.2019.01.011

Lloyd, K. G., Alperin, M. J., and Teske, A. (2011). Environmental evidence for net methane production and oxidation in putative ANaerobic MEthanotrophic (ANME) archaea. *Environ. Microbiol.* 13, 2548–2564. doi: 10.1111/j.1462-2920.2011.02526.x

Louca, S., Hawley, A. K., Katsev, S., Torres-Beltran, M., Bhatia, M. P., Kheirandish, S., et al. (2016). Integrating biogeochemistry with multiomic sequence information in a model oxygen minimum zone. *Proc. Natl. Acad. Sci. U.S.A.* 113, E5925–E5933. doi: 10.1073/pnas.1602897113

Luesken, F. A., Van Alen, T. A., Van Der Biezen, E., Frijters, C., Toonen, G., Kampman, C., et al. (2011). Diversity and enrichment of nitrite-dependent anaerobic methane oxidizing bacteria from wastewater sludge. *Appl. Microbiol. Biotechnol.* 92, 845–854. doi: 10.1007/s00253-011-3361-9

Luesken, F. A., Wu, M. L., Op den Camp, H. J. M., Keltjens, J. T., Stunnenberg, H., Francoijs, K.-J., et al. (2012). Effect of oxygen on the anaerobic methanotroph "Candidatus Methylomirabilis oxyfera": kinetic and transcriptional analysis. *Environ. Microbiol.* 14, 1024–1034. doi: 10.1111/j.1462-2920.2011.02682.x

Lüke, C., and Frenzel, P. (2011). Potential of pmoA amplicon pyrosequencing for methanotroph diversity studies. *Appl. Environ. Microbiol.* 77, 6305–6309. doi: 10.1128/AEM.05355-11

Maltby, J., Sommer, S., Dale, A. W., and Treude, T. (2016). Microbial methanogenesis in the sulfate-reducing zone of surface sediments traversing the *Peruvian margin*. *Biogeosciences* 13, 283–299. doi: 10.5194/bg-13-283-2016

Martinez-Cruz, K., Leewis, M. C., Herriott, I. C., Sepulveda-Jauregui, A., Anthony, K. W., Thalasso, F., et al. (2017). Anaerobic oxidation of methane by aerobic methanotrophs in sub-Arctic lake sediments. *Sci. Total Environ.* 607–608, 23–31. doi: 10.1016/j.scitotenv.2017.06.187

Metcalf, W. W., Griffin, B. M., Cicchillo, R. M., Gao, J., Janga, S. C., Cooke, H. A., et al. (2012). Synthesis of methylphosphonic acid by marine microbes: a source for methane in the aerobic ocean. *Science* 337, 1104–1107. doi: 10.1126/science.1219875

Meulepas, R. J. W., Jagersma, C. G., Khadem, A. F., Stams, A. J. M., and Lens, P. N. L. (2010). Effect of methanogenic substrates on anaerobic oxidation of methane and sulfate reduction by an anaerobic methanotrophic enrichment. *Appl. Microbiol. Biotechnol.* 87, 1499–1506. doi: 10.1007/s00253-010-2597-0

Middelburg, J. J., and Levin, L. A. (2009). Coastal hypoxia and sediment biogeochemistry. *Biogeosciences* 6, 1273–1293. doi: 10.5194/bg-6-1273-2009

Mitterer, R. M. (2010). Methanogenesis and sulfate reduction in marine sediments: a new model. *Earth Planet. Sci. Lett.* 295, 358–366. doi: 10.1016/j.epsl.2010.04.009

Mogollón, J. M., Dale, A. W., Fossing, H., and Regnier, P. (2012). Timescales for the development of methanogenesis and free gas layers in recently-deposited sediments of Arkona Basin (Baltic Sea). *Biogeosciences* 9, 1915–1933. doi: 10.5194/bg-9-1915-2012

Morris, N., Alldred, M., Zarnoch, C., and Alter, E. (2019). Composition of estuarine sediment microbiome from a chronosequence of restored urban salt marshes. *bioRxiv* [Pre-print]. doi: 10.1101/641274

Myllykangas, J. P., Hietanen, S., and Jilbert, T. (2020a). Legacy effects of eutrophication on modern methane dynamics in a boreal estuary. *Estuaries Coasts* 43, 189–206. doi: 10.1007/s12237-019-00677-0

Myllykangas, J. P., Rissanen, A. J., Hietanen, S., and Jilbert, T. (2020b). Influence of electron acceptor availability and microbial community structure on sedimentary methane oxidation in a boreal estuary. *Biogeochemistry* 148, 291–309. doi: 10.1007/s10533-020-00660-z

Narrowe, A. B., Borton, M. A., Hoyt, D. W., Smith, G. J., Daly, R. A., Angle, J. C., et al. (2019). Uncovering the diversity and activity of methylotrophic methanogens in freshwater wetland soils. *mSystems* 4:e00320-19. doi: 10.1128/mSystems.00320-19

Nauhaus, K., Treude, T., Boetius, A., and Kruger, M. (2005). Environmental regulation of the anaerobic oxidation of methane: a comparison of ANME-I and ANME-II communities. *Environ. Microbiol.* 7, 98–106. doi: 10.1111/j.1462-2920.2004.00669.x

Nie, W.-B., Ding, J., Xie, G.-J., Yang, L., Peng, L., Tan, X., et al. (2020). Anaerobic oxidation of methane coupled with dissimilatory nitrate reduction to ammonium fuels anaerobic ammonium oxidation. *Environ. Sci. Technol.* [Epub ahead of print]. doi: 10.1021/acs.est.0c02664

Op den Camp, H. J. M., Islam, T., Stott, M. B., Harhangi, H. R., Hynes, A., Schouten, S., et al. (2009). Environmental, genomic and taxonomic perspectives on methanotrophic Verrucomicrobia. *Environ. Microbiol. Rep.* 1, 293–306. doi: 10.1111/j.1758-2229.2009.00022.x

Orphan, V. J., Hinrichs, K. U., Ussler, W., Paull, C. K., Taylor, L. T., Sylva, S. P., et al. (2001). Comparative analysis of methane-oxidizing archaea and sulfate-reducing bacteria in anoxic marine sediments. *Appl. Environ. Microbiol.* 67, 1922–1934. doi: 10.1128/AEM.67.4.1922-1934.2001

Orphan, V. J., House, C. H., Hinrichs, K. U., McKeegan, K. D., and DeLong, E. F.(2002). Multiple archaeal groups mediate methane oxidation in anoxic cold seep sediments. *Proc. Natl. Acad. Sci. U. S. A.* 99, 7663–7668. doi: 10.1073/pnas.072210299

Padilla, C. C., Bertagnolli, A. D., Bristow, L. A., Sarode, N., Glass, J. B., Thamdrup, B., et al. (2017). Metagenomic binning recovers a transcriptionally active gammaproteobacterium linking methanotrophy to partial denitrification in an anoxic oxygen minimum zone. *Front. Mar. Sci.* 4:23. doi: 10.3389/fmars.2017.00023

Padilla, C. C., Bristow, L. A., Sarode, N., Garcia-Robledo, E., Gómez Ramírez, E., Benson, C. R., et al. (2016). NC10 bacteria in marine oxygen minimum zones. *ISME J.* 10, 2067–2071. doi: 10.1038/ismej.2015.262

Parks, D. H., Chuvochina, M., and Chaumeil, P. A. (2020). A complete domain-to-species taxonomy for Bacteria and Archaea. *Nat. Biotechnol.* 38, 1079–1086.

Petersen, J. M., and Dubilier, N. (2009). Methanotrophic symbioses in marine invertebrates. *Environ. Microbiol. Rep.* 1, 319–335. doi: 10.1111/j.1758-2229.2009.00081.x

Petro, C., Starnawski, P., Schramm, A., and Kjeldsen, K. U. (2017). Microbial community assembly in marine sediments. *Aquat. Microb. Ecol. Inter Res.* 79, 177–195. doi: 10.3354/ame01826

Raghoebarsing, A. A., Pol, A., Van De Pas-Schoonen, K. T., Smolders, A. J. P., Ettwig, K. F., Rijpstra, W. I. C., et al. (2006). A microbial consortium couples anaerobic methane oxidation to denitrification. *Nature* 440, 918–921. doi: 10.1038/nature04617

Rasigraf, O., Schmitt, J., Jetten, M. S. M., and Lüke, C. (2017). Metagenomic potential for and diversity of N-cycle driving microorganisms in the Bothnian Sea sediment. *MicrobiologyOpen* 6:e00475. doi: 10.1002/mbo3.475

Rasigraf, O., van Helmond, N. A. G. M., Frank, J., Lenstra, W. K., Egger, M., Slomp, C. P., et al. (2020). Microbial community composition and functional potential in Bothnian Sea sediments is linked to Fe and S dynamics and the quality of organic matter. *Limnol. Oceanogr.* 65, S113–S133. doi: 10.1002/lno.11371

Reeburgh, W. S. (2007). Oceanic methane biogeochemistry. *Chem. Rev.* 107, 486–513. doi: 10.1021/cr050362v

Reed, D. C., Algar, C. K., Huber, J. A., and Dick, G. J. (2014). Gene-centric approach to integrating environmental genomics and biogeochemical models. *Proc. Natl. Acad. Sci. U.S.A.* 111, 1879–1884. doi: 10.1073/pnas.1313713111

Reed, D. C., Gustafsson, B. G., and Slomp, C. P. (2016). Shelf-to-basin iron shuttling enhances vivianite formation in deep Baltic Sea sediments. *Earth Planet. Sci. Lett.* 434, 241–251. doi: 10.1016/j.epsl.2015.11.033

Regnier, P., Dale, A. W., Arndt, S., LaRowe, D. E., Mogollón, J., and Van Cappellen, P. (2011). Quantitative analysis of anaerobic oxidation of methane (AOM) in marine sediments: a modeling perspective. *Earth Sci. Rev.* 106, 105–130. doi: 10.1016/j.earscirev.2011.01.002

Reyes, C., Dellwig, O., Dähnke, K., Gehre, M., Noriega-Ortega, B. E., Böttcher, M. E., et al. (2016). Bacterial communities potentially involved in iron-cycling in Baltic Sea and North Sea sediments revealed by pyrosequencing. *FEMS Microbiol. Ecol.* 92:fiw054. doi: 10.1093/femsec/fiw054

Reyes, C., Schneider, D., Lipka, M., Thürmer, A., Böttcher, M. E., and Friedrich, M. W. (2017). Nitrogen metabolism genes from temperate marine sediments. *Mar. Biotechnol.* 19, 175–190. doi: 10.1007/s10126-017-9741-0

Rissanen, A. J., Peura, S., Mpamah, P. A., Taipale, S., Tiirola, M., Biasi, C., et al. (2019). Vertical stratification of bacteria and archaea in sediments of a small boreal humic lake. *FEMS Microbiol. Lett.* 366:fnz044. doi: 10.1093/femsle/fnz044

Rooze, J., Egger, M., Tsandev, I., and Slomp, C. P. (2016). Iron-dependent anaerobic oxidation of methane in coastal surface sediments: potential controls and impact. *Limnol. Oceanogr.* 61, S267–S282. doi: 10.1002/lno.10275

Saito, M. A., Bertrand, E. M., Duffy, M. E., Gaylord, D. A., Held, N. A., Hervey, W. J., et al. (2019). Progress and challenges in ocean metaproteomics and proposed best practices for data sharing. *J. Proteome Res.* 18, 1461–1476. doi: 10.1021/acs.jproteome.8b00761

Schade, J. D., Bailio, J., and McDowell, W. H. (2016). Greenhouse gas flux from headwater streams in New Hampshire, USA: patterns and drivers. *Limnol. Oceanogr.* 61, S165–S174. doi: 10.1002/lno.10337

Scheller, S., Yu, H., Chadwick, G. L., McGlynn, S. E., and Orphan, V. J. (2016). Artificial electron acceptors decouple archaeal methane oxidation from sulfate reduction. *Science* 351, 703–707. doi: 10.1126/science.aad7154

Schönheit, P., Kristjansson, J. K., and Thauer, R. K. (1982). Kinetic mechanism for the ability of sulfate reducers to out-compete methanogens for acetate. *Arch. Microbiol.* 132, 285–288. doi: 10.1007/BF00407967

Schulz, S., Matsuyama, H., and Conrad, R. (2006). Temperature dependence of methane production from different precursors in a profundal sediment (Lake Constance). *FEMS Microbiol. Ecol.* 22, 207–213. doi: 10.1111/j.1574-6941.1997.tb00372.x

Segarra, K. E. A., Comerford, C., Slaughter, J., and Joye, S. B. (2013). Impact of electron acceptor availability on the anaerobic oxidation of methane in coastal freshwater and brackish wetland sediments. *Geochim. Cosmochim. Acta* 115, 15–30. doi: 10.1016/j.gca.2013.03.029

Sela-Adler, M., Ronen, Z., Herut, B., Antler, G., Vigderovich, H., Eckert, W., et al. (2017). Co-existence of methanogenesis and sulfate reduction with common substrates in sulfate-rich estuarine sediments. *Front. Microbiol.* 8:766. doi: 10.3389/fmicb.2017.00766

Shen, L., Hu, B., Liu, S., Chai, X., He, Z., Ren, H., et al. (2016). Anaerobic methane oxidation coupled to nitrite reduction can be a potential methane sink in coastal environments. *Appl. Microbiol. Biotechnol.* 100, 7171–7180. doi: 10.1007/s00253-016-7627-0

Shen, L., Wu, H., and Gao, Z. (2015). Distribution and environmental significance of nitrite-dependent anaerobic methane-oxidising bacteria in natural ecosystems. *Appl. Microbiol. Biotechnol.* 99, 133–142. doi: 10.1007/s00253-014-6200-y

Sieczko, A. K., Demeter, K., Singer, G. A., Tritthart, M., Preiner, S., Mayr, M., et al. (2016). Aquatic methane dynamics in a human-impacted river-floodplain of the Danube. *Limnol. Oceanogr.* 61, S175–S187. doi: 10.1002/lno.10346

Sivan, O., Adler, M., Pearson, A., Gelman, F., Bar-Or, I., John, S. G., et al. (2011). Geochemical evidence for iron-mediated anaerobic oxidation of methane. *Limnol. Oceanogr.* 56, 1536–1544. doi: 10.4319/lo.2011.56.4.1536

Sivan, O., Shusta, S. S., and Valentine, D. L. (2016). Methanogens rapidly transition from methane production to iron reduction. *Geobiology* 14, 190–203. doi: 10.1111/gbi.12172

Steinle, L., Maltby, J., Treude, T., Kock, A., Bange, H. W., Engbersen, N., et al. (2017). Effects of low oxygen concentrations on aerobic methane oxidation in seasonally hypoxic coastal waters. *Biogeosciences* 14, 1631–1645. doi: 10.5194/bg-14-1631-2017

Stokke, R., Roalkvam, I., Lanzen, A., Haflidason, H., and Steen, I. H. (2012). Integrated metagenomic and metaproteomic analyses of an ANME-1-dominated community in marine cold seep sediments. *Environ. Microbiol.* 14, 1333–1346. doi: 10.1111/j.1462-2920.2012.02716.x

Sturm, A., Fowle, D. A., Jones, C., Leslie, K., Nomosatryo, S., Henny, C., et al. (2019). Rates and pathways of CH4 oxidation in ferruginous Lake Matano, Indonesia. *Geobiology* 17, 294–307. doi: 10.1111/gbi.12325

Su, G., Zopfi, J., Yao, H., Steinle, L., Niemann, H., and Lehmann, M. F. (2020). Manganese/iron-supported sulfate-dependent anaerobic oxidation of methane by archaea in lake sediments. *Limnol. Oceanogr.* 65, 863–875. doi: 10.1002/lno.11354

Sundby, B. (2006). Transient state diagenesis in continental margin muds. *Mar. Chem.* 102, 2–12. doi: 10.1016/j.marchem.2005.09.016

Swan, B. K., Ehrhardt, C. J., Reifel, K. M., Moreno, L. I., and Valentine, D. L. (2010). Archaeal and bacterial communities respond differently to environmental gradients in anoxic sediments of a california hypersaline lake, the Salton Sea. *Appl. Environ. Microbiol.* 76, 757–768. doi: 10.1128/AEM.02409-09

Tavormina, P. L., Ussler, W., and Orphan, V. J. (2008). Planktonic and sediment-associated aerobic methanotrophs in two seep systems along the North American margin. *Appl. Environ. Microbiol.* 74, 3985–3995. doi: 10.1128/AEM.00069-08

Thamdrup, B., Steinsdóttir, H. G. R., Bertagnolli, A. D., Padilla, C. C., Patin, N. V., Garcia-Robledo, E., et al. (2019). Anaerobic methane oxidation is an important sink for methane in the oceans largest oxygen minimum zone. *Limnol. Oceanogr.* 64, 2569–2585. doi: 10.1002/lno.11235

Thang, N. M., Brüchert, V., Formolo, M., Wegener, G., Ginters, L., Jørgensen, B. B., et al. (2013). The impact of sediment and carbon fluxes on the biogeochemistry of methane and sulfur in littoral baltic sea sediments (Himmerfjärden, Sweden). *Estuaries Coasts* 36, 98–115. doi: 10.1007/s12237-012-9557-0

Thomas, F., Morris, J. T., Wigand, C., and Sievert, S. M. (2019). Short-term effect of simulated salt marsh restoration by sand-amendment on sediment bacterial communities. *PLoS One* 14:e0215767. doi: 10.1371/journal.pone.0215767

Timmers, P. H. A., Gieteling, J., Widjaja-Greefkes, H. C. A., Plugge, C. M., Stams, A. J. M., Lens, P. N. L., et al. (2015). Growth of anaerobic methane-oxidizing archaea and sulfate-reducing bacteria in a high-pressure membrane capsule bioreactor. *Appl. Environ. Microbiol.* 81, 1286–1296. doi: 10.1128/AEM.03255-14

Tu, T.-H., Wu, L.-W., Lin, Y.-S., Imachi, H., Lin, L.-H., and Wang, P.-L. (2017). Microbial community composition and functional capacity in a terrestrial ferruginous, sulfate-depleted mud volcano. *Front. Microbiol.* 8:2137. doi: 10.3389/fmicb.2017.02137

Vaksmaa, A., Guerrero-Cruz, S., van Alen, T. A., Cremers, G., Ettwig, K. F., Lüke, C., et al. (2017). Enrichment of anaerobic nitrate-dependent methanotrophic "Candidatus *Methanoperedens nitroreducens*" archaea from an Italian paddy field soil. *Appl. Microbiol. Biotechnol.* 101, 7075–7084. doi: 10.1007/s00253-017-8416-0

Valenzuela, E. I., Prieto-Davó, A., López-Lozano, N. E., Hernández-Eligio, A., Vega-Alvarado, L., Juárez, K., et al. (2017). Anaerobic methane oxidation driven by microbial reduction of natural organic matter in a tropical wetland. *Appl. Environ. Microbiol.* 83:e00645-17. doi: 10.1128/AEM.00645-17

van Grinsven, S., Sinninghe Damsté, J. S., and Villanueva, L. (2020). Assessing the effect of humic substances and Fe(III) as potential electron acceptors for anaerobic methane oxidation in a marine anoxic system. *Microorganisms* 8:1288. doi: 10.3390/microorganisms8091288

Vekeman, B., Kerckhof, F.-M., Cremers, G., de Vos, P., Vandamme, P., Boon, N., et al. (2016a). New Methyloceanibacter diversity from North Sea sediments includes methanotroph containing solely the soluble methane monooxygenase. *Environ. Microbiol.* 18, 4523–4536. doi: 10.1111/1462-2920.13485

Vekeman, B., Speth, D., Wille, J., Cremers, G., De Vos, P., Op den Camp, H. J. M., et al. (2016b). Genome characteristics of two novel type I methanotrophs

enriched from north sea sediments containing exclusively a lanthanide-dependent XoxF5-type methanol dehydrogenase. *Microb. Ecol.* 72, 503–509. doi: 10.1007/s00248-016-0808-7

Versantvoort, W., Guerrero-Castillo, S., Wessels, J. C. T., van Niftrik, L. A. M. P., Jetten, M. S. M., Brandt, U., et al. (2019). Complexome analysis of the nitrite-dependent methanotroph *Methylomirabilis lanthanidiphila*. *Biochim. Biophys. Acta Bioenerget.* 1860, 734–744. doi: 10.1016/j.bbabio.2019.07.011

Versantvoort, W., Guerrero-Cruz, S., Speth, D. R., Frank, J., Gambelli, L., Cremers, G., et al. (2018). Comparative genomics of *Candidatus Methylomirabilis* species and description of Ca. *Methylomirabilis lanthanidiphila*. *Front. Microbiol.* 9:1672. doi: 10.3389/fmicb.2018.01672

Vigneron, A., Alsop, E. B., Cruaud, P., Philibert, G., King, B., and Baksmaty, L. (2017). Comparative metagenomics of hydrocarbon and methane seeps of the Gulf of Mexico. *Sci. Rep.* 7, 1–12. doi: 10.1038/s41598-017-16375-5

Vigneron, A., Alsop, E. B., Cruaud, P., Philibert, G., King, B., Baksmaty, L., et al. (2019). Contrasting pathways for anaerobic methane oxidation in gulf of mexico cold seep sediments. *mSystems* 4:e00091-18. doi: 10.1128/msystems.00091-18

Vuillemin, A., Horn, F., Friese, A., Winkel, M., Alawi, M., Wagner, D., et al. (2018). Metabolic potential of microbial communities from ferruginous sediments. *Environ. Microbiol.* 20, 4297–4313. doi: 10.1111/1462-2920.14343

Wang, B., Wei, Q., Chen, J., and Xie, L. (2012). Annual cycle of hypoxia off the Changjiang (Yangtze River) Estuary. *Mar. Environ. Res.* 77, 1–5. doi: 10.1016/j.marenvres.2011.12.007

Wang, J., Cai, C., Li, Y., Hua, M., Wang, J., Yang, H., et al. (2019). Denitrifying anaerobic methane oxidation: a previously overlooked methane sink in intertidal zone. *Environ. Sci. Technol.* 53, 203–212. doi: 10.1021/acs.est.8b05742

Wang, Y., Feng, X., Natarajan, V. P., Xiao, X., and Wang, F. (2019). Diverse anaerobic methane- and multi-carbon alkane-metabolizing archaea coexist and show activity in Guaymas Basin hydrothermal sediment. *Environ. Microbiol.* 21, 1344–1355. doi: 10.1111/1462-2920.14568

Weber, T., Wiseman, N. A., and Kock, A. (2019). Global ocean methane emissions dominated by shallow coastal waters. *Nat. Commun.* 10:4584. doi: 10.1038/s41467-019-12541-7

Webster, G., OSullivan, L. A., Meng, Y., Williams, A. S., Sass, A. M., Watkins, A. J., et al. (2015). Archaeal community diversity and abundance changes along a natural salinity gradient in estuarine sediments. *FEMS Microbiol. Ecol.* 91:fiu025. doi: 10.1093/femsec/fiu025

Wells, N. S., Chen, J. J., Maher, D. T., Huang, P., Erler, D. V., Hipsey, M., et al. (2020). Changing sediment and surface water processes increase CH4 emissions from human-impacted estuaries. *Geochim. Cosmochim. Acta* 280, 130–147. doi: 10.1016/j.gca.2020.04.020

Welte, C. U., Rasigraf, O., Vaksmaa, A., Versantvoort, W., Arshad, A., Op den Camp, H. J. M., et al. (2016). Nitrate- and nitrite-dependent anaerobic oxidation of methane. *Environ. Microbiol. Rep.* 8, 941–955. doi: 10.1111/1758-2229.12487

Wen, X., Yang, S., Horn, F., Winkel, M., Wagner, D., and Liebner, S. (2017). Global biogeographic analysis of methanogenic archaea identifies community-shaping environmental factors of natural environments. *Front. Microbiol.* 8:1339. doi: 10.3389/fmicb.2017.01339

Westermann, P., Ahring, B. K., and Mah, R. A. (1989). Temperature compensation in methanosarcina barkeri by modulation of hydrogen and acetate affinity. *Appl. Environ. Microbiol.* 55, 1262–1266. doi: 10.1128/aem.55.5.1262-1266.1989

Xiao, K.-Q., Beulig, F., Røy, H., Jørgensen, B. B., and Risgaard-Petersen, N. (2018). Methylotrophic methanogenesis fuels cryptic methane cycling in marine surface sediment. *Limnol. Oceanogr.* 63, 1519–1527. doi: 10.1002/lno.10788

Xie, F., Ma, A., Zhou, H., Liang, Y., Yin, J., Ma, K., et al. (2020). Niche differentiation of denitrifying anaerobic methane oxidizing bacteria and archaea leads to effective methane filtration in a Tibetan alpine wetland. *Environ. Int.* 140:105764. doi: 10.1016/j.envint.2020.105764

Xu, L., Zhuang, G.-C., Montgomery, A., Liang, Q., Joye, S. B., and Wang, F. (2020). Methyl-compounds driven benthic carbon cycling in the sulfate-reducing sediments of South China Sea. *Environ. Microbiol.* doi: 10.1111/1462-2920.15110 [Online ahead of print].

Yvon-Durocher, G., Allen, A. P., Bastviken, D., Conrad, R., Gudasz, C., St-Pierre, A., et al. (2014). Methane fluxes show consistent temperature dependence across microbial to ecosystem scales. *Nature* 507, 488–491. doi: 10.1038/nature13164

Zhang, Y., Zhang, X., Wang, F., Xia, W., and Jia, Z. (2020). Exogenous nitrogen addition inhibits sulfate-mediated anaerobic oxidation of methane in estuarine coastal sediments. *Ecol. Eng.* 158:106021. doi: 10.1016/j.ecoleng.2020.106021

Zheng, Y., Wang, H., Liu, Y., Zhu, B., Li, J., Yang, Y., et al. (2020). Methane-dependent mineral reduction by aerobic methanotrophs under hypoxia. *Environ. Sci. Technol. Lett.* 7, 606–612. doi: 10.1021/acs.estlett.0c00436

Zhou, Z., Pan, J., Wang, F., Gu, J.-D., and Li, M. (2018). Bathyarchaeota: globally distributed metabolic generalists in anoxic environments. *FEMS Microbiol. Rev.* 42, 639–655. doi: 10.1093/femsre/fuy023

Zhu, Y., Purdy, K. J., Eyice, Ö, Shen, L., Harpenslager, S. F., Yvon-Durocher, G., et al. (2020). Disproportionate increase in freshwater methane emissions induced by experimental warming. *Nat. Clim. Change* 10, 685–690. doi: 10.1038/s41558-020-0824-y

Zhuang, G. C., Elling, F. J., Nigro, L. M., Samarkin, V., Joye, S. B., Teske, A., et al. (2016). Multiple evidence for methylotrophic methanogenesis as the dominant methanogenic pathway in hypersaline sediments from the Orca Basin, Gulf of Mexico. *Geochim. Cosmochim. Acta* 187, 1–20. doi: 10.1016/j.gca.2016.05.005

Zhuang, G. C., Lin, Y. S., Bowles, M. W., Heuer, V. B., Lever, M. A., Elvert, M., et al. (2017). Distribution and isotopic composition of trimethylamine, dimethylsulfide and dimethylsulfoniopropionate in marine sediments. *Mar. Chem.* 196, 35–46. doi: 10.1016/j.marchem.2017.07.007

Zhuang, G. C., Montgomery, A., Sibert, R. J., Rogener, M. K., Samarkin, V. A., and Joye, S. B. (2018). Effects of pressure, methane concentration, sulfate reduction activity, and temperature on methane production in surface sediments of the Gulf of Mexico. *Limnol. Oceanogr.* 63, 2080–2092. doi: 10.1002/lno.10925

Conflict of Interest: The authors declare that the research was conducted in the absence of any commercial or financial relationships that could be construed as a potential conflict of interest.

frontiers in Marine Science

ORIGINAL RESEARCH
published: 24 March 2021
doi: 10.3389/fmars.2021.633314

Comparison of Oyster Aquaculture Methods and Their Potential to Enhance Microbial Nitrogen Removal From Coastal Ecosystems

*Paraskevi Mara[1], Virginia P. Edgcomb[1], Taylor R. Sehein[2], David Beaudoin[1], Chuck Martinsen[3], Christina Lovely[3], Bridget Belcher[4], Rebecca Cox[1], Meghan Curran[4], Claire Farnan[4], Peter Giannini[4], Sarah Lott[1], Kyle Paquette[4], Anna Pinckney[4], Natalie Schafer[4], Tonna-Marie Surgeon-Rogers[5] and Daniel R. Rogers[4]**

[1] Department of Geology and Geophysics, Woods Hole Oceanographic Institution, Woods Hole, MA, United States, [2] MIT-WHOI Joint Program in Biological Oceanography, Cambridge and Woods Hole, MA, United States, [3] Marine and Environmental Services, Falmouth, MA, United States, [4] Laboratory of Biogeochemistry, Department of Chemistry, Stonehill College, Easton, MA, United States, [5] Waquoit Bay National Estuarine Research Reserve, Waquoit, MA, United States

OPEN ACCESS

Edited by:
Konstantinos Ar. Kormas, University of Thessaly, Greece

Reviewed by:
Élise Lacoste, University of French Polynesia, French Polynesia
Sokratis Papaspyrou, University of Cádiz, Spain
Ashley Smyth, University of Florida, United States

***Correspondence:**
Daniel R. Rogers
drogers2@stonehill.edu

Specialty section:
This article was submitted to Aquatic Microbiology, a section of the journal Frontiers in Marine Science

Received: *25 November 2020*
Accepted: *11 February 2021*
Published: *24 March 2021*

Citation:
Mara P, Edgcomb VP, Sehein TR, Beaudoin D, Martinsen C, Lovely C, Belcher B, Cox R, Curran M, Farnan C, Giannini P, Lott S, Paquette K, Pinckney A, Schafer N, Surgeon-Rogers T-M and Rogers DR (2021) Comparison of Oyster Aquaculture Methods and Their Potential to Enhance Microbial Nitrogen Removal From Coastal Ecosystems. Front. Mar. Sci. 8:633314. doi: 10.3389/fmars.2021.633314

Coastal ecosystems are impacted by excessive nutrient inputs that cause degradation of water quality and impairments of ecosystem functioning. Regulatory and management efforts to enhance nutrient export from coastal ecosystems include sustainable oyster aquaculture that removes nitrogen in the form of oyster biomass and increases particulate export to underlying sediments where increased organic material may enhance microbial denitrification. To better understand the impacts of oyster aquaculture on nitrogen removal, we examined bacterial processes in sediments underlying three of the most common aquaculture methods that vary in the proximity of oysters to the sediments. Sediment samples underlying sites managed with these different aquaculture methods were examined using the 16S rRNA gene to assess microbial community structure, gene expression analyses to examine nitrogen and sulfur cycling genes, and nitrogen gas flux measurements. All sites were located in the same hydrodynamic setting within Waquoit Bay, MA during 2018 and 2019. Although sediments under the different oyster farming practices showed similar communities, ordination analysis revealed discrete community groups formed along the sampling season. Measured N_2 fluxes and expression of key genes involved in denitrification, anaerobic ammonium oxidation (anammox), and dissimilatory nitrate reduction to ammonium (DNRA) increased during mid-summer and into fall in both years primarily under bottom cages. While all three oyster growing methods enhanced nitrogen removal relative to the control site, gene expression data indicate that the nitrogen retaining process of DNRA is particularly enhanced after end of July under bottom cages, and to a lesser extent, under suspended and floating bags. The choice of gear can also potentially increase processes that induce nitrogen retention in the form of ammonia in the underlying sediments over time, thus causing deviations from predicted nitrogen removal. If nitrogen removal is a primary objective, monitoring for these shifts is essential for making decisions about siting and size of aquaculture sites from year to year.

Keywords: nitrogen removal, oyster cultures, denitrification, anammox, DNRA

INTRODUCTION

Coastal bays and estuaries receive excessive nutrient inputs from anthropogenic activities that have profound negative effects upon water quality (Smith, 2003). Over the past decades the use of chemical fertilizers has expanded, and population densities have increased along coastal zones. These have accelerated nutrient pollution and eutrophication has become a broad-scale concern for nearshore coastal and estuarine ecosystems (Howarth et al., 2011; Glibert et al., 2018; and discussed in Clements and Comeau, 2019). Coastal communities are now challenged to meet goals to decrease nitrogen inputs to coastal waters. Nitrogen controls primary production in coastal ecosystems and nitrogen in the form of nitrate (a common fertilizer component) can serve as a nutrient for many aquatic microorganisms that can utilize it as an energy source under both aerobic and anaerobic conditions (Howarth, 1988). Excessive inputs of nitrate can result in reduced oxygen levels (hypoxia) (Rabalais et al., 2014), enhanced algal growth, and increased duration and severity of harmful algal blooms (HABs) (Anderson et al., 2002; Glibert et al., 2005). The altered balance between nitrogen inputs and exports has potentially severe ecological and economic impacts and requires appropriate management to reduce eutrophication in coastal ecosystems (Humphries et al., 2016; Clements and Comeau, 2019).

Coastal areas in New England are impacted by nitrogen loads carried by sewage outfalls and river discharges, but the primary source of excess nitrogen is groundwater contaminated with septic fluids, fertilizers, and other contaminants that contribute to eutrophication (Correll et al., 1992; Valiela et al., 1997). While sewering can address significant fractions of these inputs, additional mitigation tools are needed to extract nutrients from coastal ecosystems. One potential tool for removing nitrogen from coastal estuaries and bays is shellfish aquaculture, and specifically oyster farming. Oysters are filter-feeders and their harvesting can remove nutrients from the water column because oysters filter blooms of primary producers and convert those nutrients into oyster biomass. As such, the harvesting of oysters can be beneficial for nitrogen removal, so-called "bio-extraction," in New England's estuaries and bays (Feinman et al., 2018; Clements and Comeau, 2019). The efficiency of oysters to assimilate and digest various sources of organic matter varies over the season which can lead to significant amounts of undigested particulate organic nitrogen (PON) being transported via their feces and pseudofeces to the sediment surface (Newell and Jordan, 1983). This biodeposition may enhance the microbial process of denitrification in underlying sediments (Kellogg et al., 2013). Denitrification releases nitrogen from the ecosystem in the form of nitrogen gas (N_2) and this process naturally occurs in marine sediments. Oyster biodeposits can alter sediment chemistry since they contain twice as much the concentrations of carbon, nitrogen, and phosphorus compared to particles settling-out naturally from the water column (Jordan, 1987) and thus enhance denitrification rates of sediment bacterial communities (Newell et al., 2002).

Denitrification is a four-step metabolic process that converts nitrate to N_2. The denitrification genes are assembled in clusters and encode functions for nitrate (*narG*/*napA*), nitrite (*nirS*/*nirK*), nitric oxide (*norB*/*norC*), and nitrous oxide (*nosZ*) reduction largely unique to denitrifying bacteria (Zumft, 1997). The process occurs in the membranes and the periplasm of the microbes and constitutes one of the basic energy flow pathways under anaerobic conditions. The energy for microbial denitrification in marine sediments derives from organic matter oxidation under suboxic (near-zero O_2 values) or anoxic conditions by facultative heterotrophic anaerobes that use nitrate, nitrite, and nitrous oxide as terminal electron acceptors (Tiedje, 1988; Devol, 2015). Nitrate availability is important for denitrification, although denitrifiers are equipped with nitrate reduction enzymes (NapA and NarG) that share the same function but are induced at low (*napA* at <0.5 mM nitrate) and higher nitrate (*narG* at >1 mM of nitrate) concentrations based on experimental studies (Wang et al., 1999).

The importance of sediment denitrification underneath oyster aquaculture sites has been extensively debated, with studies suggesting different levels of significance of the process (Ray et al., 2020 and references therein). Rates measured at both bottom-planted and off-bottom oyster aquaculture sites in New England showed increased denitrification (Humphries et al., 2016; Vieillard, 2017; Feinman et al., 2018) that occasionally was comparable to the denitrification rates of restored oyster reefs (Humphries et al., 2016). This suggests that oyster farm biodeposits (e.g., faces, pseudofaces, particles) could enhance bacterial denitrification in marine sediments (Feinman et al., 2018), perhaps at rates equal to that of wild oyster beds.

Oyster biodeposits might also have the potential to promote alternative anaerobic metabolic processes, including dissimilatory nitrate reduction to ammonium (DNRA) or anaerobic ammonium oxidation (anammox). The process of DNRA reduces nitrate to nitrite (*narG*) and then nitrite to ammonium via the ammonia-forming nitrite reductase NrfA. DNRA is an active nitrate reduction process that can dominate over dentification in sediments below farmed bivalves, and it generates ammonium that can be partially regenerated into the water column (Nizzoli et al., 2006; Carlsson et al., 2012; Murphy et al., 2016). Enhanced fluxes of benthically produced ammonium into the water column has been documented below oyster aquaculture sites (Mazouni et al., 1996; Chapelle et al., 2000; Higgins et al., 2013; Lunstrum et al., 2018) may lead to retention rather than removal of reactive nitrogen (Lunstrum et al., 2018). However, to date, DNRA rates have been measured in association with three oyster aquaculture studies that show DNRA can either dominate over benthic denitrification (Erler et al., 2017; Lunstrum et al., 2018) or can have an insignificant (if any) role (Vieillard, 2017). The factors that control the competition between DNRA and denitrification and the impact oyster aquaculture can have on the balance of these processes needs further study (Burgin and Hamilton, 2007). Both processes are found across many different microbial lineages (Burgin and Hamilton, 2007; Braker et al., 2010) and there has been some suggestion that increased hydrogen sulfide concentrations in the environment may favor DNRA over denitrification (An and Gardner, 2002).

The impact of oyster biodeposits on sediment anaerobic ammonia oxidation is also not extensively characterized. Under anaerobic conditions anammox converts nitrite and ammonia to N_2 that is removed from the marine sediments (Devol, 2015). Anammox usually involves the reduction of nitrite to nitric oxide (*nirS*/*nirK*) which is used for the oxidation of ammonia to hydrazine (Kartal and Keltjens, 2016). The last step of anammox involves hydrazine oxidoreductase (*hzo*) that oxidizes hydrazine to nitrogen gas (Hu et al., 2019). Both DNRA and anammox are strictly anaerobic processes that can be inhibited at oxygen concentrations as low as ∼1–2 μM (Mohan and Cole, 2007; Dalsgaard et al., 2014). Direct measurements of denitrification and anammox rates in sediments underneath bivalve farming have estimated that the contribution of anammox to nitrogen removal is minor (Carlsson et al., 2012; Erler et al., 2017; Lunstrum et al., 2018).

Microbial denitrification and other nitrogen cycling processes can be influenced by redox changes and sediment oxygen demand (SOD), temperature and salinity, availability of organic matter, and local hydrodynamics (Hoellein and Zarnoch, 2014). Also, the oyster stocking density and the available space for oyster aquaculturing can affect the quantity and quality of particles and thus impact nitrogen removal via "bio-extraction" and denitrification (Carmichael et al., 2012). Redox changes induced via hydrogen sulfide concentrations can alter rates of denitrification, DNRA, and anammox. The sulfur cycle via the oxidation and/or reduction of sulfides, sulfur intermediates, as well as via disproportionation influences the nitrogen cycle in marine sediments (e.g., Caffrey et al., 2019 and references therein; Jørgensen et al., 2019). Diverse aquaculture settings can potentially influence the above parameters and thus enhance or inhibit different nitrogen cycling processes in the underlying sediments. The type of gear used for aquaculture can also have an impact. Oyster aquaculture systems utilized in areas of New England include surface or floating bags, suspended oysters (oyster are suspended under a buoy), and bottom cage oysters (5–6 cm above the sediments). In this study, we examined net N_2 release from sediments under different oyster aquaculture systems, whether the presence of oyster aquaculture altered sediment microbial community composition, and we investigated evidence for expression of genes involved in bacterial nitrogen metabolisms that impact N removal, including bacterial denitrification, anammox, and potentially, chemolithotrophic DNRA. We hypothesized that overall nitrogen production and individual nitrogen cycling processes might be differentially affected by different oyster culturing systems that hold oysters at different distances from the sediment, resulting in differences in net N_2 release from underlying sediments. To test this hypothesis, we installed three different farming practices that included floating and suspended bags, and bottom cages within the same hydrodynamic setting in Waquoit Bay, MA, United States during the aquaculture season in two consecutive years. We collected sediment cores for 16S rRNA gene analyses, quantitative reverse transcription PCR (RT-qPCR), of denitrification, anammox, dissimilatory nitrate reduction to ammonium and sulfur oxidation genes, and metatranscriptome analyses addressing dissimilatory sulfate reduction (*dsr* genes). We also monitored nitrogen production fluxes under the different aquaculture sites. Waquoit Bay is typical of the setting of many oyster aquaculture sites in the region.

MATERIALS AND METHODS

Site Description

Our study site was established in Waquoit Bay, Falmouth Massachusetts (41°34′49″N, 70°31′27″W; Waquoit, MA, United States), within the boundaries of the Waquoit Bay National Estuarine Research Reserve in an area relatively undisturbed by human impacts. Waquoit Bay is a shallow bay encompassing approximately 825 acres. The bay has an average depth of 0.79 m (with a maximum depth of 2.7 m and tidal height of ∼0.5 m) and is tidally flushed through a narrow opening (∼115 m) to Vineyard Sound to the south of the study site (∼3.2 km) with salinity ranging from 0 (in the tributaries) to 32 PSU, with the highest salinities occurring in the center of the bay. Nitrogen loading is a major concern in the bay and is likely the driver behind the collapse of the Waquoit Bay eelgrass population over recent decades. Nitrogen enters the bay through atmospheric deposition, rivers (e.g., Childs River and Great River) and groundwater (accounting for 50%–80% of the N-load) (Talbot et al., 2003; Kroeger et al., 2006; Bowen et al., 2007). Our study site was carefully selected to best allow us to isolate the effects of using different aquaculture gear by co-locating sites for each of the three types of aquaculture gear as well as our control site at a location where all would be in the same hydrodynamic setting (exposure to winds, waves, and currents), have the same sediment characteristics, be the same distance from shore, and in the same depth of water in an area free of seagrass beds.

Experimental Design

We used three commercially available oyster growth methods (surface, suspended, and bottom oyster aquaculture methods) that result in different proximity of oysters to the sediment. The different oyster methods were first installed in early March 2018 and 2019, with each treatment site covering an area of 80 m^2 (Floating Bags), 108 m^2 (Oyster Gro'), or 108 m^2 (Bottom Cages) (**Figure 1**). Year old oysters were added in late April of each year. Oysters and all gear were removed in October 2018 and 2019 for over wintering.

Between each gear type deployment there was a 5 m gap. For the Bottom Cage (BC) method we deployed 1.2 × 0.9 × 0.4 m^3 cages that rested on the bottom and held the oysters 5–6 cm above the sediment. The BC setups allowed oysters to grow on the ocean bottom similar to wild oysters. The Floating Bag (FB) method utilized 0.5 × 0.8 m^2 rigid floating bags with 6 mm^2 mesh, attached to foam floats and aligned into a floating system that ensured adequate water circulation. The suspended Oyster Gro' method (OG) utilized 0.46 × 0.89 m^2 rigid grow-out bags with 6 mm^2 mesh held within rigid metal wire frames suspended below buoys that allowed the oysters to be held about 30 cm below the sea surface and 0.5–2.0 m above the seafloor, depending on the tide. The BC oysters were constantly on the seafloor,

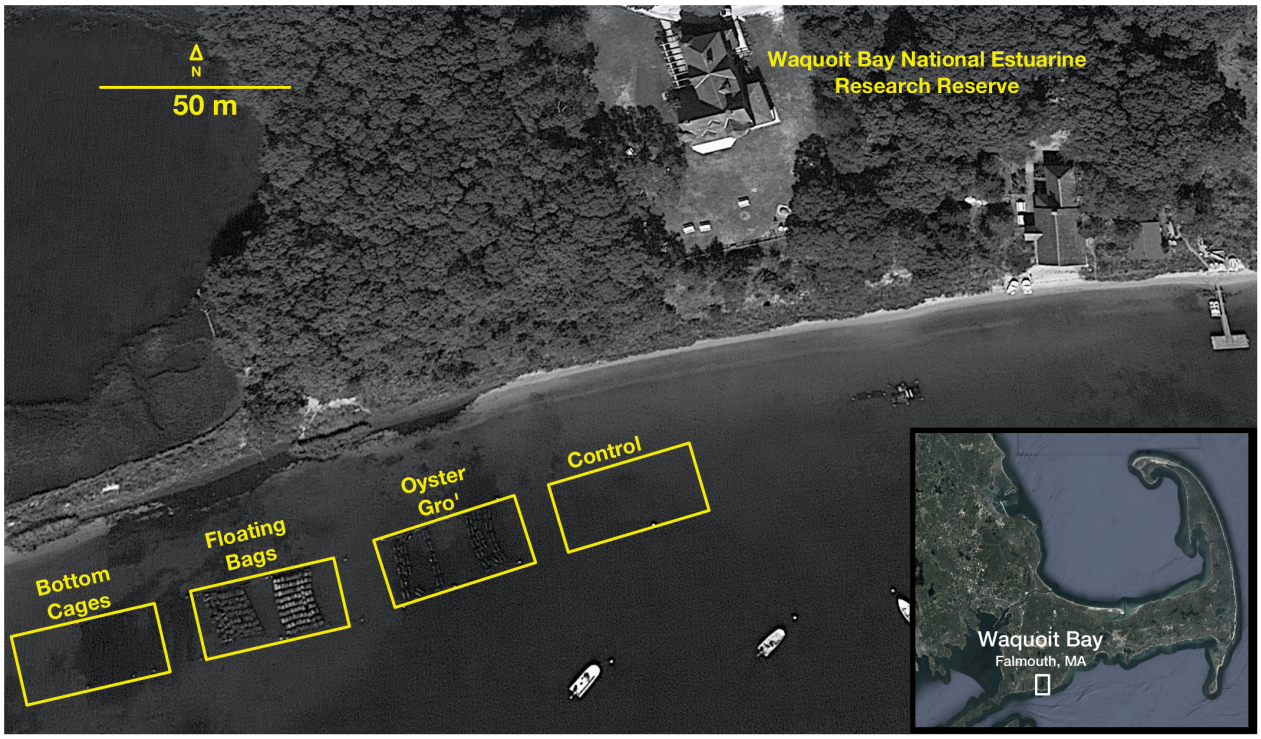

FIGURE 1 | Aerial image of oyster deployments and the sediment sampling sites in Waquoit Bay, MA (41°34′49″N, 70°31′27″W). Within the yellow box from left to right are the bottom cages, the floating bags, and the floating Oyster Gro cages (Image from Google Earth).

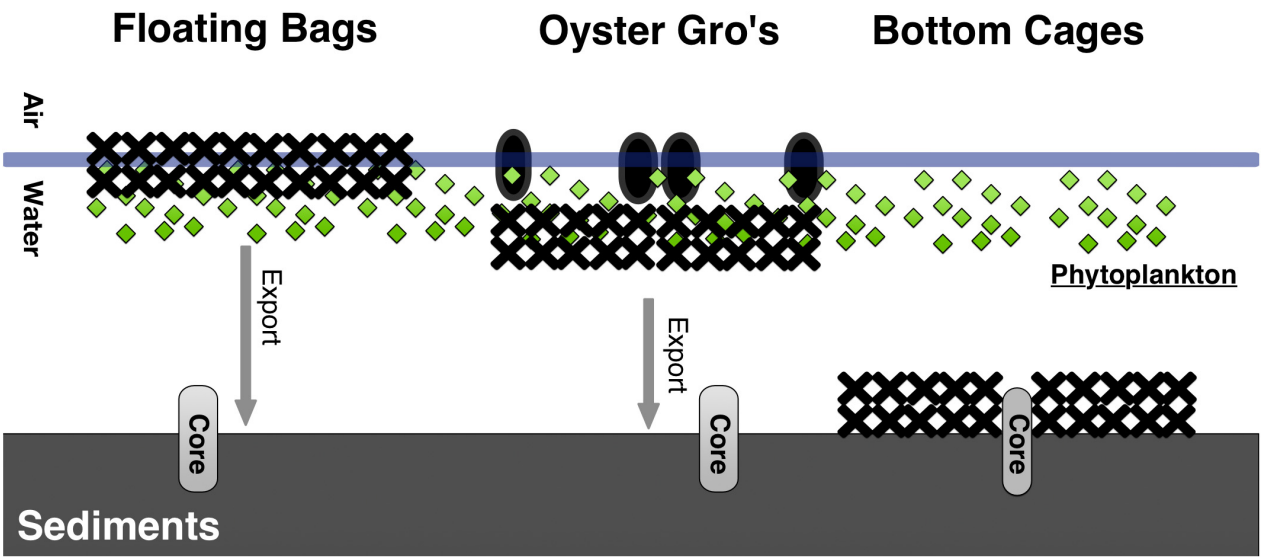

FIGURE 2 | Schematic for the three different oyster aquaculture gear tested and their proximity to the sediment in Waquoit Bay. The Floating Bags and Oyster Gro's were approximately 1–3 m and 0.5–2.0 m above the seafloor, depending on the tide, respectively.

while the FB and OG gear were exposed to intertidal changes but always in the water (**Figure 2**). For each growth method initial stocking weights of 1-year old oysters were 2.28 kg of oysters, targeting approximately 225 oysters per bag. This resulted with ∼200 kg of oysters initially in the FB, ∼205 kg in the OG and BC. Bottom cages and Oyster Gro' systems hold six bags per unit. Our experimental design also included a control site (**Figure 1**). As mentioned, all sites (including the control site) were separated by approximately 5 m to limit effects of lateral transport of biodeposits between sites.

Sample Collection

Samples were collected bi-weekly during 2018 (May–September) and 2019 (April–October). Water column profiles for dissolved oxygen, temperature, and salinity were obtained in 15 cm intervals along the water column (max depth 60 cm) using a YSI Pro2030 handheld meter (YSI, Inc., yellow Springs, OH, United States) (**Supplementary Table S1**). We collected three sediment cores as biological replicates under each oyster method site and at the control site using a pole coring device (Aquatic Research Instruments, Hope, ID, United States) and polycarbonate core liners (internal diameter, 9.5 cm; total length, 0.5 m). All triplicate cores were collected near the center of each site (avoiding edge effects), directly under FB's, OG's, or BC's, 0.5–3 m apart to limit spatial dependence between replicate cores (**Figure 1**). The top 3 cm of each core were sectioned immediately (within 5 min) in the field and homogenized for RNA, DNA, and porewater nutrient analyses. An extra set of two sediment cores per study site were collected for the measurements of N_2 fluxes using flux chambers (see below). The same number of sediment cores were collected from our control site.

Nutrient, Total Carbon, and Nitrogen Analyses

Replicate bottom water samples (∼50 ml) were collected from each core, filtered through a 0.45 μm sterivex filter (Fisher Scientific, United States) and frozen until analysis for nitrate, nitrite, and ammonium. Porewaters were collected from the upper 3-cm of sediments into 50 ml Falcon tubes. The Falcon tubes were stored on ice in the field and then at 10°C in the laboratory. For nitrate and nitrite measurements, 10 g of sediment were placed in Macrosep centrifuge tubes with a 0.45 μm membrane (Fisher Scientific, United States) and centrifuged for 5 min at 3000 rpm. The resulting filtrate was analyzed colorimetrically for nitrate + nitrite (NO_x) using a salt compensated resorcinol method (Zhang and Fischer, 2006). Nitrite was measured colorimetrically according to Pai et al. (1990). Extractable ammonium was measured by incubating 10 g of sediment with 10 ml of a 1 M KCl and separating sediments from the aqueous solution using the 0.45 μm Macrosep tubes. The resultant ammonium was measured using the phenolhypochlorite method (Solorzano, 1969). Standards were salt matched and analyzed along with samples. The remaining sediments were oven-dried (80°C), ground with a mortar and pestle (<250 μm), weighed and encapsulated in Al cups, and analyzed for total carbon and total nitrogen using a Micro-Dumas (flash) combustion method at the Stable Isotope Ecology Laboratory at the University of Georgia.

Flux Chambers and N_2/Ar Measurements

The replicate sediment cores were collected to measure N_2 fluxes. Collected cores from each site were submerged in a cooler containing site water and allowed to equilibrate for at least 1 h. After equilibration, cores were sealed with a cap that contained a magnetic stir bar and an oxygen optode (PSt3 sensor) attached to an Oxy10 SMA meter (PreSens Precision Sensing GmbH, Germany), that allowed real-time monitoring of oxygen concentrations using the PreSens Measurement Studio 2 software. The temperature of the incubation water was monitored continually. The sediment height and water height (no headspace) were recorded. Initial N_2/Ar samples (t_0) were collected with no headspace into 12-ml exetainers (739 W, Labco Ltd, Austin, TX, United States) containing 300 μl of saturated $ZnCl_2$ (for preservation) from the incubation waters immediately after capping all the cores. Cores were incubated in the dark until 20%–25% of the oxygen in the overlying waters had been consumed. Then the overlying water from the core was collected into exetainers with no headspace as before and 50 ml of water was filtered through a 0.45 μm sterivex filter and prepared for NO_x and ammonium analysis as described above. Exetainers were refrigerated (below *in situ* temperatures) until analysis. N_2/Ar was measured on a membrane inlet mass spectrometer equipped with a water bath on the inlet, set to match sample collection temperature, a liquid nitrogen trap for CO_2, a Cu-reduction column heated to 600°C to remove O_2, and a quadrupole mass analyzer (RGA100, Stanford Research Systems, Sunnyvale, CA, United States). N_2/Ar standards were made by equilibrating salinity matched waters at 4°C, room temperature (as measured, typically 21°C) and 30°C. Standards were analyzed every 10–15 samples to correct for any instrument drift. Excess N_2 production was calculated as production above background (t_0 samples as described above), scaled to water volume and normalized to incubation time (each core had the same surface area). All results for experimental site cores were compared to N_2 production from the control cores.

RNA and DNA Samples

We collected and homogenized the top 3 cm of each sediment core in ethanol-sterilized weigh boats. Homogenized sediments were aliquoted to sterile 15-ml Falcon tubes and 5-ml cryovials for subsequent extraction of bacterial RNA and DNA back in the laboratory. The RNA and DNA samples were flash frozen immediately with liquid nitrogen in the field and were stored to −80°C at the lab. All the RNA and DNA extractions occurred the day following the sampling.

RNA Extractions and Metatranscriptome Analysis

We extracted 2 g of sediment for each sample in a UV-sterilized clean hood using the RNeasy PowerSoil® Total RNA Isolation Kit (Qiagen, United States) following the manufacturer's protocol. To remove traces of contaminating DNA we treated our RNA extracts twice (2 × 30 min) with TURBO DNA-free™ (Invitrogen, United States) as suggested by the manufacturer. To confirm absence of DNA from the RNA solutions we ran a PCR reaction using the bacterial primers BACT 1369F and PROK 1541F targeting the 16S rRNA. Each 25 μl reaction contained 0.5 U μl^{-1} *Taq* DNA Polymerase (Thermo Fisher Scientific), 1 × *Taq* DNA Polymerase reaction buffer (Thermo Fisher Scientific), 0.4 mM dNTPs (Thermo Scientific dNTP Mix),

and 4 μM of each primer (final concentrations). These reactions were performed at 94°C for 5 min, followed by 35 cycles of 94°C (30 s), 55°C (30 s), and 72°C (45 s).

We quantified our total RNA extracts using a Qubit™ RNA HS Assay Kit (Thermo Fisher Scientific) and prepared metatranscriptome libraries on selected samples using the KAPA RNA HyperPrepKit for Illumina Sequencing Platforms (Kapa Biosystems) according to manufacturer instructions. The metatranscriptome libraries were prepared only for selected samples collected from both the control site and the different oyster treatments in May (May_23), July (July_17), and September (Sep_25) 2018 and were stored at −80°C until sequencing using 150 bp paired-end Illumina NextSeq 550 (Georgia Genomics and Bioinformatics Core; University of Georgia).

Trimmomatic (v.0.32) was used to trim adapter sequences (leading = 20, trailing = 20, sliding window = 04:24, minlen = 50). Paired reads were further quality checked and trimmed using FastQC (v.0.11.7) and the FASTX-toolkit (v. 0.0.14). Downstream analyses utilized paired reads. After co-assembling reads with Trinity (v.2.6.6) (min length 150 bp) we used Bowtie2 (v.2.3.4.1) to align all sample reads and RSEM (v.1.3.0) to estimate the expression level of these reads. TMM was used to perform cross-sample normalization and to generate a TMM-normalized expression matrix. Within the Trinotate suite, TransDecoder (v.5.3.0) was used to identify coding regions within contigs and functional and taxonomic annotations were made by BLASTx and BLASTp against UniProt, Swissprot, and RefSeq non-redundant protein sequence (nr) databases (e-value threshold of 1e – 40).

RT-qPCR

Transcript abundances of denitrification, anammox, DNRA, and sulfur oxidation genes were determined with two-step quantitative RT-qPCR. The first step of RT-qPCR involved the reverse transcription of the extracted RNA into a single-stranded copy of cDNA using the QuantiTect Reverse Transcription Kit (Qiagen, United States) following the manufacturer's protocol. The cDNAs were quantified using the Qubit™ dsDNA HS Assay Kit and normalized to 10 ng reaction^{-1} to avoid concentration-related PCR variations. We performed the quantitative PCR amplification steps of RT-qPCR in triplicate to all genes of interest on a StepOnePlus Real Time PCR (ThermoFisher, United States) using the SsoAdvanced Universal SYBR Green Supermix (Bio-Rad, United States). PCR protocols included 95°C (10 min) followed by 40 cycles of 95°C (30 s), annealing temperatures indicated in **Supplementary Table S2** for 60 s, 72°C (30 s), and 85°C for 15 s. A melt curve was produced after each analysis. We generated the RT-qPCR standard curves with 10^1–10^7 dilutions of linearized plasmids containing known sequences of the targeted genes. The RT-qPCR efficiency ranged from 95% to 105% for all reactions, resulting in linear standard curves ($r^2 = 0.99\%$).

Genes involved in denitrification (*narG*, *nirS*/*nirK*, and *nosZ*), sulfur oxidation (*soxA* and *soxB*), DNRA (*nrfA*), and anammox (*hzo*) were amplified using the primers in **Supplementary Table S2**.

DNA Extractions and 16S rRNA Marker Gene Analysis

We extracted 0.5 g of sediment for each sample collected in 2018 in a UV-sterilized clean hood using the PowerSoil® DNA Isolation Kit (MOBIO) following manufacturer's instructions. Bacterial and archaeal SSU rRNA gene fragments were PCR amplified and sequenced at Georgia Genomics and Bioinformatics Core (University of Georgia). The primers used were 515F-Y (5′-GTGYCAGCMGCCGCGGTAA-3′) and 926R (5′-CCGYCAATTYMTTTRAGTTT-3′) targeting the hypervariable region 4-5 (V4-V5) of the SSU rRNA gene (Parada et al., 2016). Paired reads were quality checked and trimmed using FastQC (v. 0.11.7). We analyzed the sediment microbiome data using the QIIME2 platform (Bolyen et al., 2019), and used the DADA2 plugin provided in the QIIME2 pipeline to denoise and optimize the merging of the forward and reverse reads. Taxonomy was assigned to amplicon sequence variants (ASVs) using the scikit-learn multinomial naive Bayes classifier (q2-feature-classifier plugin; Bokulich et al., 2018) with the SILVA v132 database as the reference (Quast et al., 2013). Sequences were deposited into the National Center for Biotechnology Information (NCBI) Sequence Read Archive (SRR13101827-SRR13101797, and SAMN16838263-SAMN16838385) database under project BioProject ID PRJNA679576.

Statistical Analyses

The relative abundances of 16S rRNA data were determined by dividing the number of sequences in each taxon by the total number of sequences for each sample. These normalized relative abundances were used to estimate the average abundances of the different bacterial taxa described in **Figures 4** and **5**. We also calculated the Bray–Curtis dissimilarity index using the normalized relative abundances and performed a hierarchical clustering (complete linkage) to assess potential differences between the biological triplicates collected underneath the oyster treatments and the control site. Bray-Curtis dissimilarity index and the hierarchical clustering analyses were performed using the Vegan v2.5-6 packages in R (Dixon, 2003). We used the unweighted UniFrac distance to compare the phylogenetic similarity of the sediment bacterial communities between the different oyster culture methods. We generated the unweighted UniFrac principal component ordination plot (PCoA), in R using the package ggplot2 (Wickham, 2016). Our input data for the PCoA plot were the unweighted UniFrac PCoA results and the Shannon index feature-table generated by the QIIME2 pipeline.

We tested for the effects of the individual oyster treatments on the expression of key genes associated with nitrogen cycling, and on measurements of nitrogen flux. Seasonality may have impacted measurements, in addition to oyster treatment; therefore, two-way ANOVAs were performed to compare the measurements collected at all sites and to evaluate the effect of time. Given that marine sediments are heterogeneous by nature (e.g., random deposition of large organic particles, influences of Metazoa, and other disturbances) due to processes that occur on sub-millimeter scales, homogenized core horizons from 9.5 cm ID push core capture variation that occurs at this scale

and triplicate cores collected 0.5–3 m apart at each site are reasonably independent to justify their use in ANOVAs. All gene expression datasets were normalized by log transformation and calculations were performed in R (version 3.6.1), with ANOVAs evaluated using the car package (version 3.0-10). All residuals were checked for normality using the Shapiro-Wilk test using the shapiro.test function in the stats package (version 3.6.2), with outliers removed from datasets when necessary to maintain the assumption of normality. Sliced least squares means (LS means) were calculated via Dunnett's method using the lsmeans function in the lsmeans package, comparing each oyster treatment to the control site at each time point.

RESULTS

Nitrate, Ammonia, Sedimentary Carbon and Nitrogen, Temperature, Dissolved Oxygen, and Salinity

The average porewater nitrate (**Supplementary Figure S1A**) and ammonia concentrations in 2018 ranged from 37 to 103 mM, and 720 to 1387 μM respectively (**Supplementary Figure S1B**). Nitrate concentrations between the different oyster treatments were comparable, while nitrite concentrations were below detection in all samples. Spikes of high nitrate in samples from the OG and the control site were detected in May, June and early July, while FB showed elevated nitrate concentrations in June and early July. Porewater nitrate showed a generally negative correlation with N_2 flux but this trend was only statistically significant in 2018 under the FB and OG treatments (Pearson's correlation r −0.84 to −0.91, $p < 0.5$).

The average porewater nutrient concentrations in 2019 were generally steady over the season at all sites. The average nitrate ranged from 23.0 to 33.2 μM, presenting the highest concentrations in late June (**Supplementary Figure S2A**). Nitrite was below detection in all samples. The average ammonia concentrations were also comparable between the different oyster treatments and ranged from 355 to 493 μM (**Supplementary Figure S2B**). We detected positive correlations between ammonia and N_2 fluxes in both 2018 and 2019, however these were not significant aside from under the FB site in 2018 (Pearson correlation r 0.88, $p < 0.5$). Bottom water nutrients were consistent between sites.

Total carbon and nitrogen were measured monthly at each site during both 2018 and 2019 sampling periods (**Supplementary Table S3**). The impact of the oyster aquaculture resulted in an increase on carbon content of the underlying sediment over the course of the growing season. BC sediments showed the largest impact with %C increasing ∼14%, followed by OG (∼8%), FB (∼4%), and the C (∼3%). Literature reports average sediment grain size in the area is ∼200 μm in the upper few cm (Maio et al., 2016).

In 2018 the water column temperature at all sites ranged from ∼18°C to 28°C over the sampling period June through September (**Supplementary Table S1** and **Figure S3A**). Salinity ranged from ∼25 to 30 PSU, and dissolved oxygen ranged from ∼3.5 to 10 mg/L over the same period (**Supplementary Table S1**). In 2019 the water column temperature ranged from ∼12.5°C to 28°C over the sampling period from April to October (**Supplementary Table S1**). Salinity ranged from ∼18.5 to 26.5 PSU, and dissolved oxygen ranged from ∼0.5 to 12.5 mg/L (**Supplementary Table S1** and **Figure S3B**). The water column temperature in 2019 was positively correlated with the N_2 fluxes at all different treatment sites and the control site (Pearson correlations r 0.62–0.75, $p < 0.5$).

N_2 Production Rates

Flux chambers were used to estimate N_2 production from the sediments across the sites. In all flux chamber experiments nitrate and ammonium flux to or from the sediments was negligible compared to concentration changes over the short incubation periods. The flux chambers showed production of N_2 gas in sediments at the control as well as the different oyster aquaculture method sampling sites in 2018 and 2019 (**Figures 3A,B**). The N_2 fluxes were comparable between the control and the different oyster treatments from late May until late June in 2018 (∼0.3 mmol N m^{-2} day^{-1}). After June 2018 we observed a sudden twofold increase in N_2 production at the aquaculture sites that reached up to a fivefold increase (in the case of BCs) when compared to the control. To test for significant differences between treatments over time we used a two-way ANOVA followed by the *post hoc* LS means analysis. In 2018, the overall comparison of the treatments and time point, as well as the interaction between the two variables, was found to be statistically significant ($p < 0.05$) (**Figure 3A** and **Supplementary Table S4**).

In 2019 N_2 production rates were comparable between the control site and the different treatment sites from late April until June and showed a sharp and statistically significant increase in N_2 production (up to a fivefold increase) especially after July that continued until the end of the 2019 sampling period (**Figure 3B** and **Supplementary Table S4**).

Phylogenetic Analysis of the Bacterial Communities Underneath the Oyster Culture Treatments

The phylogenetic analysis of the bacterial communities underneath the oyster cultures and the control site was performed for the 2018 sampling period. The number of sequences per sample ranged from 1954 to 34,716, with a mean of 16,790 ± 6387 sequences. A total of 17,176 bacterial ASVs were recovered from the Waquoit sediment libraries. Hierarchical clustering of the biological triplicates from all sampling sites using the Bray–Curtis dissimilarity index revealed consistency of the microbial community structure amongst replicates for most samples (**Supplementary Figures S4, S5**).

Sediment community compositions underneath the different oyster treatments were generally similar to those at the control site. The dominant phyla at all sites were Proteobacteria, Cyanobacteria, and Bacteroidetes, while Planctomycetes was among the phyla with the lowest relative abundance at all sampling sites (**Figure 4**).

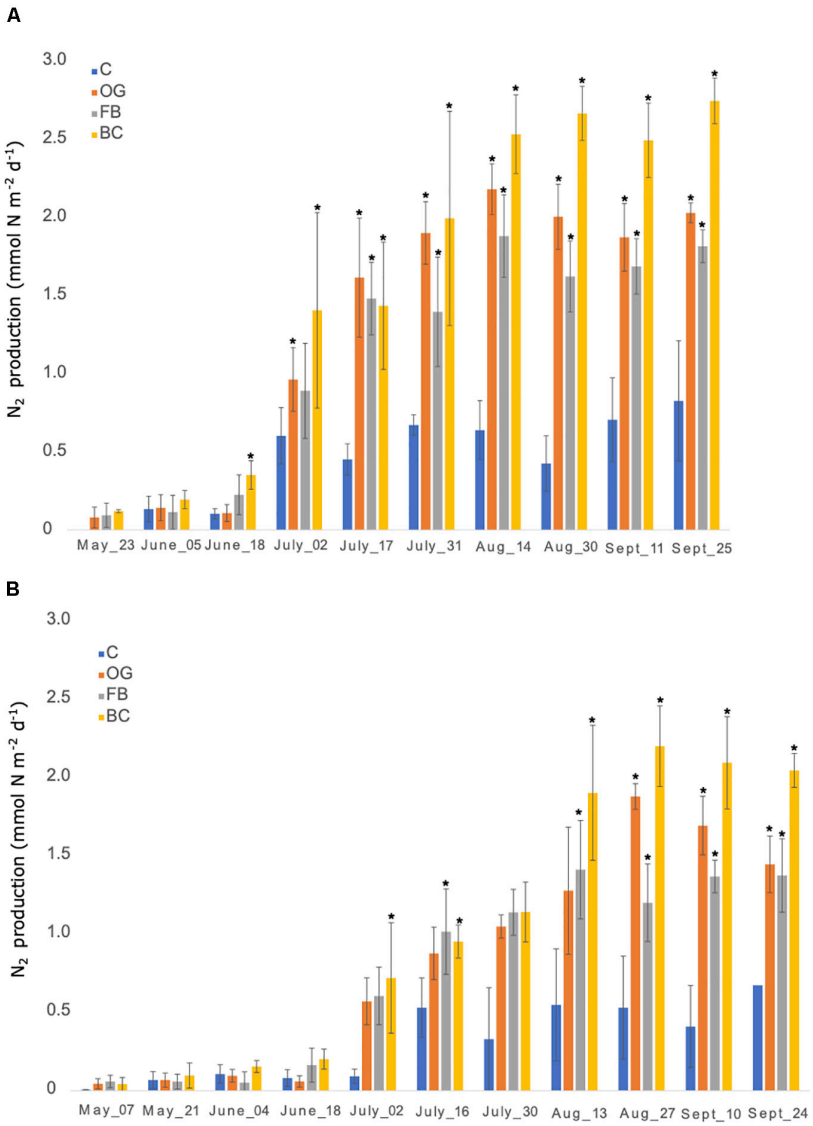

FIGURE 3 | Nitrogen production rates measured from late May until end of September 2018 **(A)** and 2019 **(B)** using *in situ* flux chambers. C, Control; OG, Oyster Gro'; FB, Floating Bags; BC, Bottom Cages. Statistically significant differences are marked with an asterisk (*t*-test, $p < 0.05$).

The relative abundance of Proteobacteria was similar, percentage-wise, between the control site and the oyster treatments throughout the sampling period (C: 41% ± 4.7%, BC: 39% ± 4.5%, OG: 38% ± 2.3%, FB: 40ˆ ± 3.9%). The relative abundance of Bacteroidetes was comparable between the control and different oyster aquaculture methods (C: 29% ± 5.2%, BC: 28% ± 5.4%, OG: 31.4% ± 6.8%, FB: 32.5% ± 11.5%). Planctomycetes had relative abundance of 1%–3% with higher abundances in the BC oyster treatment (C: 1.5% ± 0.5%, BC: 2.8% ± 2%, OG: 1.9% ± 0.3%, FB: 2.5% ± 0.6%). Regarding other less abundant phyla, Latescibacteria and Acidobacteria had relative abundances of 1.9%–2.5% and 2.5%–3%, respectively, and were comparable between the control and the oyster aquaculture sites. Spirochaetes were detected in the different oyster aquaculture treatments at relative abundances higher than 1% after the middle of July, while at the control site we detected Spirochetes only in August.

Within the Proteobacteria, the Deltaproteobacteria and Gammaproteobacteria classes were the most abundant, followed by the Alphaproteobacteria in all our samples (**Figure 5**). The ASVs affiliated with Alphaproteobacteria were primarily (∼90% of the relative abundance) within the family Mitochondria (order Rickettsiales), annotated to mitochondrial 16S rRNA gene from unicellular algae. The Gammaproteobacteria were mostly assigned to genera in Chromatiales (C: 29.3% ± 4.3%, BC: 22% ± 5.9%, OG: 29.7% ± 4.1%, FB: 22.3% ± 8.1%) and to Gammaproteobacteria incertae sedis. The most abundant classes in Deltaproteobacteria were Myxococcales (C: 9.6% ± 4%, BC: 13.6% ± 7.5%, OG: 8% ± 2.2%, FB: 15.2% ± 13.6%) and Desulfobacterales. Within Desulfobacterales, highly abundant

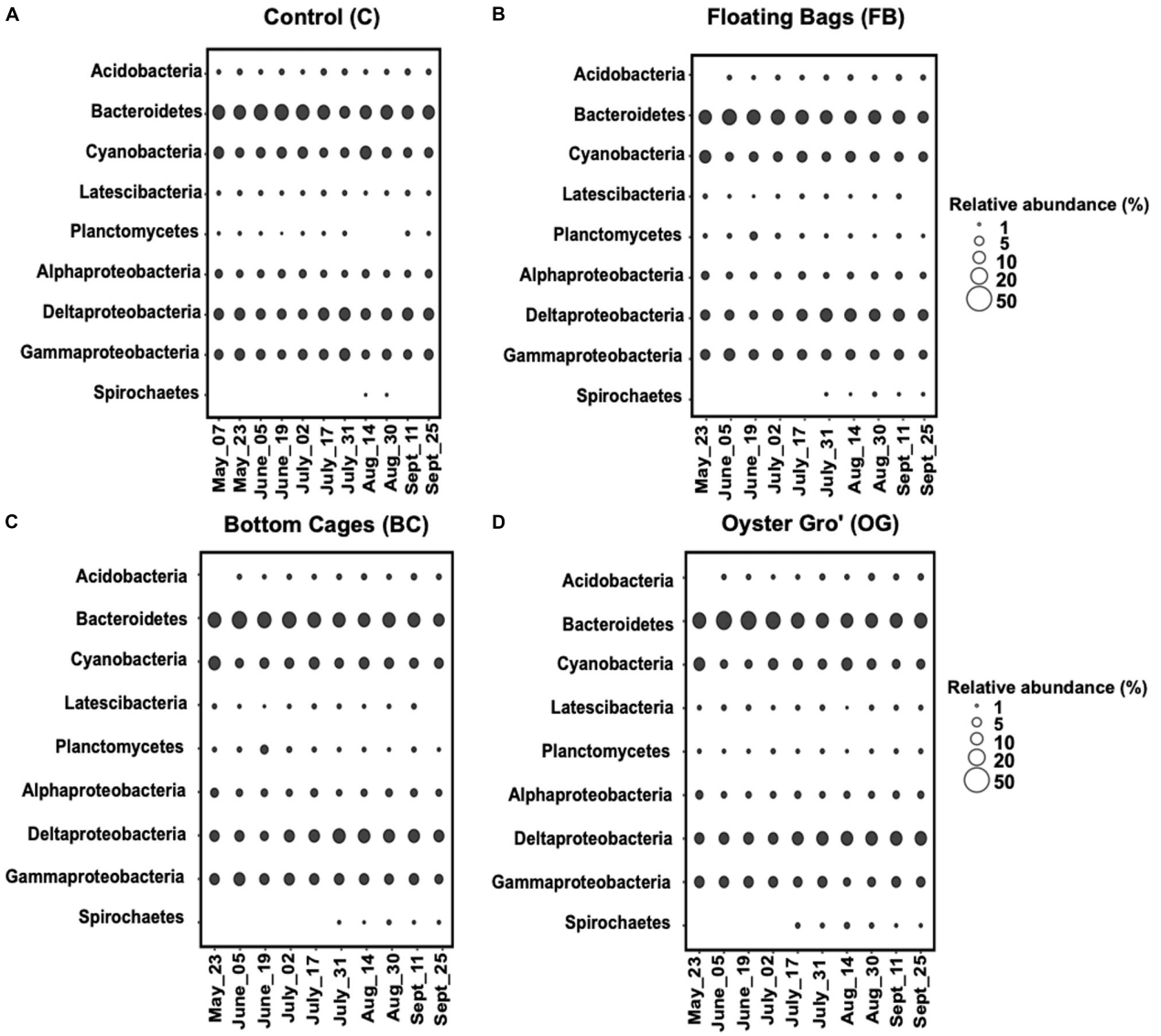

FIGURE 4 | Average relative abundance of the bacterial communities comprising over 1% at phylum level (class level for Proteobacteria) based on 16S rRNA gene sequencing per sampling date during May-September 2018. Control **(A)**, Floating Bags **(B)**, Bottom Cage **(C)**, and Oyster Gro' **(D)**. Sampling dates are presented along the *x*-axis.

taxa were in the Desulfobacteraceae family (C: 67.9% ± 6.5%, BC: 64% ± 11%, OG: 71.5% ± 7.2%, FB: 60.4% ± 14.2%). Flavobacteriales (C: 49.4% ± 12%, BC: 45.4% ± 12.7%, OG: 37.7% ± 15%, FB: 47.8% ± 13.4%) were the most abundant order within Bacteroidetes and specifically the Flavobacteriaceae family. The FB oyster site presented high (up to 68%) relative abundance of Flavobacteriales from May to June when compared to the control site and the rest of the oyster aquaculture treatments. The most abundant orders within ASVs assigned to Planctomycetes were the Phycisphaerales, Pirellulales, and Planctomycetales.

We used ordination analyses to identify possible (dis)similarities in community composition in sediments under the different oyster aquaculture treatments. The unweighted UniFRac principal coordinate analysis (PCoA) showed taxonomic overlap of the ASVs under the different oyster treatments as well as between the treatments and the control site (**Figure 6**). PCoA showed discrete phylogenetic groups that were formed at different times across the sampling season (**Figure 6**). A similar result was obtained when we generated a weighted UniFrac ordination plot using relative abundances.

RT-qPCR

Expression of Denitrification Genes

Analyses of gene expression by microbial communities can provide significant insights into microbial activities and interactions. Our RT-qPCR results for 2018 showed expression

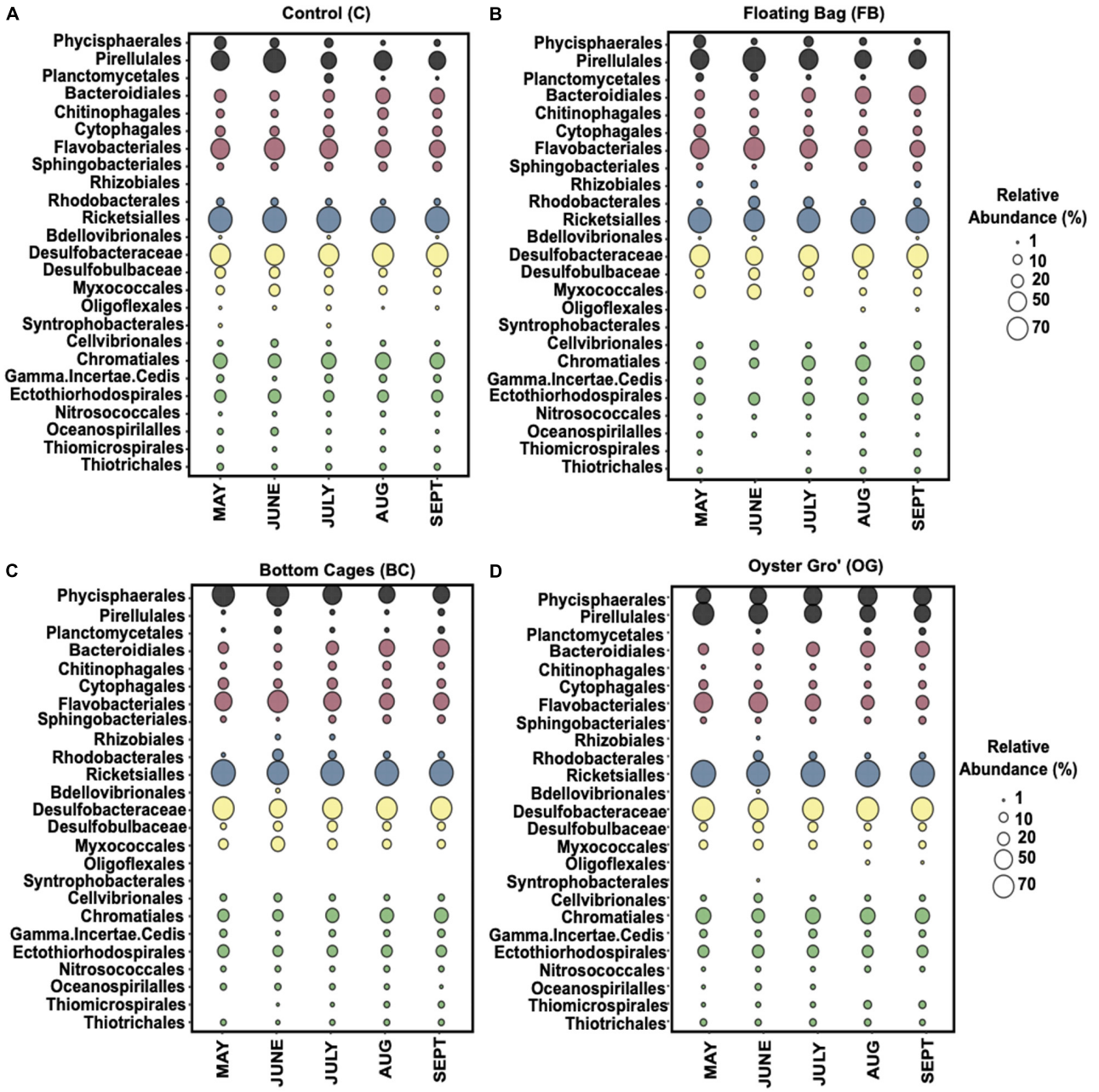

FIGURE 5 | Average relative abundance of the bacterial communities comprising over 1% at order level (family level for Deltaproteobacteria) from May until September 2018 for Control **(A)**, Floating Bags **(B)**, Bottom Cages **(C)**, and Oyster Gro' **(D)** samples based on 16S rRNA gene sequencing. Planctomycetes: black, Bacteroidetes: red, Alphaproteobacteria: blue, Deltaproteobacteria: yellow, Gammaproteobacteria: green.

of the denitrification genes *nirS*, *nirK*, *nosZ*, and *narG* in sediments from all oyster treatments and the control site (**Figure 7A**). To estimate statistically significant effects of the oyster treatments on the expression of denitrification genes, we performed a two-way ANOVA for each denitrification gene comparing the three oyster treatments and control site measurements across the time series (**Supplementary Table S5**). Findings from the least squares means (LS means) showed that *narG* expression was similar between the control and the sediment samples collected below the Bottom Cage (BC), Oyster Gro' (OG), and Floating Bag (FB) sites from May until middle of July 2018. However, at the end of July, we detected a sharp increase of *narG* expression relative to the control site under all aquaculture sites that continued until the end of September (**Figure 7A**). These increases were statistically significant when compared to the control based on the results of least squares means comparisons ($p < 0.05$). The number of *narG* transcripts detected under the different oyster

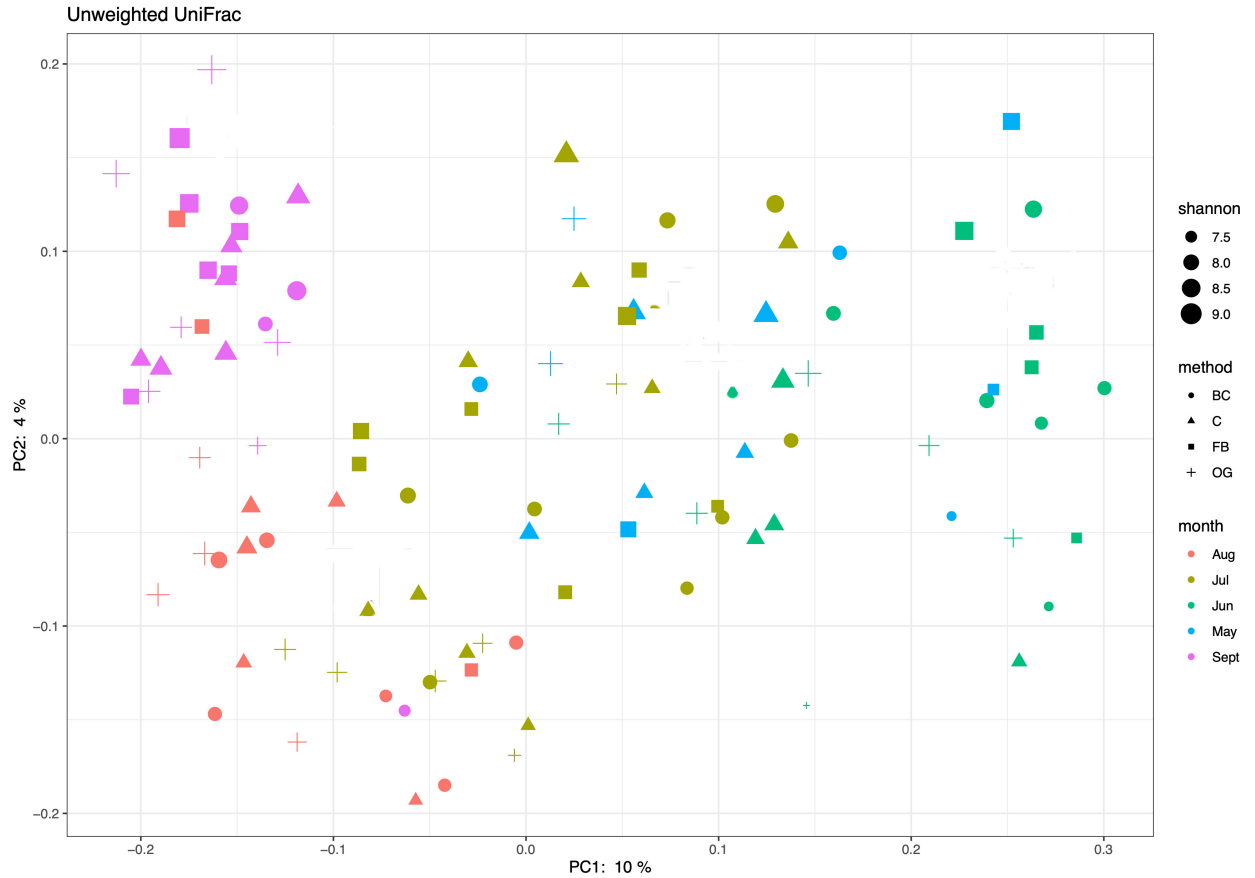

FIGURE 6 | Principal coordinates analysis (PCoA) of bacterial phylogenetic similarity based on the unweighted UniFrac results and the Shannon index.

treatments after the end of July was higher when compared to the number of copies detected earlier in the sampling period (May until mid of July 2018; **Supplementary Figure S6**). Elevated expression of *narG* after July was also detected in sediments at the control site, but was lower when compared to samples from under the aquaculture sites (**Supplementary Figure S6**). Differences in the *narG* expression were significant after July in both 2018 and 2019; however, *t*-ratios were greater in 2018, suggesting a larger deviation from the gene expression baseline detected in the control site. Elevated gene expression relative to the control was also detected for *nirS*, *nirK*, and *nosZ* (where measurable differences occurred) under the three oyster treatments (**Figure 7A** and **Supplementary Figure S6**). Expression of *nosZ* in sediments under the bottom cages was significantly lower than *nosZ* expression measured at the control site from late May to mid-July of 2018, with similar patterns observed in 2019.

Similar patterns of expression of denitrification genes were also observed in 2019 (**Figure 7B**). Sliced LS means showed that *narG* expression was significantly higher under all treatments when comparing treatments to the control site at individual time points from mid-August to late September and overall comparisons of the treatments across the time series were found to be significant (**Figure 7B** and **Supplementary Table S6**). We detected elevated gene expression of *nosZ* under FB and OG oyster treatments that was statistically significant (primarily under the OG treatment) when compared to the control site on individual sampling days ($p < 0.05$). The two-way ANOVA results showed no statistically significant differences in *nirS* across all treatments. In 2019, *nosZ* also had significantly lower overall rates of expression in sediment samples collected under the BC.

Expression of *nrfA* (DNRA)

We estimated expression of *nrfA*, the key gene in DNRA, both in 2018 and 2019. Our results showed that differences in expression levels of *nrfA* across treatments were statistically significant when compared to the control for both sampling seasons (**Figure 8** and **Supplementary Tables S5, S6**). Closer examination of sampling dates reveals different *nrfA* expression trends between the three oyster treatments. In 2018, expression of *nrfA* was consistently elevated relative to the control site in sediments collected under the BC treatment, starting at the end of June. *nrfA* expression was also relatively elevated in samples collected under the FB site beginning in July, with statistically significant differences observed in late July through the end of sampling period. The expression levels of *nrfA* in the OG samples

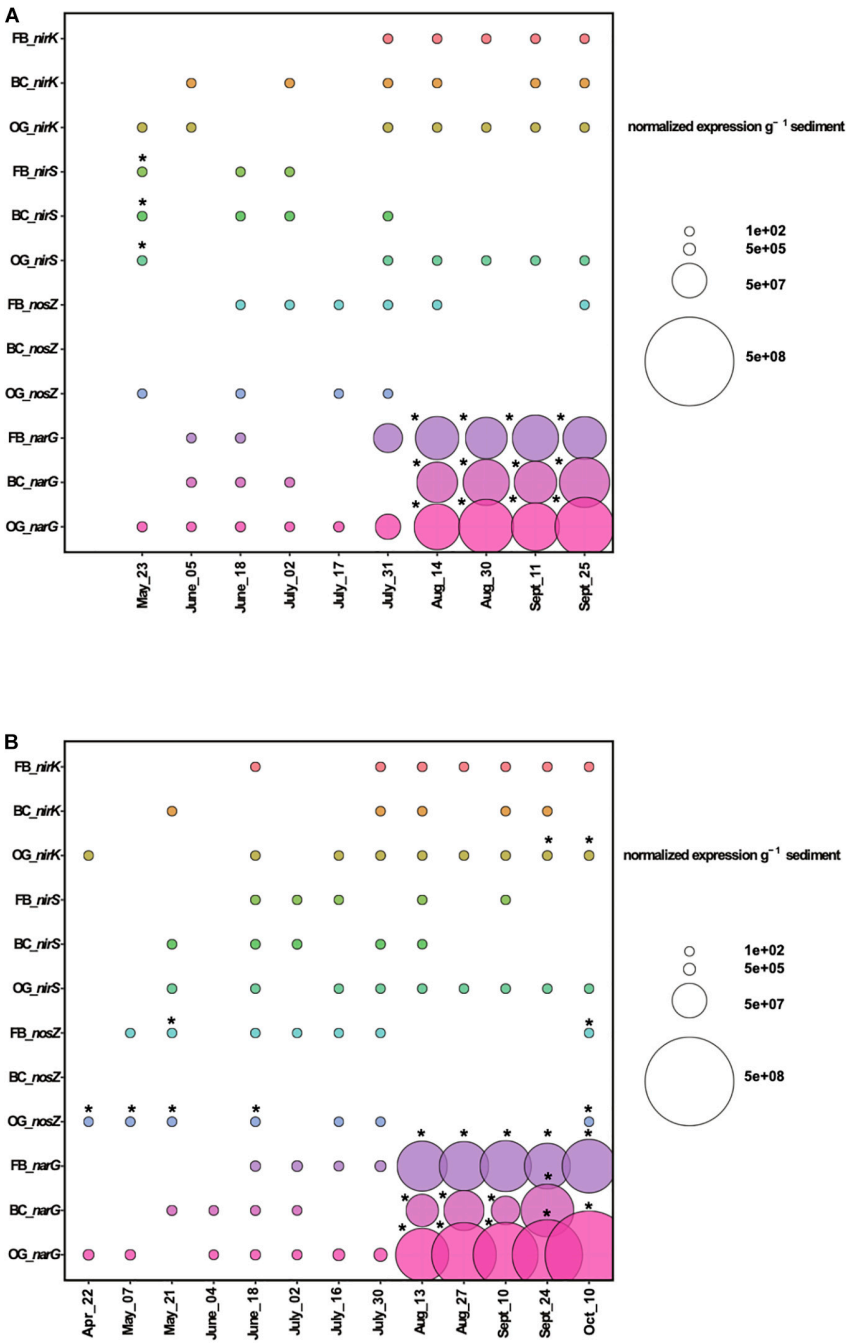

FIGURE 7 | Expression of denitrification genes above control levels (gene expression values from the control were subtracted from the values from the treatments) during 2018 **(A)** and 2019 **(B)**. FB, Floating Bags; BC, Bottom Cages and OG, Oyster Gro'. Statistically significant differences are shown with an asterisk (*t*-test, $p < 0.05$).

were significantly reduced relative to the control site ($p < 0.05$) from late July onward in 2018.

Trends in *nrfA* expression by sampling day were similar in 2019 (**Figure 8B**). We detected elevated expression of *nrfA* in BC and FB oyster treatment samples relative to the control site. OG sediment samples exhibited decreased expression relative to the control site across all sampling dates in 2019. The decreased *nrfA* expression levels were statistically significant across the time series (**Figure 8B**).

Expression of *hzo* (anammox)

We estimated the expression of *hzo* genes, responsible for the final step of anammox, across all sites (**Figure 9** and **Supplementary Tables S5, S6**). *hzo* expression across the three

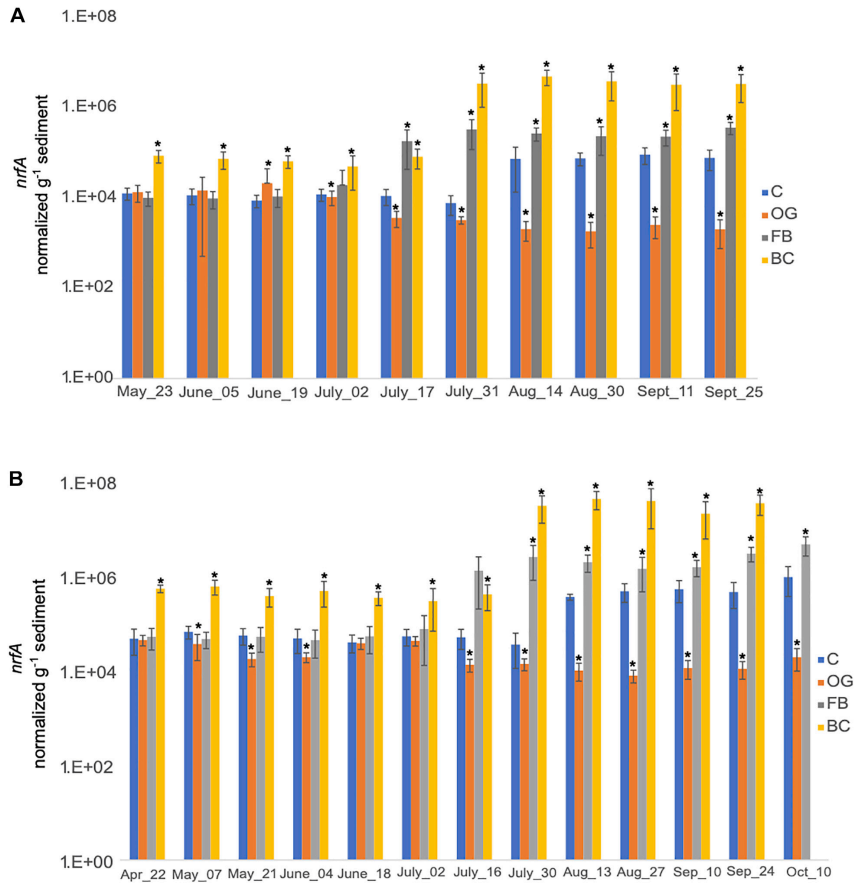

FIGURE 8 | Average copy number of *nrfA* for the three cores collected under the three oyster treatments and at the control site over the course of the sampling period in 2018 **(A)** and 2019 **(B)**. C, Control; OG, Oyster Gro'; FB, Floating Bags; BC, Bottom Cages. Statistically significant differences are marked with an asterisk (*t*-test, $p < 0.05$).

oyster treatment sites was found to be statistically significant for both 2018 and 2019 sampling seasons (**Supplementary Tables S5, S6**). In 2018, expression of *hzo* was relatively similar between the control site and the BC and FB treatments from May to late June (**Figure 9A**). Elevated expression of *hzo* was detected from mid-July through the end of the 2018 sampling period in BC sediments which was statistically significant when compared to the control. The *hzo* expression in FB sediments remained similar to the control site even after July, with the greatest change in expression levels observed in early September (**Figure 9A**). Patterns of *hzo* expression were the opposite in OG sediments relative to the other treatments and the control site. *hzo* expression in OG was slightly elevated primarily in May and early June when compared to the control and was followed by a sharp and statistically significant decrease from mid-July through the end of the 2018 sampling.

Samples collected in 2019 demonstrated similar trends with 2018. *t*-ratios indicated similar *hzo* expression between the BC, FB, and the control site from April until June, with exception in May where we detected slightly reduced expression of *hzo* in BC and FB relative to the control. A sudden and statistically significant increase in *hzo* expression levels was detected in the BC sediments from late July and through the end of the 2019 sampling period. FB sediments had similar or significantly reduced *hzo* expression across the time series. Similar to 2018, expression of *hzo* in OG oyster site was slightly elevated early in the time series (primarily in June) when compared to the control, followed by a sharp and statistically significant decrease in expression levels from the end of July through the end of 2019 sampling period.

Expression of Sulfur Oxidizing Genes (*sox* Genes)

We detected similar expression levels of sulfur oxidizing genes, *soxA* (**Figure 10A**) and *soxB* (**Figure 10B**) in samples collected underneath the different oyster aquaculture methods and the control sites. Expression of both *sox* genes showed a gradual increase in the middle of July that continued until the end of September. Slightly enhanced expression levels of *soxB* were detected in samples collected from BC and FB sediments, when compared to the controls.

Expression of *sox* genes expression in 2019 was comparable between the samples collected at the different oyster treatments

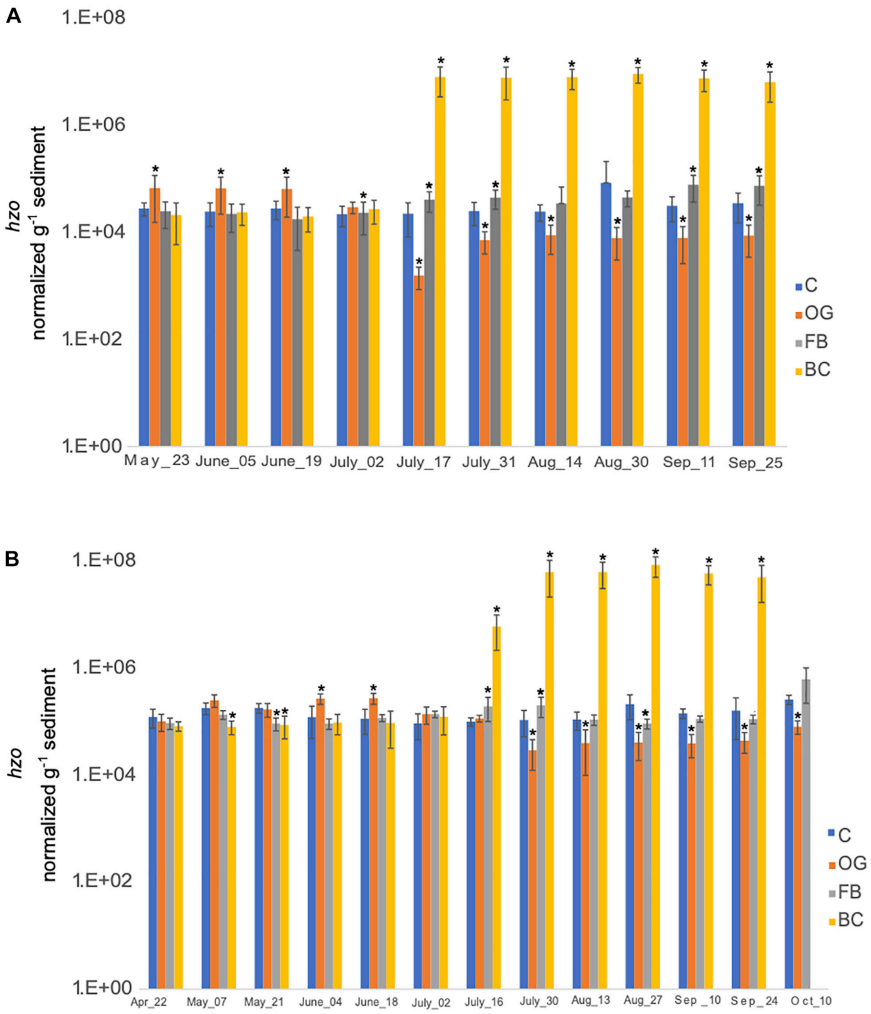

FIGURE 9 | Average copy number of *hzo* for the three cores collected under the three oyster treatments and at the control site over the course of the sampling period in 2018 **(A)** and 2019 **(B)**. C, Control; OG, Oyster Gro'; FB, Floating Bags; BC, Bottom Cages. Statistically significant differences are marked with an asterisk (*t*-test, $p < 0.05$).

and the control site. Increase in expression was detected in all samples after the middle of July (data not shown).

DISCUSSION

Excessive nitrogen loading in coastal waters is a growing topic of concern to coastal communities. Many communities see aquaculture as a potential method of removing nitrogen from the coastal waters, by growing and removing biomass. However, nitrogen removed by biomass harvesting is only part of the equation. Farming activities can also impact the sediment chemistry and microbial communities. A recent study suggests that in coastal systems with excess nitrogen loading from anthropogenic activity, oyster aquaculture may have a positive long-term effect on sediment denitrification that persists over the years (Ray et al., 2020). In most coastal sediment-hosted microbial communities nitrogen removal is a natural result of the net activities of denitrification, DNRA, and anammox processes in coastal sediments. Here we investigate how the activity of these process, as reflected by net nitrogen removal and changes in gene expression for key nitrogen cycling processes may change as function of three popular oyster aquaculture methodologies; Bottom Cages (BC), Oyster Gro' (OG), and Floating Bags (FB).

Gene Expression Within Sediment Microbial Communities and Links to Nitrogen Removal

Our analyses of expression of genes for denitrification, DNRA, and anammox showed that genes associated with nitrogen cycling respond to changes that occur in the sediments underneath the different oyster treatments. BC, OG, and FB presented distinct expression patterns of key nitrogen-cycling genes over the season. We detected a statistically significant increase in the expression of *narG* under all sites relative to the control

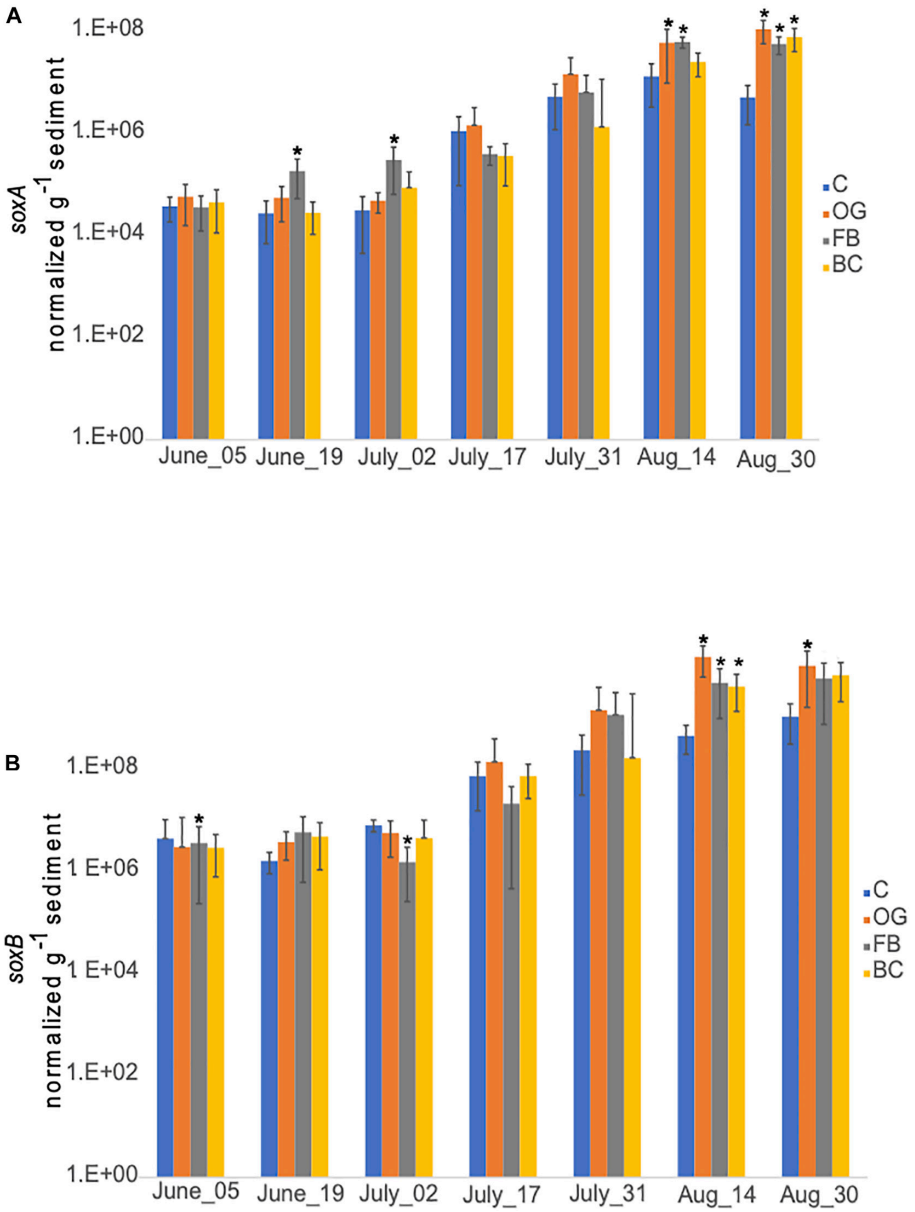

FIGURE 10 | Average copy number of *soxA* **(A)** and *soxB* **(B)** for the three cores collected under the three oyster treatments and at the control site over the course of the sampling period in 2018. C, Control; OG, Oyster Gro'; FB, Floating Bags; BC, Bottom Cages. Statistically significant differences are marked with an asterisk (*t*-test, $p < 0.05$).

site after the end of July in both years (comparisons of LS means for each sampling event). This enhanced expression of *narG* could potentially be linked to enhanced N_2 production rates and is consistent with greater and statistically significant N_2 production detected in the sediments underneath the oyster aquaculture treatments relative to the control site. Although the presence of aquaculture increased expression of *narG* and resulted in greater production of N_2 relative to background, the increase in N_2 production at all sites over the installation period indicates that environmental factors (e.g., temperature), could also contribute to the enhanced N_2 removal in Waquoit Bay. The expression of *nirS*, *nirK*, and *nosZ* were relatively consistent over the course of the growing season at all sites. Overall, our data do not show a clear link between N_2 production and the expression of *nirS*, *nirK*, and *nosZ*, although the gene expression of *nosZ* presented statistically significant differences primarily between the OG treatment and the control site. This can be partially explained by the modular nature of denitrification since it is a nitrogen cycling process that can be performed in sediments in a cooperative way by a variety of phylogenetically unrelated microorganisms that participate in different steps of the process, and to differing degrees

(Dalsgaard et al., 2014; Graf et al., 2014). Bacterial denitrifiers can host in their genome the full suite of denitrification genes or they can perform truncated denitrification that lacks the final step of the pathway (reduction of N_2O to N_2) (Braker et al., 2010; Graf et al., 2014). The expression of denitrification genes is controlled by parameters not yet fully understood that can vary among individual strains (Zumft, 1997; Wallenstein et al., 2006). Additionally, the sensitivity of denitrification gene transcripts (*nirS*, *nosZ*) to oxygen is known (Dalsgaard et al., 2014). Although our handling of sediments from the time cores were brought to shore and subsamples frozen was short (∼5–10 min), the process of subsampling may introduce enough oxygen to suppress *nirS* and *nosZ* transcription, as has been previously described (Dalsgaard et al., 2014). Collectively, these complexities illustrate the challenges of directly linking rates of nitrogen biogeochemical processes with gene expression data which can follow non-linear dynamics (Bowen et al., 2014), especially in natural ecosystems that usually host diverse bacterial communities. Finally, we need to point out that the commonly used gene-specific primer sets for RT-qPCR studies related to denitrification genes are usually designed based on sequence alignments found in publicly available database and for cultured microbes (Wallenstein et al., 2006). This can limit the RT-qPCR ability to target all variants of key denitrification genes (*nirS*, *nirK*, *nosZ*, *norB/C*), especially those deriving from uncultured taxa. Our Illumina-sequenced marker gene data (iTAGs) data showed that almost 60% of our ASVs were affiliated with uncultured taxa, which makes it difficult to assess to what degree our RT-qPCR primers were able to represent all variants of the key denitrification genes.

Our RT-qPCR data showed that the *narG* expression levels at the aquaculture sites were different when compared to those at the control site especially after July (**Figure 7** and **Supplementary Figure S6**). This indicates that the different oyster treatments were able to trigger and maintain elevated *narG* expression in the underlying sediments after July. This might have occurred due to increasing carbon and nitrogen content in the underlying sediment, via the release of oyster biodeposits which are known to deliver organic nitrogen and carbon to the sediments (Newell et al., 2002; Smyth et al., 2013). Organic matter is a prerequisite for heterotrophic denitrification since denitrifiers oxidize organic carbon inputs using nitrate as electron acceptors to gain energy. Moderate organic additions to the sediments can increase activity of benthic denitrification while high inputs of organic matter can decrease denitrification rates (Caffrey et al., 1993). The biodeposits from bivalve cultures contain 2–3 times more carbon and nitrogen than unaggregated particles (Feinman et al., 2018 and references therein) and similarly to what observed in experimental studies (Caffrey et al., 1993), their moderate or excessive release to the sediments underneath bivalve cultures can enhance or diminish denitrification (Carlsson et al., 2012). Carlsson et al. (2012) suggested that the decline of denitrification under excessive organic matter inputs from bivalve farming is due to the production of hydrogen sulfide that can inhibit denitrification (Jensen et al., 2008), nitrification (Joye and Anderson, 2008), and anaerobic ammonia oxidation (anammox) (Porubsky et al., 2009), but also can favor dissimilatory nitrate reduction to ammonium (DNRA) (Caffrey et al., 2019).

While we did not directly measure rates of DNRA, our gene expression data for *nrfA* showed that DNRA is a process that likely occurs naturally in the Waquoit Bay. However, the expression of *nrfA* increased primarily under the BC site over the season whereas *nrfA* in sediments under the OG site significantly declined in both 2018 and 2019 sampling periods (**Figures 8A,B**). The expression of *nrfA* under the FB treatments was lower than under the BC treatment and comparable to what we observed in control sediments especially before the end of July. This may indicate that DNRA is an active process in the sediments underlying oyster treatments (especially for BCs), but that the suspended (primarily), and to a lesser extent, the floating oyster culturing methods limit or inhibit DNRA. The role of DNRA has been extensively debated with regard to whether or not oyster aquaculture can promote nitrogen retention over nitrogen release (denitrification). DNRA was identified as the dominant nitrate reduction process (∼80%–96%) under suspended oyster systems, and it was suggested that limited denitrification was due to competition for nitrate between denitrification and DNRA, and the labile nature of organic matter that favors DNRA (Erler et al., 2017; Lunstrum et al., 2018). Mortazavi et al. (2015) also detected low rates of net denitrification and high ammonium fluxes in sediments underneath cages and indicated DNRA as a potential process due to the high presence of hydrogen sulfide. Vieillard (2017) found low DNRA rates (< 130 μmol m^{-2} h^{-1}) in the sediments underlying suspended nets and bottom bags/cages, with insignificant differences between oyster aquaculture sites and controls. Confounding interpretation of the role of DNRA in these systems is the observation of DNRA bacteria isolated from soils that contain "atypical" (due to their presence in non-denitrifying phyla) but functional nitrous oxide reductases genes (*nosZ*) that can contribute to nitrogen gas production (Sanford et al., 2012; Orellana et al., 2014). We do not know if these "atypical" *nosZ* genes are also expressed in marine sediment DNRA bacteria, but we argue that if they exist, then nitrogen cycling underneath bivalve cultures can be more complicated than previously anticipated.

The enhanced expression of *nrfA* detected after July, primarily in the BC oyster aquaculture, suggests that the biodeposits released from oyster treatments in close proximity to the sediment can enhance ammonium regeneration in the sediment. We hypothesize that this enhanced expression of *nrfA* especially in the BC sediments could be attributed to chemolithotrophic or fermentative DNRA, with the latter being less prominent. Fermentative DNRA couples nitrate reduction with organic matter fermentation and occurs under high carbon, non-sulfidic, and nitrate-limited conditions (Burgin and Hamilton, 2007; van den Berg et al., 2015). Oyster biodeposits, and/or active nitrification across oxic/anoxic interfaces can provide significant amounts of nitrate in the underlying sediments (Jensen et al., 1994; Newell et al., 2005 and references therein); thus, we consider that fermentative DNRA may not be the primary form of DNRA occurring underneath BC in our study. This is supported by our iTAG data that show low relative abundances (<0.5%) of fermentative bacteria that can perform

DNRA and influence the competition between denitrification and DNRA in favor of DNRA (e.g., taxa affiliated to *Clostridia*, *Vibrio*, *Desulfovibrio*, *Bacillus*, and *Pseudomonas* sp.; Burgin and Hamilton, 2007; van den Berg et al., 2017).

Chemolithotrophic DNRA can dominate under sulfidic conditions in coastal sediments since it can couple nitrate reduction to the oxidation of reduced sulfur forms, including free sulfide (H_2S, HS^-, and S^{2-}) and elemental sulfur (S^0) (Burgin and Hamilton, 2007 and references therein). While seasonal sulfide concentration dynamics are not available because we did not measure sulfide concentrations directly during both 2018 and 2019 field seasons, sediments under the BC site had visibly greater accumulations of organic material including algae, and produced a noticeable sulfidic smell from mid-summer onward. This suggests that organic matter in biodeposits released from oysters accumulates at higher concentrations under BCs, possibly enhancing sulfate reduction, and increasing production of hydrogen sulfide and other sulfur species (e.g., S^0, thiosulfates, and sulfites) below the BC site. Available metatranscriptome data was searched for expression of *dsr* genes. Expression of *dsr* genes supports the notion of active dissimilatory sulfate reduction under all treatments and also at the control site (**Supplementary Table S7**). The RT-qPCR results showed similar patterns of expression of the sulfur oxidizing genes *soxA* and *soxB*, under the different aquaculture sites and the control site (**Figure 10**). Both our metatranscriptome and RT-qPCR results indicate that sulfide production and oxidation occur naturally in Waquoit Bay sediments and also under the different oyster treatments.

Redox changes due to hydrogen sulfide accumulation can alter the rates of denitrification, anammox, and DNRA (Caffrey et al., 2019). Background hydrogen sulfide (H_2S) measured in October (2020) at our study site when the aquaculture sites were not present was 53.2 $\pm$ 2.7 μM. Caffrey et al. (2019) estimated that exposure of hypoxic sediments to low sulfide (S^{-2}) concentrations ($\sim$52 μM) can promote DNRA in the expense of denitrification, with the latter remaining still active but with lower nitrogen production rates. We believe that the possible sulfide accumulation (if occurs) in the BC oyster aquaculture method via enhanced biodeposition was not critical to inhibit oyster-mediated N_2 production via denitrification as has been previously described (Carlsson et al., 2012). A possible explanation for this can be the *in situ* biogeochemistry of the sediments in Waquoit Bay that can allow the oxidation of the sulfides that accumulate in the sediment with Mn and Fe oxides under anoxic conditions. Mn, and especially Fe, oxidants form metal-bound sulfides (e.g., iron sulfide; FeS) that do not inhibit denitrification (Brunet and Garcia-Gil, 1996). Downcore analyses of Waquoit sediments have shown black FeS underneath the oxic sediment layer (Charette et al., 2005). Mn and Fe, oxides are the dominant oxidants of sulfides in the coastal sediments with an active role on sulfur sediment dynamics (Jørgensen et al., 2019). Another possible explanation for the continuation of high N_2 production rates underneath the BC site despite the potential sulfide accumulation can be the tolerance of the *in situ* microbial community to suboptimal sulfide conditions. Microbial communities from hypoxic sediment or the oxic/anoxic interfaces of estuarine and coastal sediments seem to tolerate periodic redox fluctuations that would occur with disturbances (weather events, animal burrowing, human activities, etc.) and are able to recover from sporadic exposure to oxic or highly sulfidic conditions (Marchant et al., 2017; Caffrey et al., 2019). This can be an adaptation of the *in situ* communities to overcome tidal cycles or periodic events that affect the redox regime of the sediments. We suggest that the proximity of the oyster gear to the seafloor can influence the fate of the nitrogen transformations since it can affect oxygen circulation or promote redox changes. Our data show that DNRA appears depressed under the OG site possibly due to the increased aeration caused by that gear, as discussed below.

The same explanations can apply to the enhanced *hzo* levels that we detected underneath the BC site. *hzo* is the key gene of anaerobic ammonium oxidation (anammox), and sulfide, at micromolar concentrations, has an inhibitory effect on anammox activity (Jensen et al., 2008). However, under our BC treatments we detected enhanced expression of *hzo* coincident with seasonal expression of *narG,* indicating possibly active anammox over the sampling season despite potential sulfide accumulation. Similar *hzo* expression levels between FBs treatments and at the control site were observed for most of the 2018 and 2019 sampling periods, while statically significant depressed expression levels of both *hzo* and *nrfA* were detected almost throughout the 2018 and 2019 sampling periods under the OG treatment (**Figures 8** and **9**). This suggests that the OG equipment may introduce oxygen to the underlying sediments by creating a "piston-pumping" activity in response to wind and waves that aerate the underlying sediments. While this action has not been quantified it could limit and/or inhibit the strictly anaerobic anammox and DNRA processes. Floating bags also appear to permit enough bottom water circulation to aerate surficial sediments enough to suppress these two processes relative to BCs, although not to the extent of the OG gear. **Figure 5** shows that the control and FB and OG sites share high relative abundance of the order Pirellulales (Planctomycetes), compared to sediments below BCs. Bacterial representatives affiliated to this order can be aerobes (Dedysh et al., 2020), which can support our hypothesis of suppressed anammox activity under the OG and FB systems due to sufficient oxygen circulation underneath these gear.

Anammox is reported to have less influence than denitrification on nitrogen release from coastal ecosystems (Dalsgaard et al., 2005; Trimmer and Engström, 2011). This is consistent with observations at bivalve farming sites (Carlsson et al., 2012; Erler et al., 2017; Lunstrum et al., 2018). Our iTAGs indicate the relative abundance of Planctomycetes in our sediments is low (1%–3%); thus, we can infer that anammox makes a limited contribution to nitrogen removal in Waquoit Bay, however this requires further investigation. The potentially low anammox activity in Waquoit Bay may be insignificant when compared to the overall benefit of promoting nitrogen removal and possibly limiting or inhibiting ammonia regeneration using either the OG or FB oyster aquaculture methods. However, depending on *in situ* sediment biogeochemistry anammox activity can vary, so loss of anammox under oyster aquaculture activities might have a significant impact on overall nitrogen loss in other settings.

The possible "piston-pumping" caused by the OG gear (and to a lesser extent the FB) and consequent O_2 circulation in surficial sediments did not appear to have a negative effect on the N_2 production rates possibly induced via bacterial denitrification underneath OG and FB treatments at our study site. Denitrifiers are primarily facultative anaerobes in surficial sediments, with strict anaerobes appearing at increasing sediment depths where anoxia is more consistent (Tiquia et al., 2006). This idea is consistent with observations that denitrification in coastal sediments can be stimulated by frequent switches between oxic and anoxic conditions (influenced perhaps by tidal cycles and storm events), with denitrification occurring even under O_2 exposure (Marchant et al., 2017 and references therein). Finally, as already discussed, denitrification is a modular process where distinct groups of microorganisms can mediate different steps of the process (Dalsgaard et al., 2014; Graf et al., 2014). Thus, a metabolic strategy that can be more resistant to sporadic changes in oxygen at coastal sediments. Finally, we note that sample handling (subsampling of cores in the field and dispensing to sterile containers prior to freezing) exposes sediment microbiota to oxygen, and while handling was consistent for all samples in this study, expression of genes for some oxygen-sensitive processes may be negatively affected to an unknown degree, and thus, be higher than we report.

Bacterial Sediment Communities and Nitrogen Fluxes

The structure and composition of sediment bacterial communities were similar underneath the different aquaculture practices and the control site, and were dominated by three highly abundant phyla; Bacteroidetes, Cyanobacteria, and Proteobacteria (**Figure 4**). Bacteroidetes is a cosmopolitan phylum colonizing marine and freshwater sediments (Klier et al., 2018) with high abundances especially in coastal areas (Fernández-Gómez et al., 2013). Generally, Bacteroidetes are known for their ability to grow in association with particles and for their capacity to degrade polymers (Fernández-Gómez et al., 2013). Bacteroidetes may also be able to colonize biodeposits released from the oysters, however, this requires further investigation. Within Bacteroidetes there were five dominant orders including Bacteroidales, Flavobacteriales, Cytophagales, Chitinophagales, and Sphingobacteriales at both control and oyster aquaculture sites. Bacteroidales was the only taxon that showed a seasonal trend with elevated relative abundances after the end of June under all the examined aquaculture treatments (**Figure 5**). The seasonal increase of Bacteroidales can be due to increased presence of particles (biodeposits) and/or related to nitrogen cycling processes. For the latter we can only speculate that it is denitrification, since we know that Bacteroidetes have the *nirK*/*nirS* and *nosZ* genes in their genomes and thus, can perform specific steps of denitrification (Graf et al., 2014). These possibilities, however, require further investigation.

Proteobacteria were dominated by the classes Deltaproteobacteria, Gammaproteobacteria, and Alphaproteobacteria (**Figure 4**). Genera that belong to Proteobacteria can do denitrification *sensus stricto* (complete denitrification; they host *nir*/*nor*/*nosZ* genes in their genomes) while the majority of Proteobacteria have mainly the *nir*/*nor* genes (Graf et al., 2014). In Alphaproteobacteria, besides the family Mitochondria (order Rickettsiales) that dominated at all sites, the other less abundant taxa (<10% relative abundance) were Rhodobacterales (Rhodobacteraceae) and Rhizobiales. Members of the Rhodobacteraceae family are abundant in coastal sites with high nutrient availability and anoxic, or anoxic/sulfidic (euxinic) regimes (Pohlner et al., 2019). Genera that belong to Rhizobiales have *nirS* and *nirK* genes so they are also potential denitrifiers (Rasigraf et al., 2017).

Within Gammaproteobacteria the dominant order at all sites including our control site was Chromatiales. Genera and species affiliated to Chromatiales are sulfur oxidizers known to utilize the accumulated sulfides, or thiosulfates to produce S^0 (Imhoff, 2005). Chromatiales can proliferate when sediments are nitrate-replete, possibly performing chemolithotrophic denitrification (Aoyagi et al., 2015). Chemolithotrophic denitrification might be a naturally occurring process at the Waquoit Bay sediments, and we suggest that it can take place underneath the different oyster treatments especially after July. Other dominant orders within Gammaproteobacteria were aerobic ammonia oxidizers (Nitrosococcales; Ward and O'Mullan, 2002), heterotrophic denitrifiers (Oceanospiralles; Llorens-Marès et al., 2015; Marchant et al., 2017), and other taxa related with sulfur/hydrogen sulfide oxidation (Thiotrichales, Thiomicrospirales, and Ectothiorhodospiraceae; Robinson et al., 2016). Finally, our iTAG data showed dominant sulfate reducing microorganisms (SRM) within the order Desulfobacterales (Desulfobacteraceae) under the different oyster aquaculture treatments and at the control site.

The taxonomic composition of our bacterial communities is consistent with previous studies of Waquoit Bay (Coskun et al., 2019), and with studies of bacterial communities underneath oyster aquaculture sites (Azandégbé et al., 2012). The principal component ordination analysis (PCoA) based on bacterial phylogenetic similarity of communities collected from all sites (control and oyster aquaculture) over the season indicated discrete groups formed along the sampling season, that cannot be explained solely by observed minor differences at the class/order level. A significant portion of our ASVs (∼60%) below the order/family taxonomic levels is affiliated with "uncultured" taxa, about which little is known. The observed discrete groups could be be driven by changes in these uncultured taxa. These taxa may also contribute (together with our assigned denitrifying and anammox phyla) to elevated nitrogen production rates that occurred after the end of June in both 2018 and 2019. Some of these uncultured taxa in Waquoit Bay have been described as "microbial dark matter" with micro-aerophilic and anaerobic lifestyles, and show metabolic flexibility under anoxic and euxinic conditions (Coskun et al., 2019). This supports further the idea that bacterial communities in coastal sediments might be more tolerant than previously assumed of fluctuations in oxygen and sulfide (Marchant et al., 2017; Caffrey et al., 2019), and with

possible consequences for nitrogen cycling processes that occur underneath aquaculture sites.

Bacterial communities underlying our aquaculture systems enhanced nitrogen removal when compared to control sediments. Observable accumulations of organic material below each aquaculture site were evident, particularly under the BC's (**Supplementary Table S3**). Future investigations would benefit from photo-documentation of the time-course evolution of increasing organic material below study sites due to oyster biodeposits and biofouling of gear. Additionally, from this study we have learned that sulfide concentration data prior to site installation and then gathered throughout the season in 2 or more years at the same site would be tremendously valuable for understanding biogeochemical shifts in sediments underlying oyster aquaculture, whether biodeposits drive sediments toward sulfide concentrations that start to depress the sulfide-sensitive processes of denitrification and anammox, and start to favor DNRA. While N_2 production rates also increase over the course of the summer at the control site, this pattern is magnified at each of the treatment sites. The last two months of the growing season during both 2018 and 2019, had significant increases in N_2 flux from the sediments under each of the aquaculture treatments compared to the control sediments with the daily flux rates increasing ∼two- to four-fold over the referenced control site (**Figure 3**). The variability of flux measurements within a particular site likely represents the inherent heterogeneity of the sediments (i.e., presence/absence of bioturbators, disturbances, local concentrations of organic matter, etc.). Additionally, we observe an increase in the carbon content at each site over the growing season (**Supplementary Table S3**). The addition of carbon to the sediments is constituent with the measured N_2 production fluxes. Moreover, the overall patterns are consistent year to year. Flux rates, and carbon and nitrogen content of the sediments at our control site were on par with rates under each of our treatment sites at the beginning of the second aquaculture season (2019) when oysters were returned to the site, indicating that sediments under aquaculture sites in Waquoit Bay returned to control conditions during the winter. Taken together with the molecular data we view this system as primed for nitrogen removal, that is enhanced through the activity of the overlying oyster aquaculture. The activity of the oysters does not change the structure of the underlying microbial but rather increases the activity of the natural community, with individual gear types influencing the balance between different nitrogen cycling processes.

CONCLUSION

This study examines the effect of different oyster aquaculture methods to stimulate nitrogen removal from the underlying sediments. We show that all three aquaculture methods stimulated nitrogen removal (i.e., greater N_2 flux relative to a control site). An increase in the abundance of genes associated with nitrogen cycling was observed under our aquaculture sites which suggests that underlying microbial communities actively respond to changes caused by the deployments. A smaller magnitude seasonal increase in the expression of nitrogen cycling genes at our control site was observed. We acknowledge that our control site could be influenced by our nearby oyster deployments via the tidal cycles that can transport suspended material. However, the shallow depths and east-west fetch of the bay would minimize these influences at our control site location. Additionally, N_2 production rates were significantly different between the control site and the different treatment sites, which indicates that nitrogen removal processes are affected by released organic material from the oysters (and possibly accumulation of additional organic material under the BCs). Floating bags and the suspended oyster deployments (OG) can distribute biodeposits over larger areas than BCs, diluting the impact of denitrification and thus nitrogen removal (Lunstrum et al., 2018), but we argue OGs and FBs (to a lesser extent) can also limit DNRA because they increase oxygenation of surface sediments. The consequence of this is that OG and FB (to a lesser extent) methods can limit nitrogen retention in the overlaying sediment in the form of ammonium.

The hydrodynamic setting (water depth, bottom characteristics, exposure to wind and waves), the method of oyster cultivation, and the stocking density of the oysters, can all affect nitrogen cycling via influences on availability of organic matter, nitrate, and O_2 (Lunstrum et al., 2018). More work is needed to understand the effect of these factors on net nitrogen removal. Sulfur and sulfur-speciation can affect nitrogen cycling and therefore should be considered prior to the deployment of oysters at potential aquaculture sites where nitrogen removal is a priority. Here, we show that nitrogen removal underneath the different oyster treatments is active and that DNRA, which can be counter-productive to nitrogen removal because it leads to retention of nitrogen in sediments in the form of ammonium, can be influenced by the oyster farming method. The dynamic complexity of these many factors can be the reason behind the diverse results researchers have obtained regarding impact of oyster culturing on nitrogen removal from coastal settings. Monitoring of sulfide and organic content of sediments at aquaculture sites can help stakeholders to predict whether anticipated nitrogen removal rates at their site will follow patterns observed in Waquoit Bay, or whether nitrogen-retaining processes may be favored over time. One way to combat nitrogen retention that should be the topic of further study is the relocation of the aquaculture site in subsequent years to optimize microbially mediated nitrogen removal.

DATA AVAILABILITY STATEMENT

Amplicon and RNA-Seq sequences were deposited into NCBI SRA BioProject # PRJNA579576 under accessions SRR13101311–SRR13101212 and SRR13101827–SRR13101797 respectively.

AUTHOR CONTRIBUTIONS

PM wrote the first version of the draft with contributions from DR and VE. PM, DR, VE, and TS incorporated changes after reviewers suggestions. VE, CM, and DR conceived and planned the experiments. CM and CL installed the aquaculture systems. PM, VE, DB, RC, MC, CF, PG, SL, KP, AP, NS, and DR conducted field and laboratory analyses. TS contributed to statistical analyses. TR was the collaboration lead. All authors contributed to the article and approved the submitted version.

FUNDING

This work was supported by the National Oceanic and Atmospheric Administration and National Estuarine Research Reserve System Science Collaborative, award NAI4NOS4190145 (subaward 3004686666) to DR and VE.

ACKNOWLEDGMENTS

We acknowledge Dr. Andrew Solow at WHOI for invaluable advice on applications of statistical analyses to our data. We would also like to acknowledge Dr. Maria G. Pachiadaki (WHOI) for her assistance with metatranscriptome and iTAG analyses and graphics. Dr. Lindsay Hinkle, Adam Ziegler, Fatima Seuffert (Stonehill College), and Nan Trowbridge (NOSAMS, WHOI) for their field assistance.

SUPPLEMENTARY MATERIAL

The Supplementary Material for this article can be found online at: https://www.frontiersin.org/articles/10.3389/fmars.2021.633314/full#supplementary-material

Supplementary Figure 1 | Average porewater nitrate **(A)** and ammonia **(B)** concentrations in 2018.

Supplementary Figure 2 | Average porewater nitrate **(A)** and ammonia **(B)** concentrations in 2019.

Supplementary Figure 3 | Water temperature, salinity, and oxygen measurements at 30 cm depth in 2018 **(A)** and 2019 **(B)**. Uniform/consistent values were recorded at other depths in both years (**Supplementary Table S1**).

Supplementary Figure 4 | Hierarchical clustering of the three biological replicates from Control **(A)** and Floating Bags **(B)** oyster treatments using the Bray–Curtis dissimilarity index.

Supplementary Figure 5 | Hierarchical clustering of the three biological replicates from the Bottom Cages **(A)** and the Oyster Gro' **(B)** oyster treatments using the Bray–Curtis dissimilarity index.

Supplementary Figure 6 | Average normalized abundance of denitrification genes expressed in the underlying sediments of the three oyster deployments during the biweekly sampling over the 2018 **(A–D)** and 2019 **(A–D)** sampling periods.

REFERENCES

An, S., and Gardner, W. S. (2002). Dissimilatory nitrate reduction to ammonium (DNRA) as a nitrogen link, versus denitrification as a sink in a shallow estuary. *Mar. Ecol. Prog. Ser.* 237, 41–50. doi: 10.3354/meps237041

Anderson, D. M., Glibert, P. M., and Burkholder, J. M. (2002). Harmful algal blooms and eutrophication: nutrient sources, composition, and consequences. *Estuaries* 25, 704–726. doi: 10.1007/bf02804901

Aoyagi, T., Kimura, M., Yamada, N., Navarro, R. R., Itoh, H., Ogata, A., et al. (2015). Dynamic transition of chemolithotrophic sulfur-oxidizing bacteria in response to amendment with nitrate in deposited marine sediments. *Front. Microbiol.* 6:426. doi: 10.3389/fmicb.2015.00426

Azandégbé, A., Poly, F., Andrieux-Loyer, F., Kérouel, R., Philippon, X., and Nicolas, J. L. (2012). Influence of oyster culture on biogeochemistry and bacterial community structure at the sediment-water interface. *FEMS Microbiol. Ecol.* 82, 102–117. doi: 10.1111/j.1574-6941.2012.01410.x

Bokulich, N. A., Kaehler, B. D., Rideout, J. R., Dillon, M., Bolyen, E., Knight, R., et al. (2018). Optimizing taxonomic classification of marker-gene amplicon sequences with QIIME 2's q2-feature-classifier plugin. *Microbiome* 6:90.

Bolyen, E., Rideout, J. R., Dillon, M. R., Bokulich, N. A., Abnet, C. C., Al-Ghalith, G. A., et al. (2019). Reproducible, interactive, scalable and extensible microbiome data science using QIIME 2. *Nat. Biotechnol.* 37, 852–857.

Bowen, J. L., Babbin, A. R., Kearns, P. J., and Ward, B. B. (2014). Connecting the dots: linking nitrogen cycle gene expression to nitrogen fluxes in marine sediment mesocosms. *Front. Microbiol.* 5:429. doi: 10.3389/fmicb.2014.00429

Bowen, J. L., Kroeger, K. D., Tomasky, G., Pabich, W. J., Cole, M. L., Carmichael, R. H., et al. (2007). A review of land-sea coupling by groundwater discharge of nitrogen to New England estuaries: mechanisms and effects. *J. Appl. Geochem.* 22, 175–191. doi: 10.1016/j.apgeochem.2006.09.002

Braker, G., Fesefeldt, A., and Witzel, K. P. (1998). Development of PCR primer systems for amplification of nitrite reductase genes (*nirK* and *nirS*) to detect denitrifying bacteria in environmental samples. *Appl. Environ. Microbiol.* 64, 3769–3775. doi: 10.1128/aem.64.10.3769-3775.1998

Braker, G., Schwarz, J., and Conrad, R. (2010). Influence of temperature on the composition and activity of denitrifying soil communities. *FEMS Microbiol Ecol.* 73, 134–148.

Bru, D., Sarr, A., and Philippot, L. (2007). Relative abundances of *proteobacteria*l membrane-bound and periplasmic nitrate reductases in selected environments. *Appl. Environ. Microbiol.* 73, 5971–5974. doi: 10.1128/aem.00643-07

Brunet, R. C., and Garcia-Gil, L. J. (1996). Sulfide-induced dissimilatory nitrate reduction to ammonia in anaerobic freshwater sediments. *FEMS Microbiol. Ecol.* 21, 131–138. doi: 10.1111/j.1574-6941.1996.tb00340.x

Burgin, A. J., and Hamilton, S. K. (2007). Have we overemphasized the role of denitrification in aquatic ecosystems? A review of nitrate removal pathways. *Front. Ecol. Environ.* 5, 89–96. doi: 10.1890/1540-9295(2007)5[89:hwotro]2.0.co;2

Caffrey, J., Sloth, N., Kaspar, H., and Blackburn, T. (1993). Effect of organic loading on nitrification and denitrification in a marine sediment microcosm. *FEMS Microb. Ecol.* 12, 159–167. doi: 10.1111/j.1574-6941.1993.tb00028.x

Caffrey, J. M., Bonaglia, S., and Conley, D. J. (2019). Short exposure to oxygen and sulfide alters nitrification, denitrification, and DNRA activity in seasonally hypoxic estuarine sediments. *FEMS Microbiol. Lett.* 366:fny288.

Cannon, J., Sanford, R. A., Connor, L., Yang, W. H., and Chee-Sanford, J. (2019). Optimization of PCR primers to detect phylogenetically diverse *nrfA* genes associated with nitrite ammonification. *J. Microb. Meth.* 160, 49–59. doi: 10.1016/j.mimet.2019.03.020

Carlsson, M., Engström, P., Lindahl, O., Ljungqvist, L., Petersen, J., Svanberg, L., et al. (2012). Effects of mussel farms on the benthic nitrogen cycle on the Swedish west coast. *Aquac. Int.* 2, 177–191. doi: 10.3354/aei00039

Carmichael, R. H., Walton, W., and Clark, H. (2012). Bivalve-enhanced nitrogen removal from coastal estuaries. *Can. J. Fish. Aquat. Sci.* 69, 1131–1149. doi: 10.1139/f2012-057

Chapelle, A., Menesguen, A., Deslous-Paoli, J.-M., Souchu, P., Mazouni, N., Vaquer, A., et al. (2000). Modelling nitrogen, primary production and oxygen in a Mediterranean lagoon: impact of oysters farming and inputs from the watershed. *Ecol. Model.* 127, 161–181. doi: 10.1016/s0304-3800(99)00206-9

Charette, M. A., Sholkovitz, E. R., and Hansel, C. M. (2005). Trace element cycling in a subterranean estuary: part 1. Geochemistry of the permeable sediments. *Geochim. Cosmochim. Acta* 69, 2095–2109. doi: 10.1016/j.gca.2004.10.024

Clements, J. C., and Comeau, L. A. (2019). Nitrogen removal potential of shellfish aquaculture harvests in eastern Canada: a comparison of culture methods. *Aquac. Rep.* 13:100183. doi: 10.1016/j.aqrep.2019.100183

Correll, D. L., Jordan, T. E., and Weller, D. E. (1992). Nutrient flux in a landscape: effects of coastal land use and terrestrial community mosaic on nutrient transport to coastal waters. *Estuaries* 15, 431–442. doi: 10.2307/1352388

Coskun, ÖK., Özen, V., Wankel, S. D., and Orsi, W. D. (2019). Quantifying population-specific growth in benthic bacterial communities under low oxygen using $H_2{}^{18}O$. *ISME J.* 13, 1546–1559. doi: 10.1038/s41396-019-0373-4

Dalsgaard, T., Stewart, F. J., Thamdrup, B., De Brabandere, L., Revsbech, N. P., Ulloa, O., et al. (2014). Oxygen at nanomolar levels reversibly suppresses process rates and gene expression in anammox and denitrification in the oxygen minimum zone off Northern Chile. *mBio* 5:e01966-14.

Dalsgaard, T., Thamdrup, B., and Canfield, D. E. (2005). Anaerobic ammonium oxidation (anammox) in the marine environment. *Res. Microbiol.* 156, 457–464. doi: 10.1016/j.resmic.2005.01.011

Dedysh, S. N., Kulichevskaya, I. R., Beletsky, A. V., Ivanova, A. A., Rijpstra, I. C., Damsté, S. J. S., et al. (2020). *Lacipirellula parvula* gen. nov., sp. nov., representing a lineage of planctomycetes widespread in low-oxygen habitats, description of the family *Lacipirellulaceae* fam. nov. and proposal of the orders *Pirellulales* ord. nov., *Gemmatales* ord. nov. and *Isosphaerales* ord. nov. *Syst. Appl. Microbiol.* 43:126050. doi: 10.1016/j.syapm.2019.126050

Devol, A. H. (2015). Denitrification, anammox, and N_2 production in marine sediments. *Ann. Rev. Mar. Sci.* 7, 403–423. doi: 10.1146/annurev-marine-010213-135040

Dixon, R. (2003). VEGAN, a package of R functions for community ecology. *J. Veg. Sci.* 14, 927–930. doi: 10.1111/j.1654-1103.2003.tb02228.x

Erler, D. V., Welsh, D. T., Bennet, W. W., Meziane, T., Hubas, C., Nizzoli, D., et al. (2017). The impact of suspended oyster farming on nitrogen cycling and nitrous oxide production in a sub-tropical Australian estuary. *Estuar. Coast. Shelf Sci.* 192, 117–127. doi: 10.1016/j.ecss.2017.05.007

Feinman, S. G., Farah, Y. R., Bauer, J. M., and Bowen, J. L. (2018). The influence of oyster farming on sediment bacterial communities. *Estuar. Coast.* 41, 800–814. doi: 10.1007/s12237-017-0301-7

Fernández-Gómez, B., Richter, M., Schüler, M., Pinhassi, J., Acinas, S. G., González, J. M., et al. (2013). Ecology of marine bacteroidetes: a comparative genomics approach. *ISME J.* 7, 1026–1037. doi: 10.1038/ismej.2012.169

Glibert, P. M., Anderson, D. A., Gentien, P., Granéli, E., and Sellner, K. G. (2005). The global, complex phenomena of harmful algal blooms. *J. Oceanogr.* 18, 136–147. doi: 10.5670/oceanog.2005.49

Glibert, P. M., Heil, C. A., Wilkerson, F. P., and Dugdale, R. C. (2018). "Nutrients and harmful algal blooms: dynamic kinetics and flexible nutrition," in *Global Ecology and Oceanography of Harmful Algal Blooms. Ecological Studies (Analysis and Synthesis)*, eds P. Glibert, E. Berdalet, M. Burford, G. Pitcher, and M. Zhou (Cham: Springer Nature). doi: 10.1007/978-3-319-70069-4_6

Graf, D. R. H., Jones, C. M., and Hallin, S. (2014). Intergenomic comparisons highlight modularity of the denitrification pathway and underpin the importance of community structure for N_2O emissions. *PLoS One* 9:e114118. doi: 10.1371/journal.pone.0114118

Henry, S., Baudouin, E., Lopez-Gutierrez, J. C., Martin-Laurent, F., Brauman, A., and Philippot, L. (2004). Quantification of denitrifying bacteria in soils by nirK gene targeted real-time PCR. *J. Microbiol. Methods* 59, 327–335. doi: 10.1016/j.mimet.2004.07.002

Higgins, C., Tobias, C., Piehler, M., Smyth, A., Dame, R., Stephenson, K., et al. (2013). Effect of aquacultured oyster biodeposition on sediment N_2 production in Chesapeake Bay. *Mar. Ecol. Progr. Ser.* 473, 7–27. doi: 10.3354/meps10062

Hoellein, T. J., and Zarnoch, C. B. (2014). Oysters in an Eastern Estuary. *Bull. Ecol. Soc. Am.* 95, 82–84. doi: 10.1890/0012-9623-95.1.82

Howarth, R., Chan, F., Conley, D. J., Garnier, J., Doney, S. C., Marino, R., et al. (2011). Coupled biogeochemical cycles: eutrophication and hypoxia in temperate estuaries and coastal marine ecosystems. *Front. Ecol. Environ.* 9, 18–26. doi: 10.1890/100008

Howarth, R. W. (1988). Nutrient limitation of net primary production in marine ecosystems. *Annu. Rev. Ecol. Evol. Syst.* 19, 89–110. doi: 10.1146/annurev.es.19.110188.000513

Hu, Z., Wessels, H. J. C. T., van Alen, T., Jetten, M. S. M., and Kartal, B. (2019). Nitric oxide-dependent anaerobic ammonium oxidation. *Nat. Commun.* 10:1244.

Humphries, A. T., Ayvazian, S. G., Carey, J. C., Hancock, B. T., Grabbert, S., Cobb, D., et al. (2016). Directly measured denitrification reveals oyster aquaculture and restored oyster reefs remove nitrogen at comparable high rates. *Front. Mar. Sci.* 3:74. doi: 10.3389/fmars.2016.00074

Imhoff, J. F. (2005). "Order I. *Chromatiales* ord. nov," in *Bergey's Manual of Systematic Bacteriology, (The Proteobacteria), Part B (The Gamma proteobacteria)*, 2nd Edn, Vol. 2, eds D. J. Brenner, N. R. Krieg, J. T. Staley, and G. T. Garrity (New York: Springer), 1–3. doi: 10.1002/9781118960608.obm00096

Jensen, K., Sloth, N. P., Rixaard-Petersen, N., Rysgaard, S., and Revsbech, N. P. (1994). Regulationof the coupling between nitrification and denitrification in sediment as studied with a microsensor for nitrate. *Appl. Environ. Microbial.* 60, 2094–2100.

Jensen, M. M., Kuypers, M. M., Gaute, L., and Thamdrup, B. (2008). Rates and regulation of anaerobic ammonium oxidation and denitrification in the Black Sea. *Limnol. Oceanogr.* 53, 23–36. doi: 10.4319/lo.2008.53.1.0023

Jordan, S. J. (1987). *Sedimentation and Remineralization Associated with Biodeposition by the American Oyster Crassostrea virginica (Gmelin)*. Doctoral thesis, University of Maryland, College Park, MD.

Jørgensen, B. B., Findlay, A. J., and Pellerin, A. (2019). The biogeochemical sulfur cycle of marine sediments. *Front. Microbiol.* 10:849. doi: 10.3389/fmicb.2019.00849

Joye, S. B., and Anderson, I. C. (2008). "Nitrogen cycling in coastal sediments," in *Nitrogen in the Marine Environment*, 2nd Edn, eds D. G. Capone, D. A. Bronk, M. R. Mulholland, and E. J. Carpenter (Amsterdam: Academic Press), 868–915.

Kartal, B., and Keltjens, J. T. (2016). Anammox biochemistry: a tale of Heme c Proteins. *Trends Biochem Sci.* 41, 998–1011. doi: 10.1016/j.tibs.2016.08.015

Kellogg, L. M., Cornwell, J. C., Owens, M. S., and Paynter, K. T. (2013). Denitrification and nutrient assimilation on a restored oyster reef. *Mar. Ecol. Prog. Ser.* 480, 1–19. doi: 10.3354/meps10331

Klier, J., Dellwig, O., Leipe, T., Jürgens, K., and Herlemann, D. (2018). Benthic bacterial community composition in the oligohaline-marine transition of surface sediments in the Baltic Sea based on rRNA analysis. *Front. Microbiol.* 9:236. doi: 10.3389/fmicb.2018.00236

Krishnani, K. K., Gopikrishna, G., Pillai, S. M., and Gupta, B. P. (2010). Abundance of sulphur-oxidizing bacteria in coastal aquaculture using *soxB* gene analyses. *Aquac. Res.* 41, 1290–1301. doi: 10.1111/j.1365-2109.2009.02415.x

Kroeger, K. D., Cole, M. L., York, J. K., and Valiela, I. (2006). Nitrogen loads to estuaries from waste water plumes: modeling and isotopic approaches. *Ground Water* 44, 188–200. doi: 10.1111/j.1745-6584.2005.00130.x

Li, M., and Gu, J.-D. (2011). Advances in methods for detection of anaerobic ammonium oxidizing (anammox) bacteria. *Appl. Microbiol. Biotechnol.* 90, 1241–1252. doi: 10.1007/s00253-011-3230-6

Llorens-Marès, T., Yooseph, S., Goll, J., Hoffman, J., Vila-Costa, M., Borrego, C. M., et al. (2015). Connecting biodiversity and potential functional role in modern euxinic environments by microbial metagenomics. *ISME J.* 9, 1648–1661. doi: 10.1038/ismej.2014.254

Lunstrum, A., McGlathery, K., and Smyth, A. (2018). Oyster (*Crassostrea virginica*) aquaculture shifts sediment nitrogen processes toward mineralization over denitrification. *Estuar. Coast.* 41, 1130–1146. doi: 10.1007/s12237-017-0327-x

Maio, C. V., Donnelly, J. P., Sullivan, R., Madsen, S. M., Weidman, C. R., Gontz, A. M., et al. (2016). Sediment dynamics and hydrographic conditions during storm passage, Waquoit Bay, Massachusetts. *Mar. Geol.* 381, 67–86. doi: 10.1016/j.margeo.2016.07.004

Marchant, H. K., Ahmerkamp, S., Lavik, G., Tegetmeyer, H. E., Graf, J., Klatt, J. M., et al. (2017). Denitrifying community in coastal sediments performs aerobic and anaerobic respiration simultaneously. *ISME J.* 11, 1799–1812. doi: 10.1038/ismej.2017.51

Mazouni, N., Gaertner, J.-C., Deslous-Paoli, J.-M., Landrein, S., and Geringer d'Oedenberg, M. (1996). Nutrient and oxygen exchanges at the water-sediment interface in a shellfish farming lagoon (Thau, France). *J. Exp. Mar. Biol. Ecol.* 205, 91–113. doi: 10.1016/s0022-0981(96)02594-4

Mohan, S. B., and Cole, J. A. (2007). "The dissimilatory reduction of nitrate to ammonia by anaerobic bacteria," in *Biology of the Nitrogen Cycle*, eds H. Bohe, S. Ferguson, and W. E. Newton (Amsterdam: Elsevier), 93. doi: 10.1016/b978-044452857-5.50008-4

Mortazavi, B., Ortmann, A. C., Wang, L., and Bernard, R. (2015). Evaluating the impact of oyster (*Crassostrea virginica*) gardening on sediment nitrogen cycling in a subtropical estuary. *Bull. Mar. Sci.* 91, 323–341. doi: 10.5343/bms.2014.1060

Mosier, A. C., and Francis, C. A. (2010). Denitrifier abundance and activity across the San Francisco Bay estuary. *Environ. Microb. Rep.* 2, 667–676. doi: 10.1111/j.1758-2229.2010.00156.x

Mukhopadhyaya, P. N., Deb, C., Lahiri, C., and Roy, P. (2000). A *soxA* gene, encoding a diheme cytochrome c, and a *sox* locus, essential for sulfur oxidation in a new sulfur lithotrophic bacterium. *J. Bacteriol.* 182, 4278–4287. doi: 10.1128/jb.182.15.4278-4287.2000

Murphy, A. E., Anderson, I. C., Smyth, A. R., Song, B., and Luckenbach, M. W. (2016). Microbial nitrogen processing in hard clam (*Mercenaria mercenaria*) aquaculture sediments: the relative importance of denitrification and dissimilatory nitrate reduction to ammonium (DNRA). *Limn. Ocean.* 61, 1589–1604. doi: 10.1002/lno.10305

Newell, R. I. E., Cornwell, J. C., and Owens, M. S. (2002). Influence of simulated bivalve biodeposition and microphytobenthos on sediment nitrogen dynamics: a laboratory study. *Limn. Ocean.* 47, 1367–1379. doi: 10.4319/lo.2002.47.5.1367

Newell, R. I. E., Fisher, T. R., Holyoke, R. R., and Cornwell, J. C. (2005). "Influence of eastern oysters on nitrogen and phosphorus regeneration in Chesapeake Bay, USA," in *The Comparative Roles of Suspension-Feeders in Ecosystems, NATO Science Series IV: Earth and Environmental Series*, Vol. 47, eds R. F. Dame and S. Olenin (Dordrecht: Springer).

Newell, R. I. E., and Jordan, S. J. (1983). Preferential ingestion of organic material by the American Oyster *Crassostrea virginica*. *Mar. Ecol. Prog. Ser.* 13, 47–53. doi: 10.3354/meps013047

Nizzoli, D., Welsh, D. T., Fano, E. A., and Viaroli, P. (2006). Impact of clam and mussel farming on benthic metabolism and nitrogen cycling, with emphasis on nitrate reduction pathways. *Mar. Ecol. Progr. Ser.* 315, 151–165. doi: 10.3354/meps315151

Orellana, L. H., Rodriguez, R. L. M., Higgins, S., Chee-Sanford, J. C., Sanford, R. A., Ritalahti, K. M., et al. (2014). Detecting nitrous oxide reductase (NosZ) genes in soil metagenomes: method development and implications for the nitrogen cycle. *mBio* 5:e001193-14.

Pai, S.-C., Yang, C.-C., and Riley, J. P. (1990). Formation kinetics of the pink azo dye in the determination of nitrite in natural waters. *Anal. Chim. Acta* 232, 345–349. doi: 10.1016/s0003-2670(00)81252-0

Parada, A., Needham, D. M., and Fuhrman, J. A. (2016). Every base matters: assessing small subunit rRNA primers for marine microbiomes with mock communities, time series and global field samples. *Environ. Microbiol.* 18, 1403–1414. doi: 10.1111/1462-2920.13023

Pohlner, M., Dlugosch, L., Wemheuer, B., Mills, H., Engelen, B., and Reese, B. K. (2019). The majority of active Rhodobacteraceae in marine sediments belong to uncultured genera: a molecular approach to link their distribution to environmental conditions. *Front. Microbiol.* 10:659. doi: 10.3389/fmicb.2019.00659

Porubsky, W. P., Weston, N. B., and Joye, S. B. (2009). Benthic metabolism and the fate of dissolved inorganic nitrogen in intertidal sediments. *Estuar. Coast. Shelf. Sci.* 83, 392–402. doi: 10.1016/j.ecss.2009.04.012

Quast, C., Pruesse, E., Yilmaz, P., Gerken, J., Schweer, T., Yarza, P., et al. (2013). The SILVA ribosomal RNA gene database project: improved data processing and web-based tools. *Nucleic Acids Res.* 41, D590–D596.

Rabalais, N. N., Cai, W.-J., Carstensen, J., Conley, D. J., Fry, B., Hu, X., et al. (2014). Eutrophication-driven deoxygenation in the coastal ocean. *J. Oceanogr.* 27, 172–183. doi: 10.5670/oceanog.2014.21

Rasigraf, O., Schmitt, J., Jetten, M., and Lüke, C. (2017). Metagenomic potential for and diversity of N-cycle driving microorganisms in the Bothnian Sea sediment. *Microbiol. Open* 6:e00475. doi: 10.1002/mbo3.475

Ray, N. E., Al-Haj, A. N., and Fulweiler, R. W. (2020). Sediment biogeochemistry along an oyster aquaculture chronosequence. *Mar. Ecol. Prog. Ser.* 646, 13–27. doi: 10.3354/meps13377

Robinson, G., Caldwell, G. S., Wade, M. J., Free, A., Jones, C., and Stead, S. M. (2016). Profiling bacterial communities associated with sediment-based aquaculture bioremediation systems under contrasting redox regimes. *Sci. Rep.* 6:38850.

Sanford, R. A., Wagner, D. D., Wu, Q., Chee-Sanford, J. C., Thomas, S. H., Cruz-García, C., et al. (2012). Unexpected nondenitrifier nitrous oxide reductase gene diversity and abundance in soils. *Proc. Natl. Acad. Sci. U.S.A.* 109, 19709–19714. doi: 10.1073/pnas.1211238109

Smith, V. H. (2003). Eutrophication of freshwater and coastal marine ecosystems a global problem. *Environ. Sci. Pollut. Res.* 10, 126–139. doi: 10.1065/espr2002.12.142

Smyth, A. R., Geraldi, N. R., and Piehler, M. F. (2013). Oyster-mediated benthic-pelagic coupling modifies nitrogen pools and processes. *Mar. Ecol. Prog. Ser.* 493, 23–30. doi: 10.3354/meps10516

Solorzano, L. (1969). Determination of ammonia in natural waters by the phenolhypochlorite method. *Limnol. Oceanogr.* 14, 799–801. doi: 10.4319/lo.1969.14.5.0799

Talbot, J. M., Kroeger, K. D., Rago, A., Allen, M. C., Charette, M. A., and Abraham, D. M. (2003). Nitrogen flux and speciation through the subterranean estuary of Waquoit Bay, Massachusetts. *Biol. Bull. Mar. Biol. Lab. Woods Hole* 205:246.

Tiedje, J. M. (1988). "Ecology of denitrification and dissimilatory nitrate reduction to ammonium," in *Biology of Anaerobic Microorganisms*, ed. A. J. B. Zehnder (New York, NY: John Wiley & Sons), 179–244.

Tiquia, S. M., Masson, S. A., and Devol, A. (2006). Vertical distribution of nitrite reductase genes (*nirS*) in continental margin sediments of the Gulf of Mexico. *FEMS Microbiol. Ecol.* 58, 464–475. doi: 10.1111/j.1574-6941.2006.00173.x

Tourna, M., Maclean, P., Condron, L., O'Callaghan, M., and Wakelin, S. A. (2014). Links between sulphur oxidation and sulphur-oxidising bacteria abundance and diversity in soil microcosms based on *soxB* functional gene analysis. *FEMS Microbiol. Ecol.* 3, 538–549. doi: 10.1111/1574-6941.12323

Trimmer, M., and Engström, P. (2011). "Distribution, activity, and ecology of anammox bacteria in aquatic environments," in *Nitrification*, eds B. B. Ward, D. J. Arp, and M. G. Klotz (New York, NY: ASM Press), 201–236. doi: 10.1128/9781555817145.ch9

Valiela, I., McClelland, J., Hauxwell, J., Behr, P. J., Hersh, D., and Foreman, K. (1997). Macroalgal blooms in shallow estuaries: controls and ecophysiological and ecosystem consequences. *Limnol. Oceanogr.* 42, 1105–1118. doi: 10.4319/lo.1997.42.5_part_2.1105

van den Berg, E., van Dongen, U., Abbas, B., and van Loosdrecht, M. M. C. (2015). Enrichment of DNRA bacteria in a continuous culture. *ISME J.* 9, 2153–2161. doi: 10.1038/ismej.2015.26

van den Berg, E. M., Elisário, M. P., Kuenen, J. G., Kleerebezem, R., and van Loosdrecht, M. C. M. (2017). Fermentative bacteria influence the competition between denitrifiers and DNRA bacteria. *Front. Microbiol.* 8:1684. doi: 10.3389/fmicb.2017.01684

Vieillard, A. (2017). *Impacts of New England Oyster Aquaculture on Sediment Nitrogen Cycling: Implications for Nitrogen Removal and Retention.* Master thesis, University of Connecticut, Storrs CT.

Wallenstein, M. D., Myrold, D. D., Firestone, M., and Voytek, M. (2006). Environmental controls on denitrifying communities and denitrification rates: insights from molecular methods. *Ecol. Appl.* 16, 2143–2152. doi: 10.1890/1051-0761(2006)016[2143:ecodca]2.0.co;2

Wang, H., Tseng, C. P., and Gunsalus, R. P. (1999). The *napF* and *narG* nitrate reductase operons in *Escherichia coli* are differentially expressed in response to submicromolar concentrations of nitrate but not nitrite. *J. Bacteriol.* 181, 5303–5308. doi: 10.1128/jb.181.17.5303-5308.1999

Ward, B. B., and O'Mullan, G. D. (2002). Worldwide distribution of *Nitrosococcus oceani*, a marine ammonia-oxidizing gamma-proteobacterium, detected by PCR and sequencing of 16S rRNA and *amoA* genes. *Appl. Environ. Microbiol.* 68, 4153–4157. doi: 10.1128/aem.68.8.4153-4157.2002

Wickham, H. (2016). *ggplot2: Elegant Graphics for Data Analysis*. New York, NY: Springer-Verlag.

Zhang, J.-Z., and Fischer, C. J. (2006). A simplified resorcinol method for direct spectrophotometric determination of nitrate in seawater. *Mar. Chem.* 99, 220–226. doi: 10.1016/j.marchem.2005.09.008

Zumft, W. G. (1997). Cell biology and molecular basis of denitrification. *Microbiol. Mol. Biol. Rev.* 61, 533–616. doi: 10.1128/.61.4.533-616.1997

Conflict of Interest: The authors declare that the research was conducted in the absence of any commercial or financial relationships that could be construed as a potential conflict of interest.

frontiers in Marine Science

ORIGINAL RESEARCH
published: 06 September 2021
doi: 10.3389/fmars.2021.656300

Seasonal Variations in the Biodiversity, Ecological Strategy, and Specialization of Diatoms and Copepods in a Coastal System With *Phaeocystis* Blooms: The Key Role of Trait Trade-Offs

Elsa Breton[1], Urania Christaki[1], Benoit Sautour[2], Oscar Demonio[3], Dimitra-Ioli Skouroliakou[1], Gregory Beaugrand[1], Laurent Seuront[1,4,5], Loïck Kléparski[1,6], Adrien Poquet[1,7], Antoine Nowaczyk[8], Muriel Crouvoisier[1], Sophie Ferreira[9], David Pecqueur[10], Christophe Salmeron[10], Jean-Michel Brylinski[1], Arnaud Lheureux[8] and Eric Goberville[3]*

[1] Univ. Littoral Côte d'Opale, CNRS, Univ. Lille, UMR 8187 LOG, Wimereux, France, [2] Univ. Bordeaux, CNRS, UMR 5805 EPOC, Rue Geoffroy Saint Hilaire – Bâtiment, Pessac, France, [3] Unité Biologie des Organismes et Ecosystémes Aquatiques (BOREA), Muséum National d'Histoire Naturelle, CNRS, IRD, Sorbonne Université, Université de Caen Normandie, Université des Antilles, Paris, France, [4] Department of Marine Resources and Energy, Tokyo University of Marine Science and Technology, Tokyo, Japan, [5] Department of Zoology and Entomology, Rhodes University, Grahamstown, South Africa, [6] Marine Biological Association, Citadel Hill, Plymouth, United Kingdom, [7] Univ. Côte d'Azur, CNRS, INSERM, IRCAN, Medical School of Nice, Nice, France, [8] Univ. Bordeaux, CNRS, UMR 5805 EPOC, Station Marine d'Arcachon, Arcachon, France, [9] Observatoire Océanologique de Banyuls s/mer, FR 3724 – Laboratoire Arago – SU/CNRS, Banyuls-sur-Mer, France, [10] Univ. Bordeaux, CNRS, OASU, UMS 2567 POREA, Allée Geoffroy Saint-Hilaire, Pessac, France

Although eutrophication induced by anthropogenic nutrient enrichment is a driver of shifts in community composition and eventually a threat to marine biodiversity, the causes and consequences on ecosystem functioning remain greatly unknown. In this study, by applying a trait-based approach and measuring niche breadth of diatoms and copepods, the drivers and underlying mechanisms of the seasonal species succession of these ecological communities in a coastal system dominated in spring by *Phaeocystis* blooms were explored. It is suggested that the seasonal succession of diatoms and copepods is the result of several trade-offs among functional traits that are controlled by the seasonal abiotic and biotic pressure encountered by the plankton communities. The results of this study highlight that a trade-off between competition and predator, i.e., weak competitors are better protected against predation, plays an important role in promoting plankton species richness and triggers the *Phaeocystis* bloom. As often observed in eutrophicated ecosystems, only the biotic homogenization of the copepod community and the shift in the diet of copepods toward *Phaeocystis* detrital materials have been detected during the *Phaeocystis* bloom. The diatom and copepod communities respond synchronously to fluctuating resources and biotic conditions by successively selecting species with specific traits. This study confirms the key role of competition and predation in controlling annual plankton succession.

Keywords: diatoms, copepods, *Phaeocystis*, biodiversity, functional traits, seasonality, trade-off

OPEN ACCESS

Edited by:
Maria Moustaka-Gouni, Aristotle University of Thessaloniki, Greece

Reviewed by:
Jun Sun, China University of Geosciences, China
Fabio Benedetti, ETH Zürich, Switzerland
Benjamin Alric, Centre National de la Recherche Scientifique (CNRS), France

****Correspondence:***
Elsa Breton
elsa.breton@univ-littoral.fr

Specialty section:
This article was submitted to Aquatic Microbiology, a section of the journal Frontiers in Marine Science

Received: *20 January 2021*
Accepted: *30 July 2021*
Published: *06 September 2021*

Citation:
Breton E, Christaki U, Sautour B, Demonio O, Skouroliakou D-I, Beaugrand G, Seuront L, Kléparski L, Poquet A, Nowaczyk A, Crouvoisier M, Ferreira S, Pecqueur D, Salmeron C, Brylinski J-M, Lheureux A and Goberville E (2021) Seasonal Variations in the Biodiversity, Ecological Strategy, and Specialization of Diatoms and Copepods in a Coastal System With Phaeocystis Blooms: The Key Role of Trait Trade-Offs. Front. Mar. Sci. 8:656300. doi: 10.3389/fmars.2021.656300

INTRODUCTION

Coastal eutrophication induced by anthropogenic nutrient enrichment is one of the major threats to biodiversity (Vitousek et al., 1997; Halpern et al., 2008; Howarth, 2008). However, assessing the impact of eutrophication on biodiversity is a difficult task, because the multiple drivers shaping biodiversity interact and operate at different interconnected temporal and spatial scales (e.g., White et al., 2010; Dray et al., 2012; Hill et al., 2016). Eutrophication may not only cause excessive blooms of opportunistic species, species loss (Smith and Schindler, 2009) but also, subtle changes in functional trait composition; and may even lead to a loss of functional diversity (FD) caused by a biotic homogenization by favoring generalist (species with broad environmental tolerances) over specialist (species well adapted to particular habitats) species: the latter showed narrower niche breadth and a lower tolerance to high nutrient levels (e.g., Clavel et al., 2011; Nelson et al., 2013; Villéger et al., 2014; Wengrat et al., 2018; Chihoub et al., 2020). Functional traits are biological characteristics that influence the performance and survival of organisms (Violle et al., 2007). Biotic changes may alter biodiversity by selecting species that possess functional traits that confer to them a selecting advantage. For instance, light limitation, which typically occurs under high primary production events, may select species with morphological features that allow them to enhance their buoyancy (Naselli-Flores et al., 2021 and references therein). Communities mainly composed of functionally redundant species may improve ecosystem resilience and stability (e.g., Biggs et al., 2020), but the loss of FD and/or specialist species may deteriorate ecosystem functioning (Olden et al., 2004; Pan et al., 2016; Alexander et al., 2017). Understanding how functional traits relate to associated ecological strategies (i.e., a combination of functional attributes reflecting how species cope with their environment) and ecological specialization across productivity gradients, which defines the degree of tolerance to changing environmental conditions, is, therefore, important to better measure ecosystem functioning and health.

Over the last decade, trait-based approaches have been increasingly used in plankton ecology to understand the drivers of biodiversity changes along environmental gradients and to propose ecological generalities and predictions across ecosystems. Because functional traits mediate the responses of the species to their abiotic and biotic environment (Violle et al., 2007), they help to: (i) better understand how organisms interact with their surrounding environment; and (ii) identify key processes that influence biodiversity such as trait trade-offs (e.g., Kneitel and Chase, 2004; Litchman et al., 2007). While functional identity informs on competitiveness and ecological strategies (e.g., predation avoidance, Shipley, 2010; Muscarella and Uriarte, 2016), FD, in combination with null modeling, informs on the degree of functional convergence of a community and detects mechanisms of community assembly (e.g., abiotic filtering and competitive interactions, Mason et al., 2013). As it may influence conclusions, trait choice is a critical issue (Zhu et al., 2017) when: studying resource traits (e.g., nutrient uptake and light absorption); under-dispersion of traits reflects environmental filtering and/or hierarchical competition (Mayfield and Levine, 2010); and over-dispersion of traits is related to a competition governed by niche differences (Macarthur and Levins, 1967; Cornwell and Ackerly, 2009). When focusing on defense traits against predation (e.g., setae and toxin production), under-dispersion is related to a high predation pressure by generalists, and over-dispersion to a high predation pressure by specialists (Cavender-Bares et al., 2009).

The Eastern English Channel (EEC) is a well-mixed meso-eutrophic sea undergoing multiple environmental disturbances such as temperature rise (McLean et al., 2019) and nutrient enrichment, mainly from the Seine and Somme rivers (Thieu et al., 2009) as a result of anthropogenic activities in the watersheds, especially intensive agriculture practices (e.g., Garnier et al., 2019). This nutrient enrichment is known to trigger the recurrent spring *Phaeocystis* blooms of EEC (Lancelot et al., 1987; Lancelot, 1995; Breton et al., 2000, Breton et al., 2017; Grattepanche et al., 2011a,b; Bonato et al., 2016; Ménesguen et al., 2018). By affecting the diatom and copepod communities, two interacting key compartments of the ecosystem trophodynamics (Smetacek, 1999; Tréguer and Pondaven, 2000; Beaugrand et al., 2003; Kiørboe, 2011; Mitra et al., 2014; Steinberg and Landry, 2017), this prymnesiophyte can disrupt the structure of the food web (Schoemann et al., 2005; Nejstgaard et al., 2007), especially during the late winter/spring and summer/autumn periods (Gasparini et al., 2000; Antajan, 2004).

By applying a functional trait-based approach to diatom and copepod communities collected over the period 2007–2013, and by measuring niche breadth of resources used and environmental conditions tolerated both at the species- and community level, the aims were to: (i) understand how diatoms and copepods in coastal waters of the EEC respond to seasonally changing environmental conditions; (ii) determine what drives plankton species richness and ecological specialization; and (iii) test whether taxonomic (species richness) and FD [functional richness (FRic), functional evenness (FEve), and functional divergence (Rao Quadratic entropy, RaoQ)] of plankton communities were affected by *Phaeocystis* blooms. Protozooplankton biomass (i.e., the sum of heterotrophic dinoflagellate, ciliate, and tintinnid biomass) and co-occurring phytoplankton groups were also considered in this study because of: (i) the diverse trophic regimes and feeding strategies of copepods depend on their food environment (Kleppel, 1993); (ii) diatoms may also be the prey of other predators other than copepods (e.g., Grattepanche et al., 2011b); and (iii) knowledge of the whole community composition may help to better depict trade-offs.

MATERIALS AND METHODS

Datasets

Hydrological and phytoplankton samples were collected at high tide at coastal station "C" (50°40′75 N; 1°31′17 E, 20–25 m maximum depth), which belongs to the French monitoring network SOMLIT[1]. Sampling was carried out on an average of every 3 weeks from February 2007 to December 2013. Subsurface (2 m depth) temperature (SST, °C) and salinity (S) were

[1] www.somlit.fr

measured with a conductivity temperature depth (CTD) Seabird profiler equipped with photosynthetically active radiation (PAR, E m^{-2} d^{-1}) sensor (QSP 2300; Biospherical Instruments Inc.). Dissolved inorganic phosphorous (DIP, μM), inorganic silica (DSi, μM), and inorganic nitrogen [the sum of nitrates, nitrites, and ammonium; (DIN, μM)], total suspended matter (TSM, mg L^{-1}), chlorophyll *a* (Chla, μg L^{-1}), particulate organic carbon (POC, μgC L^{-1}), phytoplankton, and protozooplankton were measured by means of a Niskin Water Sampler (8 L). Nutrient concentrations were quantified according to Aminot and Kérouel (2004) using autoanalyzer systems (Technicon, Alliance, and Seal Instruments), except for ammonium concentrations (NH4), which were assessed by fluorimetry according to Holmes et al. (1999) and Taylor et al. (2007). TSM was determined by filtrating a known volume of seawater through 47 mm precombusted and preweighed glass fiber filters (Whatman, GF/F, 47 mm), and drying it at 50°C for 24 h. POC was determined using a NA2100 Frisons CHN analyzer after filtration of 100–500 ml subsamples through precombusted glass fiber filters (Whatman, GF/F, 25 mm), then dried for at least 48 h at 50°C and exposed to HCl 1 N vapors for 5 h. Chla was estimated by fluorometry (Lorenzen, 1967) from subsample (100–250 ml) of seawater filtrated through glass fiber filters (Whatman, GF/F, 25 mm) and free of pigment (extraction in acetone 90% in the dark at 4°C for 12 h). The minimal volume values corresponded to the *Phaeocystis* bloom period that leads quickly to filter clogging. The maximal volume value corresponds to the maximal value fixed by the SOMLIT network. The average daily PAR experienced by phytoplankton in the water column, for 6 days before sampling, was obtained from a diffuse fraction (kd, m^{-1}) and global solar radiation (GSR, Wh m^{-2}) from the Copernicus Atmosphere Monitoring Service (CAMS) radiation service[2] using the formula of Riley (1957). GSR was converted into PAR by assuming PAR to be 50% of GSR and by considering 1 W m^{-2} = 0.36 E m^{-2} d^{-1} (Morel and Smith, 1974). Wind stress (Pa) and direction (i.e., eastward and northward components of horizontal winds), as proxies of regional turbulence (e.g., MacKenzie and Leggett, 1991), were obtained from the National Center for Atmospheric Research (NCAR, United States)[3] and the National Centers for Environmental Prediction (NCEP, United States). Subsurface and near-bottom environmental values were averaged for niche analysis (refer below "Ecological specialization").

Copepods were collected on 96 separate occasions (sampling frequency of 4 weeks) with vertical hauls from the bottom (ca. ∼ 20–25 m depth) to the surface using a 200-μm mesh size working party (WP) 2 plankton net. The volume filtered was measured with a Tsurumi – Seiki (TSK) *flowmeter* (Tokyo Seimitsu Co. Ltd) and mounted on the mouth of the net (0.25 m^2 mouth area). The volume of filtered seawater varied between 1 and 11 m^3, the lowest values being recorded during the *Phaeocystis* bloom (from mid-April to mid-May) as a result of rapid net clogging. All copepod samples were preserved with 4% formaldehyde buffered with borax. The composition and abundance of copepods were determined under stereomicroscopy (Nikon SMZ1500) with 10–100x magnification in Dollfus chambers according to the determination key provided by Rose (1933). Copepod carbon biomass was calculated from (i) the median of the minimum and maximum weights for the CV and CVI copepodite stages; and (ii) the regression equations relating wet weight and dry weight (mg) to carbon (mg C, Wiebe, 1988). The minimum and maximum weights were estimated from the range values of copepodite length reviewed by Conway (2006) for the North Atlantic sector and species-specific length-weight relationships (Durbin and Durbin, 1978; Cohen and Lough, 1981; Williams and Robins, 1982; Dam and Peterson, 1991; Zakaria et al., 2018). The list of the copepod species identified in this study, the final carbon conversion factor values and their corresponding frequencies (%) and average biomasses (μgC L^{-1}), are shown in **Supplementary Table 1**. Diatom, *Phaeocystis*, and dinoflagellate samples were fixed with Lugol-glutaraldehyde solution (1% v/v, a fixative that does not disrupt *Phaeocystis* colonies; Breton et al., 2006) and were kept at 4°C in the dark until microscopy analysis. Other protozooplankton samples, i.e., ciliates and tintinnids, were fixed with formaldehyde (Grattepanche et al., 2011a). Samples were examined using an inverted microscope (Nikon Eclipse TE2000-S) with 100–400x magnification after sedimentation in 5–25 ml and 25–100 ml Hydrobios chambers for phytoplankton and protozooplankton, respectively. Identifications were identified at the species level when possible, according to taxonomic literature (Halse and Syvertsen, 1996; Hoppenrath et al., 2009, for phytoplankton; Schiller, 1931–1937; Maar et al., 2002; Gómez and Souissi, 2007, for heterotrophic dinoflagellates; Kofoid and Campbell, 1929; Plankton Ciliate Project, 2002, for ciliates). For *Synechococcus* spp., picoeukaryotes, and cryptophytes, 5 ml samples were fixed with glutaraldehyde (1.33% v/v) and kept at −80°C until flow cytometry analysis (FACScan, BD Biosciences, Marie et al., 1999). Biovolumes were estimated using standard geometric forms according to Hillebrand et al. (1999). The number of *Phaeocystis* cells in the colonial stage of life was counted according to biovolume measurements of the colonies (Rousseau et al., 1990). Carbon biomass (μgC l^{-1}) of phytoplankton and heterotrophic dinoflagellates was calculated using the carbon conversion factors of Menden-Deuer and Lessard (2000). For *Phaeocystis* solitary cells, *Synechococcus* spp., and picoeukaryotes, the values of 89.5 pg C $cell^{-1}$ (van Rijssel et al., 1997), 154 fg $cell^{-1}$, and 1319 fg $cell^{-1}$ (Buitenhuis et al., 2012) were used, respectively. For flagellated and solitary colonial cells, only discriminated since 2007, the carbon conversion factors of 10.8 and 14.15 pg C/cell were applied, respectively (refer **Table 1** in Schoemann et al., 2005). The biomass of ciliates and tintinnids was calculated using a conversion factor of 0.19 pg μm^{-3} (Putt and Stoecker, 1989; refer **Supplementary Tables 1–4** and **Supplementary Data** for species list and biomass estimates).

Phytoplankton and Copepod Species Traits

Information on resource traits is scarce in the literature for most phytoplankton species (Litchman and Klausmeier, 2008; Breton et al., 2017). Consequently, an *a posteriori* approach

[2]http://www.soda-pro.com/web-services/radiation/cams-radiation-service
[3]https://psl.noaa.gov/data/gridded/data.ncep.html

TABLE 1 | List of the diatom and copepod traits used in this study and their functional meaning.

Traits	Type[a]	Range/Category	Ecological process/Functional meaning	References
Phytoplankton/diatoms				
Biovolume	Numerical (R and D)		The "master trait" for resource acquisition, reproduction, and predator avoidance	Litchman and Klausmeier, 2008
S/V cell ratio	Numerical (*R*)	0.02–4.62μm^{-1}	Competitive ability under nutrient limitation, silica requirement	Grover, 1989; Karp-Boss et al., 1996; Leynaert et al., 2004; Takabayashi et al., 2006; Musielak et al., 2009; Lovecchio et al., 2019
Coloniality	Ordinal (R and D)	0: No, 1: <5 cells, 2:[5–20], 3:[20, 100], 4:>100	Competitive ability under nutrient limitation	Grover, 1989; Karp-Boss et al., 1996; Takabayashi et al., 2006; Musielak et al., 2009; Bjærke et al., 2015; Lovecchio et al., 2019
		0: <500; 1:>501μm	vulnerability to predation	Djeghri et al., 2019
Apparent degree of signification	Ordinal (R and D)	1: Slightly, 2: Medium, 3: Heavily	Silica requirement, vulnerability to predation	Martin-Jézéquel et al., 2000; Martin-Jézéquel and Lopez, 2003; Pančić et al., 2019
Tychopelagic/Benthic occurrence	Binary	0: Pelagic; 1: Tychopelagic/Benthic	Use of resources and habitat	
Maximum Linear Dimension (MLD)	Numerical (R and D)	3–447 μm	Cell buoyancy, vulnerability to photo-inhibition	Grover, 1989; Key et al., 2010; Schwaderer et al., 2011; Naselli-Flores et al., 2021
			Capacity at capturing the fluctuating light and persisting in subsurface waters	Naselli-Flores et al., 2021
Defense	Ordinal (D)	0–4 (0: No defence, 4 many defence traits)[b]	Predator avoidance	Pančić and Kiørboe, 2018
Copepods				
Maximum size	Numerical (R and D)	1: ≤1 mm, 2: [1; 2], and 3: >2 mm	Feeding, growth, reproduction, survival	Litchman et al., 2013
Trophic regime	Fuzzy coded (R)	Carnivory, Herbivory, Detritivory, Omnivory[c]	Feeding, growth, reproduction, survival	Litchman et al., 2013
Feeding mode	Ordinal (R and D)	0: Passive, 0.5: Mixed, 1: Active	Feeding, survival	Kiørboe, 2011; Litchman et al., 2013

[a] *R and D: Resource and Defense trait, respectively.*
[b] *See **Supplementary Table 3** and **Supplementary Data**.*
[c] *See Chihoub et al. (2020) for more details.*

to defining resource use and requirement traits was used. For each species, biovolume (V, μm^3), maximum linear dimension (MLD, μm), and the surface to biovolume cell ratio (S/V ratio) were calculated from the median values of a series of microscopic measures over the entire 1996–2019 diatom datasets acquired at Station "C" (Breton unpublished data). The apparent degree of silicification (1: slight; 2: medium; 3: heavy) and Tychopelagic/benthic habit (0: pelagic; 1: tychopelagic/benthic) was based on information from phytoplankton taxonomic literature (e.g., Halse and Syvertsen, 1996; Hoppenrath et al., 2009). The potential degree of coloniality (0: None; 1: <5 cells; 2: 5–20 cells; 3: >20 cells) was assessed through the cultivation of each diatom species under F/20 medium and with a light: dark cycle of 12:12 h at an irradiance of 400 μmol photons m^{-2} s^{-1} (Daylight HQIT-WD 250 W F, OSRAM GmbH, Munich, Germany).

Biovolume is a key trait because it relates to the various ecophysiological attributes for resource acquisition, reproduction, and predator avoidance (Litchman and Klausmeier, 2008; **Table 1**). Species with high S/V cell ratio and long cellular chain length that favor cell suspension in the water column and increase nutrient flux have a great competitive ability under nutrient limitation (Grover, 1989; Karp-Boss et al., 1996; Takabayashi et al., 2006; Musielak et al., 2009; Lovecchio et al., 2019). Higher S/V cell ratio and weaker silicified species have also been related to lower silica requirement under laboratory conditions [(Leynaert et al., 2004) and to DSi limitation (Martin-Jézéquel et al., 2000; Martin-Jézéquel and Lopez, 2003)]. Cell elongation enhances both cell buoyancy (Grover, 1989; Naselli-Flores et al., 2021) and protection against photoinhibition, especially for larger cells (Key et al., 2010; Schwaderer et al., 2011). The binary trait "Tychopelagic/benthic habit" may be informative of resource use and requirement, as benthic diatoms are often highly photosynthetic efficient species and potentially facultative heterotrophs (Cahoon, 1999). This trait may be also an indicator of ecosystem health, as demonstrated by the positive relationship between the FD of benthic diatoms and the productivity of coastal waters in the Baltic Sea (Virta et al., 2019). Besides reflecting resource use and/or requirement, prey biovolume (Litchman and Klausmeier, 2008), the degree of coloniality (Bjærke et al., 2015), and the apparent degree of silicification (Pančić et al., 2019) mirror ecological processes/functions linked to predation. By including: (i) the capacity to produce mucous or toxins; (ii) the presence of

setae and/or spicules (that also favor buoyancy; Van den Hoek et al., 1995); (iii) the degree of silicification; and (iv) coloniality, the composite of defense traits reflect alteration of copepod grazing (Pančić and Kiørboe, 2018). The composite trait was obtained by summing the scores of each of these traits (refer **Supplementary Table 5** and **Supplementary Data**).

The carbon-to-chlorophyll ratio for phytoplankton (C/Chl*a* ratio, in μgC μgChla^{-1}) and timing of bloom initiation of diatoms (in months) were then calculated. Although not being traits *per se* (Litchman and Klausmeier, 2008), they are the outcome of processes linking the actual traits of species and the alleviation, or accentuation, of external limiting factors, such as grazing pressure or nutrients/light availability (Thackeray et al., 2008; Jakobsen and Markager, 2016). The C/Chl*a* ratio was calculated using microscopic counts and the cell carbon was computed from the equations of Menden-Deuer and Lessard (2000). Timing of bloom initiation of diatoms at Station "C" (refer **Supplementary Data**) was based on the cumulative biomass-based threshold method (Brody et al., 2013), using mean monthly diatom abundances over the period 1996–2019 and a limit value of 20%.

For copepods: (i) maximum size (mm); (ii) trophic preference (herbivory, carnivory, detritivory, and omnivory); and (iii) feeding mode (0: passive, 1: active, and 0.5: mixed feeding) were selected, as they directly/indirectly influence species fitness through growth, reproduction, and/or survival (Litchman et al., 2013; Kiørboe and Hirst, 2014). Most of them are responsive to changes in environmental conditions (McGinty et al., 2018). Data were obtained from the copepod trait database constructed by Benedetti et al. (2016) and completed by Brun et al. (2017), and references therein. For each copepod species, all available information on species size was compiled, and the maximum size value as representative of adult species was kept, note that sexual dimorphism was not considered. The degree of herbivory (carnivory, detritivory, or omnivory) was coded following Mondy and Usseglio-Polatera (2014). In this study, a coefficient of (i) 1/3 for omnivore; (ii) 2/3 for omnivore-herbivory (dominance of herbivory in copepod diet) or 2/3 for omnivore-carnivory (dominance of carnivory in copepod diet), with 1/4 for the two other diet categories; and (iii) 1 for species with carnivore/herbivore/detritivore diets, and 0 for the two other diet categories (refer Chihoub et al., 2020 for more details) was applied.

FD Metrics

In this study, four metrics (Step 1, refer **Supplementary Figure 1** for a description of the five main steps of the statistical method) to characterize the functional structure and diversity of diatom and copepod communities were used as follows: (i) community-weighted mean (CWM); (ii) FRic, (iii) FEve; and (iv) Rao Quadratic entropy (RaoQ) as a proxy of functional divergence. CWM, the mean trait value among each community weighted by the relative biomass of each species (Garnier et al., 2004), is a proxy of functional identity. FRic corresponds to the volume of functional niche space filled by a species within a community (Villéger et al., 2008). FEve corresponds to the regularity with which species biomass in a community is distributed along the minimum spanning tree that links all species in the multidimensional trait space (Mason et al., 2005). RaoQ is the sum of pairwise distances between species, weighted by the relative biomass within the multidimensional trait space. This index was selected over the functional divergence metric for its stronger ability to detect assembly rules (Botta-Dukát, 2005; Botta-Dukát and Czúcz, 2016). The FD indices of the diatom community were calculated from the biovolume, the apparent degree of silicification, coloniality, the S/V cell ratio, MLD, and defense traits (as shown in **Supplementary Table 5**). For each observation (i.e., sampling unit), functional metrics were computed on log-transformed species biomass, to reduce a potential influence of outliers, using the R package (R version 3.5.3, 2019) "FD" (Laliberté and Legendre, 2010). A preliminary principal coordinate analysis (PCoA; "vegan" package; and Oksanen et al., 2011) was performed to calculate the multidimensional trait space for each sampling day and FD was calculated from a dissimilarity matrix calculated using both the PCoA axis, as new functional traits, and the Gower distance (Gower, 1971). The Gower distance allows us to combine traits of different types, including ordinal (Podani, 1999; **Table 1**). A square root transformation ("sqrt"), or a Lingoes correction for negative values (Lingoes, 1971), was applied when the distance matrix "species × species" was not Euclidean. The quality of the functional space (i.e., the similarity between the functional space and initial functional trait values) based on the corrected distance matrix varied from 0.64 to 0.94. The inference of environmental filtering and biotic interactions (Step 2, **Supplementary Figure 1**) was estimated from the deviation [standardized effect size (SES); Gotelli and McCabe, 2002] between functional metrics calculated on a given (i.e., observed) diatom community and functional values obtained from a random community: for each sampling date, trait data were randomized 999 times ("permatfull" in the "vegan" package), while maintaining species richness and abundance constant. SES was calculated as follows:

$$SES = \frac{x_{obs} - \bar{x}_{ran}}{\sigma_{ran}} \quad (1)$$

where x_{obs} is the observed values of the functional metric at a given date; $\bar{x}_{ran}$ is the mean, and σ_{ran} is the SD of the FD of randomly assembled communities. Assuming a normal distribution of the random communities, the traits derived from the sampling dates falling into the 95th (or higher) percentile of the random distribution were considered "over-dispersed" (i.e., niche differentiation being the major process driving community assembly) and trait falling into the 5th (or lower) percentile were considered "under-dispersed" (i.e., environmental filtering as the major process).

Ecological Specialization

Ecological specialization (Step 3, **Supplementary Figure 1**) was estimated by means of the multidimensional outlying mean index (OMI, hereafter called "environmental tolerance," Dolédec et al., 2000) and unidimensional niche breadth analysis using the "ade4" (Chessel et al., 2004; Dray et al., 2007) and "hypervolume" packages (Blonder et al., 2014). The OMI was selected because it does not rely on any expected species response curves to environmental gradients and outperforms classical

methods such as canonical correspondence or redundancy analysis (Dolédec et al., 2000). The OMI analysis seeks combinations of environmental variables that maximize average species marginality, i.e., the squared Euclidean distance between the mean environmental conditions used by a species and the mean environmental conditions available to this species. Hypervolume estimates the niche breadth of one or several dimensions from the calculation of uni or multivariate kernel density. This method captures irregular shapes and does not require a specific density function, unlike OMI analysis that requires normal distribution: estimation of the hypervolume is, therefore, more accurate when high-dimensional or holey datasets are considered. An accurate estimate of kernel density requires high amounts of trait/environmental data, which rises as dimensionality increases, however (e.g., about >67 and >770 for three and five dimensions, respectively, Silverman, 1986). For a comprehensive assessment of environmental gradients, the calculation was, therefore, based on the ecological specialization of long-term diatom and copepods datasets, collected between 1996 and 2019 at the station "C," and from 2001 to 2017, respectively, in the downstream part of the Gironde estuary (Breton et al., 2000; Schapira et al., 2008; Breton et al., 2017; Richirt et al., 2019).

Environmental tolerance was based on species biomass, considering: (i) SST, S, Pa, nutrients, and PAR for diatoms; and (ii) SST, S, Pa, TSM, and POC for copepods. Unidimensional niche breadth related to resources (DIN, DIP, DSi, and light for diatoms; TSM and POC for copepods) was determined from kernel density using the environmental conditions encountered by species when present with a Silverman bandwidth estimator and a 0% quantile threshold (Blonder et al., 2014). An increase in these two indices of ecological specialization mirrors an decrease in the degree of specialization of the diatom or copepod community. Trophic homogenization within the copepod community was assessed from trophic preferences and feeding mode, as recommended by Mondy and Usseglio-Polatera (2014). For each copepod species and trophic trait, we first calculated the taxon specialization index (TSI) using the Gini-Simpson index (Gini, 1912; Simpson, 1949). Each TSI, where the trophic preference (the feeding mode) describes the degree of omnivory (the capacity to alternate between passive and active feeding), was then scaled by its respective minimum and maximum values to account for the different number of categories among traits (Mondy and Usseglio-Polatera, 2014). The community specialization index (CSI) was finally computed as the CWMs of each TSI: a value of 0 (1) corresponds to truly generalists (truly specialists).

All analyses were performed with R (R Development Core Team), version 3.5.3.

Exploratory Analyses

First, box plots (Step 4, **Supplementary Figure 1**) were computed combined with a locally weighted scatterplot smoothing (LOESS; Jacoby, 2000) curve in association with a 95% confidence interval (function "geom_smooth," package "ggplot2," Wickham, 2016) to depict the seasonal variations. Monthly differences were assessed by a Kruskal–Wallis test, followed by a *post hoc* Nemenyi test (Legendre and Legendre, 1998; package "PMCMRplus," Pohlert, 2014). To explore and summarize seasonal changes in the abiotic environment, a principal component analysis (PCA) was performed with the "ade4" package. To explore seasonal variations in both the mean values of key biological traits and in the degree of ecological specialization of the diatom and copepod communities, a PCoA (Step 4, **Supplementary Figure 1**) was computed on a community dissimilarity matrix (Gower distance) using monthly data of niche breadth and CWMs of different functional attributes. The coupling (Step 5, **Supplementary Figure 1**) between the environment and key biological attributes (species biomass, functional structure, ecological specialization, and FD of diatoms and copepods) was then estimated by computing two separated co-inertia analysis (COIA; Dolédec and Chessel, 1994; Dray et al., 2003) on monthly means using the "ade4" package. Prior to all multivariate analysis, and for each variable, skewness of the data was removed to reach normality and all variables were to have a mean of zero and a SD of one ("caret" package; Kuhn et al., 2016). The principle of COIA consists of finding co-inertia axis by maximizing the covariance between the row coordinates of two matrices (in this study, the environmental variables and either diatoms or copepods). It defines axis that simultaneously explain the highest possible variance in each of the two matrices and describes their closest common structure. First, a PCA was performed on each matrix, and then applied the COIA (Dray et al., 2003). Explanatory environmental variables were: Pa and direction, S, SST, DIN, DIP, DSi, and protozooplankton biomass. While PAR and copepods biomass were included as additional explanatory environmental variables for diatoms, diatom biomass was added, the defense trait against predation (expressed as CWM) for copepods, and the abundance of their main predators (i.e., Chaetognaths, fish larvae and jellyfish; Hirst and Kiørboe, 2002). The COIA was sequentially built for: (i) environment vs. diatoms; and (ii) environment vs. copepods, with a manual backward selection of the significant variables to obtain the highest coupling coefficients, the strength of the coupling being based on the multidimensional correlation coefficient (RV; Robert and Escoufier, 1976). The variables included in the final COIA were selected (i) only if they displayed a significant seasonal trend in box-plots (refer the final list above), and depending on both (ii) the RV value and (iii) the contribution of variables to the construction of the co-inertia axis. The latter was estimated by means of Pearson correlation calculated between the variables and the scores of samplings on the COIA axis. Although the loadings describe how each variable contributes to each co-inertia axis, such information can be retrieved by the correlation coefficient between the variables and the co-inertia axis. A Monte Carlo permutation procedure (1,000 permutations) was applied to compute the RV and statistical significance. For PCA, PCoA, and COIA analyses, an ascending hierarchical classification (AHC) was used with Ward's aggregation criterion on the two first component coordinates ("hclust" function of the "ade4" package) to reveal monthly clusters.

A variation partitioning (VP) analysis (Step 5, **Supplementary Figure 1**; "vegan" package; Borcard et al., 1992; Legendre and Legendre, 2012) was finally performed to estimate

the contribution of *Phaeocystis* blooms, water masses, hydrometeorological (Pa and/or direction as proxies), and local environmental conditions (S, nutrients, PAR, and predator and/or prey biomass) on changes in the functional structure (i.e., the CWMs), ecological specialization (i.e., environmental tolerance and niche breadths), and FD (SES-RaoQ) of the diatom and copepod communities. To explain variations in species richness of the diatom and copepod communities, the contribution of assembly rules was added using SES-RaoQ as a proxy. SES-RaoQ is known to be the most appropriate FD index (Botta-Dukát and Czúcz, 2016) to detect both environmental filtering (trait convergence) and competition based on niche difference (trait divergence). As for the COIA, variables that attest to the hydrometeorological and local environmental conditions (abiotic and prey biomass) were selected backward to obtain the lowest residual proportion. To explore the effect of *Phaeocystis* blooms on species richness, functional structure, ecological specialization, and FD of the diatom community, a Kruskal–Wallis test was performed using different classes of *Phaeocystis* biomass [1: <100; 2: (100, 500); 3: (500, 1000); 4: >1,000 μgC L^{-1}] coming from the 1996 to 2019 dataset (refer "Ecological specialization").

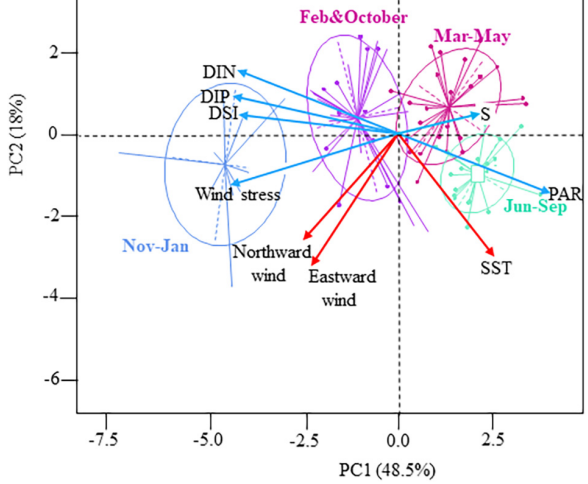

FIGURE 1 | Principal Component Analysis showing the seasonal variations of the abiotic environment in coastal waters of the eastern English Channel over the period 2007–2013. Projection of the variables and of the observations (from January to December) on the factorial map (Eigenvalues are given into brackets, 66.5% of the total inertia). Blue and red arrows: significant Pearson correlation with the first (PC1) and second (PC2) principal components. Blue, purple, pink and green ellipses: Hierarchical Agglomerative Clustering (HAC) of the observations on the factorial map using the Ward's linkage. Photosynthetic Active Radiation (PAR m^{-2} d^{-1}), Salinity (S, n.u), Sea Surface Temperature (SST, °C), Dissolved Inorganic Nitrogen (DIN, μM), Phosphorus (DIP, μM), Silica (DSi, μM), Northward and Eastward winds (m s^{-1}).

RESULTS

Abiotic Environment and Plankton Composition and Biomass

The first principal component (PC1, 48.5% of the total variance) showed a seasonal gradient from relatively high turbulent (Pa as a proxy), less saline, nutrient-rich (DIN, DIP, and DSi), and poor PAR winter conditions to calm and relatively lighted, but nutrient-limited (DSi < 2 μM, DIN < 1 μM, and DIP < 0.2 μM), and saline summer conditions (**Figure 1** and **Supplementary Figure 2**). The second principal component (PC2, 18% of the total variance) was mainly driven by wind direction (both north and eastward winds) and SST, suggesting that SST increased as north and eastward winds increased. The temperature-salinity diagrams mainly discriminated water masses according to temperature (**Supplementary Figure 3**). The vertical structure of water masses also showed seasonal variations; the spring-summer water masses (from March to August) being saltier and colder at the bottom depth; autumn-winter conditions (from September to February) were reversed.

Phytoplankton biomass was mainly composed of diatoms, except when *Phaeocystis* colonies prevailed (from March to mid-May, **Figure 2A**). Zooplankton biomass was mainly composed of copepods, except during the seasonal outburst of the meroplankton that was mainly composed of Echinodermata (in May, mainly *Pluteus* larvae, **Figure 2B**). While a slight decrease was observed during the peak of *Phaeocystis*, the biomass of diatoms followed the same seasonal dynamics as protozooplankton (sum of heterotrophic dinoflagellates and ciliates) and copepods (**Figures 3A–D**). Protozooplankton and copepod biomass progressively increased from winter months to May–June (**Figures 3C,D**), before decreasing. The C/Chl*a* ratio showed strong seasonal variations, with maxima in April–May and minima in winter (**Figure 3E**).

Functional Structure and Ecological Specialization of the Diatom and Copepod Communities

Seasonal variations in the functional structure and ecological specialization of the diatom community characterized with LOESS over the period 2007–2013 (**Supplementary Figures 4A,C,E,G,I,K,M,O** and **Supplementary Figures 5A,C,E,G,I,K**) were similar to those obtained over the period 1996–2019 (**Supplementary Figures 4B,D,F,H,J,L,N,P** and **5B,D,F,H,J,L**). However, Nemenyi tests revealed that monthly changes were more pronounced when using the 24-year time series. The PC1 of the PCoA (PCoA1; 51% of the total variance) (**Figure 4A**) suggested a seasonal shift in the functional structure and ecological specialization of diatom communities from the autumn fall winter to the spring period. This shift was characterized by a seesawing from communities exhibiting high silicification, low S/V ratio, presence of tychopelagic/benthic species, PAR specialization, and generalists relative to nutrient use, to more environmentally tolerant diatom communities (from May to July). During early spring and the *Phaeocystis* bloom period, communities exhibited an intermediate position

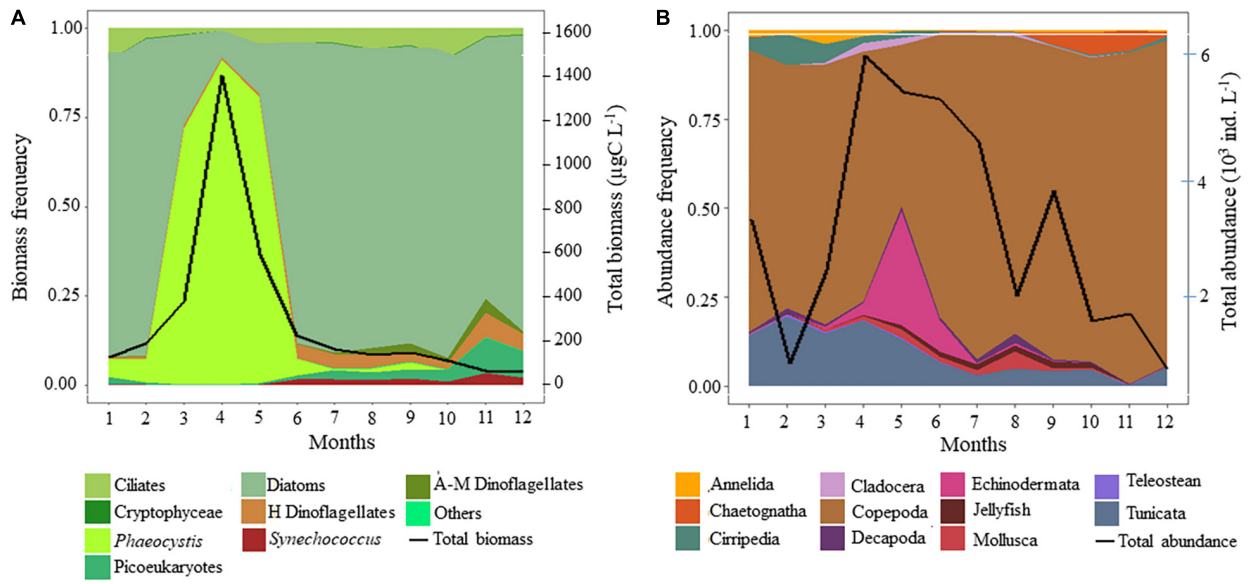

FIGURE 2 | Seasonal variations in panel **(A)** phytoplankton composition (carbon biomass frequency) and total phytoplankton biomass (black line, µgC L^{-1}), and **(B)** zooplankton composition (abundance frequency) and total zooplankton abundance (black line,10^3 ind. L^{-1}). A-M, Auto- Mixotrophic; H, Heterotrophic. Teleostean included fish larvae and eggs. Jellyfish included Cnidaria and Ctenaria.

(**Figure 4A**). The PC2 (PCoA2; 15% of the total variance) revealed that large-size diatom species with defense against predation prevailed from January to March and in October (**Figure 4A**). Although weakly associated with the first two principal components, we detected, for both time series, that CWM-MLD values peaked during the maximum of the *Phaeocystis* bloom (i.e., April; **Supplementary Figures 4E,F**).

For copepods, the PCoA (the PCoA1 and PCoA2 explaining 56% and 22% of the total inertia, respectively, **Figure 4B**) showed that the communities were mainly composed, from February to May, of large omnivorous active feeders (i.e., high CWM-feeding mode values), omnivores with a relatively high propensity to detritivory and environmentally tolerant species, and generalists for TSM and POC. A contrasting pattern between the CWM-omnivorous and the CSI-trophic regime was detected. From June to September, communities were mainly composed of small and passive feeders with a low propensity to detritivory and specialists for both TSM and POC. In October, carnivorous copepods, with specialized feeding modes and specialized environmental requirements, dominated the community.

Accordingly, the CSIs of copepods for trophic regime and feeding mode had high values. Concerning the functional structure of the copepod community (**Supplementary Figures 6A–M**), significant monthly changes were only seen for maximum size (**Supplementary Figure 6A**) and feeding mode (**Supplementary Figure 6B**).

Species Richness and FD of Diatom and Copepod Communities

The annual cycle of diatom species richness exhibited a bimodal pattern (**Figure 5A** and **Supplementary Figure 7A**), with a peak in February–March and September–October. No significant monthly change was detected (Nemenyi test, $p > 0.05$). The annual cycle of copepod species richness was unimodal, peaking in August–September (**Figure 5B**). No monthly variation was detected between the volume of filtered seawater and copepod species richness ($N = 96$, $r^2 = 10^{-5}$, $p > 0.05$).

Patterns of FD of the diatom community (**Figures 5C–H**, refer **Supplementary Table 5** and "diatom.defense.traits" in **Supplementary Data** for more details on the calculation), differed among functional indices, independently of the sampling period (**Supplementary Figures 7B–G**). FRic (SES-FRic, **Figures 5C,D** and **Supplementary Figures 7B,C**) and divergence (SES-RaoQ, **Figures 5E,F** and **Supplementary Figures 7D,E**) for resource use and predation avoidance were lower than expected by chance. FEve values (SES-FEve, **Figures 5G,H** and **Supplementary Figures 7F,G**) were also not different from those expected by chance. The SES-FRic and SES-RaoQ were significantly negatively correlated to species richness for both resource use and predation avoidance (SES-FRic: $r = -1$, $p < 0.001$ and $r = -0.98$, $p < 0.001$, respectively; SES-RaoQ: $r = -0.78$, $p < 0.001$, $r = -0.77$, $p < 0.001$, respectively). SES-FEve was not correlated with species richness ($r = 0.21$, $p > 0.05$ and $r = 0.01$, $p > 0.05$, respectively).

For copepods, the SES-FRic (**Figure 5I**) and SES-RaoQ (**Figure 5J**) were also significantly negatively correlated with species richness, but to a lesser extent ($r = -0.43$, $p < 0.001$, $r = -0.34$, $p < 0.001$, respectively). Omnivory and herbivory, because of their respective high significant correlation with detritivory ($r = 0.9$, $p < 0.001$) and carnivory ($r = -0.91$, $p < 0.001$), were discarded from the calculation. The SES-FRic (**Figure 5I**) values for copepods were not different from those expected by chance. SES-RaoQ (**Figure 5J**) and SES-FEve

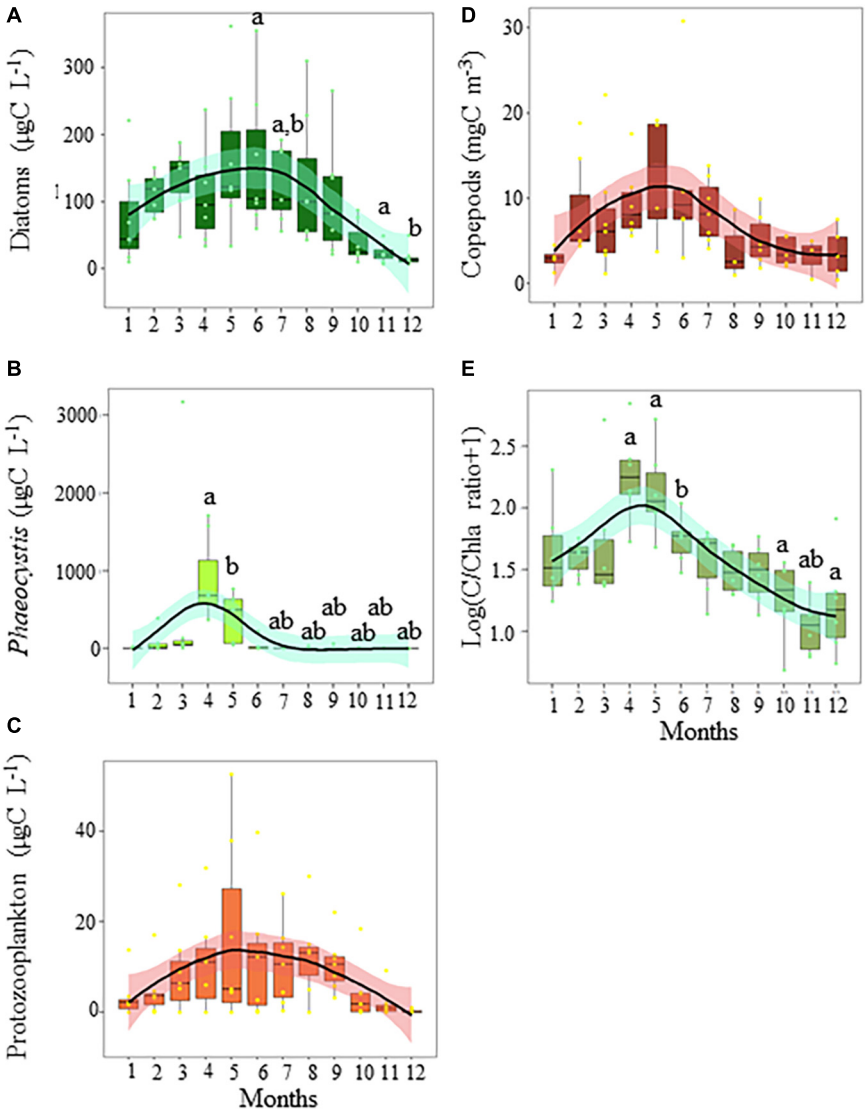

FIGURE 3 | Seasonal variations in the biomass (mgC L^{-1}) of panel **(A)** diatoms, **(B)** *Phaeocystis*, **(C)** protozooplankton (ciliates and dinoflagellates), **(D)** copepods (mgC m^{-3}), and **(E)** the C/Chla ratio in coastal waters of the eastern English Channel over the period 2007–2013. Black horizontal line inside box: median; box: first to third quartiles; whiskers: 1.5 times the interquartile range (IQR); dots: monthly data including outliers (>1.5 times IQR). The labels a and b show significant differences between months ($p = 0.05$, Nemenyi test). The solid line and ribbon represent LOESS smoothing and the 95% confidence interval, respectively.

(**Figure 5K**) values were mostly lower and higher, respectively, than expected by chance. FD indices did not show seasonal patterns (e.g., note the large 95% confidence intervals of the LOESS fits in **Figures 5I–K** and **Supplementary Figure 6A–M**).

Relationships Between the Functional Structure, Ecological Specialization, and FD, and the Abiotic and Biotic Environment

Co-inertia analysis showed a significant coupling (n = 63, RV = 0.49, $p = 10^{-3}$) between the structure of diatom communities and abiotic/biotic conditions (**Figures 6A,B**, **Supplementary Figures 8A,B**, and **Supplementary Table 6A**). A seasonal pattern was delineated by the COIA (**Supplementary Figures 8A,B**). Although all environmental parameters were significant in structuring the seasonality of diatom communities, some were more important than others (**Supplementary Table 6A**). The first COIA axis (explaining 86% of the total inertia, **Figure 6A**) showed that diatom communities, composed predominantly of slightly silicified species, with a relative high S/V cell ratio, and the ability to form colonies, were associated to calm weather conditions and more saline seawater with relatively higher PAR, but low nutrients. Diatom communities, with mainly specialist species for nutrients but generalists for PAR, were also sensitive to environmental variations (relatively

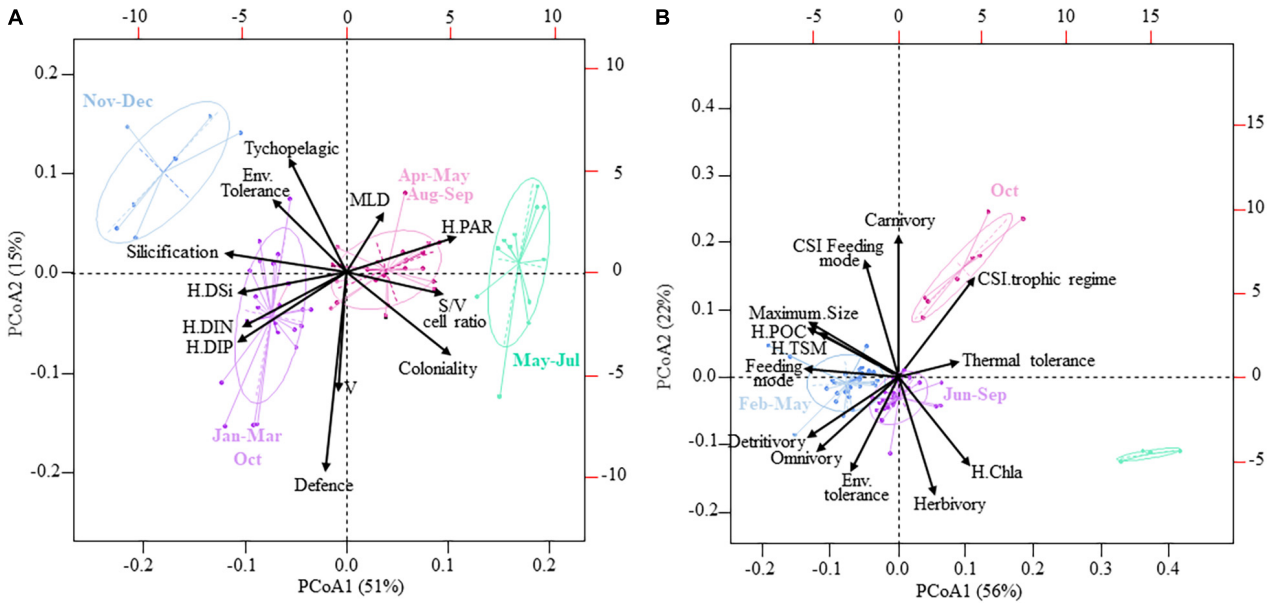

FIGURE 4 | Principal coordinates analysis (PCoA) of the functional structure and ecological specialization of the **(A)** diatom and **(B)** copepod community in coastal waters of the eastern English Channel over the period 2007–2013. The percentage of the total variance explained by each axis is shown in parentheses. Months are grouped together following the results of a Hierarchical Agglomerative Clustering (HAC) using the Ward's linkage and the two first coordinates of the PCoA. Each point represents a monthly averaged community sample. The ellipses show a 95% confidence level. H, niche breadth; PAR, Photosynthetic Active Radiation; DIN, DIP, DSi, Dissolved Inorganic Nitrogen and Phosphorous, and Silica; Chla, Chlorophyll *a*; S/V cell ratio, Surface to Volume cell ratio; MLD, Maximum Linear Dimension; Env. Tolerance, environmental tolerance; CSI, Community Specialization Index; TSM, Total Suspended Matter; POC, Particulate Organic Carbon. Thermal tolerance in panel **(A)** is not shown given its central position on the PCoA plane.

low "Tol" values); slightly silicified species bloomed later in the year. According to the second COIA axis (8% of the total inertia; **Figure 6A**), most diatoms with high defense levels against predation and DIN generalists were associated with colder seawater, rich in *Phaeocystis* biomass and characterized by a high C/Chla ratio, and large-bodied generalist omnivore copepod species. Under such conditions, diatom biomass was maximal. The third COIA axis (3% of the total inertia; **Figure 6B**) showed that species-rich diatom communities, characterized by the dominance of small MLD species, were associated with copepod communities dominated by specialist species. The SES-FRic and SES-RaoQ of the diatom community were the lowest for both resource use and predation avoidance (**Figure 6B**).

The coupling strength between functional structure (i.e., the CWMs), ecological specialization (i.e., environmental tolerance and niche breadth), and FD (SES-RaoQ and SES-FRic) of copepods, and environmental conditions (refer section "Materials and Methods") was low but significant (n = 63, RV = 0.36, p = 0.001, **Figure 6C**). The seasonality of the coupling was unclear (**Supplementary Figure 8C**). The first co-inertia axis (explaining 84% of the total inertia) revealed that large, active-feeding, and omnivore copepod species (i.e., low CSI-trophic regime values) were associated with relative calm weather conditions, more saline *Phaeocystis*-rich waters, characterized by higher proportions of diatoms with defense levels against predation (**Figure 6C** and **Supplementary Table 6B**), and relative high abundance of jellyfish and fish larvae, but low abundance of chaetognaths. Copepods were tolerant to environmental fluctuations, with a propensity to detritivory. The second co-inertia axis (12% of the total inertia) exhibited that species-rich copepod communities were mainly composed of passive-feeding and trophic specialist species (i.e., high CSI-trophic regime values) with a low propensity to detritivory. Copepod species were also sensitive to environmental variations, especially under warm conditions and a high protozooplankton and jellyfish biomass (**Figure 6C**); this coincides with the lowest SES-FRic and SES-RaoQ values occurring in the copepod communities.

Variation partitioning analysis (VP, **Figure 7A**) exhibited that seasonal variations of the functional structure and ecological specialization of the diatom and copepod communities were not related to seasonal changes in environmental conditions, as shown by the high residual values. It was detected that the local environment contributed the most to the explained variance (i.e., 49%) in the functional structure and ecological specialization of the diatom community (adjusted r^2 = 0.18, p = 0.001, i.e., 18% of the total variations of the diatom community), followed by hydrometeorological features (3%, p = 0.001) and the interaction between the local environment and hydrometeorological features is 16% (**Figure 7A**). The variations in the structure of the diatom community were also explained, but to a lesser extent, by the *Phaeocystis* bloom (1%, p = 0.001), predator biomass, and size (1%, p = 0.001), and their interactions (2%). The *Phaeocystis* bloom was the most contributing process to the functional structure and ecological specialization of the copepod community (15%, p = 0.001, **Figure 7B**). Hydrometeorological

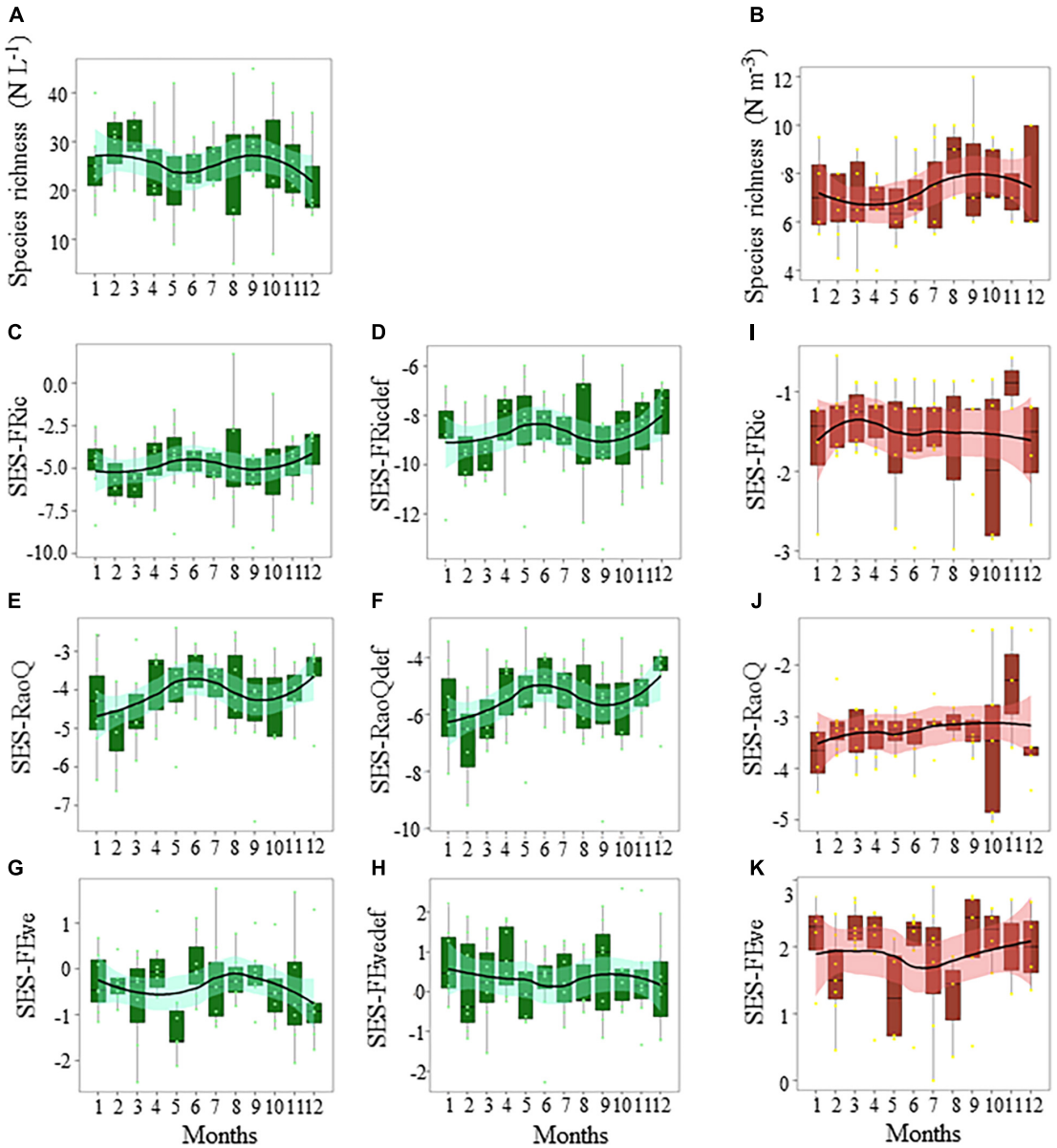

FIGURE 5 | Seasonal variations in the panels **(A,B)** species richness, **(C–E)** functional richness (SES-Fric), **(E,F,J)** functional divergence (SES-RaoQ), and **(G,H,K)** functional evenness (SES-Feve) of the diatom (**A–H**, in green) and copepod (**B,I–K**, in red) community in coastal waters of the eastern English Channel over the period 2007–2013. Def: defence traits against predation. Black horizontal line inside box: median; box: first to third quartiles; whiskers: 1.5 times the interquartile range (IQR); dots: monthly data including outliers (>1.5 times IQR). The solid line and ribbon represent LOESS smoothing and the 95% confidence interval. No difference between months ($p > 0.05$, Nemenyi test) was found between boxes for any of the variables.

features (5%, $p < 0.05$) and their interaction with the *Phaeocystis* bloom (4%), and the interaction between the local environment and predators (3%), played a minor role. In contrast to the functional structure and ecological specialization of diatom and copepod communities, the proportion of unexplained variance was low (3%) for diatom species richness. Diatom species richness was mainly explained by the convergence of a combination of traits: SES-RaoQ decreased as species richness decreased (92% of the total variations in diatom species richness, $p = 0.001$, **Figure 7C**). As for the functional structure and ecological specialization, most of the variations of copepod species richness remained unexplained (69%), and the most contributing drivers are both the convergence of a combination of traits (**Figure 7D**) and its indirect influence through interaction with the local environment (27%).

Phaeocystis biomass had no significant effect on the diatom species richness, biomass, FD (i.e., SES-FRic, SES-FEve, and SES-RaoQ), ecological specialization (i.e., niche breadths), or the functional structure (i.e., CWMs) of the diatom community (**Supplementary Figure 9**).

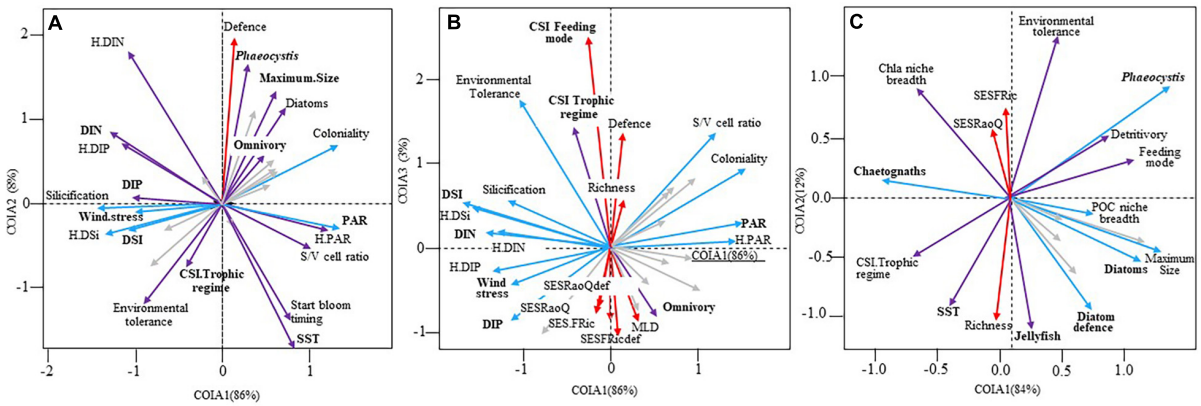

FIGURE 6 | Projection of the environmental variables, species richness, functional structure, ecological specialization and functional diversity of **(A,B)** diatoms ($N = 63$, $RV = 0.49$, $p = 10^{-3}$) and **(C)** copepods ($N = 63$, $RV = 0.36$, $p = 10^{-3}$) on the factorial maps (**A:** 1–2, **B:** 1–3 and **C:** 1–2) of the co-inertia analysis performed on the diatom and copepod community in coastal waters of the eastern English Channel over the period 2007–2013. Bold labels: "environmental" variables. Only the variables that contribute the most to the construction of the axes are labelled (see **Supplementary Table 6** for details). Gray arrows: no or low ($r < 0.5$) significant Pearson correlation between the variables and the first (blue arrows), second (red arrows) or both first and second or third (purple arrows) co-inertia axes. PAR, Photosynthetic Active Radiation; DIN, DIP, DSi, Dissolved Inorganic Nitrogen, Phosphorous, and Silica; SST, Sea Surface Temperature; S/V ratio, Surface to Volume cell ratio; MLD, Maximum Linear Dimension; CSI, Community Specialization Index; SES-FRic, the functional richness, SES-RaoQ, the functional divergence; def., defence against predation.

DISCUSSION

In this study, we investigated the challenging questions of linking the seasonal succession of planktonic organisms with resource and defense traits, and the identification of the conditions that shape species richness. The results showed that the diatom and copepod communities of the EEC respond synchronously to varying abiotic and biotic conditions. We highlighted that some environmental drivers acted on some trait combinations, through environmental filtering, leading to temporal succession in species composition. Such a pattern was possible through the expression of several well-established functional trait trade-offs that allowed us to optimize the fitness of a species in a particular environment. The results strongly suggested that the competition-defense trade-off (e.g., Hillebrand et al., 2000; Chase et al., 2002), a mechanism that favors weak competitors, better protected against predation, played a key role, not only in driving diatom and copepod species richness but also in triggering the *Phaeocystis* bloom (as shown below). We also revealed the key role of nutrient levels and competition for nutrients, and of prey-predator interactions in the seasonal succession of diatoms and copepods in the coastal waters of the EEC.

The seasonal succession of trait values within the diatom community along with the seasonal gradient of resource, turbulence, and grazing intensity, resulted from several trait trade-off effects: (i) a trade-off in the competitive ability for light vs. nutrients (i.e., S/V cell ratio, coloniality, and specialization for nutrients in opposition to silicification and specialization for light; as shown in **Figure 4A**; Huisman and Weissing, 1994; Leibold, 1997; Klausmeier and Litchman, 2001); (ii) a defense-competition trade-off (e.g., Hillebrand et al., 2000; Chase et al., 2002); and (iii) an opportunistic-gleaner strategy trade-off (Grover, 1990). We revealed a clear opposition in the dominance between *r*- and K-strategists: species with high maximum growth rate and photosynthetic efficiency adapted to low light but high nutrient and turbulent conditions on the one hand (e.g., diatoms: Armbrust, 2009, and *Phaeocystis* colony: Rousseau et al., 2007; Seuront et al., 2007; Nissen and Vogt, 2021), and species which have low maximum growth rate but high competitiveness for nutrients, such as *Synechococcus* and picoeukaryotes (Stawiarski, 2014), on the other hand. The defense-competition trade-off was deduced from the fact that the diatom communities with the highest proportion of level against predation species matched with periods of (i) high grazing intensity [i.e., late winter/spring (February–March) and late summer/autumn (September–October)] (Gasparini et al., 2000; Stelfox-Widdicombe et al., 2000; Antajan, 2004; Grattepanche et al., 2011b); and (ii) low competitiveness for nutrients (i.e., high silicification but low specialization for nutrients and low S/V cell ratio). The association between the defensive trait and cell biovolume was consistent with this functional trait trade-off (**Figure 4A**). To invest in defensive traits against predation, is generally metabolically costly, in such a way that prey with high defense levels has generally lower maximum growth rate, maximum resource uptake, and/or resource uptake affinity (Pančić and Kiørboe, 2018; Cadier et al., 2019; Ehrlich et al., 2020), all these types of defense costs being related to cell biovolume (Litchman and Klausmeier, 2008; Marañón, 2015).

We observed seasonal successions of copepod species of varying maximum size values, feeding strategies, trophic regimes, and vulnerability to predation along a seasonal gradient of turbulence, food level and composition, and predator abundance (**Figures 2A,B**, **3A–D**, **4B**, **6C**), in line with a competition-defense trade-off. Actively feeding copepods feed more efficiently on non-motile than on motile preys (i.e., competitive specialists), but they are more at predation risk

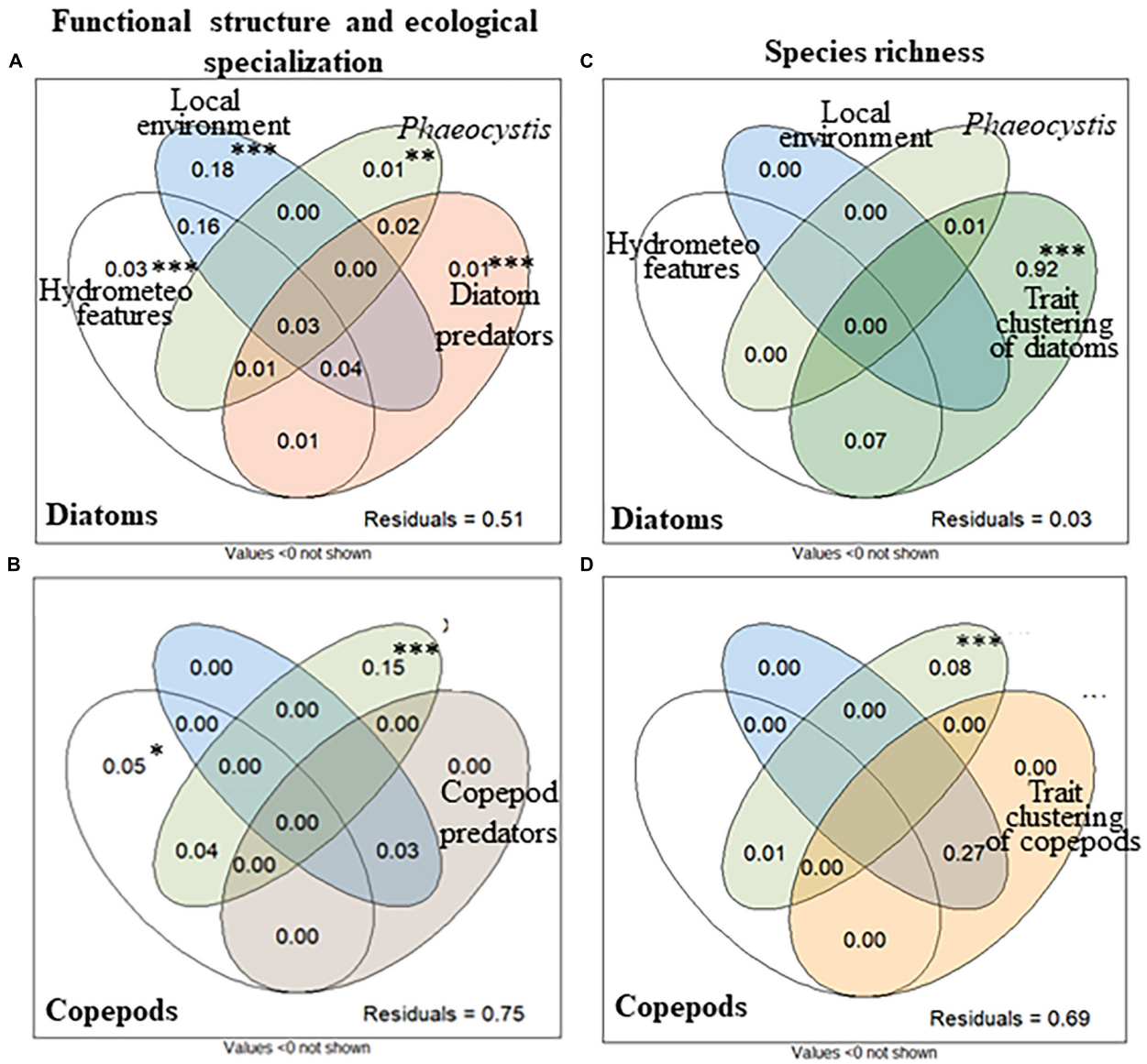

FIGURE 7 | Variation partitioning of the effect of water masses movement and hydrometeorological features (wind stress and direction, white circle), local environment (abiotic and prey biomass, blue circle), *Phaeocystis* biomass (light green circle), predator patterns (light brown: maximum.size of copepods, and biomass of copepods and protozooplankton for diatoms; dark brown: biomass of fish larvae, chaetognaths and jellyfish for copepods), biotic interaction (trait clustering as a proxy; dark green: diatoms, orange: copepods; using SES-RaoQ), the interactions, and the residual proportion on the **(A,B)** functional structure and the ecological specialization and **(C,D)** species richness of the **(A,C)** diatom and **(B,D)** copepod communities in coastal waters of the eastern English Channel over the period 2007–2013. Proportions of variations [adjusted r^2 calculated from redundancy analysis (rda)] in the response variables explained by the explanatory ones are shown. The statistical significance of proportions is calculated by permutation test for rda (***$p = 0.001$, **$p = 0.005$, and *$p < 0.05$). Variance values below are not shown. Note that the shared partitions cannot be tested for statistical significance.

than ambush feeders (i.e., defense specialists) (Almeda et al., 2018). This suggests that the shift toward the dominance of ambush copepod feeders (i.e., predators) during summer might result from strong predation pressure on active-feeding copepods by zooplanktivorous organisms, especially jellyfish (i.e., Cnidaria and Ctenaria). The increasing abundance of jellyfish during summer (**Figure 6C**) is known to exert strong top-down control on copepods (Hirst and Kiørboe, 2002). Ambush copepod feeders, mainly carnivores (**Figure 4B**), were also smaller, and with a lower metabolic cost (Kiørboe, 2011 and references therein) than actively feeding copepods. The presumed strong predation pressure of jellyfish on active-feeding copepods, in combination with the shift toward dominance of motile prey, might also explain the shift in maximum size and diet change that we observed for the copepod community from July (**Supplementary Figures 6A,C–F**). The dominance of active feeding-current feeders observed during the first quarter is consistent with the dominance of non-motile prey of high

food level (i.e., the spring bloom), their higher metabolic needs (Kiørboe, 2011 and references therein), and a lower abundance of zooplanktivore predators (**Figure 6C**). The prevalence of omnivory in winter and spring, which results from higher detritivory, is consistent with the high quantity of detrital material in winter, and both *Phaeocystis* aggregates and ghost colonies in spring (Becquevort et al., 1998; Mari et al., 2005). The significant decline in the grazing rate of copepods, often reported during a *Phaeocystis* bloom (Gasparini et al., 2000; Nejstgaard et al., 2007 and references therein), might result from a shift in the diet of copepods toward *Phaeocystis* detrital material.

We hypothesize that the increase in diatom species richness in early spring and autumn resulted from high grazing pressure by generalist copepods, which grazed the dominant highly competitive diatoms that displayed weak defensive traits. Annual maxima of diatom species richness (**Figure 5A** and **Supplementary Figure 7A**) matched with periods of annual maxima of defense level (**Figure 6B** and **Supplementary Figures 4O,P**) and high grazing pressure occurred at this time of the year (Gasparini et al., 2000; Antajan, 2004). Seasonal variations in diatom species richness were inversely related to functional divergence linked to resource and defense (SES-RaoQ and SES-RaoQdef) (**Figures 5A,E,F** and **Supplementary Figures 7A,D,E**). This indicates that species richness increased as the diatom community converged toward species of similar traits for resource and defense. Trait convergence, which results from abiotic stress (Cornwell and Ackerly, 2009) and/or competitive dominance and ensuing species exclusion (Mayfield and Levine, 2010), is unlikely given the increase in diatom biomass and species richness in early spring and autumn. Cavender-Bares et al. (2009) demonstrated that generalist consumers are expected to cluster prey communities toward species with high defense levels. Although we observed a pattern in line with Cavender-Bares et al. (2009) during the spring period, the autumnal peak in diatom species richness that we observed in the data was associated with specialist ambush and carnivore feeders: such a discrepancy may result from the high predation pressure exerted by jellyfish on generalist and actively feeding copepods (**Figure 6C**), which are more vulnerable to predation in comparison to passive ambush feeders (Kiørboe, 2011 and references therein). Copepod species richness also peaked in autumn, when the copepod community converged toward species of the similar maximum size, trophic preference, and feeding mode (**Figure 6C**) and when we observed dominance of copepod species less vulnerable to predation (i.e., passive ambush feeders; Kiørboe, 2011 and references therein, Almeda et al., 2018; refer also "feeding mode" in **Figure 6C** and **Supplementary Table 6**). However, the seasonal succession of copepod species was by far less evident than for diatoms. The lack of identification of the different copepodite stages, with sizes varying by one order of magnitude between the different copepodite stages (i.e., CI–CVI, Durbin and Durbin, 1978; Cohen and Lough, 1981), probably explained the result. Moreover, copepods live much longer than diatom cells (several months/up to 1 year for copepods, but a few days for diatoms) and their traits enable them to survive in unfavorable conditions. Large unexplained variance (>50%), as we quantified in the VP analysis, is common in ecological studies (Brasil et al., 2020 and references therein) and is often the result of (i) unmeasured environmental drivers, such as trace metals (Chappell et al., 2019); and (ii) potential antagonistic responses among species within a community (Brasil et al., 2020). Brasil et al. (2020) have also recently provided evidence that the assessment of biodiversity and FD is influenced by the presence/lack of rare species: rarity can contribute to large residuals when varpart models are computed. The uncertainty in plankton counts [estimated to be 10% for diatoms based on the table of Lund et al. (1958), and 3–40% for zooplankton (Mack et al., 2012; Kwong and Pakhomov, 2021) with an average of 30% (Frontier, 1969)] could have contributed to the large unexplained discrepancies found in the VP analyses (Brasil et al., 2020). Uncertainty in the species carbon conversion factors that we used for the calculation may have also influenced the estimations and the initial assumptions on how to capture the biological responses, such as linearity of the relationships between the response and explanatory matrices or statistical normality.

Despite potential shortcomings inherent to both the nature of the data and methodological assumptions, we characterized the important role of prey-predator interaction in shaping autumnal copepod community as a consequence of a strong predation pressure by jellyfish on the actively feeding copepods, which in turn induces relaxation of prey-prey competitive interactions. Because of the dominance of phytoplankton r- strategists in spring and autumn, generalist consumers might have grazed mainly on the dominant diatom species that displayed higher growth rates than diatom species with strongly defended cells. Several studies have suggested that species coexistence is possible only under both high grazing pressure and nutrient level conditions to allow the strongly grazed species to regrow after grazing (e.g., Proulx and Mazumder, 1998; Leibold, 1999; Worm et al., 2002). This could explain why diatom species richness declined in summer when nutrients are growth-limiting and the grazing pressure much lower than in spring and autumn (Gasparini et al., 2000; Stelfox-Widdicombe et al., 2000; Antajan, 2004; Grattepanche et al., 2011b). The defense-competition trade-offs could have reduced the frequency of well-defended, but poor-competitive, species and reduced diatom species richness in nutrient-limiting conditions that favor competitive exclusion. The relatively high S/V cell ratio and chain length values, but lowest silicification and defense level, observed in summer, reinforce this idea of the prevalence of competitive exclusion during this period. The concomitant shift toward niche differentiation through the tendency toward a decrease in functional divergence (e.g., Cornwell and Ackerly, 2009), according to the principle of limiting similarity (Macarthur and Levins, 1967), also suggested competitive exclusion. Such shift toward niche differentiation, paralleled by a decrease in species richness, started in April from the maximum of the *Phaeocystis* bloom. It suggests that the unbalancing of the defense-competition trade-off toward competitive exclusion began at the time *Phaeocystis* is a poor competitor for nitrate (Lancelot et al., 1998), has, in average, a lower maximum growth rate than diatoms (e.g., Breton et al., 2017 and reference therein), but strong protection against grazing by forming colonies that grow larger in the presence of predators (Jakobsen and Tang, 2002; Long et al., 2007; Nejstgaard et al., 2007, and references therein). *Phaeocystis* might have consequently benefited from the grazing

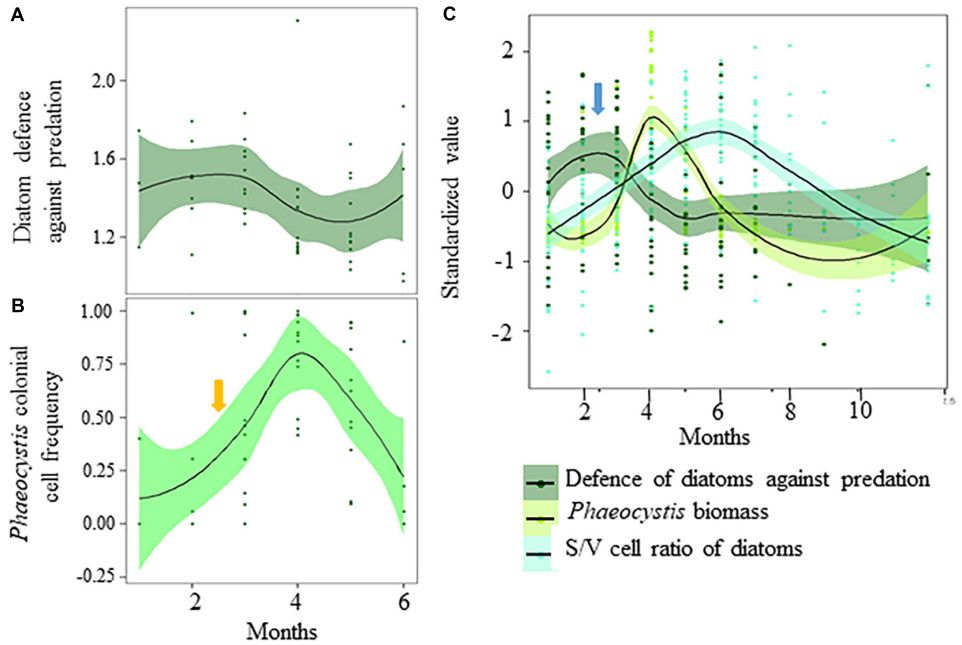

FIGURE 8 | Winter-spring variations in panel **(A)** the Community-Weight mean of Defence against predation of the diatom community (standardized value; black line and dark green shading), and **(B,C)** *Phaeocystis* colonial cell frequency and biomass (standardized value; black line and green shading) in coastal waters of the eastern English Channel over the **(A,B)** 2007–2019 and **(C)** 1996–2019. The solid line and ribbon represent LOESS smoothing and the 95% confidence interval, respectively. Standardized values were calculated per year. Note that **(A)** the seasonal maximum of the defense trait value, **(B)** the start of the transformation of *Phaeocystis* flagellate cells into colonial cells embedded into a mucopolysaccharide matrix (orange arrow) and **(C)** the start *Phaeocystis* bloom timing (blue arrow) are synchronised. Note that the S/V cell ratio of diatoms as proxy of competitiveness is low at this time **(C)**.

preference of generalists toward poor-defended, but highly competitive, species (**Figure 8**). The seasonal maximum of the defense trait value (**Figure 8A**), the start of the transformation of *Phaeocystis* flagellate cells into colonial cells embedded into a mucopolysaccharide matrix (**Figure 8B**, orange arrow), as well as the timing of bloom initiation of *Phaeocystis* (**Figure 8C**, blue arrow), were synchronized. The results highlight the potential key role in the defense-competition trade-off besides nutrient level in triggering the *Phaeocystis* bloom, and more generally, the cardinal role of generalist consumers in the initiation of the bloom. As observed for other ecological communities [Chihoub et al., 2020 (copepods); Wengrat et al., 2018 (diatoms); Villéger et al., 2014; Menezes et al., 2015; Alexander et al., 2017 (fish); Rogalski et al., 2017 (daphniids); Donohue et al., 2009; Zhang et al., 2019 (benthic invertebrates)], eutrophication favors biotic homogenization, which in turn may favor blooms of inedible species such as *Phaeocystis*. We did not detect any negative effect of the *Phaeocystis* bloom on the plankton community (**Supplementary Figure 9**), but a shift of the copepod community toward biotic homogenization was detected.

CONCLUSION

The application of a trait-based approach, combined with the assessment of ecological specialization, has made possible a better understanding of seasonal succession and biodiversity patterns in plankton along gradients of resources, turbulence, and grazing pressure. We have shown that species succession is driven by different trade-offs among functional traits, under the functional constraints dictated by the environmental pressure encountered by plankton communities across the seasons. We suggest that the competition-defense trade-off plays an important role in promoting plankton species richness and in triggering the *Phaeocystis* bloom in coastal waters of the EEC. By successively favoring species with ecological strategies that match environmental conditions, the diatom and copepod communities in coastal waters of the EEC respond synchronously to varying resources and biotic conditions.

DATA AVAILABILITY STATEMENT

The raw data supporting the conclusions of this article are available by the authors in **Supplementary Data**.

AUTHOR CONTRIBUTIONS

EB, BS, and EG conceptualized the study. EB and EG performed the investigation on methodology. EB, BS, D-IS, DP, CS, MC, SF, J-MB, and AL provided the abiotic and biological data. EB, AP, OD, and EG performed the data analysis. EB, UC, EG, BS, LK, GB, and LS contributed to the manuscript writing. All authors contributed to the article and approved the submitted version.

FUNDING

This work was a contribution of the project EVOLECO-NUPHY supported by the French National program LEFE (Les Enveloppes Fluides et l'Environnement).

ACKNOWLEDGMENTS

We acknowledge the three reviewers for their constructive comments, which allowed us to greatly improve the manuscript. We thank the crews who helped during long-term monitoring downstream of the Gironde estuary (2001–2017) and in coastal waters of the eastern English Channel (1996–2019), and the SOMLIT teams for sampling and physicochemical measurements and analysis, especially N. Degros, E. Lecuyer, and H. Derriennic. We also thank the students T. Rault and G. Parmentier for copepod identification and counts and S. Bosc and P. Faye for their contribution to diatom cell measurements. This work is dedicated to J.-M. Dewarumez, who managed SOMLIT at Wimereux, and P. Lebleu, who performed sampling in the Gironde estuary.

SUPPLEMENTARY MATERIAL

The Supplementary Material for this article can be found online at: https://www.frontiersin.org/articles/10.3389/fmars.2021.656300/full#supplementary-material

REFERENCES

Alexander, T. J., Vonlanthen, P., and Seehausen, O. (2017). Does eutrophication-driven evolution change aquatic ecosystems? *Philos. Trans. R. Soc. B Biol. Sci.* 19:372. doi: 10.1098/rstb.2016.0041

Almeda, R., van Someren Gréve, H., Kiørboe, T. (2018). Prey perception mechanism determines maximum clearance rates of planktonic copepods. *Limnol. Oceanogr.* 63, 2695–2707. doi: 10.1002/lno.10969

Aminot, A., and Kérouel, R. (2004). *Hydrologie des Écosystèmes Marins: Paramètres et Analyses*. Brest: Ifreme.

Antajan, E. (2004). *Responses of Calanoid Copepods to Changes in Phytoplankton Dominance in the Diatoms - Phaeocystis Globosa Dominated Belgium Coastal Waters*. Ph.D. thesis. Brussel: Vrije Universiteit Brussel, 142.

Armbrust, E. V. (2009). The life of diatoms in the world's oceans. *Nature* 459, 185–192. doi: 10.1038/nature08057

Beaugrand, G., Brander, K. M., Lindley, J. A., Souissi, S., Reid, P. C. (2003). Plankton effect on cod recruitment in the North Sea. *Nature* 426, 661–664. doi: 10.1038/nature02164

Becquevort, S., Rousseau, V., and Lancelot, C. (1998). Major and comparable roles for free-living and attached bacteria in the degradation of *Phaeocystis*-derived organic matter in coastal waters of the North Sea. *Aquat. Microb. Ecol.* 14, 39–48. doi: 10.3354/ame014039

Benedetti, F., Gasparini, S., and Ayata, S. D. (2016). Identifying copepod functional groups from species functional traits. *J. Plankton Res.* 38, 159–166. doi: 10.1093/plankt/fbv096

Bjærke, O., Jonsson, P. R., Alam, A., and Selander, E. (2015), Is chain length in phytoplankton regulated to evade predation? *J. Plankton Res.* 37, 1110–1119. doi: 10.1093/plankt/fbv076

Biggs, C. R., Yeager, L. A., Bolser, D. G., Bonsell, C., Dichiera, A. M., Hou, Z., et al. (2020). Does functional redundancy affect ecological stability and resilience? A review and meta-analysis. *Ecosphere* 11: e03184. doi: 10.1002/ecs2.3184

Blonder, B., Lamanna, C., Violle, C. and Enquist, B. J. (2014). The n-dimensional hypervolume. *Global Ecol. Biogeogr.* 23, 595–609. doi: 10.1111/geb.12146

Bonato, S., Breton, E., Didry, M., Lizon, F. (2016). Spatio-temporal patterns in phytoplankton assemblages in coastal-offshore gradients using flow cytometry: a case study in the eastern English Channel. *J. Mar. Syst.* 156, 76–85. doi: 10.1016/j.jmarsys.2015.11.009

Borcard, D. P, Legendre, P, Drapeau, P. (1992). Partialling out the spatial component of ecological variation. *Ecology* 73, 1045–1055. doi: 10.2307/1940179

Botta-Dukát, Z. (2005), Rao's quadratic entropy as a measure of functional diversity based on multiple traits. *J. Veg. Sci.* 16, 533–540. doi: 10.1111/j.1654-1103.2005.tb02393.x

Botta-Dukát, Z. and Czúcz, B. (2016). Testing the ability of functional diversity indices to detect trait convergence and divergence using individual-based simulation. *Methods Ecol. Evol.* 7, 114–126.

Brasil, L. S., Vieira, T. B., Andrade, A. F. A. (2020). The importance of common and the irrelevance of rare species for partition the variation of community matrix: implications for sampling and conservation. *Sci. Rep.* 10:19777.doi: 10.1038/s41598-020-76833-5

Breton E., Brunet C., Sautour B., and Brylinski, J. M. (2000). Annual variations of phytoplankton biomass in the eastern English Channel: comparison by pigment signatures and microscopic counts. *J. Plankton Res.* 22, 1423–1440. doi: 10.1093/plankt/22.8.1423

Breton, E., Rousseau, V., Parent, J. Y., Ozer, J., and Lancelot, C. (2006). Hydroclimatic modulation of diatom/*Phaeocystis* blooms in nutrient-enriched Belgian coastal waters (North Sea). *Limnol. Oceanogr.* 51, 1401–1409. doi: 10.4319/lo.2006.51.3.1401

Breton, E., Christaki, U., Bonato, S., Didry, M., and Artigas, L. F. (2017). Functional trait variation and nitrogen use efficiency in temperate coastal phytoplankton. *Mar. Ecol. Prog. Ser.* 563, 35–49. doi: 10.3354/meps11974

Brody, S. R., Lozier, M. S., and Dunne, J. P. (2013). A comparison of methods to determine phytoplankton bloom initiation. *J. Geophys. Res. Oceans*, 118, 2345–2357. doi: 10.1002/jgrc.20167

Brun, P., Payne, R., and Kiørboe, T. (2017). A trait database for marine copepods. *Earth Syst. Sci. Data* 9, 99–113. doi: 10.5194/essd-2016-30

Buitenhuis, E. T., Li, W. K. W., Vaulot D., Lomas M. W. (2012). Picophytoplankton biomass distribution in the global ocean. *Earth Syst. Sci. Data* 4, 37–46. doi: 10.5194/essd-4-37-2012

Cadier, M., Andersen, K. H., Visser, A. W. and Kiørboe, T. (2019). Competition–defense tradeoff increases the diversity of microbial plankton communities and dampens trophic cascades. *Oikos* 128, 1027–1040. doi: 10.1111/oik.06101

Cahoon, L. B. (1999). The role of benthic microalgae in neritic ecosystems. *Oceanogr. Mar. Biol. Annu. Rev.* 37, 47–86.

Cavender-Bares, J., Kozak, K. H., Fine, P. V. A., and Kembel, S. W. (2009). The merging of community ecology and phylogenetic biology. *Ecol. Lett.* 12, 693–715. doi: 10.1111/j.1461-0248.2009.01314.x

Chappell, P. D., Armbrust, E. V., Barbeau, K. A., Bundy, R. M., Moffett, J. W., Vedamati, J., and Jenkins, B. D. (2019). Patterns of diatom diversity correlate with dissolved trace metal concentrations and longitudinal position in the northeast Pacific coastal offshore transition zone. *Mar. Ecol. Prog. Ser.* 563, 35–49.

Chase, J. M., Abrams, P. A., Grover, J. P., Diehl, S., Chesson, P., Holt, R. D. et al. (2002). The interaction between predation and competition: a review and synthesis. *Ecol. Lett.* 5, 302–315. doi: 10.1046/j.1461-0248.2002.00315.x

Chessel, D., Dufour, A. B., and Thioulouse, J. (2004). The ade4 package-I-One-table methods. *R. News* 4, 5–10.

Chihoub, S., Christaki, U., Chelgham, S., Amara, R., Ramdane, Z., Zebboudj, A., Rachik, S., and Breton, E. (2020). Coastal eutrophication as a potential driver of functional homogenization of copepod species assemblages in the Mediterranean Sea. *Ecol. Ind.* 115:106388. doi: 10.1016/j.ecolind.2020.106388

Clavel, J., Julliard, R., and Devictor, V. (2011). Worldwide decline of specialist species: toward a global functional homogenization? *Front. Ecol. Environ.* 9, 222–228. doi: 10.1890/080216

Cohen, R. E. and Lough, R. G. (1981). Length-weight relationships for several copepods dominant in the Georges BankGulf of Maine area. *J. Northw. Atl. Fish. Sci.* 2, 47–52. doi: 10.2960/J.v2.a4

Conway, D. V. P. (2006). Identification of the copepodite developmental stages of twenty-six North Atlantic copepods. *J. Mar. Biolog. Assoc. U.K.* 21, 1–28.

Cornwell, W. K. and Ackerly, D. D. (2009). Community assembly and shifts in plant trait distributions across an environmental gradient in coastal California. *Ecol. Monogr.* 79, 109–126. doi: 10.1890/07-1134.1

Dam, H. G. and Peterson, W. T. (1991). *In situ* feeding behaviour of the copepod *Temora longicornis*: effects of seasonal changes in chlorophyll size fractions and female size. *Mar. Ecol. Prog. Ser.* 71, 113–123. doi: 10.3354/meps071113

Djeghri, N., Atkinson, A., Fileman, E. S., Harmer, R. A., Widdicombe, C. E., McEvoy, A. J., Cornwell, L., Mayor, D. J. (2019). High Prey-predator size ratios and unselective feeding in copepods: a seasonal comparison of five species with contrasting feeding modes, *Prog. Oceanogr*.177:102039. doi: 10.1016/j.pocean.2018.11.005

Dolédec, S., and Chessel, D. (1994). Co-inertia analysis: an alternative method for studying species–environment relationships. *Freshw. Biol.* 31, 277–294. doi: 10.1016/0269-7491(87)90079-0

Dolédec, S., Chessel, D. and Gimaret-Carpentier, C. (2000). Niche separation in community analysis: a new method. *Ecology* 81, 2914–2927. doi: 10.1890/0012-96582000081

Donohue, I., Jackson, A. L., Pusch, M. T., and Irvine, K. (2009). Nutrient enrichment homogenizes lake benthic assemblages at local and regional scales. *Ecology* 90, 3470–3477. doi: 10.1890/09-0415.1

Dray, S., Chessel, D., and Thioulouse, J. (2003). Co-inertia analysis and the linking of ecological data tables. *Ecology* 84, 3078–3089. doi: 10.1890/03-0178

Dray, S., Dufour, A.B., and Chessel, D. (2007). The ade4 Package-II: two-table and K-table methods. *R. News* 7, 47–52.

Dray, S., Pélissier, R., Couteron, P., Fortin, M., Legendre, P., Peres-Neto, P. R., et al. (2012). Community ecology in the age of multivariate multiscale spatial analysis. *Ecol. Monogr.* 82, 257–275. doi: 10.1890/11-1183.1

Durbin, E. G. and Durbin, A. G. (1978). Length and weight relationships of *Acartia clausi* from Narragansett Bay, R.I. *Limnol. Oceanogr.* 23, 958–969 doi: 10.4319/lo.1978.23.5.0958

Ehrlich, E., Kath, N. J., and Gaedke, U. (2020). The shape of a defense-growth trade-off governs seasonal trait dynamics in natural phytoplankton. *ISME J.* 14, 1451–1462. doi: 10.1038/s41396-020-0619-1

Frontier, S. (1969). Sur une méthode d'analyse faunistique rapide du zooplancton. exp. mar. *Biol. Ecol.* 3, 18–26.

Garnier, E., Cortez, J., Billes, G., Navas, M. L., Roumet, C., Debussche, M., Laurent, G., Blanchard, A., Aubry, D., Bellmann, A., Neill, C., and Toussaint, J. P. (2004). Plant functional markers capture ecosystem properties during secondary succession. *Ecology* 85, 2630–2637. doi: 10.1890/03-0799

Garnier, J., Riou, P., Le Gendre, R., Ramarson, A., Billen, G, Cugier, P., Schapira, M., Théry, S., Thieu, V., Ménesguen, A. (2019). Managing the agri-food system of watersheds to combat coastal eutrophication: a land-to-sea modelling approach to the french coastal english channel. Geosciences 9:441. doi: 10.3390/geosciences9100441

Gasparini, S., Daro, M. H., Antajan, E., Tackx, M., Rousseau, V., Parent, J. Y., and Lancelot, C. (2000). Mesozooplankton grazing during the *Phaeocystis globosa* bloom in the Southern Bight of the North Sea. *J. Sea Res.* 43, 345–356. doi: 10.1016/S1385-1101(00)00016-2

Gini, C., (1912). «Variabilità e Mutabilità», Studi Economico-Giuridici dell'Univ. Di Cagliari 3, 1–158. doi: 10.2307/2340052

Gómez, F. and Souissi, S. (2007). The distribution and life cycle of the dinoflagellate Spatulodinium pseudonoctiluca (Dinophyceae, Noctilucales) in the northeastern English Channel. *C. R. Biologies*, 330, 231–236. doi: 10.1016/j.crvi.2007.02.002

Gotelli, N. J. and McCabe, D. J. (2002). Species co-occurrence: a meta-analysis of J. M. Diamond's assembly rules model. *Ecology* 83, 2091–2096. doi: 10.1890/0012-96582002083

Gower, J. C. (1971). A general coefficient of similarity and some of its properties. *Biometrics* 27:857. doi: 10.2307/2528823

Grattepanche, J. D., Breton, E., Brylinski, J. M., Lecuyer, E., and Christaki, U. (2011a). Succession of primary producers and micrograzers in a coastal ecosystem dominated by *Phaeocystis globosa* blooms. *J. Plankton Res.* 33, 37–50. doi: 10.1093/plankt/fbq097

Grattepanche, J. D., Vincent, D., Breton, E., and Christaki, U. (2011b). Microzooplankton herbivory during the diatom-*Phaeocystis* spring succession in the eastern English Channel. *J. Exp. Mar. Biol. Ecol.* 404, 87–97. doi: 10.1016/j.jembe.2011.04.004

Grover, J. P. (1989). Influence of cell shape and size on algal competitive ability. *J. Phycology* 25, 402–405. doi: 10.1111/j.1529-8817.1989.tb00138.x

Grover, J. (1990). Resource competition in a variable environment: phytoplankton growing according to Monod's model. *Am. Nat.* 136, 771–789. doi: 10.1086/285131

Halpern, B. S., Walbridge, S., Selkoe, K. A., Kappel, C. V., Micheli, F. (2008). A global map of human impact on marine ecosystems. *Science* 319, 948–952. doi: 10.1126/science.1149345

Halse, G. R., and Syvertsen, E. E. (1996). "Chapter 2 - marine diatoms". ed C.R. *Tomas. Identifying Marine Diatoms and Dinoflagellates* (Cambridge, MA: Academic Press), 5–385.

Hill, S. L., Harfoot, M., Purvis, A., Purves, D. W., Collen, B., Newbold, T., Burgess, N. D. and Mace, G. M. (2016). Reconciling biodiversity indicators to guide understanding and action. *Conserv. Lett.* 9, 405–412. doi: 10.1111/conl.12291

Hillebrand, H., Worm, B., and Lotze, H. K. (2000). Marine microbenthic community structure regulated by nitrogen loading and grazing pressure. *Mar. Ecol. Prog. Ser.* 204, 27–38. doi: 10.3354/meps204027

Hillebrand, H., Dürselen, C. D., Kirschtel, D., Pollingher, U., and Zohary, T. (1999). Biovolume calculation for pelagic and benthic microalgae, *J. Phycol.* 35, 403–424. doi: 10.1046/j.1529-8817.1999.3520403.x

Hirst, A. G., and Kiørboe, T. (2002). Mortality of marine planktonic copepods: global rates and patterns. *Mar. Ecol. Prog. Ser.* 230, 195–209. doi: 10.3354/meps230195

Holmes, R. M., Aminot, A., Kérouel, R., Hooker, B. A., and Peterson, B. J. (1999). A simple and precise method for measuring ammonium in marine and freshwater ecosystems. *Can. J. Fish Aquat. Sci.* 56, 1801–1808. doi: 10.1139/f99-128

Hoppenrath, M., Elbrächter, M., Drebes, G. (2009). *Marine Phytoplankton. Selected Microphytoplankton From the North Sea Around Helgoland and Sylt, E.* Stuttgart: Schweizerbartsche Verlagsbuchhandlung, 264.

Howarth, R. W. (2008). Coastal nitrogen pollution: a review of sources and trends globally and regionally. *Harmful Algae* 8, 14–20. doi: 10.1016/j.hal.2008.08.015

Huisman, J. and Weissing, F. J. (1994). Light-limited growth and competition for light in well-mixed aquatic environments: an elementary model. *Ecology* 75, 507–520. doi: 10.2307/1939554

Jacoby, W. G. (2000). LOESS: a nonparametric, graphical tool for depicting relationships between variables. *Electoral Stud.* 19, 577–613. doi: 10.1016/S0261-3794(99)00028-1

Jakobsen, H. H., and Tang, K. W. (2002). Effects of protozoan grazing on colony formation in *Phaeocystis globosa* (Prymnesiophyceae) and the potential costs and benefits. *Aquat. Microb. Ecol.*, 27, 261–273. doi : 10.3354/ame027261

Jakobsen, H. H., and Markager, S. (2016). Carbon-to-chlorophyll ratio for phytoplankton in temperate coastal waters: seasonal patterns and relationship to nutrients. *Limnol. Oceanogr.* 61, 1853–1868. doi: 10.1002/lno.10338

Karp-Boss, L., Boss, E., and Jumars, P. A. (1996). Nutrient fluxes to planktonic osmotrophs in the presence of fluid motion. *Oceanogr. Mar. Biol.* 34, 71–107.

Key, T., McCarthy, A., Campbell, D. A., Six, C., Roy S. (2010). Cell size trade-offs govern light exploitation strategies in marine phytoplankton. *Environ. Microbiol.* 12, 95–104. doi: 10.1111/j.1462-2920.2009.02046.x

Kiørboe, T. (2011). How zooplankton feed: mechanisms, traits and trade-offs. *Biol. Rev.* 86, 311–339. doi: 10.1111/j.1469-185X.2010.00148.x

Kiørboe, T. and Hirst, A. G. (2014). Shifts in mass scaling of respiration, feeding, and growth rates across life-form transitions in marine pelagic organisms. *Am. Nat.* 183, 118–130. doi :10.1086/675241

Klausmeier, C. A. and Litchman, E. (2001). Algal games: the vertical distribution of phytoplankton in poorly mixed water columns. *Limnol. Oceanogr.* 46, 1998–2007. doi: 10.4319/lo.2001.46.8.1998

Kleppel, G. (1993). On the diets of calanoid copepods. *Mar. Ecol. Prog. Ser.* 99, 183–195.

Kneitel, J. M. and Chase, J. M. (2004). Trade-offs in community ecology: linking spatial scales and species coexistence. *Ecol. Lett.* 7, 69–80. doi: 10.1046/j.1461-0248.2003.00551.x

Kofoid, C. A. and Campbell, A. S. (1929). A conspectus of the marine and freshwater Ciliata belonging to the suborder Tintinnoinea with descriptions of new species, principally from the Agassiz Expedition to the eastern tropical Pacific, 1904–05. *Univ. Calif. Publ. Zool.* 34:403.

Kuhn, M., Wing, J., Weston, S., Williams, A., Keefer, C., Engelhardt, A., et al. (2016). *caret: Classification and Regression Training. R package version 6.0-71*. Available online at: https://CRAN.R-project.org/package=caret

Kwong, L. E, and Pakhomov, A. E. (2021). Zooplankton size spectra and production assessed by two different nets in the subarctic Northeast Pacific, *J. Plankton Res.* 43, 527–545. doi: 10.1093/plankt/fbab039

Laliberté, E. and Legendre, P. (2010). A distance-based framework for measuring functional diversity from multiple traits. *Ecology* 91, 299–305. doi: 10.1890/08-2244.1

Lancelot, C. (1995). The mucilage phenomenon in the continental coastal waters of the North Sea. *Sci. Tot. Environ. Mar. Mucilages* 165, 83–102. doi: 10.1016/0048-9697(95)04545-

Lancelot, C., Billen, G., Sournia, A., Weisse, T., Colijn, F., Veldhuis, M. J. W., et al. (1987). *Phaeocystis* blooms and nutrient enrichment in the continental coastal zones of the North Sea. *Ambio* 16, 38–46. doi: 10.1016/0198-0254(87)90379-7

Lancelot, C., Keller, M. D., Rousseau, V., Smith, W. O. Jr., and Mathot S. (1998). "Autoecology of the marine haptophyte *Phaeocystis* sp," in *Physiological Ecology of Harmful Algal Blooms NATO ASI Series*, eds D. M. Anderson, A. D. Cembella, and G. M. Hallegraeff (Berlin: Springer Verlag), 209–224

Legendre, P. and Legendre, L. (1998). *Numerical Ecology*, 2nd edn. Amsterdam: Elsevier ScienceBV.

Legendre, P. and Legendre, L. (2012). *Numerical Ecology: Developments in Environmental Modelling*, Vol. 24. Amsterdam: Elsevier Science and Technology.

Leibold, M.A. (1997). Do nutrient-competition models predict nutrient availabilities in limnetic ecosystems? *Oecologia* 110, 132–142. doi: 10.1007/s004420050141

Leibold, M. A. (1999). Biodiversity and nutrient enrichment in pond plankton communities. *Evol. Ecol. Res.* 1, 73–95.

Leynaert, A, Bucciarelli, E., Claquin, P., Dugdale, R. C., Martin-Jézéquel, V., Pondaven, P., and Ragueneau, O. (2004). Effect of iron deficiency on diatom cell size and silicic acid uptake kinetics. *Limnol. Oceanogr.* 49, 1134–1143. doi: 10.4319/lo.2004.49.4.1134

Lingoes, J. C. (1971). Some boundary conditions for a monotone analysis of symmetric matrices. *Psychometrika* 36, 195–203. doi: 10.1007/BF02291398

Litchman, E, Klausmeier, C. A, Schofield, O. M, Falkowski, P.G (2007). The role of functional traits and trade-offs in structuring phytoplankton communities: scaling from cellular to ecosystem level. *Ecol. Lett.* 10, 1170–1181. doi: 10.1111/j.1461-0248.2007.01117.x

Litchman, E., and Klausmeier, C. A. (2008). Trait-based community ecology of phytoplankton. *Annu. Rev. Ecol. Evol. Syst.* 39, 615-639. doi: 10.1146/annurev.ecolsys.39.110707.173549

Litchman, E., Ohman, M. D., and Kiørboe, T. (2013). Trait-based approaches to zooplankton communities. *J. Plankton Res.* 35, 473–484.

Long, J. D., Smalley, G. W., Barsby, T., Anderson, J. T; and Hay, M. E. (2007). Chemical cues induce consumer-specific defenses in a bloom forming marine phytoplankton. *Proc. Natl. Acad. Sci. U.S.A.* 104, 10512–10517.

Lorenzen, C. J. (1967). Determination of chlorophyll and pheopigments: spectrophotometric equations. *Limnol. Oceanogr.* 12, 343–346. doi: 10.4319/lo.1967.12.2.0343

Lovecchio, S., Climent, E., Stocker, R., and Durham, W. M. (2019). Chain formation can enhance the vertical migration of phytoplankton through turbulence. *Sci. Adv.* 5:eaaw7879. doi: 10.1126/sciadv.aaw7879

Lund, J. W. G., Kipling, C., and Le Cren, E. D. (1958). The inverted microscope method of estimating algal numbers and the statistical basis of estimations by counting. *Hydrobiologia* 11, 143–170. doi: 10.1007/BF00007865

Maar, M., Nielsen, T. G., Richardson, K. (2002). Spatial and temporal variability of food web structure during the spring bloom in the Skagerrak. *Mar. Ecol. Prog. Ser.* 239, 11–29.

Mack, H. R., Conroy, J. D., Blocksom, K. A., Stein, R. A., and Ludsin, S. A. (2012). A comparative analysis of zooplankton field collection and sample enumeration methods. *Limnol. Oceanogr. Methods* 10:41. doi: 10.4319/lom.2012.10.41

Marañón, E. (2015). Cell size as a key determinant of phytoplankton metabolism and community structure. *Annu. Rev. Mar. Sci.* 7, 241–264. doi: 10.1146/annurev-marine-010814-015955

Mari, X., Rassoulzadegan, F., Brussaard, C., and Wassmann, P. (2005). Dynamics of transparent exopolymeric particles (TEP) production by *Phaeocystis globosa* under N- or P limitation: a controlling factor of the retention/export balance? *Harmful Algae* 4, 895–914. doi: 10.1016/j.hal.2004.12.014

Marie, D., Brussaard, C. P. D., Partensky, F., and Vaulot, D. (1999). "Flow cytometric analysis of phytoplankton, bacteria and viruses," in *Current Protocols in Cytometry*, Vol. 11, ed. J. P. Robinson (New York: John Wiley & Sons), 1–15.

Martin-Jézéquel, V., and Lopez, P. J. (2003). Silicon – a central metabolite for diatom growth and morphogenesis. *Prog. Mol. Subcell. Biol.* 33, 99–124. doi: 10.1007/978-3-642-55486-5_4

Martin-Jézéquel, V., Hildebrand, M., Brzezinski, M. A. (2000). Silicon metabolism in diatoms: implications for growth. *J. Phycology* 36, 821–840. doi: 10.1104/pp.107.107094

Mason, N.W., de Bello, F., Mouillot, D., Pavoine, S., and Dray, S. (2013). A guide for using functional diversity indices to reveal changes in assembly processes along ecological gradients. *J. Veg. Sci.* 24, 794–806. doi: 10.1111/jvs.12013

Mayfield, M. M., and Levine, J. M. (2010). Opposing effects of competitive exclusion on the phylogenetic structure of communities. *Ecol. Lett.* 13, 1085–1093. doi: 10.1111/j.1461-0248.2010.01509.x

Macarthur, R., and Levins, R. (1967). Limiting similarity, convergence, and divergence of coexisting Species. *Am. Nat.* 101, 377–385. doi: 10.1086/282505

McGinty, N., Barton A. D., Record, N. R., Finkel, Z. V., and Irwin, A. J. (2018). Traits structure copepod niches in the North Atlantic and Southern Ocean. *Mar. Ecol. Prog. Ser.* 601, 109–126. doi: 10.3354/meps12660

MacKenzie, B. R., and Leggett, W. C. (1991). Quantifying the contribution of small-scale turbulence to the encounter rates between larval fish and their zooplankton prey: effects of wind and tide. *Mar. Ecol. Prog. Ser.* 73, 149–160. doi: 10.3354/meps213229

Mason, N. W. H., Mouillot, D., Lee, W. G., and Wilson, J. B. (2005). Functional richness, functional evenness and functional divergence: the primary components of functional diversity. *Oikos* 111, 112–118. doi: 10.1111/j.0030-1299.2005.13886.x

McLean, M. J., Mouillot, D., Goascoz, N., Schlaich, I., and Auber, A. (2019). Functional reorganization of marine fish nurseries under climate warming. *Glob. Chang. Biol.* 25, 660–674. doi: 10.1111/gcb.14501

Menden-Deuer, S., and Lessard, E. J. (2000). Carbon to volume relationships for dinoflagellates, diatoms, and other protist plankton. *Limnol. Oceanogr.* 45, 569–579. doi: 10.4319/lo.2000.45.3.0569

Ménesguen, A., Desmit, X., Dulière, V., Lacroix, G., Thouvenin, B., Thieu, V., Dussauze, M. (2018). How to avoid eutrophication in coastal seas? A new approach to derive river-specific combined nitrate and phosphate maximum concentrations. *Sci. Tot. Environ.* 628, 400–414. doi: 10.1016/j.scitotenv.2018.02.025

Menezes, R. F., Borchsenius, F., Svenning, J. C., Davidson, T. A., Søndergaard, M., Lauridsen, T. L., Landkildehus, F., and Jeppesen, E. (2015). Homogenization of fish assemblages in different lake depth strata at local and regional scales. *Fresh. Biol.* 60, 745–757. doi: 10.1111/fwb.12526

Mitra, A., Castellani, C., Gentleman, W. C., Jónasdóttir, S. H., Flynn, K. J, Bode, A., et al. (2014). Bridging the gap between marine biogeochemical and fisheries sciences; configuring the zooplankton link. *Prog. Oceanogr.* 129, 176–199. doi: 10.1016/j.pocean.2014.04.025

Mondy, C. P., and Usseglio-Polatera, P. (2014). Using fuzzy-coded traits to elucidate the nonrandom role of anthropogenic stress in the functional homogenisation of invertebrate assemblages. *Fresh. Biol.* 59, 584–600. doi: 10.1111/fwb.12289

Morel, A., and Smith, R. C. (1974). Relation between total quanta and total energy for aquatic photosynthesis. *Limnol. Oceanogr.* 19, 591–600. doi: 10.4319/lo.1974.19.4.0591

Muscarella, R., and Uriarte, M. (2016). Do community-weighted mean functional traits reflect optimal strategies? *Proc. Biol. Sci.* 283:20152434. doi: 10.1098/rspb.2015.2434

Musielak, M. M., Karp-Boss, L., Jumars, P. A., and Fauci, L. J. (2009). Nutrient transport and acquisition by diatom chains in a moving fluid. *J. Fluid Mech.* 638, 401–421.

Naselli-Flores, L., Zohary, T., and Padisák, J. (2021). Life in suspension and its impact on phytoplankton morphology: an homage to Colin S. Reynolds. *Hydrobiologia* 848, 7–30. doi: 10.1007/s10750-020-04217-x

Nejstgaard, J. C., Tang, K., Steinke, M., Dutz, J., Koski, M., Antajan, E., and Long, J. (2007). Zooplankton grazing on *Phaeocystis*: a quantitative review and future challenges. *Biogeochemistry* 83, 147–172. doi: 10.1007/s10533-007-9098-y

Nelson, C. E., Danuta, M. B., and Bradley, J. C. (2013). Consistency and sensitivity of stream periphyton community structural and functional responses to nutrient enrichment. *Ecol. Appl.* 23, 159–173. doi: 10.1890/12-0295.1

Nissen, C., and Vogt, M. (2021). Factors controlling the competition between Phaeocystis and diatoms in the Southern Ocean and implications for carbon export fluxes. *Biogeosciences* 18, 251–283. doi: 10.5194/bg-18-251-2021

Oksanen, J., Blanchet, G. F, Kindt, R., Legendre, P. (2011). *Vegan: Community Ecology Package*. Available online at: http://cran.r-project.org/web/packages/vegan/index.html

Olden, J. D., Poff, N. L., Douglas, M. R., Douglas, M. E., and Fausch, K. D. (2004). Ecological and evolutionary consequences of biotic homogenization. *Trends Ecol. Evol.* 19, 18–24. doi: 10.1016/j.tree.2003.09.010

Pan, Q., Tian, D., Naeem, S., Auerswald, K., Elser, J.J., Bai, Y., et al. (2016). Effects of functional diversity loss on ecosystem functions are influenced by compensation. *Ecology* 97: 2293-2302. doi: 10.1002/ecy.1460

Pančić, M., and Kiørboe, T. (2018). Phytoplankton defense mechanisms: traits and trade-offs. *Biological Reviews* 93: 1269–1303. doi: 10.1111/brv.12395

Pančić, M, Torres, R. R., Almeda, R, Kiørboe, T. (2019). Silicified cell walls as a defensive trait in diatoms. *Proc. Biol. Sci.* 24:20190184. doi: 10.1098/rspb.2019.0184

Plankton Ciliate Project (2002). *Plankton Ciliate Project. University of Liverpool*. Available online at: http://www.liv.ac.uk/ciliate/intro.htm

Podani, J. (1999). Extending Gower's general coefficient of similarity to ordinal characters. *Taxon* 48, 331–340. doi: 10.2307/1224438

Pohlert, T. (2014). *The Pairwise Multiple Comparison of Mean Ranks Package (PMCMR). R package*. Available online at: http://CRAN.R-project.org/package=PMCMR

Proulx, M. and Mazumder, A. (1998), Reversal of grazing impact on plant species richness in nutrient-poor vs. nutrient-rich ecosystems. Ecology 79, 2581–2592.

Putt, M., and Stoecker, D. K. (1989). An experimentally determined carbon: volume ratio for marine "oligotrichous" ciliates from estuarine and coastal waters. *Limnol. Oceanogr.*, 34, 1097–1103. doi: 10.4319/lo.1989.34.6.1097

R version 3.5.3 (2019). "Great Truth", the R Foundation for Statistical Computing Platform: i386-w64-mingw32/i386 (32-bit). Vienna: R Foundation for Statistical Computing.

Richirt, J., Goberville, E., Ruiz-Gonzalez, V., and Sautour, B. (2019). Local changes in copepod composition and diversity in two coastal systems of Western Europe, Estuar. Coast. Mar. Sci. 227:106304. doi: 10.1016/j.ecss.2019.106304

Riley, G. A. (1957). Phytoplankton of the north central Sargasso Sea. *Limnol. Oceanogr.* 2, 252–270. doi: 10.1002/lno.1957.2.3.0252

Robert P., and Escoufier Y. (1976). A unifying tool for linear multivariate statistical methods: the RV-coefficient. J. Appl. Stat., 25, 257–265.

Rogalski, M. A., Skelly, D. K., and Leavitt, P. R. (2017). Daphniid zooplankton assemblage shifts in response to eutrophication and metal contamination during the Anthropocene. *P. Roy. Soc. B Biol. Sci.*, 284:20170865. doi: 10.1098/rspb.2017.0865

Rose, M. (1933). *Copépodes pélagiques. – Faune de France*, Vol. 26, ed. P. Lechevalier (Paris), 374. Available online at: https://faunedefrance.org/bibliotheque/docs/M.ROSE(FdeFr26)Copepodes-pelagiques.pdf

Rousseau, V., Mathot, S., and Lancelot, C. (1990). Calculating carbon biomass of *Phaeocystis* sp. from microscopic observations. *Mar. Biol.* 107, 305–314. doi : 10.1007/BF01319830

Rousseau, V., Chrétiennot-Dinet, M. J., Jacobsen, A., Verity, P., and Whipple, S. (2007). The life cycle of *Phaeocystis*: state of knowledge and presumptive role in ecology. Biogeochemistry 83, 29–47. doi: 10.1007/s10533-007-9085-3

Schapira, M., Vincent, D., Gentilhomme, V., and Seuront, L. (2008). Temporal patterns of phytoplankton assemblages, size spectra and diversity during the wane of a *Phaeocystis globosa* spring bloom in hydrologically contrasted coastal waters. *J. Mar. Biol. Assoc.* U. K. 88, 649–662. doi: 10.1017/S0025315408001306

Schiller, J. (1931–1937). "Dinoflagellatae (Peridinineae) in monographischer Behandlung," in *Kryptogamen-Flora von Deutschland, Österreichs und der Schweiz. Akad, (Vol. 10 (3): Teil 1 (1–3) (1931–1933): Teil 2 (1–4) (1935–1937))* ed L. Rabenhorst (Leipzig: Verlag).

Schoemann, V., Becquevort, S., Stefels, J., Rousseau, V., and Lancelot, C. (2005). *Phaeocystis* blooms in the global ocean and their controlling mechanisms: a review. *J. Sea Res.* 53, 43–66. doi: 10.1016/j.seares.2004.01.008

Schwaderer, A. S., Yoshiyama, K., De Tezanos Pinto, P., Swenson, N. G., Klausmeier, C. A., and Litchman, E. (2011). Eco-evolutionary differences in light utilization traits and distributions of freshwater phytoplankton. *Limnol. Oceanogr.* 56, 589–598. doi: 10.4319/lo.2011.56.2.0589

Seuront, L., Lacheze, C., Doubell, M. J., Seymour, J. R., Van DongenVogels, V., Newton, K., Alderkamp, A. C., and Mitchell, J. G. (2007). The influence of *Phaeocystis globosa* on microscale spatial patterns of chlorphyll a and bulk-phase seawater viscosity. Biogeochemistry 83, 173–188.

Shipley, B. (2010). *From Plant Traits to Vegetation Structure: Chance and Selection in the Assembly of Ecological Communities*. Cambridge: Cambridge University Press.

Silverman, B. W. (1986). *Density Estimation for Statistics and Data Analysis*. London: Chapman and Hall.

Simpson, E. H. (1949). Measurement of diversity. *Nature* 163:688.

Smetacek, V. (1999). Diatoms and the ocean carbon cycle. *Protist* 150, 25–32. doi: 10.1016/S1434-4610(99)70006-4

Smith, V. H., and Schindler, D. W. (2009). Eutrophication science: where do we go from here? *Trends Ecol. Evol.* 24, 201–207. doi: 10.1016/j.tree.2008.11.009

Stawiarski, B. (2014). *The Physiological Response of Picophytoplankton to Light, Temperature and Nutrients Including Climate Change Model Simulations*. Ph.D. thesis. Norwich: Universityof East Anglia

Steinberg, D. K., and Landry, M. R. (2017). Zooplankton and the ocean carbon cycle. *Annu. Rev. Mar. Sci.* 9, 413–444. doi: 10.1146/annurev-marine-010814-015924

Stelfox-Widdicombe, C. E., Edwards, E. S., Burkill, P. H., and Sleigh, M. A. (2000). Microzooplankton grazing activity in the temperate and sub-tropical NE Atlantic: summer 1996. *Mar. Ecol. Prog. Ser.* 208, 10–12.

Takabayashi, M., Lew, K., Johnson, A., Marchi, A., Dugdale, R., and Wilkerson, F. P. (2006). The effect of nutrient availability and temperature on chain length of the diatom *Skeletonema costatum*. *J. Plankton Res.* 28, 831–840.

Taylor, B. W., Keep, C. F., Hall, R. O. Jr., Koch, B. J., Tronstad, L. M., Flecker, A., et al. (2007). Improving the fluorometric ammonium method: matrix effects, background fluorescence, and standard additions. *J. N. Am. Benthol. Soc.* 26, 167–177. doi: 10.1899/0887-3593200726

Thackeray, S. J., Jones, I. D. and Maberly, S. C. (2008). Long-term change in the phenology of spring phytoplankton: species-specific responses to nutrient enrichment and climatic change. *J. Ecol.* 96, 523–535. doi: 10.1111/j.1365-2745.2008.01355.x

Thieu, V., Billen, G., and Garnier, J. (2009). Nutrient transfer in three contrasting NW European watersheds: the seine, somme, and scheldt rivers. A comparative application of the Seneque/Riverstrahler model. *Water Res.* 43, 1740–1748.

Tréguer, P., and Pondaven, P. (2000). Global change: silica control of carbon dioxide. *Nature* 406, 358–359. doi: 10.1038/35019236

Van den Hoek, C., Mann, D. G. and Jahns, H. M. (1995). *Algae: An Introduction to Phycology*. Cambridge, MA: Cambridge University Press.

van Rijssel, M., Hamm, C., and Gieskes, W. (1997). *Phaeocystis globosa*(Prymnesiophyceae) colonies: hollow structures built with small amounts of polysaccharides. *Eur. J. Phycol.* 32, 185–192. doi: 10.1080/09670269710001737119

Villéger S., Mason N. W. H., and Mouillot, D. (2008). New multidimensional functional diversity indices for a multifaceted framework in functional ecology. *Ecology* 89, 2290–2301. 10.1890/07-1206.1.

Villéger, S., Grenouillet, G., and Brosse, S. (2014).Functional homogenization exceeds taxonomic homogenization among European fish assemblages. *Global Ecol. Biogeogr.* 23, 1450–1460. doi: 10.1111/geb.12226

Violle, C., Navas, M. L., Vile, D., Kazakou, E., Fortunel, C., Hummel, I.,et al. (2007). Let the concept of trait be functional! *Oikos* 116, 882–892. doi: 10.1111/j.0030-1299.2007.15559.x

Virta, L., Gammal, J., Järnström, M., Bernard, G., Soininen, J., Norkko, J., et al. (2019). The diversity of benthic diatoms affects ecosystem productivity in heterogeneous coastal environments. *Ecology* 100:e02765. doi: 10.1002/ecy.2765

Vitousek, P. M., Mooney, H. A., and Lubchenco, J. (1997). Human domination of Earth's ecosystems. *Science* 277, 494–499. doi: 10.1126/science.277.5325.494

Wengrat, S., Padial, A. A., Jeppesen, E., Davidson, T. A., Fontana, L., Costa-Boddeker, S., and Bicudo, D. C. (2018). Paleolimnological records reveal biotic homogenization driven by eutrophication in tropical reservoirs. *J. Paleolimnol.* 60, 299–309.

White, E. P., Ernest, S. K. M., Adler, P. B., Hurlbert, A. H., and Lyons, S. K. (2010). Integrating spatial and temporal approaches to understanding species richness. *Phil. Trans. R. Soc. B* 365, 3633–3643. doi: 10.1098/rstb.2010.0280

Wickham, H. (2016). *ggplot2: Elegant Graphics for Data Analysis*. New York, NY: Springer-Verlag New York.

Wiebe, P. H. (1988). Functional regression equations for zooplankton displacement volume, wet weight, dry weight, and carbon: a correction. *Fish. Bull.* 86, 833–835.

Williams, R., and Robins, D. B. (1982). Effects of preservation on wet weight, dry weight, nitrogen and carbon contents of *Calanus helgolandicus* (Crustacea: copepoda). *Mar. Biol.* 71, 271–281.

Worm, B., Lotze, H., Hillebrand, H. (2002). Consumer versus resource control of species diversity and ecosystem functioning. *Nature* 417, 848–851. doi: 10.1038/nature00830

Zakaria, H. Y., Hassan, A. M., El-Naggar, H. A., and Abo-Senna, F. M. (2018). Biomass determination based on the individual volume of the dominant copepod species in the Western Egyptian Mediterranean Coast. *Egyptian J. Aquatic Res.* 44, 89–99. doi: 10.1016/j.ejar.2018.05.002

Zhang, Y., Cheng, L., Li, K., Zhang, L., Cai, Y., Wang, X., et al. (2019). Nutrient enrichment homogenizes taxonomic and functional diversity of benthic macroinvertebrate assemblages in shallow lakes. *Limnol. Oceanogr.* 64, 1047–1058. doi: 10.1002/lno.11096

Zhu, L., Fu, B., Zhu, H. (2017). Trait choice profoundly affected the ecological conclusions drawn from functional diversity measures. *Sci. Rep.* 7:3643. doi: 10.1038/s41598-017-03812-8

Conflict of Interest: The authors declare that the research was conducted in the absence of any commercial or financial relationships that could be construed as a potential conflict of interest.

Publisher's Note: All claims expressed in this article are solely those of the authors and do not necessarily represent those of their affiliated organizations, or those of the publisher, the editors and the reviewers. Any product that may be evaluated in this article, or claim that may be made by its manufacturer, is not guaranteed or endorsed by the publisher.

frontiers in Microbiology

ORIGINAL RESEARCH
published: 08 October 2021
doi: 10.3389/fmicb.2021.661177

Legacy Metal Contaminants and Excess Nutrients in Low Flow Estuarine Embayments Alter Composition and Function of Benthic Bacterial Communities

Simone C. Birrer[1,2†], Franziska Wemheuer[1,2†], Katherine A. Dafforn[1,2,3], Paul E. Gribben[2,4], Peter D. Steinberg[2,4], Stuart L. Simpson[5], Jaimie Potts[6], Peter Scanes[6], Martina A. Doblin[2,7] and Emma L. Johnston[1,2]*

[1] Evolution and Ecology Research Centre, School of Biological, Earth and Environmental Sciences, University of New South Wales, Kensington, NSW, Australia, [2] Sydney Institute of Marine Science, Mosman, NSW, Australia, [3] Department of Earth and Environmental Sciences, Macquarie University, North Ryde, NSW, Australia, [4] Centre for Marine Science and Innovation, School of Biological, Earth and Environmental Sciences, University of New South Wales, Kensington, NSW, Australia, [5] CSIRO Land and Water, Centre for Environmental Contaminants Research, Canberra, ACT, Australia, [6] Coastal Waters Unit, Science Division, NSW Department of Planning, Industry and Environment, Sydney, NSW, Australia, [7] Climate Change Cluster, University of Technology, Sydney, NSW, Australia

OPEN ACCESS

Edited by:
Savvas Genitsaris, National and Kapodistrian University of Athens, Greece

Reviewed by:
Guangshan Wei, Sun Yat-sen University, China
Jun Gong, Sun Yat-sen University, China

***Correspondence:**
Katherine A. Dafforn
katherine.dafforn@mq.edu.au

[†]These authors have contributed equally to this work

Specialty section:
This article was submitted to Aquatic Microbiology, a section of the journal Frontiers in Microbiology

Received: *30 January 2021*
Accepted: *09 September 2021*
Published: *08 October 2021*

Citation:
Birrer SC, Wemheuer F, Dafforn KA, Gribben PE, Steinberg PD, Simpson SL, Potts J, Scanes P, Doblin MA and Johnston EL (2021) Legacy Metal Contaminants and Excess Nutrients in Low Flow Estuarine Embayments Alter Composition and Function of Benthic Bacterial Communities. Front. Microbiol. 12:661177. doi: 10.3389/fmicb.2021.661177

Coastal systems such as estuaries are threatened by multiple anthropogenic stressors worldwide. However, how these stressors and estuarine hydrology shape benthic bacterial communities and their functions remains poorly known. Here, we surveyed sediment bacterial communities in poorly flushed embayments and well flushed channels in Sydney Harbour, Australia, using 16S rRNA gene sequencing. Sediment samples were collected monthly during the Austral summer-autumn 2014 at increasing distance from a large storm drain in each channel and embayment. Bacterial communities differed significantly between sites that varied in proximity to storm drains, with a gradient of change apparent for sites within embayments. We explored this pattern for embayment sites with analysis of RNA-Seq gene expression patterns and found higher expression of multiple genes involved in bacterial stress response far from storm drains, suggesting that bacterial communities close to storm drains may be more tolerant of localised anthropogenic stressors. Several bacterial groups also differed close to and far from storm drains, suggesting their potential utility as bioindicators to monitor contaminants in estuarine sediments. Overall, our study provides useful insights into changes in the composition and functioning of benthic bacterial communities as a result of multiple anthropogenic stressors in differing hydrological conditions.

Keywords: hydrology, sediment, bacteria, 16S rRNA, RNAseq, multiple stressors, estuary

INTRODUCTION

Estuaries are diverse and productive ecosystems that support many human activities. However, the diversity and functioning of these ecosystems are increasingly threatened by multiple anthropogenic stressors including contamination and habitat modification (Johnston et al., 2015a; Mayer-Pinto et al., 2017; Vadillo Gonzalez et al., 2019). Industrial contamination and pulses of

stormwater carrying urban contaminants are some of the greatest threats to estuarine health and stability. Upon entering the waterway, the distribution and concentrations of contaminants in estuaries is largely dependent on hydrological conditions (Birch and Rochford, 2010; Mayer-Pinto et al., 2015; Machado et al., 2016; Nystrand et al., 2016). Specifically, under low flow conditions, any contaminants entering a waterway are likely to be retained for longer compared to the rapid transit and dilution that occur under high flow conditions (Sutherland et al., 2017). Hotspots of contamination have been documented where low flow estuarine environments exist naturally, such as at the ends of embayments (Birch and Rochford, 2010; Sutherland et al., 2017), or those created by built structures such as break-walls surrounding marinas (Floerl and Inglis, 2003; Johnston, 2011; Sim et al., 2015). Understanding the consequences of these hydrological differences for the distribution and potential impacts of contaminants is important to manage the health and stability of estuarine ecosystems.

Bacterial communities play a key role in ecosystem stability and functioning (Falkowski et al., 2008). Moreover, several bacteria are important for the biodegradation of contaminants such as excess nutrients, or petroleum hydrocarbons and speciation of metals (Hammack and Edenborn, 1992; Das and Chandran, 2011). Allison and Martiny (2008) proposed that changes in microbial communities in response to different environmental disturbances may directly influence ecosystem functions. Due to their importance for ecosystem function and their sensitivity to altered environmental conditions, bacterial communities can be used to monitor environmental perturbations (Sun et al., 2012; Aylagas et al., 2017; Glasl et al., 2017). It is therefore important to identify factors that influence bacterial communities and, as a result, alter the ecosystem functions they provide (Sun et al., 2013).

In the past decade, bacterial communities in coastal sediments and their responses toward anthropogenic stressors have received significant attention (Liu et al., 2014; Lawes et al., 2017; Beale et al., 2018; Birrer et al., 2018; Su et al., 2018). For instance, significant changes in bacterial community composition and predicted functions in surface sediments of Hangzhou Bay (China) in response to nutrients and metal contaminants were recorded by Su et al. (2018). In another study, the community composition and richness of benthic bacterial communities in chemically polluted sites along the coast of Italy were altered by polychlorinated biphenyls (PCBs), polycyclic aromatic hydrocarbons (PAHs) and metals (Quero et al., 2015). Sun et al. (2013) investigated the response of sediment bacterial communities to contaminant disturbance across six estuaries with differing levels of modification along the coast of New South Wales, Australia. They observed that sediment metals and silt content explained most of the variation seen in the community composition, while PAHs explained little of the variance. However, functional responses of bacterial communities in estuarine sediments to multiple urban stressors (e.g., metals and excess nutrients) are still not well-understood, as many previous studies have focused on community changes only (but see Lu et al., 2017; Birrer et al., 2018; Su et al., 2018).

The aim of the present study was to investigate how the diversity, community composition and functions of benthic bacteria in Sydney Harbour (Australia) change in relation to multiple contaminants and estuarine hydrology. Sydney Harbour is one of the largest estuaries in the world and a hotspot for biological diversity (Johnston et al., 2015b; Mayer-Pinto et al., 2015). In a previous study, Sutherland et al. (2017) assessed contaminant hotspots and biogeochemical processes in sediment communities at four locations in Sydney Harbour that were either poorly flushed (low flow and high retention) embayments or well-flushed (high flow and low retention) channels. For this purpose, sediment samples were taken monthly from two embayment and two channel locations at increasing distances (approximately 0, 200, and 1,000 m away) from a large storm drain. The authors observed significant differences in biogeochemical processes between the two retention types and changes in benthic metabolism with distance from storm drains. They suggested that embayments are particularly vulnerable to the negative effects of contaminant retention, while the apparent resilience of fast-flowing channels may mean that these locations are more suitable for handling stormwater inputs due to the potential for rapid dilution and transit.

In the present study, we assessed benthic bacterial communities by Illumina (MiSeq) sequencing targeting the bacterial 16S rRNA genes using the same sediment samples analysed by Sutherland et al. (2017). We further examined differences in gene expression patterns and in the composition of the potentially active bacterial community targeting embayment sediments at sites close to and far from storm drains by RNA-Seq analysis. Our main hypotheses were that bacterial alpha diversity measures and community composition differ between channels and embayments, and bacterial community structure and function in embayment systems differ depending on proximity to storm drains.

MATERIALS AND METHODS

Sampling Design

Sediment samples were collected monthly in the Austral summer-autumn between February 2014 and June 2014 (four sampling times) in Sydney Harbour (Port Jackson; 33°50'S, 151°15'E, **Figure 1**). Sydney Harbour is a drowned river valley (Roy et al., 2001) situated on the temperate south-east coast of New South Wales, Australia. It comprises a complex network of embayments and inlets connected through channels adjacent to a winding and increasingly larger channel opening to the Tasman Sea. Over the past 200 years, human activities including the dredging of shipping channels and land reclamation have extensively modified the bathymetry and shoreline of Sydney Harbour (Birch et al., 2009). Past urban stormwater inflows and historical industrial practices have left a legacy of contamination in surrounding sediments (Chariton et al., 2010; Dafforn et al., 2012).

Four locations in the central portion of Sydney Harbour were randomly selected to represent different hydrology and water retention (**Figure 1**). Two locations were in well-flushed channels with low retention (Lane Cover River and Upper Parramatta

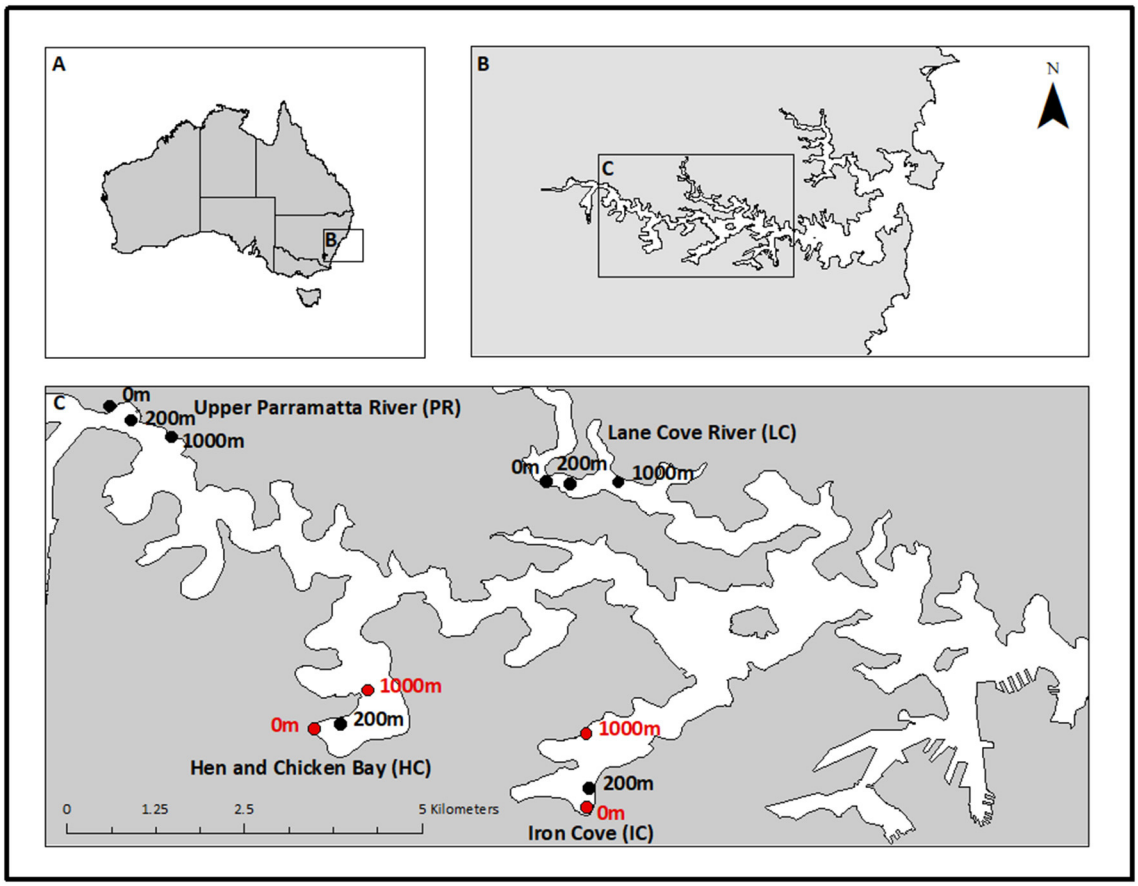

FIGURE 1 | Sampling locations in Sydney Harbour, New South Wales, Australia. Map shows **(A)** Australia, **(B)** Sydney Harbour estuary, and **(C)** locations sampled within the estuary. The Upper Parramatta River (100 km^2; PR) and Lane Cove River (80 km^2; LC) locations are well flushed channels with low retention. The embayments Hen and Chicken Bay (< 10 km^2; HC) and Iron Cove (14 km^2; IC) experience very little flushing and were therefore selected as high retention sites. Samples were taken monthly from February to May 2014. Sampling sites within each location ($n = 3$) are indicated by approximate proximity to a large storm drain (i.e., 0, 200, 1,000 m). Sites highlighted in red were selected for metatranscriptomics analysis (collected in February and March).

River) and two locations were in poorly flushed embayments with high retention (Hen and Chicken Bay and Iron Cove River). The embayments contain high concentrations of contaminants (Irvine and Birch, 1998). Within each location, sampling was done at increasing distances from major stormwater outlets (0, 200, and 1,000 m), representing a potential gradient away from a contaminant hotspot. The three distances were selected based on hydrodynamic modelling by Lee et al. (2011) who described freshwater-plume penetration into the Sydney Harbour estuary during significant rainfall events (> 50 mm/day).

Sample Collection and Chemical Analyses

Sediment samples were collected during relatively dry conditions (<5 mm rainfall/day, Bureau of Meteorology, 2014). As a consequence, ongoing stormwater inputs into the estuary were minimal (<0.1 m^3/s) (Birch and Rochford, 2010). The sampling and chemical analyses were described in detail by Sutherland et al. (2017). In brief, surficial sediments (<5 cm depth) were collected subtidally using a Van Veen sediment grab from a water depth of approximately 1.5–2.5 m at each distance. Two sediment grabs per distance were collected approximately 3 m apart and sub-sampled for the surface (<2 mm depth) microbial community in sterile, DNase- and RNase-free 2 mL cryo tubes. The surface 2 mm of sediment was sampled for the bacteria to target the most oxygenated layer that would be in contact with both the water and sediment to allow for comparisons with physicochemical measures collected from both media. To ensure that the transcription was directly related to environmental conditions, sediment samples for molecular analyses were immediately frozen in liquid nitrogen in the field. Samples remained in liquid nitrogen until returning to the laboratory and were then stored at −80°C until extractions were performed within 4 weeks of sampling.

The remaining grab sample was then homogenised in a clean tray and sub-sampled for metal, carbon, nitrogen and grain size analyses. Sediments from the whole grab (i.e., 0–5 cm depth) were used to determine sediment properties because a greater quantity is required compared to the microbial analysis. Plasticware used to collect sediment for metal analyses was previously soaked in 5% HNO_3 for a minimum of 24 h and then rinsed in deionised

water (Milli-Q™). Samples were kept in the dark on ice for transport to the laboratory. Samples for chemical analyses were frozen at −20°C. In brief, total organic carbon and total nitrogen were analysed at Isoenvironmental (South Africa) using 5–20 mg of dried, homogenised sample in a 20-20 IRMS linked to an ANCA SL element analyser (Europa Scientific). Metal analyses followed Dafforn et al. (2012). Sediments were oven-dried (50°C) and homogenised to a fine powder with mortar and pestle before microwave digestion according to method 3051A (USEPA, 2007). Metal concentrations were analysed using ICP-AES (Perkin Elmer, OptimaOptima7300DV, USA). Grain size analyses were performed on wet sediments using a Malvern laser particle size analyser (Mastersizer 2000, USA) and the percentage of silt content (% < 63 μm) was calculated. All environmental properties are provided as **Supplementary Table 1**.

Extraction and Purification of Nucleic Acids

Environmental RNA and DNA were extracted from 2 g of wet sediment using the RNA PowerSoil® Total RNA Isolation Kit and the RNA PowerSoil® DNA Elution Accessory Kit (Mo Bio Laboratories Inc., Carlsbad, CA, USA, now Qiagen), respectively, according to the manufacturer recommendations (http://www.qiagen.com, accessed 25/01/21). Extracted DNA was purified using Agencourt AMPure XP (Agencourt Bioscience Corporation, Beverly, MA, USA) following manufacturer recommendations (https://www.beckmancoulter.com/wsrportal/techdocs?docname=B37419, accessed 25/01/21). DNA concentrations of all purified samples were quantified using a NanoDrop ND-1000 spectrophotometer (NanoDrop Technologies, Wilmington, DE, USA). To remove residual DNA from RNA samples, the TURBO DNA-free™ Kit (Life Technologies, Carlsbad, CA, USA) was used following manufacturer recommendations for routine DNase treatment (https://assets.thermofisher.com/TFS-Assets/LSG/manuals/1907M_turbodnafree_UG.pdf, accessed 21/01/21). Subsequently, RNA was purified with the Agencourt® RNAClean® XP (Agencourt Bioscience Corporation, Beverly, MA, USA). The RNA integrity number (RIN) was measured for each sample to control for RNA degradation. The mean RIN for all samples was 7.72, where a RIN of 10 represents no degradation.

The absence of DNA in RNA samples was confirmed by PCR using the primers 515FB (5′-GTGYCAGCMGCCGCGGTAA-3′) and 806RB (5′-GGACTACNVGGGTWTCTAAT-3′) from the earth microbiome project (https://earthmicrobiome.org/protocols-and-standards/16s/, accessed 25/01/21). The PCR reaction mixture (50 μL) contained 10 μL of five-fold MyTaq Reaction Buffer (Bioline, Alexandria, NSW), 0.4 μM of each primer, 1 U of MyTaq DNA Polymerase (Bioline, Alexandria, NSW), and approximately 10 ng of purified RNA as template. The following thermal cycling scheme was used: initial denaturation at 95°C for 2 min, 28 cycles of denaturation at 95°C for 30 s, annealing at 50°C for 30 s, followed by extension at 72°C for 1 min. The final extension was carried out at 72°C for 2 min. Negative controls were performed by using the reaction mixture without template. Genomic DNA from *Escherichia coli* DH5α was used in the positive control. The success of the PCR was controlled by gel electrophoresis. No PCR signals were detected for the RNA samples.

Sequencing and Processing of the 16S rRNA Gene Data

Bacterial communities in sediments were assessed by paired-end sequencing targeting the 16S rRNA gene at the Molecular Research DNA (MRDNA) Lab (https://www.mrdnalab.com, Shallowater, TX, USA). The V2-V3 region was amplified with primers 104F (Bertilsson et al., 2002) and 530R (Lane, 1991) for consistency with our previous research to provide comparable results to the bacterial diversity investigations undertaken in the same estuary (Sun et al., 2013). PCRs were done using the HotStarTaq *Plus* Master Mix Kit (Qiagen, Valencia, CA, USA) under the following conditions: 94°C for 3 min, followed by 28 cycles of 94°C for 30 s, 53°C for 40 s, and 72°C for 1 min, after which a final elongation step at 72°C for 5 min was performed. After amplification, PCR products were checked in 2% agarose gel to determine the success of amplification and the relative intensity of bands. Samples were pooled together in equal proportions based on their molecular weight and DNA concentrations. Pooled samples were purified using calibrated Agencourt AMPure XP beads (Agencourt Bioscience Corporation, Beverly, MA, USA). The purified PCR products were used to prepare DNA library by following Illumina TruSeq DNA library preparation protocol using the MiSeq reagent kit V2 (Illumina Inc., San Diego, CA, USA). Sequencing was performed at the MRDNA lab (https://www.mrdnalab.com, Shallowater, TX, USA) on a MiSeq Sequencing platform (Illumina Inc., San Diego, CA, USA) following the manufacturer recommendations.

Obtained sequencing data were initially quality filtered with the Trimmomatic tool version 0.36 (Bolger et al., 2014). Low quality reads were truncated if the quality dropped below 10 in a sliding window of 4 bp. Subsequently, all reads shorter than 100 bp and orphan reads were removed. Remaining sequences were subsequently processed with USEARCH version 10.240 (Edgar, 2010). Paired-end reads were merged and quality-filtered. Filtering included the removal of reads shorter than 350 bp or longer than 470 bp as well as the removal of low-quality reads (maximum number of expected errors >1 or 1 ambiguous base). Processed sequences of all samples were concatenated into one file and subsequently dereplicated into unique sequences. Obtained unique sequences were denoised and clustered into zero-radius operational taxonomic units (zOTUs) with the *unoise3* algorithm implemented in USEARCH (Edgar, 2010).

Chimeric sequences were removed *de novo* using the UCHIME algorithm during clustering (Edgar et al., 2011). Additionally, the *unoise3* algorithm removed all unique sequences which appeared <8 times in the entire data set. Remaining chimeric sequences were removed using UCHIME (Edgar et al., 2011) in reference mode with the SILVA SSU Ref NR 99 132 database (Quast et al., 2013). To assign taxonomy of bacteria, unique and chimaera-free sequences were classified by BLAST alignment (Camacho et al., 2009) against the SILVA

database with an e value cutoff of 1e-20. Processed sequences were mapped onto zOTU sequences to calculate the distribution and abundance of each zOTU in every sample using the *otutab* command with *maxrejects* and *maxaccepts* options disabled. All non-bacterial zOTUs were removed based on their taxonomic classification in the SILVA database. In addition, all zOTUs consisting of one single sequence (singletons) were removed prior to statistical analysis. The final OTU table is provided as **Supplementary Table 2**. Sequence characteristics are provided for each sample in **Supplementary Table 3**.

Sequencing and Processing of Metatranscriptomic Data

Based on patterns in the bacterial community composition observed from the amplicon sequencing, sediment samples collected at 0 and 1,000 m from the storm drain in the embayments at two sampling times (Feb/Mar 2014, $n = 16$) were selected for RNA sequencing. RNA libraries with fragment lengths of approximately 200 bp were prepared. Prior to library preparation, the quality of the total RNA samples was assessed on a Bioanalyzer 2100 using an RNA 6000 Nano Chip (Agilent Technologies, Santa Clara, CA, USA). Sample quantitation was carried out using Invitrogen's Ribogreen assay (Invitrogen, Carlsbad, Ca, USA). Library preparation was then performed according to the TruSeq Stranded mRNA protocol (Illumina Inc., San Diego, CA, USA) with the following modifications: the oligo-dT mRNA purification step was omitted and instead, 200 ng of total RNA were directly added to the Elution2-Frag-Prime step. The amplification step of the PCR was performed according to the manufacturer's recommendations, but the number of amplification cycles was reduced to 12. Each library was uniquely tagged with one of Illumina's TruSeq LT RNA barcodes and quantified using Invitrogen's Picogreen assay (Invitrogen, Carlsbad, Ca, USA). The average library size was determined on a Bioanalyzer 2100, using a DNA 7500 chip (Agilent Technologies, Santa Clara, CA, USA). Library concentrations were then diluted to 2 nM, and the concentrations were validated by qPCR on a ViiA-7 real-time thermocycler (Applied Biosystems, Foster City, CA, USA), using qPCR primers recommended in Illumina's qPCR protocol, and Illumina's PhiX control library as standard. The libraries were then pooled at equimolar concentrations and sequenced across two lanes on an Illumina HiSeq2500 sequencer in rapid mode at a read-length of 100 bp paired-end as recommend by the manufacturer. Sequencing was performed at the Singapore Centre for Environmental Life Sciences Engineering (SCELSE).

Generated sequencing data were initially quality filtered and residual adaptor sequences were removed with Trimmomatic version 0.36 (Bolger et al., 2014). The quality of the RNA data and the absence of adaptor sequences were controlled using FastQC version 0.11.7 (Andrews, 2010). Ribosomal RNA (rRNA) was removed *in silico* using SortMeRNA version 2.1 (Kopylova et al., 2012). Residual sequences were assembled using rnaSPAdes version 3.12.0 (Bankevich et al., 2012). The occurrences and abundance of each assembled transcript was determined by mapping the unassembled reads on the assembled transcripts using Bowtie version 2.3.2 (Langmead and Salzberg, 2012) with RSEM version 1.3.0 (Ferrari et al., 2011). Because RSEM cannot handle paired and unpaired data simultaneously, they were mapped individually, and the mean expected count was calculated from both assemblies taking the numbers of paired and unpaired reads into account. mRNA reads of all samples were assembled together and individual reads of each sample were mapped on obtained contigs. As we only compared transcription levels of individual genes between samples, gene length did not differ and thus was not considered in the analysis.

Prodigal version 2.6.3 (Hyatt et al., 2010) was used to predict open reading frames (ORFs) and protein sequences. Predicted protein sequences were functionally annotated using UPRoC version 1.2 (Meinicke, 2014) and the KEGG database (Kanehisa, 2002) implemented in UPRoC. To taxonomically classify assembled transcripts, we used Kaiju version 1.6.2 (Menzel et al., 2016) and the NCBI NR release with eukaryotic sequences (2018-02-23). Only bacterial transcripts were considered in the functional analysis. To obtain a deeper, PCR-unbiased insight into the active community, rRNA sequences identified with SortMeRNA were mapped on unique and chimaera-free sequences obtained from the 16S rRNA amplicon data using bowtie2 (Langmead and Salzberg, 2012). The final zOTU and transcript tables for the active bacterial community dataset can be found in **Supplementary Table 4**.

Statistical Analyses

All statistical analyses were performed in R version 3.4.0 (R Core Team, 2018) as well as in PRIMER 7 with the PERMANOVA add-on (PRIMER-E, Plymouth Marine Laboratory, UK). Differences were considered as statistically significant with $p \leq 0.05$.

Environmental data (water and sediment characteristics) were normalised prior to statistical analyses. Multivariate datasets were initially explored with pairwise correlations between variables (Draftsman Plot). Where variables were strongly correlated ($r > 0.9$), a single variable was selected as representative for further analyses (e.g., Zn was strongly correlated with Al, As, Cd, Fe, Ni, Pb). Principal Components Analysis (PCA) was performed on normalised data to visualise relationships between retention type and proximity to storm drain as well as their interaction on environmental properties.

Differences in sequencing depth were tested by Kruskal-Wallis test. There were no significant differences in library size among distances, locations or sampling month. Hence, data were not normalised prior to further analyses (except for the alpha diversity analysis). Alpha diversity indices (richness, Shannon index of diversity, Faith's phylogenetic diversity, Chao1 and Michaelis-Menten Fit) were calculated using the R packages *vegan* 2.4.-4 (Oksanen et al., 2017), *picante* version 1.7 (Kembel et al., 2010) and *drc* version 3.0-1 (Ritz et al., 2015). Sample coverage was estimated using the Michaelis-Menten Fit calculated in R (Hughes et al., 2001). For this purpose, richness and rarefaction curves were calculated using the *specnumber* and *rarecurve* function, respectively, in *picante*. The Michaelis-Menten Fit was subsequently calculated from generated rarefaction curves using the *MM2* model within the *drc* package. Faith's phylogenetic diversity was generated

using Fasttree version 2.1.10 (Price et al., 2010). Prior to tree calculation, sequences were aligned using PyNAST against the aligned version of the SILVA database. All alpha diversity indices were calculated 10 times. The OTU tables were rarefied to 29,919 sequences in each iteration using the *rrarefy* function in *vegan*. The average of all iterations was used for further statistical analyses. Bacterial alpha diversity values are provided as **Supplementary Table 3**.

Changes in alpha diversity values, environmental properties and abundant bacterial families/genera were evaluated by linear mixed effects models using the R packages *lmerTest* version 3.0-1 (Kuznetsova et al., 2018) and *MuMIn* version 1.42.1 (Barton, 2018). As fixed effects, we entered retention type (two levels: channel, embayment) and proximity to storm drain (three levels: 0, 200, 1,000 m) as well as their interaction term into each model. The random factors considered in each model were sampling month (four levels: February, March, April, May) and location (nested within retention: LC, PR, HC, IC). The exception was for water properties, where months were the replicates. A reduced model including proximity to storm drain (0 and 1,000 m) and location (HC and IC) was applied to abundant bacterial genera from the entire (amplicon) and active (rRNA) datasets. The best model was chosen according to lowest Akaike information criterion (AIC). The sample size was relatively small in comparison to the number of estimated parameters. As a consequence, AICc was used for model selection in the R package *MuMIn* (2018). Visual inspection of residual plots did not reveal any obvious deviations from homoscedasticity or normality. The final model was calculated using the function *lmer* provided within "lmerTest" with restricted maximum likelihood.

P-values were obtained by likelihood ratio tests of the full model against models without each of the fixed effects. Significance levels for fixed factors and their interaction are based on *F*-values, calculated by a type III analysis of variance with Satterthwaite approximation for degrees of freedom within the R package *lmerTest* (Kuznetsova et al., 2018). Statistically significant results were followed up with Tukey's HSD comparison tests, with *p*-value adjustment ($p < 0.01$) due to multiple comparisons. For random factors, an ANOVA-like table with likelihood ratio test statistics was generated using the *ranova* function in R package *lmerTest* (Kuznetsova et al., 2018).

Overall patterns of the entire bacterial community composition were analysed by permutational multivariate analysis of variance (PERMANOVA; Typ III) with 999 random permutations using the PRIMER 7 statistical package with the PERMANOVA + add-on (PRIMER-E, Plymouth Marine Laboratory, UK). The factors considered in each model were retention type (two levels: channel, embayment), proximity to storm drain (three levels: 0, 200, 1,000 m) as well as their interaction term, and sampling month (two levels: February, March) and location (nested within retention: HC, IC). analyses were done with Bray-Curtis dissimilarity measures. Differences in community composition among the distance gradient in each retention type (retention type * proximity to storm drain) were tested using pairwise tests. Bacterial zOTUs were analysed with the environmental properties using distance-based linear modelling (DistLM). R^2 selection criteria and all specified selection procedure were used in the analysis. Results were visualised with distance-based redundancy analysis (dbRDA).

Potential differences in the composition of the active bacterial community as well as of transcripts were investigated by PERMANOVA with 1000 random permutations using the *vegdist* and *adonis* function within the *vegan* package in R using Bray-Curtis dissimilarities. Differences in community composition were tested using pairwise PERMANOVA (https://github.com/bwemheu/pairwise.adonis). Transcripts being differently expressed between the two investigated distances were detected using DESeq2 (Love et al., 2014). Prior to testing for differential abundance, an independent philtre was used to exclude genes absent with <10 counts in the entire data set. We controlled the false discovery rate using the *Benjamini–Hochberg* procedure for multiple comparisons (FDR = 0.1).

To identify bacterial zOTUs that were differentially associated with sediments close to or far from storm drains in embayments, multi-pattern analyses were applied with functions *multipatt* and *r.g* from the *indicspecies* package (De Cáceres and Legendre, 2009). To enhance reliability of the indicator analysis, only bacterial zOTUs found in at least two samples and with an abundance ≥ 0.001 in the active bacterial community were considered. In addition, we performed this analysis for the entire bacterial community using the same samples as for the metatranscriptomic analysis. The results of the indicator analysis with regard to the distance gradient are provided as **Supplementary Table 5**.

Sequence Data Deposition

Sequence data were deposited in the sequence read archive (Ghosh et al., 2006) of the National Center for Biotechnology Information (NCBI) under accession numbers SUB7398817 (amplicons) and SUB7403872 (metatranscriptomes).

RESULTS

General Sediment Characteristics

To investigate the effect of multiple anthropogenic stressors and estuarine hydrology on benthic bacterial communities, a total of 96 sediment samples were collected in embayments and channels once a month in the Austral summer-autumn between February 2014 and June 2014 (**Figure 1** and **Supplementary Table 1**). Environmental properties were checked for co-linearity with a Draftsman Plot and the dataset was reduced to include temperature, salinity, Co, Cr, Cu, Ni, Zn (as representative of Al, As, Cd, Fe, Pb), %TOC, %TN and silt content. We analysed the effect of retention type and proximity to storm drain as well as their interaction on water and sediment properties with linear mixed-effect models (**Table 1**) and visualised these differences with Principal Components Analysis (PCA) ordination (**Supplementary Figure 1** and **Supplementary Table 1**). The first two axes of the PCA ordination explained 63.4% of the total variance. PC1 explained 45.6%, mainly in relation to higher metal concentrations and silt content in the sediments 0 m and 200 m away from storm drains in embayments. PC2 explained 17.8%, mainly in relation to higher %TOC and %TN in embayments compared to channels. Channel sediments and

TABLE 1 | Environmental characteristics (mean ± sd).

	Embayment			Channel		
	0 m	200 m	1,000 m	0 m	200 m	1,000 m
Co (mg/kg)	6.5 ± 3.2^{a}	6.8 ± 2.2^{a}	3.4 ± 1.6^{b}	5.6 ± 2.8^{ab}	3.8 ± 3.2^{b}	5.2 ± 2.2^{ab}
Cr (mg/kg)	61.5 ± 31.8^{ab}	99.1 ± 55.9^{a}	46 ± 40.2^{b}	53.9 ± 55.5^{ab}	46.2 ± 54.2^{b}	55.1 ± 45.5^{ab}
Cu (mg/kg)	238 ± 119^{a}	323 ± 166^{a}	124 ± 122^{b}	60.6 ± 34.3^{b}	42.4 ± 32.5^{b}	73.5 ± 29.2^{b}
Ni (mg/kg)	16.5 ± 8.2^{a}	16.2 ± 6.8^{a}	6.4 ± 4^{b}	10.3 ± 5.4^{ab}	7.1 ± 6.1^{b}	9.8 ± 4.9^{b}
Zn (mg/kg)	920 ± 580^{a}	819 ± 406^{a}	251 ± 142.8^{b}	288 ± 220^{b}	197 ± 173^{b}	293 ± 157^{b}
TN (%)	0.3 ± 0.1^{a}	0.3 ± 0.1^{a}	0.1 ± 0.1^{b}	0.1 ± 0.1^{b}	0.1 ± 0.1^{b}	0.2 ± 0.1^{b}
TOC (%)	6.4 ± 2.3^{a}	4.3 ± 1.3^{ab}	1.7 ± 0.7^{c}	2.8 ± 1.3^{bc}	2.6 ± 1.9^{bc}	4 ± 4^{b}
Silt content [<63 μm (%)]	72.2 ± 22.7^{c}	97 ± 2.2^{a}	79.8 ± 14.5^{bc}	78.8 ± 15.1^{bc}	80.7 ± 15.7^{bc}	89.4 ± 8.6^{ab}
Temperature (°C)	22.2 ± 3.3	22.2 ± 3.3	22.1 ± 3.1	22.1 ± 3.2	22.1 ± 3.3	22.2 ± 3.3
Salinity	34.2 ± 1.3	34.2 ± 1.2	34.2 ± 1.3	33.2 ± 1.7	33.1 ± 1.8	33.4 ± 1.7

Sediment samples and water properties were measured at increasing distance from storm drains (0, 200, and 1,000 m away) in embayments and channels. Significant differences ($p \leq 0.05$) of water and sediment properties among all sites are indicated with different lowercase letters. Parameters included water quality measurements (temperature, salinity), sediment metals (Co, Cr, Cu, Ni, and Zn), sediment properties [total nitrogen (TN), total organic carbon (TOC), and silt content (% <63 μm)]. For all results of the statistical analyses see ***Supplementary Table 6****.*

those from embayments collected at 1,000 m from storm drains clustered together.

These results are supported by the statistical analyses. In general, sediment properties differed with retention type and distance from storm drain (**Table 1** and **Supplementary Table 6**). Specifically, in embayments we observed significantly lower concentrations of several metals such as Cu, Ni, and Zn in 1,000 m samples compared to those from 0 and 200 m samples. We also observed greater organic carbon and nitrogen content in embayment sediments 0 and 200 m away from the storm drain compared to 1,000 m sediments. In contrast, metal concentrations, total organic carbon and total nitrogen did not differ with distance from storm drains in channels and tended to be similar to samples collected at 1,000 m in embayments. The silt content (grain size) did not differ between channel and embayment sediments and was variable with distance within these retention types. Sediment properties also varied spatially (i.e., among locations within retention type), but showed almost no temporal variation (i.e., among sampling times). Water temperature and salinity were consistent among retention types and with distance from storm drains although there was some spatial variation among locations within retention type.

Sediment Bacterial Community Composition

A total of 4,538,134 sequences with a mean of 47,272 (range: 29,919 to 69,706) sequences per sample were obtained after merging, quality filtering, denoising and removal of chimeric and non-bacterial sequences as well as singletons (**Supplementary Table 3**). Sequences were assigned to 15,954 bacterial zOTUs (**Supplementary Table 2**). A calculated rarefaction curve (**Supplementary Figure 2A**) as well as Michaelis-Menten Fit (**Supplementary Table 3**) confirmed that the sampling efforts of all samples were sufficient to represent the majority of the bacterial diversity (coverage: 77.4%). Species accumulation curves further indicated that more than 94% of all zOTUs (maximum number of zOTUs calculated = 16,928) were recovered by the surveying effort (**Supplementary Figure 2B**).

Six phyla dominated (>1% of all sequences across all samples) the entire bacterial community and accounted for more than 97% of all sequences analysed in this study (**Supplementary Table 2**). Approximately 60% of sequences across all samples were affiliated to *Proteobacteria* with *Gammaproteobacteria* (32.02%) as the predominant class, followed by *Deltaproteobacteria* (24.02%) and *Alphaproteobacteria* (3.39%). The other abundant phyla observed in this study were *Chloroflexi* (21.70%), *Bacteroidetes* (7.40%), *Actinobacteria* (3.22%), *Acidobacteria* (2.95%), and *Epsilonbacteraeota* (1.77%). The five dominant bacterial families were *Desulfobulbaceae* (11.58%), *Anaerolineaceae* (11.39%), *Woeseiaceae* (9.90%), *Desulfobacteraceae* (7.66%), and *Flavobacteriaceae* (4.58%; **Figure 2**).

Bacterial Communities Differ in Relation to Estuarine Hydrology and Proximity to Storm Drain

We used linear mixed-effects models and pairwise comparisons to investigate the hypothesis that bacterial communities would differ between channels and embayments and would differ with proximity to storm drain only in embayments. Bacterial diversity, richness and Faith's PD varied as a result of the interactive effect of retention type and proximity to storm drain, and there was also significant spatial (among locations) and temporal (among sampling times) variation (**Figure 3** and **Supplementary Table 6**). OTU richness, diversity and Faith's PD tended to be lowest in the 0 m samples from embayments compared to 200 and 1,000 m away from the storm drain (**Figure 3** and **Table 2**). Similarly, bacterial diversity tended to be lower in 0 m samples of embayments compared to 0 m samples of channels, although this was not significant (**Figure 3** and

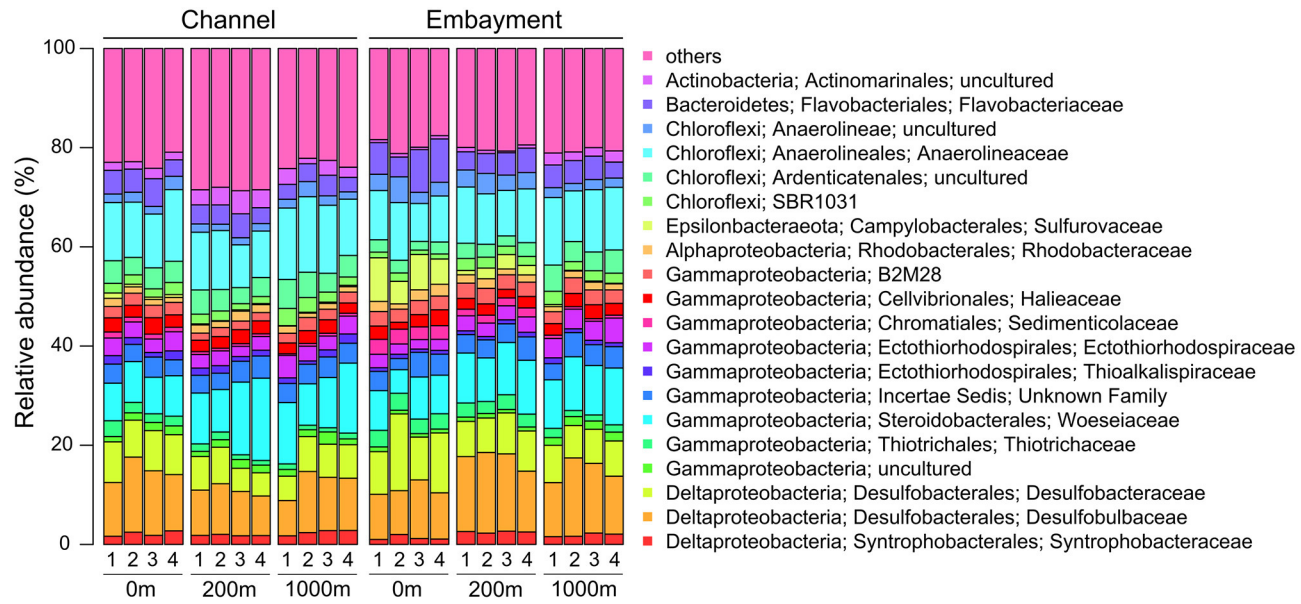

FIGURE 2 | Abundant bacterial families in embayment and channel sediments as determined by 16S rRNA gene amplicon sequencing. Only families with an average abundance >1% in the entire data set are shown. 1, February; 2, March; 3, April; 4, May.

Table 2). In contrast, sediments sampled in channels did not differ in diversity with distance from storm drains (**Figure 3** and **Table 2**). Sediments for microbial analyses were collected from the surface (<2 mm depth) to reflect exposure to changes in both the dynamic water column and more stable sediments. This may be why the microbial communities varied over time, but the sediment properties were generally constant.

Several predominant families differed with distance from stormdrains, with the strongest patterns occurring in embayments (**Supplementary Figure 3** and **Supplementary Table 7**). *Flavobacteriaceae*, *Sulfurovaceae*, *Desulfobacteraceae, Sedimenticolaceae,* and *Thiotrichaceae* were most abundant next to storm drains and decreased in relative abundance with distance from the storm drain. The opposite trend was observed for *Desulfobulbaceae, Woeseiaceae, Actinomarinales, Ardenticatenales,* SBR1031, *Syntrophobacteraceae,* B2M28, *Ectothiorhodospiraceae* and *Thioalkalispiraceae*. In contrast, the relative abundances of the *Anaerolineaceae*, *Rhodobacteraceae,* and *Halieaceae*, were similar among retention types. Hence, we analysed the influence of proximity to storm drain and retention type as well as their interaction on bacterial community composition by permutational multivariate analysis of variance (PERMANOVA) and dbRDA analyses based on Bray-Curtis dissimilarities (**Figure 4** and **Supplementary Table 6**). We observed a clear separation of sediment bacterial communities by proximity to storm drain, which was more pronounced for embayment than channel communities ($p > 0.001$, **Figure 4**). This was detected even accounting for significant spatial (among locations within retention type) and temporal (among sampling times) variation in bacterial community composition (**Supplementary Table 6**).

Bacterial Communities in Channels and Embayments Are Related to Different Environmental Variables

To identify the potential drivers of bacterial community composition in channels and embayments, we performed separate statistical analyses for each retention type. Fitting the environmental variables to the bacterial zOTUs with dbRDA revealed metal concentrations, total nitrogen, total organic carbon and silt content in the sediments explained 42% of the variation in bacterial communities in embayments (**Figure 4A**, **Table 3**, and **Supplementary Table 8**) and 39% in channels (**Figure 4B**, **Table 3**, and **Supplementary Table 8**). Fewer environmental properties measured in this study were significant predictors of bacterial community composition in channels compared to embayments (**Figure 4**, **Table 3**, and **Supplementary Table 8**). Notably, several important sediment properties (Zn and total nitrogen) were only significant predictors of bacterial community composition in embayments.

Active Bacterial Community in Embayments Differed With Proximity to Storm Drain

We analysed samples collected close to and far from storm drains in two locations (Hen and Chicken Bay and Iron Cove) over 2 months (February and March 2014) by metatranscriptomics to test for differences in the community composition of the active bacteria among sites. Active bacterial communities across all samples were dominated by a few bacterial genera, such as *Thiogranum* (7.60%), *Woeseia* (6.82%), the Sva0081 sediment group (5.23%) and the B2M28 group (4.06%) (**Figure 5** and

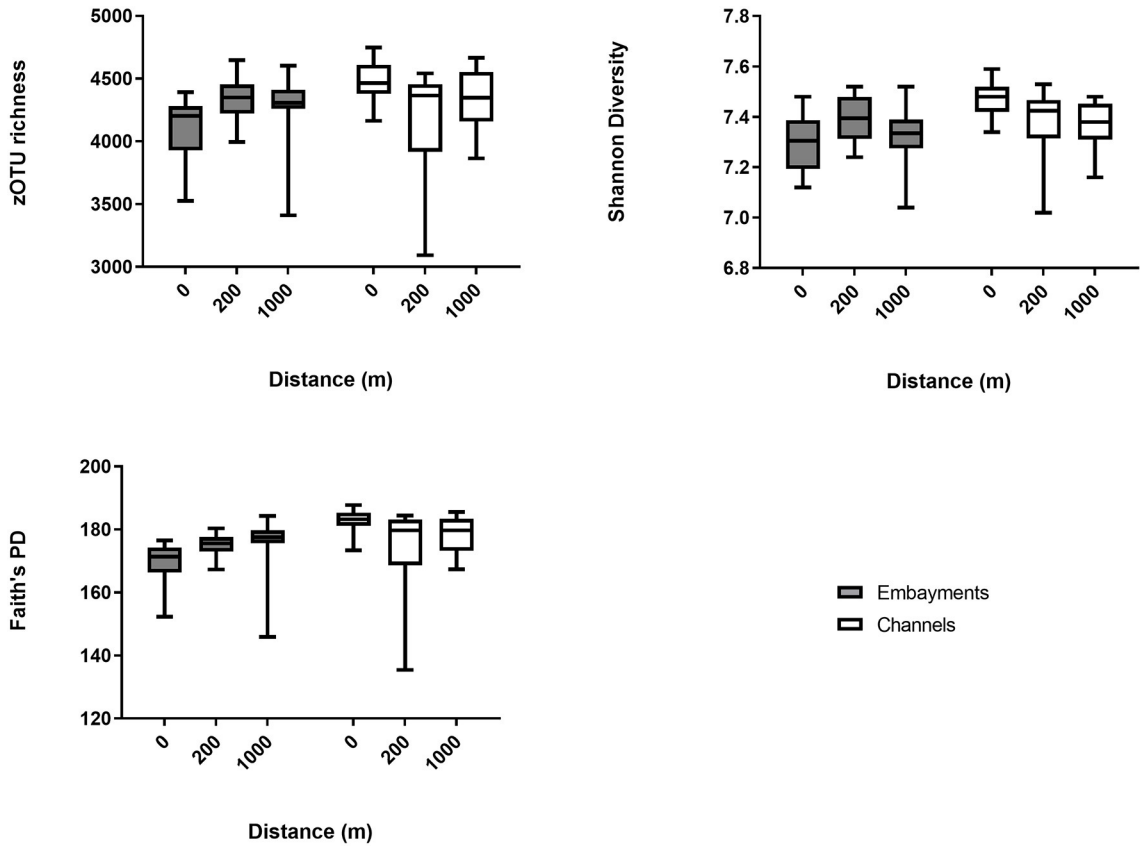

FIGURE 3 | Alpha diversity measures (mean ± min/max) for benthic bacterial communities. Bacterial diversity was measured at increasing distance from storm drains (0, 200, and 1,000 m away) in embayments and channels. For all results of the statistical analyses (see **Table 2**).

TABLE 2 | Statistical results of the pairwise comparisons investigating differences in bacterial (a) richness, (b) diversity and (c) Faith's PD.

Comparison	Richness		Diversity		Faith's PD	
	t-value	*p*-value	*t*-value	*p*-value	*t*-value	*p*-value
Embayment 0 m vs. Channel 0 m	2.16	0.1336	3.27	0.0343	2.70	0.0827
Embayment 0 m vs. Embayment 200 m	−3.10	**0.0028**	−2.83	**0.0060**	−2.51	0.0145
Embayment 0 m vs. Embayment 1,000 m	−2.49	0.0151	−1.02	0.3102	−2.91	**0.0049**
Embayment 0 m vs. Channel 200 m	−0.53	0.6410	−1.61	0.1887	−1.10	0.3605
Embayment 0 m vs. Channel 1,000 m	−1.34	0.2844	−1.44	0.2294	−1.63	0.2108
Embayment 200 m vs. Embayment 1,000 m	0.61	0.5444	1.81	0.0744	−0.40	0.6918
Embayment 200 m vs. Channel 0 m	0.83	0.4769	1.47	0.2202	1.55	0.2294
Embayment 200 m vs. Channel 200 m	−0.81	0.4875	−0.19	0.8587	−0.05	0.9603
Embayment 200 m vs. Channel 1,000 m	−0.01	0.9908	0.36	0.7375	−0.48	0.6668
Embayment 1,000 m vs. Channel 0 m	1.09	0.3667	2.62	0.0632	1.36	0.2752
Embayment 1,000 m vs. Channel 200 m	−0.54	0.6294	0.96	0.3960	−0.24	0.8293
Embayment 1,000 m vs. Channel 1,000 m	0.27	0.8044	0.79	0.4780	0.30	0.7871
Channel 0 m vs. Channel 200 m	3.81	**0.0003**	2.62	0.0108	3.48	**0.0009**
Channel 0 m vs. Channel 1,000 m	1.90	0.0616	2.89	**0.0051**	2.32	**0.0233**
Channel 200 m vs. Channel 1,000 m	−1.91	0.0606	0.27	0.7890	−1.17	0.2478

Bacterial communities were sampled at increasing distance from storm drains (0, 200, and 1,000 m away) in embayments and channels. Significant differences ($p \leq 0.01$) are indicated in bold.

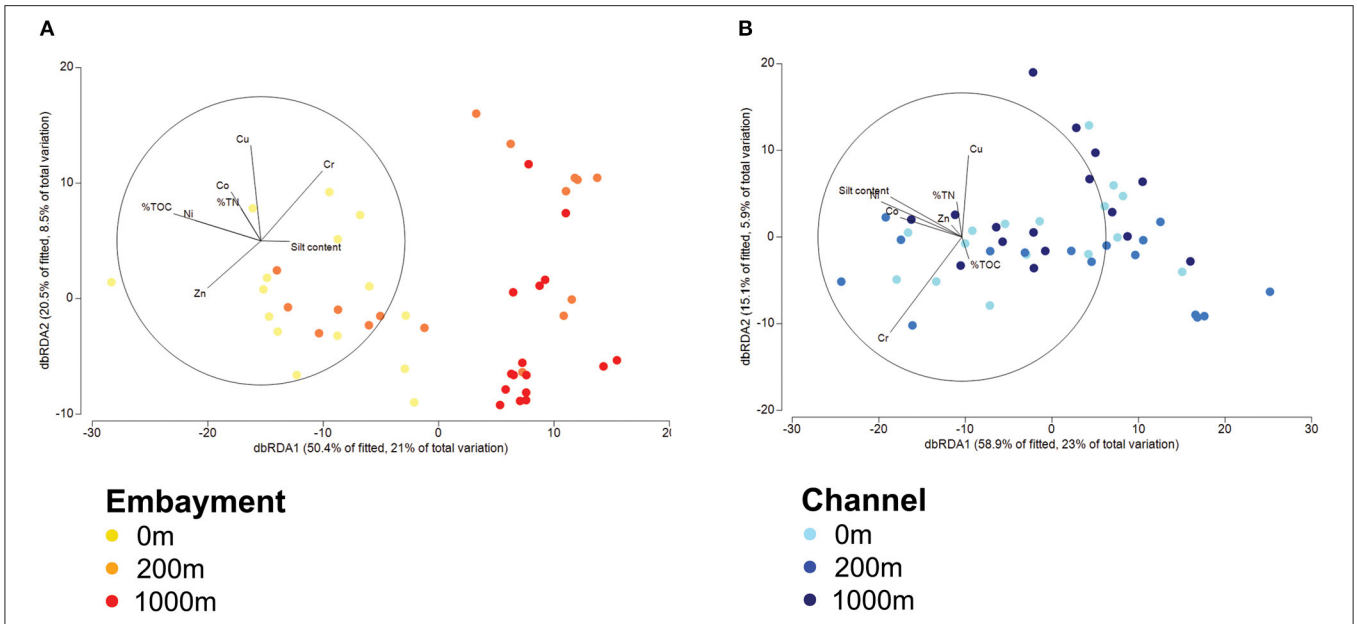

FIGURE 4 | Distance-based redundancy analysis (dbRDA) of bacterial communities in embayments **(A)** and channels **(B)** with regard to the distance from storm drains fitted to predictor variables. Ordination is colour-coded by site (proximity to storm drain) and retention type. Blue symbols are channel locations and orange symbols are embayment locations. The gradient in colour from lighter to darker represents the distances 0, 200, 1,000 m from a storm drain. Lengths of vector overlays indicate the relative influences of fitted predictor variables.

TABLE 3 | Statistical results of the PERMANOVA investigating potential drivers of benthic bacterial community composition.

	Channels		Embayments	
	Pseudo-F	***p*-value**	***Pseudo-F***	***p*-value**
Distance (m)	1.86	**0.0004**	2.31	**0.0001**
Al (mg/kg)	8.25	**0.0001**	4.93	**0.0001**
As (mg/kg)	3.00	**0.0002**	5.26	**0.0001**
Cd (mg/kg)	4.31	**0.0001**	8.77	**0.0001**
Co (mg/kg)	2.72	**0.001**	2.24	**0.0002**
Cr (mg/kg)	4.04	**0.0001**	2.29	**0.0001**
Cu (mg/kg)	1.30	0.1303	3.98	**0.0001**
Fe (mg/kg)	1.40	0.078	1.94	**0.0012**
Mn (mg/kg)	1.88	**0.0087**	2.24	**0.0002**
Ni (mg/kg)	1.26	0.1529	1.97	**0.0017**
Pb (mg/kg)	1.72	**0.0208**	2.12	**0.0002**
Zn (mg/kg)	1.19	0.2081	2.57	**0.0001**
TN (%)	1.51	0.0597	3.05	**0.0001**
TOC (%)	1.98	**0.0054**	1.24	0.1397
Silt content (% <63 μm)	3.25	**0.0002**	1.08	0.3239

Bacterial community composition was measured at increasing distance from storm drains (0, 200, and 1,000 m away) in embayments and channels. Significant differences ($p \leq 0.05$) along the distance gradient in channels and embayments are indicated in bold.

Supplementary Table 4). At the DNA level, uncultured bacteria of the *Desulfobulbaceae* (10.90%) and *Anaerolineaceae* (11.20%) were predominant. Other abundant genera were, for example, *Woeseia* (8.30%), uncultured members of the Sva0081 sediment group (5.84%) and *Thiogranum* (3.08%). Several bacterial genera including *Lutimonas*, *Actibacter,* or *Sulfurovum* were abundant (>1% of the abundance in the DNA dataset) in the entire bacterial community, but rare (<1% of the abundance in the RNA dataset) in the active bacterial community. In contrast, *Sedimenticola*, *Desulfosarcina*, *Desulfatiglans,* and members of the OM190 group were highly abundant in the active, but not in the entire bacterial community.

Several of the predominant bacterial genera also differed in their relative abundances with distance from storm drains

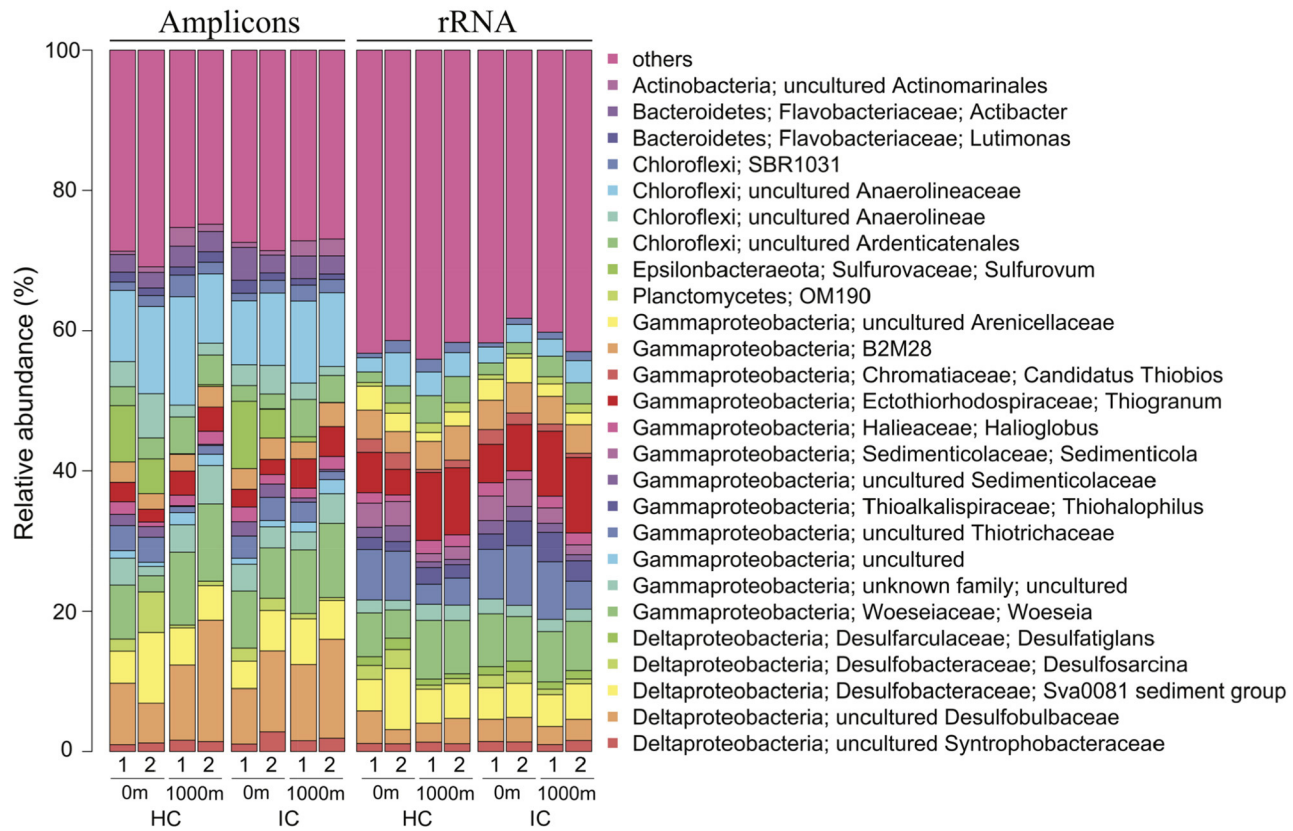

FIGURE 5 | Abundant bacterial genera in embayments. Only genera with an average abundance > 1% in the 16S rRNA gene amplicon sequencing (entire) or in the rRNA (active) dataset, respectively, are shown. Entire and active bacterial communities were assessed by barcoding and mapping of rRNA reads on denoised unique sequences, respectively. HC, Hen and Chicken Bay; IC, Iron Cove; 1, February; 2, March.

(**Supplementary Figures 4, 5** and **Supplementary Table 9**). Consequently, we performed an indicator species analysis to identify bacterial zOTUs significantly associated with 0 and 1,000 m in embayments (**Figure 6** and **Supplementary Table 5**). The number of bacterial zOTUs that differed with proximity to a stormdrain was higher in the entire (DNA) community compared to the active (RNA) bacterial community. Several bacteria including two zOTUs belonging to *Lutimonas vermicola* and three zOTUs of the genus *Sulfurovum* were significantly associated with 0 m samples of embayments, whereas others including zOTUs belonging to the genera *Halioglobus*, *Woeseia* and *Thiogranum* were uniquely associated with 1,000 m samples. In the rRNA dataset, three zOTUs belonging to Candidatus *Electrothrix*, one zOTU affiliated with Candidatus *Electrothrix aarhusiensis* as well as uncultured members of the *Sedimenticolaceae* and *Thiotrichaceae* were significantly associated with 0 m samples. Two zOTUs belonging to BD2-11 terrestrial group, OM190, the Pla3 lineage, *Geothermobacter* and *Thiohalophilus* showed unique associations with 1,000 m samples.

The active bacterial community differed significantly with proximity to storm drain and this was consistent among sampling times (**Figure 7A**). Specifically, the bacterial community composition differed significantly between sites close to and far from storm drains in February ($p = 0.03$, $R^2 = 38.6\%$) and March ($p = 0.03$, $R^2 = 38.6\%$) and this pattern was consistent among locations (**Figure 7A**).

We further expected that gene expression of bacterial communities in embayments would differ between sediments close to and far from storm drains. To investigate this, we performed ordination analyses based on Bray-Curtis dissimilarities for assembled non-rRNA transcripts with known functional annotation (**Figure 7B**). We found a clear separation by proximity to storm drain and sampling month. Similar results were obtained when investigating all assembled transcripts as well as transcripts without known functional annotation. Statistical analysis by PERMANOVA revealed that the compositon of assembled transcripts with known functional annotation differed with distance from storm drains ($p = 0.001$, $R^2 = 7.06\%$) and sampling time ($p = 0.04$, $R^2 = 7.20\%$). In addition, these transcripts differed significantly among sites in February ($p = 0.03$, $R^2 = 16.5\%$) and March ($p = 0.04$, $R^2 = 16.9\%$).

We additionally identified 56 bacterial transcripts that were differentially expressed ($p \leq 0.001$) between 0 and 1,000 m samples (**Figure 8**). The majority of these transcripts belonged

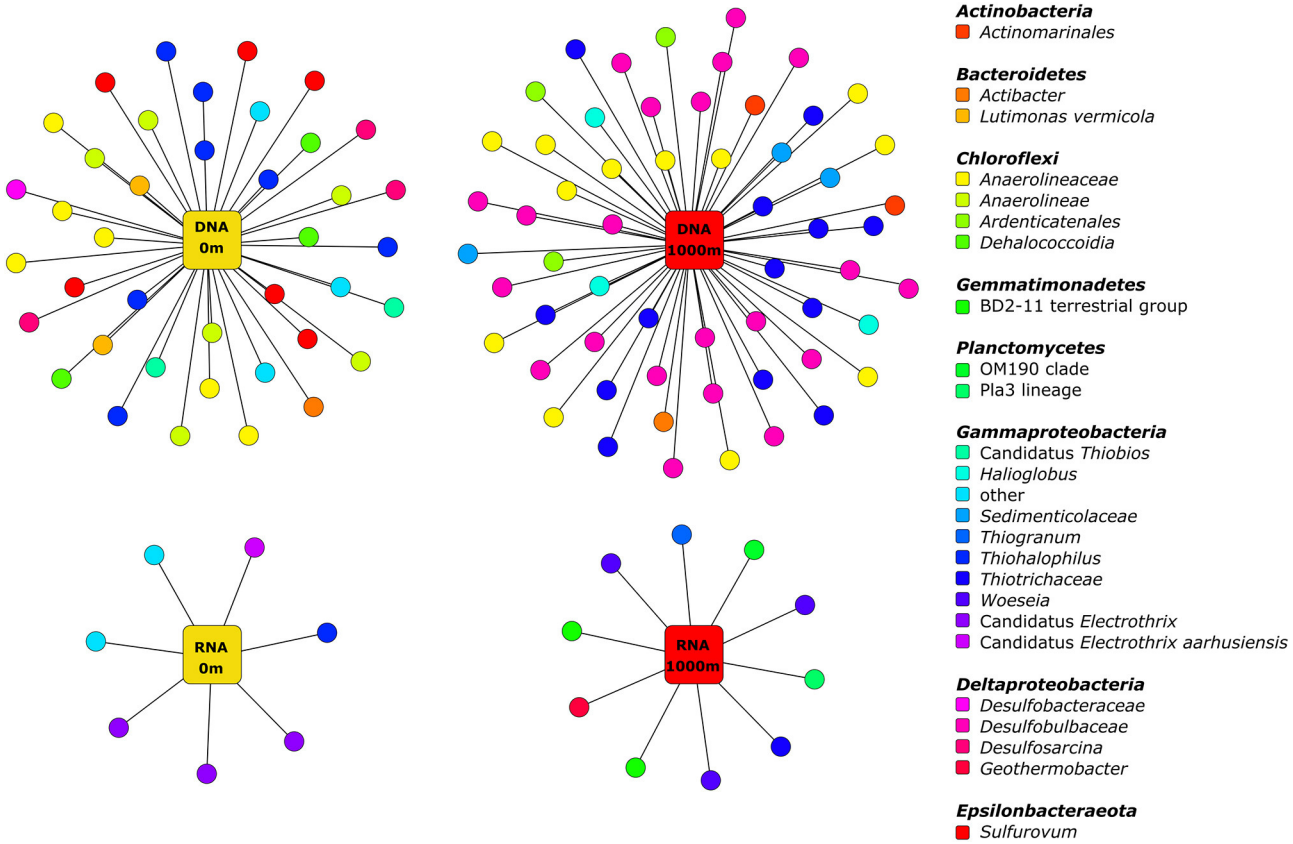

FIGURE 6 | Bipartite association network of significantly associated bacterial taxa close to and far from storm strains in embayment sediments. Only uniquely associated taxa from entire (DNA) and active (RNA) bacterial communities are shown. For further information see **Supplementary Table 5**.

to the HSP20 family (Heat shock proteins). Most transcripts encoding for the HSP20 family as well as multiple transcripts including those encoding for iron(III) transport system substrate-binding protein (K02012), nitrite reductase (NO-forming)/hydroxylamine reductase (K15864) and spore coat protein A (manganese oxidase; K06324) were expressed more at 1,000 m sites than other sites closer to stormwater outlets. By contrast, higher expressions of transcripts encoding for formyl-CoA transferase (K07749]) were detected in embayments close to storm drains. The transcripts for peptide/nickel transport system substrate-binding protein and for adenylylsulfate reductase, subunit A (K00394) and subunit B (K00395), were expressed significantly more at sites close to the storm drain at Hen and Chicken Bay, while a significantly higher expression of transcripts encoding for the arylsulfatase (K01130) were detected in Iron Cove samples collected at 1,000 m.

DISCUSSION

Over the past decade, the growing problem of contamination in marine systems, particularly urban estuaries, has resulted in an increase in research focused on understanding the impact of anthropogenic stressors such as metals or excess nutrients on bacterial communities (e.g., Liu et al., 2014; Beale et al., 2018; Birrer et al., 2018; Su et al., 2018). To date, most studies have focused on changes in diversity and community composition. Consequently, the functional responses of these communities to contaminant stressors are poorly understood. Here, we showed that alpha diversity measures and the composition of bacterial communities were affected by the hydrology that influences retention of water and sediment contaminants. We further demonstrated that bacterial communities in embayments differed more among the distance gradient from storm drains than in channels. These findings support our hypotheses that bacterial communities in channels and embayment systems respond differently to proximity to stormwater inputs. Further we found that the composition and functions of the active bacterial community in embayments differed between sites close to and far from storm drains. In addition, we found greater expression of several genes involved in bacterial stress response at sites further away from than close to storm drains. These findings suggest that bacterial communities in sites close to storm drains may be better adapted to anthropogenic stressors.

Relationships Between Estuarine Hydrology and Benthic Bacterial Diversity

Ecological monitoring studies in soft sediments have traditionally used diversity metrics as indicators of anthropogenic disturbance

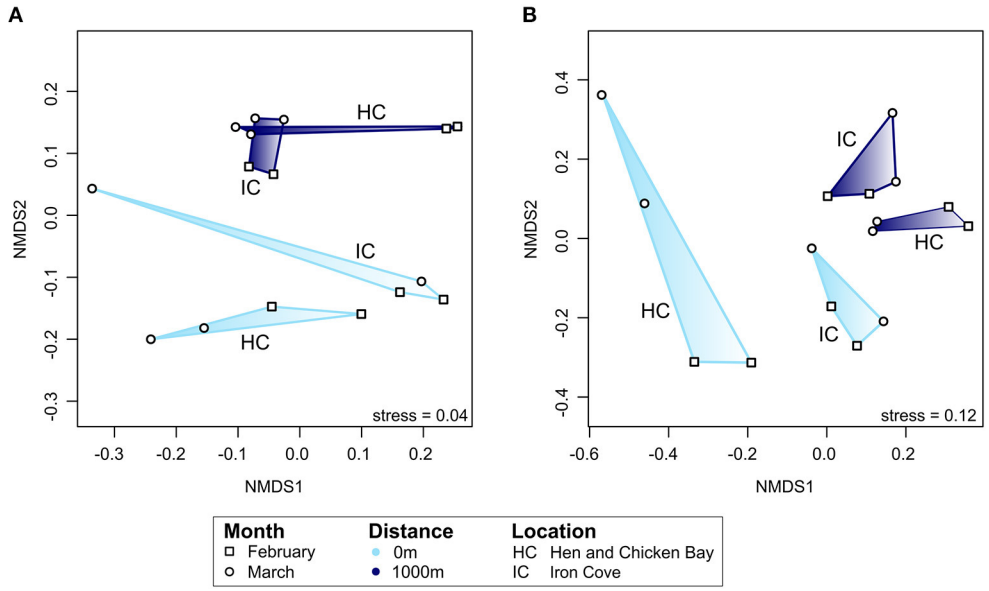

FIGURE 7 | Ordination analyses of the composition of the active bacterial community [rRNA; **(A)**] and assembled non-rRNA transcripts **(B)**. Only transcripts with known functional annotation were included in the analysis. Ordination is based on Bray-Curtis dissimilarities between samples and is colour-coded by distance from storm drain. Different symbols represent the two sampling months, February or March. Note that the nMDS axes have different scales for each ordination. The ordination plot for all (total) non-rRNA transcripts and those transcripts without known functional annotation can be found as **Supplementary Figure 6**. Data included in **Supplementary Table 4**. IC, Iron Cove; HC, Hen and Chicken Bay.

with the expectation that effects of contaminants might include decreased richness and evenness of communities (Johnston and Roberts, 2009). Our previous work has established that bacteria are as sensitive, if not more sensitive than archaea and eukaryotic microbes to the stressors examined in this study (Sun et al., 2012, 2013; Birrer et al., 2018, 2019). Here we showed that alpha diversity measures and the overall composition of bacterial communities were affected by retention type (hydrology). Specifically, bacterial diversity tended to be lower in the embayments compared to channels and was lowest in proximity to storm drains. This pattern of reduced diversity occurred where contaminant concentrations including Cu, Ni, Pb, and Zn were highest, and sediments were also highly enriched with organic carbon and nitrogen. Thus, contaminants accumulating in the sediments adjacent to stormdrains in poorly flushed embayments may be contributing to loss of sensitive species and increased dominance of more tolerant taxa (Johnston and Roberts, 2009). Some specific groups of bacteria also differed with respect to retention type. We found that *Desulfobacteraceae* and *Desulfobulbaceae* were more abundant in embayments, with *Desulfobacteraceae* most abundant next to storm drains. Members of the families Desulfobacteraceae and Desulfobulbaceae are well known sulphate-reducing bacteria (Leloup et al., 2005; Gittel et al., 2008). Sulphate-reducing bacteria display a certain degree of metal tolerance as a secondary outcome of their metabolism (Valls and De Lorenzo, 2002). Our findings highlight the abundance of sulphate-reducing bacteria in embayments in Sydney Harbour and how their distributions might be related to hydrological conditions in estuaries. While Sydney Harbour is a large and complex natural harbour, future studies that include multiple estuaries under a range of rainfall conditions would be useful to investigate the broader applicability of our findings.

Legacy Contamination Near Storm Drains in Embayments Linked to Altered Bacterial Community Composition and Functioning

Our analyses also revealed that benthic bacterial communities were related to various natural and anthropogenic properties such as metals and nutrients in both channels and embayments. A study by Yan et al. (2018) observed that TN and TC of the sediment samples significantly affected bacterial communities in mudflat sediments from the Dongtan wetland of Chongming Island. Partly in line with our and the above-mentioned study, TN had no effect on benthic bacterial communities along the Pearl Estuary (China), while TOC significantly correlated with these communities (Liu et al., 2014). Interestingly, in our study metal concentrations better predicted bacterial community composition in embayments than channels. Specifically, bacteria from embayments but not in channels differed among the distance gradient from storm drains and we observed significantly lower concentrations of several metals and nutrients in embayment samples 1,000 m away from the storm drain compared to those from 0 and 200 m. This supports our hypothesis that bacterial communities in channel and embayment systems respond differently to proximity to legacy stormwater contamination, and is in agreement with previous

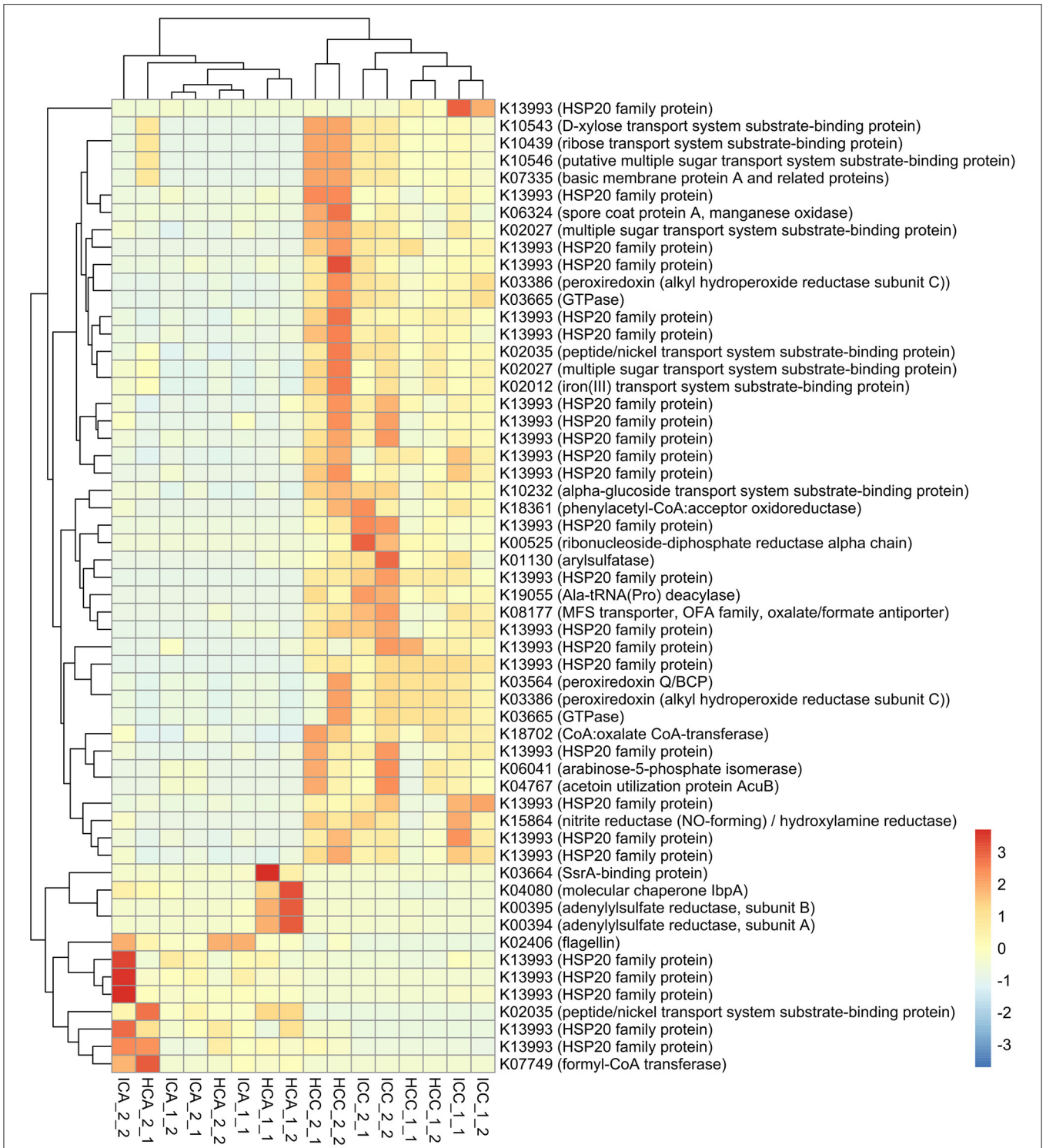

FIGURE 8 | Heatmap showing transcripts which were differentially expressed between 0 and 1,000 m samples of embayments. IC, Iron Cove; HC, Hen and Chicken Bay; A, 0 m; C, 1,000 m; 1_1, February Replicate 1; 1_2, February Replicate 2; 2_1, March Replicate 1; 2_2, March Replicate 2. The colour scale refers to log2 fold change normalised to the mean in each sample.

observations that nutrients and metals accumulate close to input sources (Liebens, 2001; Birch and Rochford, 2010). Differences may be occurring because the bacterial community living in close proximity to storm drains in embayments has recruited under prevailing contaminant concentrations. Thus, high metal concentrations may have selected for those microorganisms

more tolerant to metals as proposed by Gillan et al. (2005). Alternatively, the effect of metals on the bacterial community may be altered by the presence of excess nutrients in a so-called "antagonistic" interaction of multiple stressors. This might be supported by the higher total nitrogen and total organic carbon content found at 0 and 200 m in embayments compared to other embayment and channel sediments although only total nitrogen was a significant predictor of community composition. It should also be acknowledged that the microbial communities were sampled from the surface sediments (<2 mm depth) and thus variation may also reflect water or sediment properties that were not measured here such as light attenuation and pore water, respectively. However, experimental studies by the authors have identified direct causal impacts of metals and nutrients in sediments changing microbial communities (Birrer et al., 2018, 2019), and these stressor variables were statistically correlated with changes in this survey study and related studies (Sun et al., 2012, 2013; Dafforn et al., 2014).

In this study, the predominant genera between entire and active bacterial community differed significantly, which is in line with previous studies (Campbell and Kirchman, 2013; Wemheuer et al., 2017). While we cannot directly compare active and entire bacterial communities, as we used different approaches for the assessment, we observed that the uniquely associated zOTUs based on RNA-Seq analysis differed from those based on 16S rRNA gene sequencing. Nonetheless, consistent with our hypotheses and patterns in the entire bacterial community, the composition and functions of the active bacterial community in embayments differ between sites close to and far from storm drains. Such shifts may be explained by differences in metal and nutrient concentrations observed in the present study. Similarly to our study, significant changes in bacterial community composition and predicted functions, such as altered activity of genes involved in the nitrogen cycle as a response to anthropogenic activities, were recorded in a recent study on bacterial communities in surface sediments of Hangzhou Bay (Su et al., 2018). Dell'anno et al. (2003) showed in their study on the impact of metal contaminants on bacterial activities in coastal marine sediments that bacterial metabolism and turnover was inhibited by high metal concentrations. Our results together with previous studies (Wemheuer et al., 2015; Su et al., 2018) suggest that shifts in bacterial community composition result in altered community function.

Given the significant contamination found at sites close to storm drains, we also expected that the communities present would be highly stressed. Instead we found that several genes involved in bacterial stress response were more expressed at sites further away from storm drains. Further analysis revealed that the majority of differentially expressed transcripts belonged to the Hsp20 family. Heat shock proteins are involved in a universal molecular stress response and play an important role for cell growth and viability (Jung and Lee, 2012; Li, 2017). Previous studies showed that Hsp20 is involved in cellular defence under environmental stress conditions. In a study on the marine ciliate Euplotes crassu, many Hsps such as Hsp20 were up-regulated after metal exposure (Kim et al., 2018). Interestingly, these previous findings do not match our patterns in stress responses since metal concentrations tended to be higher near storm drains in embayments. However, this could be because the communities living in these degraded conditions are already tolerant to the contaminants present or less tolerant taxa have been subject to environmental filtering.

In addition to transcripts involved in stress response, we identified several other differentially expressed transcripts involved in the sulphur cycle such as the adenylylsulfate reductase (adenosine 5′-phosphosulfate [APS] reductase) or the arylsulfatase. The adenylylsulfate reductase plays an important role in catalysing APS to sulfite in the dissimilatory sulphate reduction pathway and thus represents a key enzyme in the energy metabolism of sulphate-reducing prokaryotes. The higher expression of adenylylsulfate reductase close to the storm drain in Hen and Chicken Bay may be related to higher organic content. In another study on arylsulfatase activity and arylsulfatase-producing bacteria in sediment samples collected from marine, estuarine and mangrove biotopes, higher substrate concentrations tended to inhibit the arylsulfatase activity (Chandramohan et al., 1974). This is supported by the present study, as a significantly higher expression of transcripts encoding for the arylsulfatase were detected in Iron Cove samples collected at 1,000 m where organic enrichment was lower.

In total, 96 and 16 sediment samples were analysed by 16S rRNA gene sequencing and RNA-Seq analysis, respectively. Calculated rarefaction and species accumulation curves confirmed that the library size was large enough to reflect the bacterial diversity in sediments investigated in the amplicon-based dataset. Nonetheless, the results of the current study are only valid for the proportion of the bacterial community covered by the surveying effort.

Bacterial Indicators for Biomonitoring at Storm Drains

Biomonitoring indicators need to fulfil several objectives (Rainbow, 1995). Firstly, they should be sensitive to the stressor of interest (e.g., metals and/or nutrients) and need to provide ecologically relevant information. Secondly, biomonitoring indicators need to produce repeatable information (i.e., low variability in the results from different replicates of the same treatment) and be reproducible in other systems with different contaminant concentrations. Finally, biomonitoring indicators should be transferable from the scientific sector to monitoring programs for easy and cost-effective application (Bourlat et al., 2013). Through indicator analysis, we identified several zOTUs belonging to the important sulphur-oxidising bacterial genera *Thiogranum* or *Sulfurovum* (Inagaki et al., 2004), which were significantly associated with 1,000 or 0 m samples, respectively. Furthermore, several bacterial zOTUs belonging to Candidatus *Electrothrix* showed unique associations with sites close to storm drains. These cable bacteria are long, multicellular filaments, that can conduct electric currents over centimetre-scale distances (Trojan et al., 2016). Taxa associated with 1,000 m sites could indicate sensitivity to elevated metal and nutrient concentrations since these decreased with distance from storm drains. Likewise, taxa significantly associated with 0 m sites might be more tolerant

to multiple anthropogenic stressors. These are initial patterns and further testing including experimental manipulation would be needed to determine if these are important bacterial indicators for contaminants in estuarine sediments and could be applied more broadly for biomonitoring.

CONCLUSION

Our results indicate that the impact of environmental properties on benthic bacterial communities is largely determined by estuarine hydrology. Furthermore, higher nutrient and metal concentrations close to storm drains in embayments are important predictors of benthic bacterial community structure and function. These patterns were detectable over and above significant spatial and temporal variation suggesting wider applicability than just Sydney Harbour. Our results therefore contribute to a better understanding of benthic bacterial responses to different retention types and associated anthropogenic stressors and have implications for future management practices in highly urbanised estuaries. An appropriate management action might be to redirect stormwater discharge points into faster flowing waters where any associated contaminants will be diluted and flushed, thus lessening any localised impacts. Future studies should assess how benthic bacterial communities and their functions in estuaries are affected upon large storm events and additional studies in estuaries with varied morphology and flushing characteristics would lend weight to our conclusions.

DATA AVAILABILITY STATEMENT

Sequence data were deposited in the sequence read archive (Ghosh et al., 2006) of the National Center for Biotechnology Information (NCBI) under accession numbers SUB7398817 (amplicons) and SUB7403872 (metatranscriptomes). All other data can be found in the **Supplementary Material**.

AUTHOR CONTRIBUTIONS

SB, KD, PG, PSt, SS, JP, PSc, MD, and EJ contributed to the experimental design. SB and KD collected the field samples. SB, FW, and KD analysed the data and wrote the manuscript text. All authors edited the manuscript text.

FUNDING

This research was funded by an ARC Linkage Grant (LP130100364) awarded to EJ, PSt, PG, MD, SS, and PSc. Fieldwork was conducted under NSW Department of Primary Industries permit number P13/0007e1.0.

ACKNOWLEDGMENTS

The authors would like to thank Tim Lachnit, Vivian Sim, volunteers and members of the Applied Marine and Estuarine Ecology laboratory for their field assistance. This paper is contribution number 279 from the Sydney Institute of Marine Science.

SUPPLEMENTARY MATERIAL

The Supplementary Material for this article can be found online at: https://www.frontiersin.org/articles/10.3389/fmicb.2021.661177/full#supplementary-material

REFERENCES

Allison, S. D., and Martiny, J. B. H. (2008). Resistance, resilience, and redundancy in microbial communities. *Proc. Natl. Acad. Sci. U.S.A.* 105, 11512–11519. doi: 10.1073/pnas.0801925105

Andrews, S. (2010). *FastQC: A Quality Control Tool for High Throughput Sequence Data*. Available online at: http://www.bioinformatics.babraham.ac.uk/projects/fastqc/

Aylagas, E., Borja, Á., Tangherlini, M., Dell'anno, A., Corinaldesi, C., Michell, C. T., et al. (2017). A bacterial community-based index to assess the ecological status of estuarine and coastal environments. *Mar. Pollut. Bull.* 114, 679–688. doi: 10.1016/j.marpolbul.2016.10.050

Bankevich, A., Nurk, S., Antipov, D., Gurevich, A. A., Dvorkin, M., Kulikov, A. S., et al. (2012). SPAdes: a new genome assembly algorithm and its applications to single-cell sequencing. *J. Comput. Biol.* 19, 455–477. doi: 10.1089/cmb.2012.0021

Barton, K. (2018). *MuMIn: Multi-Model Inference*. R package version 1.42.1. Available online at: https://CRAN.R-project.org/package=MuMIn

Beale, D. J., Crosswell, J., Karpe, A. V., Metcalfe, S. S., Morrison, P. D., Staley, C., et al. (2018). Seasonal metabolic analysis of marine sediments collected from Moreton Bay in South East Queensland, Australia, using a multi-omics-based approach. *Sci. Tot. Environ.* 631–632, 1328–1341. doi: 10.1016/j.scitotenv.2018.03.106

Bertilsson, S., Cavanaugh, C. M., and Polz, M. F. (2002). Sequencing-independent method to generate oligonucleotide probes targeting a variable region in bacterial 16S rRNA by PCR with detachable primers. *Appl. Environ. Microbiol.* 68:6077. doi: 10.1128/AEM.68.12.6077-6086.2002

Birch, G., and Rochford, L. (2010). Stormwater metal loading to a well-mixed/stratified estuary (Sydney Estuary, Australia) and management implications. *Environ. Monitor. Assess.* 169, 531–551. doi: 10.1007/s10661-009-1195-z

Birch, G. F., Murray, O., Johnson, I., and Wilson, A. (2009). Reclamation in Sydney Estuary, 1788-2002. *Austral. Geogr.* 40, 347–368. doi: 10.1080/00049180903127788

Birrer, S. C., Dafforn, K. A., Simpson, S. L., Kelaher, B. P., Potts, J., Scanes, P., et al. (2018). Interactive effects of multiple stressors revealed by sequencing total (DNA) and active (RNA) components of experimental sediment microbial communities. *Sci. Tot. Environ.* 637–638, 1383–1394. doi: 10.1016/j.scitotenv.2018.05.065

Birrer, S. C., Dafforn, K. A., Sun, M. Y., Williams, R. B. H., Potts, J., Scanes, P., et al. (2019). Using meta-omics of contaminated sediments to monitor changes in pathways relevant to climate regulation. *Environ. Microbiol.* 21, 389–401. doi: 10.1111/1462-2920.14470

Bolger, A. M., Lohse, M., and Usadel, B. (2014). Trimmomatic: a flexible trimmer for Illumina sequence data. *Bioinformatics* 30, 2114–2120. doi: 10.1093/bioinformatics/btu170

Bourlat, S. J., Borja, A., Gilbert, J., Taylor, M. I., Davies, N., Weisberg, S. B., et al. (2013). Genomics in marine monitoring: New opportunities for assessing marine health status. *Mar. Pollut. Bull.* 74, 19–31. doi: 10.1016/j.marpolbul.2013.05.042

Bureau of Meteorology (2014). *'Climate Data Online'*. Available online at: http://www.bom.gov.au/climate/data/index.shtml (accessed September 21, 2021).

Camacho, C., Coulouris, G., Avagyan, V., Ma, N., Papadopoulos, J., Bealer, K., et al. (2009). BLAST+: architecture and applications. *BMC Bioinformatics* 10:421. doi: 10.1186/1471-2105-10-421

Campbell, B. J., and Kirchman, D. L. (2013). Bacterial diversity, community structure and potential growth rates along an estuarine salinity gradient. *ISME J.* 7, 210–220. doi: 10.1038/ismej.2012.93

Chandramohan, D., Devendran, K., and Natarajan, R. (1974). Arylsulfatase activity in marine sediments. *Mar. Biol.* 27, 89–92. doi: 10.1007/BF00394764

Chariton, A. A., Court, L. N., Hartley, D. M., Colloff, M. J., and Hardy, C. M. (2010). Ecological assessment of estuarine sediments by pyrosequencing eukaryotic ribosomal DNA. *Front. Ecol. Environ.* 8, 233–238. doi: 10.1890/090115

Dafforn, K. A., Baird, D. J., Chariton, A. A., Sun, M. Y., Brown, M. V., Simpson, S. L., et al. (2014). "Chapter 1: Faster, higher and stronger? The pros and cons of molecular faunal data for assessing ecosystem condition," in *Advances in Ecological Research*, eds G. Woodward, A. J. Dumbrell, D. J. Baird, and M. Hajibabaei (London: Academic Press), 1–40. doi: 10.1016/B978-0-08-099970-8.00003-8

Dafforn, K. A., Simpson, S. L., Kelaher, B. P., Clark, G. F., Komyakova, V., Wong, C. K. C., et al. (2012). The challenge of choosing environmental indicators of anthropogenic impacts in estuaries. *Environ. Pollut.* 163, 207–217. doi: 10.1016/j.envpol.2011.12.029

Das, N., and Chandran, P. (2011). Microbial degradation of petroleum hydrocarbon contaminants: an overview. *Biotechnol. Res. Int.* 2011:941810. doi: 10.4061/2011/941810

De Cáceres, M., and Legendre, P. (2009). Associations between species and groups of sites: indices and statistical inference. *Ecology* 90, 3566–3574. doi: 10.1890/08-1823.1

Dell'anno, A., Mei, M., Ianni, C., and Danovaro, R. (2003). Impact of bioavailable heavy metals on bacterial activities in coastal marine sediments. *World J. Microbiol. Biotechnol.* 19, 93–100. doi: 10.1023/A:1022581632116

Edgar, R. C. (2010). Search and clustering orders of magnitude faster than BLAST. *Bioinformatics* 26, 2460–2461. doi: 10.1093/bioinformatics/btq461

Edgar, R. C., Haas, B. J., Clemente, J. C., Quince, C., and Knight, R. (2011). UCHIME improves sensitivity and speed of chimera detection. *Bioinformatics* 27, 2194–2200. doi: 10.1093/bioinformatics/btr381

Falkowski, P. G., Fenchel, T., and Delong, E. F. (2008). The microbial engines that drive Earth's biogeochemical cycles. *Science* 320, 1034–1039. doi: 10.1126/science.1153213

Ferrari, M. C. O., Mccormick, M. I., Munday, P. L., Meekan, M. G., Dixson, D. L., Lonnstedt, Ö., et al. (2011). Putting prey and predator into the CO2 equation - qualitative and quantitative effects of ocean acidification on predator-prey interactions. *Ecol. Lett.* 14, 1143–1148. doi: 10.1111/j.1461-0248.2011.01683.x

Floerl, O., and Inglis, G. J. (2003). Boat harbour design can exacerbate hull fouling. *Austral Ecol.* 28, 116–127. doi: 10.1046/j.1442-9993.2003.01254.x

Ghosh, P. K., Manna, M. C., Bandyopadhyay, K. K., Tripathi, A. K., Wanjari, R. H., Hati, K. M., et al. (2006). Interspecific interaction and nutrient use in soybean/sorghum intercropping system. *Agron. J.* 98, 1097–1108. doi: 10.2134/agronj2005.0328

Gillan, D. C., Danis, B., Pernet, P., Joly, G., and Dubois, P. (2005). Structure of sediment-associated microbial communities along a heavy-metal contamination gradient in the marine environment. *Appl. Environ. Microbiol.* 71, 679–690. doi: 10.1128/AEM.71.2.679-690.2005

Gittel, A., Mußmann, M., Sass, H., Cypionka, H., and Könneke, M. (2008). Identity and abundance of active sulfate-reducing bacteria in deep tidal flat sediments determined by directed cultivation and CARD-FISH analysis. *Environ. Microbiol.* 10, 2645–2658. doi: 10.1111/j.1462-2920.2008.01686.x

Glasl, B., Webster, N. S., and Bourne, D. G. (2017). Microbial indicators as a diagnostic tool for assessing water quality and climate stress in coral reef ecosystems. *Mar. Biol.* 164:91. doi: 10.1007/s00227-017-3097-x

Hammack, R. W., and Edenborn, H. M. (1992). The removal of nickel from mine waters using bacterial sulfate reduction. *Appl. Microbiol. Biotechnol.* 37, 674–678. doi: 10.1007/BF00240748

Hughes, J. B., Hellmann, J. J., Ricketts, T. H., and Bohannan, B. J. M. (2001). Counting the uncountable: statistical approaches to estimating microbial diversity. *Appl. Environ. Microbiol.* 67, 4399–4406. doi: 10.1128/AEM.67.10.4399-4406.2001

Hyatt, D., Chen, G., Locascio, P., Land, M., Larimer, F., and Hauser, L. (2010). Prodigal: prokaryotic gene recognition and translation initiation site identification. *BMC Bioinformatics* 11:119. doi: 10.1186/1471-2105-11-119

Inagaki, F., Takai, K., Nealson, K. H., and Horikoshi, K. (2004). *Sulfurovum lithotrophicum* gen. nov., sp. nov., a novel sulfur-oxidizing chemolithoautotroph within the ε-Proteobacteria isolated from Okinawa Trough hydrothermal sediments. *Int. J. Syst. Evol. Microbiol.* 54, 1477–1482. doi: 10.1099/ijs.0.03042-0

Irvine, I., and Birch, G. F. (1998). Distribution of heavy metals in surficial sediments of Port Jackson, Sydney, Australia. *Aust. J. Earth Sci.* 45, 297–304. doi: 10.1080/08120099808728388

Johnston, E. (2011). "Tolerance to contaminants: evidence from chronically-exposed populations of aquatic organisms," in *Tolerance to Environmental Contaminants*, eds C. Amiard-Triquet, P. S. Rainbow, and M. Romeo (Boca Raton, FL: CRC Press), 25–46. doi: 10.1201/b10519-3

Johnston, E. L., Mayer-Pinto, M., and Crowe, T. P. (2015a). Contaminant effects on ecosystem functioning: a review. *J. Appl. Ecol.* 52, 140–149. doi: 10.1111/1365-2664.12355

Johnston, E. L., Mayer-Pinto, M., Hutchings, P. A., Marzinelli, E. M., Ahyong, S. T., Birch, G., et al. (2015b). Sydney Harbour: what we do and do not know about a highly diverse estuary. *Mar. Freshw. Res.* 66, 1073–1087. doi: 10.1071/MF15159

Johnston, E. L., and Roberts, D. A. (2009). Contaminants reduce the richness and evenness of marine communities: a review and meta-analysis. *Environ. Pollut.* 157, 1745–1752. doi: 10.1016/j.envpol.2009.02.017

Jung, M.-Y., and Lee, Y.-M. (2012). Expression profiles of heat shock protein gene families in the monogonont rotifer Brachionus koreanus - exposed to copper and cadmium. *Toxicol. Environ. Health Sci.* 4, 235–242. doi: 10.1007/s13530-012-0141-6

Kanehisa, M. (2002). "The KEGG database," in *'In Silico' Simulation of Biological Processes: Novartis Foundation Symposium* (New Jersey), 91–103. doi: 10.1002/0470857897.ch8

Kembel, S. W., Cowan, P. D., Helmus, M. R., Cornwell, W. K., Morlon, H., Ackerly, D. D., et al. (2010). Picante: R tools for integrating phylogenies and ecology. *Bioinformatics* 26, 1463–1464. doi: 10.1093/bioinformatics/btq166

Kim, B.-M., Rhee, J.-S., Choi, I.-Y., and Lee, Y.-M. (2018). Transcriptional profiling of antioxidant defense system and heat shock protein (HSP) families in the cadmium- and copper-exposed marine ciliate Euplotes crassu. *Genes Genomics* 40, 85–98. doi: 10.1007/s13258-017-0611-y

Kopylova, E., Noé, L., and Touzet, H. (2012). SortMeRNA: fast and accurate filtering of ribosomal RNAs in metatranscriptomic data. *Bioinformatics* 28, 3211–3217. doi: 10.1093/bioinformatics/bts611

Kuznetsova, A., Brockhoff, P. B., and Christensen, R. H. B. (2018). *Package 'lmerTest' Version 3.0-1: Tests in Linear Mixed Effects Models*.

Lane, D. (1991). "16S/23S rRNA Sequencing," in *Nucleic Acid Techniques in Bacterial Systematics*. eds. E. Stackebrandt and M. Goodfellow (Hoboken, NY: Wiley Publishing), 115–175.

Langmead, B., and Salzberg, S. L. (2012). Fast gapped-read alignment with Bowtie 2. *Nat. Methods* 9, 357–359. doi: 10.1038/nmeth.1923

Lawes, J. C., Dafforn, K. A., Clark, G. F., Brown, M. V., and Johnston, E. L. (2017). Multiple stressors in sediments impact adjacent hard substrate habitats and across biological domains. *Sci. Tot. Environ.* 592, 295–305. doi: 10.1016/j.scitotenv.2017.03.083

Lee, S. B., Birch, G. F., and Lemckert, C. (2011). Field and modelling investigations of fresh-water plume behaviour in response to infrequent high-precipitation events, Sydney Estuary, Australia. *J. Estuar. Coast. Shelf Sci.* 92, 380–402. doi: 10.1016/j.ecss.2011.01.013

Leloup, J., Petit, F., Boust, D., Deloffre, J., Bally, G., Clarisse, O., et al. (2005). Dynamics of sulfate-reducing microorganisms (dsrAB genes) in two contrasting mudflats of the seine estuary (France). *Microb. Ecol.* 50, 307–314. doi: 10.1007/s00248-004-0034-6

Li, P. (2017). "Heat shock proteins in aquaculture disease immunology and stress response of crustaceans," in *Heat Shock Proteins in Veterinary Medicine and Sciences*, eds A. A. Asea and P. Kaur (Cham: Springer International Publishing), 275–320. doi: 10.1007/978-3-319-73377-7_10

Liebens, J. (2001). *Heavy metal contamination of sediments in stormwater management systems: The effect of land use, particle* size, and age.

Liu, J., Yang, H., Zhao, M., and Zhang, X.-H. (2014). Spatial distribution patterns of benthic microbial communities along the Pearl Estuary,

China. *Syst. Appl. Microbiol.* 37, 578–589. doi: 10.1016/j.syapm.2014.10.005

Love, M. I., Huber, W., and Anders, S. (2014). Moderated estimation of fold change and dispersion for RNA-seq data with DESeq2. *Genome Biol.* 15, 550–550. doi: 10.1186/s13059-014-0550-8

Lu, X.-M., Chen, C., and Zheng, T.-L. (2017). Metagenomic insights into effects of chemical pollutants on microbial community composition and function in estuarine sediments receiving polluted river water. *Microb. Ecol.* 73, 791–800. doi: 10.1007/s00248-016-0868-8

Machado, A., Spencer, K., Kloas, W., Toffolon, M., and Zarfl, C. (2016). Metal fate and effects in estuaries: a review and conceptual model for better understanding of toxicity. *Sci. Tot. Environ.* 541, 268–281. doi: 10.1016/j.scitotenv.2015.09.045

Mayer-Pinto, M., Cole, V., Johnston, E., Bugnot, A., Hurst, H., Airoldi, L., et al. (2017). Functional and structural responses to marine urbanisation. *Environ. Res. Lett.* 13:014009. doi: 10.1088/1748-9326/aa98a5

Mayer-Pinto, M., Johnston, E. L., Hutchings, P. A., Marzinelli, E. M., Ahyong, S. T., Birch, G., et al. (2015). Sydney Harbour: a review of anthropogenic impacts on the biodiversity and ecosystem function of one of the world's largest natural harbours. *Mar. Freshw. Res.* 66, 1088–1105. doi: 10.1071/MF15157

Meinicke, P. (2014). UProC: tools for ultra-fast protein domain classification. *Bioinformatics* 31, 1382–1388. doi: 10.1093/bioinformatics/btu843

Menzel, P., Ng, K. L., and Krogh, A. (2016). Fast and sensitive taxonomic classification for metagenomics with Kaiju. *Nat. Commun.* 7:11257. doi: 10.1038/ncomms11257

Nystrand, M. I., and Österholm, P., Yu, C., and Åström, M. (2016). Distribution and speciation of metals, phosphorus, sulfate and organic material in brackish estuary water affected by acid sulfate soils. *Applied Geochemistry* 66, 264–274. doi: 10.1016/j.apgeochem.2016.01.003

Oksanen, J., Blanchet, F. G., Kindt, R., Legendre, P., Minchin, P. R., O'hara, R. B., et al. (2017). *Vegan: Community Ecology Package*. R package version 2.4.-4.

Price, M. N., Dehal, P. S., and Arkin, A. P. (2010). FastTree 2 - approximately maximum-likelihood trees for large alignments. *PLoS ONE* 5:e9490. doi: 10.1371/journal.pone.0009490

Quast, C., Pruesse, E., Yilmaz, P., Gerken, J., Schweer, T., Yarza, P., et al. (2013). The SILVA ribosomal RNA gene database project: improved data processing and web-based tools. *Nucleic Acids Res.* 41, D590–D596. doi: 10.1093/nar/gks1219

Quero, G. M., Cassin, D., Botter, M., Perini, L., and Luna, G. M. (2015). Patterns of benthic bacterial diversity in coastal areas contaminated by heavy metals, polycyclic aromatic hydrocarbons (PAHs) and polychlorinated biphenyls (PCBs). *Front. Microbiol.* 6:1053. doi: 10.3389/fmicb,.2015.01053

R Core Team (2018). *R: A Language and Environment for Statistical Computing*. Vienna: R Foundation for Statistical Computing.

Rainbow, P. S. (1995). Biomonitoring of heavy metal availability in the marine environment. *Mar. Pollut. Bull.* 31, 183–192. doi: 10.1016/0025-326X(95)00116-5

Ritz, C., Baty, F., Streibig, J. C., and Gerhard, D. (2015). Dose-response analysis using R. *PLoS ONE* 10:e0146021. doi: 10.1371/journal.pone.0146021

Roy, P. S., Williams, R. J., Jones, A. R., Yassini, I., Gibbs, P. J., Coates, B., et al. (2001). Structure and function of south-east Australian estuaries. *Estuar. Coast. Shelf Sci.* 53, 351–384. doi: 10.1006/ecss.2001.0796

Sim, V. X. Y., Dafforn, K. A., Simpson, S. L., Kelaher, B. P., and Johnston, E. L. (2015). Sediment contaminants and infauna associated with recreational boating structures in a multi-use marine park. *PLoS ONE* 10:e0130537. doi: 10.1371/journal.pone.0130537

Su, Z., Dai, T., Tang, Y., Tao, Y., Huang, B., Mu, Q., et al. (2018). Sediment bacterial community structures and their predicted functions implied the impacts from natural processes and anthropogenic activities in coastal area. *Mar. Pollut. Bull.* 131, 481–495. doi: 10.1016/j.marpolbul.2018.04.052

Sun, M. Y., Dafforn, K. A., Brown, M. V., and Johnston, E. L. (2012). Bacterial communities are sensitive indicators of contaminant stress. *Mar. Pollut. Bull.* 64, 1029–1038. doi: 10.1016/j.marpolbul.2012.01.035

Sun, M. Y., Dafforn, K. A., Johnston, E. L., and Brown, M. V. (2013). Core sediment bacteria drive community response to anthropogenic contamination over multiple environmental gradients. *Environ. Microbiol.* 15, 2517–2531. doi: 10.1111/1462-2920.12133

Sutherland, M. D., Dafforn, K. A., Scanes, P., Potts, J., Simpson, S. L., Sim, V. X. Y., et al. (2017). Links between contaminant hotspots in low flow estuarine systems and altered sediment biogeochemical processes. *Estuar. Coast. Shelf Sci.* 198, 497–507. doi: 10.1016/j.ecss.2016.08.029

Trojan, D., Schreiber, L., Bjerg, J. T., Bøggild, A., Yang, T., Kjeldsen, K. U., et al. (2016). A taxonomic framework for cable bacteria and proposal of the candidate genera Electrothrix and Electronema. *Syst. Appl. Microbiol.* 39, 297–306. doi: 10.1016/j.syapm.2016.05.006

USEPA (2007). *Method 3051A Microwave Assisted Acid Digestion of Sediments, Sludges and Oils*. Washington, DC: US Environmental Protection Agency.

Vadillo Gonzalez, S., Johnston, E., Gribben, P. E., and Dafforn, K. (2019). The application of bioturbators for aquatic bioremediation: review and meta-analysis. *Environ. Pollut.* 250, 426–436. doi: 10.1016/j.envpol.2019.04.023

Valls, M., and De Lorenzo, V. (2002). Exploiting the genetic and biochemical capacities of bacteria for the remediation of heavy metal pollution. *FEMS Microbiol. Rev.* 26, 327–338. doi: 10.1016/S0168-6445(02)00114-6

Wemheuer, B., Wemheuer, F., Hollensteiner, J., Meyer, F.-D., Voget, S., and Daniel, R. (2015). The green impact: bacterioplankton response towards a phytoplankton spring bloom in the southern North Sea assessed by comparative metagenomic and metatranscriptomic approaches. *Front. Microbiol.* 6:805. doi: 10.3389/fmicb.2015.00805

Wemheuer, B., Wemheuer, F., Meier, D., Billerbeck, S., Giebel, H.-A., Simon, M., et al. (2017). Linking compositional and functional predictions to decipher the biogeochemical significance in DFAA turnover of abundant bacterioplankton lineages in the North Sea. *Microorganisms* 5:68. doi: 10.3390/microorganisms5040068

Yan, Y.-W., Jiang, Q.-Y., Wang, J.-G., Zhu, T., Zou, B., Qiu, Q.-F., et al. (2018). Microbial communities and diversities in mudflat sediments analyzed using a modified metatranscriptomic method. *Front. Microbiol.* 9:93. doi: 10.3389/fmicb.2018.00093

Conflict of Interest: The authors declare that the research was conducted in the absence of any commercial or financial relationships that could be construed as a potential conflict of interest.

Advantages of publishing in Frontiers

OPEN ACCESS
Articles are free to read for greatest visibility and readership

FAST PUBLICATION
Around 90 days from submission to decision

HIGH QUALITY PEER-REVIEW
Rigorous, collaborative, and constructive peer-review

TRANSPARENT PEER-REVIEW
Editors and reviewers acknowledged by name on published articles

Frontiers
Avenue du Tribunal-Fédéral 34
1005 Lausanne | Switzerland

Visit us: www.frontiersin.org
Contact us: frontiersin.org/about/contact

REPRODUCIBILITY OF RESEARCH
Support open data and methods to enhance research reproducibility

DIGITAL PUBLISHING
Articles designed for optimal readership across devices

FOLLOW US
@frontiersin

IMPACT METRICS
Advanced article metrics track visibility across digital media

EXTENSIVE PROMOTION
Marketing and promotion of impactful research

LOOP RESEARCH NETWORK
Our network increases your article's readership